Demonstration of Innovative Applications of Technology for Cost Reductions to the CT-121 FGD Process

DOE ICCT PROJECT DE-FC22-90PC89650

FINAL REPORT

Volume 6-B of 6: Appendices

Project Sponsors

Southern Company
US Department of Energy
Electric Power Research Institute

Issue Date: January 1997

Demonstration of Innovative Applications of Technology for Cost Reductions to the CT-121 FGD Process

Volume 6-B of 6: Appendices

Final Report, January 1997

Contents

"Design Calculations for 42' Diameter x 36'-6 JBR"
ERSHIGS Corporation

"FRP Acoustic Emission Inspection Report"
Physical Acoustics Corporation

"Strain Monitoring Final Report
Consulting and Testing Services

"Abrasion and Corrosive Coupons for JBR and Ductwork"
Southern Company Services, Inc.

Project Manager

David P. Burford
Southern Company
Southern Company Services, Inc.
44 Inverness Center Parkway
Suite 230
Birmingham, Alabama 35242

Project Sponsors

Southern Company
US Department of Energy
Electric Power Research Institute

"Design Calculations for 42' Diameter x 36'-6 JBR"

ERSHIGS Corporation

ERSHIGS
P. O. Box 1707
Bellingham, WA 98227

Design calculations for 42' Diameter X 36'-6 JBR

Southern Companies Services
Chiyoda Thoroughbred - 121
Georga Power Co. Yates Plant
Contract 195-89-005

Ershigs, Inc.
Job No. 3095

James Jarvis, P.E.
Feb. 1991

Table Of Contents

(1) Design basis:

Design pressure.....	+43" w.c. (1.6 psi)
Hydrostatic.....	14' liquid
Specific Gravity.....	1.2
Differential pressure on decks....	20" w.c. (0.75 psi)
Deposit on upper deck.....	10 psf
Slurry level on lower deck.....	6" (50psf)
Weight of gas spargers.....	20 lbs. ea.
Deposit on gas spargers.....	20 lbs. ea.
Total weight of gas spargers.....	40 lbs. ea.

(2) Design factors of safety:

(a) Operating loads strength limited.... 10 to 1 factor of safety

(b) Operating loads strain limited..... 0.001 in./in. max. strain

(c) Operating loads critical in buckling... 5 to 1

(d) Wind loads..... 5 to 1

(e) Seismic loads.... 3 to 1

(3) Laminate properties:

(a) Filament Wound Shell:

0 to 10'	Thickness.....	t = 1.10"
	Hoop modulus....	Eh = 3017000 psi
	Axial modulus...	Ea = 939500 psi
10' to 20'	Thickness.....	t = 0.94"
	Hoop modulus...	Eh = 2911000 psi
	Axial modulus..	Ea = 997300 psi
20' to 28'-6"	Thickness.....	t = 0.82"
	Hoop modulus...	Eh = 2961000 psi
	Axial modulus..	Ea = 915600 psi
28'-6" to 36'-6"	Thickness.....	t =0.74"
	Hoop modulus...	Eh = 2888000 psi
	Axial modulus..	Ea = 949800 psi

Note: Detailed laminate calculations are shown on the following computer printouts.

(b) Contact Molded Laminates:

Reference: Ashland Chemical technical data sheet for Hetron FR 992 vinyl ester resin, May 1989

Tensile Strength.....	25200 psi
Tensile Modulus.....	1380000 psi
Compressive Strength..	22500 psi

02-19-1991 09:47:07
TITLE/COMMENTS: Southern Companies Services

LAYER #		E11 PSI	E22 PSI	G12 PSI	NU12	NU21	ANGLE DEG	THICK IN
1.	C GLASS	5.00E+05	5.00E+05	4.00E+05	0.200	0.200	0.0	0.010
2.	1.5 OZ. MAT	9.00E+05	9.00E+05	4.00E+05	0.200	0.200	0.0	0.043
3.	1.5 OZ. MAT	9.00E+05	9.00E+05	4.00E+05	0.200	0.200	0.0	0.043
4.	FW 90/113YLD	4.30E+06	5.00E+05	4.00E+05	0.200	0.023	90.0	0.031
5.		4.30E+06	5.00E+05	4.00E+05	0.200	0.023	-90.0	0.031
6.	.75 OZ. MAT	9.00E+05	9.00E+05	4.00E+05	0.200	0.200	0.0	0.015
7.	FW 90/113YLD	4.30E+06	5.00E+05	4.00E+05	0.200	0.023	90.0	0.031
8.		4.30E+06	5.00E+05	4.00E+05	0.200	0.023	-90.0	0.031
9.	.75 OZ. MAT	9.00E+05	9.00E+05	4.00E+05	0.200	0.200	0.0	0.015
10.	FW 90/113YLD	4.30E+06	5.00E+05	4.00E+05	0.200	0.023	90.0	0.031
11.		4.30E+06	5.00E+05	4.00E+05	0.200	0.023	-90.0	0.031
12.	.75 OZ. MAT	9.00E+05	9.00E+05	4.00E+05	0.200	0.200	0.0	0.015
13.	15.6 UNI/FW	4.30E+06	6.00E+05	2.00E+05	0.100	0.014	0.0	0.030
14.	.75 OZ. MAT	9.00E+05	9.00E+05	4.00E+05	0.200	0.200	0.0	0.015
15.	FW 90/113YLD	4.30E+06	5.00E+05	4.00E+05	0.200	0.023	90.0	0.031
16.		4.30E+06	5.00E+05	4.00E+05	0.200	0.023	-90.0	0.031
17.	.75 OZ. MAT	9.00E+05	9.00E+05	4.00E+05	0.200	0.200	0.0	0.015
18.	FW 90/113YLD	4.30E+06	5.00E+05	4.00E+05	0.200	0.023	90.0	0.031
19.		4.30E+06	5.00E+05	4.00E+05	0.200	0.023	-90.0	0.031
20.	.75 OZ. MAT	9.00E+05	9.00E+05	4.00E+05	0.200	0.200	0.0	0.015
21.	FW 90/113YLD	4.30E+06	5.00E+05	4.00E+05	0.200	0.023	90.0	0.031
22.		4.30E+06	5.00E+05	4.00E+05	0.200	0.023	-90.0	0.031
23.	.75 OZ. MAT	9.00E+05	9.00E+05	4.00E+05	0.200	0.200	0.0	0.015
24.	15.6 UNI/FW	4.30E+06	6.00E+05	2.00E+05	0.100	0.014	0.0	0.030
25.	.75 OZ. MAT	9.00E+05	9.00E+05	4.00E+05	0.200	0.200	0.0	0.015
26.	FW 90/113YLD	4.30E+06	5.00E+05	4.00E+05	0.200	0.023	90.0	0.031
27.		4.30E+06	5.00E+05	4.00E+05	0.200	0.023	-90.0	0.031
28.	.75 OZ. MAT	9.00E+05	9.00E+05	4.00E+05	0.200	0.200	0.0	0.015
29.	FW 90/113YLD	4.30E+06	5.00E+05	4.00E+05	0.200	0.023	90.0	0.031
30.		4.30E+06	5.00E+05	4.00E+05	0.200	0.023	-90.0	0.031
31.	.75 OZ. MAT	9.00E+05	9.00E+05	4.00E+05	0.200	0.200	0.0	0.015
32.	FW 90/113YLD	4.30E+06	5.00E+05	4.00E+05	0.200	0.023	90.0	0.031
33.		4.30E+06	5.00E+05	4.00E+05	0.200	0.023	-90.0	0.031
34.	.75 OZ. MAT	9.00E+05	9.00E+05	4.00E+05	0.200	0.200	0.0	0.015
35.	15.6 UNI/FW	4.30E+06	6.00E+05	2.00E+05	0.100	0.014	0.0	0.030
36.	.75 OZ. MAT	9.00E+05	9.00E+05	4.00E+05	0.200	0.200	0.0	0.015
37.	FW 90/113YLD	4.30E+06	5.00E+05	4.00E+05	0.200	0.023	90.0	0.031
38.		4.30E+06	5.00E+05	4.00E+05	0.200	0.023	-90.0	0.031
39.	.75 OZ. MAT	9.00E+05	9.00E+05	4.00E+05	0.200	0.200	0.0	0.015
40.	FW 90/113YLD	4.30E+06	5.00E+05	4.00E+05	0.200	0.023	90.0	0.031
41.		4.30E+06	5.00E+05	4.00E+05	0.200	0.023	-90.0	0.031
42.	.75 OZ. MAT	9.00E+05	9.00E+05	4.00E+05	0.200	0.200	0.0	0.015
43.	.75 OZ. MAT	9.00E+05	9.00E+05	4.00E+05	0.200	0.200	0.0	0.015

02-19-1991
TITLE/COMMENTS: Southern Companies Services

TOTAL LAMINATE THICKNESS = 1.0930 IN.

AXIAL TENSILE MODULUS .. = 9.395E+05 PSI

HOOP TENSILE MODULUS ... = 3.017E+06 PSI

POISSON RATIO (XY) ..... = 0.130

POISSON RATIO (YX) ..... = 0.040

AXIAL FLEXURAL MODULUS = 8.472E+05 PSI

HOOP FLEXURAL MODULUS .. = 2.709E+06 PSI

?-19-1991 09:47:07
TTLE/COMMENTS: Southern Companies Services

A11	A12	A16	A22	A26	A66
1.0269E+06	1.3328E+05	0.0000E+00	3.2972E+06	0.0000E+00	4.1920E+05
B11	**B12**	**B16**	**B22**	**B26**	**B66**
-1.5088E-01	4.0346E+03	-8.1945E-04	-1.0819E+04	-7.0384E-03	7.8021E+03
D11	**D12**	**D16**	**D22**	**D26**	**D66**
9.2189E+04	1.4545E+04	1.8556E-05	2.9479E+05	1.5938E-04	4.2659E+04

A11*	A12*	A16*	A22*	A26*	A66*
9.7894E-07	-3.9571E-08	0.0000E+00	3.0489E-07	0.0000E+00	2.3855E-06
B11*	**B12***	**B16***	**B22***	**B26***	**B66***
6.6471E-04	2.4788E-04	2.9343E-10	9.2698E-09	2.6043E-11	1.2817E-04
D11*	**D12***	**D16***	**D22***	**D26***	**D66***
1.0932E-05	-5.3940E-07	-2.7401E-15	3.4188E-06	-1.2538E-14	2.3442E-05

02-19-1991 10:00:42
TITLE/COMMENTS: Southern Companies Services

LAYER		E11 PSI	E22 PSI	G12 PSI	NU12	NU21	ANGLE DEG	THICK IN
1.	C GLASS	5.00E+05	5.00E+05	4.00E+05	0.200	0.200	0.0	0.01
2.	1.5 OZ. MAT	9.00E+05	9.00E+05	4.00E+05	0.200	0.200	0.0	0.04
3.	1.5 OZ. MAT	9.00E+05	9.00E+05	4.00E+05	0.200	0.200	0.0	0.04
4.	FW 90/113YLD	4.30E+06	5.00E+05	4.00E+05	0.200	0.023	90.0	0.03
5.		4.30E+06	5.00E+05	4.00E+05	0.200	0.023	-90.0	0.03
6.	.75 OZ. MAT	9.00E+05	9.00E+05	4.00E+05	0.200	0.200	0.0	0.01
7.	FW 90/113YLD	4.30E+06	5.00E+05	4.00E+05	0.200	0.023	90.0	0.03
8.		4.30E+06	5.00E+05	4.00E+05	0.200	0.023	-90.0	0.03
9.	.75 OZ. MAT	9.00E+05	9.00E+05	4.00E+05	0.200	0.200	0.0	0.01
10.	FW 90/113YLD	4.30E+06	5.00E+05	4.00E+05	0.200	0.023	90.0	0.03
11.		4.30E+06	5.00E+05	4.00E+05	0.200	0.023	-90.0	0.03
12.	.75 OZ. MAT	9.00E+05	9.00E+05	4.00E+05	0.200	0.200	0.0	0.01
13.	15.6 UNI/FW	4.30E+06	6.00E+05	2.00E+05	0.100	0.014	0.0	0.03
14.	.75 OZ. MAT	9.00E+05	9.00E+05	4.00E+05	0.200	0.200	0.0	0.01
15.	FW 90/113YLD	4.30E+06	5.00E+05	4.00E+05	0.200	0.023	90.0	0.03
16.		4.30E+06	5.00E+05	4.00E+05	0.200	0.023	-90.0	0.03
17.	.75 OZ. MAT	9.00E+05	9.00E+05	4.00E+05	0.200	0.200	0.0	0.01
18.	FW 90/113YLD	4.30E+06	5.00E+05	4.00E+05	0.200	0.023	90.0	0.03
19.		4.30E+06	5.00E+05	4.00E+05	0.200	0.023	-90.0	0.03
20.	.75 OZ. MAT	9.00E+05	9.00E+05	4.00E+05	0.200	0.200	0.0	0.01
21.	15.6 UNI/FW	4.30E+06	6.00E+05	2.00E+05	0.100	0.014	0.0	0.03
22.	.75 OZ. MAT	9.00E+05	9.00E+05	4.00E+05	0.200	0.200	0.0	0.01
23.	FW 90/113YLD	4.30E+06	5.00E+05	4.00E+05	0.200	0.023	90.0	0.03
24.		4.30E+06	5.00E+05	4.00E+05	0.200	0.023	-90.0	0.03
25.	.75 OZ. MAT	9.00E+05	9.00E+05	4.00E+05	0.200	0.200	0.0	0.01
26.	FW 90/113YLD	4.30E+06	5.00E+05	4.00E+05	0.200	0.023	90.0	0.03
27.		4.30E+06	5.00E+05	4.00E+05	0.200	0.023	-90.0	0.03
28.	.75 OZ. MAT	9.00E+05	9.00E+05	4.00E+05	0.200	0.200	0.0	0.01
29.	15.6 UNI/FW	4.30E+06	6.00E+05	2.00E+05	0.100	0.014	0.0	0.03
30.	.75 OZ. MAT	9.00E+05	9.00E+05	4.00E+05	0.200	0.200	0.0	0.01
31.	FW 90/113YLD	4.30E+06	5.00E+05	4.00E+05	0.200	0.023	90.0	0.03
32.		4.30E+06	5.00E+05	4.00E+05	0.200	0.023	-90.0	0.03
33.	.75 OZ. MAT	9.00E+05	9.00E+05	4.00E+05	0.200	0.200	0.0	0.01
34.	FW 90/113YLD	4.30E+06	5.00E+05	4.00E+05	0.200	0.023	90.0	0.03
35.		4.30E+06	5.00E+05	4.00E+05	0.200	0.023	-90.0	0.03
36.	.75 OZ. MAT	9.00E+05	9.00E+05	4.00E+05	0.200	0.200	0.0	0.01
37.	.75 OZ. MAT	9.00E+05	9.00E+05	4.00E+05	0.200	0.200	0.0	0.01

02-19-1991
TITLE/COMMENTS: Southern Companies Services

TOTAL LAMINATE THICKNESS = 0.9390 IN.

AXIAL TENSILE MODULUS .. = 9.973E+05 PSI

HOOP TENSILE MODULUS ... = 2.911E+06 PSI

POISSON RATIO (XY) ..... = 0.123

POISSON RATIO (YX) ..... = 0.042

AXIAL FLEXURAL MODULUS = 8.361E+05 PSI

HOOP FLEXURAL MODULUS .. = 2.628E+06 PSI

-19-1991 10:00:42
TTLE/COMMENTS: Southern Companies Services

A11	A12	A16	A22	A26	A66
9.3649E+05	1.1520E+05	0.0000E+00	2.7333E+06	0.0000E+00	3.5760E+05
B11	**B12**	**B16**	**B22**	**B26**	**B66**
-6.0059E-02	3.8140E+03	-6.7046E-04	2.9432E+03	-5.7587E-03	7.9387E+03
D11	**D12**	**D16**	**D22**	**D26**	**D66**
5.7685E+04	9.4264E+03	9.2509E-06	1.8131E+05	7.9458E-05	2.7201E+04

A11*	A12*	A16*	A22*	A26*	A66*
1.0734E-06	-4.5238E-08	0.0000E+00	3.6776E-07	0.0000E+00	2.7964E-06
B11*	**B12***	**B16***	**B22***	**B26***	**B66***
-2.0232E-04	2.6219E-04	1.7310E-10	4.1286E-09	2.2146E-11	1.2596E-04
D11*	**D12***	**D16***	**D22***	**D26***	**D66***
1.7484E-05	-9.0899E-07	-3.2909E-15	5.5626E-06	-1.5940E-14	3.6764E-05

02-19-1991 10:43:51
TITLE/COMMENTS: Southern Companies Services

#	LAYER	E11 PSI	E22 PSI	G12 PSI	NU12	NU21	ANGLE DEG	THICK IN
1.	C GLASS	5.00E+05	5.00E+05	4.00E+05	0.200	0.200	0.0	0.010
2.	1.5 OZ. MAT	9.00E+05	9.00E+05	4.00E+05	0.200	0.200	0.0	0.043
3.	1.5 OZ. MAT	9.00E+05	9.00E+05	4.00E+05	0.200	0.200	0.0	0.043
4.	FW 90/113YLD	4.30E+06	5.00E+05	4.00E+05	0.200	0.023	90.0	0.031
5.		4.30E+06	5.00E+05	4.00E+05	0.200	0.023	-90.0	0.031
6.	.75 OZ. MAT	9.00E+05	9.00E+05	4.00E+05	0.200	0.200	0.0	0.015
7.	FW 90/113YLD	4.30E+06	5.00E+05	4.00E+05	0.200	0.023	90.0	0.031
8.		4.30E+06	5.00E+05	4.00E+05	0.200	0.023	-90.0	0.031
9.	.75 OZ. MAT	9.00E+05	9.00E+05	4.00E+05	0.200	0.200	0.0	0.015
10.	FW 90/113YLD	4.30E+06	5.00E+05	4.00E+05	0.200	0.023	90.0	0.031
11.		4.30E+06	5.00E+05	4.00E+05	0.200	0.023	-90.0	0.031
12.	.75 OZ. MAT	9.00E+05	9.00E+05	4.00E+05	0.200	0.200	0.0	0.015
13.	15.6 UNI/FW	4.30E+06	6.00E+05	2.00E+05	0.100	0.014	0.0	0.030
14.	.75 OZ. MAT	9.00E+05	9.00E+05	4.00E+05	0.200	0.200	0.0	0.015
15.	FW 90/113YLD	4.30E+06	5.00E+05	4.00E+05	0.200	0.023	90.0	0.031
16.		4.30E+06	5.00E+05	4.00E+05	0.200	0.023	-90.0	0.031
17.	.75 OZ. MAT	9.00E+05	9.00E+05	4.00E+05	0.200	0.200	0.0	0.015
18.	FW 90/113YLD	4.30E+06	5.00E+05	4.00E+05	0.200	0.023	90.0	0.031
19.		4.30E+06	5.00E+05	4.00E+05	0.200	0.023	-90.0	0.031
20.	.75 OZ. MAT	9.00E+05	9.00E+05	4.00E+05	0.200	0.200	0.0	0.015
21.	FW 90/113YLD	4.30E+06	5.00E+05	4.00E+05	0.200	0.023	90.0	0.031
22.		4.30E+06	5.00E+05	4.00E+05	0.200	0.023	-90.0	0.031
23.	.75 OZ. MAT	9.00E+05	9.00E+05	4.00E+05	0.200	0.200	0.0	0.015
24.	15.6 UNI/FW	4.30E+06	6.00E+05	2.00E+05	0.100	0.014	0.0	0.030
25.	.75 OZ. MAT	9.00E+05	9.00E+05	4.00E+05	0.200	0.200	0.0	0.015
26.	FW 90/113YLD	4.30E+06	5.00E+05	4.00E+05	0.200	0.023	90.0	0.031
27.		4.30E+06	5.00E+05	4.00E+05	0.200	0.023	-90.0	0.031
28.	.75 OZ. MAT	9.00E+05	9.00E+05	4.00E+05	0.200	0.200	0.0	0.015
29.	FW 90/113YLD	4.30E+06	5.00E+05	4.00E+05	0.200	0.023	90.0	0.031
30.		4.30E+06	5.00E+05	4.00E+05	0.200	0.023	-90.0	0.031
31.	.75 OZ. MAT	9.00E+05	9.00E+05	4.00E+05	0.200	0.200	0.0	0.015
32.	.75 OZ. MAT	9.00E+05	9.00E+05	4.00E+05	0.200	0.200	0.0	0.015

TOTAL LAMINATE THICKNESS = 0.8170 IN.

AXIAL TENSILE MODULUS .. = 9.156E+05 PSI

HOOP TENSILE MODULUS ... = 2.961E+06 PSI

POISSON RATIO (XY) ..... = 0.136

POISSON RATIO (YX) ..... = 0.042

AXIAL FLEXURAL MODULUS = 8.129E+05 PSI

HOOP FLEXURAL MODULUS .. = 2.560E+06 PSI

-19-1991 10:43:51
TTLE/COMMENTS: Southern Companies Services

A11	A12	A16	A22	A26	A66
7.4804E+05	1.0154E+05	0.0000E+00	2.4193E+06	0.0000E+00	3.1480E+05
B11	**B12**	**B16**	**B22**	**B26**	**B66**
-8.0566E-02	2.7799E+03	-5.9597E-04	-1.3101E+04	-5.1189E-03	5.1603E+03
D11	**D12**	**D16**	**D22**	**D26**	**D66**
3.6944E+04	6.3090E+03	1.6339E-05	1.1634E+05	1.4034E-04	1.7969E+04

A11*	A12*	A16*	A22*	A26*	A66*
1.3445E-06	-5.6429E-08	0.0000E+00	4.1570E-07	0.0000E+00	3.1766E-06
B11*	**B12***	**B16***	**B22***	**B26***	**B66***
1.6956E-03	3.5978E-04	5.5271E-10	1.0427E-08	4.1561E-11	1.9379E-04
D11*	**D12***	**D16***	**D22***	**D26***	**D66***
2.7321E-05	-1.4816E-06	-1.3271E-14	8.6761E-06	-6.6412E-14	5.5650E-05

02-19-1991 10:48:54
TITLE/COMMENTS: Southern Companies Services

YER		E11 PSI	E22 PSI	G12 PSI	NU12	NU21	ANGLE DEG	THIC IN
1.	C GLASS	5.00E+05	5.00E+05	4.00E+05	0.200	0.200	0.0	0.01
2.	1.5 OZ. MAT	9.00E+05	9.00E+05	4.00E+05	0.200	0.200	0.0	0.04
3.	1.5 OZ. MAT	9.00E+05	9.00E+05	4.00E+05	0.200	0.200	0.0	0.04
4.	FW 90/113YLD	4.30E+06	5.00E+05	4.00E+05	0.200	0.023	90.0	0.03
5.		4.30E+06	5.00E+05	4.00E+05	0.200	0.023	-90.0	0.03
6.	.75 OZ. MAT	9.00E+05	9.00E+05	4.00E+05	0.200	0.200	0.0	0.01
7.	FW 90/113YLD	4.30E+06	5.00E+05	4.00E+05	0.200	0.023	90.0	0.03
8.		4.30E+06	5.00E+05	4.00E+05	0.200	0.023	-90.0	0.03
9.	.75 OZ. MAT	9.00E+05	9.00E+05	4.00E+05	0.200	0.200	0.0	0.01
10.	FW 90/113YLD	4.30E+06	5.00E+05	4.00E+05	0.200	0.023	90.0	0.03
11.		4.30E+06	5.00E+05	4.00E+05	0.200	0.023	-90.0	0.03
12.	.75 OZ. MAT	9.00E+05	9.00E+05	4.00E+05	0.200	0.200	0.0	0.01
13.	15.6 UNI/FW	4.30E+06	6.00E+05	2.00E+05	0.100	0.014	0.0	0.03
14.	.75 OZ. MAT	9.00E+05	9.00E+05	4.00E+05	0.200	0.200	0.0	0.01
15.	FW 90/113YLD	4.30E+06	5.00E+05	4.00E+05	0.200	0.023	90.0	0.03
16.		4.30E+06	5.00E+05	4.00E+05	0.200	0.023	-90.0	0.03
17.	.75 OZ. MAT	9.00E+05	9.00E+05	4.00E+05	0.200	0.200	0.0	0.01
18.	FW 90/113YLD	4.30E+06	5.00E+05	4.00E+05	0.200	0.023	90.0	0.03
19.		4.30E+06	5.00E+05	4.00E+05	0.200	0.023	-90.0	0.03
20.	.75 OZ. MAT	9.00E+05	9.00E+05	4.00E+05	0.200	0.200	0.0	0.01
21.	15.6 UNI/FW	4.30E+06	6.00E+05	2.00E+05	0.100	0.014	0.0	0.03
22.	.75 OZ. MAT	9.00E+05	9.00E+05	4.00E+05	0.200	0.200	0.0	0.01
23.	FW 90/113YLD	4.30E+06	5.00E+05	4.00E+05	0.200	0.023	90.0	0.03
24.		4.30E+06	5.00E+05	4.00E+05	0.200	0.023	-90.0	0.03
25.	.75 OZ. MAT	9.00E+05	9.00E+05	4.00E+05	0.200	0.200	0.0	0.01
26.	FW 90/113YLD	4.30E+06	5.00E+05	4.00E+05	0.200	0.023	90.0	0.03
27.		4.30E+06	5.00E+05	4.00E+05	0.200	0.023	-90.0	0.03
28.	.75 OZ. MAT	9.00E+05	9.00E+05	4.00E+05	0.200	0.200	0.0	0.01
29.	.75 OZ. MAT	9.00E+05	9.00E+05	4.00E+05	0.200	0.200	0.0	0.01

TOTAL LAMINATE THICKNESS = 0.7400 IN.

AXIAL TENSILE MODULUS .. = 9.498E+05 PSI

HOOP TENSILE MODULUS ... = 2.888E+06 PSI

POISSON RATIO (XY) ..... = 0.132

POISSON RATIO (YX) ..... = 0.043

AXIAL FLEXURAL MODULUS = 7.992E+05 PSI

HOOP FLEXURAL MODULUS .. = 2.501E+06 PSI

-19-1991 10:48:54
ITTLE/COMMENTS: Southern Companies Services

A11	A12	A16	A22	A26	A66
7.0283E+05	9.2500E+04	0.0000E+00	2.1374E+06	0.0000E+00	2.8400E+05
B11	**B12**	**B16**	**B22**	**B26**	**B66**
-3.9063E-03	2.6877E+03	-5.2147E-04	-5.7735E+03	-4.4790E-03	5.2840E+03
D11	**D12**	**D16**	**D22**	**D26**	**D66**
2.6987E+04	4.7676E+03	1.1459E-05	8.4472E+04	9.8420E-05	1.3422E+04

A11*	A12*	A16*	A22*	A26*	A66*
1.4310E-06	-6.1926E-08	0.0000E+00	4.7053E-07	0.0000E+00	3.5211E-06
B11*	**B12***	**B16***	**B22***	**B26***	**B66***
7.9926E-04	3.7207E-04	3.9426E-10	5.4076E-10	3.6719E-11	1.8925E-04
D11*	**D12***	**D16***	**D22***	**D26***	**D66***
3.7429E-05	-2.1125E-06	-1.6463E-14	1.1957E-05	-8.5877E-14	7.4504E-05

(4) Operating Loads:

Design Pressure..... $P := 43$ in. W.C.
$P := 0.03613 \cdot P$
$P = 1.5536$ psi
Maximum liquid level... $H := 168$ in.
Specific gravity..... $SG := 1.2$

(a) Dished Cover:

	Crown		Knuckle	
Radius.....	$Rc := 420$	in	$Rz := 25.25$	in
Thickness.....	$Tc := 0.61$	in	$Tk := 0.61$	in

Allowable stress for contact molded laminates is.....

$$\frac{25200}{10} = 2520 \quad \text{psi} \qquad \text{(10 to 1 factor of safety)}$$

Stress in crown: $\sigma c := \dfrac{P \cdot Rc}{2 \cdot Tc}$ $\sigma c = 534.8425 < 2520$ psi

Stress in knuckle: (Ref. ASME Section VIII)

$$\sigma k := \frac{0.885 \cdot P \cdot Rc}{Tk} \qquad \sigma k = 946.6712 < 2520 \text{ psi}$$

Check for buckling of knuckle (Ref. Structural Analysis Of Shells by Baker,Kovalevsky and Rish pg. 258)

$t := 0.61$ in $A := 103$ in $B := 252$ in

$$\frac{t}{A} = 0.0059 \qquad \frac{A}{B} = 0.4087$$

From fig. 10-41 of the referenced work, the ratio of critical buckling pressure to modulus is:

$Pcr/E = 13X10^{-6}$ $E := 1.38 \cdot 10^{6}$

The critical pressure is..... $Pcr := 13 \cdot 10^{-6} \cdot E$
$Pcr = 17.94$ psi

The factor of safety is... $\dfrac{17.94}{1.55} = 11.5742 > 5$ to 1

(b) Vessel Shell: Radius... R := 252 in

Component weights:

Cover.....	Wc := 10000 lbs
Shell (0 to 10').....	W1 := 16000
Shell (10 to 20').....	W2 := 14000
Shell (20 to 28').....	W3 := 12000
Shell (28 to 36').....	W4 := 11000
Upper deck (+ Deposit).....	Wu := 25000
Lower deck (+ Liquid + Spargers).	Wl := 133000
Gas Risers.....	Wr := 8500
Grating deck.....	Wg := 7000

Hoop stress at vessel base: t := 1.10 in

Hydrostatic pressure.. Ph := 0.03613·H·SG
Ph = 7.2838 psi

Total pressure..... Pt := P + Ph
Pt = 8.8374 psi

Hoop stress..... $\sigma h := \frac{Pt \cdot R}{t}$ $\sigma h = 2024.5675$ psi

Hoop modulus..... Eh := 3017000 psi

Hoop strain..... $\epsilon h := \frac{\sigma h}{Eh}$ $\epsilon h = 0.0007 < 0.001$ in/in

Axial load..... W := Wc + W1 + W2 + W3 + W4 + Wu + Wl + Wr + Wg
W = 236500 lbs

Axial stress.... $\sigma a := \frac{W}{\pi \cdot 2 \cdot R \cdot t}$ $\sigma a = 135.787$ psi

Critical buckling stress (Ref. Formulas for Stress and Strain by Roarke and Young 4th Ed. pg 555 case 15

Axial modulus..... Ea := 939500 psi

Buckling stress... $\sigma cr := \frac{0.3 \cdot Ea \cdot t}{R}$ $\sigma cr = 1230.2976$ psi

Factor of safety..... $\frac{\sigma cr}{\sigma a} = 9.0605 > 5$ to 1

(4b) Continued:

Stress at 10' above base: $t := 0.94$ $Eh := 2911000$
$Ea := 997300$ $H := 48$
$Pt := P + 0.03613 \cdot H \cdot SG$ $Pt = 3.6347$

Hoop stress..... $\sigma h := \frac{Pt \cdot R}{t}$ $\sigma h = 974.403$ psi

Hoop strain..... $\epsilon h := \frac{\sigma h}{Eh}$ $\epsilon h = 0.0003 < 0.001$ in/in

Axial load..... $W := Wc + W2 + W3 + W4 + Wu + Wl + Wr + Wg$
$W = 220500$ lbs

Axial stress..... $\sigma a := \frac{W}{\pi \cdot 2 \cdot R \cdot t}$ $\sigma a = 148.1495$ psi

Buckling stress.. $\sigma cr := \frac{0.3 \cdot Ea \cdot t}{R}$ $\sigma cr = 1116.0262$ psi

Factor of safety.... $\frac{\sigma cr}{\sigma a} = 7.5331 > 5$ to 1

Stress at 20' above base: $t := 0.82$ $Eh := 2961000$
$Ea := 915600$

Hoop stress... $\sigma h := \frac{P \cdot R}{t}$ $\sigma h = 477.4447$ psi

Hoop strain... $\epsilon h := \frac{\sigma h}{Eh}$ $\epsilon h = 0.0002 < 0.001$ in/in

Axial load... $W := Wc + W3 + W4 + Wu + Wl + Wr$
$W = 199500$ lbs

Axial stress.. $\sigma a := \frac{W}{\pi \cdot 2 \cdot R \cdot t}$ $\sigma a = 153.6557$ psi

Buckling stress... $\sigma cr := \frac{0.3 \cdot Ea \cdot t}{R}$ $\sigma cr = 893.8$ psi

Factor of safety... $\frac{\sigma cr}{\sigma a} = 5.8169 > 5$ to 1

(4b) Continued:

Stress at 28' above base: $t := 0.74$ $Eh := 2888000$
$Ea := 949800$

Hoop stress... $\sigma h := \frac{P \cdot R}{t}$ $\sigma h = 529.0604$ psi

Hoop strain... $\epsilon h := \frac{\sigma h}{Eh}$ $\epsilon h = 0.0002 < 0.001$ in/in

Axial load... $W := Wc + W4 + Wu + Wr$
$W = 54500$ lbs

Axial stress... $\sigma a := \frac{W}{\pi \cdot 2 \cdot R \cdot t}$ $\sigma a = 46.5141$ psi

Buckling stress... $\sigma cr := \frac{0.3 \cdot Ea \cdot t}{R}$ $\sigma cr = 836.7286$ psi

Factor of safety... $\frac{\sigma cr}{\sigma a} = 17.9887 > 5$ to 1

(5) Finite Element Analysis of Deck System:

(a) Load on upper deck:

Differential pressure... +0.72 psi
(ignore weight of liquid on upper deck which acts in a negative direction and counteracts the pressure load)

(b) Load on gas risers: -0.73 psi

(c) Load on lower deck:

Differential pressure..	-0.73 psi
50 psf slurry load....	-0.35
Spargers and build up.	-0.30
Total load	-1.40 psi

(d) Temperature load: 95 deg F differential

(5) Load on support posts

(a) Main post:

Inside dia.	ID := 18		in
Thickness	t := 0.78		in
Outside dia	OD := ID + 2·t		in
	OD = 19.56		in
Modulus	E := 1000000		psi
Length	L := 219		in

The maximum loads as determined by the ANSYS model were:

+8200 lbs
-21900 lbs

Tensile stress: $\sigma t := \frac{8200}{\pi \cdot ID \cdot t}$ $\sigma t = 185.907 < 2520$

Compresive buckling: $I := \frac{\pi}{64} \cdot \left[OD^4 - ID^4 \right]$

Critical load (One end pinned):

$Fcr := \frac{\pi^2 \cdot E \cdot I}{4 \cdot L^2}$ $Fcr = 1.046 \cdot 10^5$ lbs

Factor of safety: $\frac{Fcr}{21900} = 4.774$ (approx. 5 to 1)

(OK since grating deck provides lateral support)

(b) Secondary posts:

ID := 14 in
t := 0.51
OD := 15.02

Maximum loads: +4716 -5200

$\sigma t := \frac{4716}{\pi \cdot ID \cdot t}$ $\sigma t = 210.245 < 2520$

$I := \frac{\pi}{64} \cdot \left[OD^4 - ID^4 \right]$ $Fcr := \frac{\pi^2 \cdot E \cdot I}{4 \cdot L^2}$ $Fcr = 1.046 \cdot 10^5$

Factor of safety: $\frac{Fcr}{5200} = 20.107$ > 5 to 1

(5) Continued:

(A) A linear analysis was run using the Algor program. Type 6 plate/shell elements were used in a quarter symetric model. Since the vessel shell was not modeled, the outer circumference of the decks were simply supported and the beam ends fixed. Contact molded physical properties were used for the decks and beams. The lower perforated deck was modeled as a solid plate with reduced stiffness calculated from STRESS ANALYSIS OF THICK PERFORATED PLATES BY Thomas Slot. The beams were fixed in the vertical direction at the locations of the internal suppport posts. The temperature differential was not applied because the edges of the deck were restrained.

The following plots show the principle stress, stress in thw X direction and stress in the Y direction on the top and bottom surfaces of both the upper and lower decks.

The design maximum stress for these components is 2520 psi. The design maximum deflection is 1/350 of the rafter (beam) span per the Chiyoda specification.

The maximum stress level is approximately 1400 psi and is generally in the 1000 psi level in the deck plates away from the beams. The maximum deflection is 0.4"

Enclosed are two disks which contain the Algor JBR deck model (File name JBRDECK7)

(B) A rough model was made of the perforated lower deck to approximate the stress concentration around the 5.59" dia. holes. A half symtetric model of the lower deck plate bounded by the deck support beams was modeled. The outter edge of the deck was fixed as was the 22" dia. gas riser tube. A -1.4 psi pressure load was applied. The maximum stress was 2038 psi next to the gas riser tube. The Algor model is enclosed on two disks (File name PERFDEC)

(6) Seismic design:

Per section 2312 of the Uniform Building Code (1988)

Seismic Zone Factor (Table 23-I)	Z := 0.15	(Zone 2A)
Importance Factor (Table 23-L)	I := 1.25	(Essential)
Coefficient (Table 23-Q)	Rw := 4	
Coefficient (Section 2312(e)2A)	C := 2.75	(Maximum)

Shear Force (Eq. 12-1) V = (ZIC/Rw) W
W = Component Weight

Component Weights and Moment Distances:

Cover.. Wc := 10000 lbs. Distance.. Hc := 40 ft.

Upper Deck.. Wu := 25000 Hu := 28

Gas Risers.. Wr := 8500 Hr := 24

Vessel Shell.. Ws := 53000 Hs := 0.67·36 (Eq. 12.8 of UBC)

lower Deck.. Wl := 133000 Hl := 20

Grating.. Wg := 7000 Hg := 15

Operating Liquid Level (14 ft.)

Liquid Weight.. $Ww := \pi \cdot 21^2 \cdot 14 \cdot 62.4 \cdot 1.2$ $Ww = 1.4524 \cdot 10^6$ lbs.

Distance.. Hw := 0.67·14 (Eq. 12.8 of UBC)

(6) Continued:

Seismic Moments at Each Thickness

(a) At Vessel Base: Thickness.. $t := 1.10$ in.
Axial Modulus.. $Ea := 939500$ psi

Vessel Inside Diameter.. $ID := 504$ in.
Vessel Outside Diameter $OD := 506.2$ in.
Distance to Neutral Axis $c := 253.1$ in.

Shell Moment of Inertia $Is := \left[\frac{\pi}{64}\right] \cdot \left[OD^4 - ID^4\right]$

$Is = 5.5666 \cdot 10^7$ in.^{4}

Seismic Moment...

$$M := \left[\frac{Z \cdot I \cdot C}{Rw}\right] \cdot (Wc \cdot Hc + Wu \cdot Hu + Wr \cdot Hr + Ws \cdot Hs + Wl \cdot Hl + Wg \cdot Hg + Ww \cdot Hw)$$

$M = 2.4454 \cdot 10^6$ ft.-lbs.

$M := 12 \cdot M$

$M = 2.9345 \cdot 10^7$ in.-lbs.

Total Axial Stress: $\sigma := \left[M \cdot \frac{c}{Is}\right] + 136$ $\sigma = 269.4274$ psi

Critical Buckling Stress: $\sigma c := \frac{0.3 \cdot Ea \cdot t}{r}$ $\sigma c = 1230.2976$ psi

Factor of Safety: $\frac{\sigma c}{\sigma} =$ 4.5663 > 3 to 1

(b) At 10 ft. above base: Thickness $t := 0.94$ in.
Axial Modulus $Ea := 997300$ psi
Outside Diameter $OD := 505.88$ in.
Neutral Axis $c := 252.94$

Moment of Inertia: $Is := \left[\frac{\pi}{64}\right] \cdot \left[OD^4 - ID^4\right]$

$Is = 4.7524 \cdot 10^7$ in.^{4}

(6) Continued:

Weight of Liquid Above 10 ft.:

$$Ww := \pi \cdot 21^2 \cdot 4 \cdot 62.4 \cdot 1.2$$

$Ww = 414967.6957$ lbs.

$Hw := 0.67 \cdot 4$ $Hw = 2.68$ ft.

Weight of Shell Above 10 ft.: $Ws := 37000$ lbs.

$Hs := 0.67 \cdot 26$ $Hs = 17.42$ ft.

$Hc := 30$ $Hu := 18$ $Hr := 14$ $Hl := 10$ $Hg := 5$

$$M := \left[Z \cdot I \cdot \frac{C}{Rw}\right] \cdot (Wc \cdot Hc + Wu \cdot Hu + Wr \cdot Hr + Ws \cdot Hs + Wl \cdot Hl + Wg \cdot Hg + Ww \cdot Hw)$$

$M = 514420.168$ ft.-lbs. $M := 12 \cdot M$

$M = 6.173 \cdot 10^6$ in.lbs.

$$\sigma a := \frac{Wc + Wu + Wr + Ws + Wl + Wg}{\pi \cdot 2 \cdot r \cdot t}$$

$\sigma a = 148.1495$ psi

Total Axial Stress: $\sigma := \frac{M \cdot c}{Is} + \sigma a$ $\sigma = 181.0051$ psi

Critical Buckling Stress: $\sigma c := \frac{0.3 \cdot Ea \cdot t}{r}$ $\sigma c = 1116.0262$ psi

Factor Of Safety: $\frac{\sigma c}{\sigma} = 6.1657$ > 3 to 1

(c) At 20 ft. Above Base:

Thickness	$t := 0.82$	in.
Axial Modulus	$Ea := 915600$	psi
Outside Diameter	$OD := 505.64$	in.
Neutral Axis	$c := 252.82$	in.

Moment of Inertia: $Is := \left[\frac{\pi}{64}\right] \cdot \left[OD^4 - ID^4\right]$

$Is = 4.1427 \cdot 10^7$ $in.^4$

(6) Continued: Weight of Shell Above 20 ft. $Ws := 23000$

$Hs := 0.67 \cdot 16$

$Hc := 20$ $Hu := 8$ $Hr := 4$

$$M := \left[Z \cdot I \cdot \frac{C}{Rw} \right] \cdot (Wc \cdot Hc + Wu \cdot Hu + Wr \cdot Hr + Ws \cdot Hs)$$

$M = 87728.4375$ ft.-lbs $M := 12 \cdot M$ $M = 1.0527 \cdot 10^{6}$ in.-lbs

Axial Stress: $$\sigma a := \frac{Wc + Wu + Wl + Wr + Ws}{\pi \cdot 2 \cdot r \cdot t} \quad \sigma a = 153.6557$$

Total Axial Stress $$\sigma := \left[M \cdot \frac{c}{Is} \right] + \sigma a \quad \sigma = 160.0803 \text{ psi}$$

Critical Buckling Stress: $$\sigma c := \frac{0.3 \cdot Ea \cdot t}{r} \quad \sigma c = 893.8 \text{ psi}$$

Factor of Safety: $\frac{\sigma c}{\sigma} =$ 5.5834 > 3 to 1

(d) At 28 ft. Above Base:

Thickness	$t := 0.74$	in.
Axial Modulus	$Ea := 949800$	psi
Outside Diameter	$OD := 505.48$	iin.
Neutral Axis	$c := 252.74$	in.

Moment of Inertia $$Is := \left[\frac{\pi}{64} \right] \cdot \left[OD^{4} - ID^{4} \right]$$

$Is = 3.7368 \cdot 10^{7}$ in.^{4}

Weight of Shell $Ws := 11000$ lbs.

$Hs := 0.67 \cdot 8$ ft.

$Hc := 11$

Moment: $$M := \left[Z \cdot I \cdot \frac{C}{Rw} \right] \cdot (Wc \cdot Hc + Ws \cdot Hs)$$

$M = 21780$ Ft.-lbs. $M := 12 \cdot M$

$M = 261360$ in.-lbs.

Axial Stress $\sigma a := \dfrac{Wc + Ws + Wu + Wr}{\pi \cdot 2 \cdot r \cdot t}$ $\sigma a = 46.5141$

Total Axial Stress $\sigma := \left[M \cdot \dfrac{c}{Is}\right] + \sigma a$ $\sigma = 48.2818$

Critical Buckling Stress $\sigma c := \dfrac{0.3 \cdot Ea \cdot t}{r}$ $\sigma c = 836.7286$ psi

Factor of Safety $\dfrac{\sigma c}{\sigma} = \boxed{17.3301 \quad > 3 \text{ to } 1}$

(7) Wind Load Design:

Per section 2311 of the Uniform Building Code (1988)

Height, Exposure and Gust Factor	$Ce := 1.3$	Table 23-G
Pressure Coefficient	$Cq := 0.8$	Table 23-H
Stagnation Pressure	$Qs := 17$	Table 23-F
Importance Factor	$I := 1.15$	Per 2311 (i)

Design Wind Pressure:

$P := Ce \cdot Cq \cdot Qs \cdot I$ (Eq. 11-1) $P = 20.332$

Uniform Wind Load $W := P \cdot 2 \cdot \dfrac{r}{12}$ $W = 853.944$ Lbs./ft.

$W := \dfrac{W}{12}$ $W = 71.162$ lbs./in.

Moment At Base: $H := 36.5 \cdot 12$

$M := 0.5 \cdot W \cdot H^2$ $M = 6.826 \cdot 10^6$ in.-lbs

Moment at 10 ft. $H := 26 \cdot 12$

$M := 0.5 \cdot W \cdot H^2$ $M = 3.4636 \cdot 10^6$ in.-lbs.

(7) Continued

Moment at 20 ft. $H := 16 \cdot 12$ $M := 0.5 \cdot W \cdot H^2$

$M = 1.3117 \cdot 10^6$ in.-lbs.

Moment at 28 ft. $H := 8 \cdot 12$ $M := 0.5 \cdot W \cdot H^2$

$M = 327914.496$ in.-lbs.

At 20 and 28 ft. the wind load moment is larger than the seismic moment:

At 20 ft.: total Axial Stress

$$\sigma := \left[1311700 \cdot \frac{252.82}{47524000}\right] + 148 \qquad \sigma = 154.978 \text{ psi}$$

Factor of Safety $\frac{894}{155} = 5.7677 > 5$ to 1

At 28 ft. Total Axial Stress

$$\sigma := \frac{327914 \cdot 252.74}{37368000} + 48 \qquad \sigma = 50.2179 \text{ psi}$$

Factor of Safety $\frac{837}{50} = 16.74 > 5$ to 1

(8) Anchor Bolt and Hold Down Design

Anchor bolts and anchor dog design is shown on the next using the base seismic moment 29345000 in.-lbs. Only the shell and cover weight is considered to resist this moment.

Design of Base Ring & Anchor Dog

Load on Anchor Bolt

Inside diameter of vessel (in).....	d := 504
Load diameter (in).....	D := 507.2
Load Radius (in).....	R := 253.6
Bolt Circle (in).....	BC := 512
Distance from load to bolt (in).....	a := 2.0
Distance from bolt to "A" (in).....	b := 5
Bending moment at base (in*lb).....	M := 29345000
Shell weight (lb).....	W := 63000
Design Pressure (psi).....	p := 1.55
Number of anchor dogs	N := 42

$$Msr := W \cdot \frac{D}{2} \qquad Mt := M - Msr \qquad \sigma := \frac{Mt}{S} \quad \text{Where:} \quad S := \pi \cdot t \cdot R^2$$

$$\text{Therefore:} \quad \sigma := \frac{Mt}{\pi \cdot t \cdot R^2} \qquad \text{If: } \sigma * t = X \quad \text{Then} \quad X := \frac{Mt}{\pi \cdot R^2} \qquad Y := p \cdot \frac{d}{4}$$

$$P := \frac{3.14 \cdot D \cdot (X + Y)}{N} \qquad F := \frac{P \cdot (a + b)}{b}$$

Total moment at Base (in*lb).....	$Mt = 1.34 \cdot 10^7$
Load in bolt (lb).....	F = 13880.34
Load per anchor dog (lb/dog).....	P = 9914.53
Allowable load for 1.0" bolt is 15700 LBS.	

Bending in anchor dog

Width of base of Dog (in).....	B := 1.5 (2 ea. 0.75 "plts.)
Height of dog (in).....	H := 2.5

$$M := \frac{F \cdot a \cdot b}{a + b} \qquad S := \left[B \cdot \frac{H^2}{6} \right] \qquad \sigma d := \frac{M}{S}$$

Section modulus (in^3).....	S = 1.56
Bending moment (in*lb).....	M = 19829.06
Bending stress (psi).....	σd = 12690.6
Allowable stress for steel is 36000 psi	

Shear on anchor ledge

Ledge Height (in).....	h := 6
Dog Width (in).....	B1 := 4

$$A := B1 \cdot h + h \cdot h \qquad \tau := \frac{P}{A}$$

Shear Area (in^2).....	A = 60
Shear on anchor ledge (psi).....	τ = 165.24
Allowable shear is 250 psi per PS-15-69	

2,3

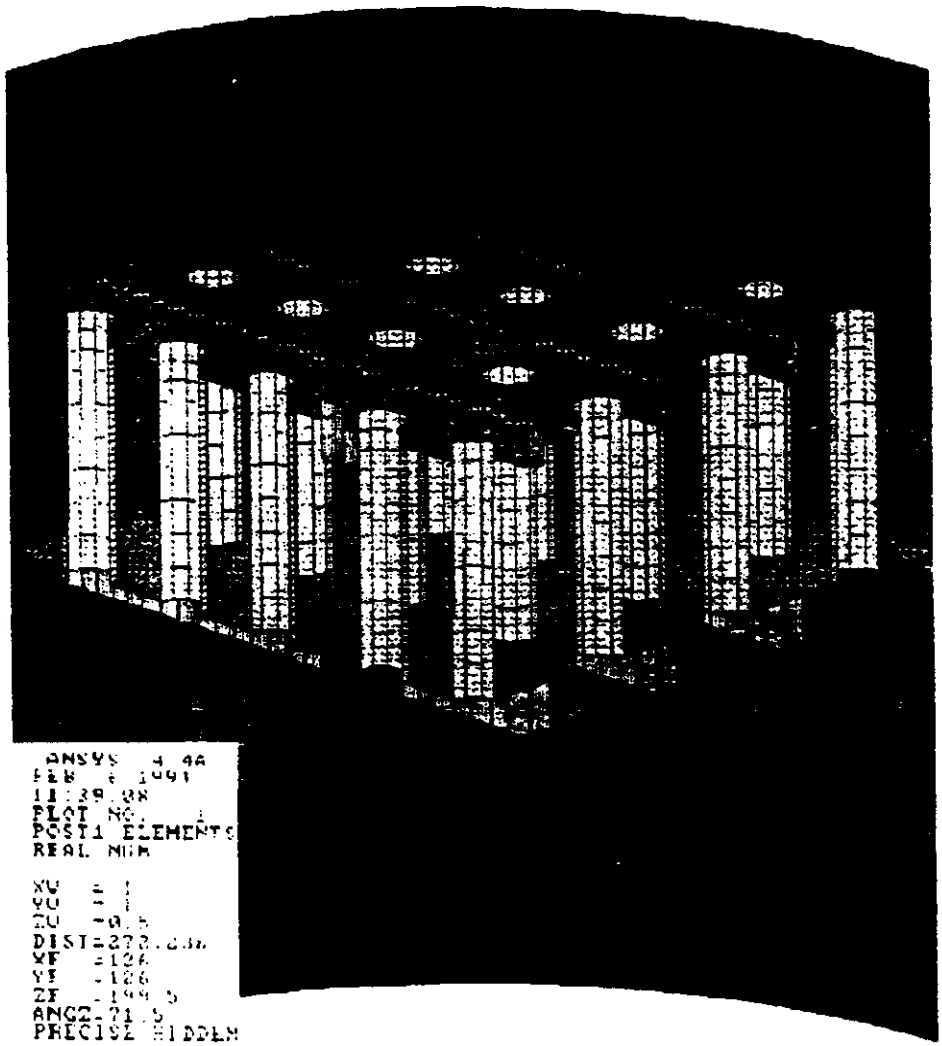

ISR Deck Analysis

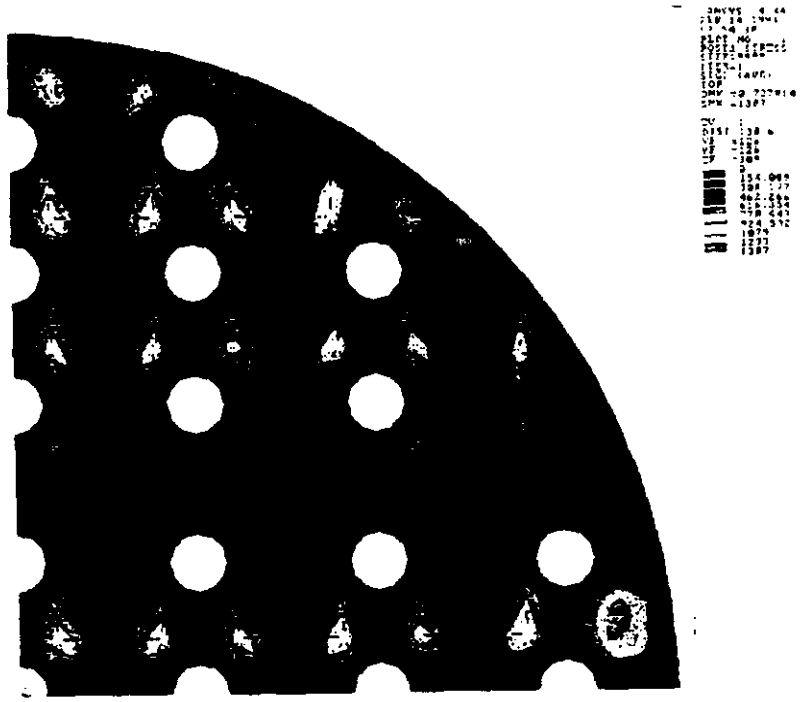

Deck - Principal stresses on top surface

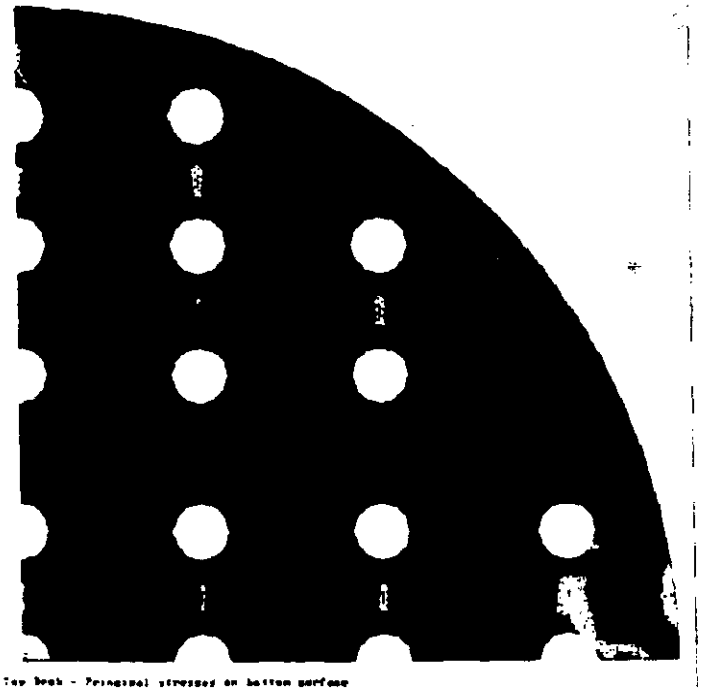

Top Deck - Principal stresses on bottom surface

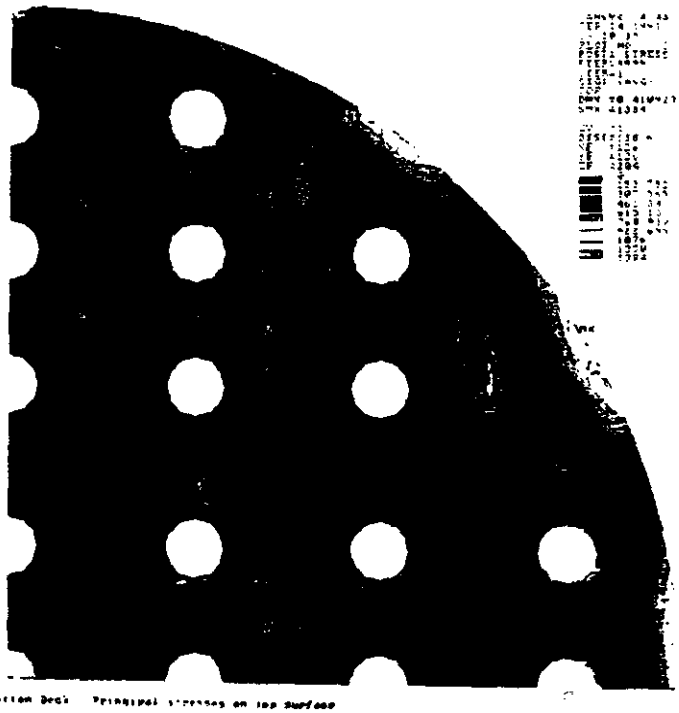

Section Deck - Principal stresses on top surface

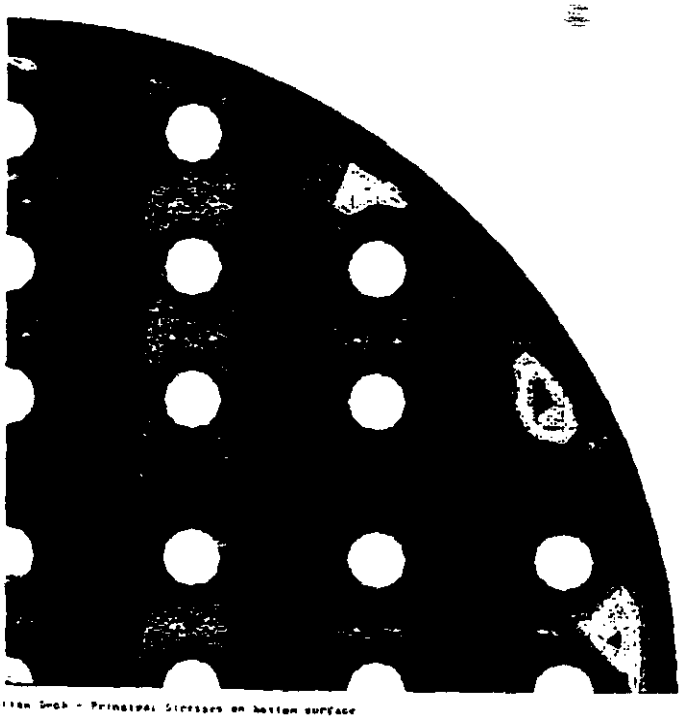

Bulkhead Deck - Principal Stresses on bottom surface

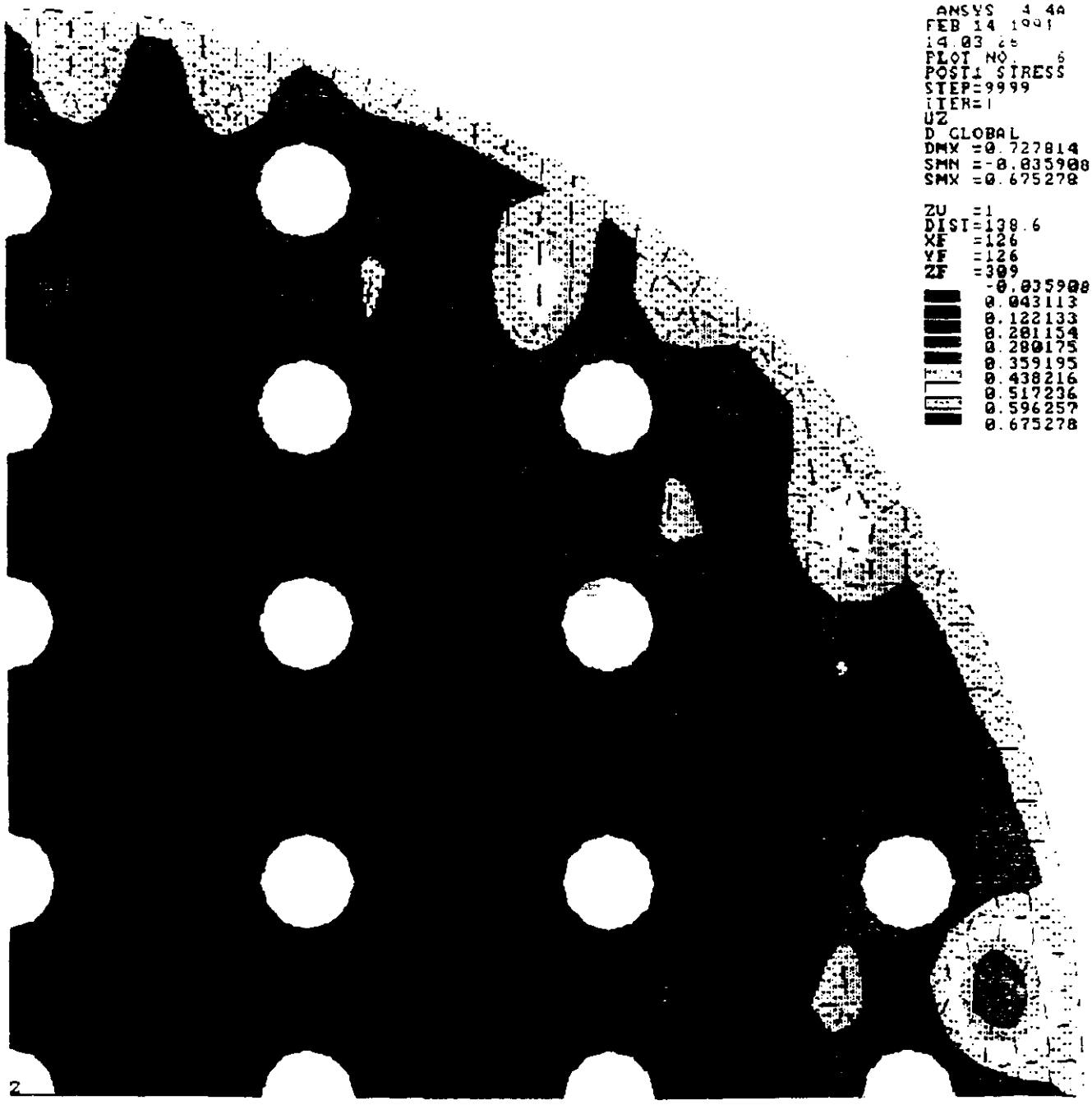

Top Deck - Displacements in Z (Vertical) Direction

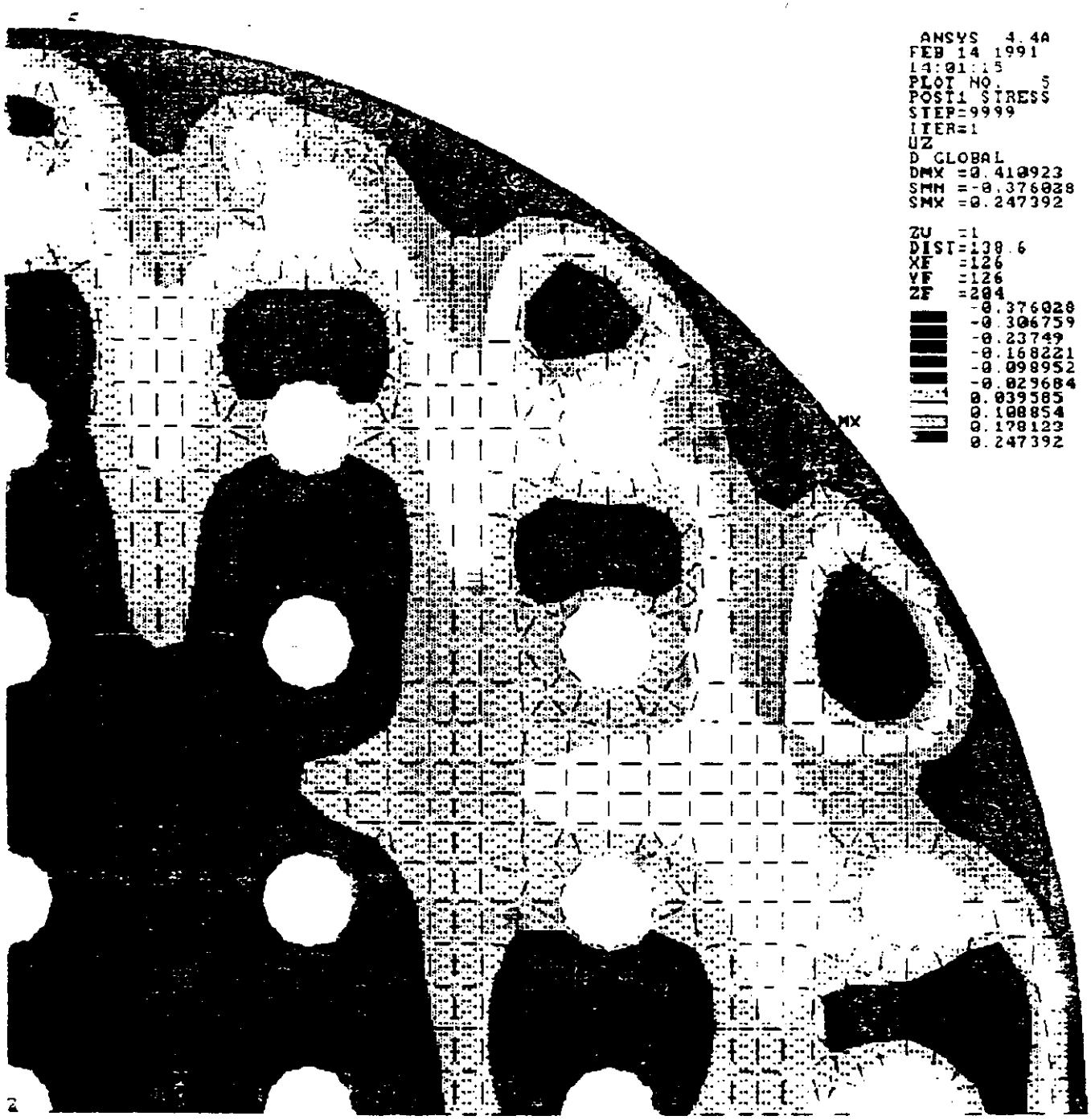

Bottom Deck - Displacements in Z (Vertical) Direction

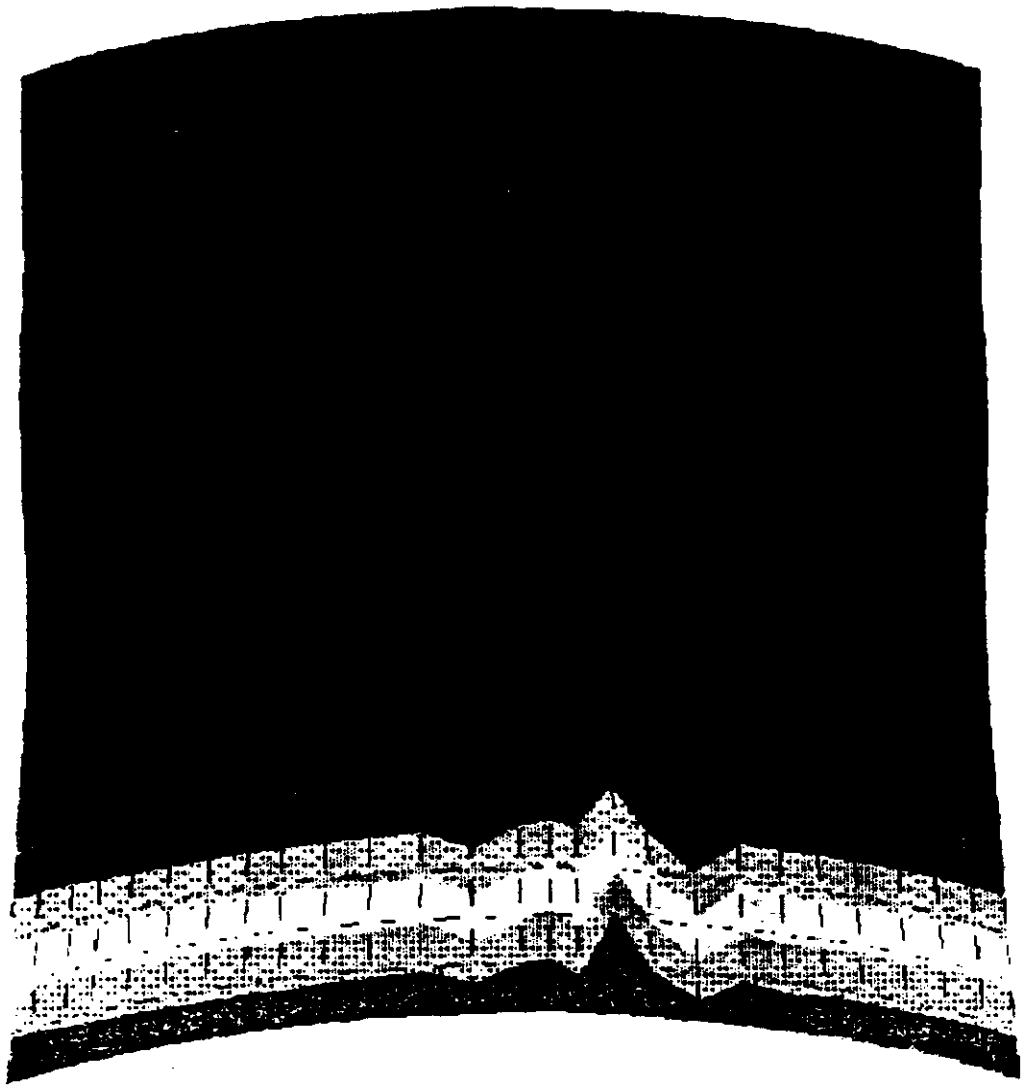

Outer Shell Principal stresses

σp
Top Deck
upper surface

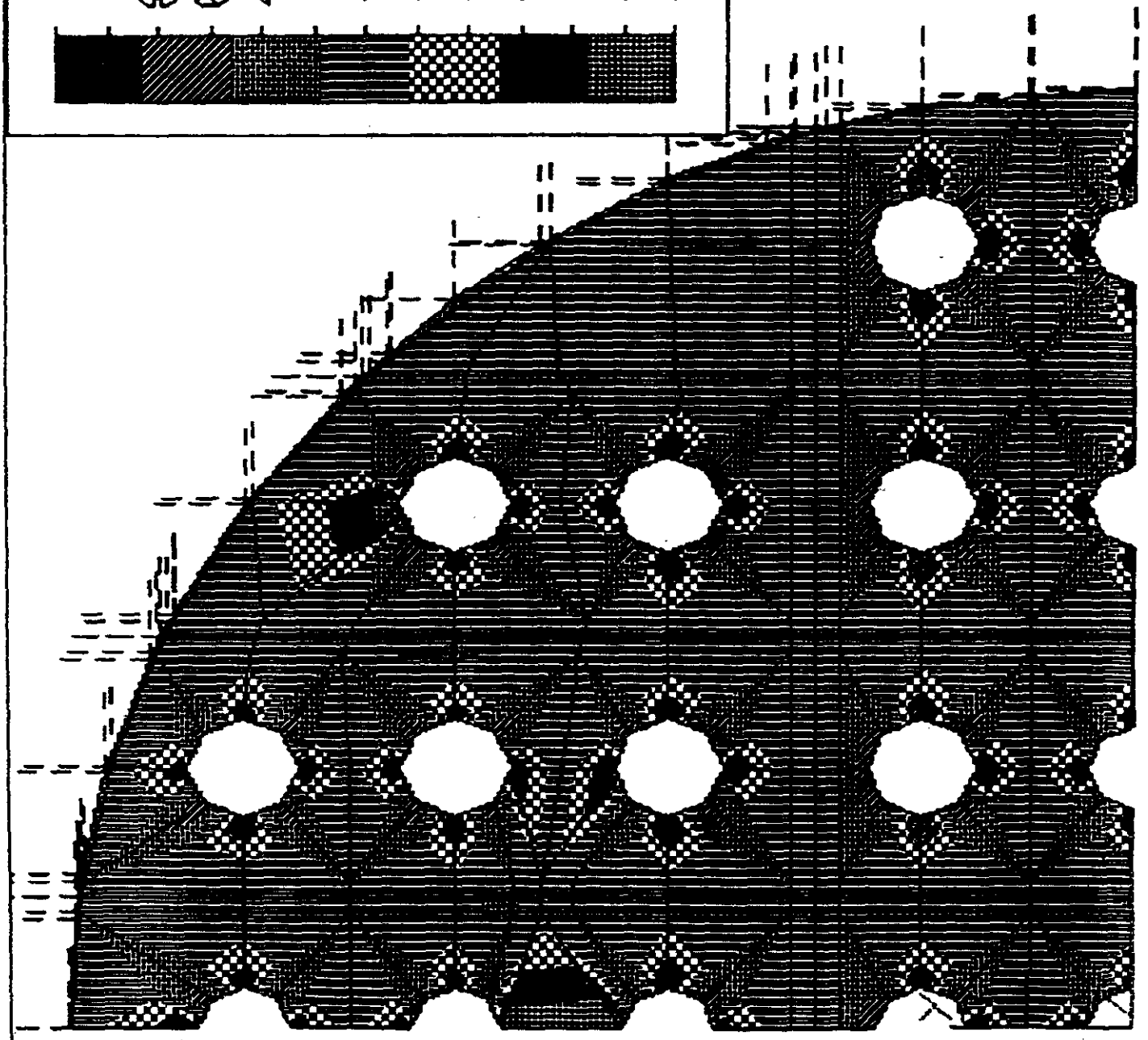

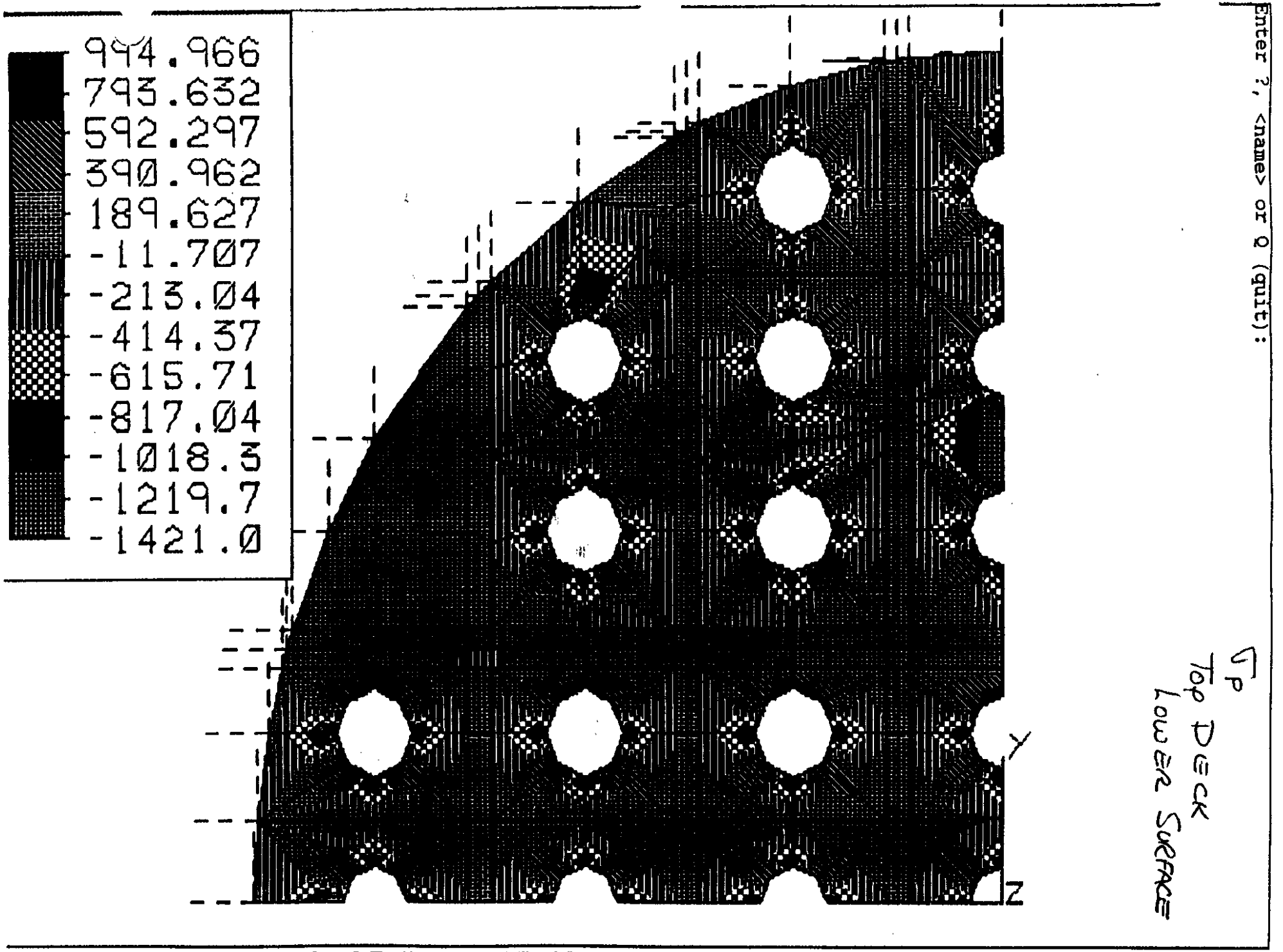

VIEWH 3.14 File: ibrdeck7 91/01/15 16:08 LC 1/ 1 Vu= 4 Lo= 180 La= -90 R= 0

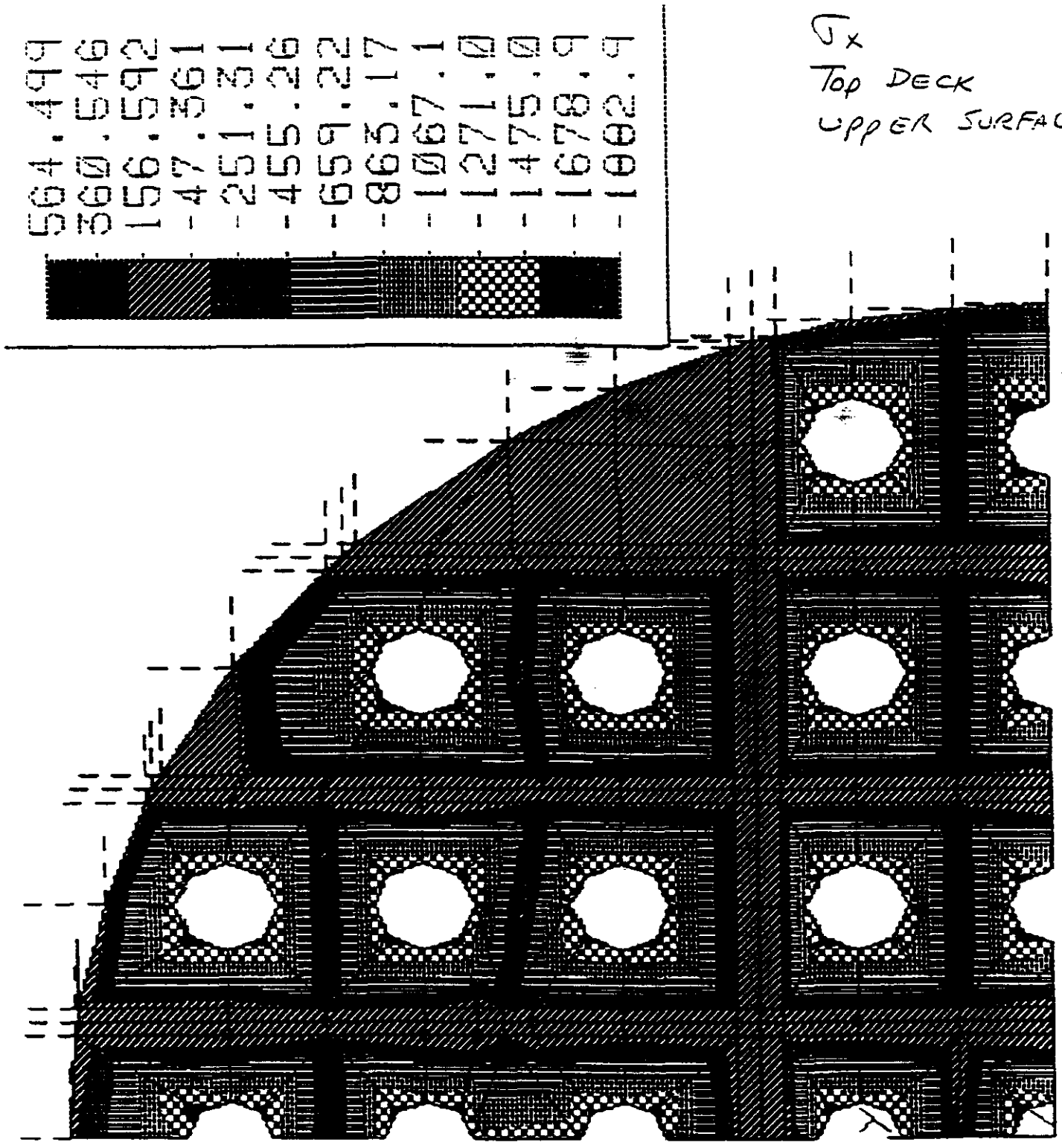
564.494
568.546
572.598
576.651
580.703
584.755
588.807
592.859
596.911
600.963
σx
Top Deck
Upper Surface

FY
TOP DECK
LOWER SURFACE

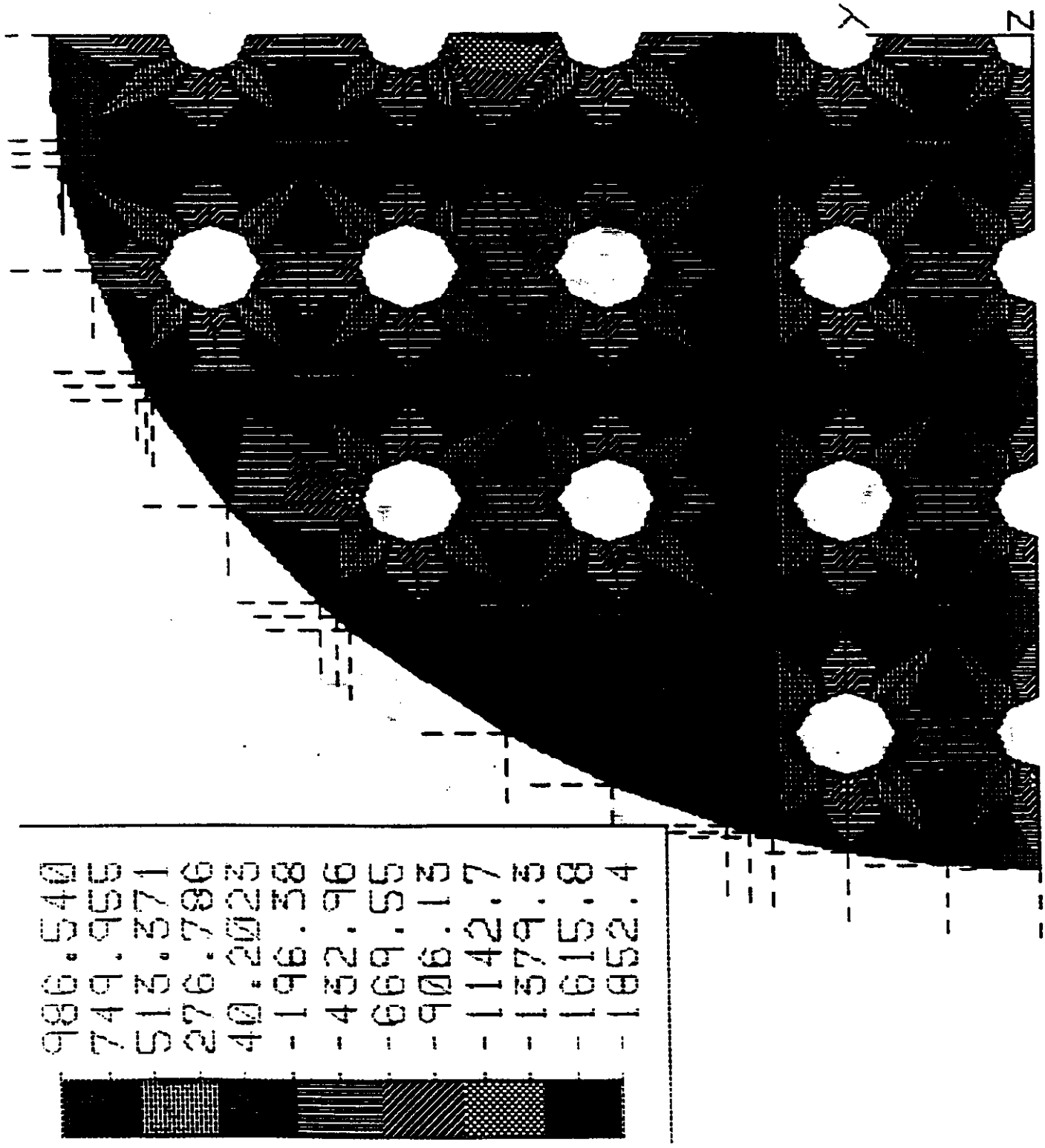

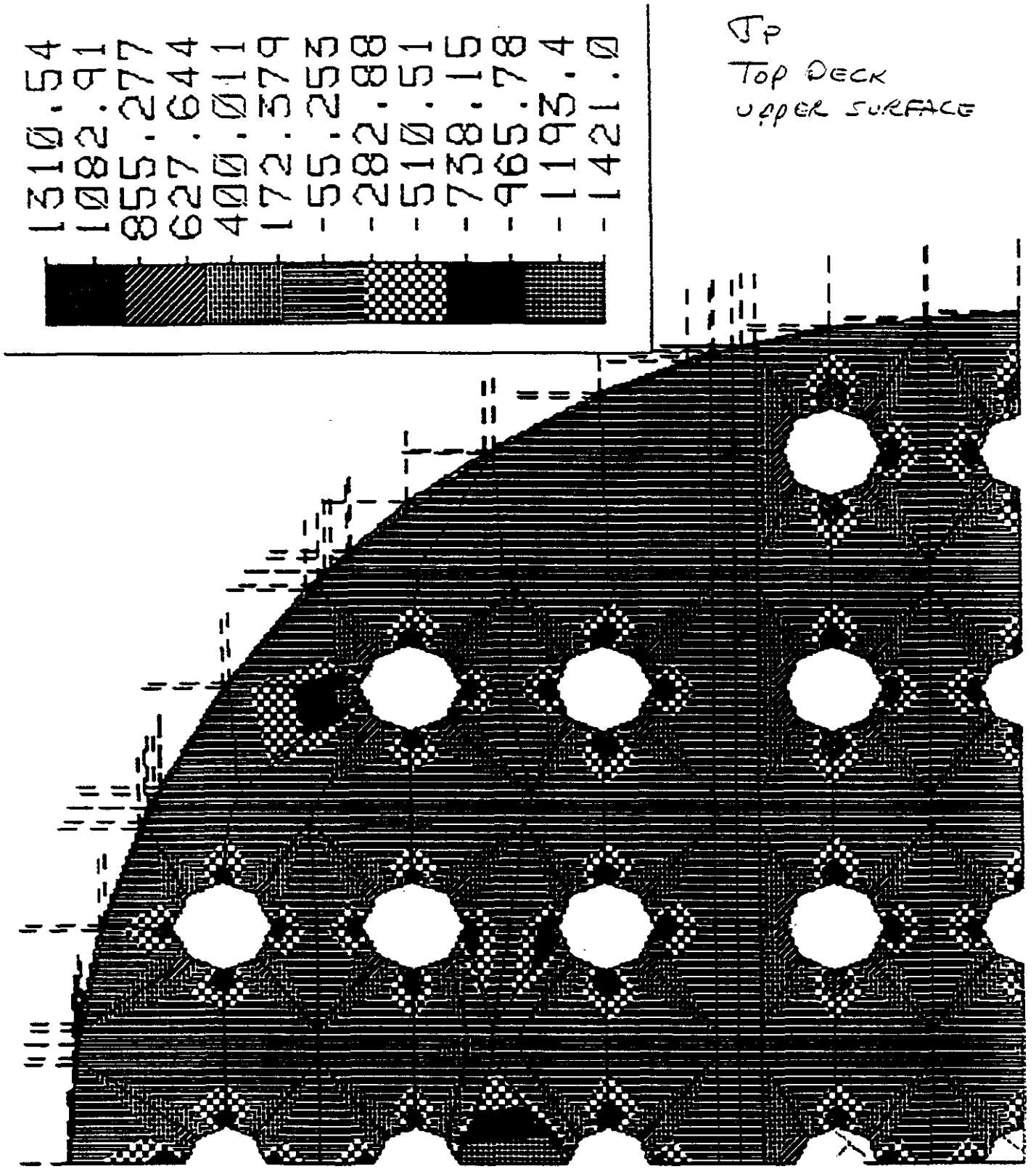
1318.54
1085.91
852.27
619.644
386.017
153.391
-79.235
-312.861
-546.487
-780.113
-1013.74
-1247.36
-1480.99
Sp
Top Deck
Upper Surface

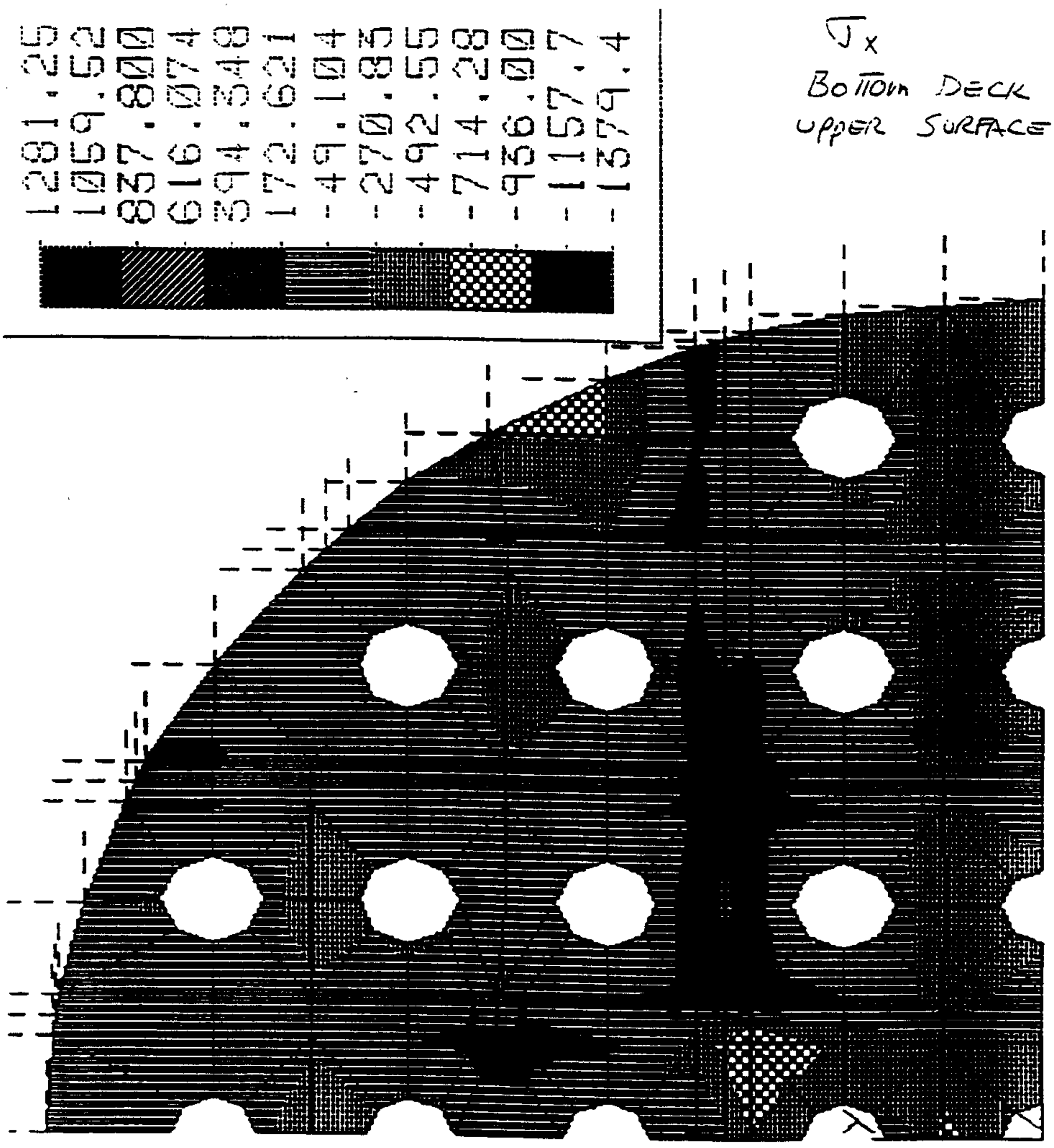
σx
Bottom Deck
upper surface

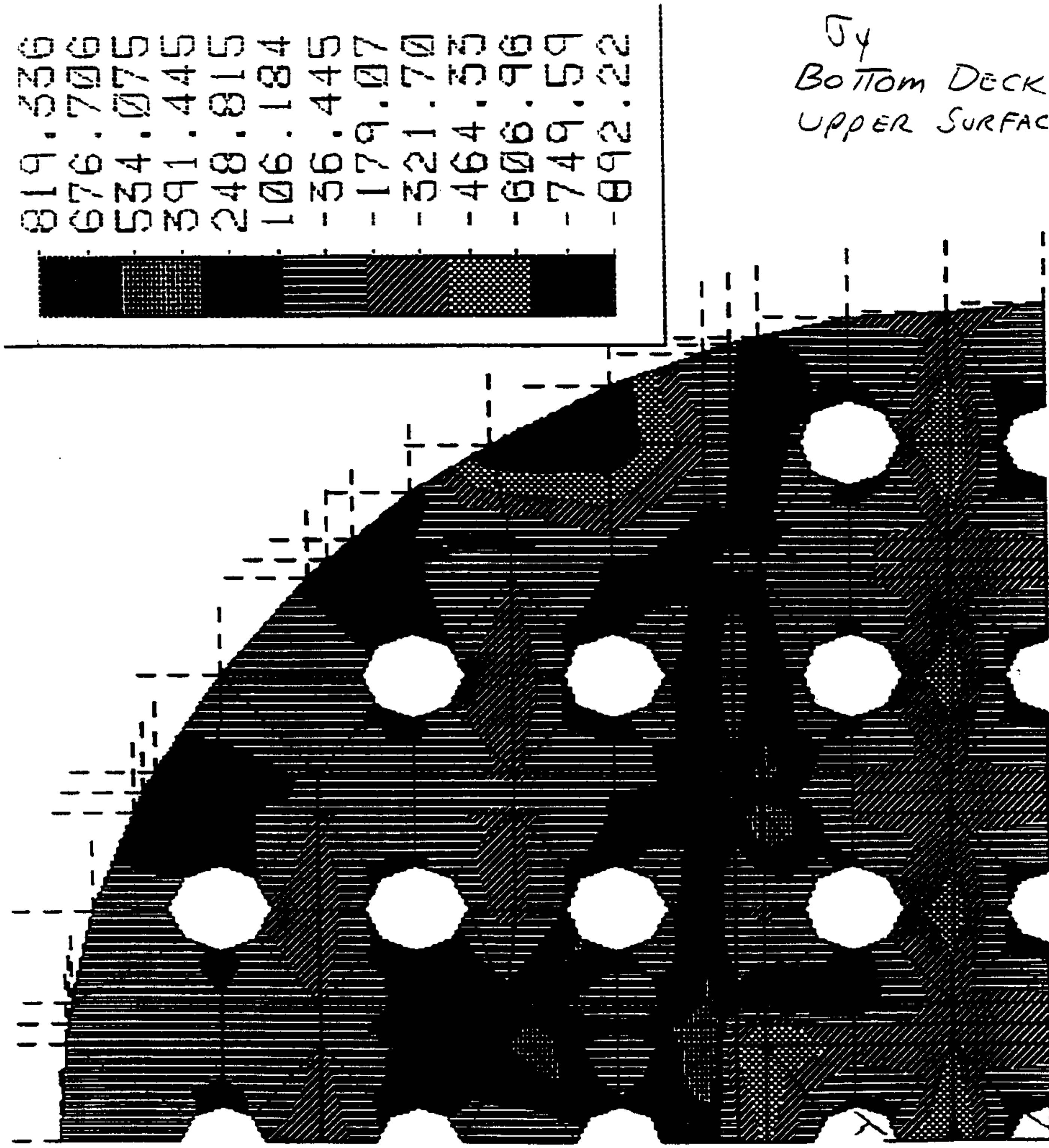

σy
Bottom Deck
Upper Surface

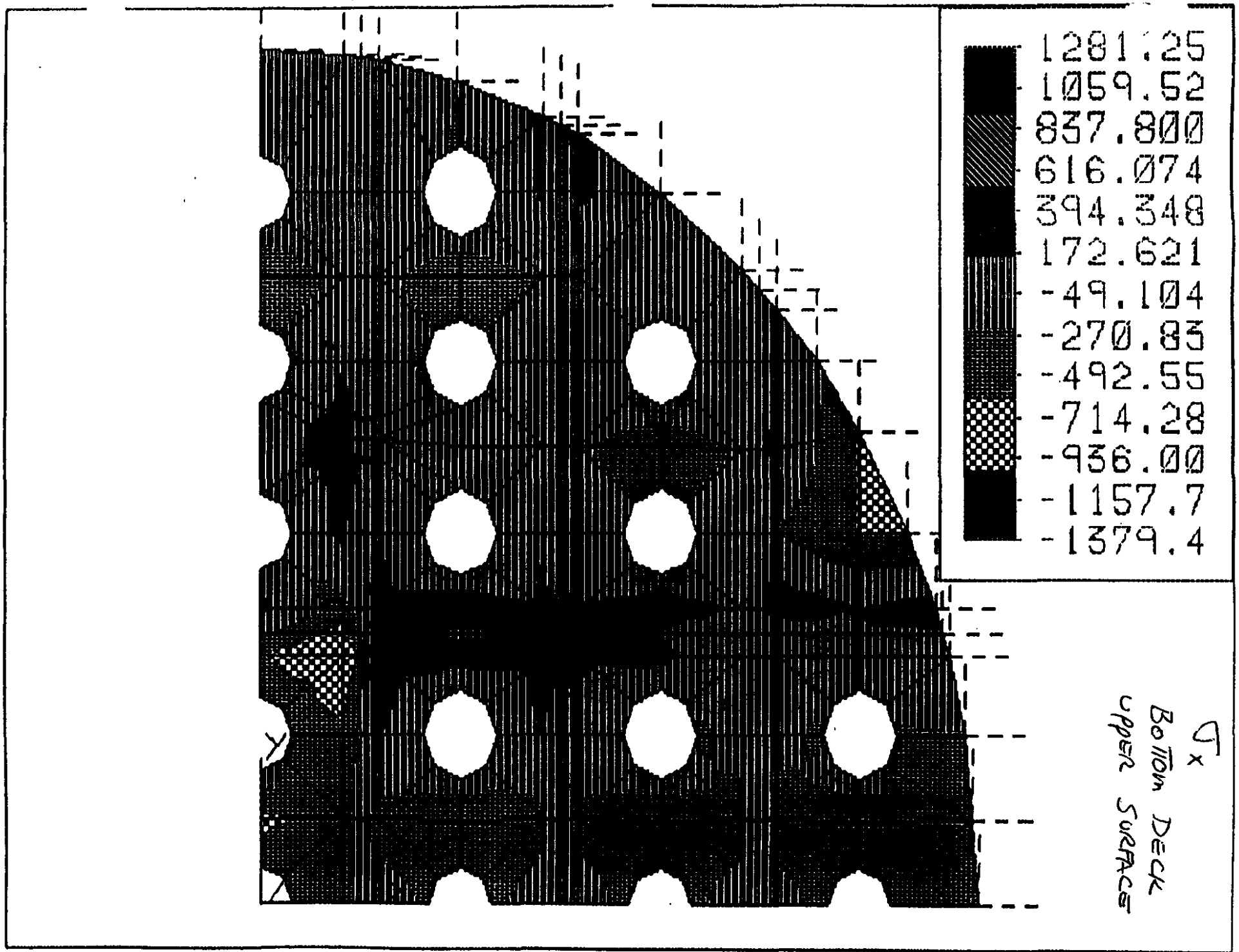

SVIEWH 3.14 File:jbrdeck7 91/01/15 16:08 LC 1/ 1 Vu= 1 Lo= 0 La= 90 R= 0

Z

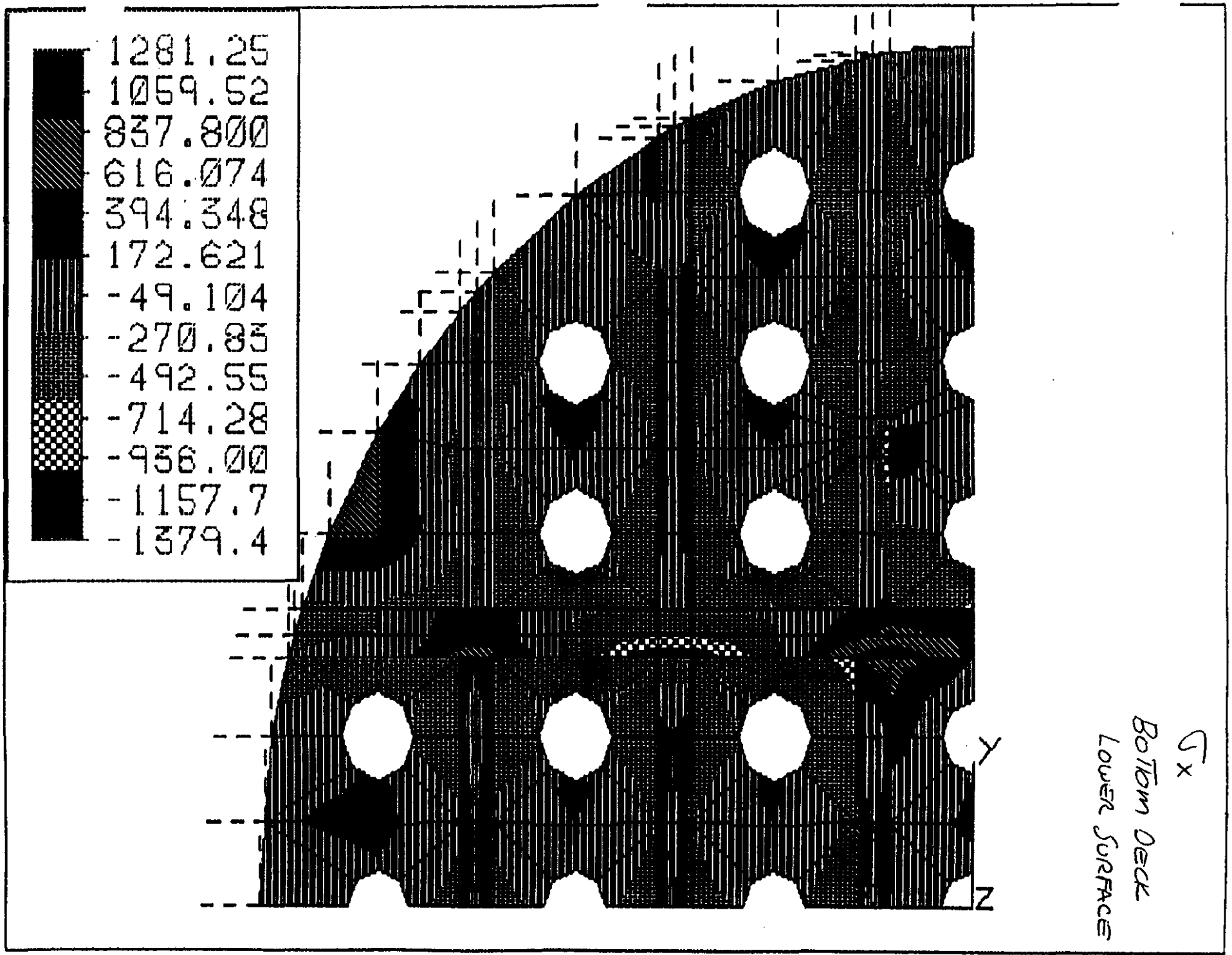

SVIEWH 3.14 File:jbrdeck7 91/01/15 16:08 LC 1/ 1 Vu= 4 Lo= 180 La= -90 R= 0

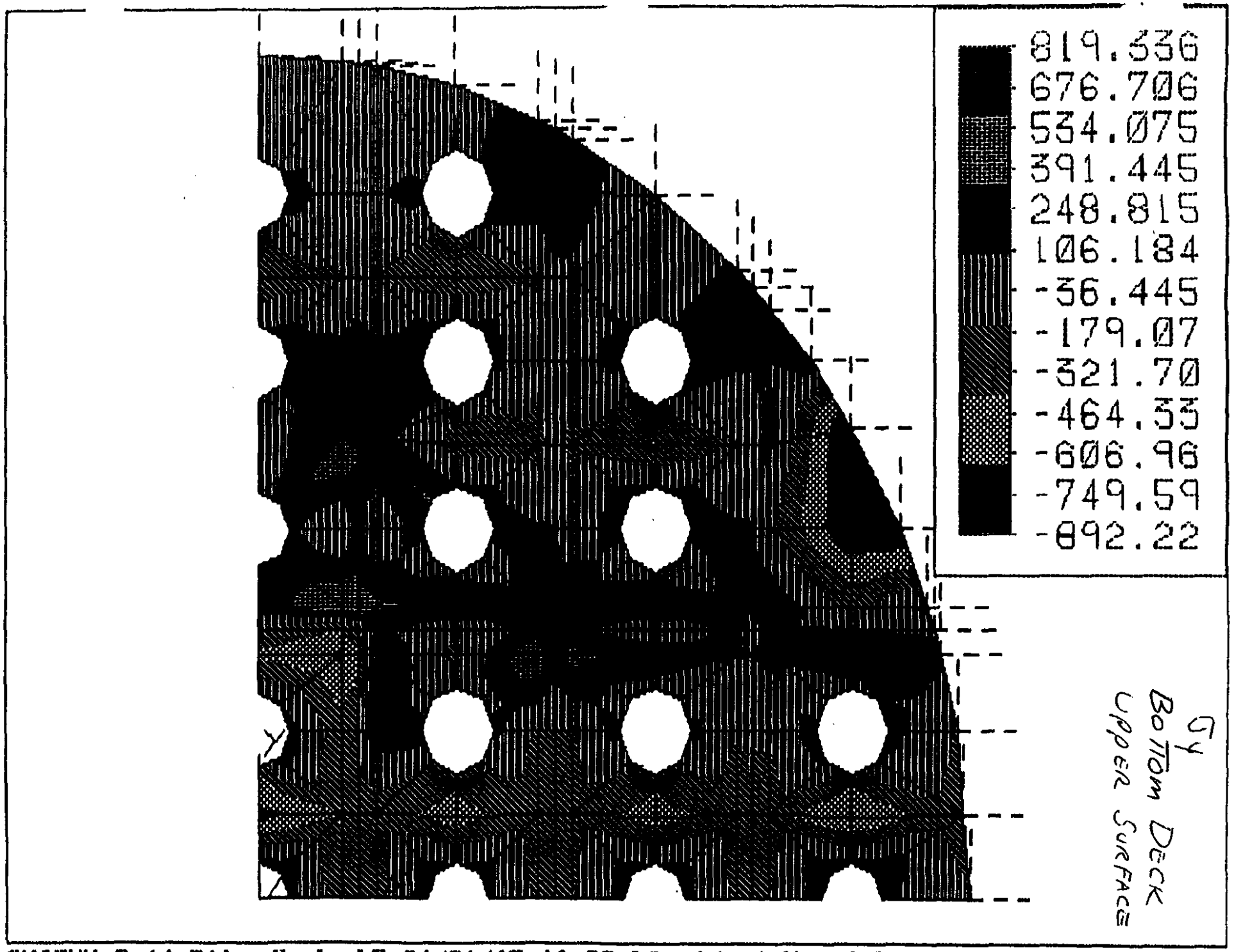

SVIEWH 3.14 File:jbrdeck7 91/01/15 16:08 LC 1/ 1 Vu= 1 Lo= 0 La= 90 R= 0

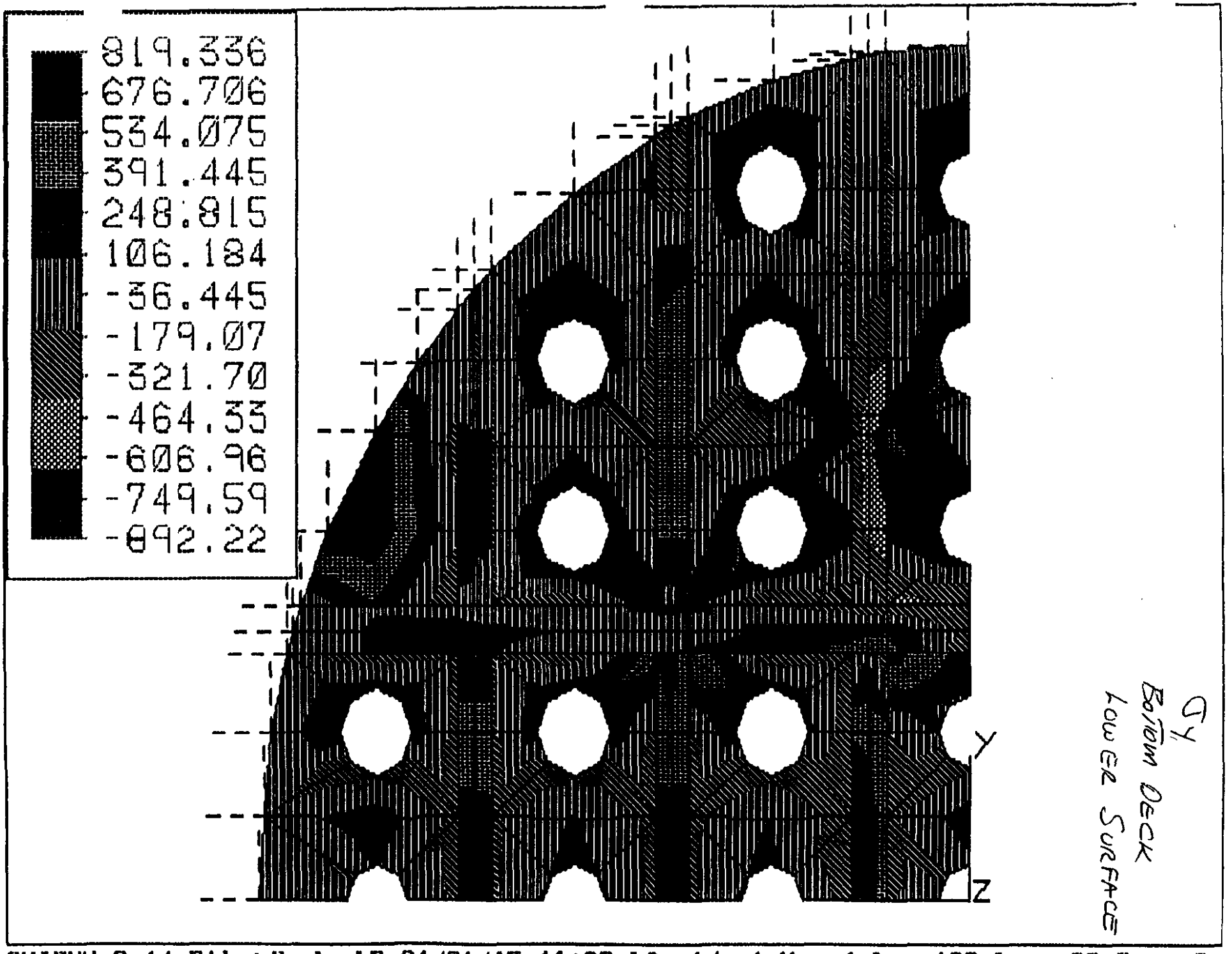
819.336
676.706
534.075
391.445
248.815
106.184
-36.445
-179.07
-321.70
-464.33
-606.96
-749.59
-892.22
Y
Z
Sy
Bottom Deck
Lower Surface
SVIEWH 3.14 File:jbrdeck7 91/01/15 16:08 LC 1/ 1 Vu= 4 Lo= 180 La= -90 R= 0

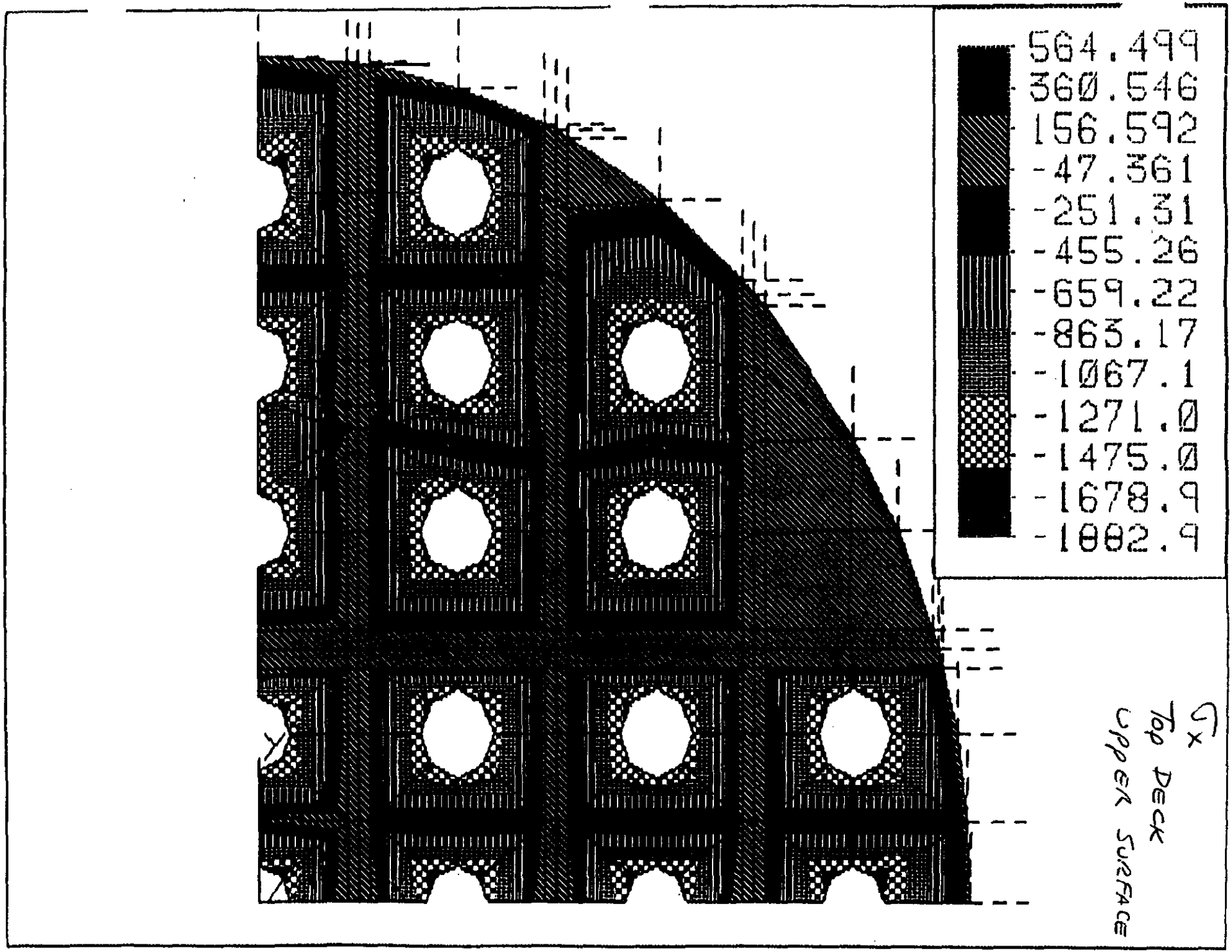

SVIEWH 3.14 File:jbrdeck7 91/01/15 16:08 LC 1/ 1 Vu= 1 Lo= 0 La= 90 R= 0

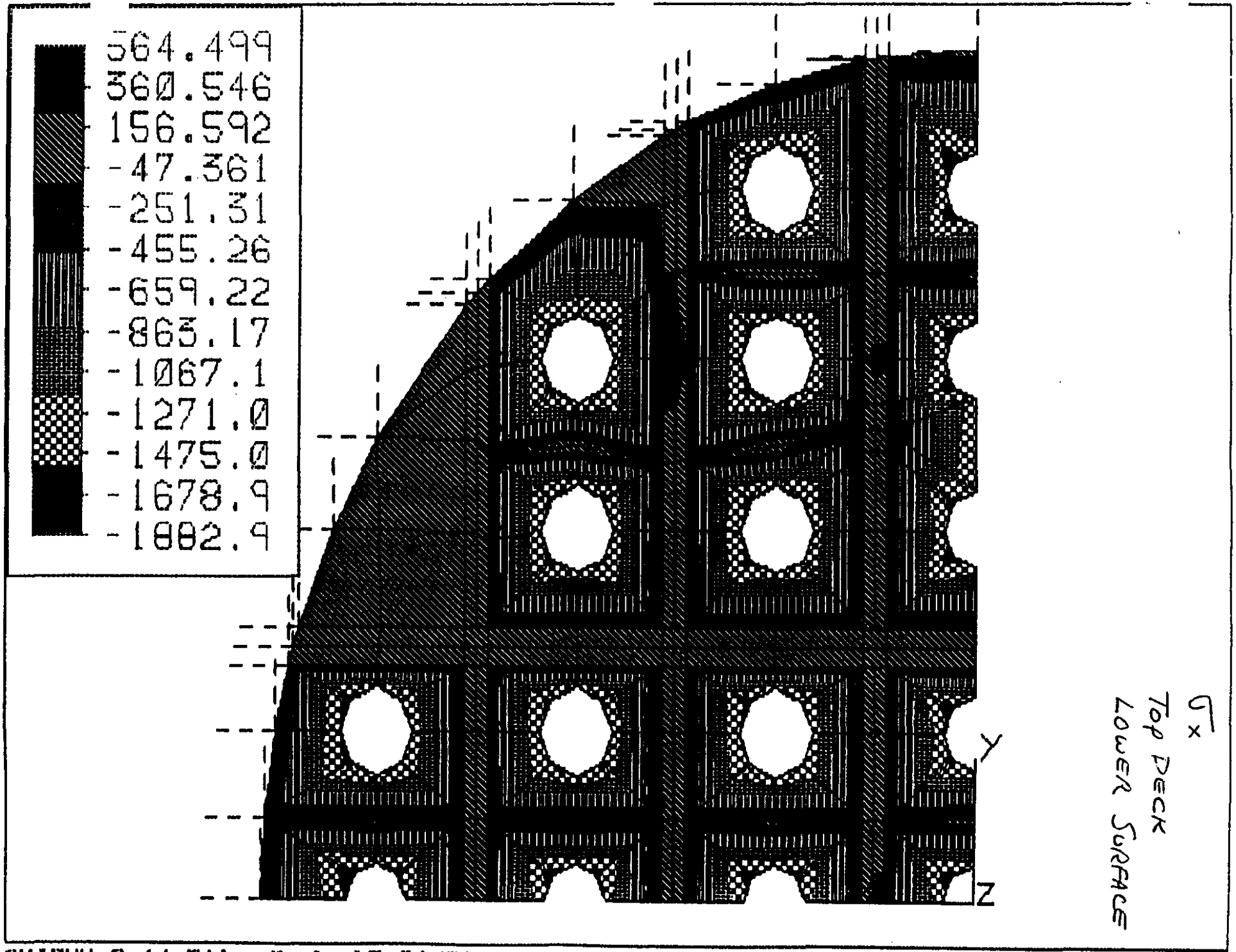

SVIEWH 3.14 File:jbrdeck7 91/01/15 16:08 LC 1/ 1 Vu= 4 Lo= 180 La= -90 R= 0

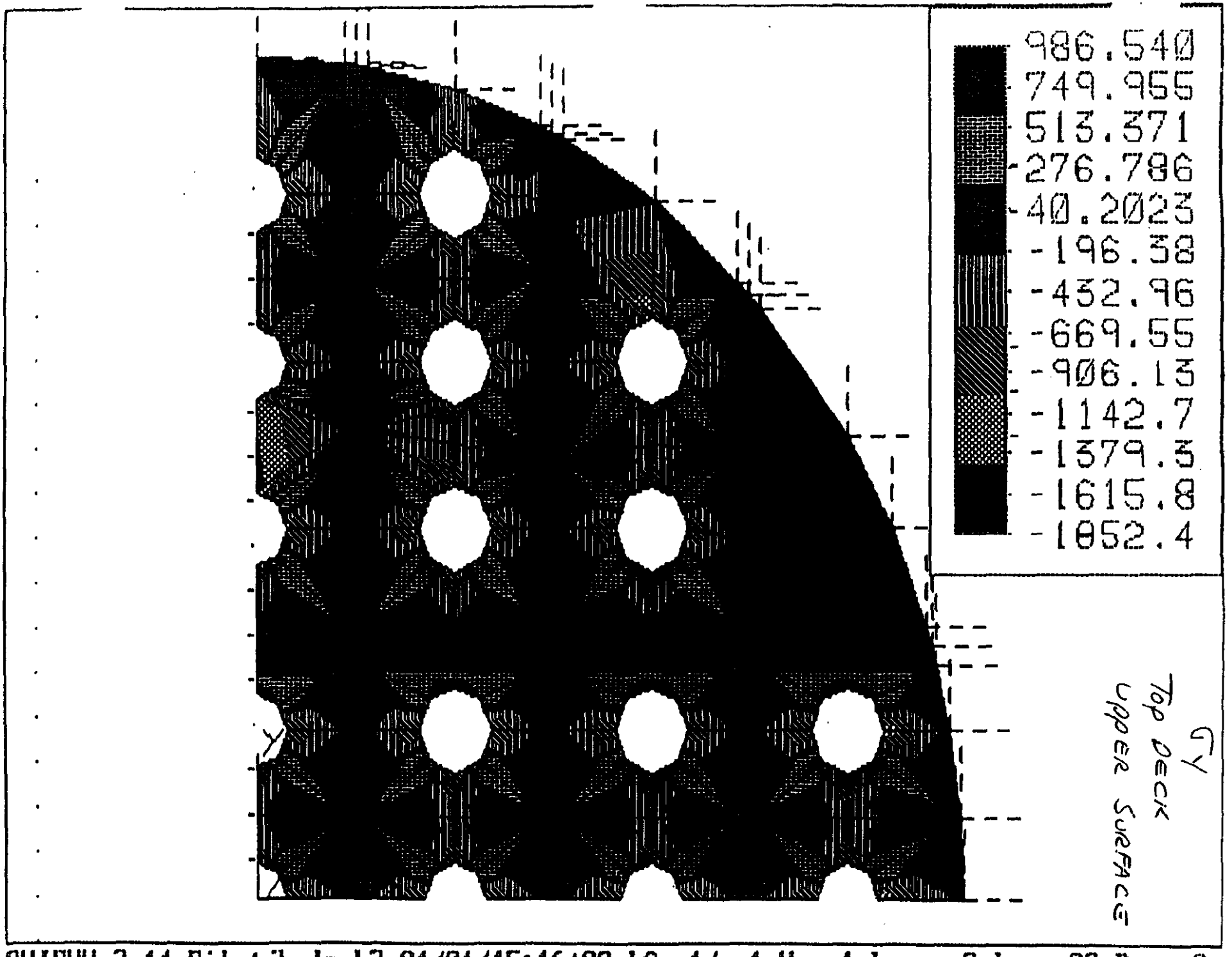

SVIEWH 3.14 File: jbrdeck7 91/01/15 16:08 LC 1/ 1 Vu= 1 Lo= 0 La= 90 R= 0

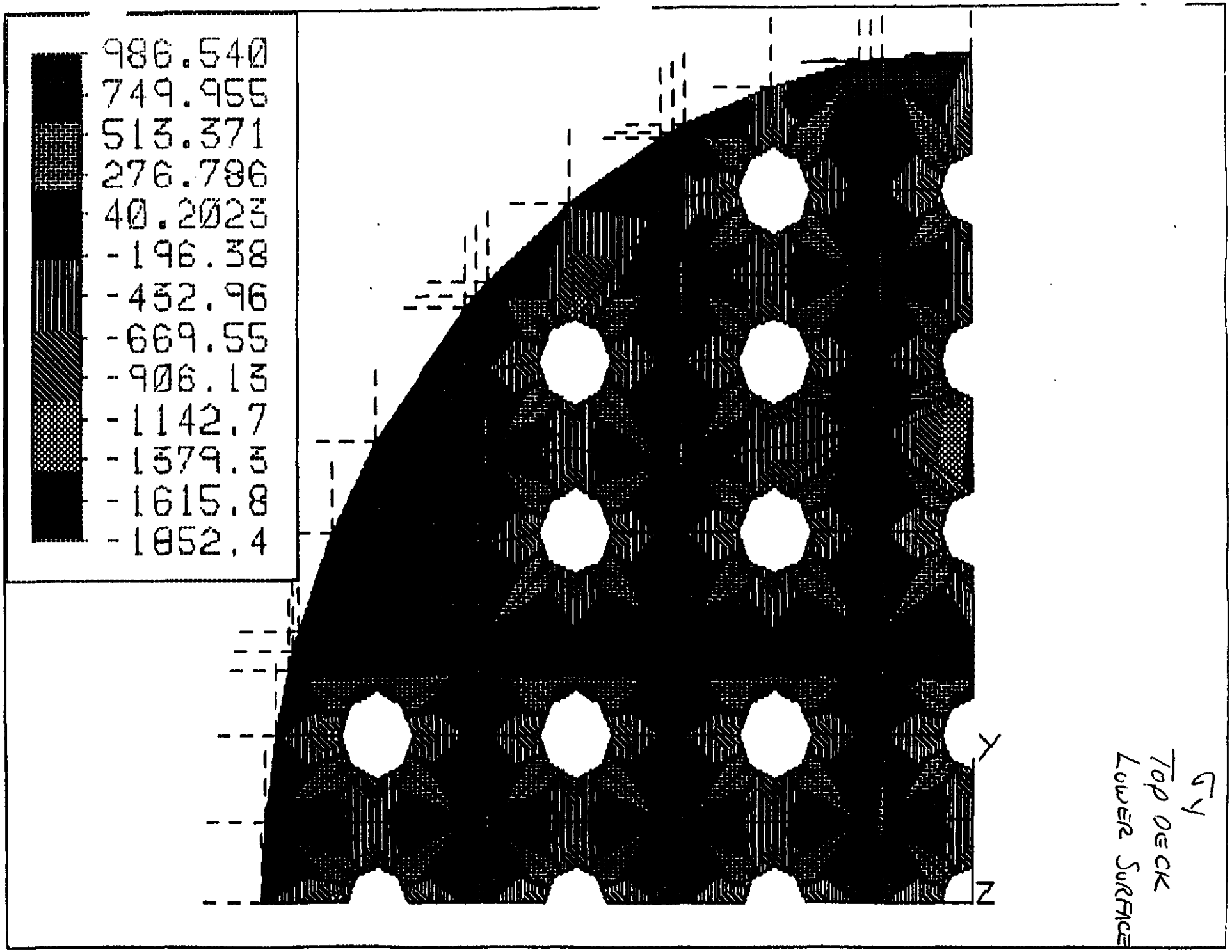

SVIEWH 3.14 File:jbrdeck7 91/01/15 16:08 LC 1/ 1 Vu= 4 Lo= 180 La= -90 R= 0

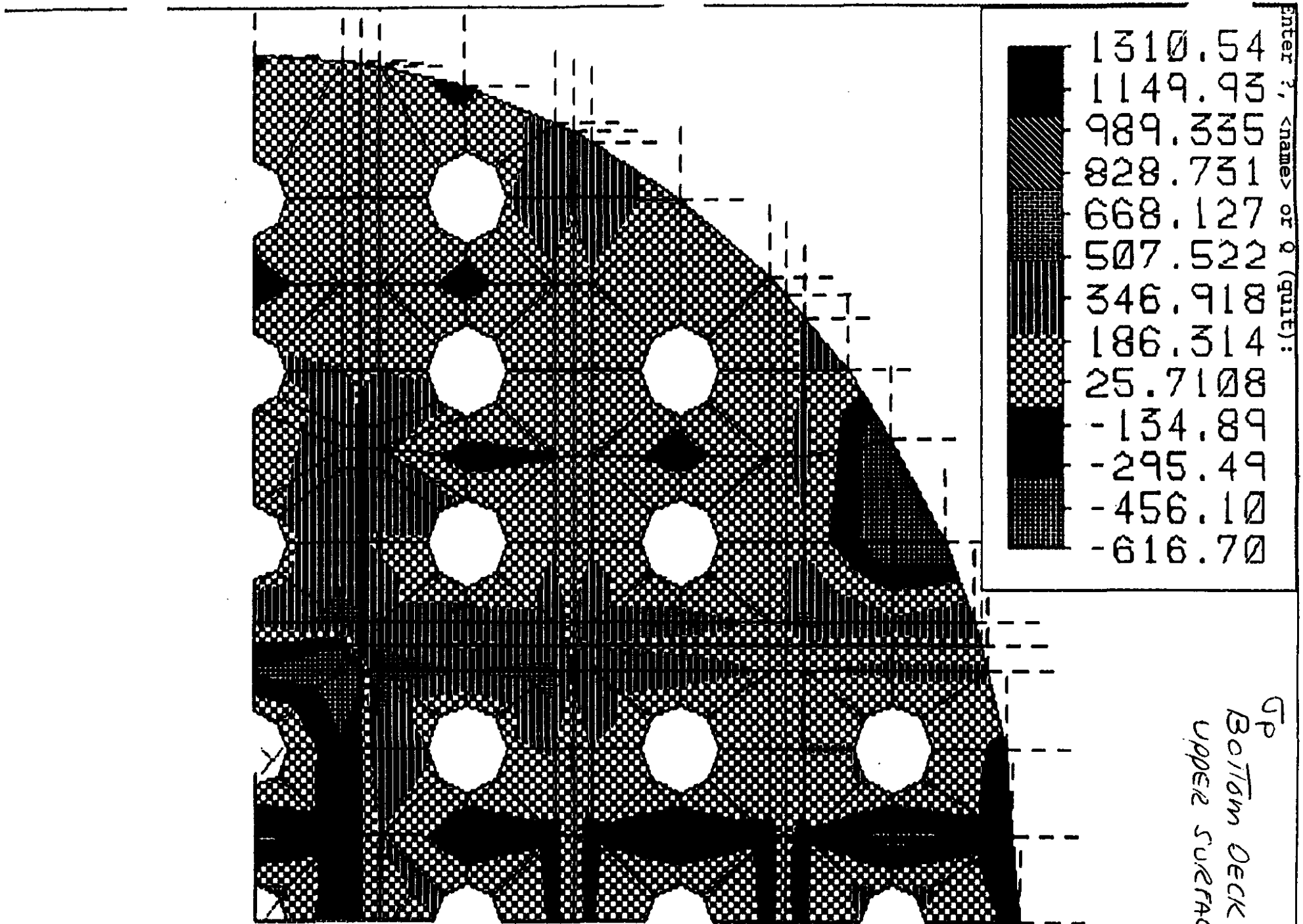

VIEWH 3.14 File:jbrdeck7 91/01/15 16:08 LC 1/ 1 Vu= 1 Lo= 0 La= 90 R= 0

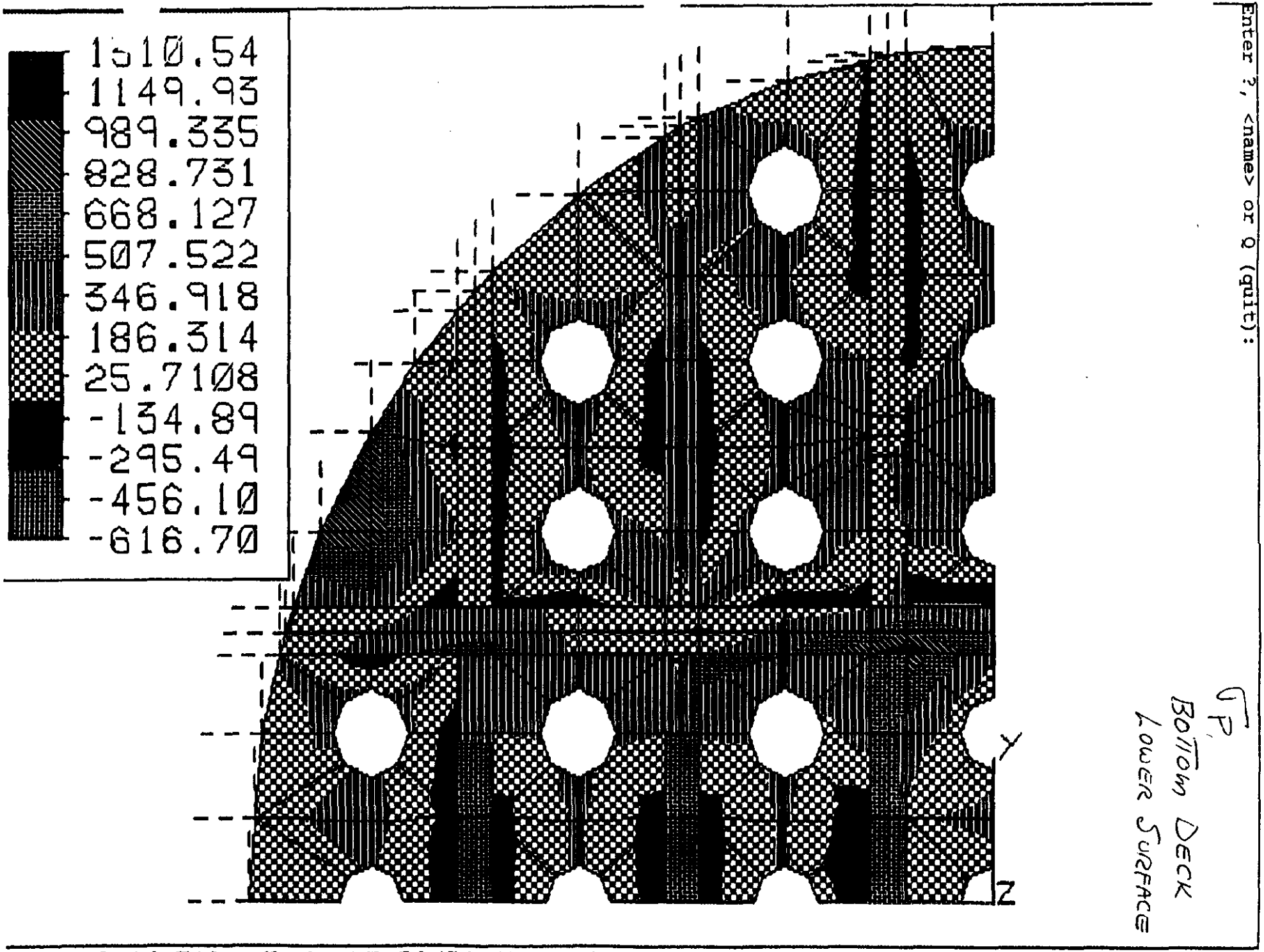

VIEWH 3.14 File: jbrdeck7 91/01/15 16:08 LC 1/ 1 Vu= 4 Ln= 180 La= -90 R= 0

REFERENCE MATERIALS

Ashland Chemicals

TECHNICAL DATA

HETRON® FR 992
Vinyl Ester Resin

ASHLAND CHEMICAL COMPANY • DIVISION OF ASHLAND OIL, INC.
BOX 2219, COLUMBUS, OHIO 43216 • (614) 889-3333

DATE: **May 1989**

FLAME RETARDANT, CORROSION RESISTANT, VINYL ESTER RESIN

DESCRIPTION: HETRON FR 992 resin is a low viscosity, unpromoted, flame retardant, vinyl ester resin containing styrene. Laminates made with HETRON FR 992 resin exhibit a flame spread of ≤25 (ASTM E84) when 3% antimony trioxide is added and a flame spread of ≤75 without antimony trioxide.

PERFORMANCE:

- Excellent flame retardancy.
- Excellent corrosion resistance to acidic and alkaline environments.
- High strength characteristics.
- Excellent impact strength and toughness.
- Fast wet-out, low drainage.

SUGGESTED USES: Corrosion resistant, reinforced thermosetting plastic equipment including filament wound, hand lay-up and spray-up tanks, pipes, duct, stacks, scrubbers, linings or other equipment handling corrosive gases, vapors or liquids where a high degree of flame retardancy is required.

ALTERNATIVE PRODUCTS: HETRON 922 non-flame retardant vinyl ester resin and HETRON 980 non-flame retardant vinyl ester resin for applications requiring higher operating temperatures and greater resistance to organics.

TYPICAL LIQUID PROPERTIES AT 77°F (25°C)

Percent Solids	60
Viscosity — Brookfield, cps	400
Appearance	Clear
Color, Gardner	5 max
Acid Value (Solids)	12
Pounds per Gallon	9.7
DOT Flash Point Range, °F	73 - 100

STANDARD PACKAGE: Nonreturnable 55 gallon drums, 500 lb net.

DOT Label Required: Flammable Liquid

CODE: 566-621

®Registered trademark, Ashland Oil, Inc.

TYPICAL PERFORMANCE DATA

(for guidance only)

TYPICAL SPI CURING CHARACTERISTICS (2.0% Luperco[1] ATC Paste Catalyst):

Gel Time, minutes	17
Total Time, minutes	25
Peak Exotherm, °F	380

TYPICAL CURING CHARACTERISTICS:

% Promoters		Catalyst[2]	Temperature	Gel Time,
6% Cobalt Naphthenate	DMA	(1.25 Lupersol DDM-9)	(°F)	(min)
0.30	0.10	1.25	60 - 70	10 - 20
0.30	0.075	1.25	70 - 80	10 - 20
0.30	0.05	1.25	80 - 90	10 - 20
0.30	0.075	1.25	60 - 70	20 - 30
0.30	0.05	1.25	70 - 80	20 - 30
0.20	0.05	1.25	80 - 90	20 - 30
0.20	0.075	1.25	60 - 70	30 - 40
0.20	0.025	1.25	70 - 80	30 - 40
0.10	0.05	1.25	80 - 90	30 - 40

CAUTION: Thoroughly mix promoters with resin before adding catalyst.

% Promoter	% Catalyst	Temperature.	Gel Time,
DMA	Luperco[1] ATC Paste	(°F)	(min)
.3	2.0	77	10 - 15
.2	2.0	77	20 - 25
.15	2.0	77	30 - 35

For all surfaces that will be exposed to air during fabrication (top-coating, lining, patching, exterior surfaces, etc.), the addition of 0.4% paraffin wax to the final resin layer is recommended. A waxed surface may interfere with secondary bonding adhesion.

Flame retardant vinyl ester resins do not demonstrate equivalent ultraviolet stability of non-halogenated vinyl ester resins. Ultraviolet stability may be improved by adding 1.0% Cyasorb[3] UV-9 ultraviolet screener to the exterior exposed surfaces where aesthetic appearance is desired.

[1]Trademark, Pennwalt Corporation. Available from Lucidol Division, Pennwalt Corporation.
[2]Witco Chemical Hi Point 90 Catalyst. Hi Point is a trademark of Witco Chemical Co.
[3]Trademark, American Cyanamid Co.

Ashland Chemicals

TYPICAL PHYSICAL PROPERTIES OF CURED CASTINGS AT 77°F
(1/8-inch)

Test	Value	Test Method
Barcol Hardness	35	ASTM D-2583
Specific Gravity	1.24	—
Tensile Strength, psi	11,700	ASTM D-638
Tensile Modulus x 10^{-5}, psi	5.2	ASTM D-638
Tensile Elongation, %	4.75	ASTM D-638
Flexural Strength, psi	20,000	ASTM D-790
Flexural Modulus, 10^{-5}, psi	5.43	ASTM D-790
Heat Deflection Temperature, °F	223	ASTM D-648

Formula: HETRON FR 992 Resin 100 parts
DMA 0.1 parts
BPO 1.0 parts

Cure: Post cured 2 hours at 100°C

TYPICAL MECHANICAL PROPERTIES OF HETRON FR 992 RESIN AT VARIOUS TEMPERATURES

Test Temp.	Approx. Thickness Inch	Glass Structure[4]	Flexural Strength, psi	Flexural Modulus, psi x 10^6	Tensile Strength, psi	Tensile Modulus, psi x 10^6	Compressive Strength, psi
25°C (77°F)	1/8	V, 2M, V	16,000	.79	12,500	1.01	26,500
	1/4	V, 2M, MRM	25,000	1.08	17,200	1.28	28,500
	3/8	V, 2M, 3(MR) M	37,300	1.38	22,250	1.56	34,000
	1/2	V, 2M, 3(MR) M, MRM	31,500	1.29	22,500	1.59	30,000
93°C (200°F)	1/8	V, 2M, V	19,000	.61	12,200	.79	20,000
	1/4	V, 2M, MRM	26,000	.94	19,200	1.20	21,000
	3/8	V, 2M, 3(MR) M	37,800	1.24	24,000	1.37	25,500
	1/2	V, 2M, 3(MR) M, MRM	31,500	1.09	25,200	1.38	22,500
121°C (250°F)	1/8	V, 2M, V	5,200	.19	9,000	.44	14,500
	1/4	V, 2M, MRM	11,200	.49	14,500	.83	16,500
	3/8	V, 2M, 3(MR) M	12,500	.66	17,000	.96	19,000
	1/2	V, 2M, 3(MR) M, MRM	16,000	.90	18,500	.99	15,000

V = 10 mil C Glass Surfacing Veil
M = 1.5 oz Chopped Strand Mat
R = 24 oz Woven Roving

Formula: HETRON FR 992 Resin 100 parts
6% Cobalt Naphthenate 0.3 parts
DMA .05 parts
Hi Point[2] 90 Catalyst 1.50 parts

Cure: Post cured 2 hours at 250°F

[4]Glass Content

1/8" - 25%
1/4" - 30%
3/8" - 37%
1/2" - 40%

TYPICAL FLAME RETARDANCY OF HETRON FR 992 RESIN FRP LAMINATES[5]

Resin	Class	ASTM E84 Flame Spread
HETRON FR 992 Resin		
With 3% antimony trioxide	I	25
With 5% antimony trioxide	I	18
Without antimony trioxide	II	75
CONTROL		
Cement Asbestos Board	I	0
Red Oak	III	100

[5]1/8" thick laminate with approximately 27% glass content.

HANDLING: HETRON FR 992 resin contains ingredients which could be harmful if mishandled. Contact with skin and eyes should be avoided and necessary protective equipment and clothing should be worn. **For important health, safety and handling information, consult Ashland's Material Safety Data Sheet before using this product.**

RECOMMENDED STORAGE: Drums — Store at temperatures below 80°F. Storage life decreases with increasing storage temperature. Avoid exposure to heat sources such as direct sunlight or steam pipes. Keep containers sealed to prevent moisture pickup and monomer loss. Rotate stock.

Bulk — Store in stainless steel tanks or tanks lined with epoxy or phenolic coatings. Observe precautions against heat and moisture (see above). Dry air sparge may be desirable to keep inhibitors activated with oxygen.

SHELF LIFE: This product has a limited shelf life. When stored in accordance with the above conditions this product has a minimum life of three months.

ERSHIGS

42' Ø -3R DISHED HEAD

83.33% CROWN - 6% KNUCKLE

MOLD DIMENSIONS

Date 9.10.90

By RC

Job No. 3095

Sht 1

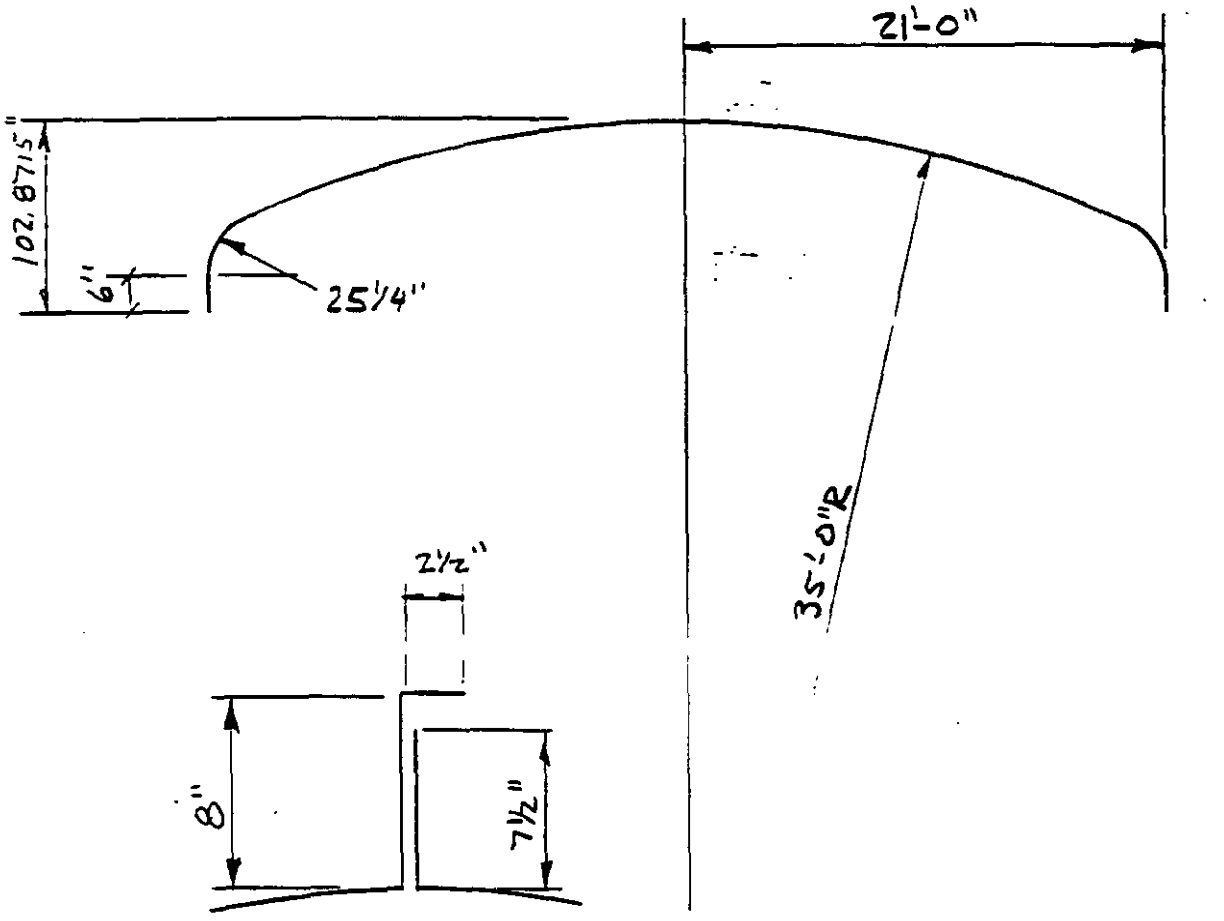

STRUCTURAL ANALYSIS OF SHELLS

E. H. BAKER
Professor of Mechanical Engineering, California State Polytechnic College at San Luis Obispo

L. KOVALEVSKY
Member of the Technical Staff Rockwell International Corp. North American Aircarft Group

F. L. RISH
Member of the Technical Staff Rockwell International Corp. Space System Group

ROBERT E. KRIEGER PUBLISHING COMPANY
HUNTINGTON, NEW YORK
1981

Uniform Internal Pressure, Complete Oblate Spheroidal Shells

When the radius ratio A/B of an oblate spheroid is less than $\sqrt{2}/2$, internal pressure produces compressive stresses in the shell and hence allows instability to occur. Theoretical values of the critical internal pressures are shown in Fig. 10-38. No experimental results are available,

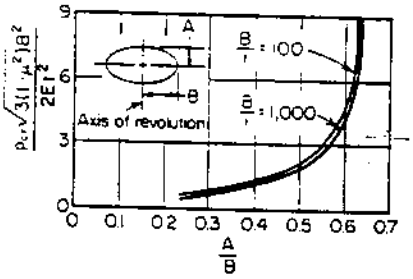

figure 10-38 *Theoretical buckling pressures of oblate spheroids under internal pressure* ($\mu = 0.3$).

but the study of imperfection sensitivity indicates that there should be good agreement between theory and experiment for shells with $0.5 < A/B < 0.7$.

Internal Pressure, Ellipsoidal and Toroidal Bulkheads

Clamped oblate spheroidal (ellipsoidal) bulkheads (Fig. 10-39) may have the ratio of length of minor and major axes A/B less than $\sqrt{2}/2$ without buckling under internal pressure, provided that the thickness exceeds a certain critical value. This problem is investigated in Ref. 10-39. Nonlinear bending theory is used to determine the prebuckling stress distribution. The regions of stability are shown in Fig. 10-40; the calculated variation of buckling pressure with thickness

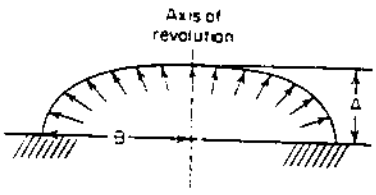

figure 10-39 *Clamped ellipsoidal bulkhead under internal pressure.*

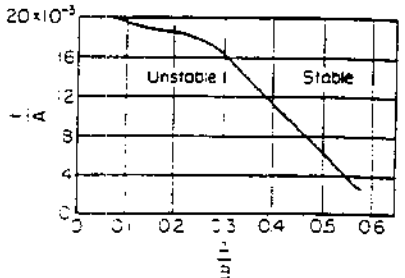

figure 10-40 *Region of stability for ellipsoidal closures subjected to internal pressure* ($\mu = 0.3$).

is shown in Fig. 10-41. The theory has not been verified by experimental results, however, and should be used with caution.

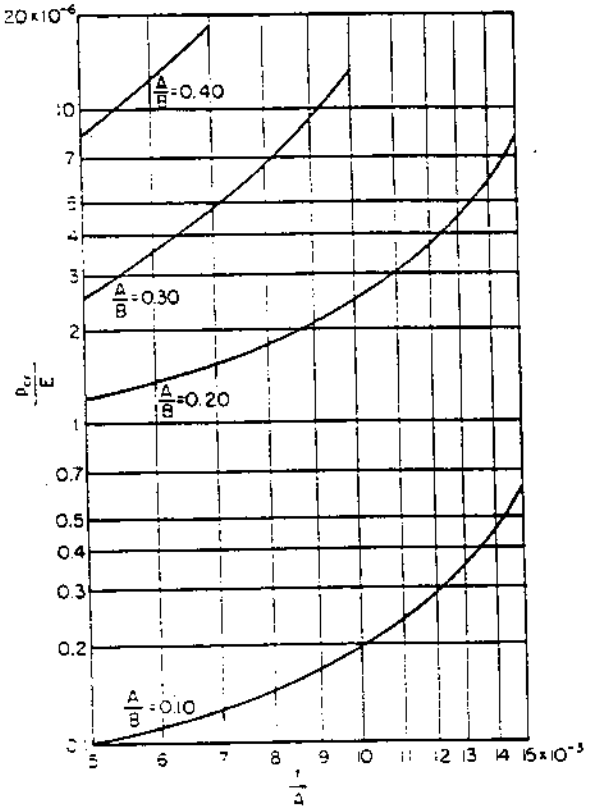

figure 10-41 *Theoretical results for clamped ellipsoidal bulkheads subjected to uniform internal pressure* ($\mu = 0.3$).

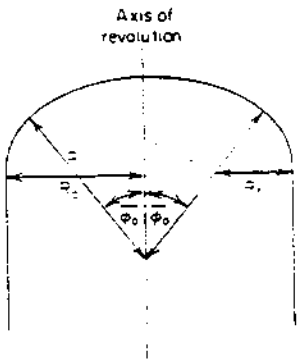

figure 10-42 *Geometry of torispherical closure.*

Formulas for Stress and Strain FIFTH EDITION

RAYMOND J. ROARK

WARREN C. YOUNG

McGraw-Hill Book Company

New York St. Louis San Francisco Auckland Düsseldorf Johannesburg Kuala Lumpur London Mexico Montreal New Delhi Panama Paris São Paulo Singapore Sydney Tokyo Toronto

		...sion combined with shear, see Refs. 28 and 31.)
 $\frac{b}{l} > 10$		
14. Curved panel under uniform shear on all edges 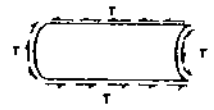	14a. All edges simply supported	$\tau' = 0.1E\frac{t}{r} + 5E\left(\frac{t}{b}\right)^2$ (Refs. 6, 27, 29)
	14b. All edges clamped	$\tau' = 0.1E\frac{t}{r} + 7.5E\left(\frac{t}{b}\right)^2$ (Ref. 6) Tests show $\tau' = 0.075E\frac{t}{r}$ for panels curved to form quadrant of a circle (Ref. 11) (See also Refs. 27, 29)
15. Thin-walled circular tube under uniform longitudinal compression (radius of tube = r)  $\frac{r}{t} > 10$	15a. Ends not constrained	$\sigma' = \frac{1}{\sqrt{3}}\frac{E}{\sqrt{1-\nu^2}}\frac{t}{r}$ (Refs. 6, 12, 13, 24) Most accurate for very long tubes, but applicable if length is several times as great as $1.72\sqrt{rt}$, which is the length of a half-wave of buckling. Tests indicate an actual buckling strength of from 40 to 60 percent of this theoretical value, or $\sigma' = 0.3E\frac{t}{r}$ approximately.
16. Thin-walled circular tube under a transverse bending moment M (radius of tube = r)  $\frac{r}{t} > 10$	16a. No constraint	$M' = K\frac{E}{1-\nu^2}rt^2$ Here the theoretical value of K for pure bending and long tubes is 0.99. The average value of K determined by tests is 1.14, and the minimum value is 0.72. Except for very short tubes, length effect is negligible and a small transverse shear produces no appreciable reduction in M'. A very short cylinder under transverse (beam) shear may fail by buckling at neutral axis when shear stress there reaches a value of about $1.25\tau'$ for case 17a (Refs. 6, 14, 15)
17. Thin-walled circular tube under a twisting moment T that produces a uniform circumferential shear stress: $\tau = \frac{T}{2\pi r^2 t}$ (length of tube = l; radius of tube = r) 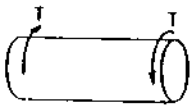 $\frac{r}{t} > 10$	17a. Ends hinged, i.e., wall free to change angle with cross section, but circular section maintained	$\tau' = \frac{E}{1-\nu^2}\left(\frac{t}{l}\right)^2(1.27 + \sqrt{9.64 + 0.466H^{1.5}})$ where $H = \sqrt{1-\nu^2}\frac{l^2}{tr}$ Tests indicate that the actual buckling stress is from 60 to 75 percent of this theoretical value, with the majority of the data points nearer 75 percent. (Refs. 6, 16, 18, 25)
	17b. Ends clamped, i.e., wall held perpendicular to cross section and circular section maintained	$\tau' = \frac{E}{1-\nu^2}\left(\frac{t}{l}\right)^2(-2.39 + \sqrt{96.9 + 0.605H^{1.5}})$ where H is given in part 17a. The statement in part a regarding actual buckling stress applies here as well. (Refs. 6, 16, 18, 25)

"FRP Acoustic Emission Inspection Report"

Physical Acoustics Corporation

PHYSICAL ACOUSTICS CORPORATION
FRP
Acoustic Emission Inspection Report

SOUTHERN COMPANY SERVICES
GEORGIA POWER PLANT, YATES FACILITY
JET BUBBLING REACTOR

Tested On
NOVEMBER 16-18, 1994

Project leader JAMES R. MITCHELL
Assisted By: DAVID L. KESLER
CHRIS B. BARBOUR

Physical Acoustics Corporation
Princeton, New Jersey

PHYSICAL ACOUSTICS CORPORATION
FRP
Acoustic Emission Inspection Report

JBR (JET BUBBLING REACTOR)

Tested On
NOVEMBER 16-18, 1994

REPORTED PREPARED
FOR
KAMYER VAKHSHOORZADEH, Ph.D
SOUTHERN COMPANY SERVICES, INC
PO BOX 2625
BIRMINGHAM, ALABAMA 35202-2625
(205)877-7805 (O), (205) 868-5367 (F)

Prepared By: JAMES R. MITCHELL
AET L-111, ASNT L1419
(203) 536-3380 (O,F)

Physical Acoustics Corporation
Princeton, New Jersey

SUMMARY AND RECOMMENDATIONS

An Acoustic Emission (AE) test was performed on a scrubber tank known as the JBR (Jet Bubbling Reactor) tank for Southern Company Services, Yates Plant. This test used the Recommended Practice for Acoustic Emission Testing of Fiberglass Reinforced Plastic Resin (RP) Tanks/Vessels, published by the Committee on Acoustic Emission from Reinforced Plastics (CARP) of the Society of the Plastics Industry.

A total of 50 AE sensors, configured as shown in Figure 1, were used to monitor the tank. Analysis of the data, after taking account of known noise incidents, showed that the tank exhibited acoustic emission data well in excess of the CARP acceptance criteria.

TABLE OF CONTENTS

1.0 INTRODUCTION

The CARP recommended practice consists of subjecting FRP equipment to increasing loads while being monitored by sensors that are sensitive to acoustic emission (transient stress waves) caused by growing flaws. The sensors are connected to instrumentation that is capable of recording and analyzing AE signals. The CARP recommended practice also provides guidelines to determine the location and severity of structural flaws with acceptance criteria as a basis to assess the structural integrity of the FRP equipment. The CARP criteria are shown in section 8 of this report.

The AE test method is designed to detect structurally significant defects and damage in FRP equipment. The damage mechanisms that are detected in FRP are as follow:

a. resin cracking
b. fiber debonding
c. fiber pullout
d. fiber breakage
e. delamination
f. bond failure in assembled joints (for example, nozzles, manways, etc.)

For a more detailed description of the test set-up and procedure see section 2 through 8 of this report. Figure 3 and appendix 1 and 2 contains data listings and activity graphs that were used to perform the final data analysis.

2.0 TANK DESCRIPTION

Vessel/Component Tested: JBR (Jet Bubble Reactor) Tank

Description: Field Erected FRP, 156F Max Temp., SPG=1.2, 80MPH Max wind load, Empty weight 235,000 pounds,

Dimension: 42 FT Diam, 28 FT High,

Insulated: NO

Capacity: 145,000 US gallons at 14 foot level.

Material of construction: Liner and structural resin: HT-992FR

Manufacturer: Ershigs, Bellingham, WA: SN D-90079 3095, PO# C-90-2148

Data of Mfg.: April 1991

Maximum Test Level: 17 Feet

Test Medium: Water

Filled From: Pumped through nozzles, 18 inches above floor

3.0 AE TEST EQUIPMENT

AE INSTRUMENTATION MFG.: Physical Acoustics Corp.

AE INSTRUMENTATION TYPE: PAC 58 CH SPARTAN-AT

SENSOR TYPE: R15I RESONANT FREQ.: 150 Khz

PREAMP TYPE: Integral

FREQUENCY BANDPASS: 100-300 Khz (Band Pass)

SENSOR ATTACHMENT METHOD: Hot Glue

4.0 INSTRUMENT SET-UP PARAMETERS

DETECTION THRESHOLD	: 48	dB
PREAMP GAIN	: 40	dB
INSTRUMENT GAIN	: 20	dB
PDT	: 100	us
HDT	: 200	us
HLT	: 500	us

5.0 AE TEST SET-UP

Attenuation: (AE source = 0.5mm Pentel lead breaks)

Sensor #5	0"	6"	12"	18"	24"
IN LINE	96 dB	83 dB	70 dB	57 dB	52 dB
45 Deg.	93 dB	75 dB	65 dB	55 dB	41 dB

Prior to the monitoring period, the complete AE system was checked to assure proper performance by injecting a signal on the surface of the tank at each sensor location with a Pentel pencil containing 0.5mm HB lead. The average amplitude of this signal was recorded by the test operator and is listed in Table 1. Under the CARP procedure, all channels should lie within 6dB of the grand average.

TABLE 1

Sensor #	dB	Sensor #	dB	Sensor #	dB
1	77	17	75	33	73
2	81	18	81	34	76
3	87	19	74	35	80
4	85	20	79	36	78
5	78	21	79	37	88
6	77	22	85	38	83
7	74	23	76	39	77
8	81	24	80	40	77
9	68	25	80	41	74
10	80	26	77	42	85
11	77	27	76	43	63
12	78	28	81	44	77
13	77	29	83	45	77
14	78	30	80	46	80
15	81	31	80	47	76
16	82	32	83	49	88

Grand Average 79 dB

Number of channels: 48

Number of sensors : 48

Sensor configuration: See Figure 1

Background noise level and character: Sporadic low level, from all channels.

Count Criterion: N = 7,735 Total counts from 130 Pentel lead breaks at a distance that gives an amplitude midway between the threshold of AE detectibility and the reference amplitude threshold.)

Threshold of AE Detectability: 48 dB

Reference Amplitude Threshold: 75 dB

NOTE: Two additional sensors were attached to drain lines which penetrate the tank floor and exit through the concrete pad. The intention was to identify leaking at the tank wall interface. This data is outside the carp procedure and will not be evaluated in this report. It will be evaluated in a future report exploring advanced analysis techniques

6.0 TEST PROCESS

A loading schedule, that followed CARP guidelines, was provided to operating personnel prior to the test. The proposed sequence included stepped loading with hold periods at 50%, 75%, 87.5%

and 100% of maximum fill height (see Figure 2). Maximum fill height was 17 FT.

The method of filling was through two 4 inch pipes located 18 inches above the tank floor.

The rise in liquid level was monitored by measuring head pressure from a pressure transducer located on a flange low on the tank wall. Hold periods were initiated as close as possible to the pre-planned levels. The operator recorded in his test log the time at the beginning and end of each hold period, and other significant events. The following is an excerpt from the test log maintained by the operator as the test was in process.

TIME LOCAL	TIME TEST (Sec.)	LOAD % OF MAX.	COMMENT
16:58:42	1620	50%	End hold period. Continue loading to 75%
17:27:12	1800	75%	Hold at 75%
18:15:30	930	75%	End hold period. Continue loading to 87.5%
18:32:13	1800	87.5%	Hold at 87.5%
19:08:29	870	87.5%	End hold period. Continue loading to 100%
19:23:33	1830	100%	Hold at 100%
49:30:00	###	100%	End hold, terminate test.

Acoustic emission detected during these loadings is shown in the three graphs of Figure 3. All three graphs have time on the x-axis. In the lower graph, each dot shows one detected acoustic emission event. The vertical height of the dot shows the amplitude (size) of the event. The middle graph shows the emission rate. "Counts" is a measure of AE activity, used for evaluating the tank. The upper graph shows which channels are detecting the emission activity. This gives information on the locations of the emission sources.

7.0 DATA INTERPRETATION

Data interpretation is the process of separating relevant from non-relevant indications, i.e. separating genuine AE from noise.

In this test, the operator identified no background noise sources outside of the tank. Components inside of the tank may have produced background noise.

Based on these identifications, the data was not filtered to remove noise before commencing with structural evaluation.

Note: A leaking nozzle was detected using advanced analysis techniques. This leak was not detected using the CARP analysis. Results of advanced analysis techniques will be described in a future report.

8.0 DATA EVALUATION

The final analysis of the data acquired during this test was conducted in the Lawrenceville, NJ., offices of the PHYSICAL ACOUSTICS CORPORATION.

Data was analyzed according to the CARP procedure, after excluding noise and background activity as far as possible, with the pass/fail criteria given below.

Acceptance Criterion	Significance Criteria	Results
1. Hits during holds None beyond 2 Min.	Measure of Continuing damage.	FAIL-1,499
2. Felicity ratio Greater than 0.95.	Measure of the severity of previously induced damage.	FAIL-0
3. Total counts less than N/2 (3868).	Measure of the overall damage during a load cycle.	FAIL-429,966
4. Hits above 75 dB less than 5.	Measure of high energy microstructural damage.	FAIL- 9

The above data summarizes the situation for the whole tank. Following the recommendations of the CARP procedure, the tank should be examined using other NDT methods, including visual, to determine the reason for the high emission levels. Visual examination of the outside wall areas which produced high levels of emission resulted in the following observations:

1) Manway, positioned between sensors 16, 17 and 1; This area produced high activity but there are no visual indications of delamination or damage. The inside of the manway should be examined carefully at the next opportunity. Note that high stresses on bolts that attach the manway can cause slipping. In the future, bolts should be tightened to the manufacturers recommendations.

2) The lower portion of the tank wall, in the area of sensors

1, 2, 3 and 4; This area produced a great deal of emission. This may be the result of a recently applied patch in the tank floor adjacent to the knuckle. The tank floor and knuckle in this area should be examined from the inside.

3) The small manway adjacent to sensor 8 produced significant activity. There is no indication of damage on the outside. The noise may have been produced by weakness in the secondary bond or possibly by loose and slipping bolts. This area should be examined visually from the inside at the next opportunity.

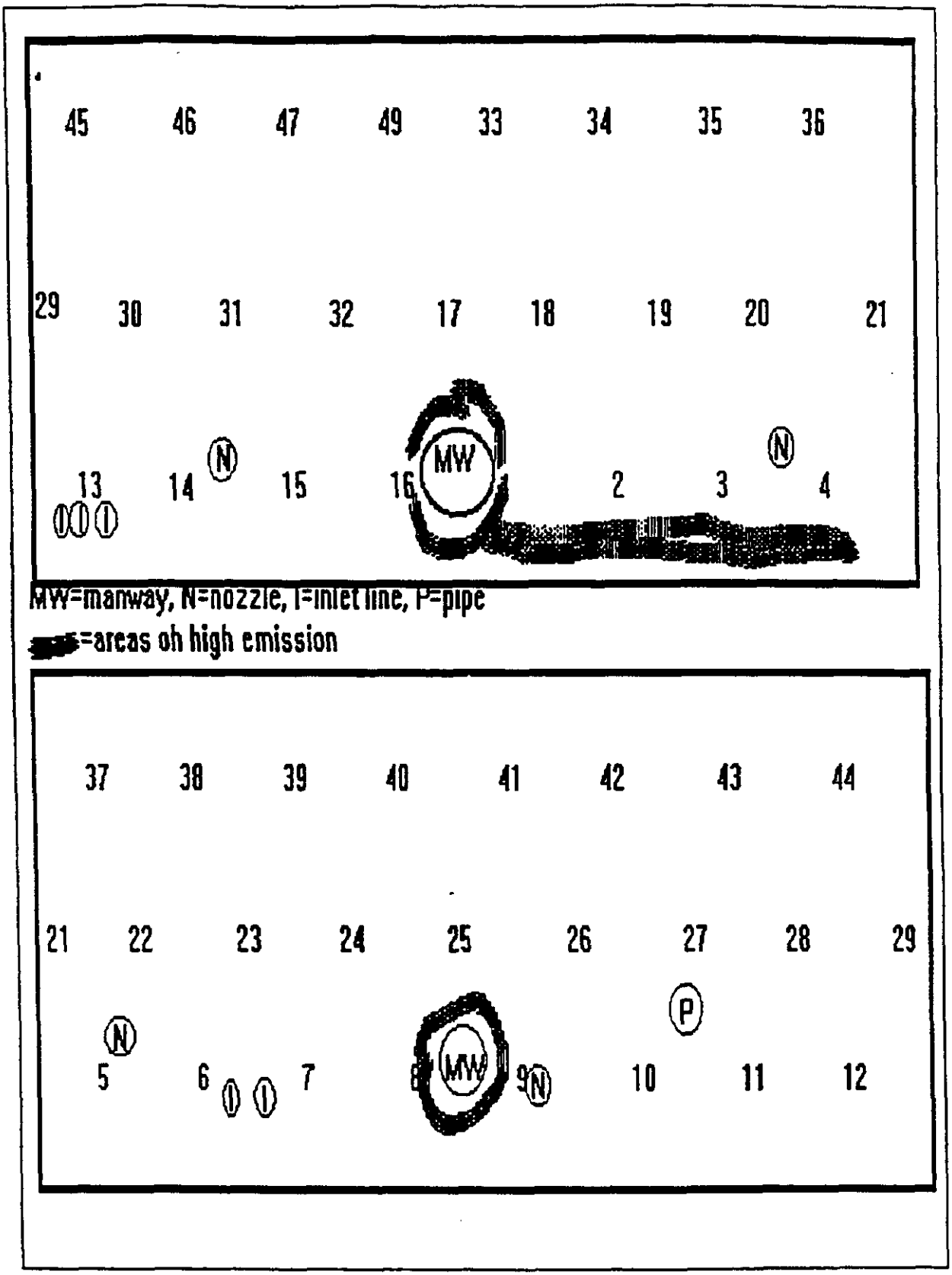

FIGURE 1
Tank Sketch and Sensor Location Map

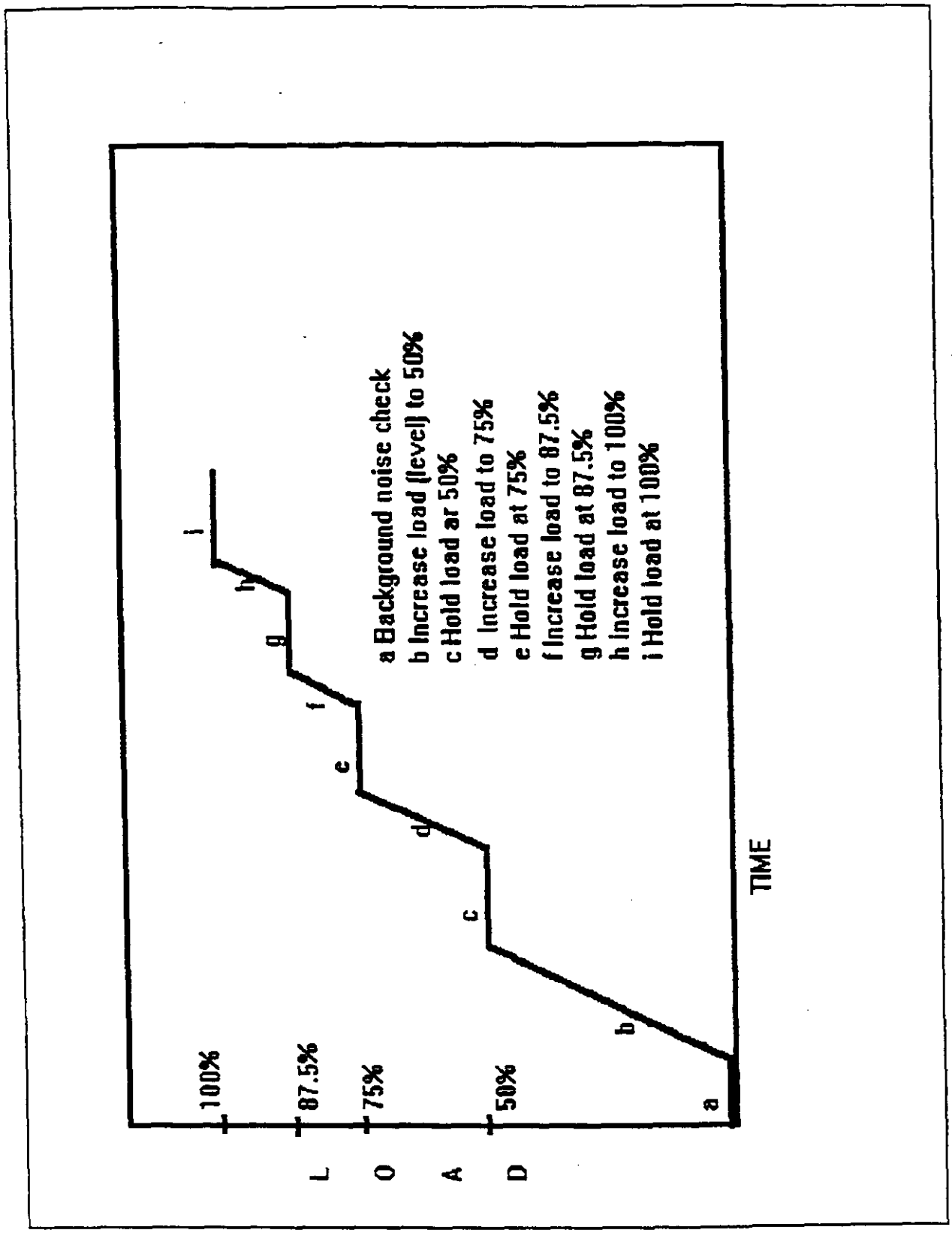

FIGURE 2
Load Ramp

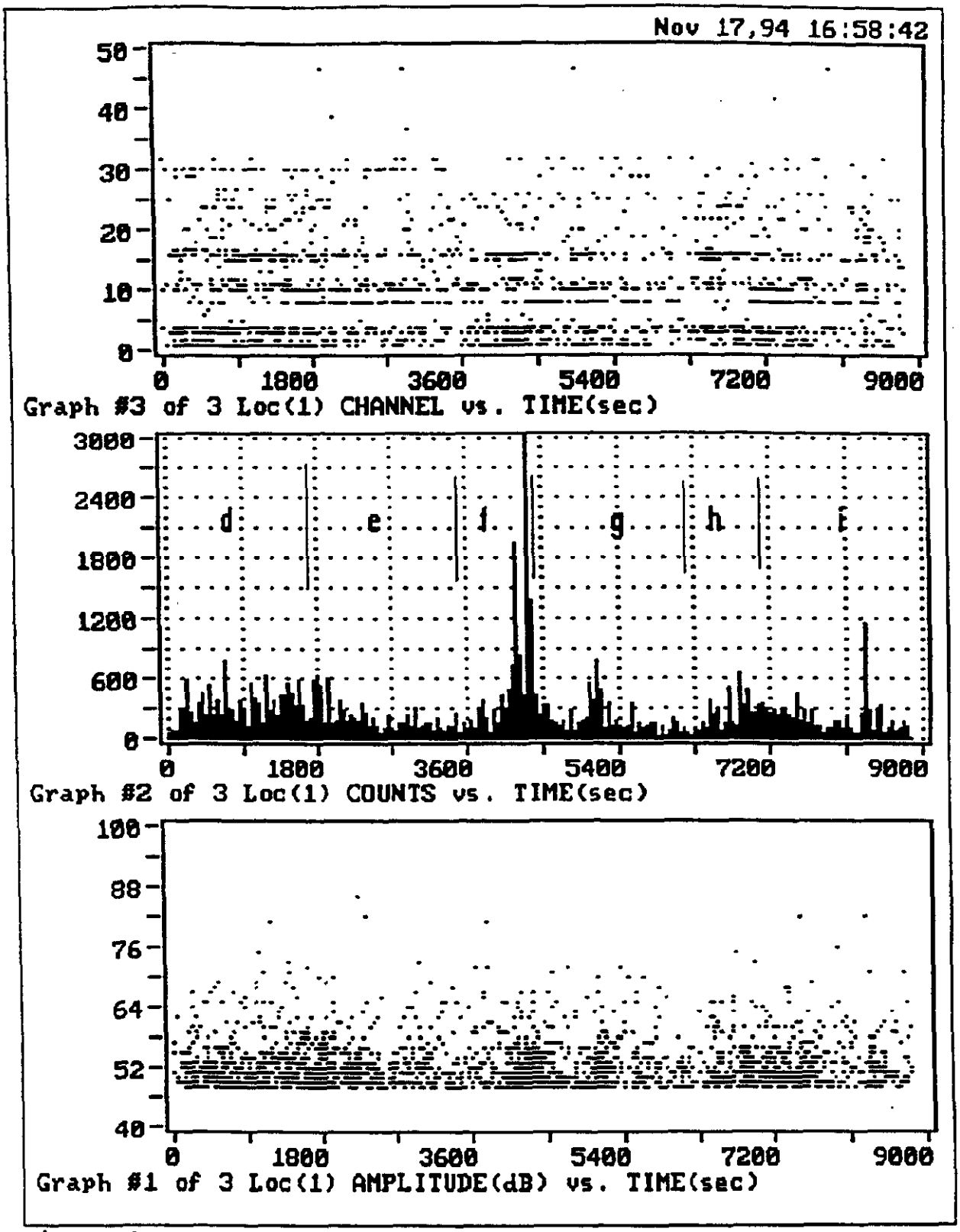

Figure 3

FIGURE 3
Acoustic Emission Data Graphs

TEST ID_____SHEET___OF___

AE ANALYSIS FILE TRACKER

ANALYSIS BY_____STRUCTURE: JBR TANK_____PROJECT_____

PART OF TEST ON THIS FORM:_____INI FILE:_____

Date	Infile	Outfile	Details of Filter &c.	
	C:\SAMSUNG\ GP2TST03	C2TST03	FILTERED TO REMOVE HITS LESS THAN 48 dB.	50-75%
	" 04	C2TST04	"	Hold 75%
	" 05	C2TST05	"	75-87.5%
	" 06	C2TST06	"	Hold 87½%
	" 07	C2TST07	"	87.5-100%
	" 03	C2TST08	"	Hold 100%
	" 09	C2TST09	"	Hold 100% 12 HRS.
	C2TST03 -08	C2TSTX.DTA	LINK ALL FILTERED FILES TO CREATE ONE COMPLETE	
			TEST FILE WITH 4333 HITS	
	JBR_TANK.RPT		WORD PERFECT FILE WITH REPORT	

JBR = JET BUBBLE REACTOR

TEST ID_____SHEET___OF___

DATA (.DTA) FILES REGISTER

DATE: 11-16-94 OPERATOR: JRM, DLL, CB PROJECT_____

PATH	FILENAME	CONTENTS	
C:\AE\	GPATTN4.DTA	(ATTNUAT.INI) LEAD BREAKS AT	
		6" INTERVALS ALONG FIBER DIRECTION	
	GPATTN5	LEAD BREAK 6" INTERVALS EVERY 30 SEC 45°	
	PERFCKDD	Done by HAND - SEE WORKSHEET	
		LB ON ALL CHANNELS, TANK EMPTY	
	GP2TST00.DTA	HOLD BACKGROUND NOISE CHECK EMPTY	
	GP2TST01.DTA	0 - 8½ ft.	
	GP2TST02.DTA	HOLD AT 50% (9'2" = ACTUAL)	
	GP2TST03.DTA	50% - 75% 8'6" TO 12'9"	
	GP2TST04.	HOLD AT 75% (13' = ACTUAL)	
	GP2TST05	75% - 87½% 12'9" - 14'10"	
	GP2TST06	HOLD AT 87½ (14'11" = ACTUAL)	
	GP2TST07	87½% - 100% 14'10" - 17'	
	GP2TST08	HOLD AT 100% 30 MIN.	
	GP2TST09	HOLD AT 100% OVERNIGHT.	

ACOUSTIC EMISSION ATTENUATION STUDY FOR F.R.P

CUSTOMER:	TANK: JBR	DATE: 11-16-94
FILE:	INI FILE: ATTNUAT.INI	

HORIZONTAL GPATTN4.DTA

DISTANCE	AMPLITUDE (db)					AVERAGE
0	95	97	96			
6"	84	83	80			
12"	69	69	72			
18"	57	56	60			
24"	53	52	49			
30"	43	48	45			
36"	43	40	43			
42"	40	40	40			

DIAGONAL GPATTN5.DTA

DISTANCE	AMPLITUDE (db)					AVERAGE
0	93	93	93			
6	75	77	74			
12	61	69	65			
18	53	56	56			
24	42	41	41			

FILE:	INI FILE:

COUNTS CRITERION DETERMINATION

BREAK #	1	2	3	4	5	6	7	8	9	10	AVERAGE	*130
	66	59	56	65	57	61	56	65	58	61	59.8	7735

Sheet No._____

SYSTEM PERFORMANCE CHECK FORM (LEAD BREAKS)

CONTINUATION SHEET JBR

DATE:_____ START/END TIMES:_____ JOB ID:_____

Sensor / Location	Amplitudes (dBae)					Av.	Sensor / Location	Amplitudes (dBae)					Av.
1	75	77	78			76.7	16	82	82	83			82.3
2	78	83	82			81	17	74	74	77			75
3 *	87	87	87			87	18	79	82	82			81
4 *	80	84	88			85.7	19	75	75	75			74.3
5	76	79	81			78.7	20	77	80	80			79
6	76	77	79			77.3	21	78	80	80			79.3
7	75	75	73			73.7	22 *	85	85	85			95
8	81	81	82			81.3	23	75	76	76			75.6
9 *	67	68	69			68	24	79	79	81			79.7
10	78	80	81			79.7	25	78	81	81			80
11	75	76	81			77.3	26	76	78	78			77.3
12	78	79	78			78.3	27	75	76	76			75.7
13	76	77	77			76.7	28	80	82	82			81.3
14	77	78	80			78.3	29	84	80	85			83
15	80	82	82			81.3	30	78	78	82			79.3

NOTES: _____

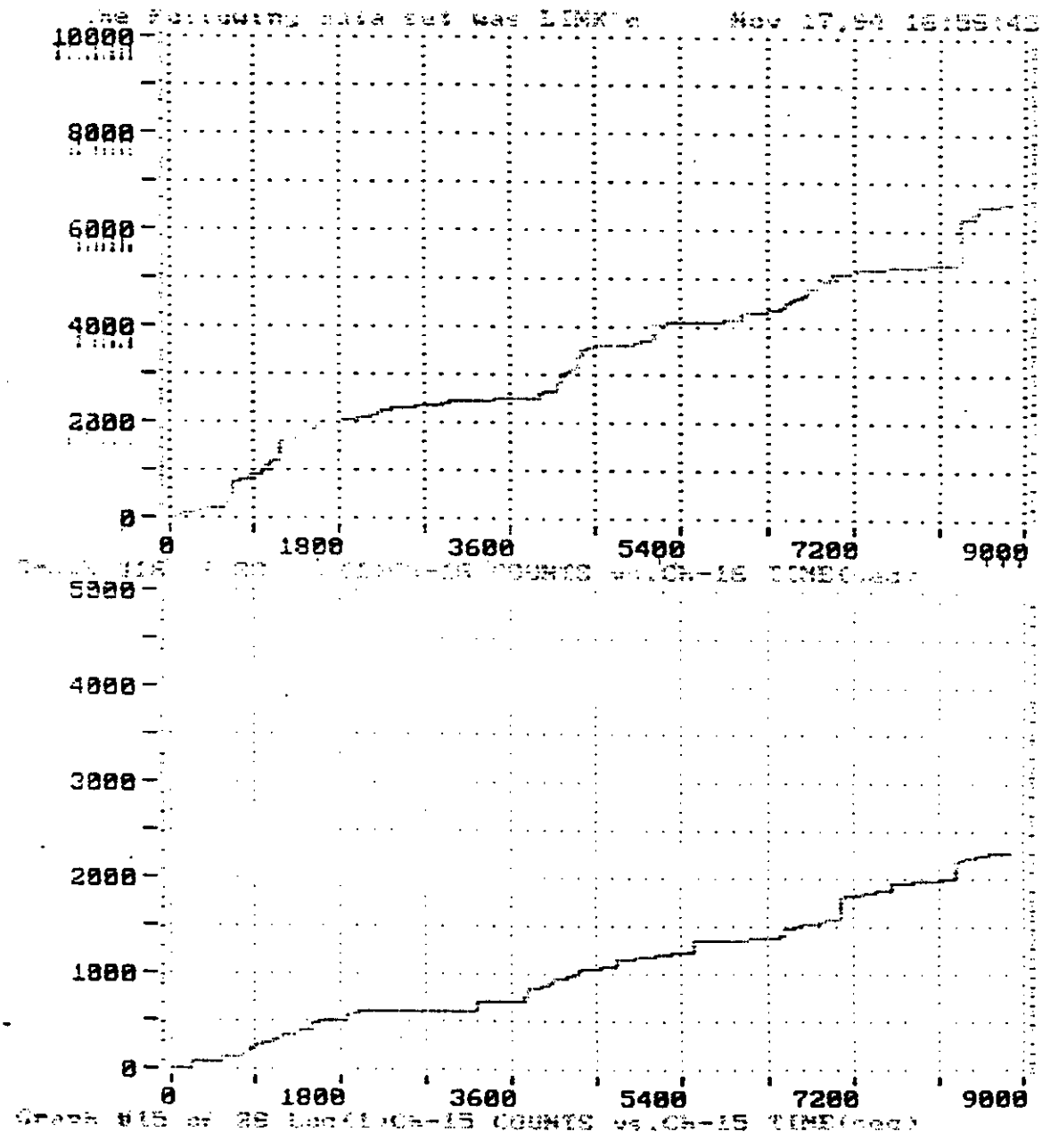
10000
8000
6000
4000
2000
0
0
1800
3600
5400
7200
9000
5000
4000
3000
2000
1000
0
0
1800
3600
5400
7200
9000

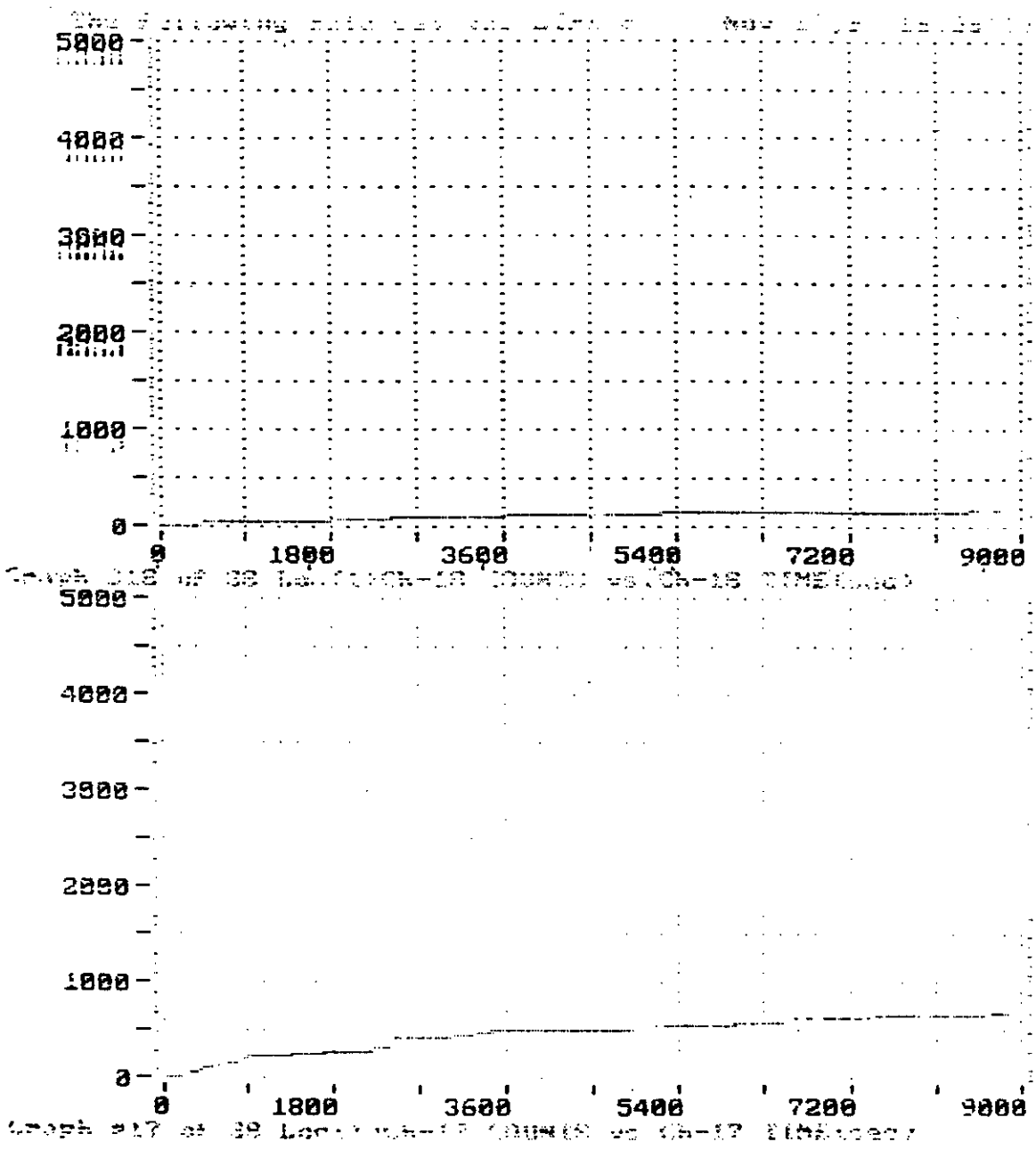
5000
4000
3000
2000
1000
0
0
1800
3600
5400
7200
9000
5000
4000
3000
2000
1000
0
0
1800
3600
5400
7200
9000

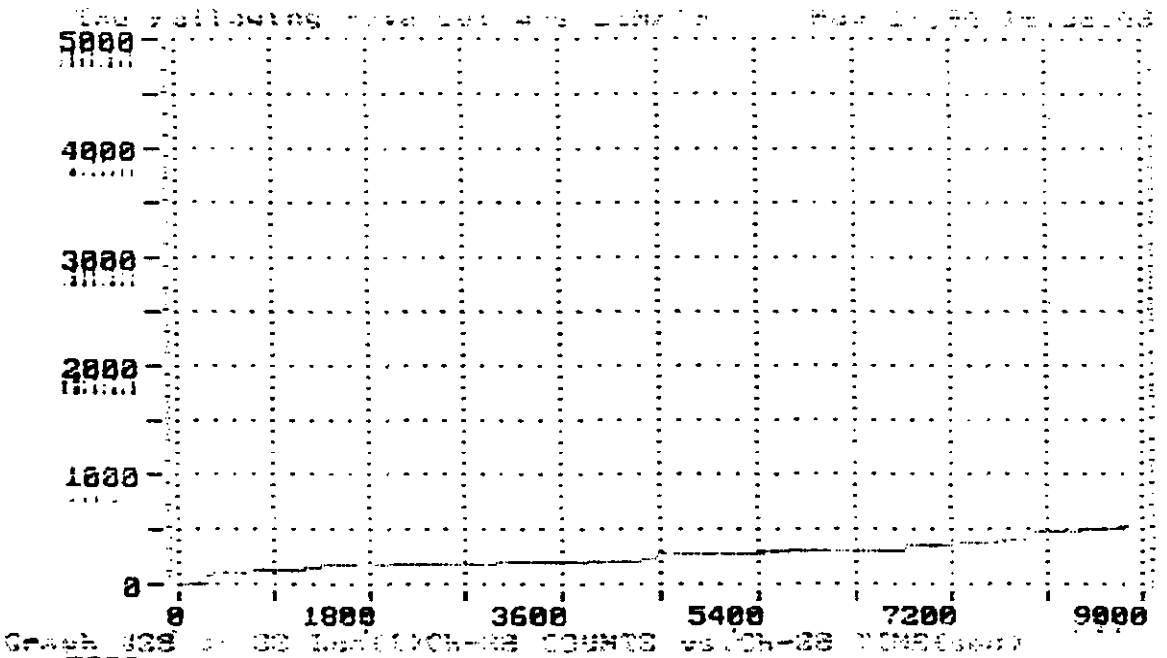
5000
4000
3000
2000
1000
0
0
1800
3600
5400
7200
9000

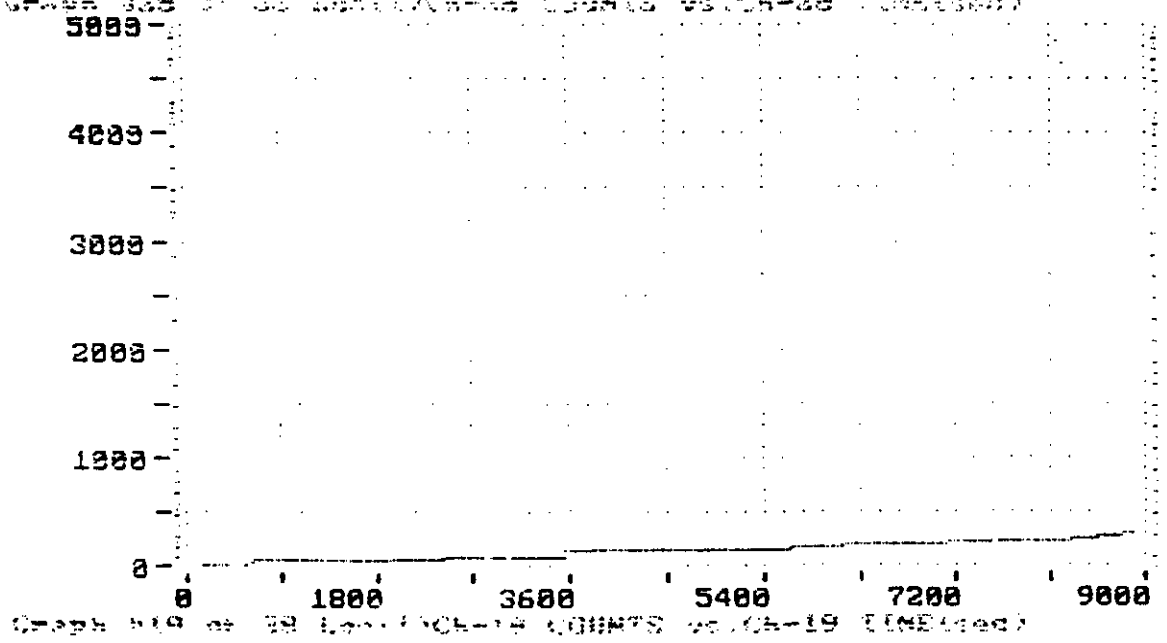
5000
4000
3000
2000
1000
0
0
1800
3600
5400
7200
9000

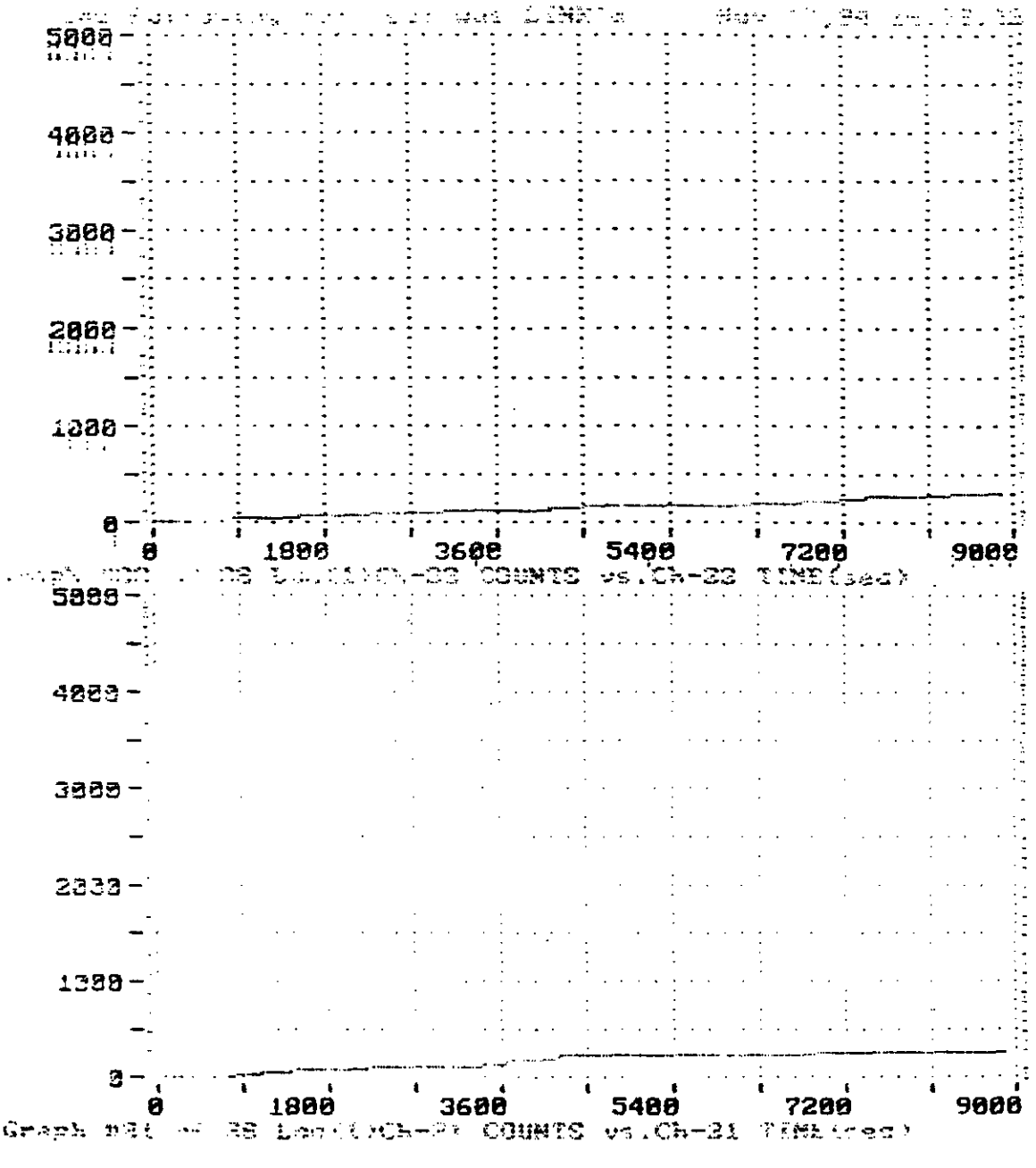
5000
4000
3000
2000
1000
0
0
1800
3600
5400
7200
9000
5000
4000
3000
2000
1000
0
0
1800
3600
5400
7200
9000

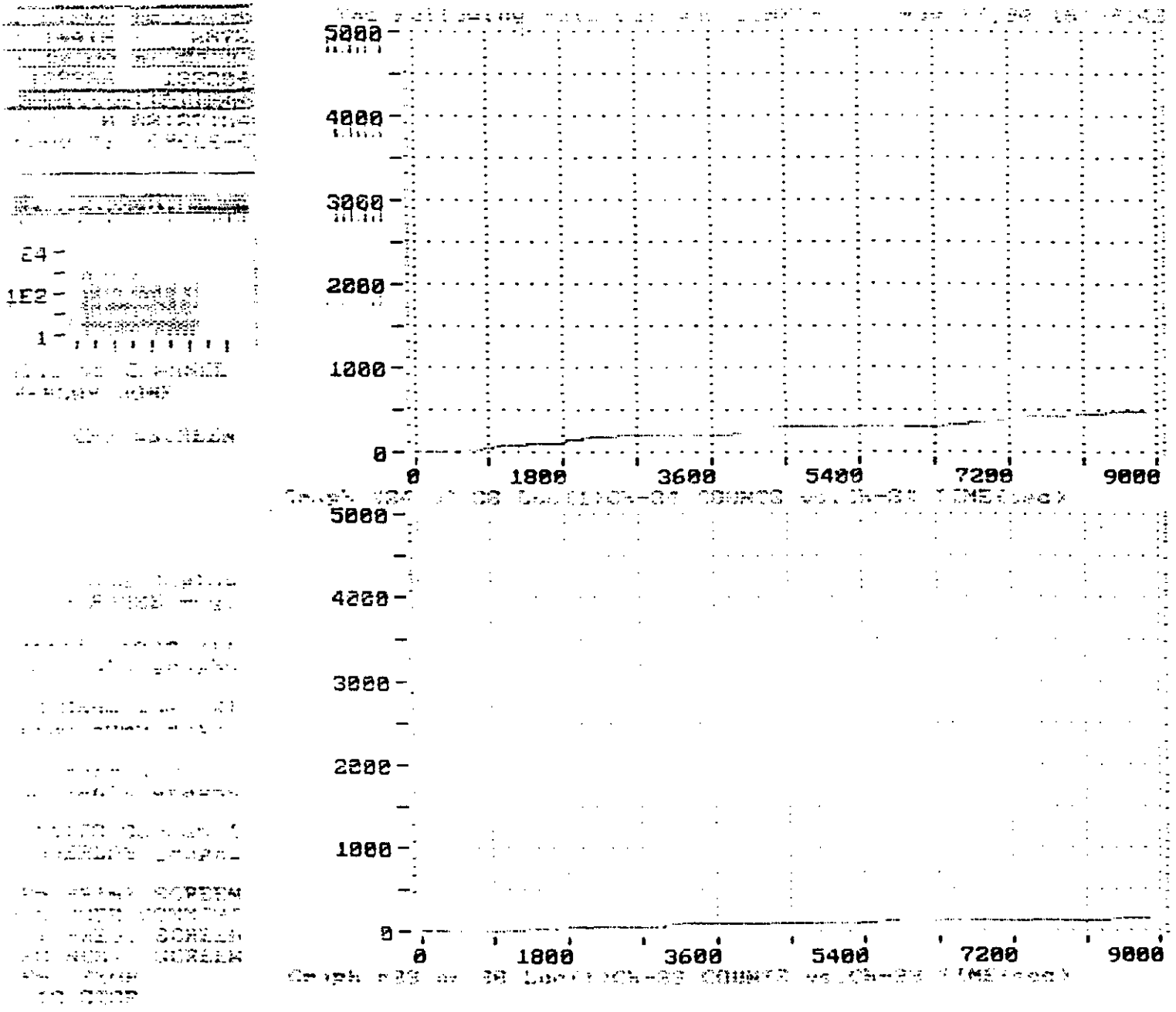
5000
4000
3000
2000
1000
0
0
1800
3600
5400
7200
9000
5000
4000
3000
2000
1000
0
0
1800
3600
5400
7200
9000

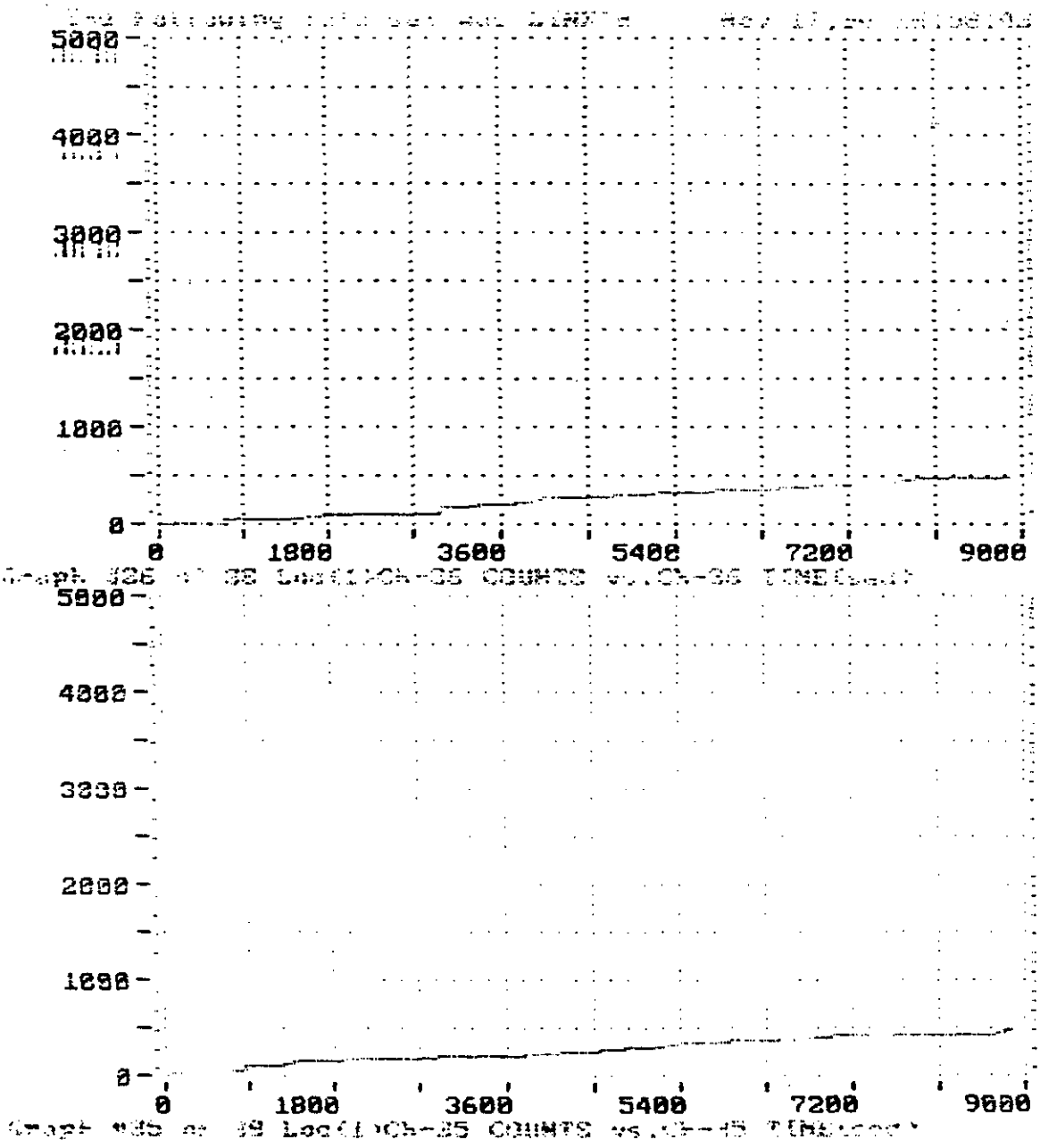
5000
4000
3000
2000
1000
0
0
1800
3600
5400
7200
9000

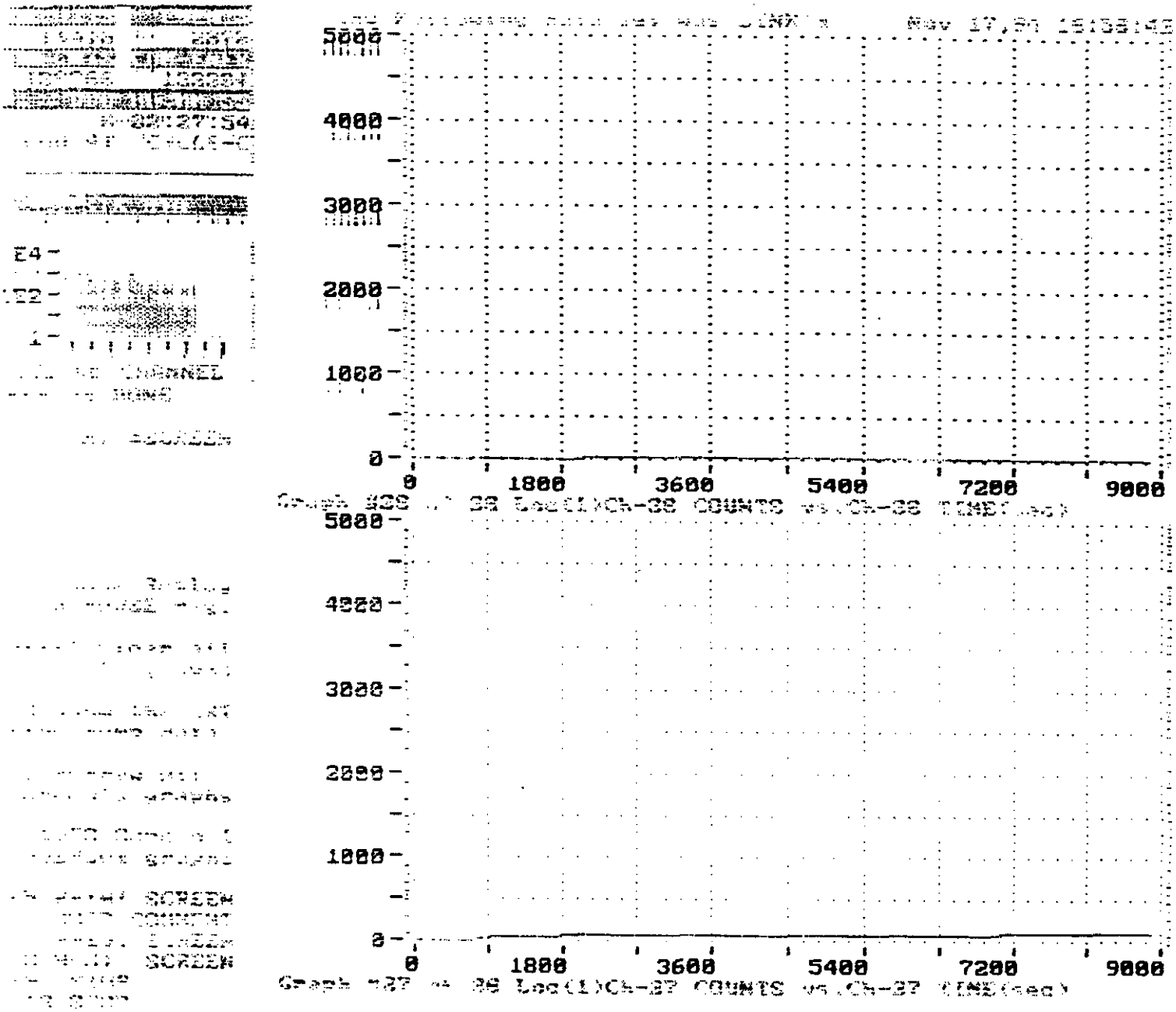
5000
4000
3000
2000
1000
0
0
1800
3600
5400
7200
9000
5000
4000
3000
2000
1000
0
0
1800
3600
5400
7200
9000

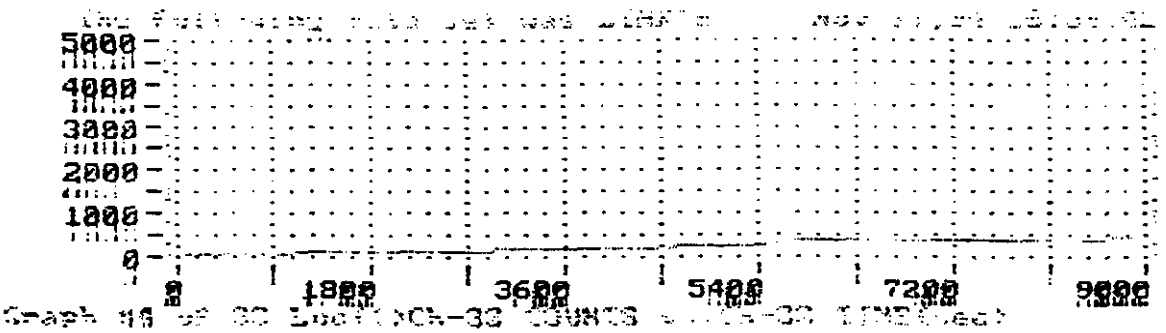
5000
4000
3000
2000
1000
0
0
1800
3600
5400
7200
9000

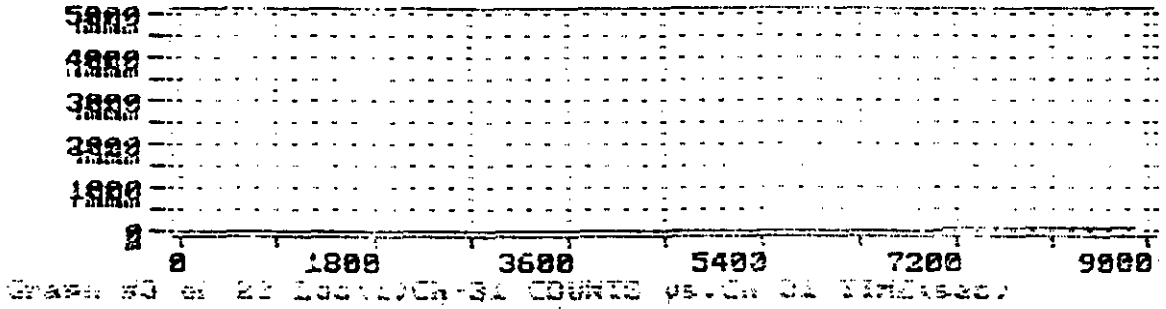
5000
4000
3000
2000
1000
0
0
1800
3600
5400
7200
9000

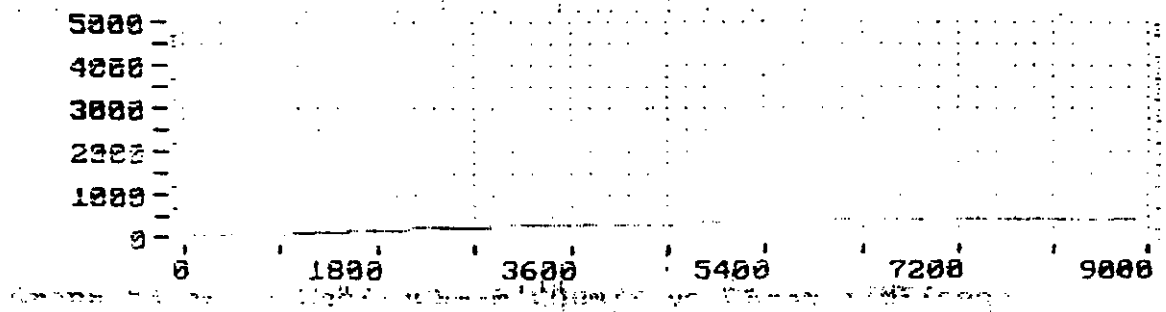
5000
4000
3000
2000
1000
0
0
1800
3600
5400
7200
9000

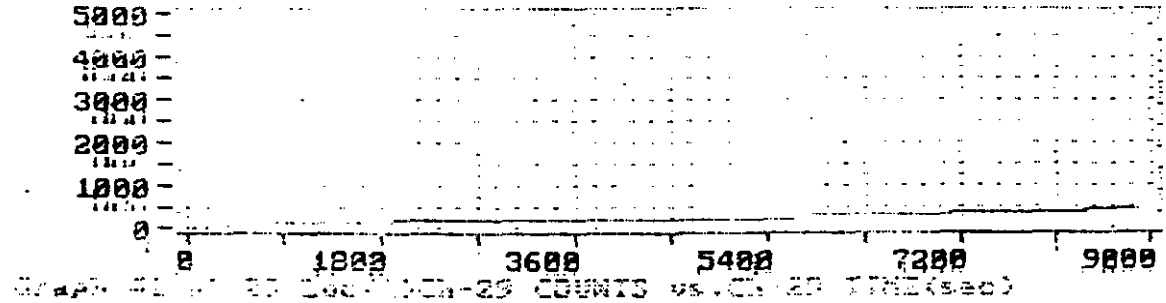
5000
4000
3000
2000
1000
0
0
1800
3600
5400
7200
9000

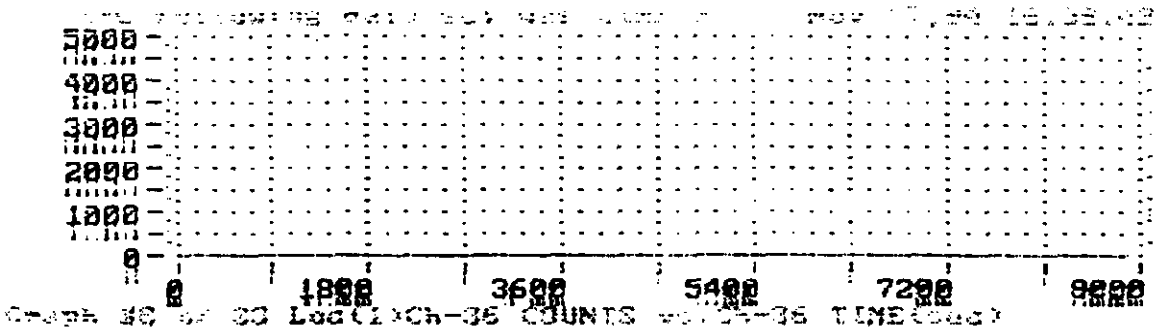

Graph #6 of 23 Loc(1)Ch-36 COUNTS vs Ch-36 TIME(sec)

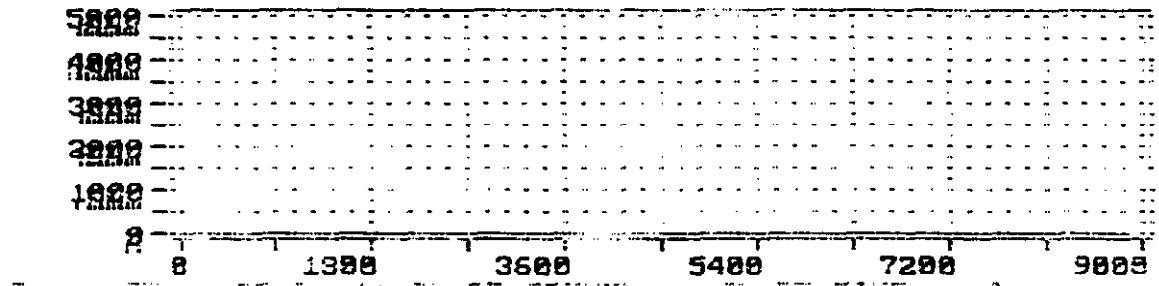

Graph #7 of 23 Loc(1)Ch-35 COUNTS vs Ch-35 TIME(sec)

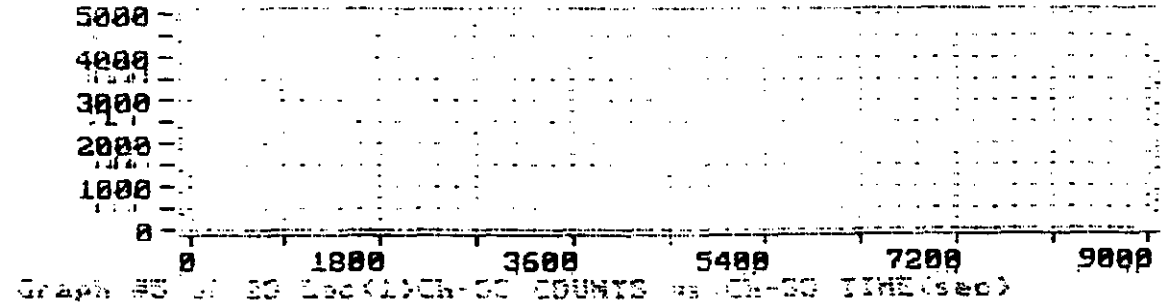

Graph #8 of 23 Loc(1)Ch-33 COUNTS vs Ch-33 TIME(sec)

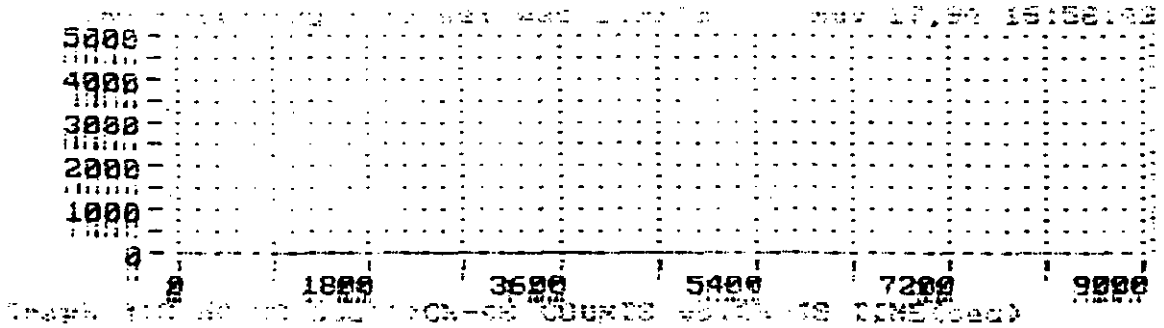
5000
4000
3000
2000
1000
0
0
1800
3600
5400
7200
9000

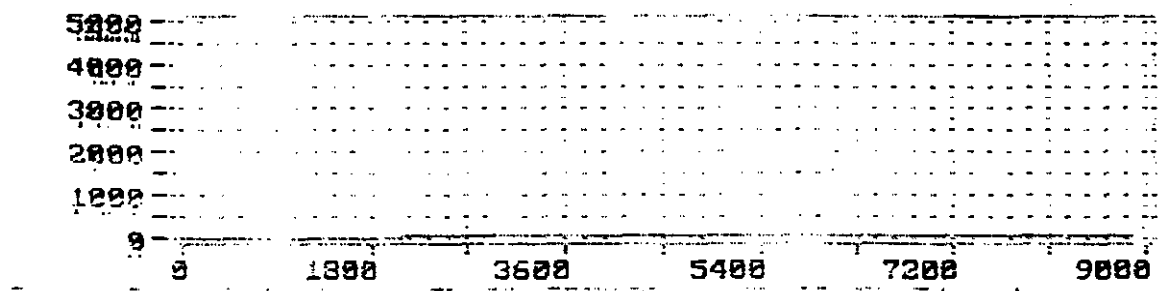
5000
4000
3000
2000
1000
0
0
1800
3600
5400
7200
9000

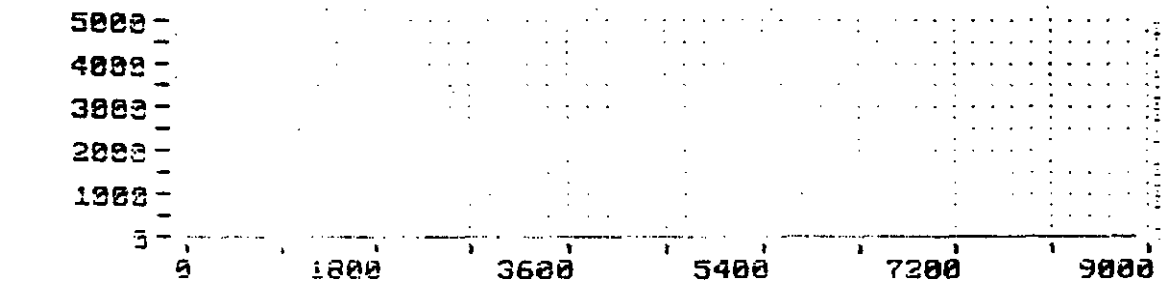
5000
4000
3000
2000
1000
0
0
1800
3600
5400
7200
9000

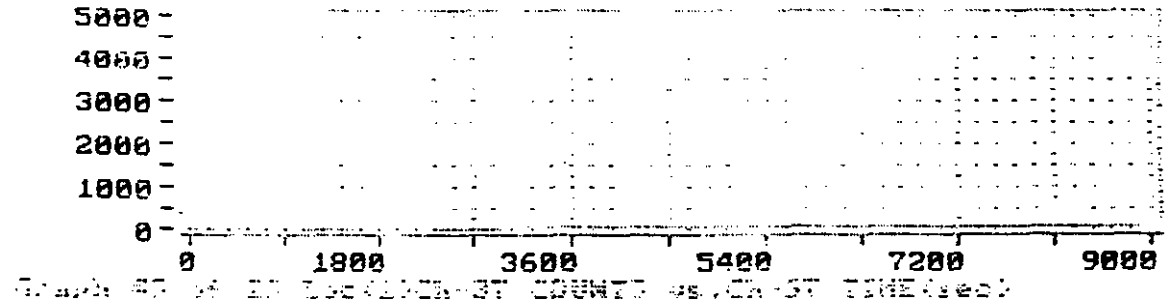
5000
4000
3000
2000
1000
0
0
1800
3600
5400
7200
9000

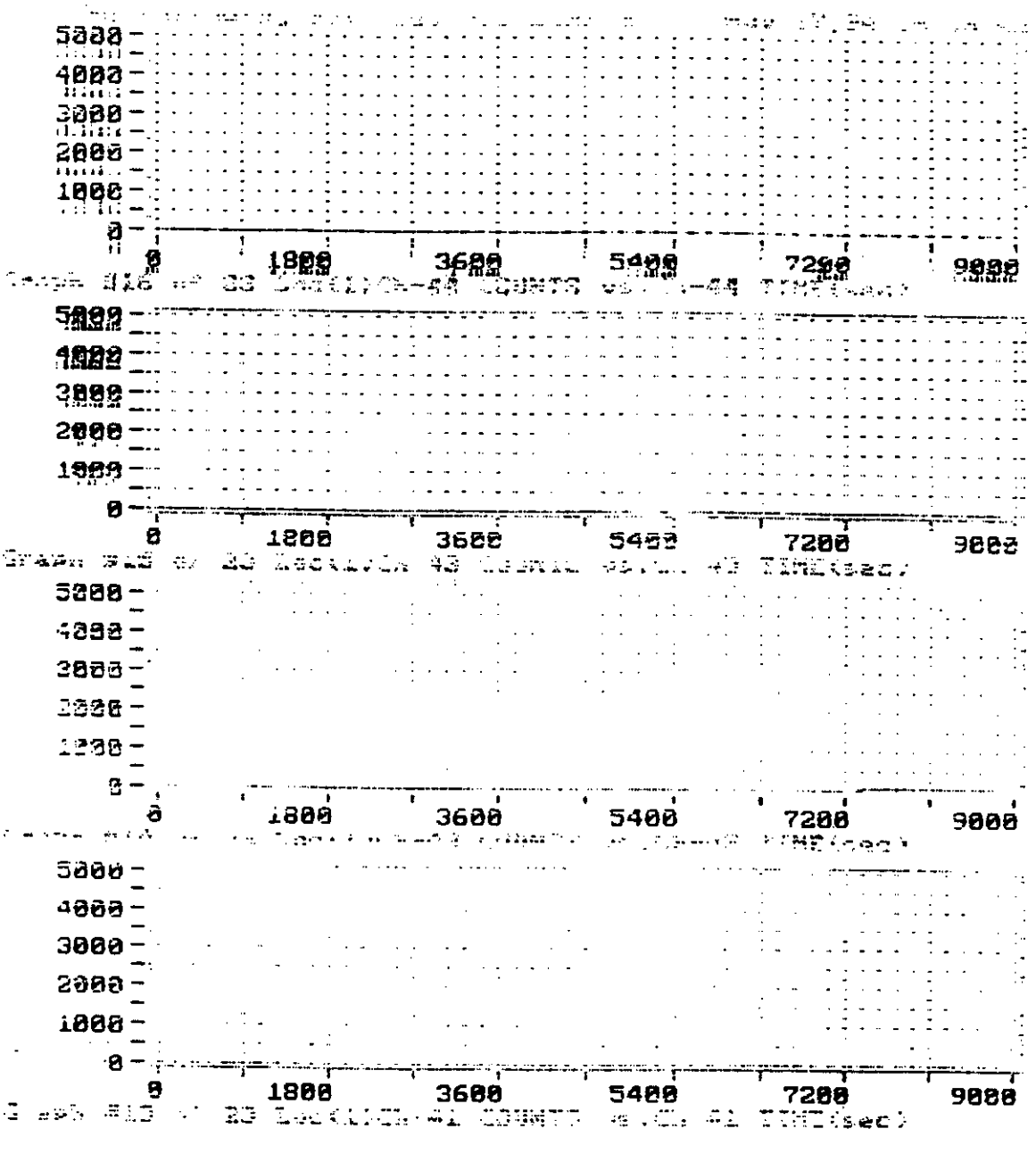
5000
4000
3000
2000
1000
0
0
1800
3600
5400
7200
9000

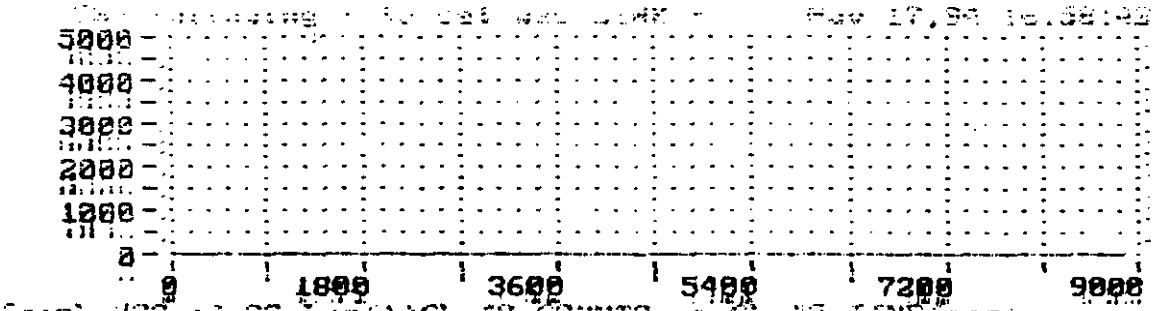
5000
4000
3000
2000
1000
0
0
1800
3600
5400
7200
9000

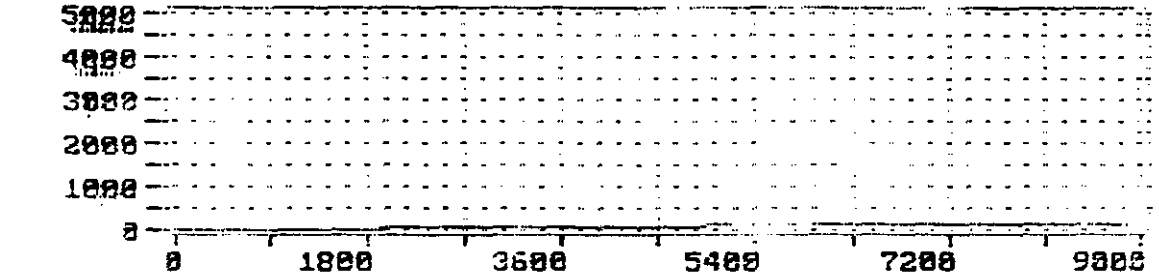
5000
4000
3000
2000
1000
0
0
1800
3600
5400
7200
9000

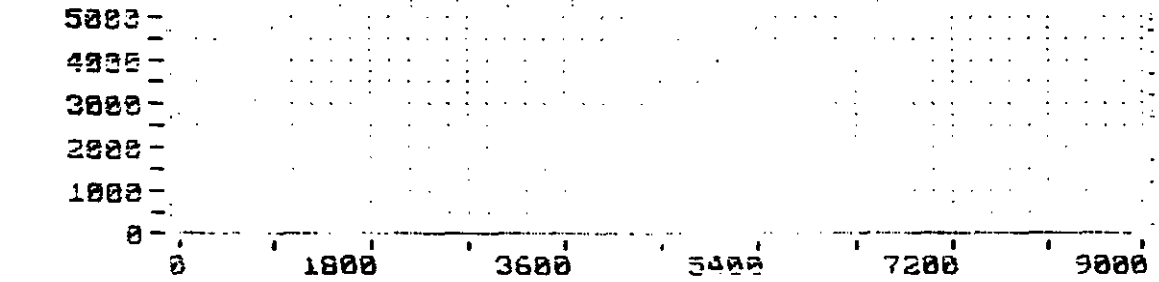
5000
4000
3000
2000
1000
0
0
1800
3600
5400
7200
9000

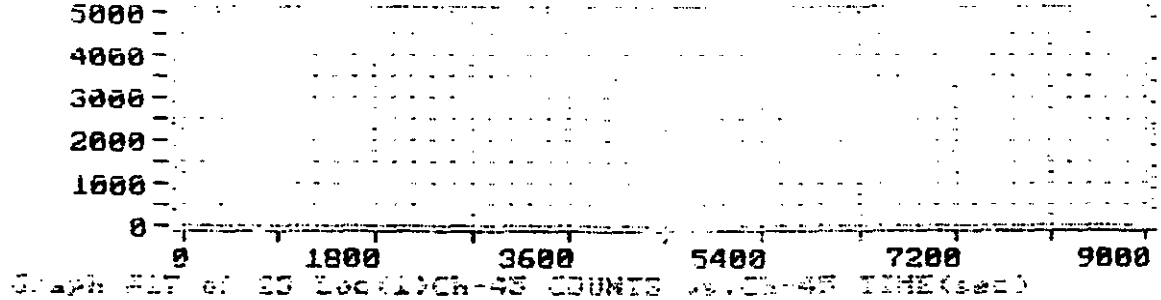
5000
4000
3000
2000
1000
0
0
1800
3600
5400
7200
9000

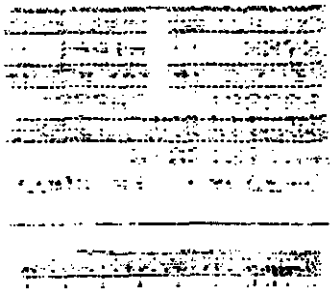

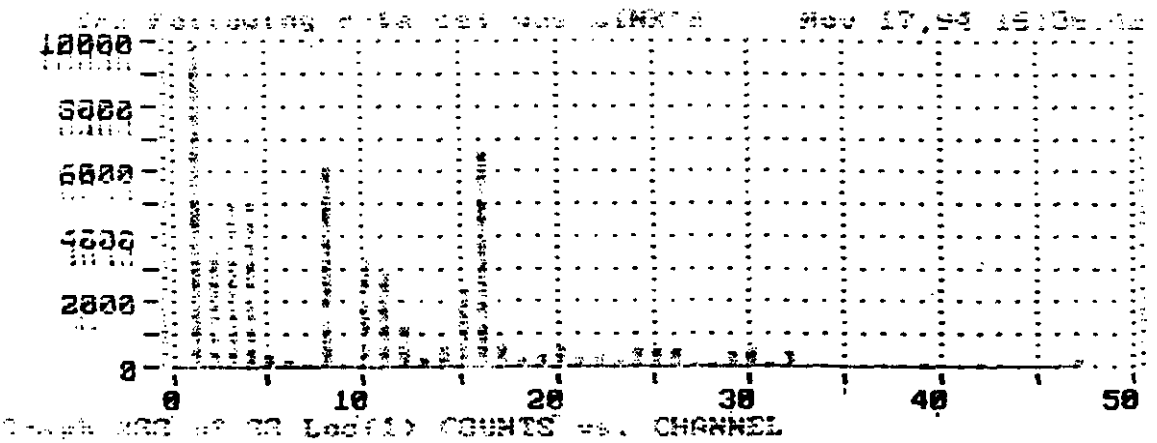

Graph #22 of 33 Log(1) COUNTS vs. CHANNEL

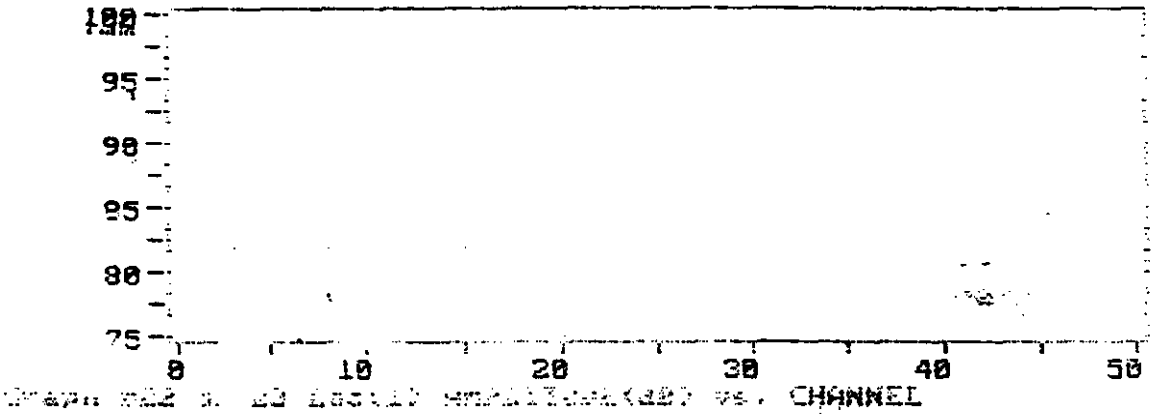

Graph #32 of 33 Log(1) AMPLITUDE(dB) vs. CHANNEL

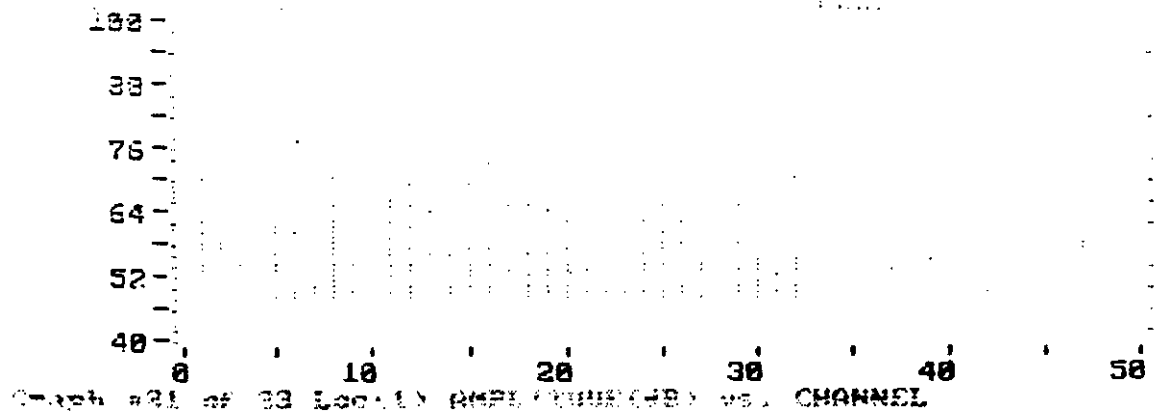

Graph #31 of 33 Log(1) AMPLITUDE(dB) vs. CHANNEL

PHYSICAL ACOUSTICS CORPORATION
FRP
Acoustic Emission Inspection Report

SOUTHERN COMPANY SERVICES
GEORGIA POWER PLANT, YATES FACILITY

LIMESTONE SLURRY STORAGE TANK

Tested On
NOVEMBER 14-15, 1994

Project leader JAMES R. MITCHELL
Assisted By: DAVID L. KESLER
CHRIS B. BARBOUR

Physical Acoustics Corporation
Princeton, New Jersey

PHYSICAL ACOUSTICS CORPORATION
FRP
Acoustic Emission Inspection Report

LIMESTONE SLURRY STORAGE TANK

Tested On
NOVEMBER 14-15, 1994

REPORTED PREPARED
FOR
KAMYER VAKHSHOORZADEH, Ph.D
SOUTHERN COMPANY SERVICES, INC
PO BOX 2625
BIRMINGHAM, ALABAMA 35202-2625
(205)877-7805 (O), (205) 868-5367 (F)

Prepared By: JAMES R. MITCHELL
AET L-111, ASNT L1419
(203) 536-3380 (O,F)

Physical Acoustics Corporation
Princeton, New Jersey

SUMMARY AND RECOMMENDATIONS

An Acoustic Emission (AE) test was performed on a limestone slurry tank for Southern Company Services, Yates Plant. This test used the Recommended Practice for Acoustic Emission Testing of Fiberglass Reinforced Plastic Resin (RP) Tanks/Vessels, published by the Committee on Acoustic Emission from Reinforced Plastics (CARP) of the Society of the Plastics Industry.

A total of 33 AE sensors, configured as shown in Figure 1, were used to monitor the tank. Analysis of the data after taking account of known noise incidents showed that the tank exhibited Acoustic Emission data well in excess of the CARP acceptance criteria.

TABLE OF CONTENTS

1.0 INTRODUCTION

The CARP recommended practice consists of subjecting FRP equipment to increasing loads while being monitored by sensors that are sensitive to acoustic emission (transient stress waves) caused by growing flaws. The sensors are connected to instrumentation that is capable of recording and analyzing AE signals. The CARP recommended practice also provides guidelines to determine the location and severity of structural flaws with acceptance criteria as a basis to assess the structural integrity of the FRP equipment. The CARP criteria are shown in section 8 of this report.

The AE test method is designed to detect structurally significant defects and damage in FRP equipment. The damage mechanisms that are detected in FRP are as follow:

a. resin cracking
b. fiber debonding
c. fiber pullout
d. fiber breakage
e. delamination
f. bond failure in assembled joints (for example, nozzles, manways, etc.)

For a more detailed description of the test set-up and procedure see section 2 through 8 of this report. Figures 3 and appendix 1, 2 contains data listings and activity graphs that were used to perform the final data analysis.

2.0 TANK DESCRIPTION

Vessel/Component Tested: Limestone Slurry Storage Tank

Description: Field Erected FRP, 110F Max Temp., SPG=1.14, 80MPH Max wind load, Empty weight 30,250 pounds,

Dimension: 28 FT Diam, 27 FT High

Insulated: NO

Capacity: 124,365 US gallons.

Material of construction: Liner and structural resin: AROPOL 7334

Manufacturer: Ershigs, Bellingham, WA: SN D-90081 3095, PO# SCS 90-C-2148

Data of Mfg.: March 1991

Maximum Test Level: 24 Feet

Test Medium: Water

Filled From: Fire Hydrant, Through low nozzle

3.0 AE TEST EQUIPMENT

AE INSTRUMENTATION MFG.: Physical Acoustics Corp.

AE INSTRUMENTATION TYPE: PAC 58 CH SPARTAN-AT

SENSOR TYPE: R15I RESONANT FREQ.: 150 kHz

PREAMP TYPE: Integral

FREQUENCY BANDPASS: 100-300 kHz (Band Pass)

SENSOR ATTACHMENT METHOD: Hot Glue

4.0 INSTRUMENT SET-UP PARAMETERS

DETECTION THRESHOLD	: 48	dB
PREAMP GAIN	: 40	dB
INSTRUMENT GAIN	: 20	dB
PDT	: 100	us
HDT	: 200	us
HLT	: 500	us

5.0 AE TEST SET-UP

Attenuation: (AE source = 0.5mm Pentel lead breaks)

Sensor #5	0"	6"	12"	18"	24"
IN LINE	97 dB	87 dB	70 dB	67 dB	61 dB
45 Deg.	95 dB	72 dB	67 dB	59 dB	50 dB

Prior to the monitoring period, the complete AE system was checked to assure proper performance by injecting a signal on the surface of the tank at each sensor location with a Pentel pencil containing 0.5mm HB lead. The average amplitude of this signal was recorded by the test operator and is listed in Table 1. Under the CARP procedure, all channels should lie within 6dB of the grand average.

TABLE 1

Sensor #	dB	Sensor #	dB	Sensor #	dB
1	80	17	83	33	73
2	67	18	85	34	--
3	68	19	75	35	--
4	76	20	76	36	--
5	70	21	77	37	--
6	68	22	76	38	--
7	69	23	77	39	--
8	73	24	71	40	--
9	72	25	72	41	--
10	77	26	79	42	--
11	77	27	68	43	--
12	83	28	73	44	--
13	84	29	80	45	--
14	78	30	76	46	--
15	81	31	75	47	--
16	74	32	79	49	--

Grand Average 75 dB

Number of channels: 33
Number of sensors : 33
Sensor configuration: See Figure 1
Background noise level and character: Sporadic low level, from all channels
Count Criterion: N = 7,969 Total counts from 130 Pentel lead breaks at a distance that gives an amplitude midway between the threshold of AE detectibility and the reference amplitude threshold.)
Threshold of AE Detectability: 48 dB
Reference Amplitude Threshold: 75 dB

6.0 TEST PROCESS

A loading schedule, that followed CARP guidelines, was provided to operating personnel prior to the test. The proposed sequence included stepped loading with hold periods at 50%, 75%, 87.5% and 100% of maximum fill height (see Figure 2). Maximum fill height was 24FT.

The method of filling was through a fire hydrant into an existing nozzle located approximately 18 inches off of the floor.

The rise in liquid level was monitored by measuring head pressure from a pressure transducer located on a flange low on the tank wall. Hold periods were initiated as close as possible to the pre-planned levels. The operator recorded in his test log the time at the beginning and end of each hold period, and other significant events. The following is an excerpt from the test log maintained by the operator as the test was in process.

TIME LOCAL	TIME TEST (Sec.)	LOAD % OF MAX.	COMMENT
###	2:23:28	50%	End hold period. Continue loading to 75%
###	00:11:33	75%	Hold at 75%
###	01:04:41	75%	End hold period. Continue loading to 87.5%
###	00:10:04	87.5%	Hold at 87.5%
###	00:52:41	87.5%	End hold period. Continue loading to 100%
###	00:30:19	100%	Hold at 100%

Acoustic emission detected during these loadings is shown in the three graphs of Figure 3. All three graphs have time on the x-axis. In the lower graph, each dot shows one detected acoustic emission event. The vertical height of the dot shows the amplitude (size) of the event. The middle graph shows the emission rate. "Counts" is a measure of AE activity, used for evaluating the tank. The upper graph shows which channels are detecting the emission activity. This gives information on the locations of the emission sources.

7.0 DATA INTERPRETATION

Data interpretation is the process of separating relevant from non-relevant indications, i.e. separating genuine AE from noise.

In this test, the operator identified background noise from operation of an ultrasonic level detector located on the walkway over the tank. The level detector was disconnected for the duration of the test. No other background noise sources outside of the tank could be identified. Components inside of the tank may have produced background noise.

8.0 DATA EVALUATION

The final analysis of the data acquired during this test was conducted in the Lawrenceville, NJ., offices of the PHYSICAL ACOUSTICS CORPORATION.

Data was analyzed according to the CARP procedure, after excluding noise and background activity as far as possible, with the pass/fail criteria given below.

Acceptance Criterion	Significance Criteria	Results
1. Hits during holds None beyond 2 Min.	Measure of Continuing damage.	FAIL-2221
2. Felicity ratio Greater than 0.95.	Measure of the severity of previously induced damage.	FAIL-0
3. Total counts less than N/2 (3868).	Measure of the overall damage during a load cycle.	FAIL-90,856
4. Hits above 75 dB less than 5.	Measure of high energy microstructural damage.	PASS-2

The above data summarizes the situation for the whole tank. Following the recommendations of the CARP procedure, the tank should be examined using other NDT methods, including visual, to determine the reason for the high emission levels. Visual examination of the outside wall areas which produced high levels of emission resulted in the following observations:

1) Manway, positioned between sensors 11, 12 and 1; This area produced high activity but there are no visual indications of delamination or damage. The inside of the manway should be examined carefully at the next opportunity. Note that high stresses on bolts that attach the manway can cause slipping. In the future, bolts should be tightened to the manufacturers recommendations.

Examination of the inside of the tank prior to the test indicated possible high stress areas including;

1) Baffels positioned at 22 foot intervals; One baffle is aligned with sensors 16 and 17. This area produced excessive emission and it is suggested that the baffle may be weak or coming loose from the wall.

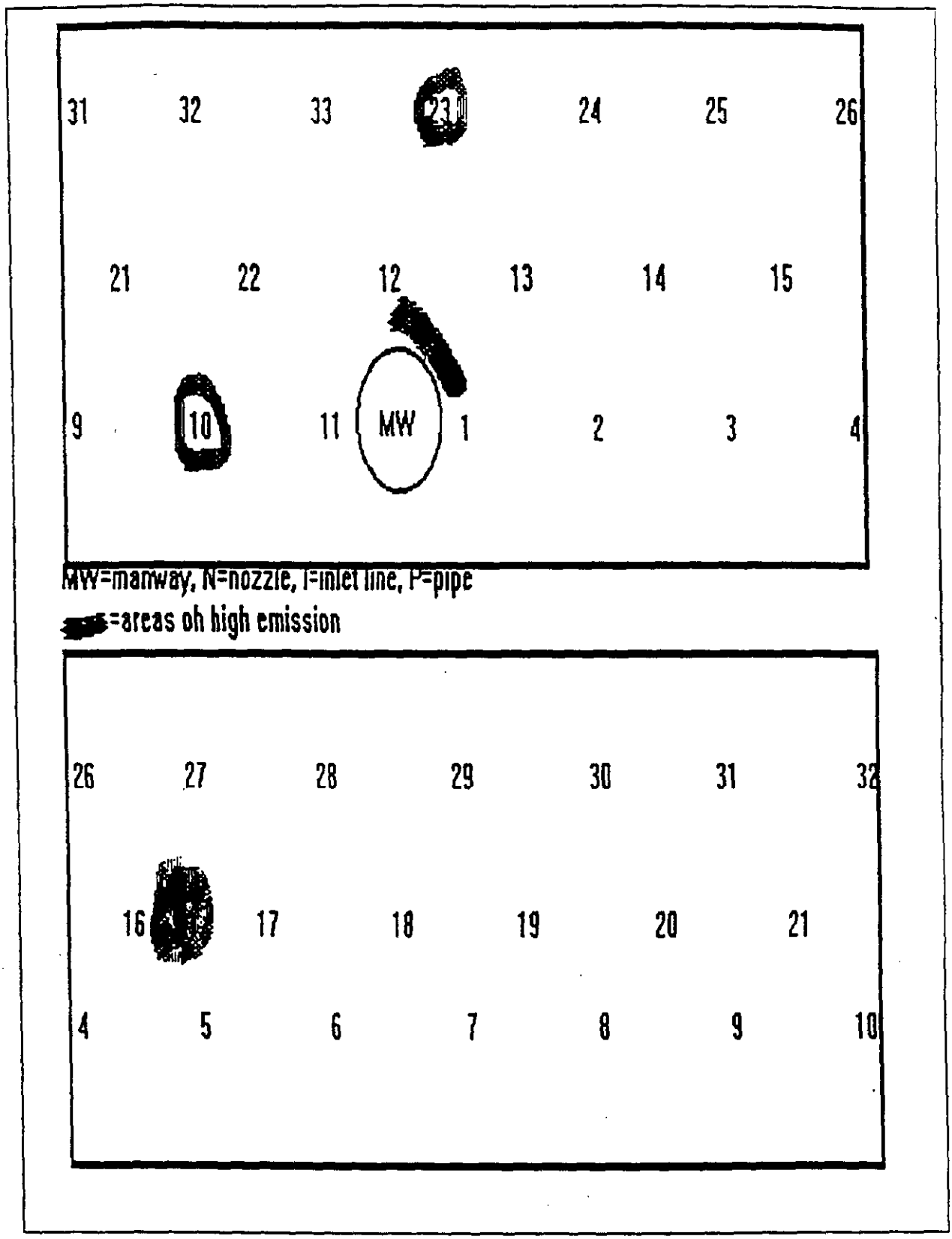

FIGURE 1
Tank Sketch and Sensor Location Map

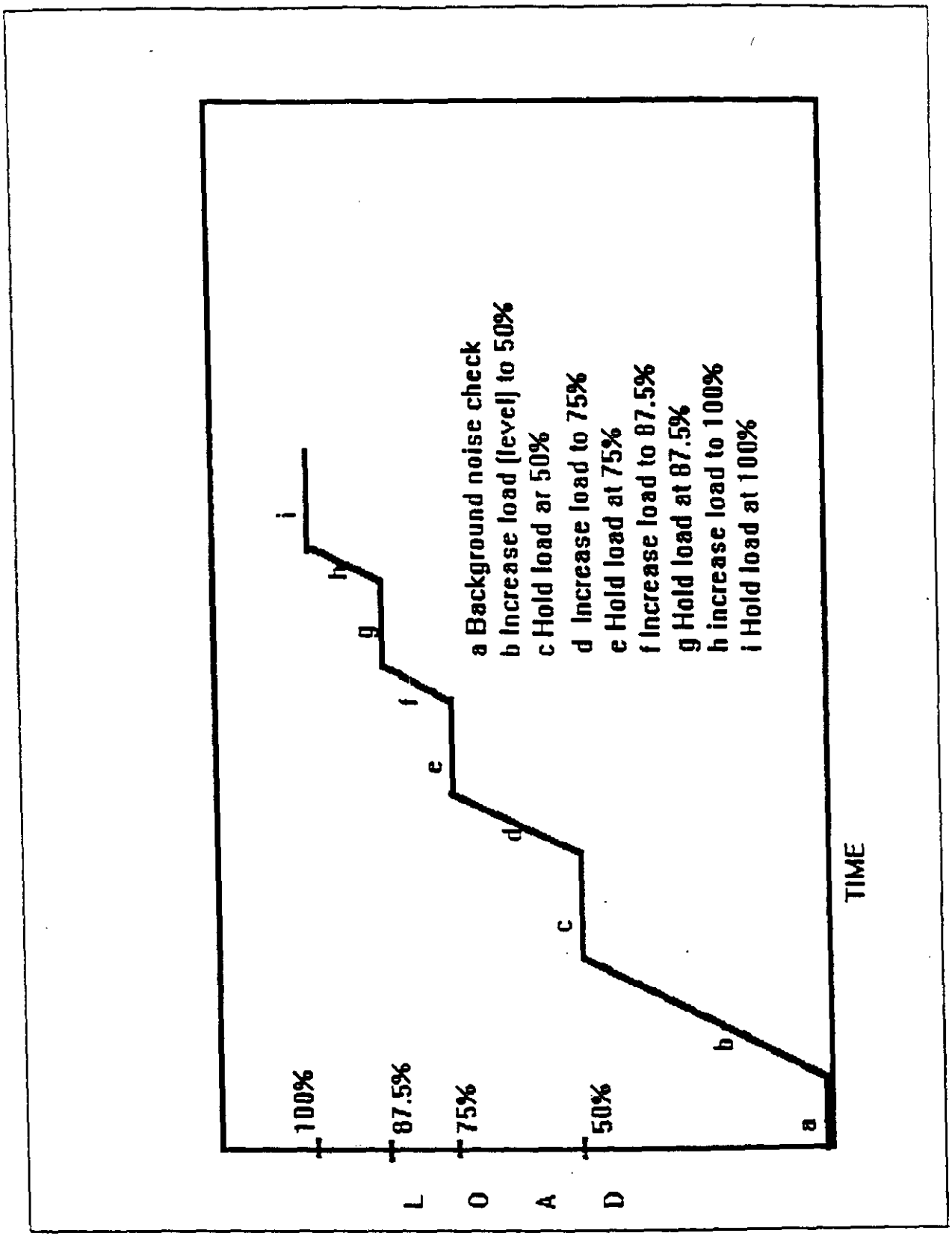

FIGURE 2
Load Ramp

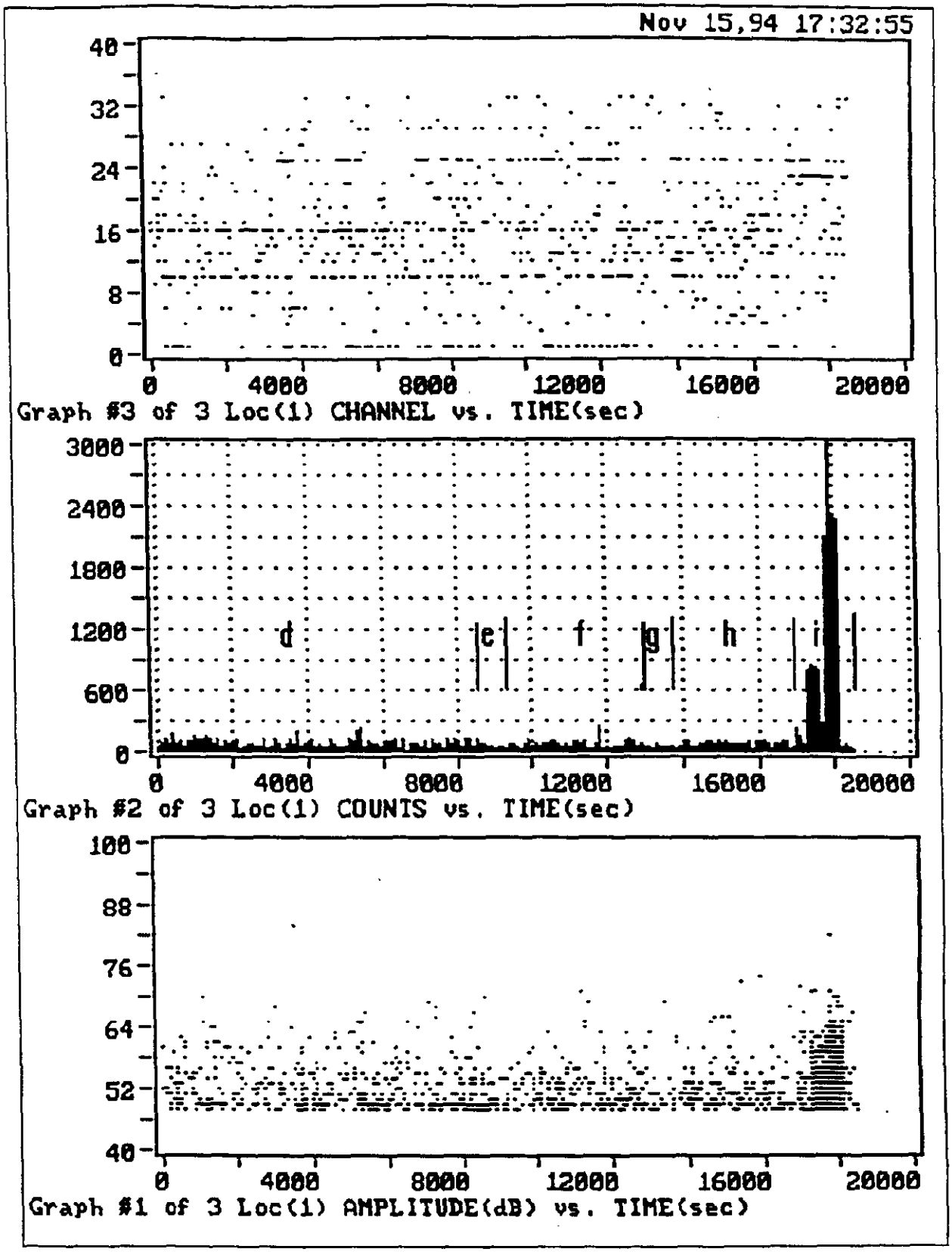

FIGURE 3
Acoustic Emission Data Graphs

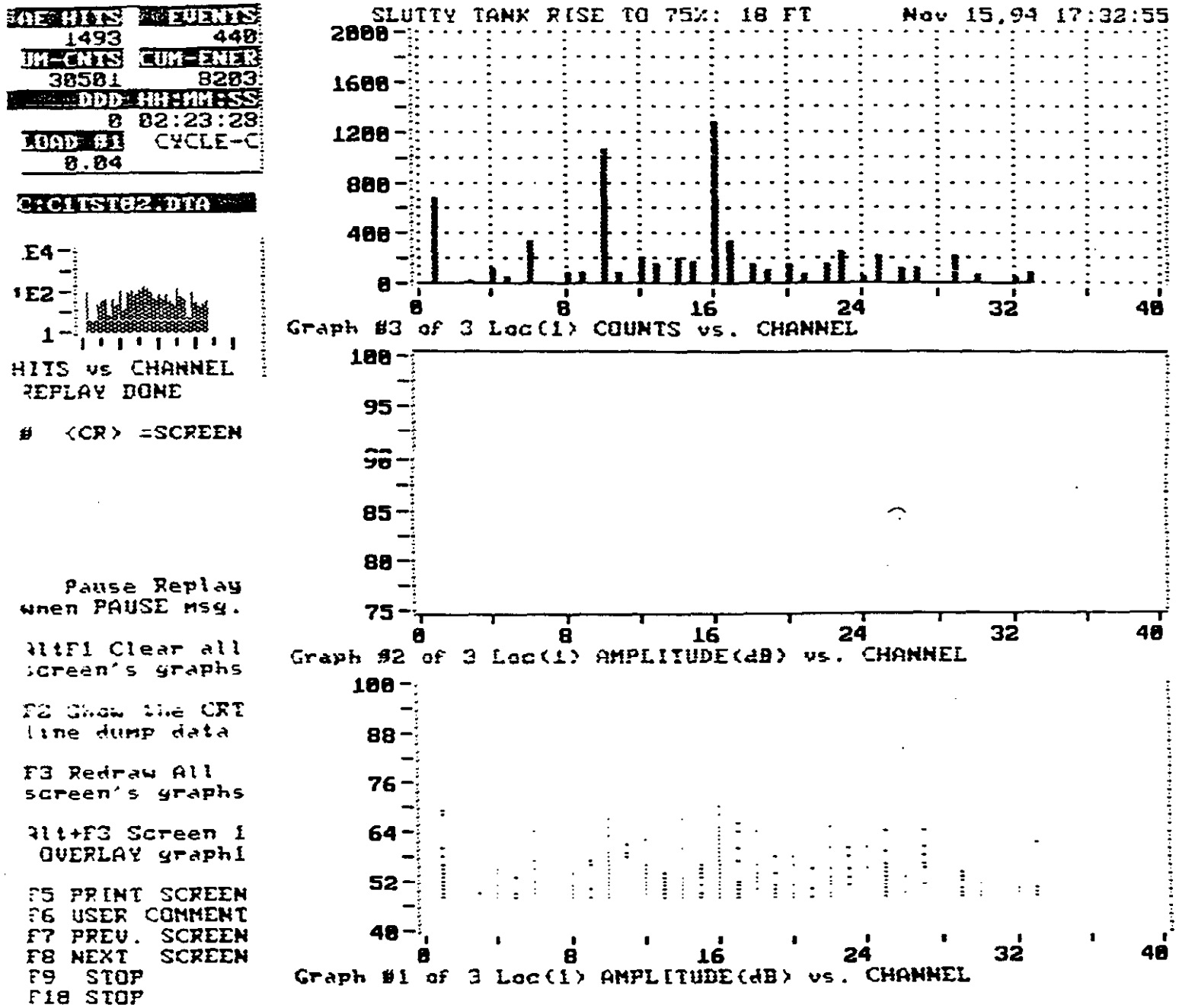
HITS
1493
EVENTS
440
CUM_CNTS
38501
CUM_ENER
8203
DDD:HH:MM:SS
0 02:23:28
LOAD 81
CYCLE-C
0.04
CRCLTST02.DTA
E4
E2
1
HITS vs CHANNEL
REPLAY DONE
<CR> =SCREEN
Pause Replay
when PAUSE msg.
Alt F1 Clear all
screen's graphs
F2 Show the CRT
line dump data
F3 Redraw All
screen's graphs
Alt+F3 Screen 1
OVERLAY graph1
F5 PRINT SCREEN
F6 USER COMMENT
F7 PREV. SCREEN
F8 NEXT SCREEN
F9 STOP
F10 STOP
SLUTTY TANK RISE TO 75%: 18 FT
Nov 15,94 17:32:55
2000
1600
1200
800
400
0
0
8
16
24
32
40
Graph #3 of 3 Loc(1) COUNTS vs. CHANNEL
100
95
90
85
80
75
0
8
16
24
32
40
Graph #2 of 3 Loc(1) AMPLITUDE(dB) vs. CHANNEL
100
88
76
64
52
40
0
8
16
24
32
40
Graph #1 of 3 Loc(1) AMPLITUDE(dB) vs. CHANNEL

RE HITS	EVENTS
105	34
IM CNTS	CUM ENER
1277	381
DDD	HH:MM:SS
0	00:11:33
LOAD #1	CYCLE-C
0.03	

HOLD AT 75% SLURRY TANK Nov 15,94 19:58:25

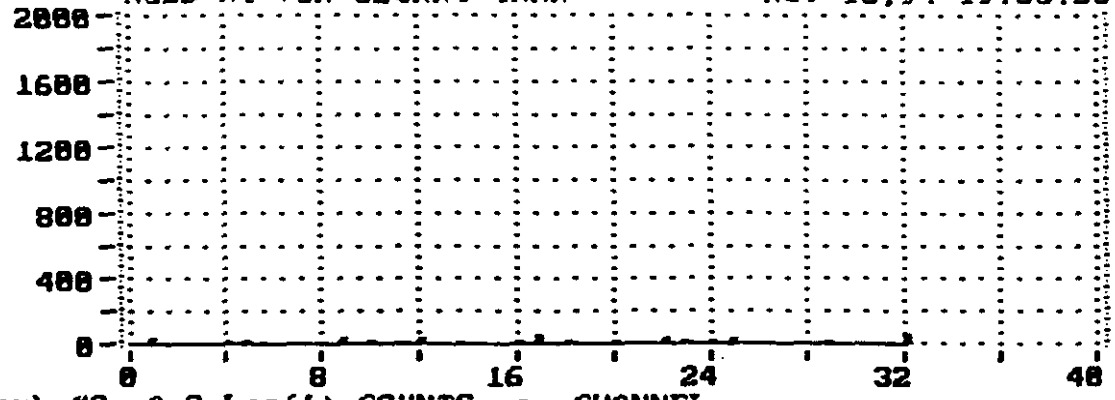

Graph #3 of 3 Loc(1) COUNTS vs. CHANNEL

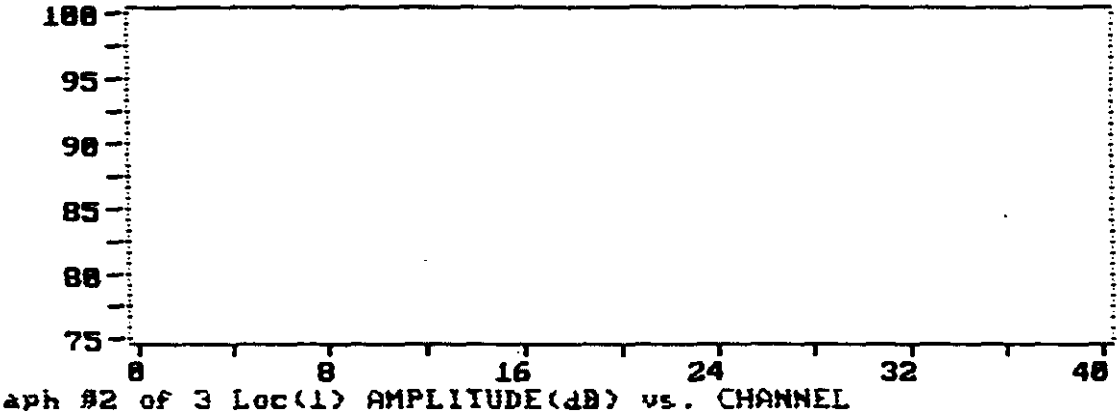

Graph #2 of 3 Loc(1) AMPLITUDE(dB) vs. CHANNEL

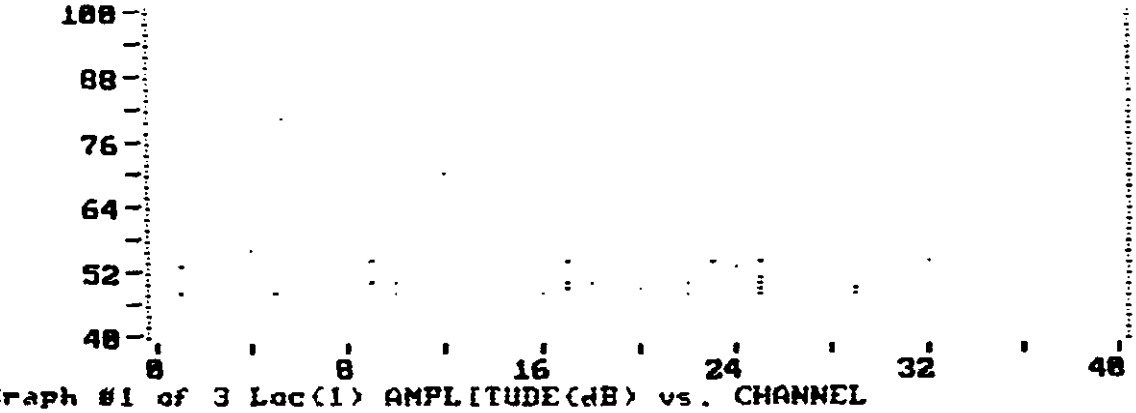

Graph #1 of 3 Loc(1) AMPLITUDE(dB) vs. CHANNEL

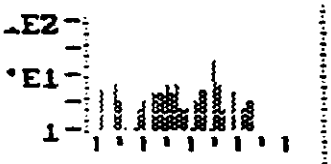

HITS vs CHANNEL
REPLAY DONE

<CR> =SCREEN

Pause Replay
...en PAUSE msg.

...tF1 Clear all
...creen's graphs

F2 Show the CRT
...ne dump data

F3 Redraw All
screen's graphs

...t+F3 Screen 1
OVERLAY graph1

...5 PRINT SCREEN
...6 USER COMMENT
...7 PREV. SCREEN
F8 NEXT SCREEN
...9 STOP
...10 STOP

AE-HITS	AE-EVENTS
638	210
M-CNTS	CUM-ENER
8766	2561
DDD	HH:MM:SS
0	01:04:41
LOAD #1	CYCLE-C
0.04	

ACITST84.DTA

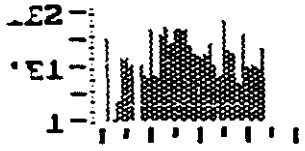

HITS vs CHANNEL
EPLAY DONE

<CR> =SCREEN

ause Replay
n PAUSE msg.

lt+F1 Clear all
creen's graphs

F2 Show the CRT
ne dump data

F3 Redraw All
screen's graphs

lt+F3 Screen 1
OVERLAY graphi

F5 PRINT SCREEN
F6 USER COMMENT
F7 PREV. SCREEN
F8 NEXT SCREEN
F9 STOP
lt8 STOP

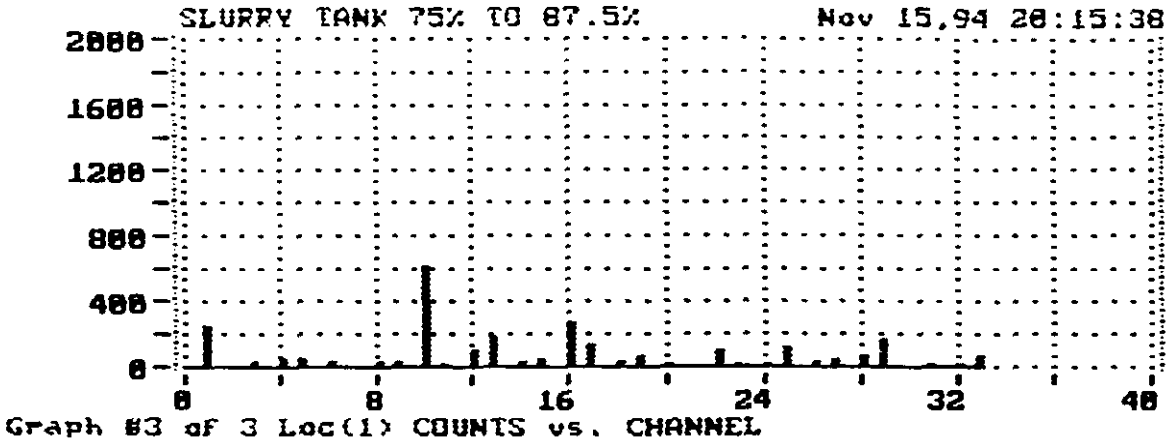

Graph #3 of 3 Loc(1) COUNTS vs. CHANNEL

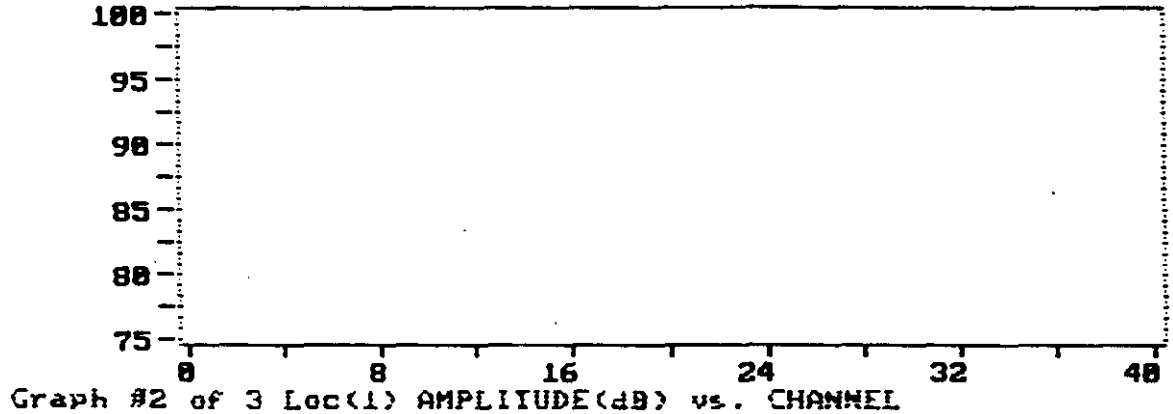

Graph #2 of 3 Loc(1) AMPLITUDE(dB) vs. CHANNEL

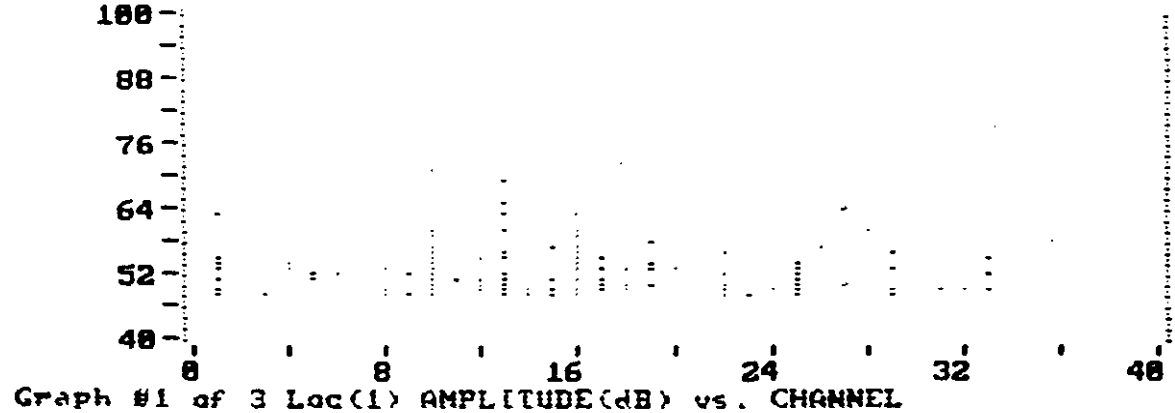

Graph #1 of 3 Loc(1) AMPLITUDE(dB) vs. CHANNEL

AE HITS	EVENTS
46	20
SUM-CNTS	SUM-ENER
678	193
DDD:HH:MM:SS	
0	00:10:04
LOAD-#1	CYCLE-C
0.04	

STATISTICS DTA

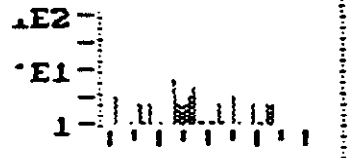

HITS vs CHANNEL
REPLAY DONE

<CR> =SCREEN

Pause Replay
...en PAUSE msg.

AltF1 Clear all
screen's graphs

F2 Show the CRT
line dump data

F3 Redraw All
screen's graphs

Alt+F3 Screen 1
OVERLAY graphi

F5 PRINT SCREEN
F6 USER COMMENT
F7 PREV. SCREEN
F8 NEXT SCREEN
F9 STOP
F10 STOP

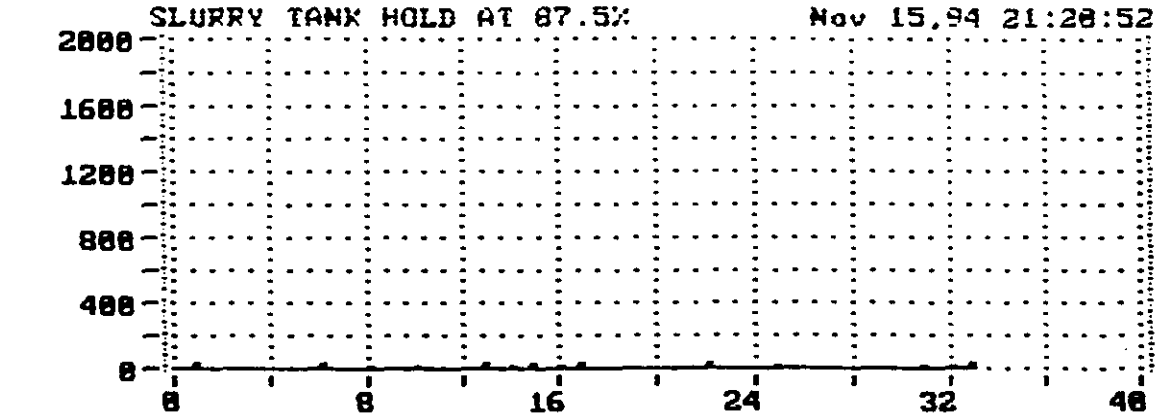

Graph #3 of 3 Loc(1) COUNTS vs. CHANNEL

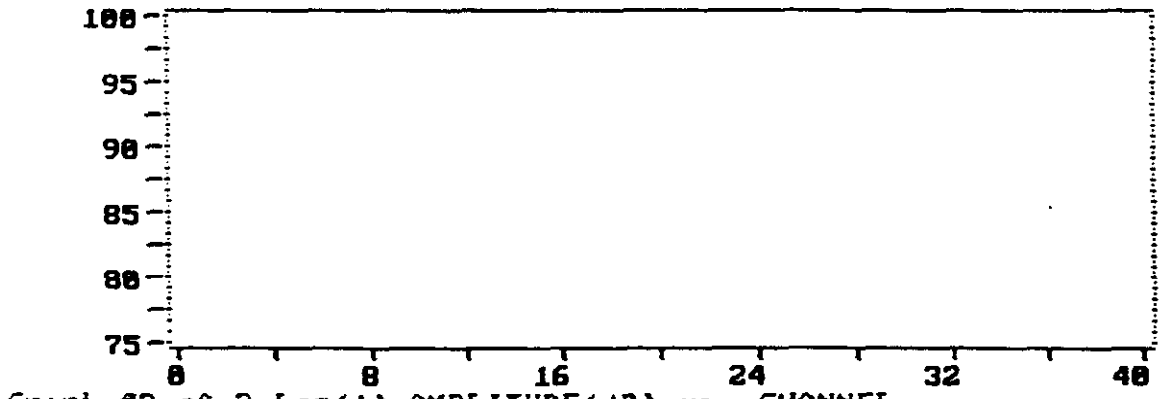

Graph #2 of 3 Loc(1) AMPLITUDE(dB) vs. CHANNEL

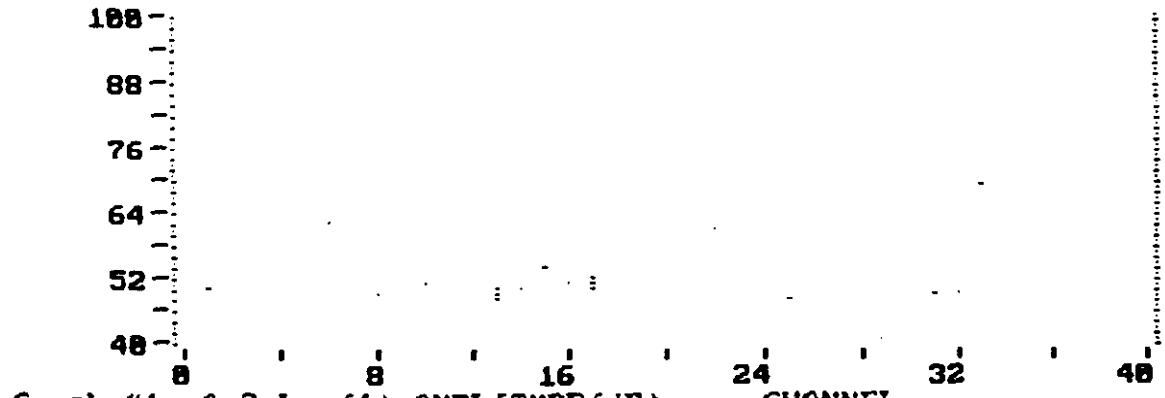

Graph #1 of 3 Loc(1) AMPLITUDE(dB) vs. CHANNEL

HITS	EVENTS
332	177
SUM-CNTS	SUM-ENER
3684	1084
DDD:HH:MM:SS	
0	00:52:41
LOAD-#1	CYCLE-C
0.04	

DAC1TS186.DTA

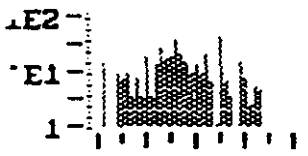

HITS vs CHANNEL
REPLAY DONE

<CR> =SCREEN

Pause Replay
when PAUSE msg.

Alt+F1 Clear all
screen's graphs

F2 Show the CRT
line dump data

F3 Redraw All
screen's graphs

Alt+F3 Screen 1
OVERLAY graphi

F5 PRINT SCREEN
F6 USER COMMENT
F7 PREV. SCREEN
F8 NEXT SCREEN
F9 STOP
F10 STOP

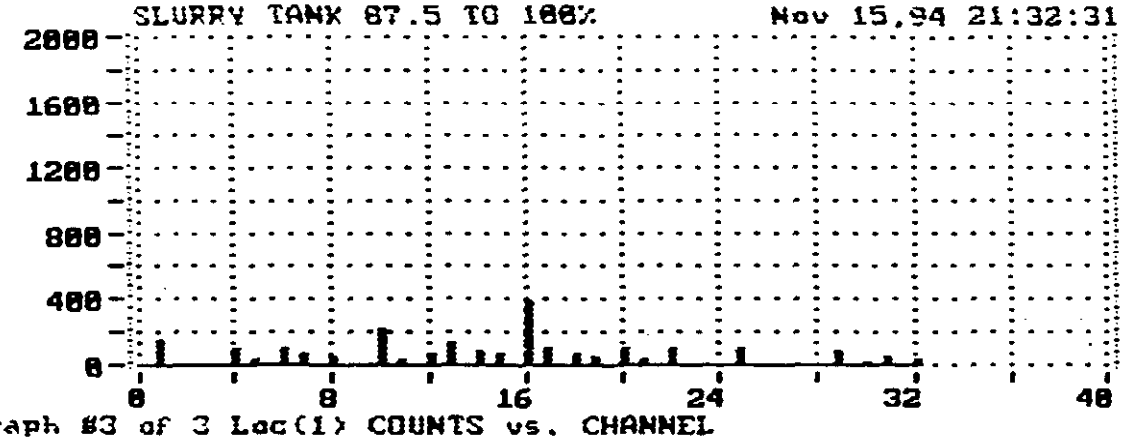

Graph #3 of 3 Loc(1) COUNTS vs. CHANNEL

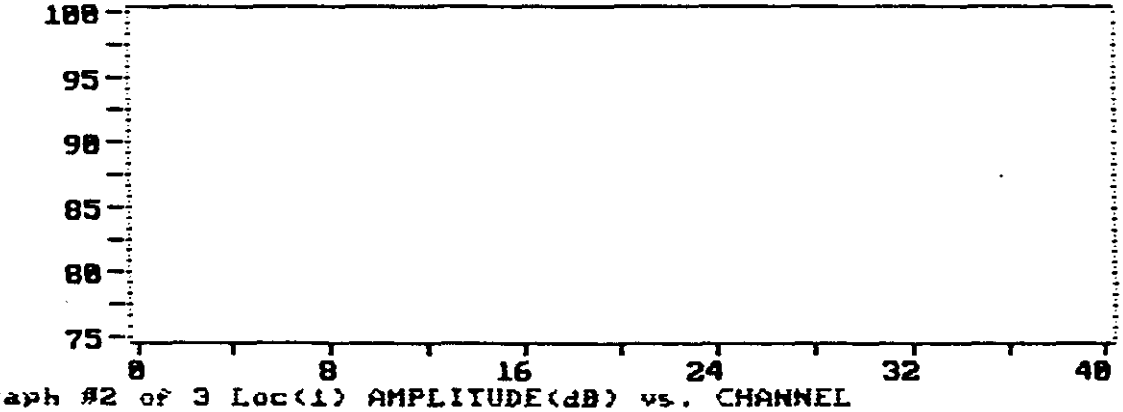

Graph #2 of 3 Loc(1) AMPLITUDE(dB) vs. CHANNEL

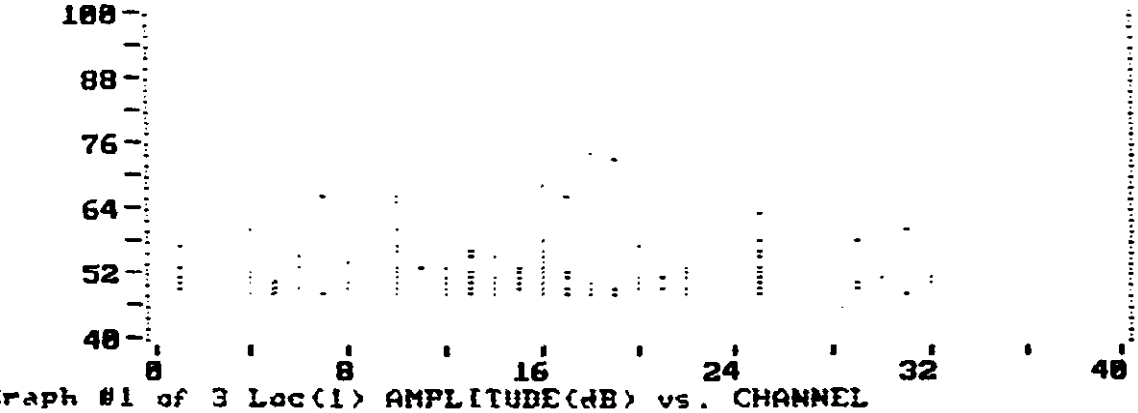

Graph #1 of 3 Loc(1) AMPLITUDE(dB) vs. CHANNEL

AE HITS	EVENTS
6382	2167
SUM-CNTS	SUM-ENER
46181	24115
DDD:HH:MM:SS	
0	00:30:19
LOAD #1	CYCLE-C
0.04	

HISTORY DATA

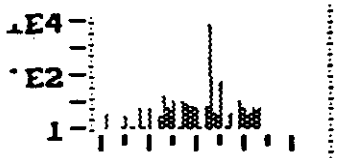

HITS vs CHANNEL
REPLAY DONE

<CR> =SCREEN

Pause Replay
when PAUSE msg.

Alt F1 Clear all
screen's graphs

F2 Show the CRT
time dump data

F3 Redraw All
screen's graphs

Alt+F3 Screen 1
OVERLAY graphi

F5 PRINT SCREEN
F6 USER COMMENT
F7 PREV. SCREEN
F8 NEXT SCREEN
F9 STOP
F10 STOP

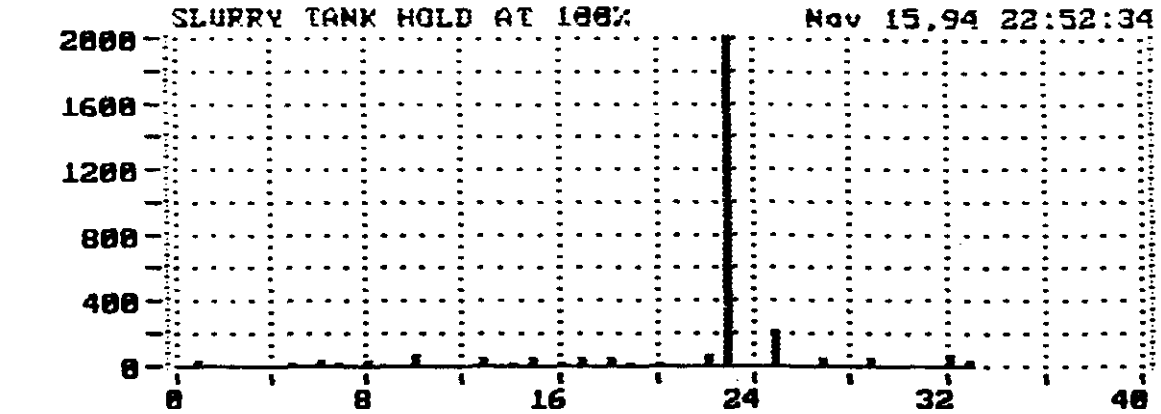

Graph #3 of 3 Loc(1) COUNTS vs. CHANNEL

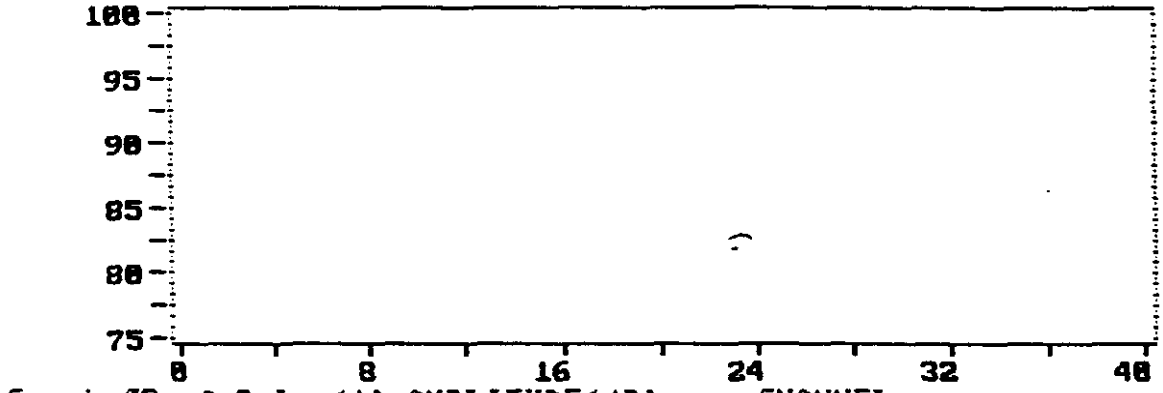

Graph #2 of 3 Loc(1) AMPLITUDE(dB) vs. CHANNEL

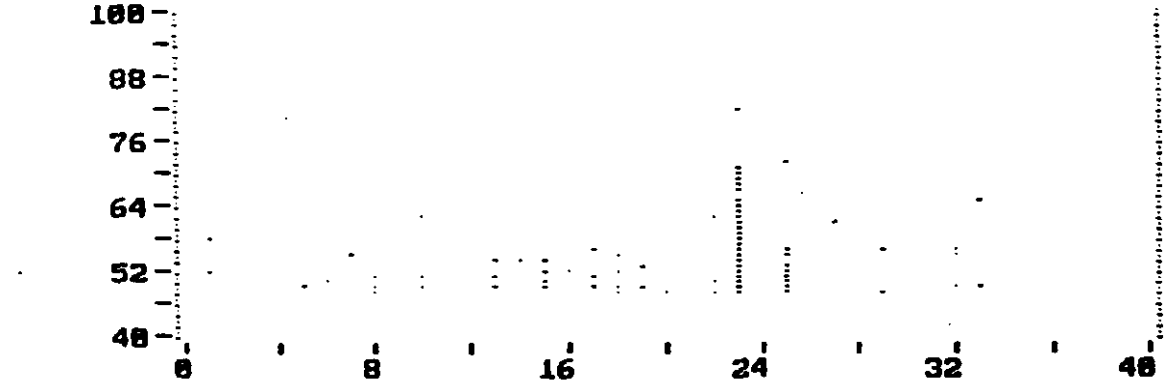

Graph #1 of 3 Loc(1) AMPLITUDE(dB) vs. CHANNEL

[illegible] HITS	[illegible] SUB HITS
5530	2505
M-CNTS	SUM-ENER
46684	45181
[illegible] DDD	HH:MM:SS
0	09:23:16
LOAD [illegible]	CYCLE-C
-0.01	

[illegible] CNTS [illegible] DTA [illegible]

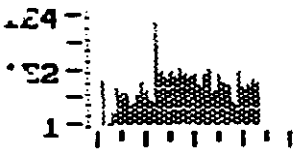

HITS vs CHANNEL
EPLAY DONE

<CR> =SCREEN

ause Replay
w..en PAUSE msg.

lt+F1 Clear all
creen's graphs

F2 Show the CRT
ine dump data

F3 Redraw All
screen's graphs

lt+F3 Screen 1
OVERLAY graphi

5 PRINT SCREEN
6 USER COMMENT
7 PREV. SCREEN
F8 NEXT SCREEN
9 STOP
10 STOP

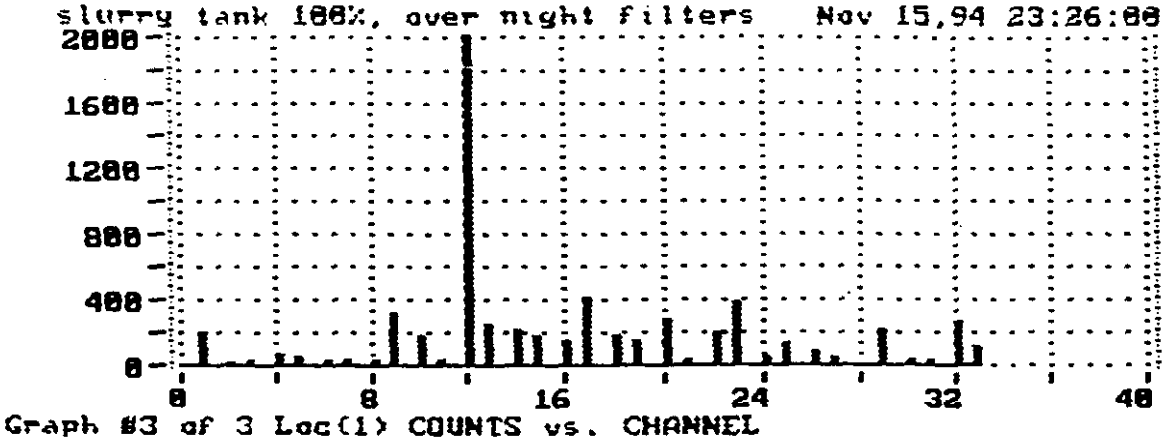

Graph #3 of 3 Loc(1) COUNTS vs. CHANNEL

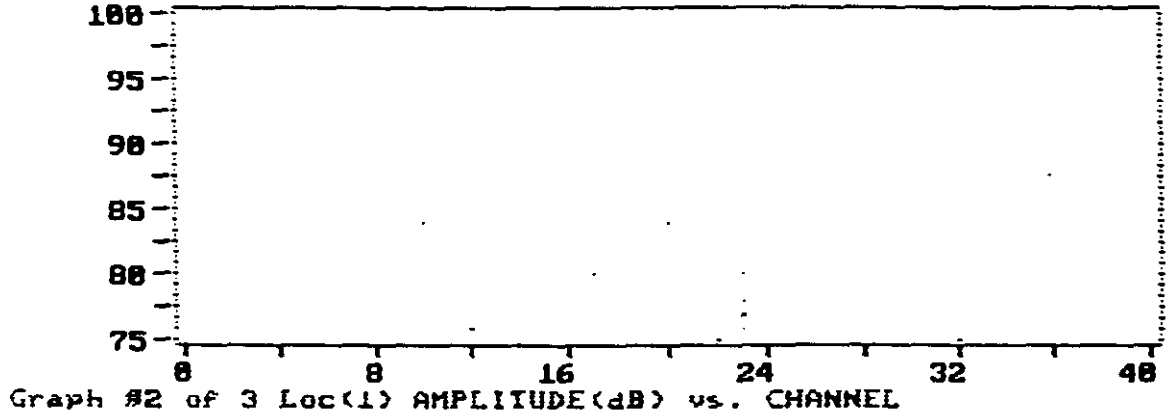

Graph #2 of 3 Loc(1) AMPLITUDE(dB) vs. CHANNEL

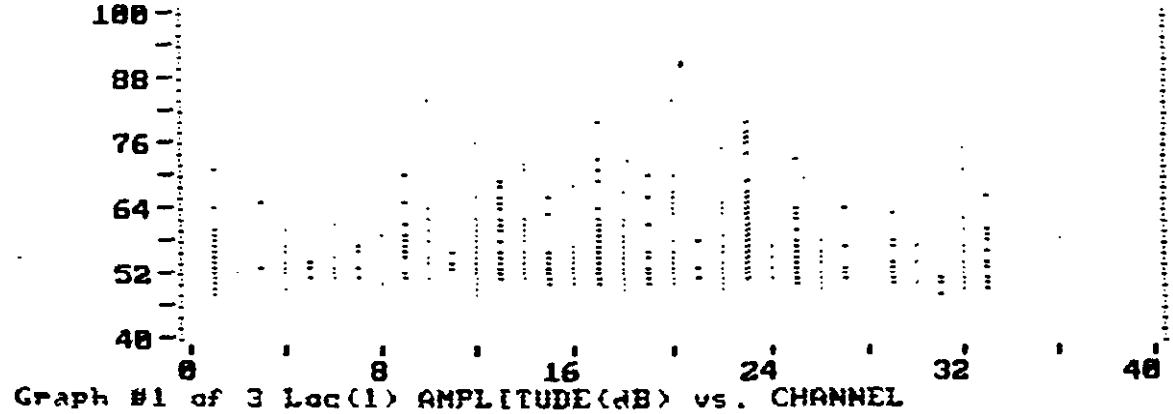

Graph #1 of 3 Loc(1) AMPLITUDE(dB) vs. CHANNEL

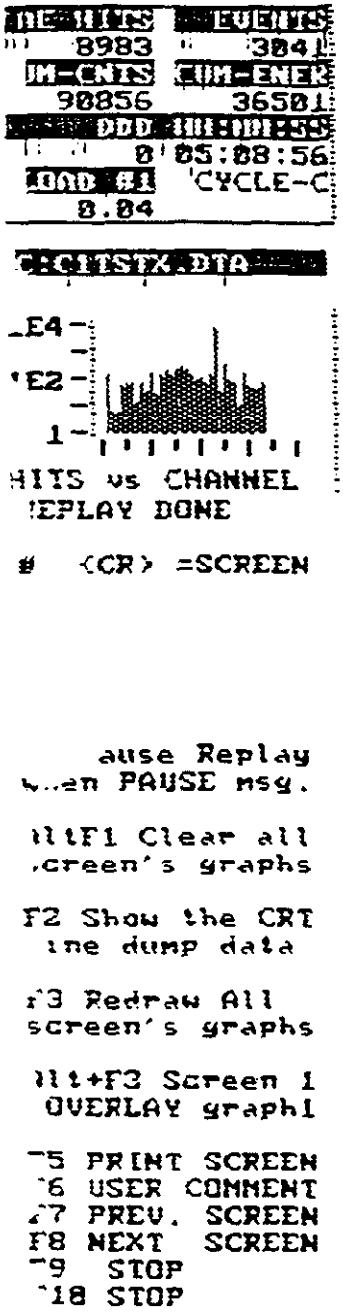

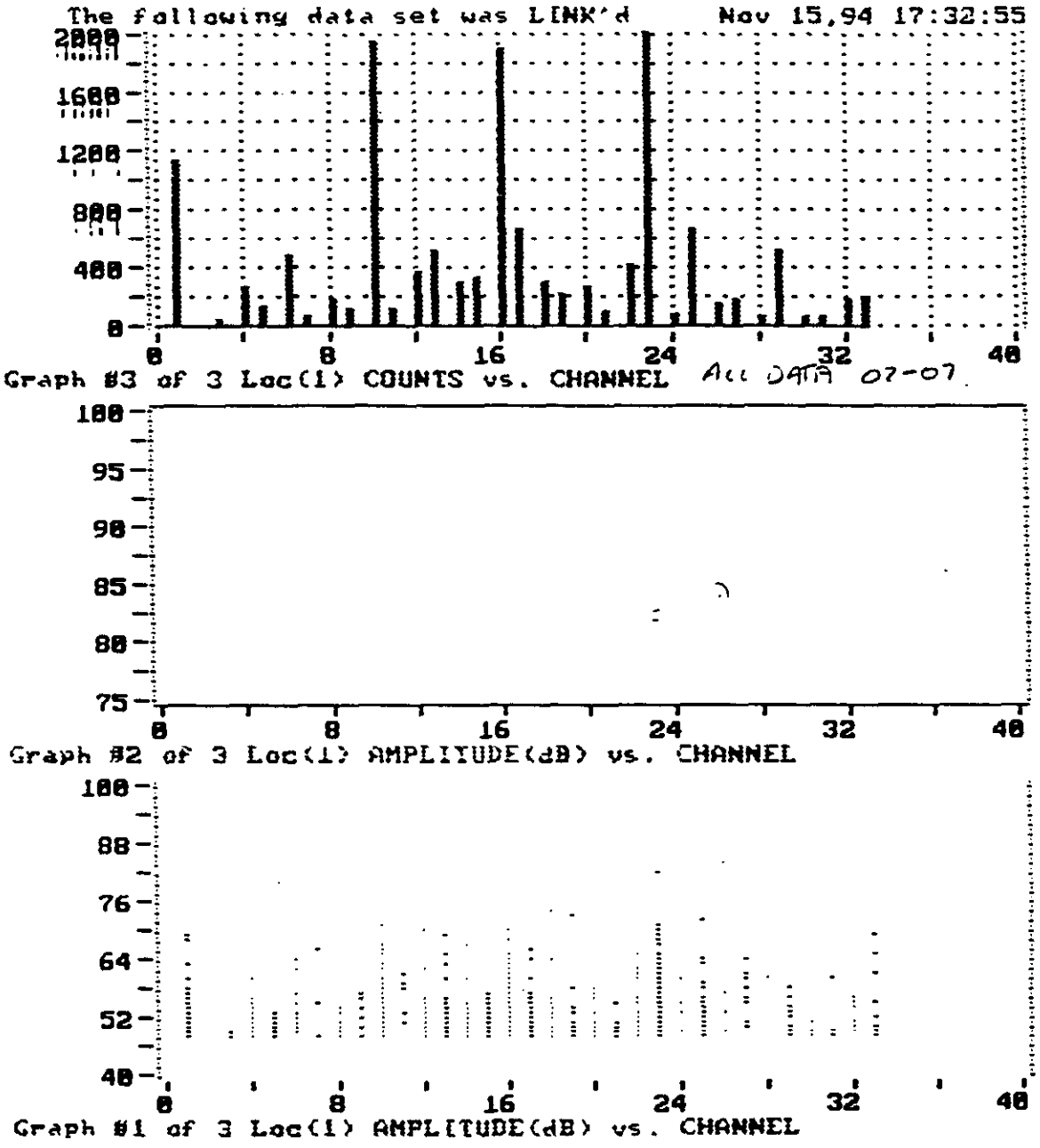

All DATA 07-07

RE-HITS	RE-EVENTS
8983	3041
M-CNTS	SIM-ENER
80856	36501

0 05:08:56

LOAD #1 CYCLE-C

REGISTER DATA

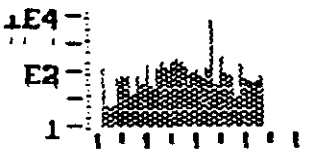

HITS vs CHANNEL
REPLAY DONE

<CR> =SCREEN

Pause Replay
when PAUSE msg.

Alt+F1 Clear all
screen's graphs

F2 Show the CRT
line dump data

F3 Redraw All
screen's graphs

Alt+F3 Screen 1
OVERLAY graph1

F5 PRINT SCREEN
F6 USER COMMENT
F7 PREV. SCREEN
F8 NEXT SCREEN
F9 STOP
F10 STOP

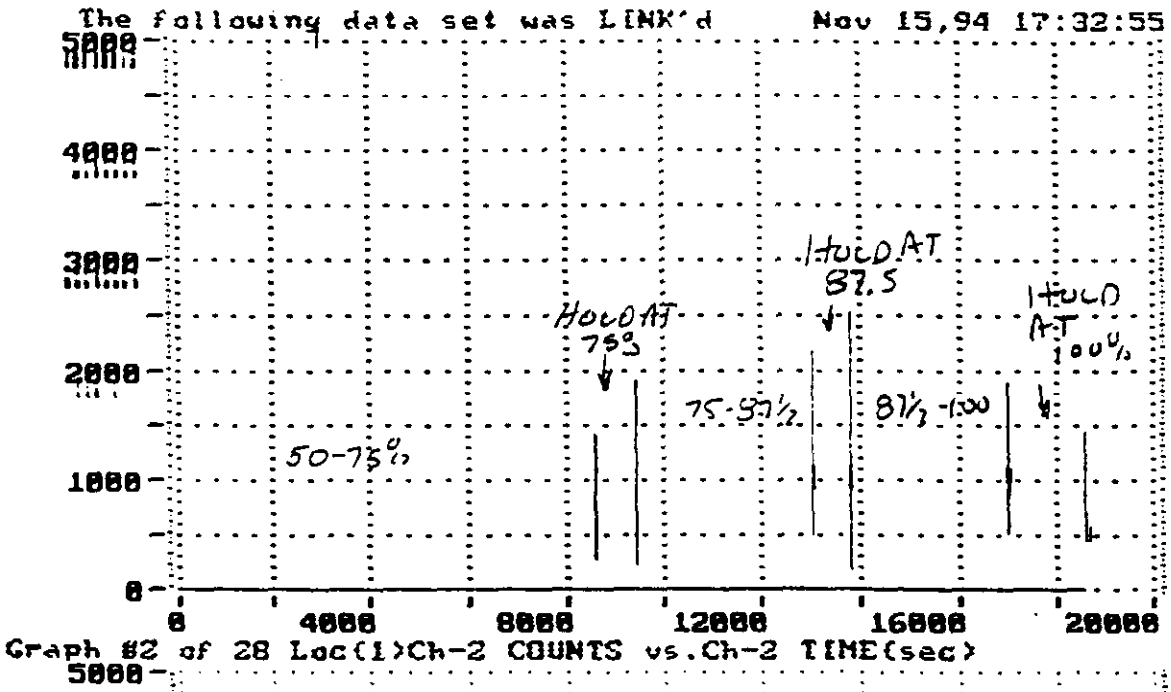

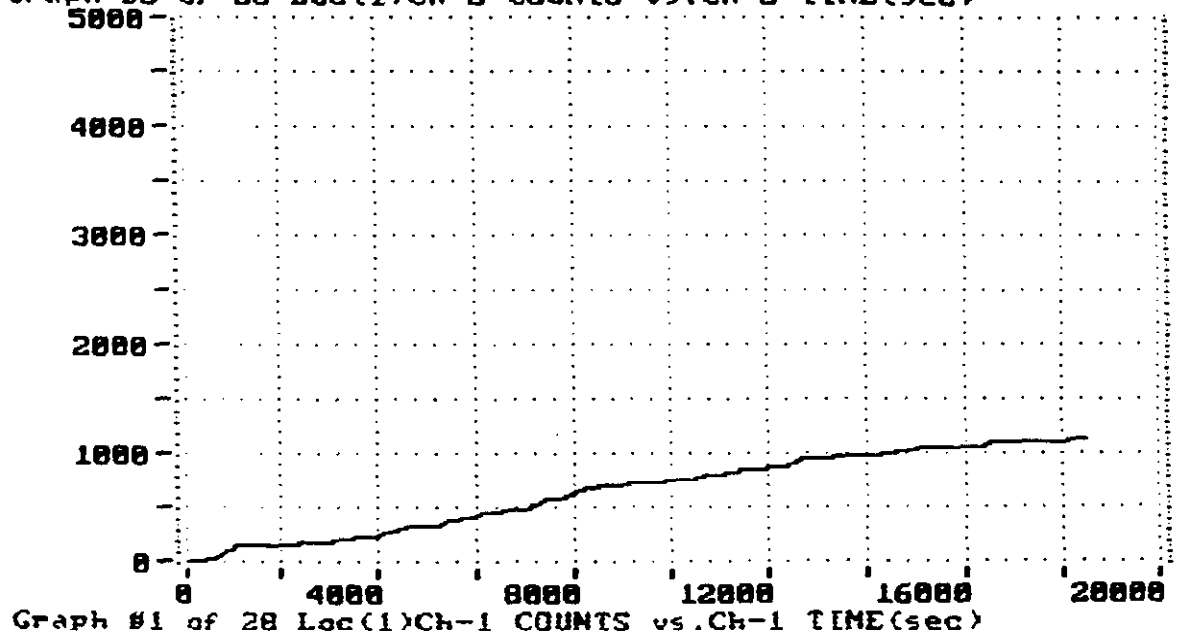

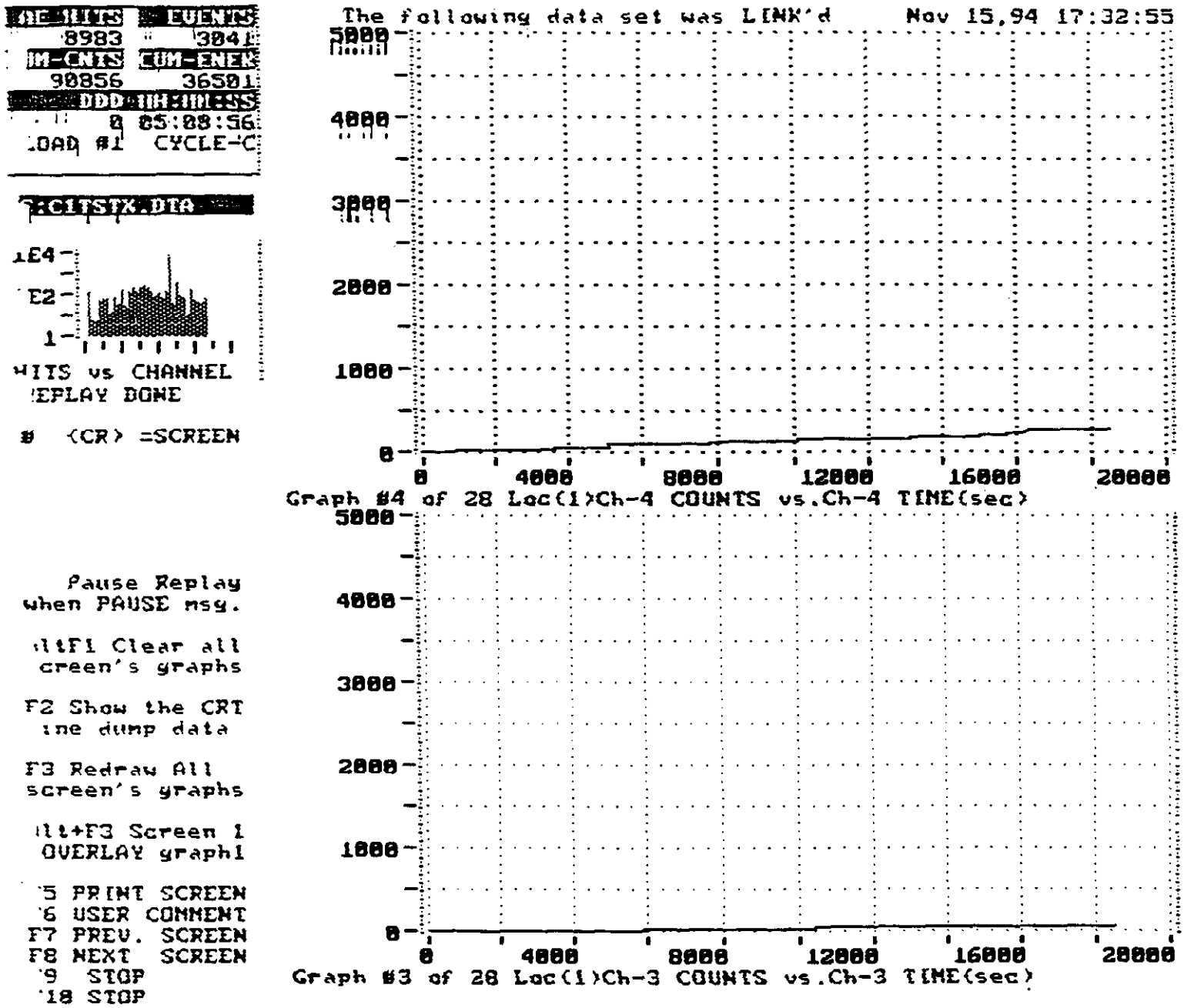
HITS
8983
EVENTS
3041
SUM-CNTS
90856
SUM-ENER
36501
DDD:HH:MM:SS
0 05:08:56
LOAD #1 CYCLE-C
HCITSTX.DTA
1E4
E2
1
HITS vs CHANNEL
REPLAY DONE
<CR> =SCREEN
The following data set was LINK'd
Nov 15,94 17:32:55
5000
4000
3000
2000
1000
0
0
4000
8000
12000
16000
20000
Graph #4 of 28 Loc(1)Ch-4 COUNTS vs.Ch-4 TIME(sec)
Pause Replay
when PAUSE msg.
Alt F1 Clear all
screen's graphs
F2 Show the CRT
time dump data
F3 Redraw All
screen's graphs
Alt+F3 Screen 1
OVERLAY graph1
F5 PRINT SCREEN
F6 USER COMMENT
F7 PREV. SCREEN
F8 NEXT SCREEN
F9 STOP
F10 STOP
5000
4000
3000
2000
1000
0
0
4000
8000
12000
16000
20000
Graph #3 of 28 Loc(1)Ch-3 COUNTS vs.Ch-3 TIME(sec)

3983	304
90856	36501

0 05:08:56

LOAD #1 CYCLE-C

HISTOGRAM DATA

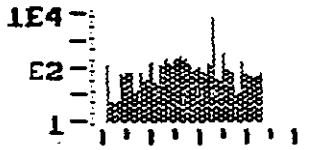

"IIS vs CHANNEL
EPLAY DONE

<CR> =SCREEN

. . Pause Replay
when PAUSE msg.

:ltF1 Clear all
screen's graphs

F2 Show the CRT
ine dump data

F3 Redraw All
screen's graphs

:lt+F3 Screen 1
OVERLAY graphi

5 PRINT SCREEN
6 USER COMMENT
F7 PREV. SCREEN
F8 NEXT SCREEN
9 STOP
10 STOP

The following data set was LINK'd Nov 15,94 17:32:55

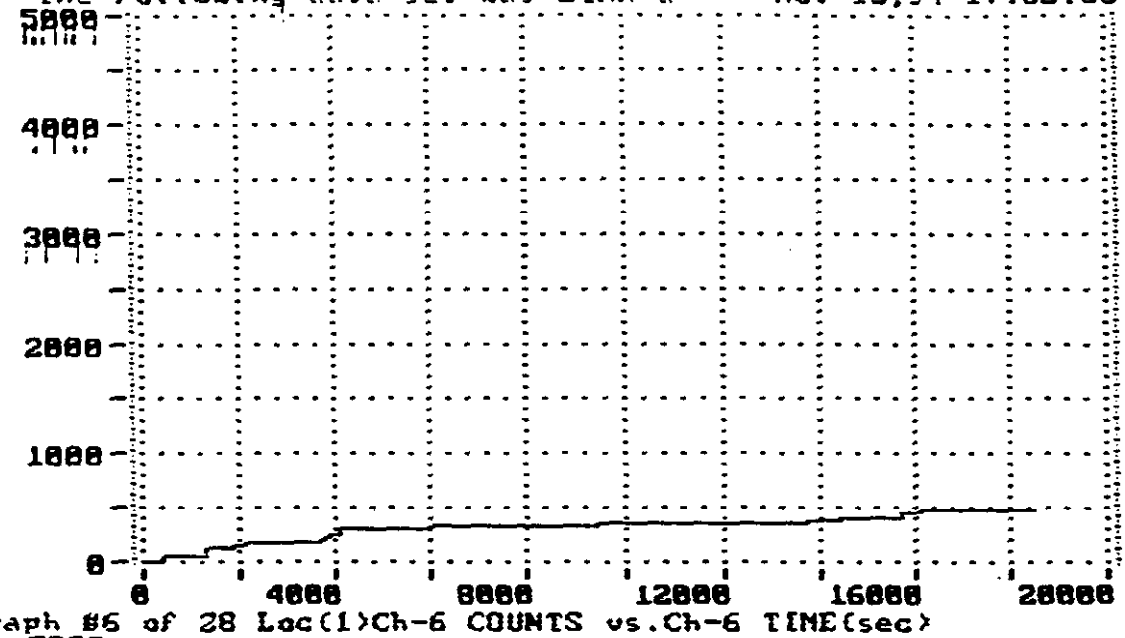

Graph #6 of 28 Loc(1)Ch-6 COUNTS vs.Ch-6 TIME(sec)

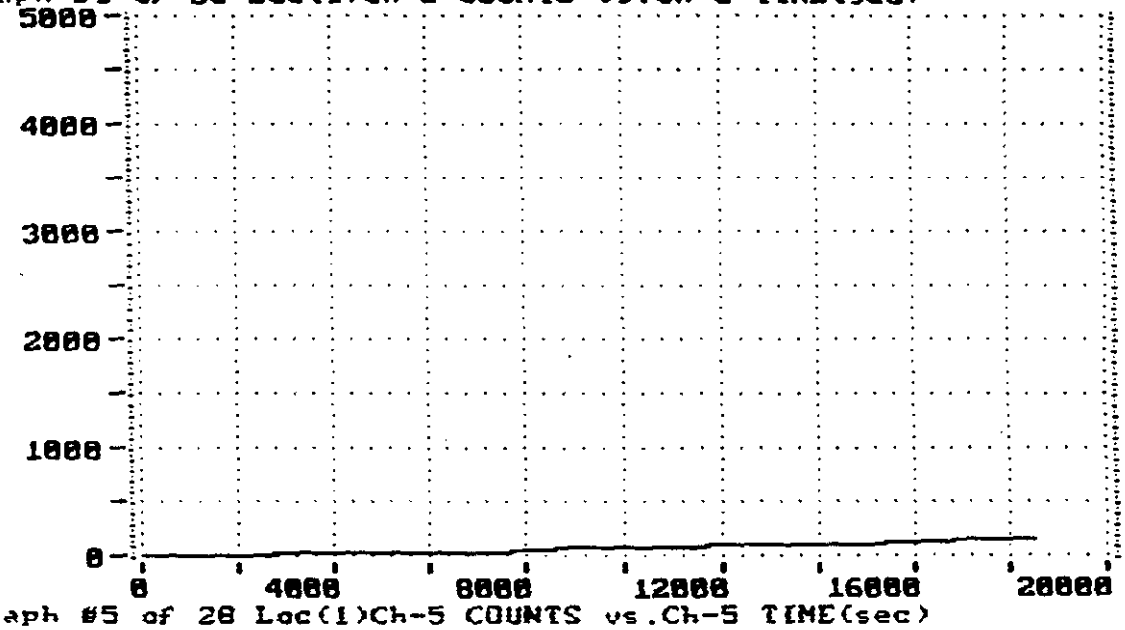

Graph #5 of 28 Loc(1)Ch-5 COUNTS vs.Ch-5 TIME(sec)

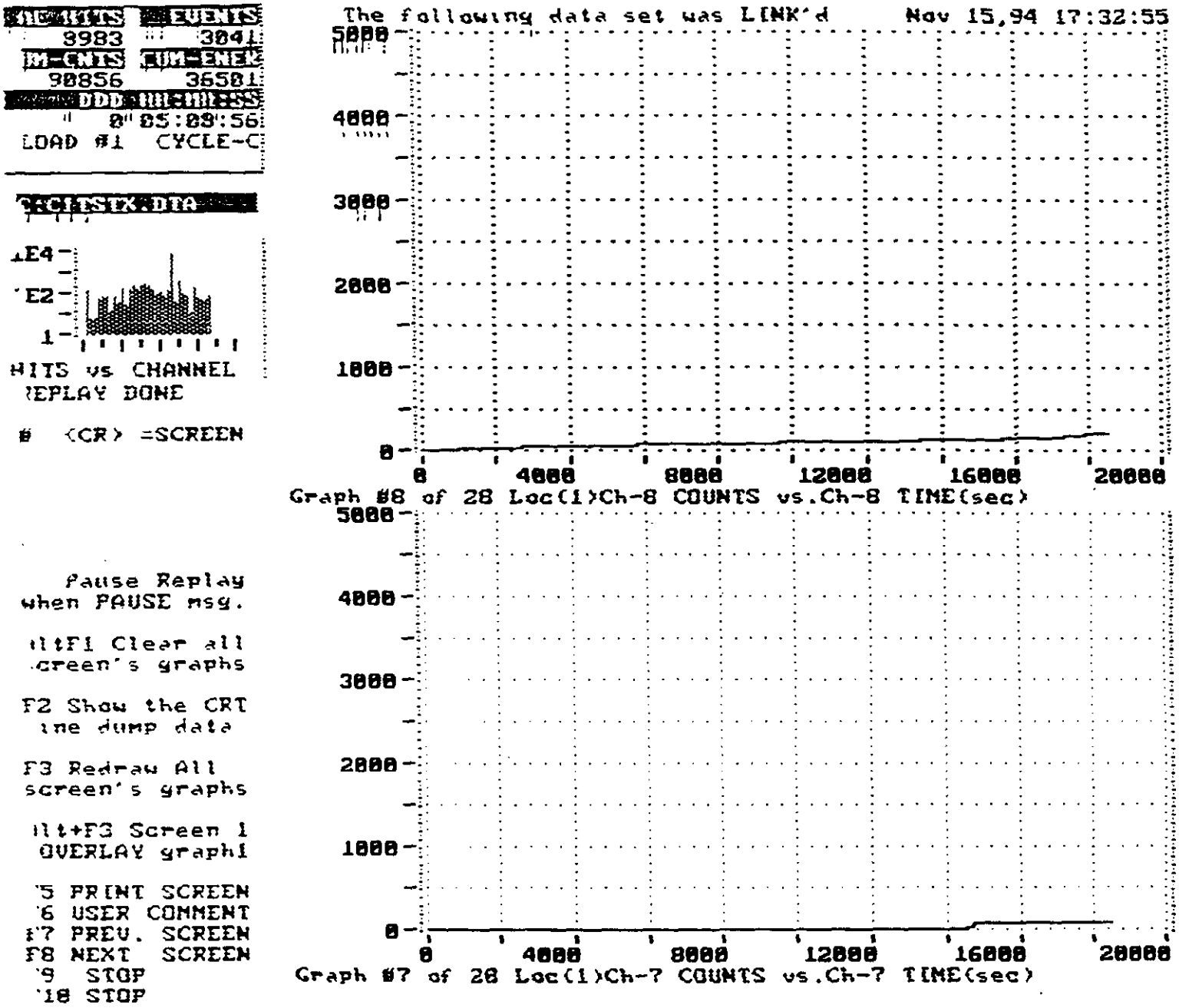
3983
3041
90856
365
0 05:09:56
LOAD #1 CYCLE-C
1E4
1E2
1
HITS vs CHANNEL
REPLAY DONE
<CR> =SCREEN
Pause Replay
when PAUSE msg.
Alt F1 Clear all
screen's graphs
F2 Show the CRT
line dump data
F3 Redraw All
screen's graphs
Alt+F3 Screen 1
OVERLAY graphi
F5 PRINT SCREEN
F6 USER COMMENT
F7 PREV. SCREEN
F8 NEXT SCREEN
F9 STOP
F10 STOP
The following data set was LINK'd
Nov 15,94 17:32:55
5000
4000
3000
2000
1000
0
0
4000
8000
12000
16000
20000
Graph #8 of 28 Loc(1)Ch-8 COUNTS vs.Ch-8 TIME(sec)
5000
4000
3000
2000
1000
0
0
4000
8000
12000
16000
20000
Graph #7 of 28 Loc(1)Ch-7 COUNTS vs.Ch-7 TIME(sec)

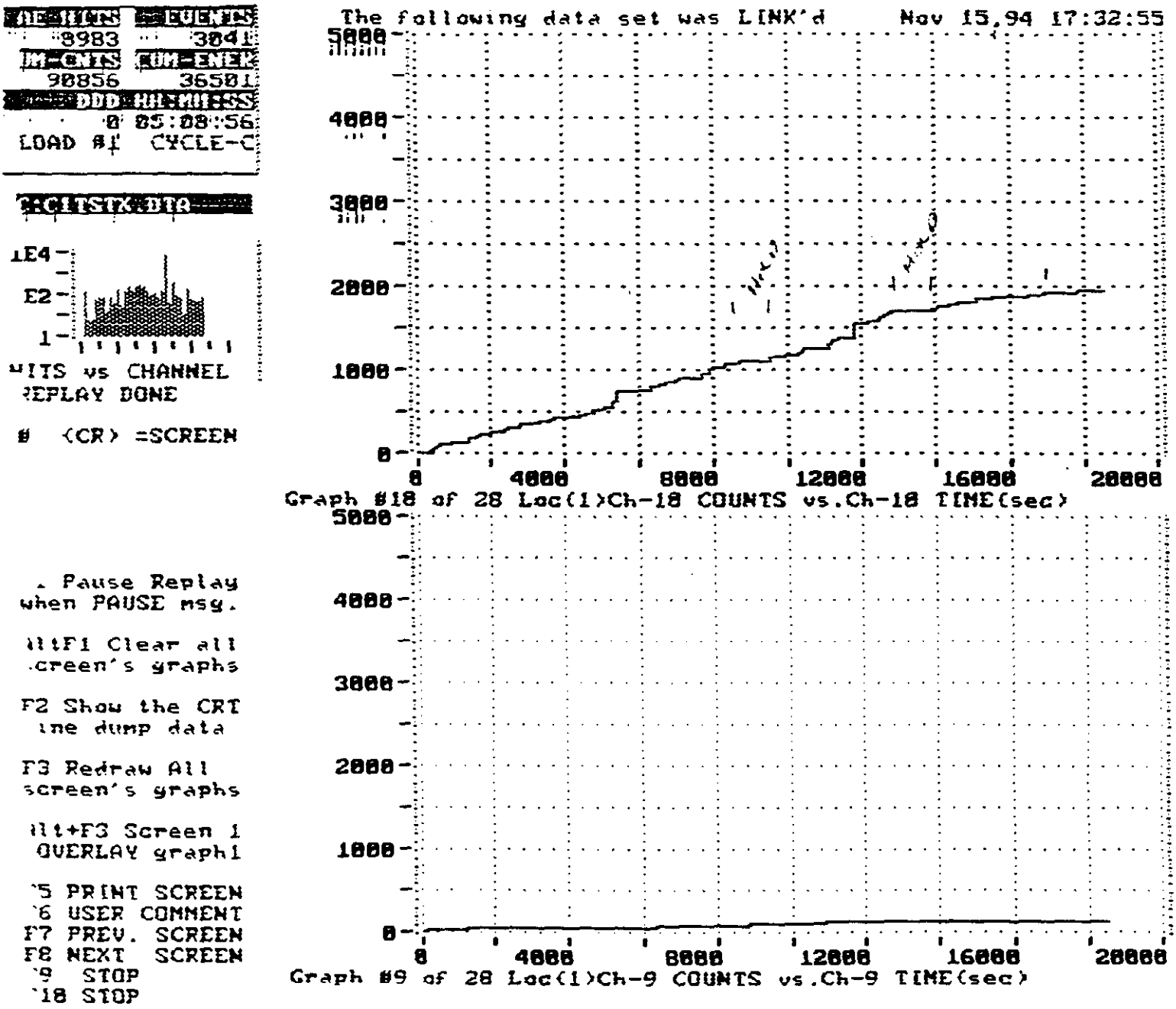
EVENTS
8983
3041
SUM-ENER
90856
36501
HH:MM:SS
0 05:08:56
LOAD #1 CYCLE-C
HISTOGRAM DATA
1E4
E2
1
ITS vs CHANNEL
REPLAY DONE
<CR> =SCREEN
Pause Replay
when PAUSE msg.
Alt-F1 Clear all
screen's graphs
F2 Show the CRT
the dump data
F3 Redraw All
screen's graphs
Alt+F3 Screen 1
OVERLAY graph1
F5 PRINT SCREEN
F6 USER COMMENT
F7 PREV. SCREEN
F8 NEXT SCREEN
F9 STOP
F10 STOP
The following data set was LINK'd
Nov 15,94 17:32:55
5000
4000
3000
2000
1000
0
0
4000
8000
12000
16000
20000
Graph #18 of 28 Loc(1)Ch-18 COUNTS vs.Ch-18 TIME(sec)
5000
4000
3000
2000
1000
0
0
4000
8000
12000
16000
20000
Graph #9 of 28 Loc(1)Ch-9 COUNTS vs.Ch-9 TIME(sec)

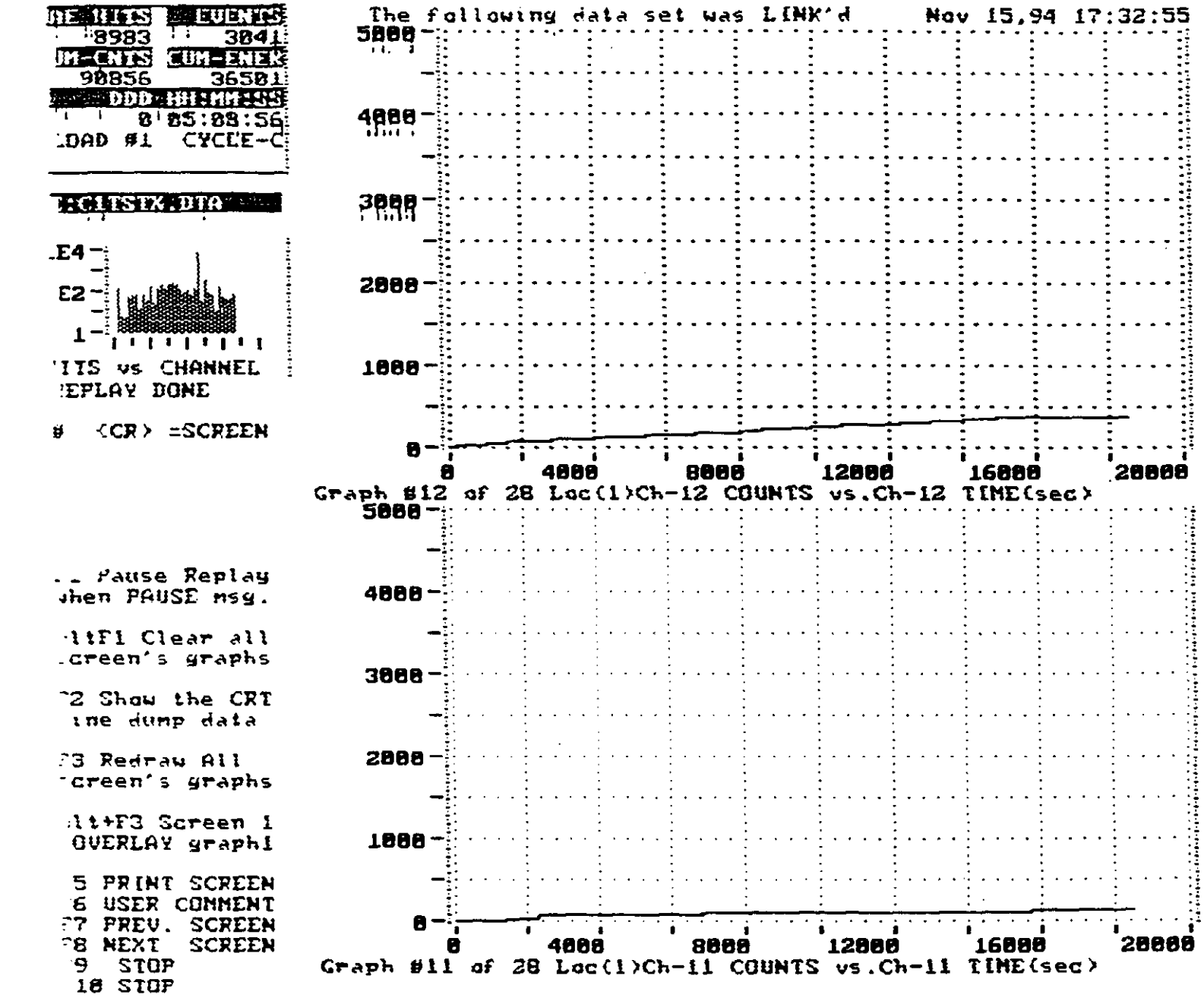
EVENTS
8983
3041
UM-CNTS
90856
36501
DDD:HH:MM:SS
0 05:08:56
LOAD #1 CYCLE-C
HISTOGRAM DATA
E4
E2
1
ITS vs CHANNEL
EPLAY DONE
<CR> =SCREEN
Pause Replay
hen PAUSE msg.
tF1 Clear all
creen's graphs
2 Show the CRT
ne dump data
3 Redraw All
creen's graphs
lt+F3 Screen 1
OVERLAY graphi
5 PRINT SCREEN
6 USER COMMENT
7 PREV. SCREEN
8 NEXT SCREEN
9 STOP
10 STOP
The following data set was LINK'd
Nov 15,94 17:32:55
5000
4000
3000
2000
1000
0
0
4000
8000
12000
16000
20000
Graph #12 of 28 Loc(1)Ch-12 COUNTS vs.Ch-12 TIME(sec)
5000
4000
3000
2000
1000
0
0
4000
8000
12000
16000
20000
Graph #11 of 28 Loc(1)Ch-11 COUNTS vs.Ch-11 TIME(sec)

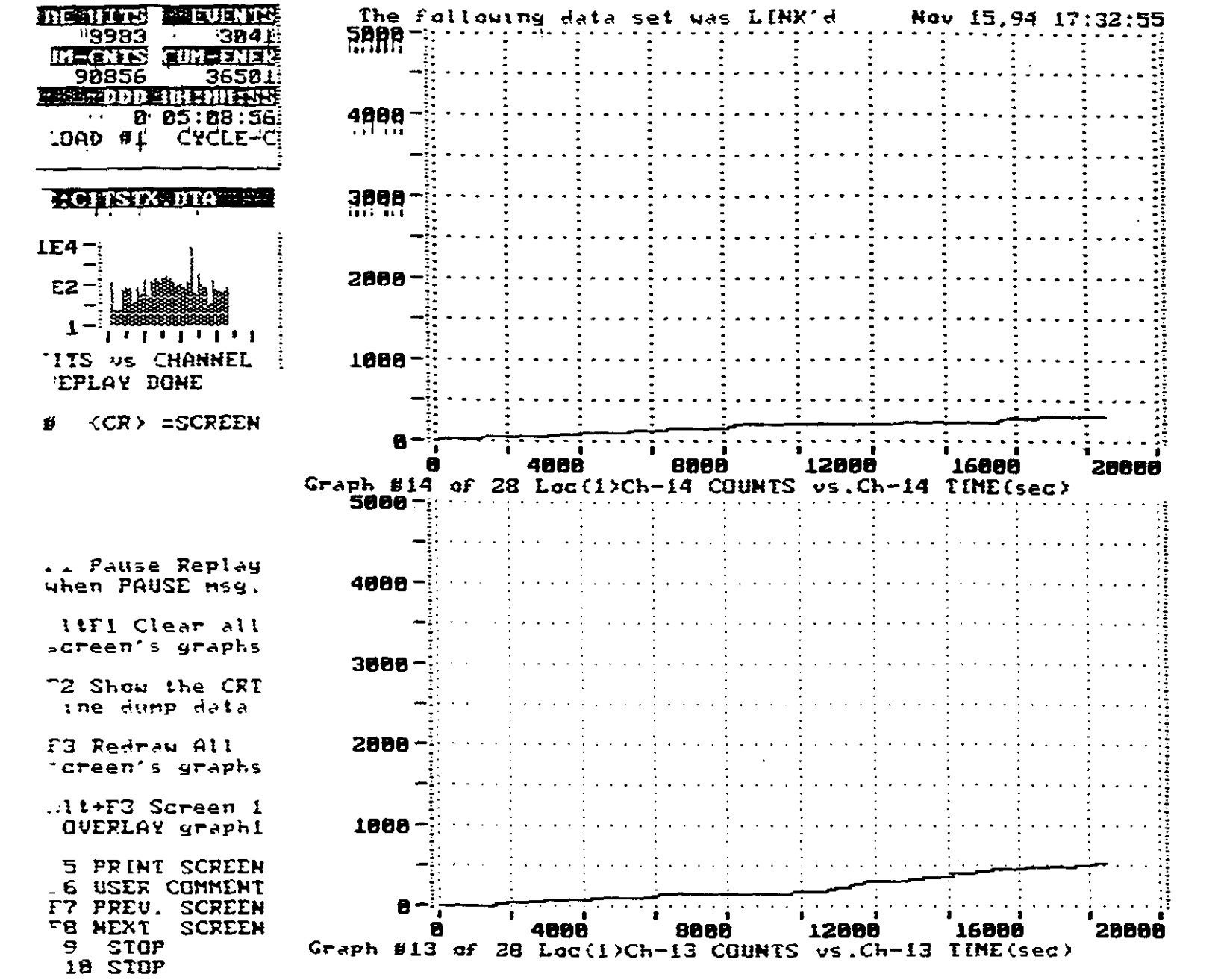
The following data set was LINK'd
Nov 15,94 17:32:55
5000
4000
3000
2000
1000
0
0
4000
8000
12000
16000
20000
Graph #14 of 28 Loc(1)Ch-14 COUNTS vs.Ch-14 TIME(sec)
Graph #13 of 28 Loc(1)Ch-13 COUNTS vs.Ch-13 TIME(sec)
1E4
E2
1
ITS vs CHANNEL
EPLAY DONE
<CR> =SCREEN
Pause Replay
when PAUSE msg.
Alt-F1 Clear all
screen's graphs
F2 Show the CRT
ine dump data
F3 Redraw All
creen's graphs
Alt+F3 Screen 1
OVERLAY graph1
5 PRINT SCREEN
6 USER COMMENT
F7 PREV. SCREEN
F8 NEXT SCREEN
9 STOP
10 STOP

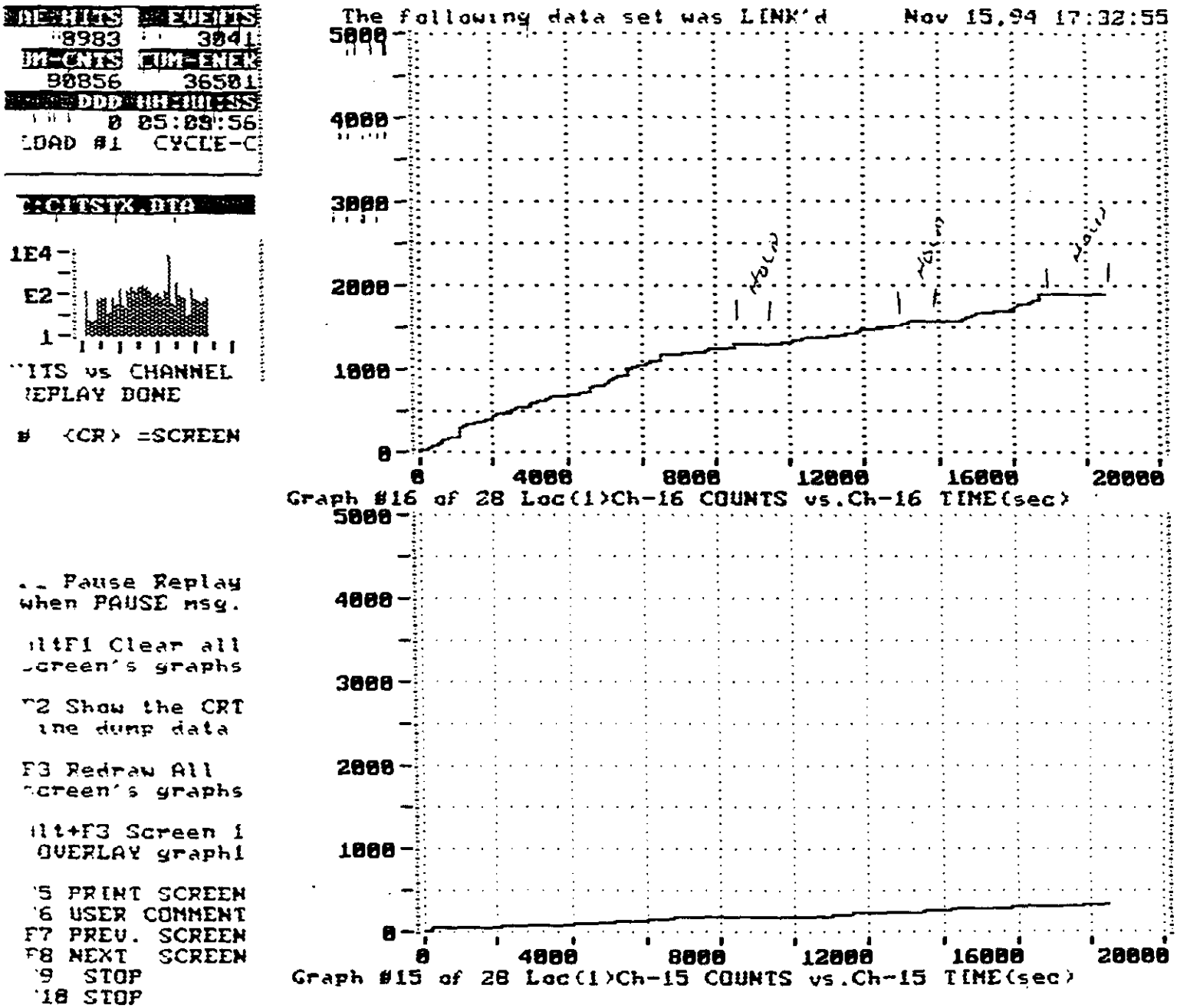
The following data set was LINK'd
Nov 15,94 17:32:55
5000
4000
3000
2000
1000
0
0
4000
8000
12000
16000
20000
Graph #16 of 28 Loc(1)Ch-16 COUNTS vs.Ch-16 TIME(sec)
Graph #15 of 28 Loc(1)Ch-15 COUNTS vs.Ch-15 TIME(sec)
1E4
E2
1
ITS vs CHANNEL
EPLAY DONE
<CR> =SCREEN
Pause Replay
when PAUSE msg.
F1 Clear all
creen's graphs
2 Show the CRT
ne dump data
F3 Redraw All
creen's graphs
lt+F3 Screen 1
OVERLAY graph1
5 PRINT SCREEN
6 USER COMMENT
F7 PREV. SCREEN
F8 NEXT SCREEN
9 STOP
10 STOP

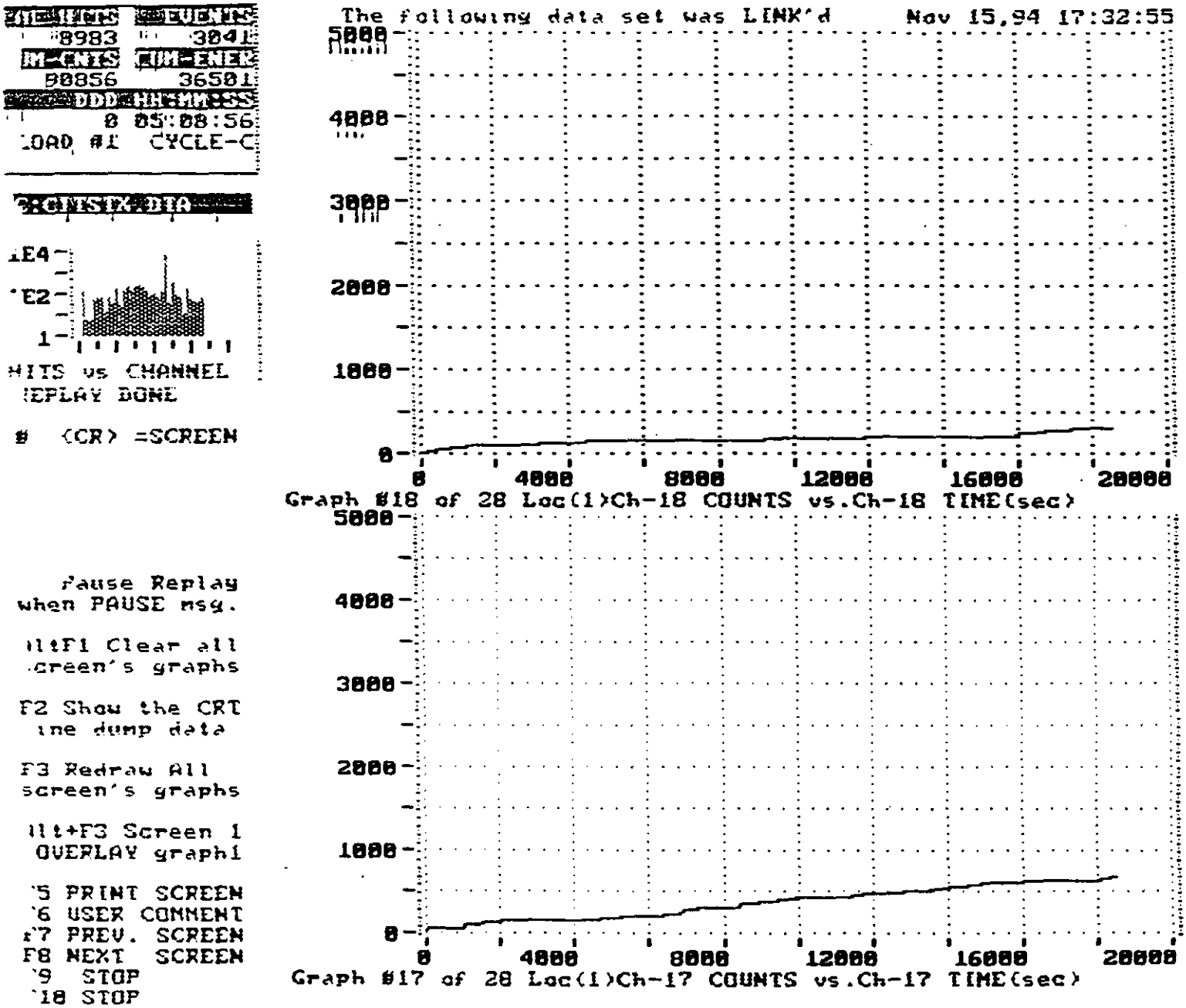
The following data set was LINK'd
Nov 15,94 17:32:55
8983
3841
80856
36501
0 05:08:56
LOAD #1 CYCLE-C
1E4
1E2
1
HITS vs CHANNEL
REPLAY DONE
<CR> =SCREEN
5000
4000
3000
2000
1000
0
0
4000
8000
12000
16000
20000
Graph #18 of 28 Loc(1)Ch-18 COUNTS vs.Ch-18 TIME(sec)
Pause Replay
when PAUSE msg.
Alt-F1 Clear all
screen's graphs
F2 Show the CRT
line dump data
F3 Redraw All
screen's graphs
Alt+F3 Screen 1
OVERLAY graph1
F5 PRINT SCREEN
F6 USER COMMENT
F7 PREV. SCREEN
F8 NEXT SCREEN
F9 STOP
F10 STOP
Graph #17 of 28 Loc(1)Ch-17 COUNTS vs.Ch-17 TIME(sec)

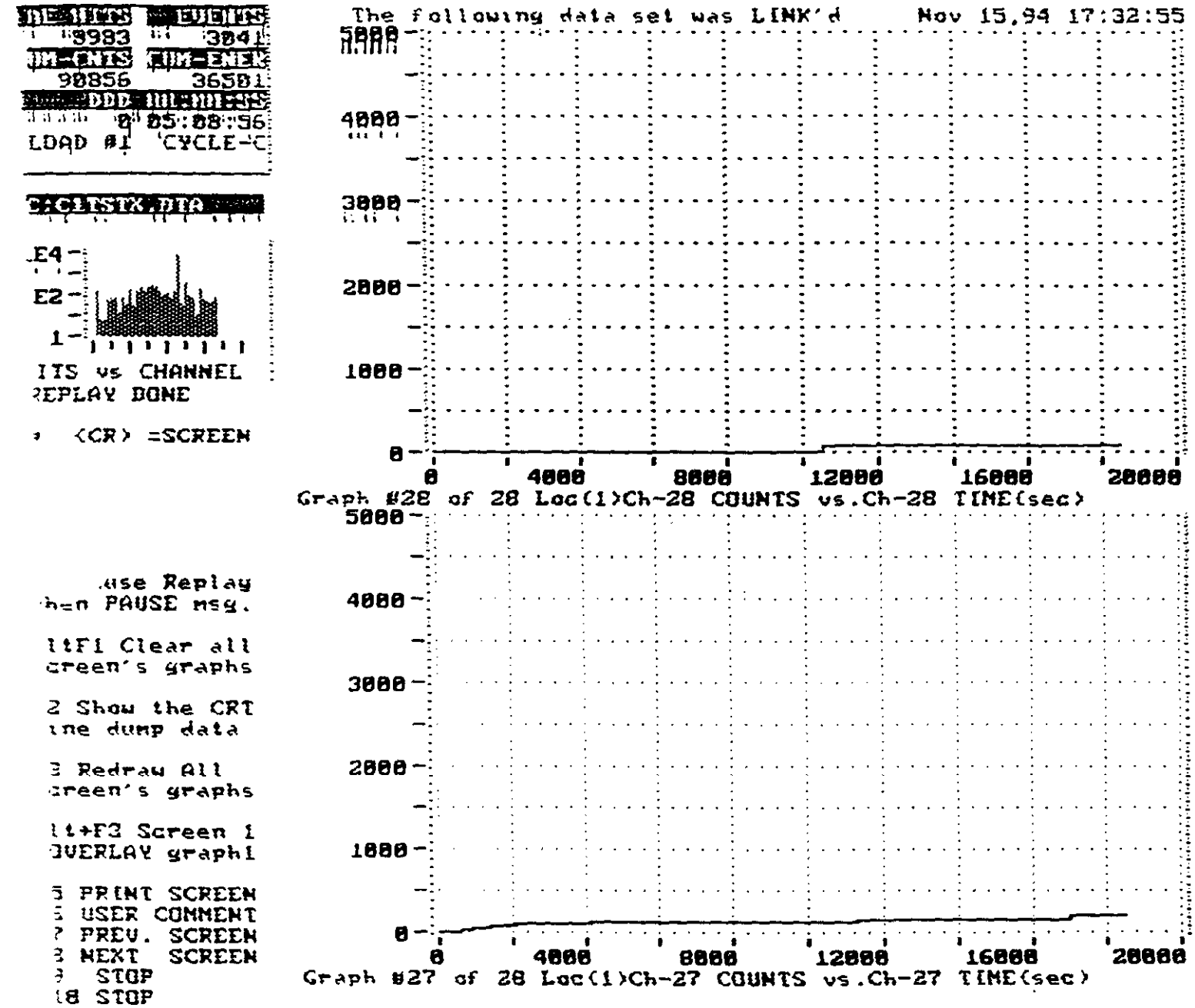
3983
3041
90856
36581
0 05:08:56
LOAD #1 CYCLE-C
E4
E2
1
ITS vs CHANNEL
REPLAY DONE
<CR> =SCREEN
use Replay
hen PAUSE msg.
tF1 Clear all
creen's graphs
2 Show the CRT
ine dump data
3 Redraw All
creen's graphs
t+F3 Screen 1
OVERLAY graphi
5 PRINT SCREEN
USER COMMENT
PREV. SCREEN
NEXT SCREEN
STOP
8 STOP
The following data set was LINK'd
Nov 15,94 17:32:55
5000
4000
3000
2000
1000
0
0
4000
8000
12000
16000
20000
Graph #28 of 28 Loc(1)Ch-28 COUNTS vs.Ch-28 TIME(sec)
5000
4000
3000
2000
1000
0
0
4000
8000
12000
16000
20000
Graph #27 of 28 Loc(1)Ch-27 COUNTS vs.Ch-27 TIME(sec)

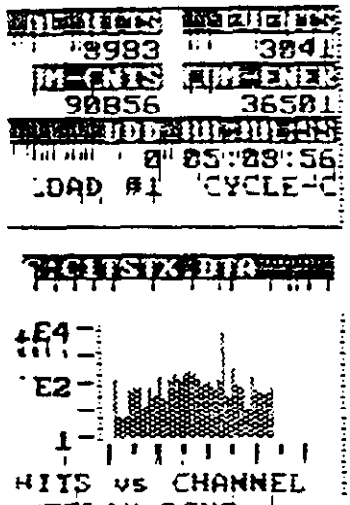

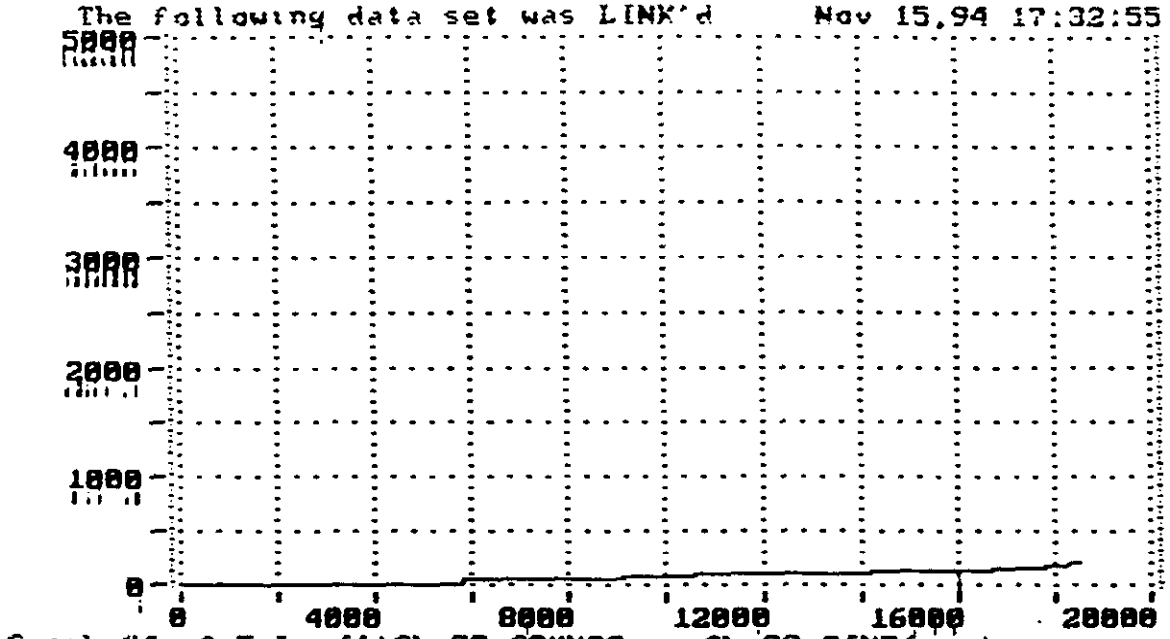

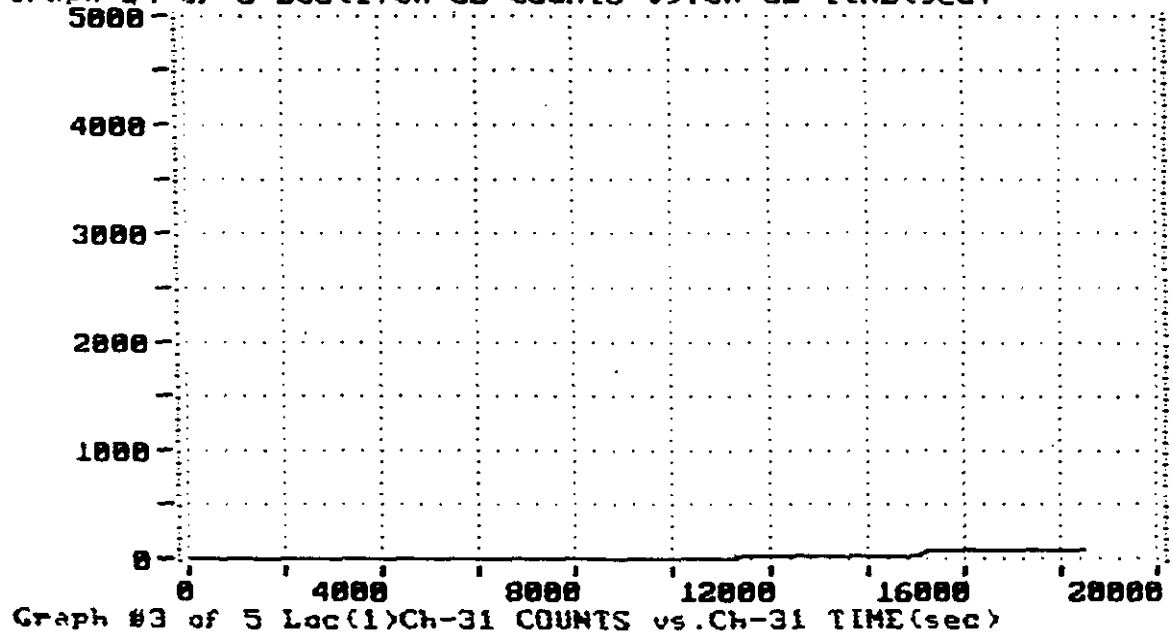

Pause Replay
when PAUSE msg.

Alt+F1 Clear all
screen's graphs

F2 Show the CRT
line dump data

F3 Redraw All
screen's graphs

Alt+F3 Screen 1
OVERLAY graphi

F5 PRINT SCREEN
F6 USER COMMENT
F7 PREV. SCREEN
F8 NEXT SCREEN
F9 STOP
F10 STOP

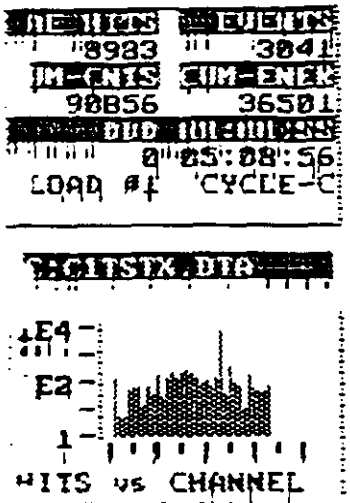

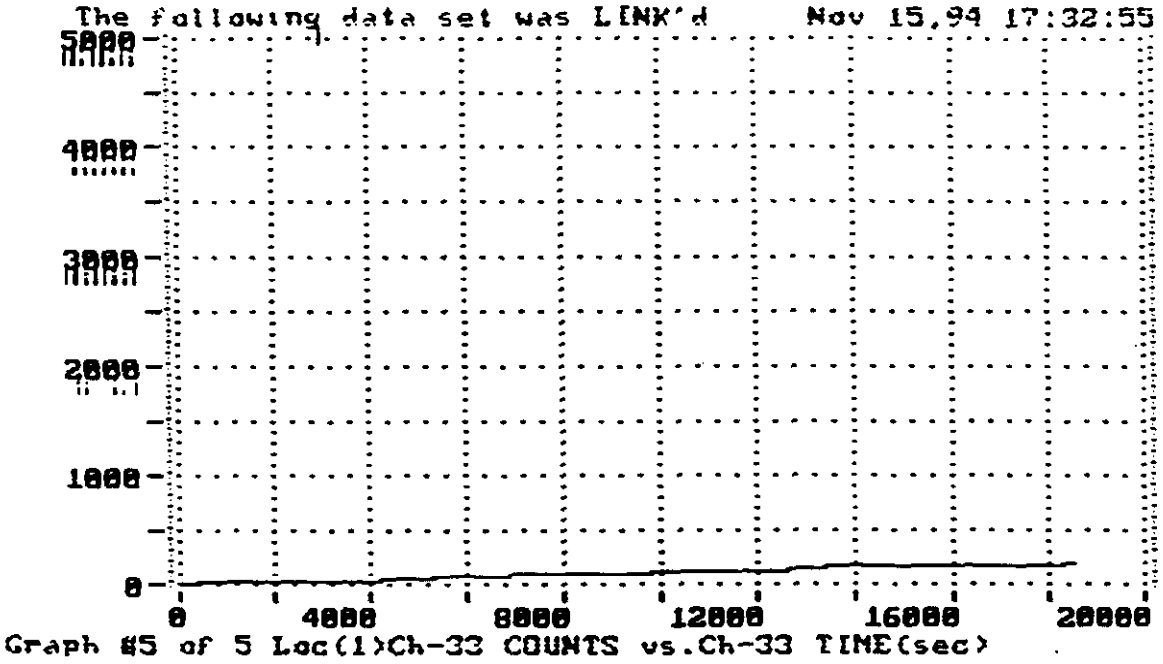

Pause Replay
when PAUSE msg.

Alt F1 Clean all
screen's graphs

F2 Show the CRT
line dump data

F3 Redraw All
screen's graphs

Alt+F3 Screen 1
OVERLAY graph1

F5 PRINT SCREEN
F6 USER COMMENT
F7 PREV. SCREEN
F8 NEXT SCREEN
F9 STOP
F10 STOP

TEST ID_____SHEET___OF___

AE ANALYSIS FILE TRACKER

ANALYSIS BY_____STRUCTURE: CHILLED DATE SLURRY TANK PROJECT_____

PART OF TEST ON THIS FORM:_____INI FILE:_____

Date	Infile	Outfile	Details of Filter &c.	
C:\SPARTAN\GPTEST02		CITST02.DTA	FILTER TO REMOVE HITS LESS THAN 48 dB	50-75%
"	03	03	" "	75% HOLD
	04	04		75%-87.5%
	05	05		87.5% HOLD
	06	06		87.5-100%
	07	07		100% HOLD
	08	08		100% OVERNIGHT HOLD.
	CITST02-07	CITSTX.DTA	LINK ALL FILTERED FILES TO CREATE ONE COMPLETE	
			TEST FILE WITH 48 dB THRESHOLD.	
	SLURTANK.PPT		WORD PERFECT FILE OF TEST REPORT	

TEST ID_____SHEET___OF___

DATA (.INI) FILES REGISTER

DATE: 11-14-94 OPERATOR: J.R. MITCHELL PROJECT GA POWER SLURRY MIX

PATH	FILENAME	CONTENTS	
C:\AE	FREFCK.INI	AE VS CH. AMP POINT PLOT VS CT.	
	ATTNUAT.INI	AE VS TIME. FOR NOISE AND 45° ATT STUDY	
	GPTEST.INI	INDEPENDENT CHANNEL ACQUISITION.	
	GPTSTZONE.INI	SAME AS GPTEST BUT SETUP FOR	
		ZONE LOCATION.	
	GPTSTTRI.INI	TWO GROUPS WINS TRANSLATE LOCATION MAXIMUM AMPLITUDE	
	GPTSTTR2.INI	MAXIMUM AMP LEFT	
	SYSCAL.INI	AMPLITRANSDUCTER VS CH. ZISI FROM PULSER WITH REST INTO EACH CH	

TEST ID_____SHEET___OF___

INITIALIZATION (DTA ~~.INI~~) FILES REGISTER

DATE: 11-14-90 OPERATOR: J. L MITCHELL PROJECT GA Power Scherer Plant
-TS-

PATH	DTA FILENAME	GPSYCAL2 CH 48-FLOW REPLACE WITH CONTENTS CH49.	
C:\AE\	GPATTN0	(ATTNUAT.INI) HORIZONTAL	
		ATTENUATION MEASUREMENT	
	GPATTN1	(ATTNUAT.INI) 45° ATTENUATION	
		MEASUREMENT	
	PERFCK00	(DONE BY HAND) ALL LEAD BREAKS	
		ON ALL CH PANELS PRIOR TO TEST	
		TANK EMPTY.	
	GPTEST01	30 MIN HOLD AT 50% 12.1 FT.	
	GPTEST02	50%-75% 12'-18'	
	GPTEST03	HOLD AT 75% 18' 2 MIN	
	GPTEST04	75-87½% 21'	
	GPTEST05	HOLD 87½%	
	GPTEST06	87½-100%, 24'	
	GPTEST07	HOLD AT 100% 24' 30 MIN.	
	GPTEST08	HOLD AT 100%, 24', OVER NIGHT	
	GPSYSCAL1,2		

PROJECT_____SHEET____OF____

FILTER (.FLT) FILES REGISTER

DATE:_____OPERATOR:_____

PATH	FILENAME	FUNCTION	
C:\AE\	GPTEST08.DTA	AMP 47-100, AF 30-200	
		N = 3-1000, RT = 5-100	

Sheet No. _____

SENSOR PERFORMANCE CHECK FORM

DATE: NOV [illegible] START/END TIMES: [illegible] JOB ID: [illegible]

OPERATOR(S) [illegible]

PENCIL TYPE: [illegible] LEAD TYPE: HB SHOE Y/N N

SYSTEM MODEL, S/N, CHANNEL Spartan

~~ROD ID~~ Plastic Plate w/ R15 COUPLANT Vacuum Grease SENSOR CABLE LENGTH 12'

DEPARTURES FROM RP-2, IF ANY: Plastic Plate instead lucite rod

Sensor Mod, #	Amplitudes (dBae)					Av.	Sensor Mod, #	Amplitudes (dBae)					Av.
5516	68						[illegible] 39	73					
BD 29	66						[illegible] 38	71					
[illegible] 27	70						[illegible] 37	71					
[illegible] 26	71						[illegible]	73					
[illegible] 10	69						[illegible] 35	72					
[illegible] 25	71						[illegible] 36	75					
[illegible]	69						A [illegible]	70					
[illegible] 91	71						[illegible] 33	72					
[illegible] 95	75						[illegible] 32	75					
[illegible] 87	71						[illegible]	77					
BD 94	72						BP 30	77					
BD 92	[illegible]						BP 32	75					

NOTES: See Sheet (2)

Sheet No. 2

SENSOR PERFORMANCE CHECK FORM

CONTINUATION SHEET

DATE: 14 Nov 94 START/END TIMES: 1230 - 2000 JOB ID: [illegible]

Sensor Mod, #	Amplitudes (dBae)					Av.	Sensor Mod, #	Amplitudes (dBae)					Av.
R0 64	76						R0 69	75					
R0 65	75						[illegible]	75					
[illegible] 31	75						R0 19	[illegible]					
R0 66	[illegible]						R0 16	67					
R0 77	72						[illegible]	[illegible]					
[illegible] 70	70						[illegible]	73					
R0 68	[illegible]						5533	72					
[illegible]	74						[illegible]	72					
R0 17	[illegible]						R0 5	73					
[illegible] 61	72						R0 [illegible]	[illegible]					
A0 91	71						R0 90	74					
[illegible] 920701	72						R0 70	76					
R0 74	71						R0 22	73					
3972	72						R0 67	72					

NOTES: See Back For Additional Sensor Mod #'s and Amplitudes

Sheet No. 1

SYSTEM PERFORMANCE CHECK FORM (LEAD BREAKS)

DATE: 14 NOV 94 START/END TIMES: 0800- JOB ID: Georgia Power (SIMRA)

TEST STRUCTURE: _____

OPERATOR(S) Jim Mitchell, Dave Kessler & Chris Pelissier

PENCIL TYPE: .5 mm LEAD TYPE: HB SHOE: NO

PENCIL-TO-SENSOR DISTANCE: 6" SENSOR MODEL: R15I

SYSTEM MODEL: Spartan PRINTOUT ID: _____

DATA FILE(S): _____ INI FILE(S): _____

Sensor / Location	Amplitudes (dBae)					Av.	Sensor / Location	Amplitudes (dBae)					Av.	
1	72	70	78			79.6	12	81	85	81			83	*1
*1 2	68	66	66			67.3	13	82	85	84			84	*2
*1 3	68	68	68			68	14	76	78	78			78	
4	76	77	75			76	15	81	81	80			80.6	
5	70	70	69			69.6	16	73	75	74			74	
*1 6	66	70	67			67.6	17	82	83	84			83	*2
7	69	69	69			69	18	82	85	85			84.6	*2
8	72	73	75			73.3	19	73	74	75			75.3	
9	72	71	71			71.6	20	78	77	74			76.3	
10	76	77	79			77.3	21	76	77	77			76.6	
11	74	73	73			76.6	22	75	76	78			76.3	

Total Avg page 1 → 75.2

NOTES: (*1) Less than 6 DB from AVG Sensors 2, 3, 6 & 27 DB.

(*2) Greater than 6 DB from AVG Sensors 12, 13, 17, & 18 DB.

PHYSICAL
ACOUSTICS
CORPORATION

ACOUSTIC EMISSION • EDDY CURRENT • RESISTIVITY • ULTRASONICS • VIBRATION • PIEZOCERAMICS • R & D APPLICATIONS

Acoustic Emission Testing of On-site Fabricated FRP Vessels Phase II

Final Report
Project R92-336
January 24, 1992

Prepared for:
Mr. Kamyer Vakhsoorzadeh
Southern Company Services
P.O. Box 2625
Birmingham, AL 35202

Prepared by:
Bruce Gilbert
Donald Pointer
Physical Acoustics Corporation
15 Princess Road
Lawrenceville, NJ 08648

Table of Contents

INTRODUCTION

Southern Company has recently constructed large fiber reinforced plastic (FRP) vessels at Plant Yates (Georgia Power Company). These FRP vessels are used as the primary parts of the CT-121 flue gas desulfurization (FGD) process. FRP was primarily selected because it provided an economic advantage over other more conventional choice of materials. To verify the integrity of the FRP construction, QC/QA testing was sought. According to the previous experience of FRP equipment users, Acoustic Emission (AE) monitoring of FRP vessels provides the most promising diagnostic tool for FRP vessels. Accordingly, Physical Acoustics Corporation (PAC) was contracted to perform the required testing and verify the integrity of the FRP vessels and their construction. To reach this goal, hydro-testing was scheduled during the pre-operation phase of the Flue gas desulfurization (FGD) process on both the Limestone Slurry (LS) and the Jet Bubble Reactor (JBR) vessels. The primary goal of the hydro-tests were:

a) Detect, locate and classify emission sources;

b) Evaluate the effectiveness of AE, if active sources are detected, distinguish emissions due to fiber cracking, fiber debonding/pull-out, resin cracking, delamination, secondary bond failures, background noise from loose parts, rubbing, etc.

c) Provide an AE baseline for both the Jet Bubble Reactor (JBR) and Limestone Slurry (LS) vessels for future AE testing.

BACKGROUND INFORMATION

The acoustic emission test personnel From Physical Acoustics (PAC) were David Kesler (AE level III), Bruce Gilbert and Donald Pointer (AE level II). The acoustic emission (AE) testing equipment was supplied by Physical Acoustics Corporation (PAC). It consisted of a 72 channel SPARTAN AT mated to an IBM PC compatible 386 host computer. The data acquisition system employed 100-300 kHz bandpass filters and was calibrated just prior to shipment to the Yates facility. The threshold for acquisition was set at a fixed value of 35 dB for all tests and later filtered to reject any signal below 47 dB. The software used was SA-LOC version 3.03 dated 1/24/91. The sensors used for this test were PAC model R15I piezoelectric sensors with an integral preamplifier and 150 kHz resonant frequency. Attenuation studies were done on each vessel to determine the sensor spacing and signal attenuation. The sensor locations on the vessels can be seen in Figures 1 & 2 of Appendix F. All sensors were mounted to the structure using a hot melt glue. Some sensors were used as guards to reject extraneous noise. Lead break calibrations were also performed just prior to each test using a Hsu-Nielsen source to verify the sensor's acoustic coupling to the structure.

Stressing of the vessels was acomplished using water at atmospheric pressure and temperature. Prior to loading, a 30 minute background noise check was performed. During this time, no appreciable data was recorded and no sources of extraneous data were identified. Stressing was accomplished at a somewhat controlled rate through a fire hose mated to the bottom of the vessel. After the initial portion of the loading, it was verified that the turbulence were not a factor during this testing. Stressing of the vessels was accomplished following standardized atmospheric vessel stressing sequences. Stress level hold periods were performed at approximately 50%, 75% & 100% of H_20 test heights for greater than 5 minutes to evaluate the integrity of the vessels.

The stressing of the JBR marked the first hydrostatic loading of the vessel. Due to the internal complexity of this vessel, and its intended operation scheme, it was impossible to apply a stressing sequence that would subject the entire vessel to a proof load. As such, only the lower level of the vessel was subjected to hydrostatic loading. This level could be stressed hydrostatically and evaluated using acoustic emission.

In April, 1991 the Limestone Slurry (LS) vessel was tested by PAC using acoustic emission NDT. Based on the findings of this initial testing, extended hold periods at the 100% stress levels were adopted for this AE testing. These extended holds were incorporated to further evaluate the response of the vessel over time. Further results of the initial testing can be found in the final report dated July 7, 1991 to Dr. Kamyer Vakhsoorzadeh.

Of importance to this testing was the replacement of the Limestone Slurry (LS) tank floor following the AE test in April. Initially this floor had been installed in prefabricated sections which were glassed together to form the final floor. The removal of the floor was initiated after warpage was realized under load. The removal was accomplished by cutting

out the majority of the floor leaving only the rim which joined the knuckle joint. The new floor was formed by spraying a cut fiber composite onto the concrete base, thus allowing the new floor to cure onto the concrete. This situation introduced the potential for extraneous AE during testing.

A final point references the post test findings from the work performed in April. During visual inspection of the LS, it was noted that some of the baffles in the LS tank had partially delaminated from the walls. Figure 3 of Appendix F, depicts this situation. To repair these anomalies, the baffles were reglassed at their connection points to the vessel walls. Another repair to the LS was made at a nozzle on the lower section of the wall. This area was also found to contain delaminations in the region of sensor number 10. A drawing of this area can be found in Figure 1 of Appendix F.

TEST LOG

PAC personnel arrived at Plant Yates Monday morning, 9/30/91. An initial coordination meeting was held in which the testing plans were reviewed by key personnel from Ershigs, Georgia Power, Plant Yates and PAC. Following this meeting the equipment was setup in the trailer adjacent to the JBR vessel. Attenuation measurements were taken on the JBR. Throughout the remainder of Monday the sensors were mounted and calibrated in preparation for the first of two AE hydrotests on the JBR.

Filling of the JBR began at approximately 9:00am Tuesday morning. Since this test was initiated by Ershigs to check for leaks coming from the vessel bottom and since work was being performed on the vessel during the loading phase; no AE was taken during the load-up portions of the test. During this time the remainder of the AE channels were installed and calibration procedures completed. Figure 2 of Appendix F shows the sensor layout. During the load-hold periods however, work on the vessel was terminated so that useful AE data could be collected. AE data was recorded during all load hold periods for at least 30 minutes. At the 100% stress level AE was recorded for an 11 hour period. This extended hold period was required by Ershigs.

On Wednesday morning the load hold at 100% on the JBR was completed and the JBR was drained. Following this, attention was directed to the Limestone Slurry (LS) tank where attenuation measurements were made. Subsequently all sensors were mounted in preparation for the loading of the LS tank. Figure 1 of Appendix F shows the sensor layout. Filling of the LS tank was initiated at 3:00 that afternoon. As prescribed, load-hold periods with AE data acquisition were performed at 50%, 75% and finally at 100%. The 100% level on the LS tank was reached at 9:00pm that evening. An extended hold period was initiated which lasted until 2:00pm on Thursday afternoon. Based on the initial findings of this hold it was decided that further evaluate of the LS tank as a function of time was warranted. Accordingly, the LS tank was left at the 100% level.

During the remainder of Thursday, the JBR was refitted with sensors for the second AE test. The sensor locations for this test were in the identical locations as specified in the first test. All sensors were calibrated and prepared for the test, which was scheduled to commence on Friday morning. Since the AE system was to be idle for the evening, it was decided to outfit the LS with a limited number of sensors in the regions of high AE activity. The sensor used were in positions 2,9,10&13. To further the evaluation, and also investigate the possibility of AE initiating from portions of the vessel near the 1st wall seam, two additional sensors were mounted above sensors 9&10. These sensors were numbered 21&22 accordingly. Their locations can be visualized Figure 1 of Appendix F. Following the setup this second test of the LS at 100% was run for greater than six hours until the following morning. Following this termination of this test, the LS tank was again left at the 100% fill level.

Immediately following the LS testing, the AE system was reconfigured for the second

loading of the JBR. At 9:00am the JBR filling was initiated. AE data was recorded at 50%, 75%, 87.5% and finally 100% stress-hold levels. The 100% level was reached at 5:30pm on Friday evening and maintained for over one hour. Following the closing of this file the JBR remained at the 100% level. Subsequently the LS tank was refitted with sensors in positions 2,9,10&13 to continue the evaluation. Over the next 12 hours both the JBR and LS vessels were monitored for acoustic emission simultaneously. The distinction between sensor arrangements and test tanks was recorded within the computer. On Saturday morning the datafiles were closed and all testing terminated. Drainage of both vessels ensued.

For the remainder of Saturday and Sunday data analysis was performed off site. By Monday morning both vessels were drained and opened for visual examination. Portions of the visual examination are included in this report. Later on Monday a debriefing meeting was held to discuss the results.

RESULTS AND DISCUSSION

The evaluation of both the Jet Bubble Recovery (JBR) and Limestone Slurry (LS) vessels was based on their ability to acoustically stabilize over time. Simply put, a stable vessel will appear acoustically dormant over time. The ability of the vessel to stabilize is contrasted by continuing or even exponentially increasing AE activity at increased stress levels. The AE technique is best applied during holding periods in the stressing schedule. It is during this time when background effects and transient phenomenona are at a minimum. One of the best ways to evaluate the data, and ultimately the integrity of the vessel, is through graphical displays. By correlating intensities of the dataset graphically an analysis of the JBR and LS vessels was possible and it is from these graphs that the results and conclusions were developed.

JET BUBBLE REACTOR (JBR)

The JBR vessel was loaded and held at the 100% stress level twice during the AE monitoring. From these loadings, two datafiles were acquired that were appropriate for analysis. The data files were both post test filtered for a fixed threshold of 47dB and any extraneous noise was eliminated. The resulting data files each yielded greater than 11 hours of hold at 100%. Figures generated for the JBR analysis can be found in Appendix A.

Figures 3 through 23 of Appendix A afford a comparison of these 2 data files. For comparison purposes similar graphs between datafiles have been included on the same page. The odd numbered plots represent the 1st load-hold while the even numbered plots represent the 2nd load-hold. For simplicity, the axis on each graph have been fixed.

Figures 3 and 4 of Appendix A show the distribution of hits among the channels. Among the most active channels during the first hold period are channels 1, 6, 8, 15, 25 and 49. It can be seen from Figure 4 of Appendix A that the activity for all channels has reduced significantly when compared to the first loading shown in Figure 3 however all channels remain active. Figures 5 and 6 of Appendix A show the amplitudes that were recorded during each hold period. During the first test there were a significant number of hits over 80dB. During the second test the amplitudes were slightly lower but still maintain values above 70dB. From Figures 7 and 8 of Appendix A it is apparent that the hit rates remains relatively constant after their initial decays. Although the decay in rate was present, the vessel never completely stopped emitting. Also of interest is the "spike" data found during the first loading. This type of emission is indicative of sudden releases of energy characteristic of damage propagation within the FRP.

Figures 9 and 10 of Appendix A indicate the energy rate recorded during the hold periods. As previously noted, the spike emission is of great concern. These spikes are from hits of middle to upper amplitudes (60 - 80 dB) and relatively long durations. Figures 11 and 12 of Appendix A show the amplitudes for all channels as a function of time. As can be seen from these plots, the amplitude levels remained relatively consistent throughout the hold

period. Figures 13 and 14 of Appendix A represent the individual channel activity versus time. From this plot it is sometimes possible to note pattern in channel activity. Figures 15 and 16 of Appendix A show the individual hit durations as a function of channel. Figure 15 appears to dominate these two plots however Figure 16 shows durations reaching 30 milliseconds which are also relatively high. A synopsis of the above graphs would highlight the long duration, and burst type emissions. The burst type emission was heavily noted during the first hold. This emission pattern decayed during the second hold however the continuing emission throughout this hold was disconcerting.

To further investigate the final status of the vessel, the last hour of data from the second hold period was scrutinized. Figures 17 through 23 of Appendix A represent this data. The figures generated for this analysis were the same as reviewed above with the exception of increased resolution to aid in the analysis. From Figure 17 it can be seen that the activity was relatively limited and scattered among the channels. Figure 19 of Appendix A indicates that the emission was also scattered as a function of time. From Figures 18 and 20 it can be seen that the amplitude ranged up to almost 60dB. The remaining figures serve to support the observation of continuing low level emission as a function of time.

To put these seemingly low levels of emission into perspective, it should be recalled that each of the data files ran for greater than 11 hours each. The standardized hold period for such a test allows a minimum of 30 minutes for vessel stabilization.

LIMESTONE SLURRY (LS)

In this section the data taken on the Limestone Slurry (LS) tank was analyzed. Comments are made on the activity of the vessel during the load-up portion of the test. Data analysis is performed on the intermediate hold periods approaching 100% and also the 60 hour hold at 100%. For analysis purposes, the data was filtered at a threshold of 47dB. This threshold was consistent with various portions of the previous report from April, 1991. Figure 1 of Appendix F shows the initial AE sensor layout for the LS vessel. As can be seen, the bottom portion of the vessel wall was heavily covered with sensors in an attempt to evaluate the knuckle joint. The decision to concentrate on this region also came as a result of the first test back in April.

LOAD-UP OF LIMESTONE SLURRY TANK

During the load-up portion of the stressing sequence AE is not typically recorded; however is certain situations useful realtime information can be gained about the vessel during these times. To evaluate this, AE requires that each individual AE channels' activity light (on the front panel of the SPARTAN AT) be scrutinized. By determining which sensors activity lights are active, a feel for the vessel can be gained on a per channel basis. This information may ultimately be used during the load-hold evaluation of the stored data.

Almost from the onset of loading, channel 3 was extremely active. After assessing the fill

rate and the lack of turbulence during fill, it was speculated that the cause of this emission could be related to the separation of the tank bottom from the cement foundation or maybe the baffle attachment to the wall. Over time the activity from this sensor decreased, however at no point during the load-up did channel 3 ever discontinue emitting. As the stress level increased, the number of active channels, as well as AE rate, continued to increase for all channels. By the time that the 100% stress level was reached, the level of AE activity on channel 3 was no longer distinct from the other channels.

INITIAL LOAD HOLD OF LIMESTONE SLURRY AT 100%

The data taken during this initial hold period represents greater than 17 hours of continuous acquisition. For reference, the standard evaluation time for an FRP vessel is 30 minutes.

Figure 1 of Appendix B shows the hits vs. time for all sensors during this load hold. As can be seen, the AE data rate follows the anticipated exponential decay with time. With time however the AE should completely decay and as portrayed in Figure 1, it does not. Further, the intersperced periods of burst type emission is of particular interest as it represents instantaneous releases of AE energy. To investigate which channels were responsible for this, Figure 22 of Appendix B was generated to display the hits vs. channel. As can be seen, sensors 2, 9, 10 and 13 were higher in activity than the remaining sensors. From this, Figure 1 through 4 of Appendix B were generated which show the hits, counts, energy and amplitude vs. time for these 4 sensors combined. Knowing which sensors were responsible for the emission it was practical to look at the AE from each channel individually. Figures 5 through 21 of Appendix B represent the hits, counts, energy and amplitudes vs. time for each of these sensor separately. It should be noted that the y-axis scales for each of these graphs was set to allow the maximum resolution for comparison purposes. When comparing like graphs between different sensors, this fact should be maintained.

From these figures it can be seen that sensors 2 and 13 are responsible for the continuing emission while sensor 9 and 10 are responsible for the burst type emission. Referring to Figures 23 and 24 of Appendix B it is apparent that channel 9 is responsible for this section of burst emission.

Referring back to Figure 1 of Appendix B (hits vs. time) it can be seen that there is a definite increase in AE activity towards the end of the figure. Upon referring back to the start of test and interpolating, it is found that the point of increase in the background rate corresponds to the time of morning which is the sunrise. From this it can be referred that the heat from the sun initiates a second stress on the vessel in the form of a thermal gradient. This gradient serves to increase the continuing AE activity thus reinforcing the notion that the AE being recorded is stress related and not just of a background effect.

SECOND HOLD OF LIMESTONE SLURRY AT 100%

Following the activity seen above, it was determined that the LS vessel should be left at the

100% stress level in order to further evaluate the continuing AE. Since the JBR was being setup for a test, the continuing efforts on the LS were scheduled as best as possible. The time period between the ending of the first data collection period and the initiation of this session was about 10 hours. Following the setup on the JBR, only the 4 most active sensors (2,9,10&13) were refitted on the LS for acquisition. To attempt to investigate the location of the AE sources on the vessel, 2 additional sensors were mounted on the LS. Their locations can be seen in Figure 1 of Appendix F. These sensors were labeled channel 21 and 22 accordingly and are positioned above 2 of the 4 initial sensors which have remained in their initial position. In this manner, the sources of emission could begin to be located on the vessel using arrival time. As can be seen from Figure 1 of Appendix C, shows the hits vs. channel as being primarily based around the region of the four original sensors. Referring to Figure 2 of this section it is observed than the emission once again does not completely died out with time. Although the data rates are fairly low, the fact remains that each of these hits was greater that the analysis threshold of 47dB. To further investigate the magnitude of these hits, Figures 3, 4 & 5 were created to look at the amplitude, count and energy distribution during this time period. From these figures we can see that there were definite periods of burst type AE activity on top of the continuing emission. Of concern are the amplitudes in the 70dB range. Figures 6 through 21 of Appendix C show the hits, counts, energy, and amplitude distribution for channels 2, 9, 10 and 13 plotted separately. From these figures, again there appears both periods continuing activity and burst type emission.

FINAL HOLD OF LIMESTONE SLURRY AT 100%

Based on the information gained above it was reasoned to once again leave the vessel at the 100% level and time permitting, continue to acquire data. Since the main concentration at this point in the schedule was to concentrate on the JBR tank, it was not until 14 hours later that the LS tank was again monitored. Both tanks were monitored for a period of greater than 15 hours through Friday evening and into Saturday morning. Due to rain on Saturday morning some of this data was filtered out. As such however, greater than 12 hours of data were considered acceptable for analysis.

The details of the acquisition are as follows; after the loading sequence up to 100% was completed on the JBR, the LS was once again outfitted with 4 sensors in positions 2, 9, 10 & 13. It was reasoned that both the JBR and the LS could be simultaneously monitored with AE at the 100% stress level. As such the AE channels used on the computer to monitor the LS were no longer 2, 9, 10 & 13 but now respectively 53, 54, 59 & 60. This was due to channels 2, 9, 10 & 13 now being used for the JBR. This in no way jeapordized the results on the LS data since the same locations on the LS were used throughout the entirety of the testing.

Figure 1 through 16 of Appendix D show the hits, counts. energy and amplitudes for each of the four channels. Once again the level of AE activity has not completely stopped and as before, there remains transient type activity. Since the time that this file was initiated

was almost 9:00pm it is inconceivable that this AE is related to the sun and the potential temperature gradient. Referring to Figures 5 through 9 of this section, we can see the counts, duration and amplitude plots for channel 54 (sensor location 9 on the vessel). Referring to approximately 10-11 hours into this test it is observed that a "spike" can be seen. This spike is of extremely high duration and relatively low amplitude. Due to the magnitude of these emissions it is obvious that the vessel is actively readjusting to the stress level.

Referring to the plots of amplitude and duration for the remaining three channels, varying trends can be seen. The origin of these sources differ greatly based on the variations in amplitude and duration. As referred to earlier, the point of this acquisition period was to determine whether the AE would eventually decay to nothing after this greatly extended hold at 100% stress level. As can be seen from the data, the emission continued and there were even burst type emissions recorded.

COMBINED DATAFILE EVALUATION OF LIMESTONE SLURRY AT 100%

To give a clear representation of the data taken from the Limestone Slurry tank over the entire 60 hour period, all of the data files have been combined to form one continuous file. The appropriate time offsets have been included between files so that the time axis on these plots is representative of the actual AE occurrances.

From this file, Figures 1 through 4 of Appendix E have been generated which show the hits, counts, energy and amplitude for the entire hold period at 100%. As can be seen from these plots, the acoustic emission activity decayed during the initial portion of the hold period, however at no point died out completely. As before, the burst type emission encountered throughout the hold period was particularly troubling due to the high amplitude AE hits and also the long duration hits. As stated above, the contrast between the high amplitude and long duration hits noted from different hits represent two different phenomenon within the vessel. Both of these occurrance can be considered detrimental to the integrity of the vessel and/or the internal structures. As stated before, the emission continued up to and through the final hold period some 60 hours after the initial hold at 100% was reached.

A further point of interest is the increased emission during daylight periods. These periods in time are marked on the appropriate figures. They are indicative of the increased thermal effect on the tank and its special ultraviolet protective coating. This thermal effect serves to further support the argument that the vessel is still actively adjusting to the stress state applied. An argument could be generated to the effect that the vessel is constantly readjusting to the thermal effect. The basis for this is explained by the movement of the tank base as the source of the emission. To discredit this hypothesis are the distinct changes in emission level noted at sunrise and again at sundown which are more indicative of a prompt adjustment to the stress. This reasoning therefore precludes the notion of continuous readjustment of the tank to stress.

CONCLUSIONS

Jet Bubble Recovery

During the testing of the JBR, two AE datafiles were primarily interpreted for results. These files contained over 11 hours each of continuous emission during two monitoring periods. Based on the emissions recorded during both of these load hold periods, it was evident that the JBR continued to emit up to, and including the last portion of the final load-hold period. Since a standardized threshold level was used for evaluation, and since the JBR was not subject to any appreciable external stresses other than the hydorstatic stress, it can be concluded that the vessel was continuing to emit due to increasing degredation of the vessel and/or internal structure at the vessel wall. Due to the sensitive nature of the AE technique, it should be noted that the levels and intensities of the emission were in no way indication of immeidate or catastrophic failure. Due to the inability of the vessel to completely stabilize over time, it can be concluded that the vessel was dynamically and adversely readjusting to the stress level. To support this conviction was the post test visual analysis of the inside of the JBR. Of interest to the AE analysis were the various portions where the internals to the JBR were attached to the vessel wall. In several areas it was noted that internal delaminations had occurred at these connection point. It is felt that the continuing AE is directly related to this phenomenon. This conclusion is further supported by the low amplitude, long duration hits that are characteristically indicative of delaminations in FRP vessels.

Limestone Slurry

Testing of the LS tank offered a unique opportunity to evaluate the vessel at the 100% stress level over a period of greater than 60 hours. During this time a large amount of data was taken to chart the response of the vessel to this constant stress level. As was the case with the JBR, the LS did not completely acoustically stabilize over time. This was confirmed not only through low level continuing emissions, but also through burst type emissions. A case in point would refer to the AE experienced by channel 54 (sensor #9 on the vessel) which was extremely long duration and realtively low amplitude. This occurrance was experienced almost 50 hours into the hold period at 100%. Once again, the conclusion being that both the low level continuing emission, in combination with the burst type emission are indicative of a vessel which is actively seeking an equilibrium state. It is anticipated that this vessel would continue to emit until such time as the entirety of the stress relief was completed.

APPENDIX A

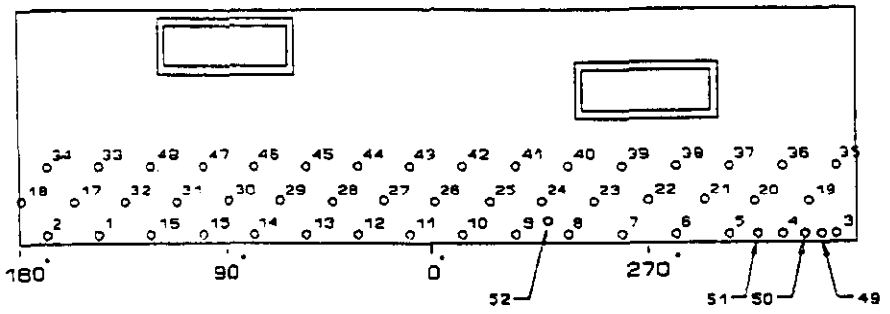

Figure 1. Sensor arrangement for Jet Bubble Reactor (JBR)

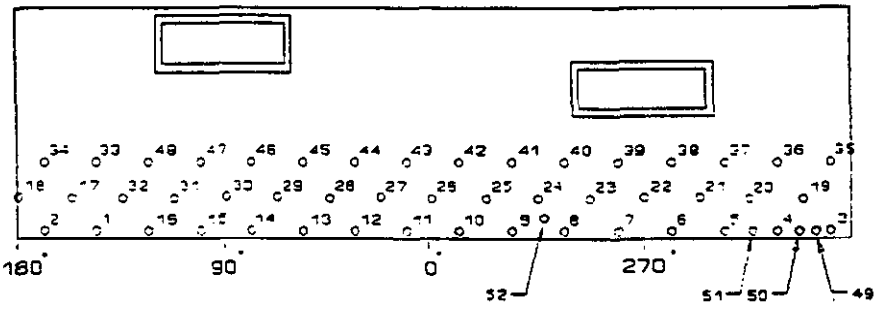

Figure 2. Sensor arrangement for Jet Bubble Reactor (JBR)

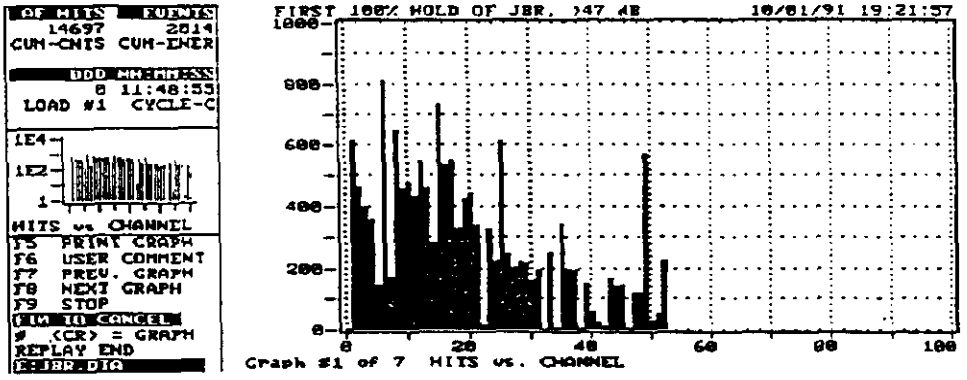

Figure 3. Hits vs Channel for first 100% hold of JBR

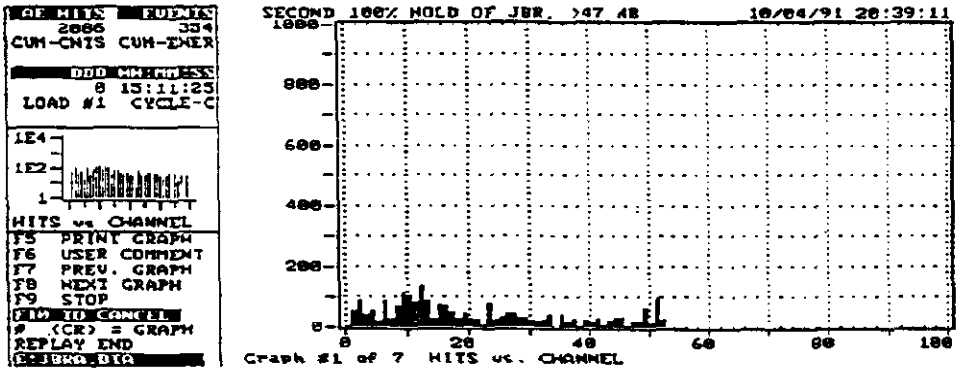

Figure 4. Hits vs Channel for second 100% hold of JBR

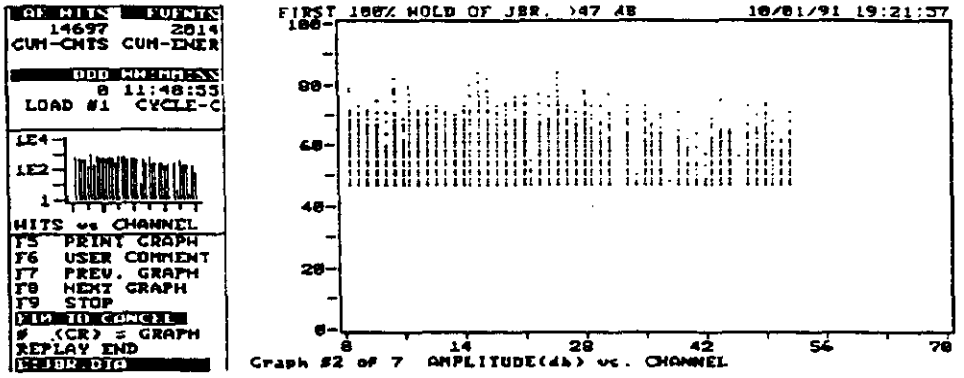

Figure 5. Amplitude vs Channel for first 100% hold of JBR

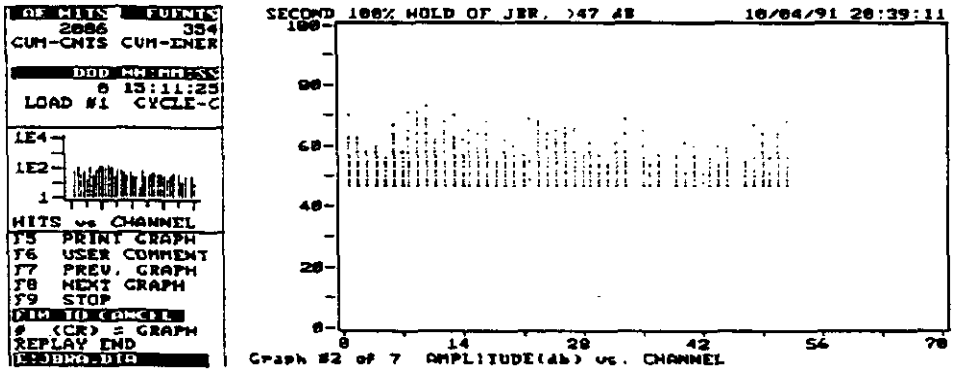

Figure 6. Amplitude vs Channel for second 100% hold of JBR

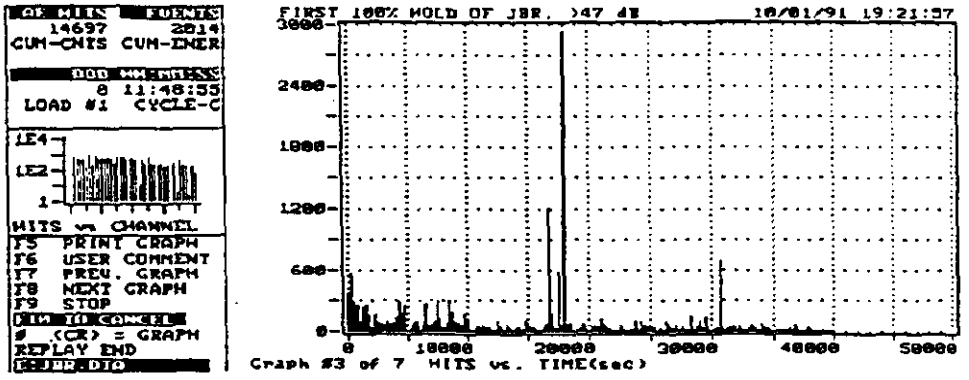

Figure 7. Hits vs Time for first 100% hold of JBR

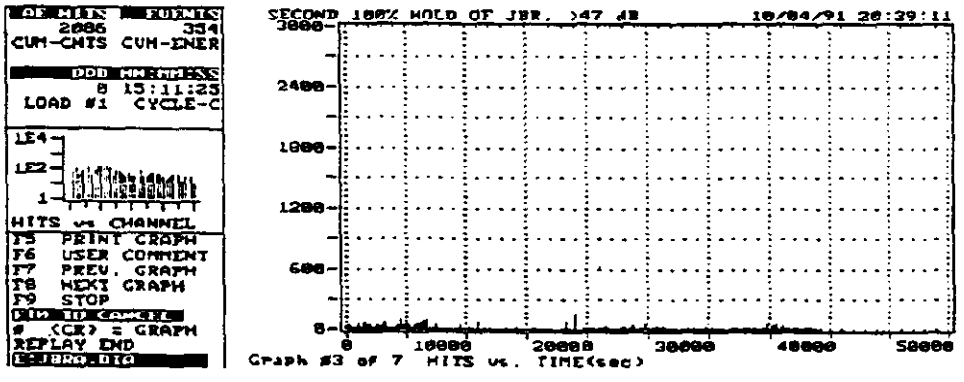

Figure 8. Hits vs Time for second 100% hold of JBR

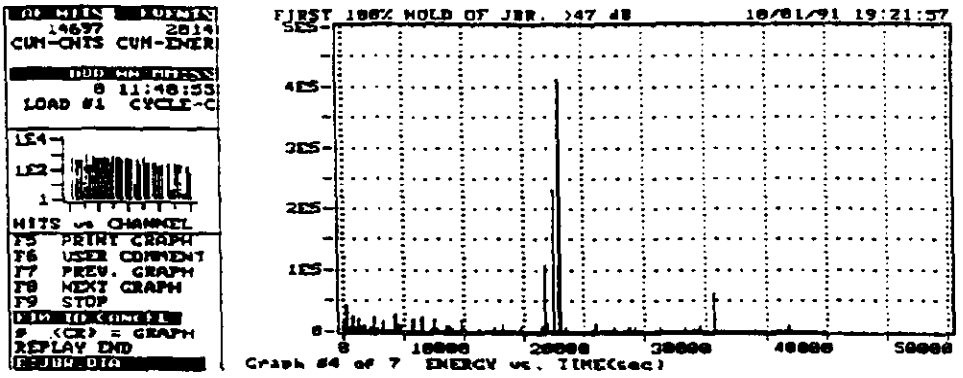

Figure 9. Energy vs Time for first 100% hold of JBR

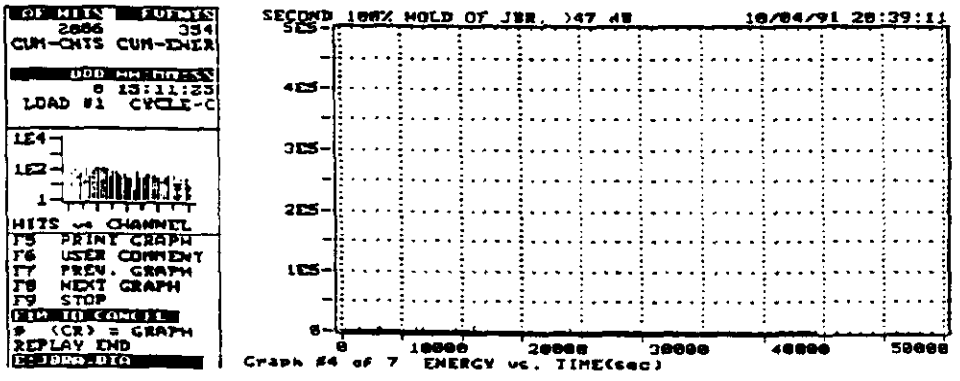

Figure 10. Energy vs Time for first 100% hold of JBR

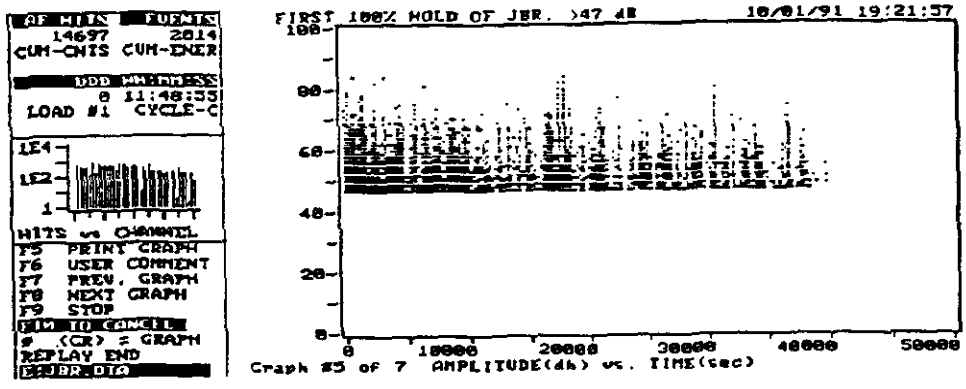

Figure 11. Amplitude vs Time for first 100% hold of JBR

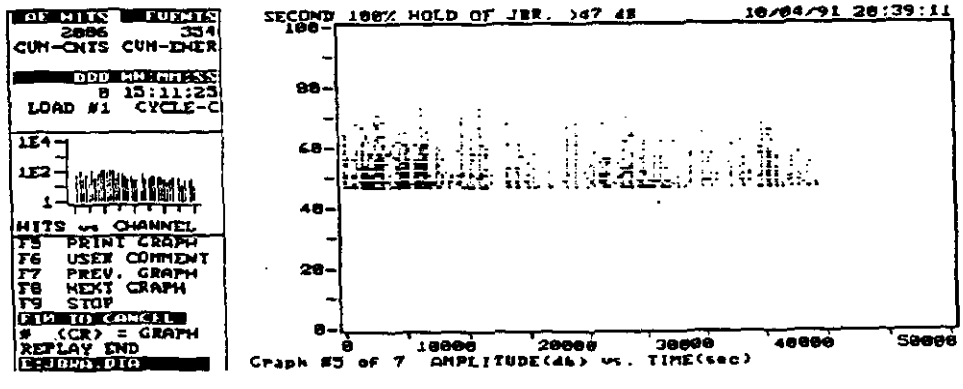

Figure 12. Amplitude vs Time for second 100% hold of JBR

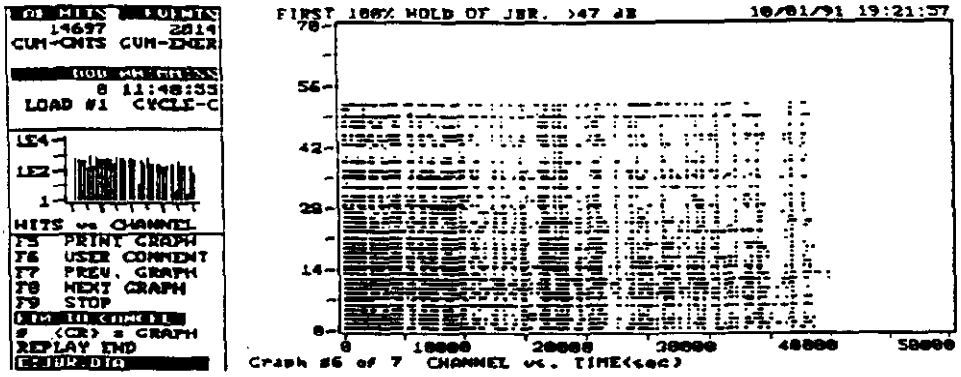

Figure 13. Channel vs Time for first 100% hold of JBR

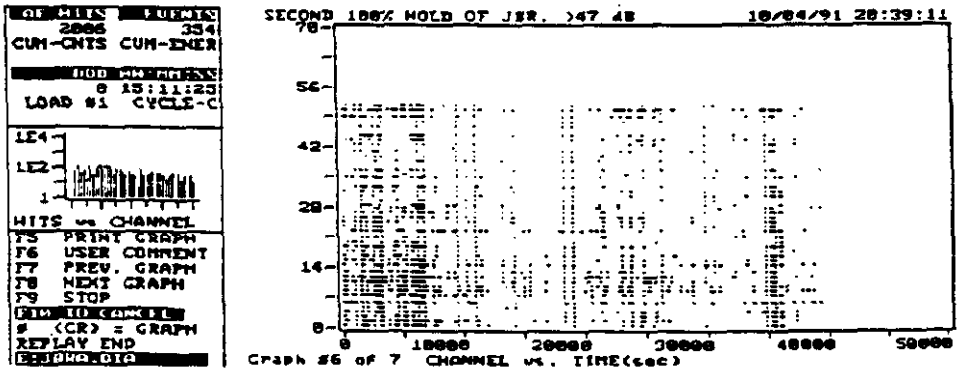

Figure 14. Channel vs Time for second 100% hold of JBR

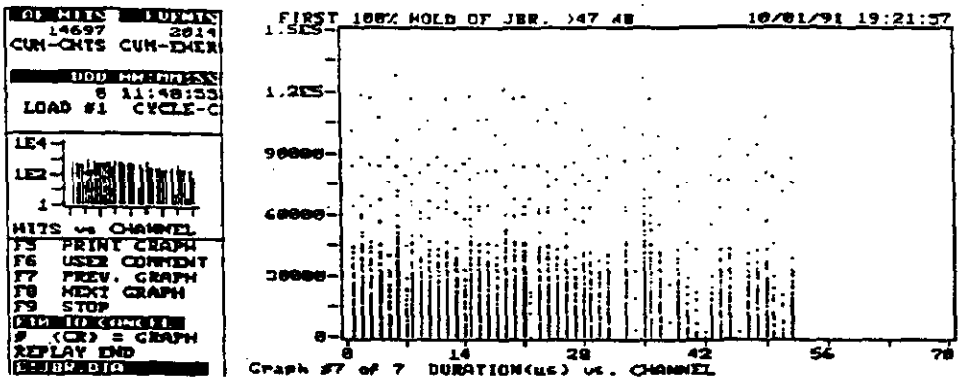

Figure 15. Duration vs Channel for first 100% hold of JBR

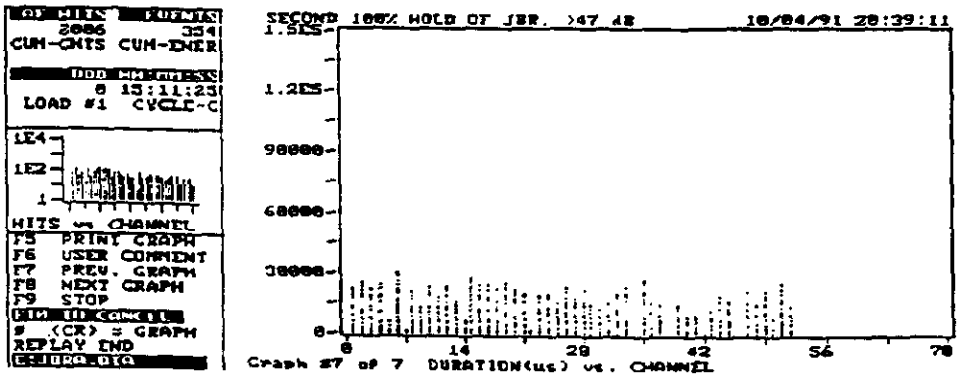

Figure 16. Duration vs Channel for second 100% hold of JBR

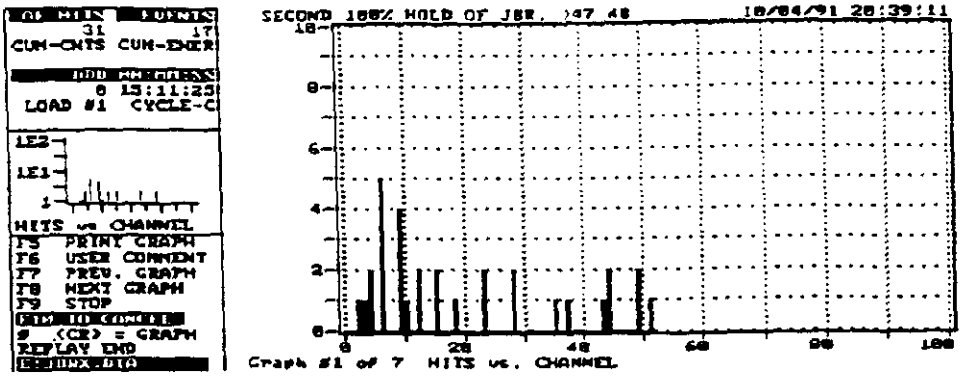

Figure 17. Hits vs Channel for final hour of JBR

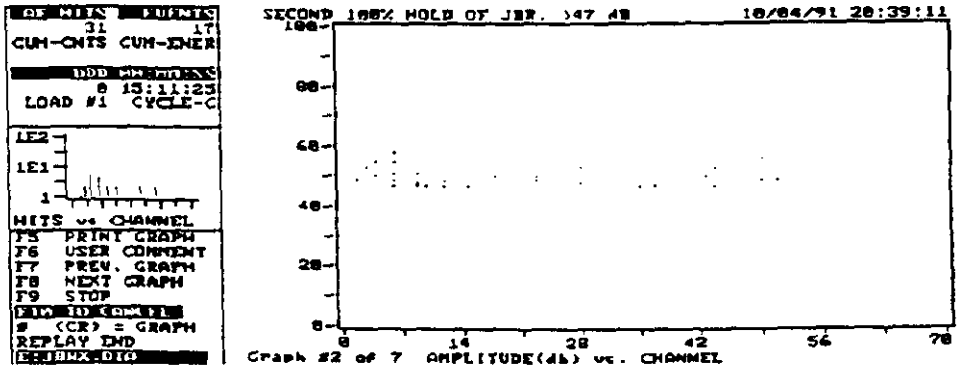

Figure 18. Amplitude vs Channel for final hour of JBR

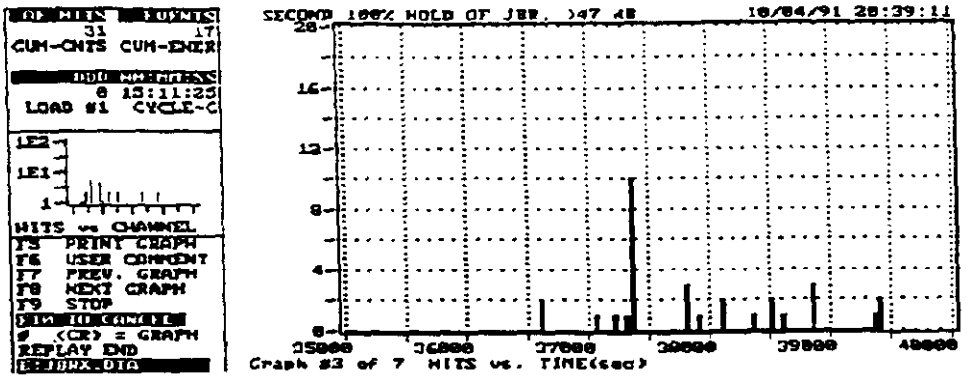

Figure 19. Hits vs Time for final hour of JBR

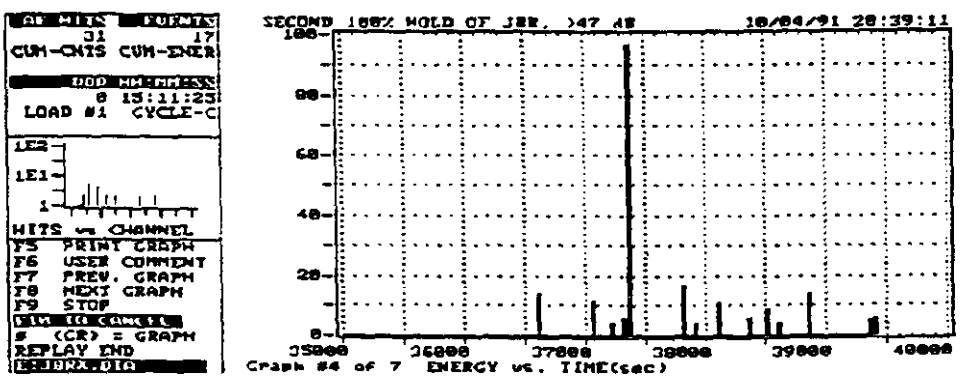

Figure 20. Energy vs Time for final hour of JBR

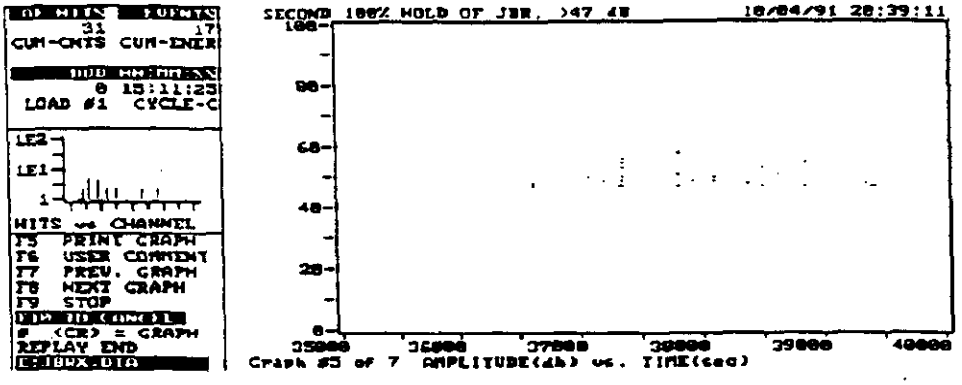

Figure 21. Amplitude vs Time for final hour of JBR

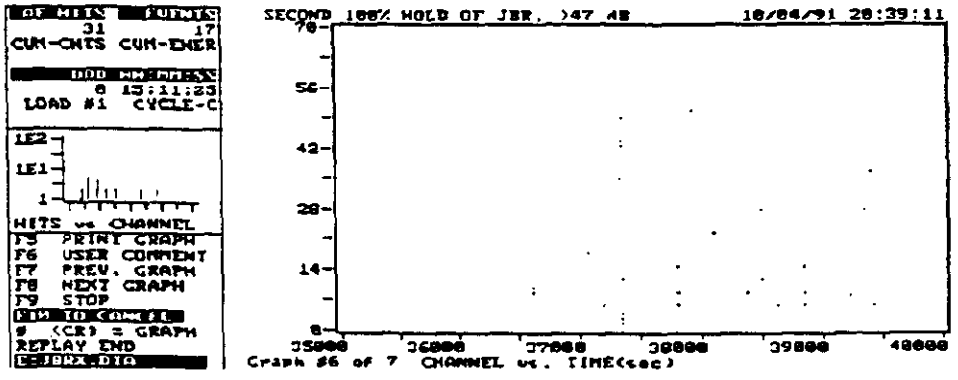

Figure 22. Channel vs Time for final hour of JBR

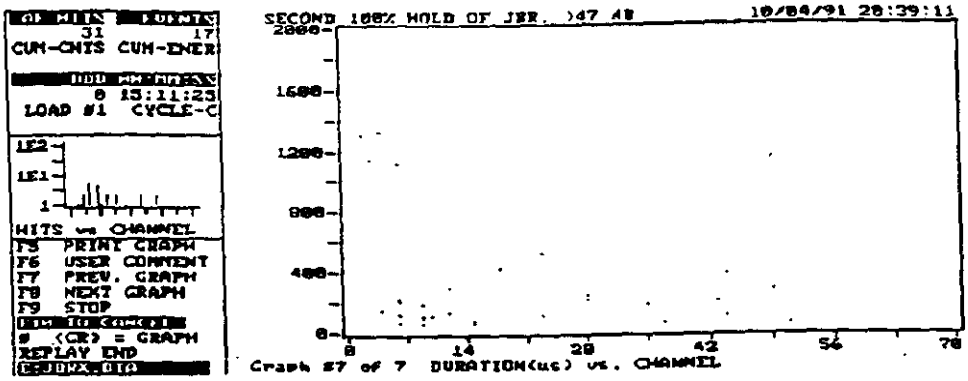

Figure 23. Duration vs Channel for final hour of JBR

APPENDIX B

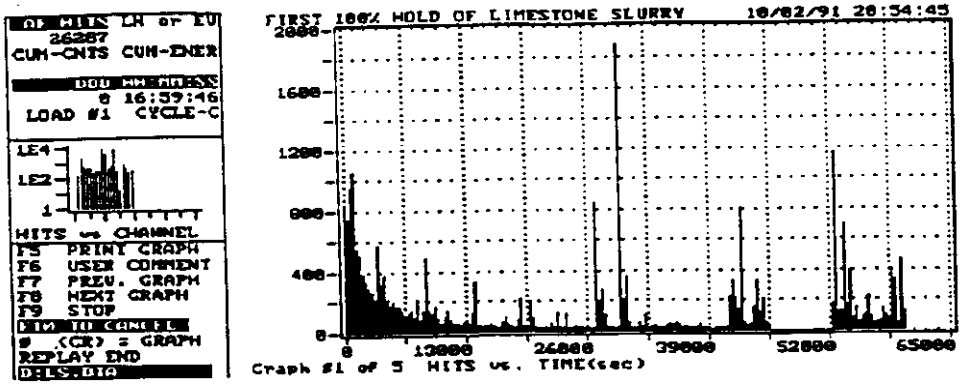

Figure 1. Hits vs Time for first 100% hold of LS

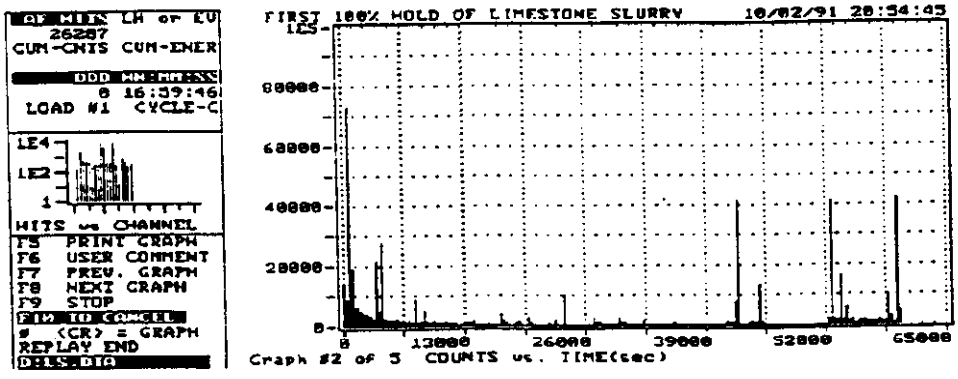

Figure 2. Counts vs Time for first 100% hold of LS

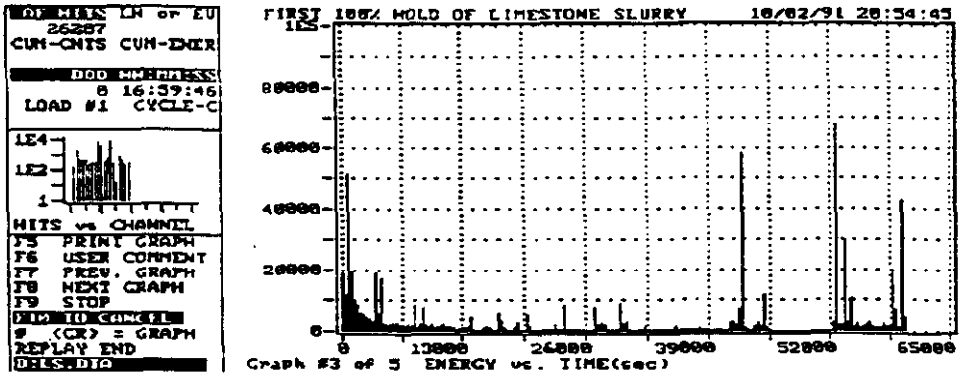

Figure 3. Energy vs Time for first 100% hold of LS

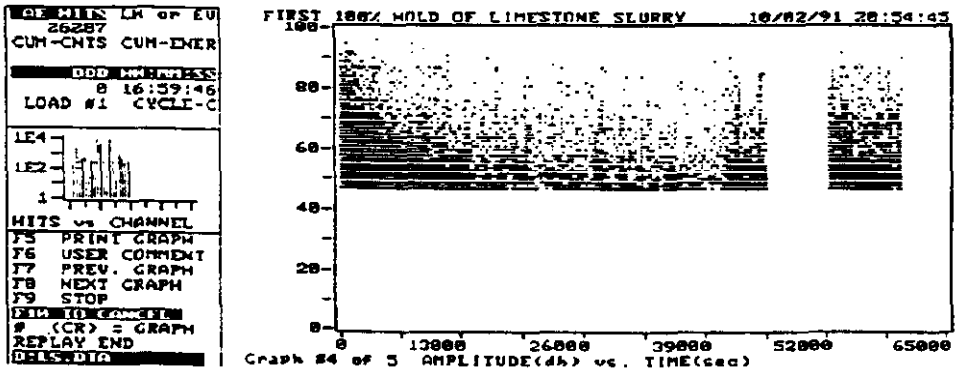

Figure 4. Amplitude vs Time for first 100% hold of LS

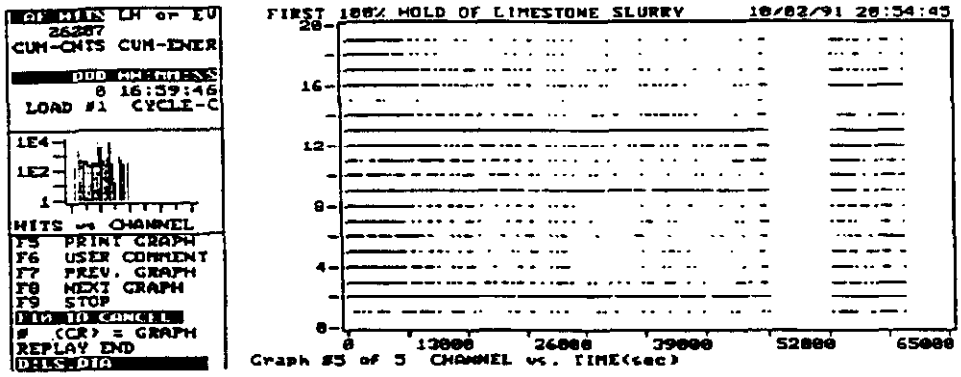

Figure 5. Channel vs Time for first 100% hold of LS

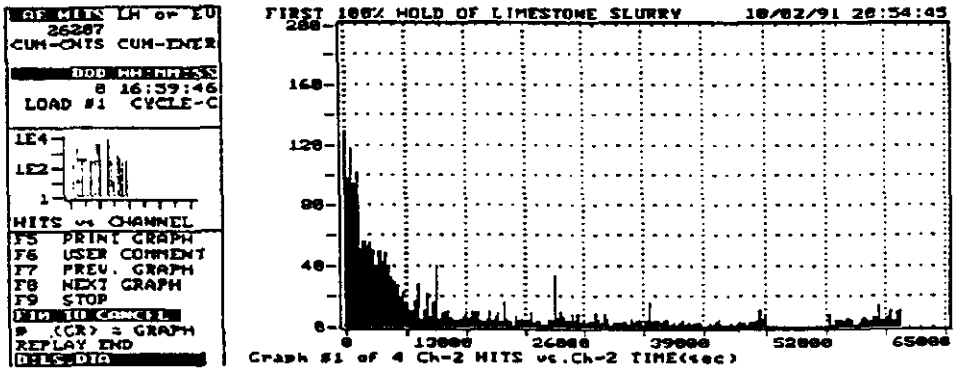

Figure 6. Channel 2 Hits vs Time for first 100% hold of LS

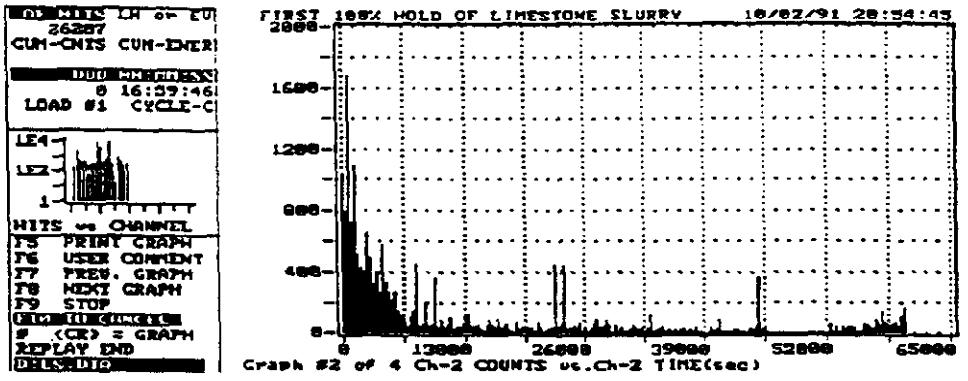

Figure 7. Channel 2 Counts vs Time for first 100% hold of LS

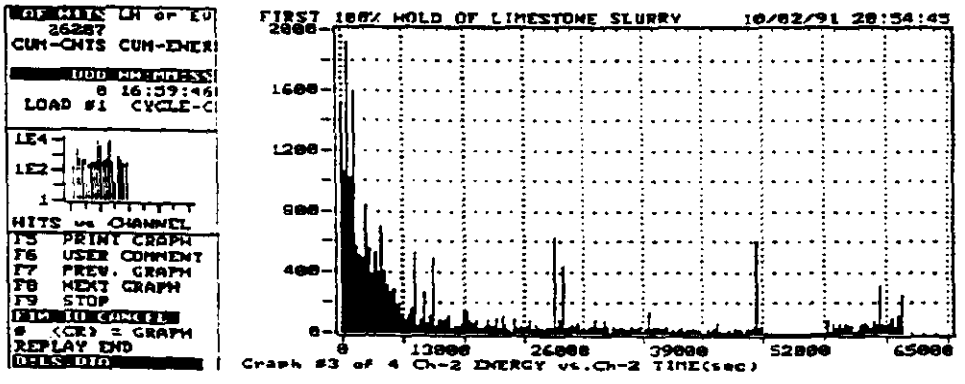

Figure 8. Channel 2 Energy vs Time for first 100% hold of LS

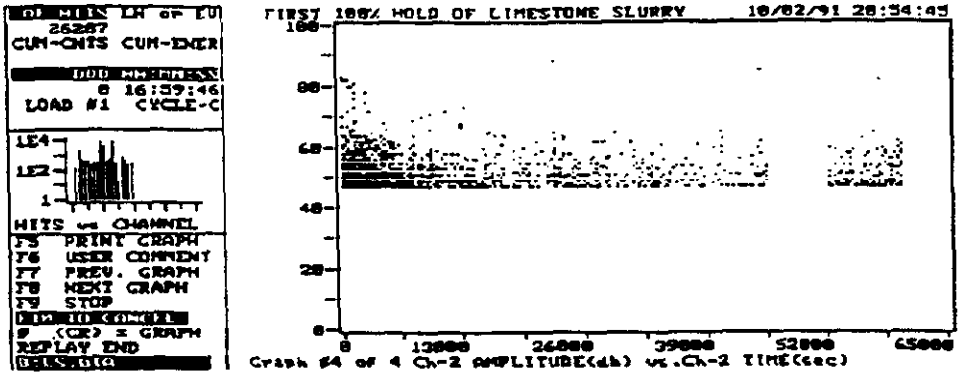

Figure 9. Channel 2 Amplitude vs Time for first 100% hold of LS

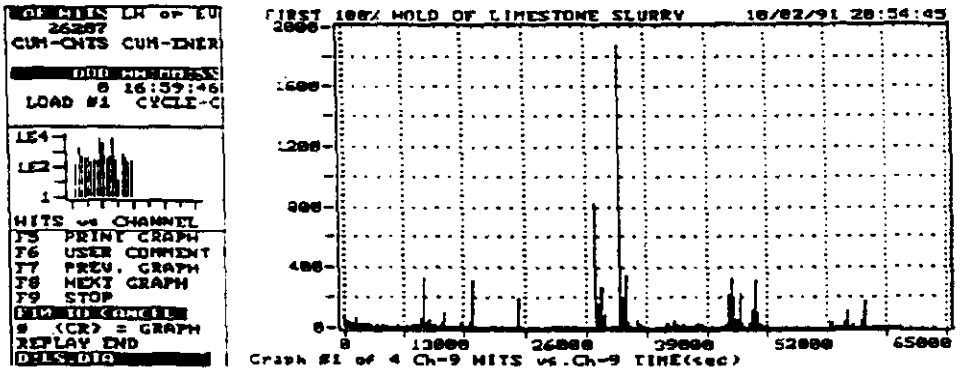

Figure 10. Channel 9 Hits vs Time for first 100% hold of LS

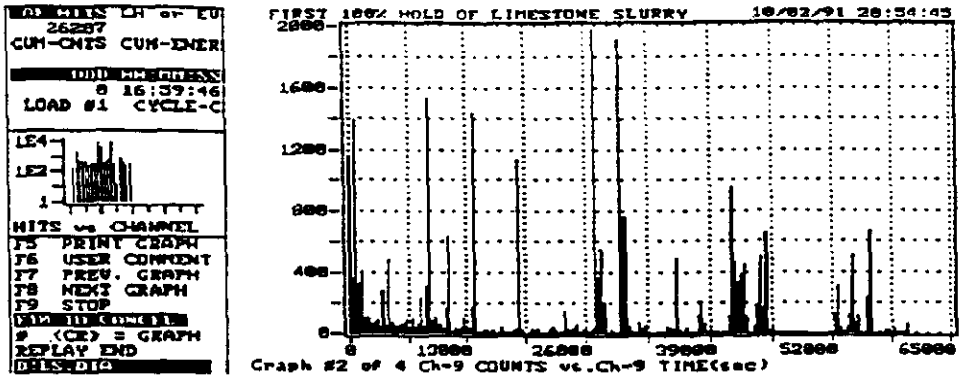

Figure 11. Channel 9 Counts vs Time for first 100% hold of LS

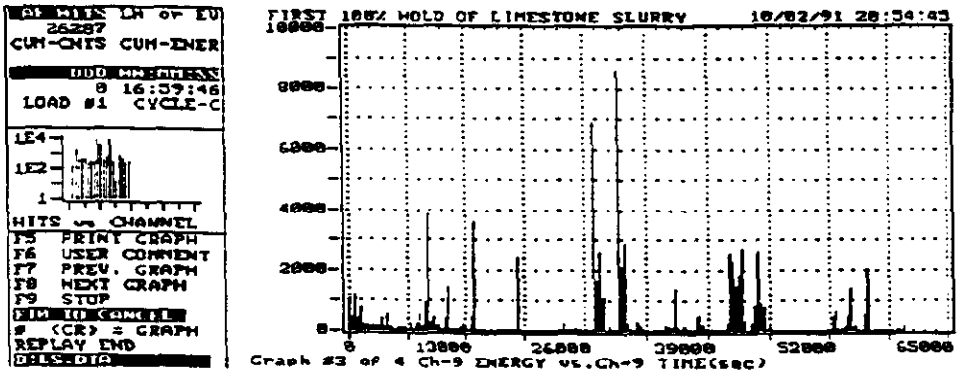

Figure 12. Channel 9 Energy vs Time for first 100% hold of LS

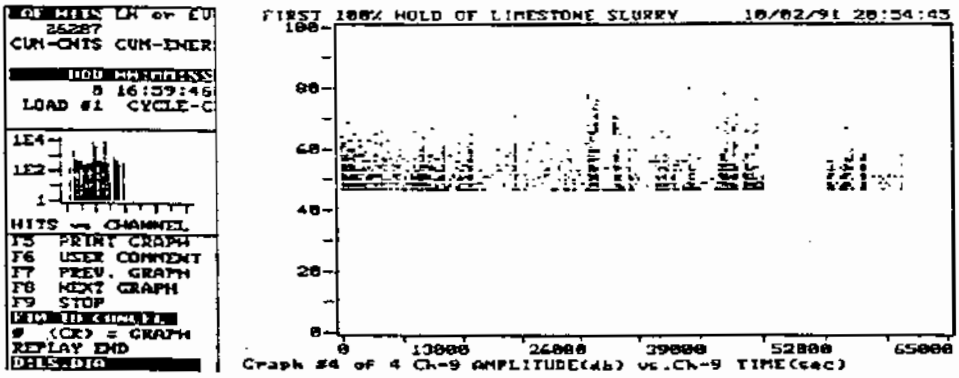

Figure 13. Channel 9 Amplitude vs Time for first 100% hold of LS

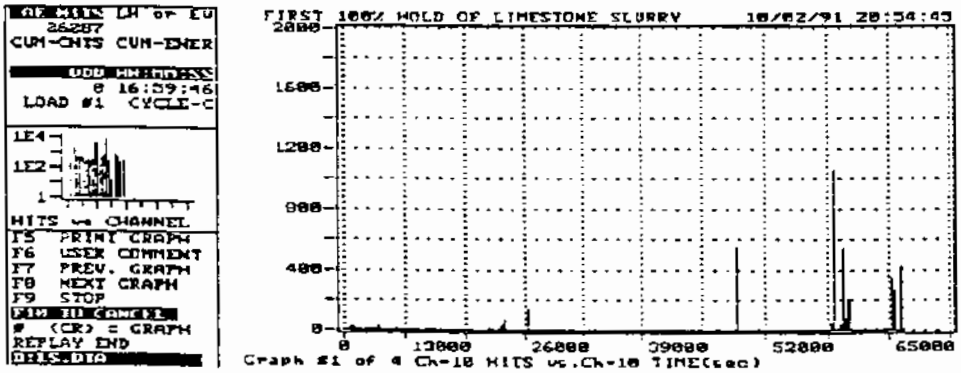

Figure 14. Channel 10 Hits vs Time for first 100% hold of LS

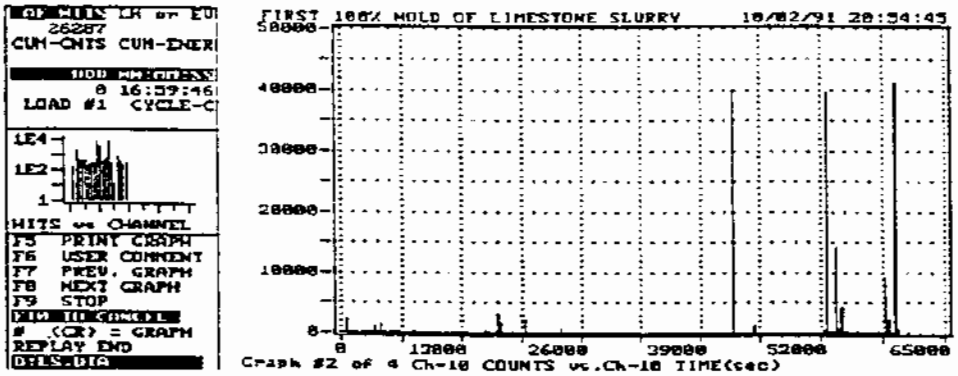

Figure 15. Channel 10 Counts vs Time for first 100% hold of LS

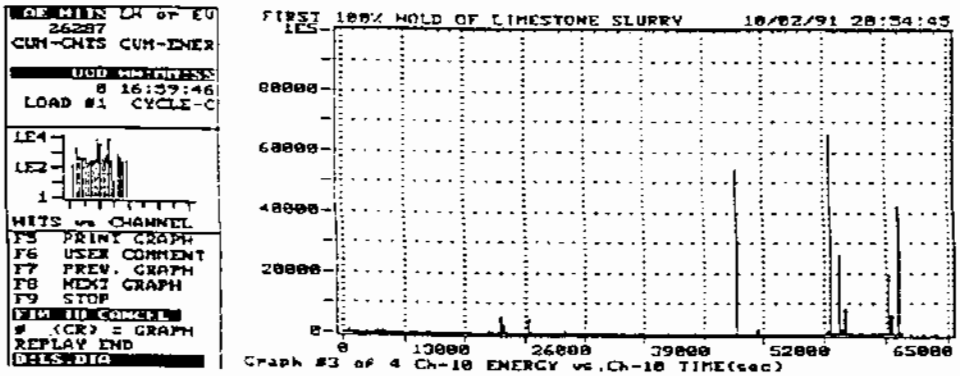

Figure 16. Channel 10 Energy vs Time for first 100% hold of LS

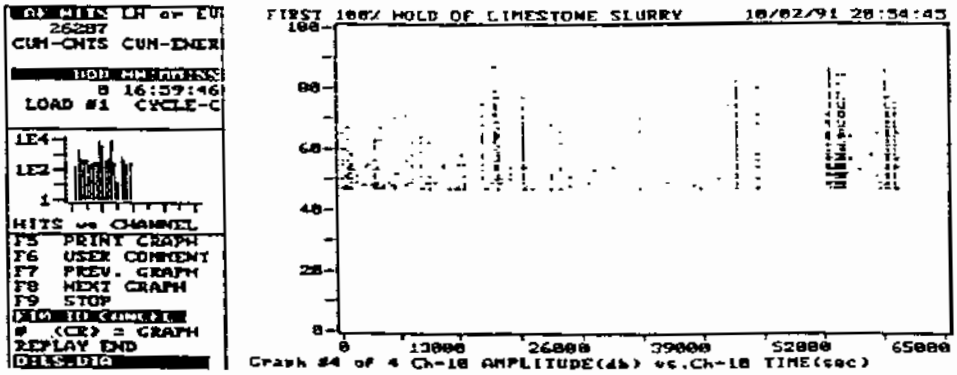

Figure 17. Channel 10 Amplitude vs Time for first 100% hold of LS

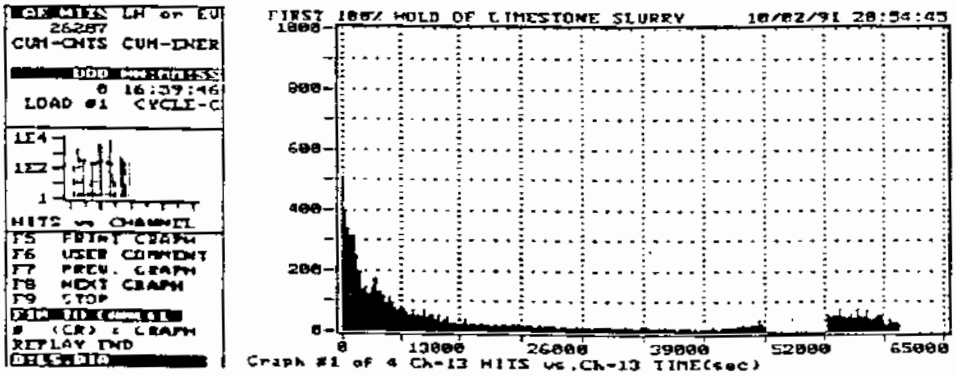

Figure 18. Channel 13 Hits vs Time for first 100% hold of LS

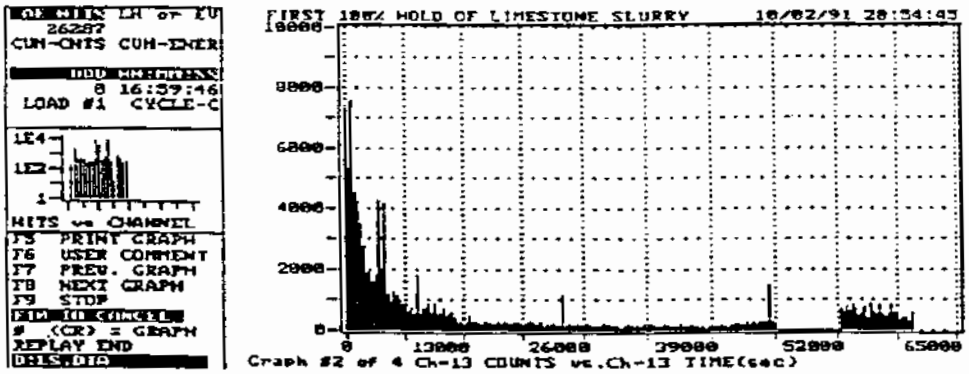

Figure 19. Channel 13 Counts vs Time for first 100% hold of LS

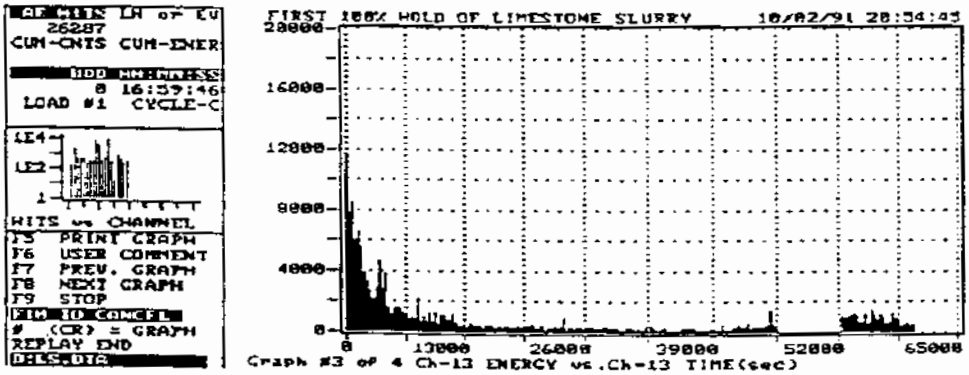

Figure 20. Channel 13 Energy vs Time for first 100% hold of LS

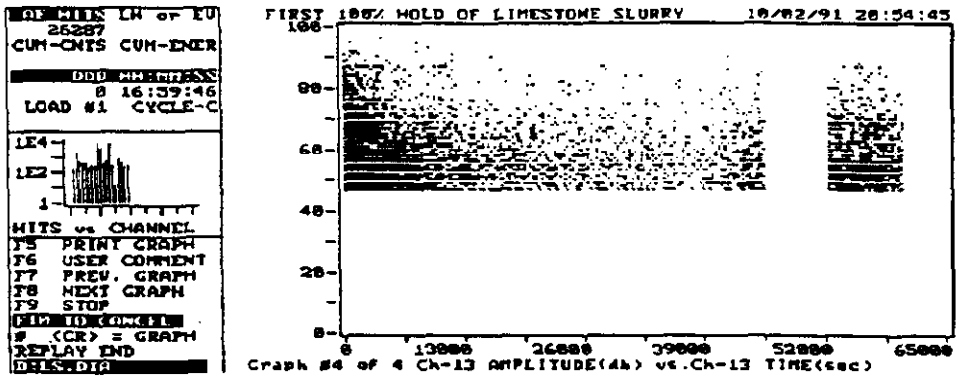

Figure 21. Channel 13 Amplitude vs Time for first 100% hold of LS

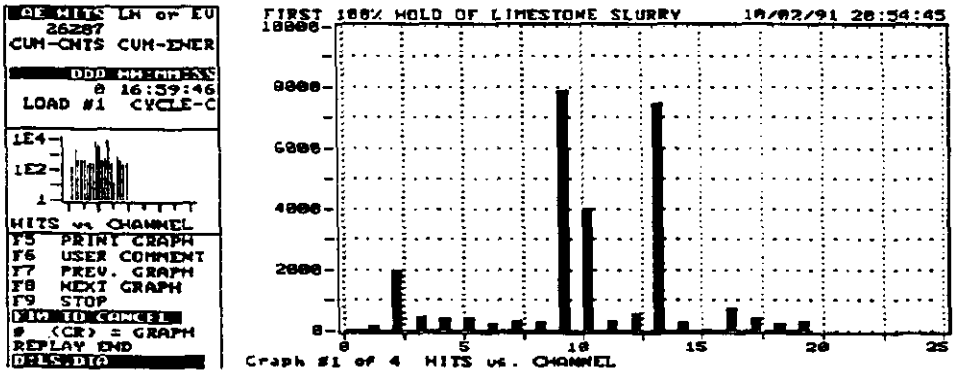

Figure 22. Hits vs Channel for first 100% hold of LS

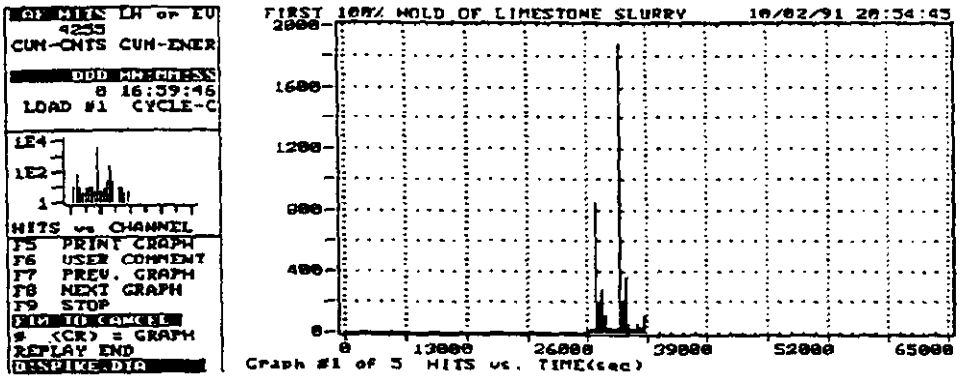

Figure 23. Hits vs Time from 26000-32500 sec, 1st 100% hold of LS

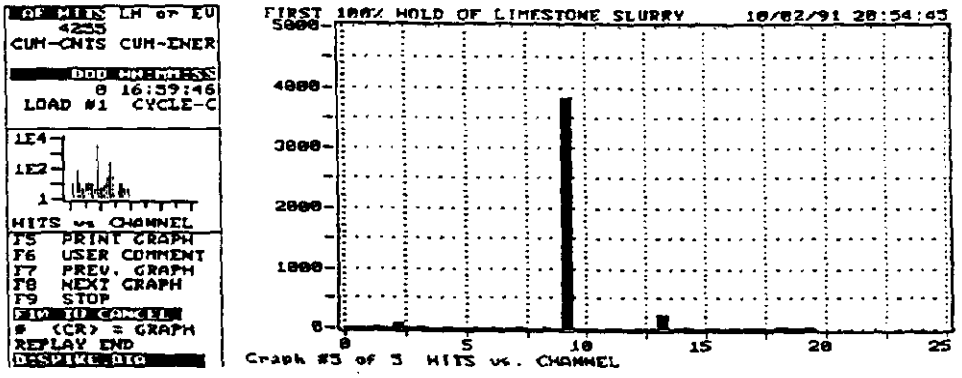

Figure 24. Hits vs Channel of 26000-32500 sec, 1st 100% hold of LS

APPENDIX C

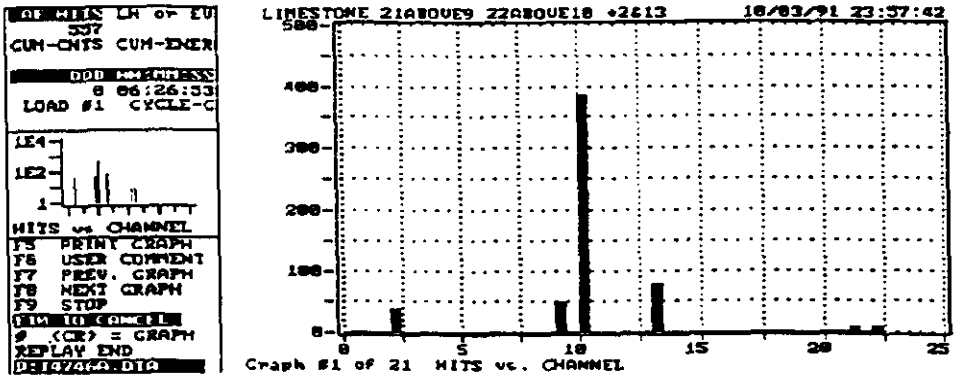

Figure 1. Hits vs Channel for second 100% hold of LS

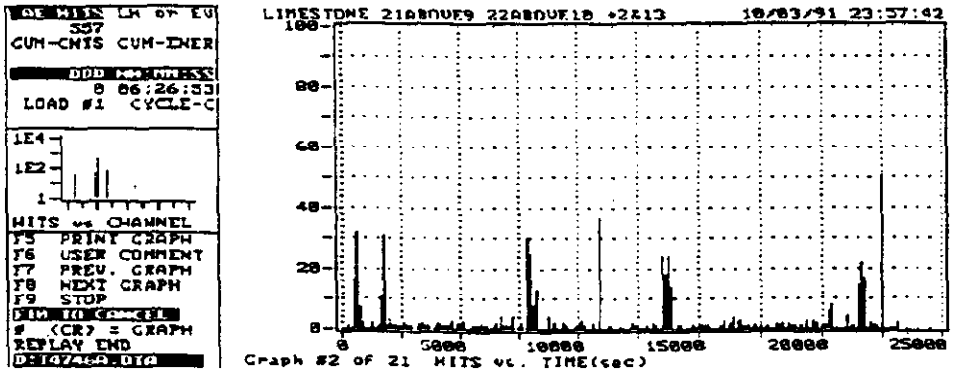

Figure 2. Hits vs Time for second 100% hold of LS

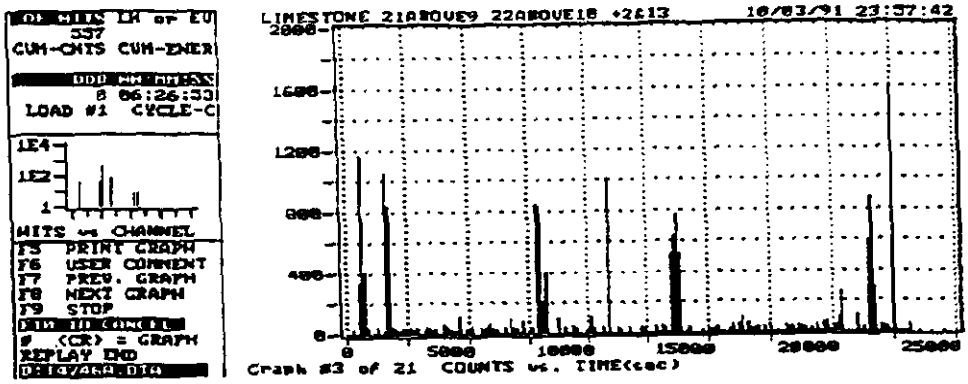

Figure 3. Counts vs Time for second 100% hold of LS

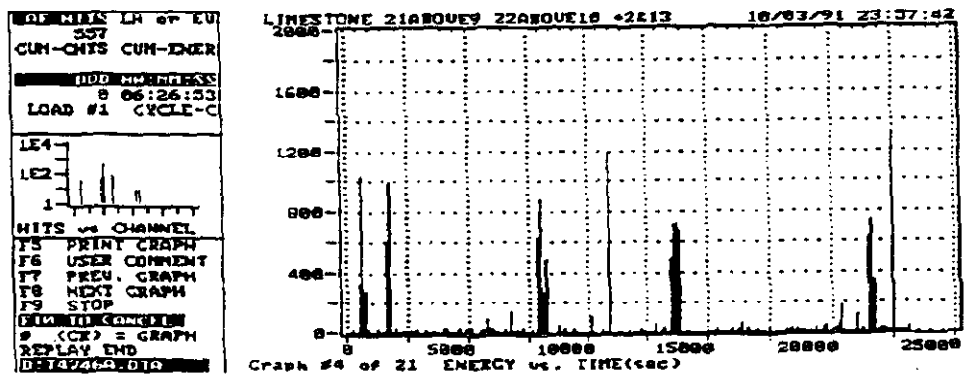

Figure 4. Energy vs Time for second 100% hold of LS

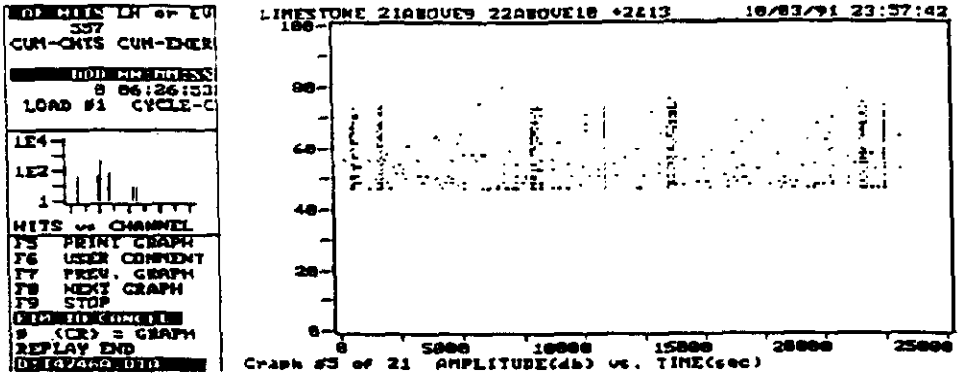

Figure 5. Amplitude vs Time for second 100% hold of LS

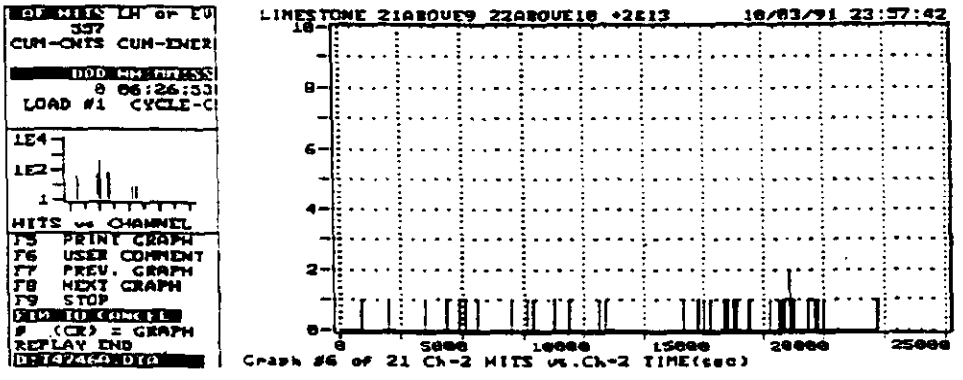

Figure 6. Channel 2 Hits vs Time for second 100% hold of LS

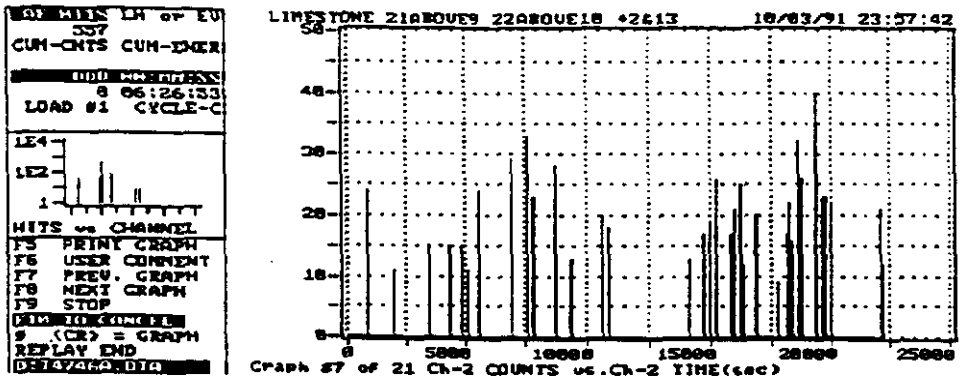

Figure 7. Channel 2 Counts vs Time for second 100% hold of LS

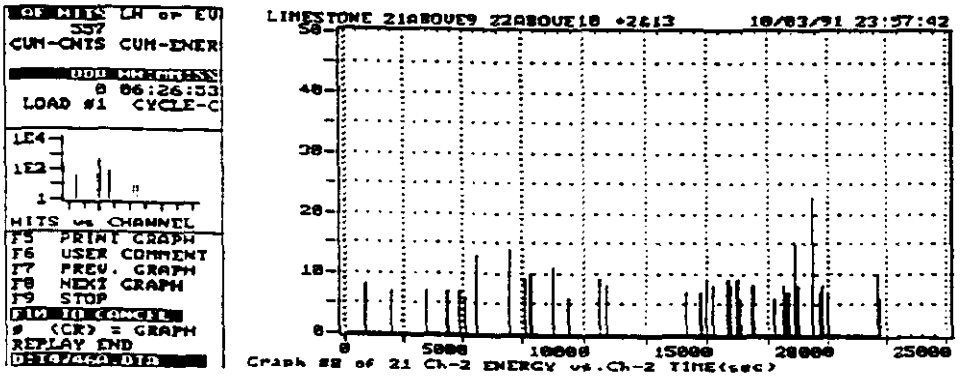

Figure 8. Channel 2 Energy vs Time for second 100% hold of LS

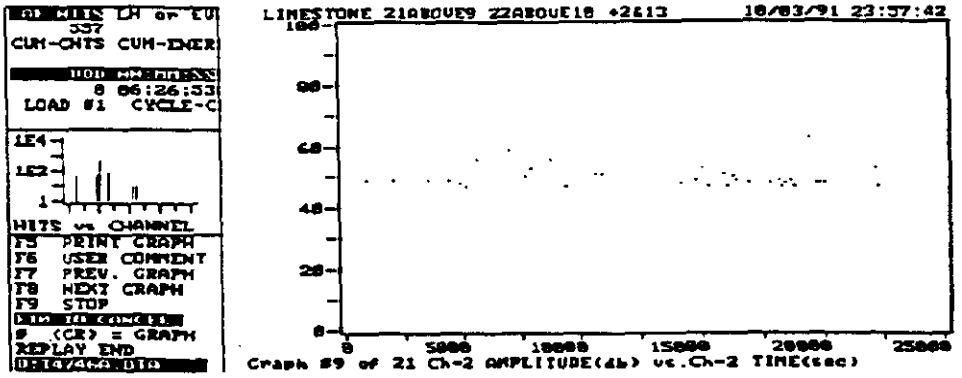

Figure 9. Channel 2 Amplitude vs Time for second 100% hold of LS

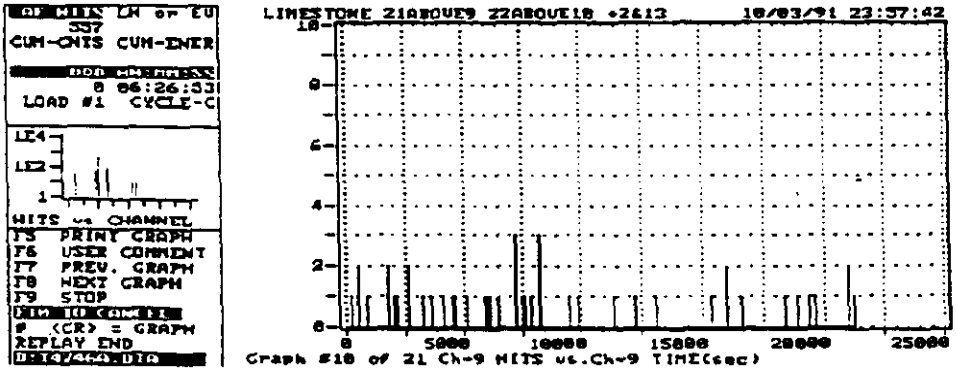

Figure 10. Channel 9 Hits vs Time for second 100% hold of LS

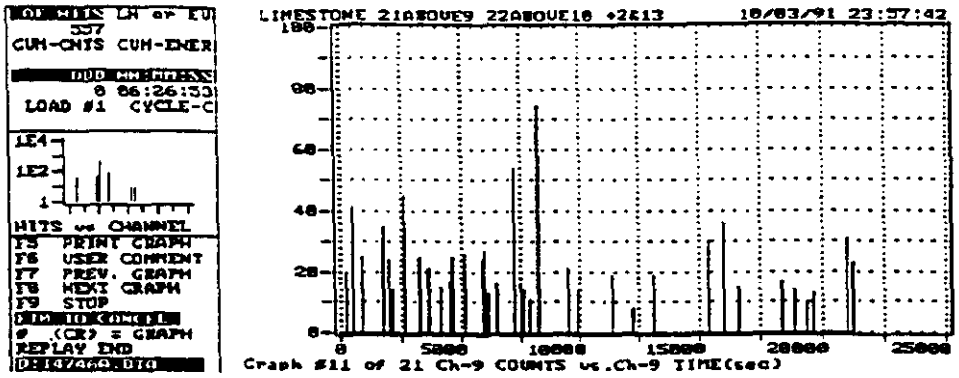

Figure 11. Channel 9 Counts vs Time for second 100% hold of LS

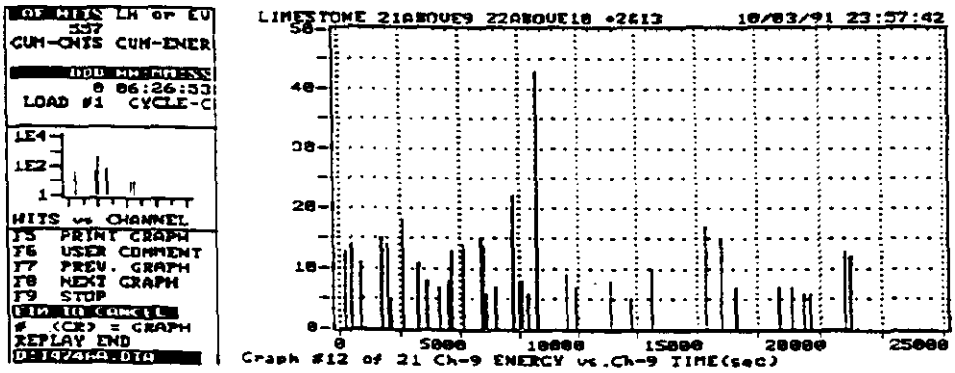

Figure 12. Channel 9 Energy vs Time for second 100% hold of LS

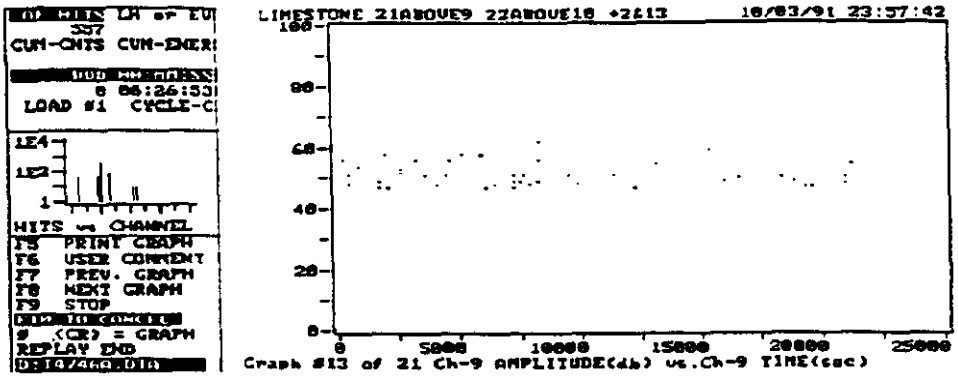

Figure 13. Channel 9 Amplitude vs Time for second 100% hold of LS

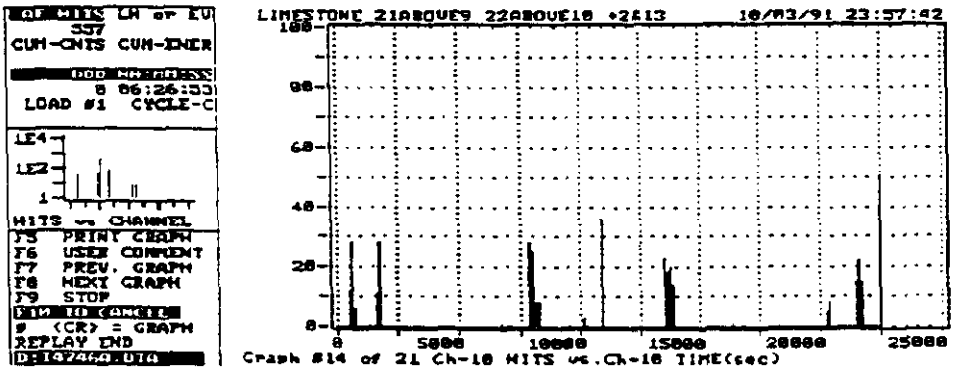

Figure 14. Channel 10 Hits vs Time for second 100% hold of LS

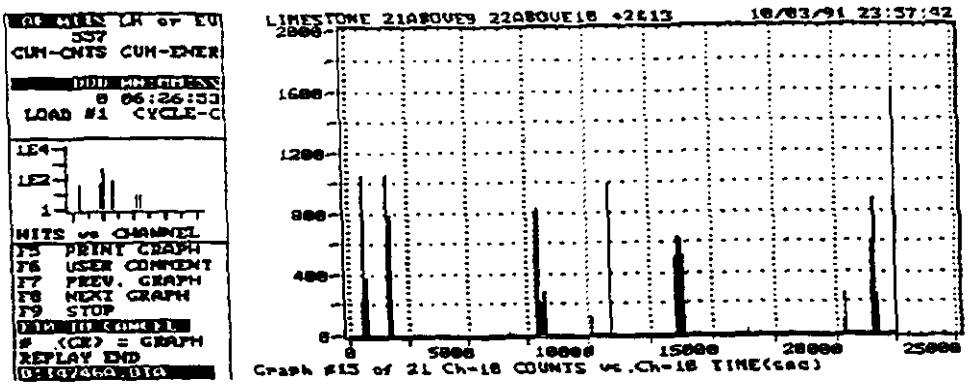

Figure 15. Channel 10 Counts vs Time for second 100% hold of LS

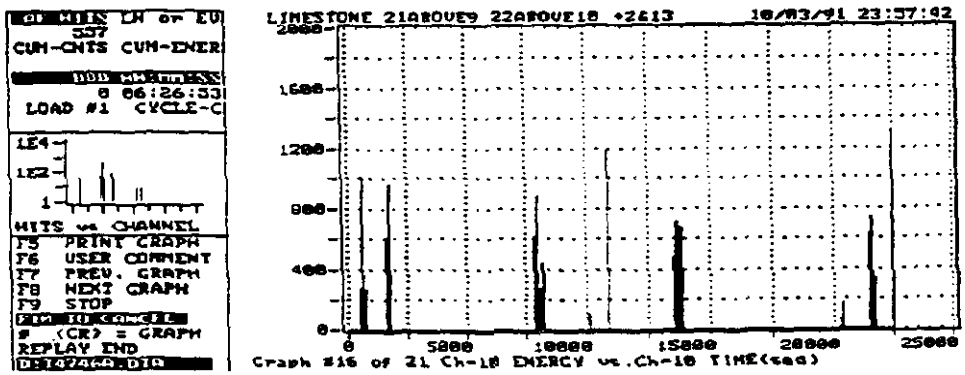

Figure 16. Channel 10 Energy vs Time for second 100% hold of LS

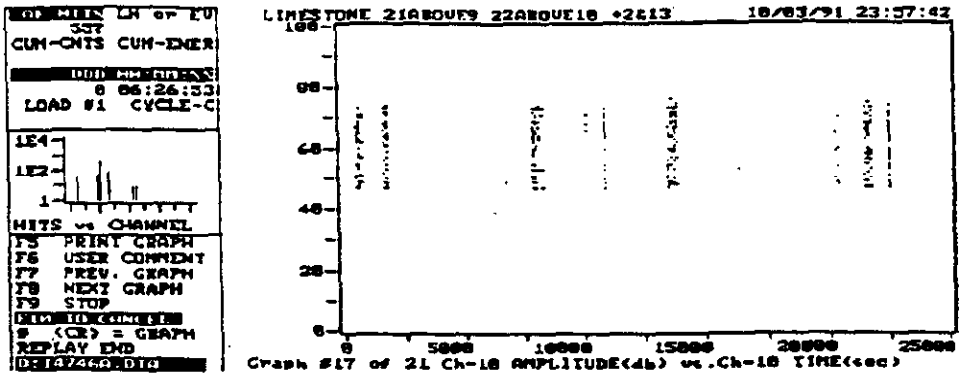

Figure 17. Channel 10 Amplitude vs Time for second 100% hold of LS

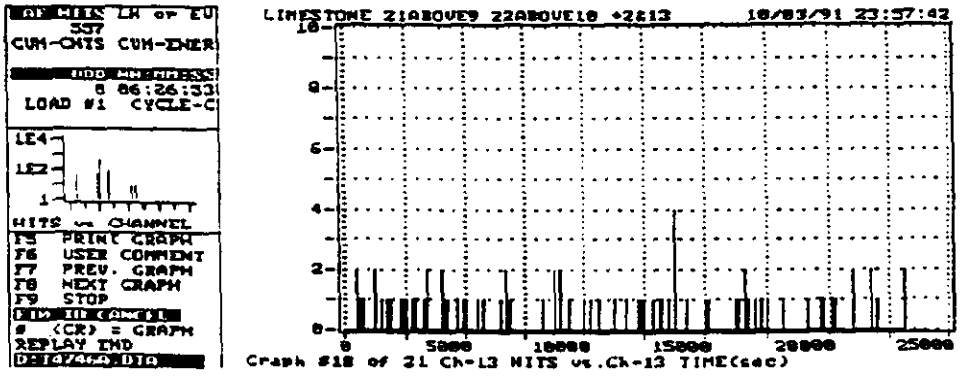

Figure 18. Channel 13 Hits vs Time for second 100% hold of LS

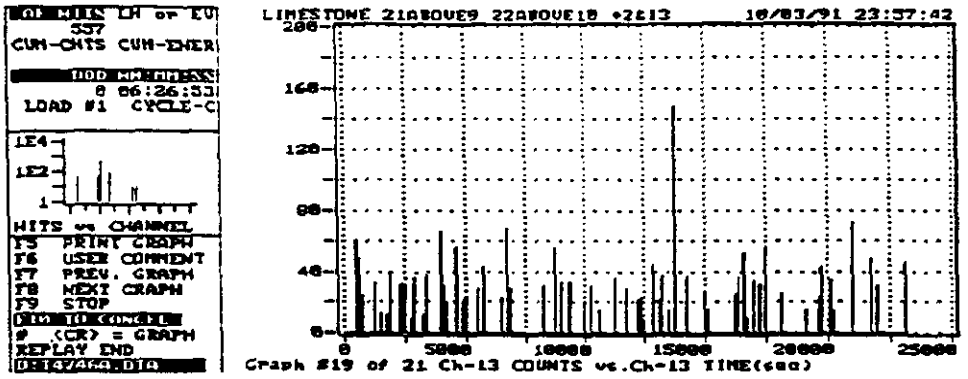

Figure 19. Channel 13 Counts vs Time for second 100% hold of LS

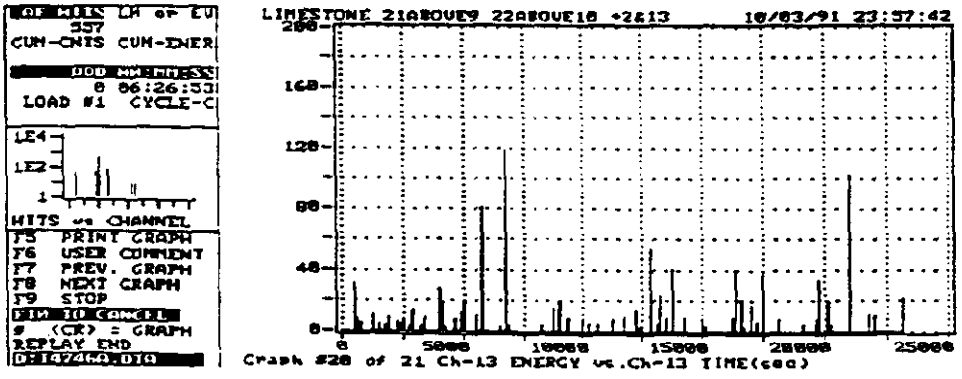

Figure 20. Channel 13 Energy vs Time for second 100% hold of LS

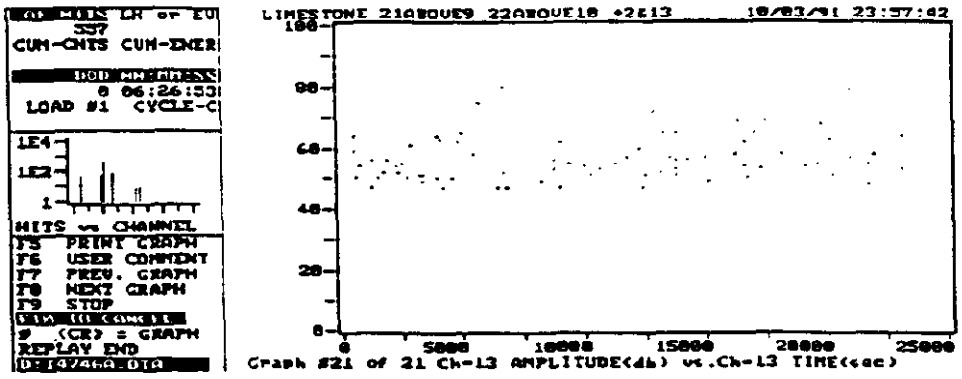

Figure 21. Channel 13 Amplitude vs Time for second 100% hold of LS

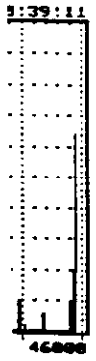

. of LS

APPENDIX D

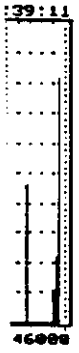

.d of LS

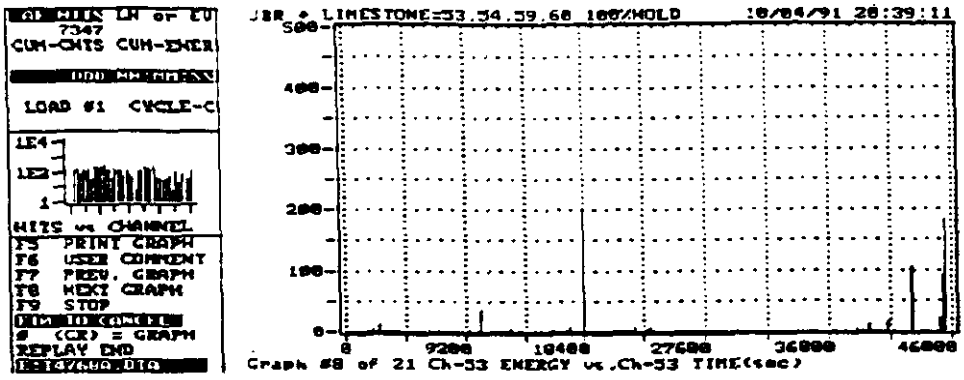

Figure 3. Channel 53 Energy vs Time for third 100% hold of LS

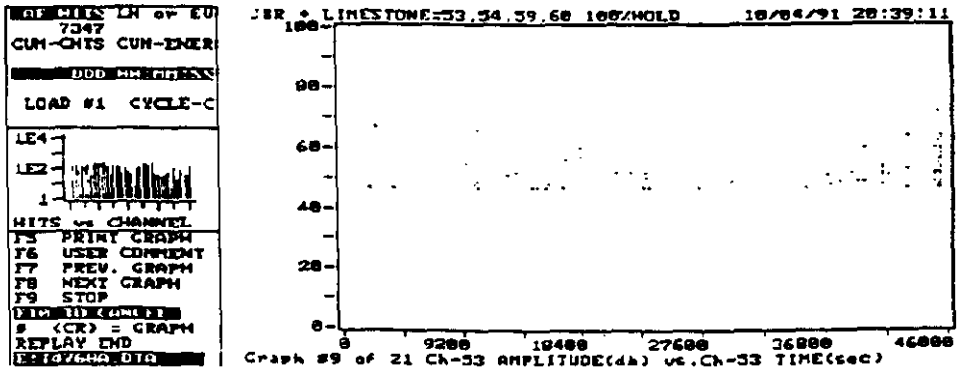

Figure 4. Channel 53 Amplitude vs Time for third 100% hold of LS

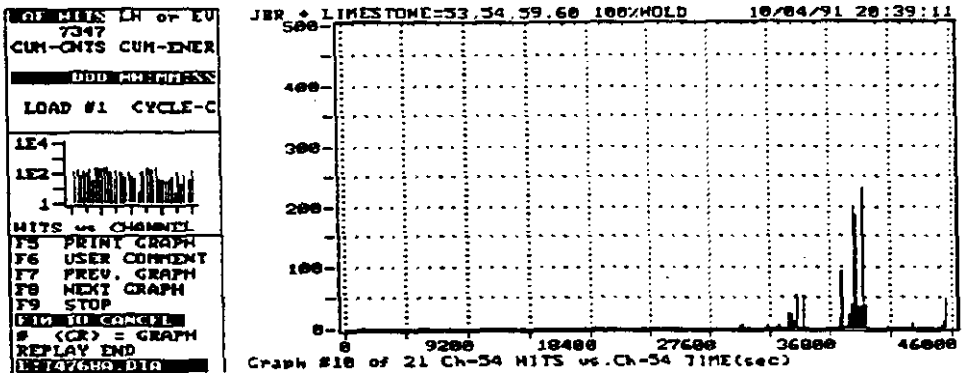

Figure 5. Channel 54 Hits vs Time for third 100% hold of LS

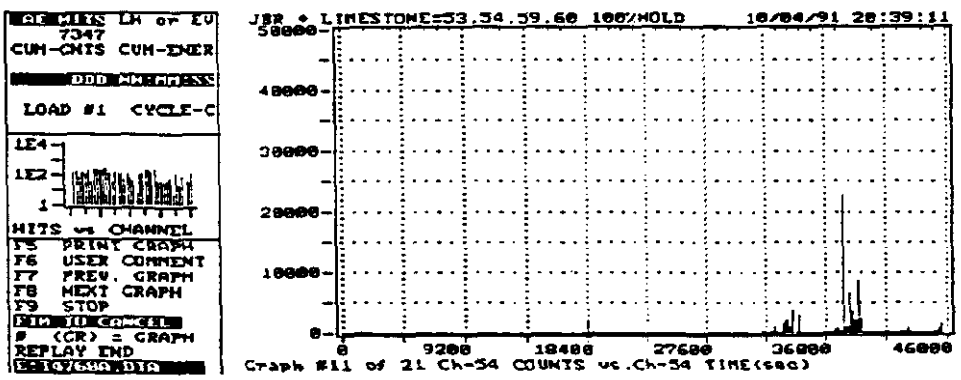

Figure 6. Channel 54 Counts vs Time for third 100% hold of LS

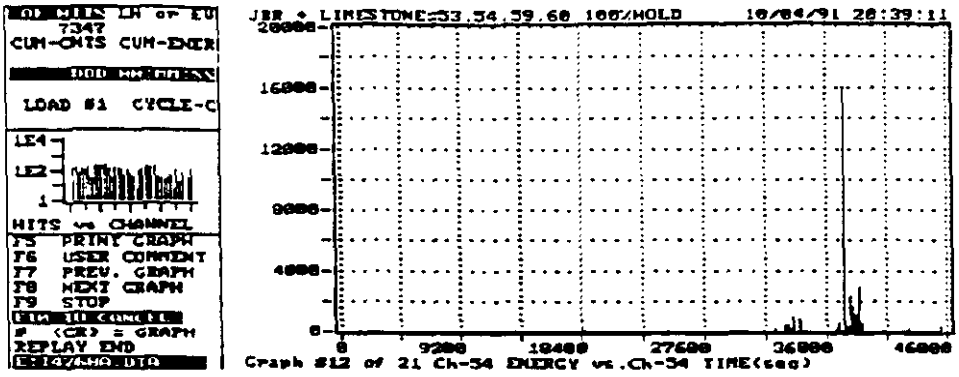

Figure 7. Channel 54 Energy vs Time for third 100% hold of LS

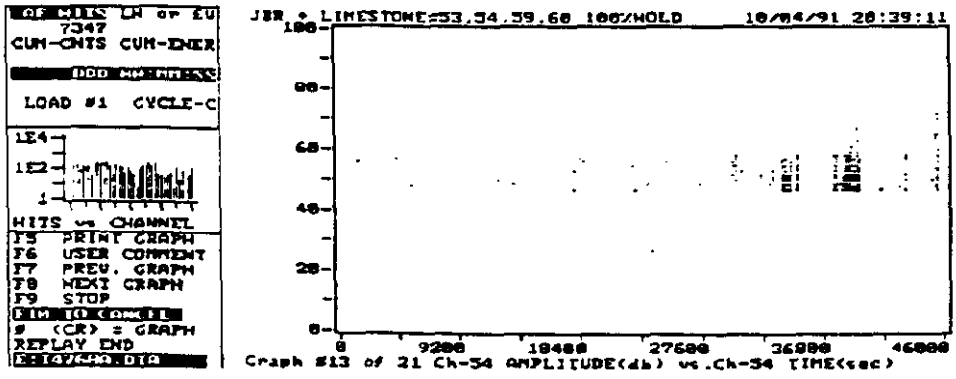

Figure 8. Channel 54 Amplitude vs Time for third 100% hold of LS

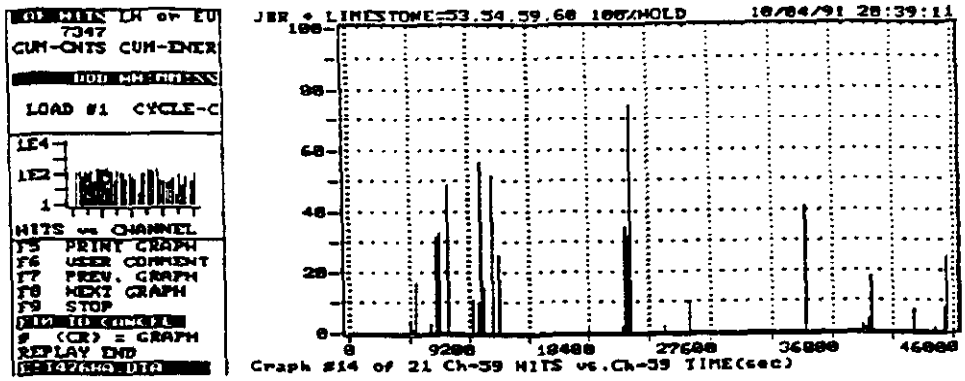

Figure 9. Channel 59 Hits vs Time for third 100% hold of LS

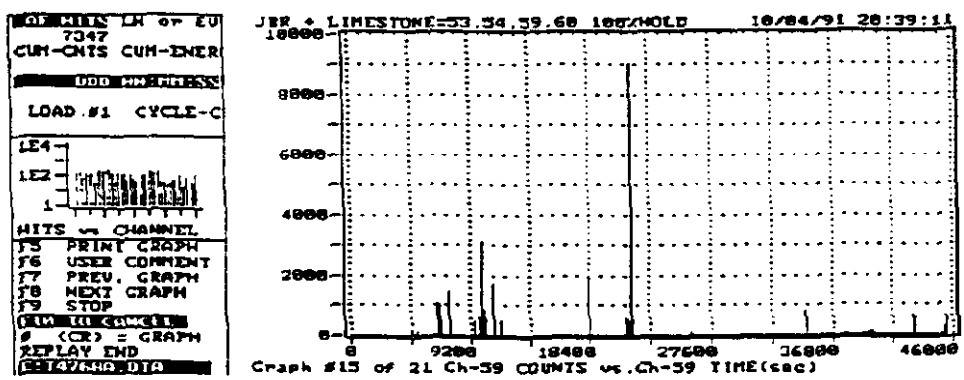

Figure 10. Channel 59 Counts vs Time for third 100% hold of LS

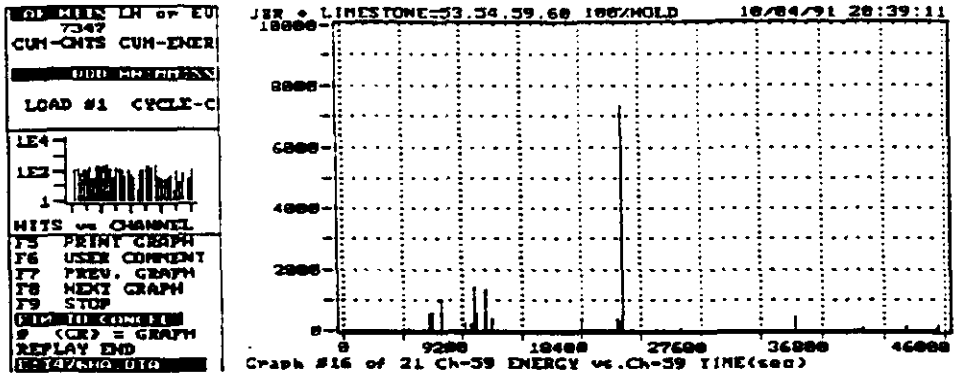

Figure 11. Channel 59 Energy vs Time for third 100% hold of LS

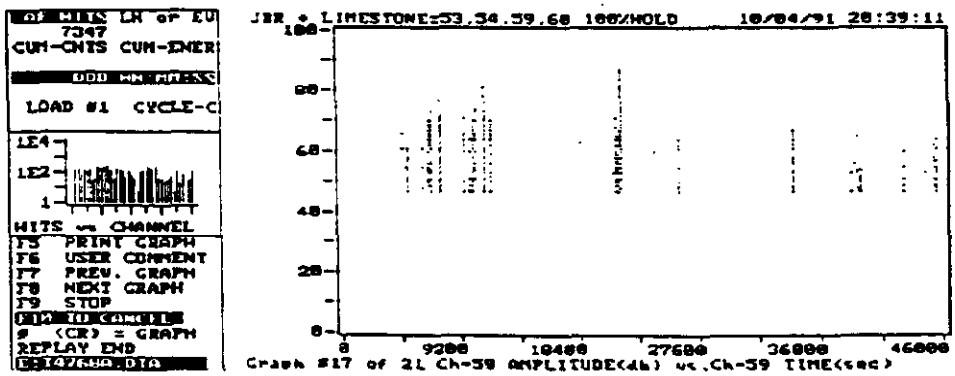

Figure 12. Channel 59 Amplitude vs Time for third 100% hold of LS

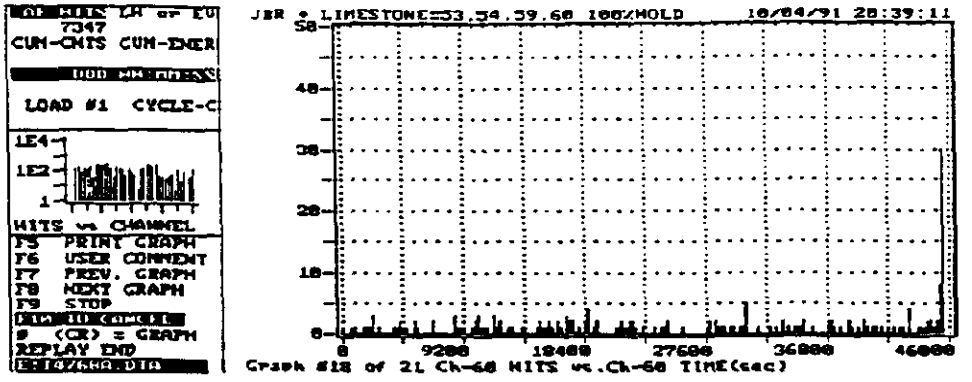

Figure 13. Channel 60 Hits vs Time for third 100% hold of LS

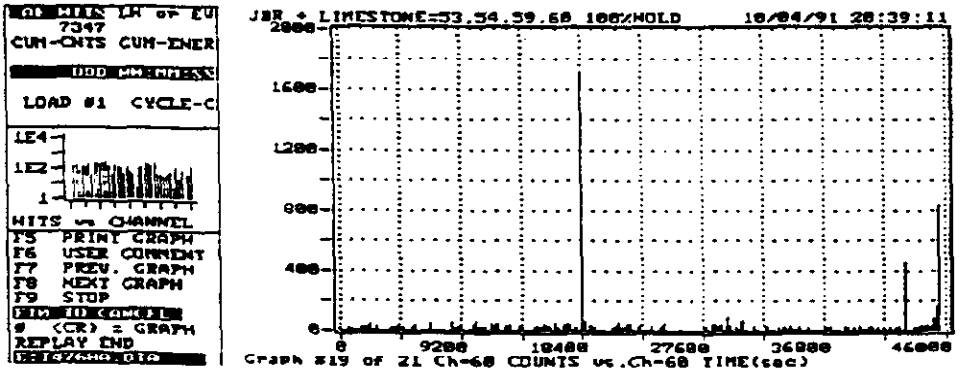

Figure 14. Channel 60 Counts vs Time for third 100% hold of LS

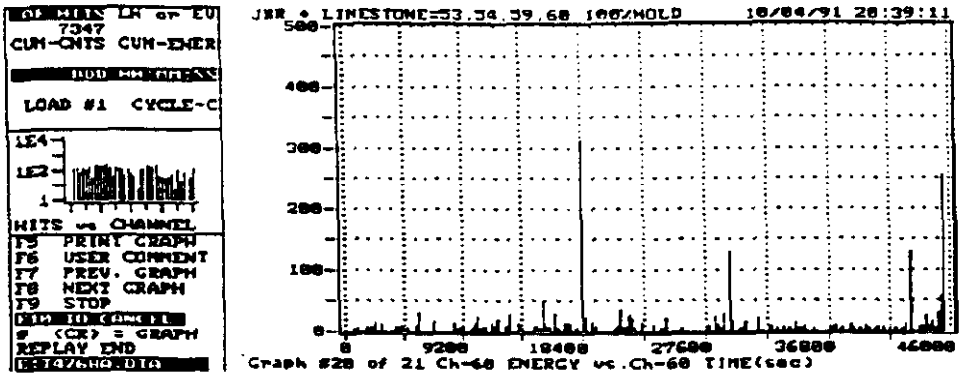

Figure 15. Channel 60 Energy vs Time for third 100% hold of LS

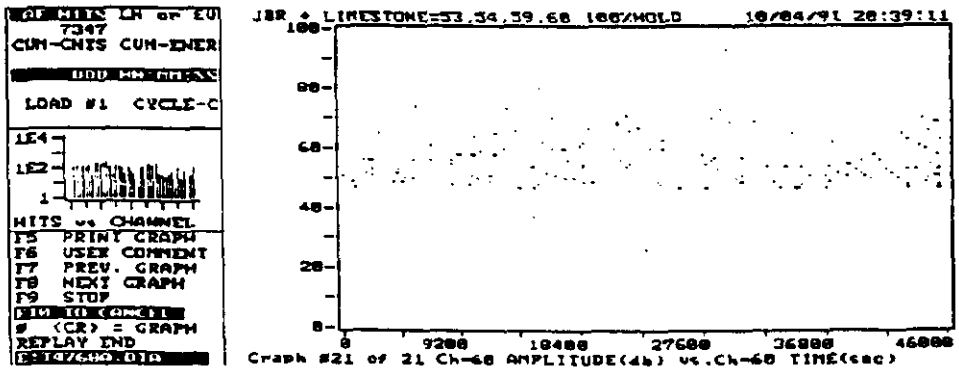

Figure 16. Channel 60 Amplitude vs Time for third 100% hold of LS

APPENDIX E

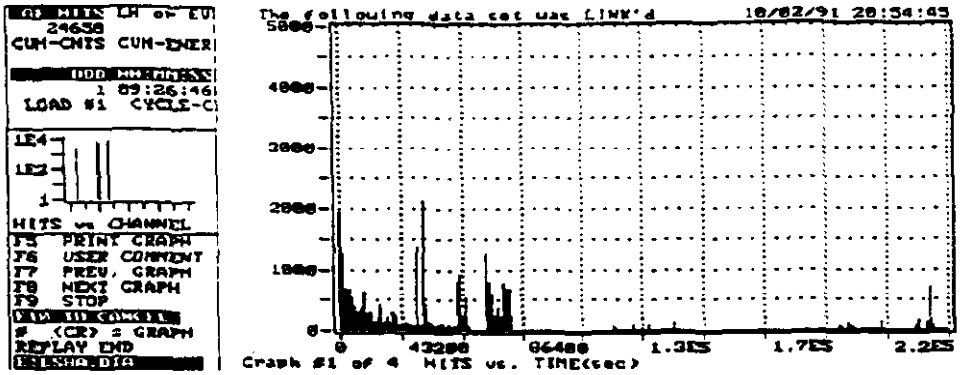

Figure 1. Hits vs Time for entire 100% hold of LS

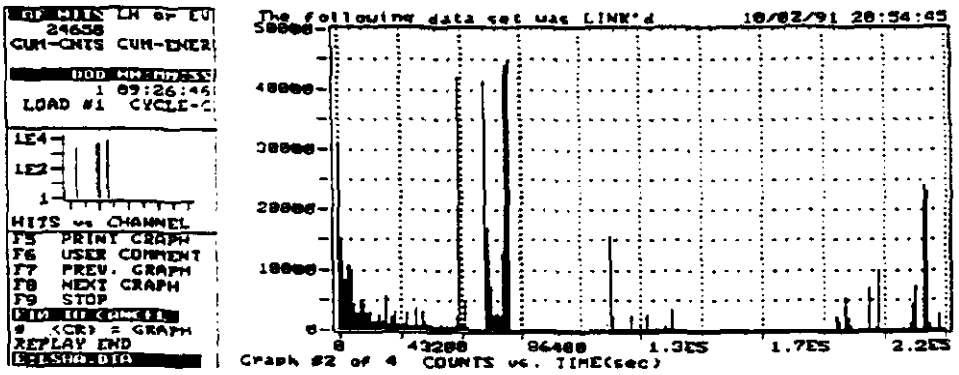

Figure 2. Counts vs Time for entire 100% hold of LS

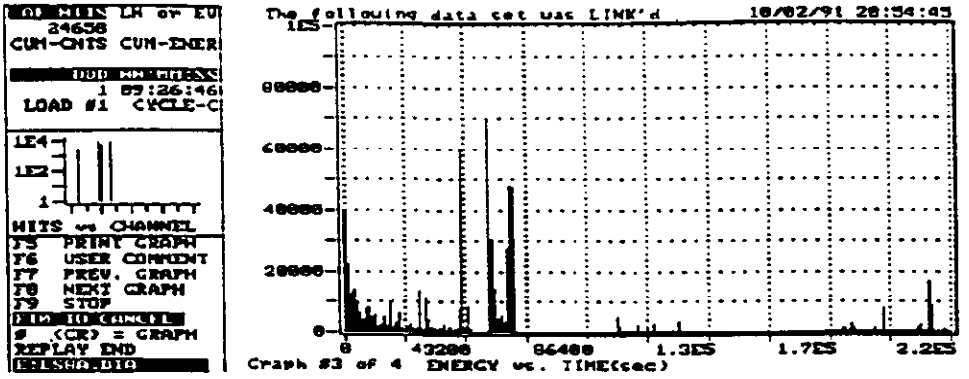

Figure 3. Energy vs Time for entire 100% hold of LS

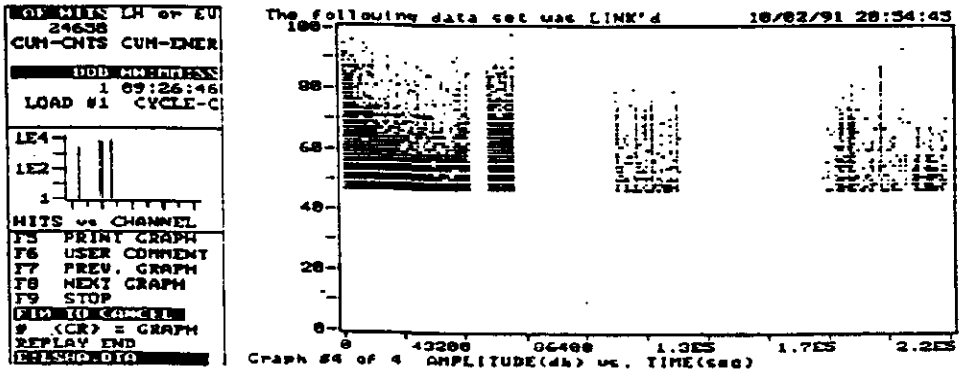

Figure 4. Amplitude vs Time for entire 100% hold of LS

APPENDIX F

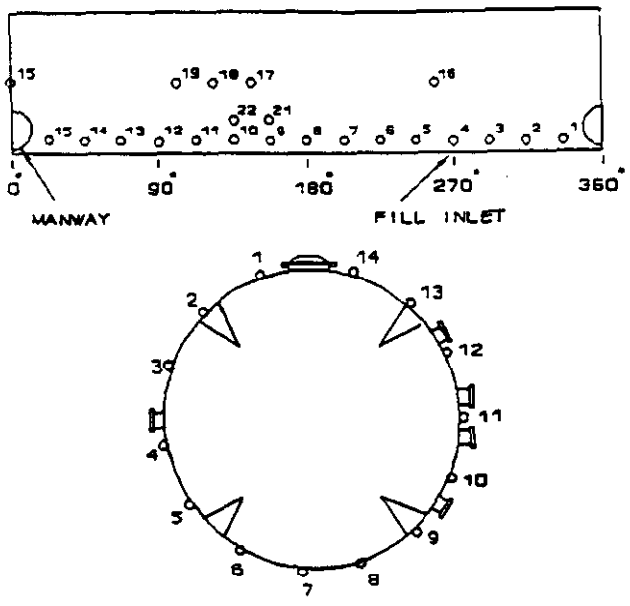

Figure 1. Sensor arrangement for Limestone Slurry Tank (LS)

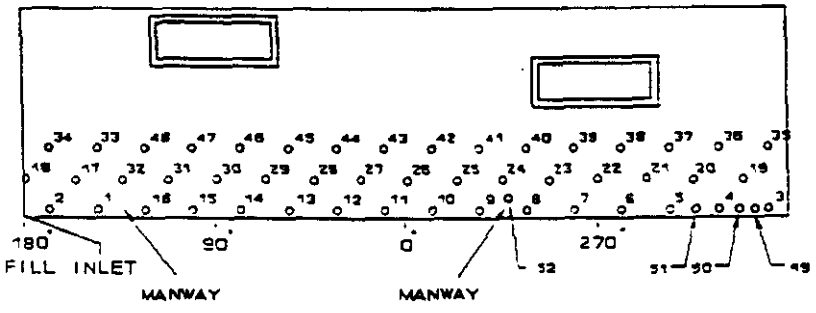

Figure 2. Sensor arrangement for Jet Bubble Reactor (JBR)

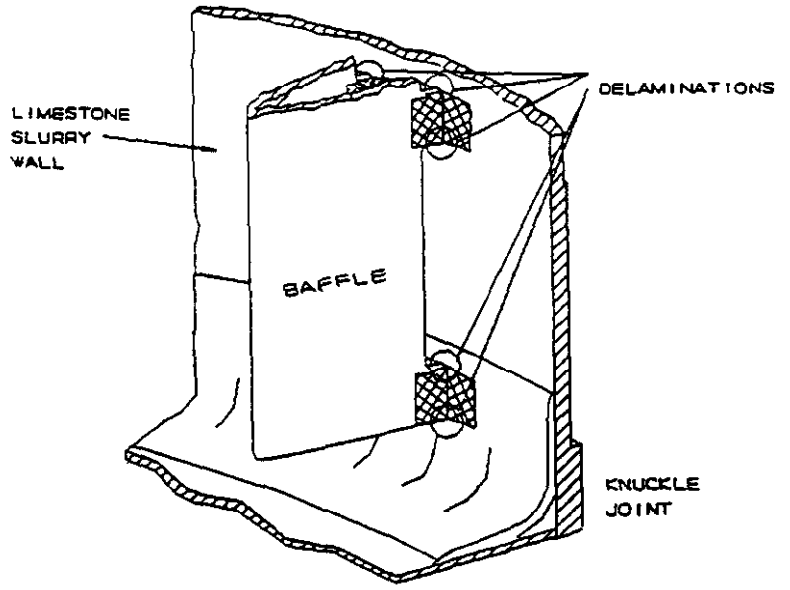

Figure 3. Detail drawing of visual delamination sites

PHYSICAL
ACOUSTICS
CORPORATION

Acoustic Emission Testing of On-site Fabricated FRP Vessels Phase II

Final Report
Project R92-336
January 24, 1992

Revised
August 21, 1992

Prepared for: Dr. Kamyer Vakhsoorzadeh
Southern Company Services
P.O. Box 2625
Birmingham, AL 35202

Prepared by: Bruce E. Gilbert

Revised by: David L. Kesler
Donald J. Pointer
Physical Acoustics Corporation
15 Princess Road
Lawrenceville, NJ 08648

Acoustic Emission Testing of On-site Fabricated FRP Vessels Phase II

Final Report
Project R92-336
January 24, 1992

Revised
August 21, 1992

Prepared for: Dr. Kamyer Vakhsoorzadeh
Southern Company Services
P.O. Box 2625
Birmingham, AL 35202

Prepared by: Bruce E. Gilbert

Revised by: David L. Kesler
Donald J. Pointer
Physical Acoustics Corporation
15 Princess Road
Lawrenceville, NJ 08648

Executive Summary

Two on-site fabricated Fiber Reinforced Plastic (FRP) vessels were tested using Acoustic Emission (AE) Non-Destructive Testing (NDT). Physical Acoustics Corporation was contracted by the Southern Company Services to perform the tests during an initial hydro test. The vessels are located at Plant Yates of the Georgia Power Company and are components in the CT-121 Flue Gas Desulfurization (FGD) process.

Both vessels were extensively tested using acoustic emission which proved its feasibility for providing "real time" monitoring of the structural integrity during proof loading. Acoustic emission also detected areas of delamination around the internal structure-to-vessel wall interface. The data obtained shows continuous emission during the testing which is indicative of a structure seeking equilibrium. An extensive data baseline has been saved for future testing of the vessels. This baseline will be compared with data obtained at a later date.

Table of Contents

1. Introduction

Southern Company Services has recently constructed two large Fiber Reinforced Plastic (FRP) vessels at Plant Yates of the Georgia Power Company. The FRP vessels are components in the CT-121 Flue Gas Desulfurization (FGD) process. To verify the integrity of the FRP, on-site construction, some form of structural testing was required. Physical Acoustics Corporation (PAC) was contracted to perform structural integrity testing using Acoustic Emission (AE) testing techniques. The AE testing was performed in conjunction with previously scheduled hydro tests.

Acoustic emission is a wide-area, nondestructive technique that "listens" to a structure as it responds to an applied stress. Acoustic emissions are high frequency stress waves which are given off by anomalies within a structure as it undergoes stress. In this instance, the stress is applied to the vessel by filling it with water. By using a global array of piezoelectric sensors, the structure as a whole can be monitored, as opposed to the local scanning techniques of traditional NDT methods.

The CT-121 system includes two FRP vessels; the Limestone Slurry (LS) tank and the Jet Bubble Reactor (JBR). The primary goals of the AE tests were:

a) Detect, locate and classify acoustic emission sources.

b) Evaluate the effectiveness of AE in distinguishing between acoustic emissions generated by fiber breakage, fiber debonding/pull-out, resin cracking, delaminations, secondary bond failures, background noise caused by internal structures, rubbing, etc.

c) Provide an AE baseline for both the Jet Bubble Reactor (JBR) and Limestone Slurry (LS) tank for future AE testing.

d) Develop quality control for this portion of FRP development/procedure.

e) Transfer of AE technology to the Southern Company research group.

2. Approach

The acoustic emission test personnel from Physical Acoustics were:

Bruce Gilbert	(AE level II)
Donald Pointer	(AE level II)
David Kesler	(AE level III)

The acoustic emission test equipment was supplied by Physical Acoustics and consisted of a PAC 72 channel SPARTAN-AT controlled by an IBM-PC compatible 386 host computer. The data acquisition system employed 100-300 kHz bandpass filters and the threshold for all tests was set at a fixed value of 35 dB. The software used was SA-LOC version 3.03 dated 1/24/91. The sensors used for this test were PAC model R15I piezoelectric transducers with integral 40 dB gain preamplifiers. Sensors were resonant at 150 kHz.

Attenuation studies were performed on each vessel to determine AE wave propagation characteristics. From this information, a sensor spacing pattern was calculated. The sensor locations on the vessels can be seen in Figures 1a & 1b of Appendix A, immediately following the text. Sensors were mounted using a hot glue adhesive (per ASTM E-650); this also doubled as the couplant. Some sensors were used as guards to detect extraneous noise. Lead break calibrations (per ASTM E-976) were performed just prior to each test using a Hsu-Nielsen source to verify the sensor's acoustic coupling to the structure.

Stressing of the vessels was accomplished using water at atmospheric pressure and temperature. Prior to loading, a 30 minute background noise check was performed. During this time, no appreciable data was recorded and no sources of extraneous data were identified. Vessel stressing was accomplished by filling the tanks from a fire hose attached to the bottom of the vessel. At approximately the 10% level, it was verified that the water turbulence would not be a source of background AE. Stressing of the vessels was accomplished following standardized atmospheric vessel stressing sequences (ASME Section 5, Article 11). Load-hold periods were performed at approximately 50%, 75% and 100% of the vessel test capacity. The load-holds lasted for greater than 5 minutes.

The stressing of the JBR marked the first hydrostatic loading of the vessel. Due to the complexity of the vessel, it was not possible to apply a stressing sequence that would subject the entire vessel to a proof load. Only the lower 50% of the vessel was subjected to hydrostatic loading and acoustic emission evaluation.

In April 1991, the Limestone Slurry (LS) tank was tested by PAC using acoustic emission. The LS vessel was retested during the second visit, along with the JBR.

3. Results

Test Notes for the Jet Bubble Reactor:

Physical Acoustics personnel arrived at Plant Yates Monday morning, 9/30/91. An initial coordination meeting was held in which the testing plans were reviewed by key personnel from Ershigs (the vessel manufacturer), Georgia Power, Plant Yates, Southern Company Services and PAC. Following this meeting the equipment was setup in the trailer adjacent to the JBR. Attenuation measurements were taken on the JBR. Throughout the remainder of Monday the sensors were mounted and calibrated in preparation for the first of two AE/hydro tests on the JBR.

Filling of the JBR began at approximately 9:00 AM Tuesday morning. This test was initiated by Ershigs to check for leaks. Since work was still being performed on the vessel during this loading phase, no AE data was taken. During this period the remaining AE sensors were installed and calibrated per ASTM E-976 (see Figure 1b for sensor locations). At the load-hold periods, work on the vessel was terminated so that useful AE data could be collected. AE data was recorded at each load-hold period. Each load-hold lasted at least 30 minutes. At the 100% load-hold level, AE data was recorded for 11 hours. This extended hold period was required by Ershigs. On Wednesday morning the load-hold at 100% on the JBR was completed and the JBR was drained.

On Thursday, October 3, the JBR was refitted with sensors for the second AE test. The sensor locations for this test were in the identical locations as specified in the first test. All sensors were calibrated and prepared for the test. The test was scheduled to commence on Friday morning.

A second loading of the JBR began Friday, October 4, at 9:00 AM. AE data was recorded at 50%, 75%, 87.5% and finally 100% load-hold levels. The 100% level was reached at 5:30 PM on Friday evening and maintained for over one hour. Upon completion of this test, the JBR remained at the 100% level.

Test Notes for the Limestone Slurry Tank:

On Wednesday morning, October 2, 1991, the AE retest of the LS tank began. Sensors were mounted (see Figure 1a for locations) and calibrated per ASTM E976. Filling of the LS tank was begun at 3:00 PM that afternoon. AE data was acquire at the 50%, 75% and 100% load-hold periods. The 100% level was reached at 9:00 PM that evening. An extended hold period was initiated which lasted until 2:00 PM on Thursday afternoon. On the basis of the initial findings of this hold, it was decided that further evaluation of the LS tank was warranted. The LS tank was left at the 100% level. The LS was refitted with a limited number of sensors in the regions of high AE activity. The sensors used were in locations 2, 9, 10 and 13. To further the evaluation, and also investigate the possibility of AE initiating from portions of the vessel near the 1st wall seam, two additional sensors were mounted above sensors 9 and 10. These sensors were

numbered 21 and 22 (see Figure 1a). Following setup, the second test of the LS tank began at the 100% load-hold level. This load-hold lasted for greater than six hours. Following the termination of this test, the LS tank was again left at the 100% load-hold level.

Test Notes for Simultaneous testing of the JBR and LS:

The LS tank was refitted with sensors in positions 2, 9, 10 and 13 to continue the evaluation. Over the next 12 hours, the JBR and LS vessels were monitored simultaneously for acoustic emissions. The distinction between sensor arrangements and test vessels was recorded within the computer. On Saturday morning, October 5, all testing terminated.

For the remainder of Saturday and Sunday data analysis was performed off site. By Monday morning both vessels were drained and opened for visual examination. Later on Monday, a debriefing meeting was held to discuss the results.

4. Discussion

Evaluation of the Jet Bubble Reactor and Limestone Slurry tank was based on their ability to become acoustically stabilized. At a fixed load, a structurally stable vessel will be acoustically dormant. An unstable vessel will continually generate acoustic activity. Towards failure, this activity may increase exponentially. This AE evaluation technique is best applied during load-hold periods in the stressing schedule. It is during these periods when background noise and transient phenomenon are at a minimum. One of the best ways to evaluate the data, and ultimately the integrity of the vessel, is through graphical displays. By graphically correlating intensities of the data set, an analysis of the JBR and LS vessels is possible. Test results and conclusions were developed from these graphs.

Jet Bubble Reactor:

The JBR vessel was loaded and held at the 100% stress level twice during the AE monitoring. From these loadings, two data files were acquired. The data files were post test filtered at a fixed threshold of 47dB to eliminate any extraneous background noise. The resulting files provided more than 11 hours of data. Figures generated for the JBR analysis can be found in Appendix A.

Figures 3 through 23 of Appendix A provide a graphical analysis of the 2 data files. For comparison purposes similar graphs between data files have been included on the same page. The odd numbered plots represent the 1st load-hold while the even numbered plots represent the 2nd load-hold. The axis on each graph has been fixed.

Figures 3 and 4 of Appendix A show the distribution of hits among the channels.

The most active channels during the first hold period are channels 1, 6, 8, 15, 25 and 49. It can be seen from Figure 4 of Appendix A that the activity for all channels was reduced significantly when compared to the first loading shown in Figure 3. However, all channels still remained active during the second loading. Activity during the second 100% load-hold indicates a Felicity Ratio of less than 1.

Figures 5 and 6 of Appendix A show the amplitudes that were recorded during each hold period. During the first test there were a significant number of hits over 80dB. During the second test the amplitudes were slightly lower but still maintain values above 70dB. Activity above the 60dB level are indications of delamination and fiber breakage.

From Figures 7 and 8 of Appendix A it is apparent that the hit rates remains relatively constant after their initial decays. Although a decay in rate was present, the vessel never completely stopped emitting. This acoustic instability indicates a continued redistribution of the stress within the vessel.

Of interest in the first loading, is the "spike" data that occurred at approximately 5 hours (18K seconds). This type of emission is indicative of sudden releases of energy characteristic of damage propagation within the FRP.

Figures 9 and 10 of Appendix A indicate the energy rate recorded during the hold periods. As previously noted, the spike emission is of great concern. These spikes are from hits of middle to upper amplitudes (60 - 80 dB) and relatively long duration.

Figures 11 and 12 of Appendix A show the amplitudes for all channels as a function of time. It can be seen from these plots that the amplitude levels remained relatively consistent throughout the hold period.

Figures 13 and 14 of Appendix A represent the individual channel activity versus time. From this plot it is sometimes possible to note pattern in channel activity.

Figures 15 and 16 of Appendix A show the individual hit duration as a function of channel. These graphs indicate long duration, burst type emissions. The burst type emission was heavily noted during the first hold. This emission pattern decayed during the second hold. The continuing long duration emission throughout the second load-hold is indicative of delimitation growth.

To further investigate the status of the vessel, the last hour of data from the second hold period was scrutinized. Figures 17 through 23 of Appendix A represent this data. The figures generated for this analysis were the same as reviewed above with the exception of increased resolution.

Figure 17 indicates that the activity was relatively limited and scattered among the channels. From figure 18 it can be seen that hits reached a maximum amplitude of 60dB. Figure 19 indicates that the emissions were also scattered throughout the hour. The remaining figures serve to support the observation of continuing low level emission as a function of time. Although activity rates and intensity have decreased significantly,

AE is still being generated. Accepted industry standards do not allow any unidentified AE activity during the first 30 minutes of the 100% load-hold.

Limestone Slurry Tank:

Comments are based on the activity of the vessel during the load-up portion of the test and the 60 hour load-hold at 100%. For analysis purposes, the data was filtered at a threshold of 47dB. This threshold was consistent with the previous test in April 1991. Figure 1a of Appendix A shows the initial AE sensor layout for the LS vessel. The bottom portion of the vessel wall was heavily covered with sensors in an attempt to evaluate the knuckle joint. The decision to concentrate on this region came as a result of the first test in April 1991. Appendix B contains a summary of graphs generated for this phase of analysis.

Load-up of Limestone Slurry Tank:

AE is not typically recorded during the load-up portion of the stressing sequence. However, in certain situations useful real-time information can be gained about the vessel. To take advantage of the loading transitions, the individual AE channel activity lights (on the front panel of the SPARTAN-AT) must be monitored. By determining which sensor activity lights are active, an understanding of how the vessel is redistributing the load can be obtained. This information may ultimately be used in conjunction with the load-hold data.

Almost from the onset of loading, channel 3 was extremely active. After insuring that the fill rate was not generating turbulence, it was speculated that the cause of this emission could be related to the separation of the tank bottom from the cement foundation. As the filling proceeded, activity from this sensor decreased. At no point during the load-up did channel 3 become completely quiet. As the stress level increased, the number of active channels, as well as AE rate per channel, continued to increase. By the time the 100% load-hold level was reached, AE activity from channel 3 was no longer distinguishable from other AE channels.

Initial Load-Hold of Limestone Slurry Tank at 100%:

The data taken during the initial load-hold represents more than 17 hours of continuous acquisition. For comparison, a standard evaluation time for an FRP vessel at the 100% load-hold level is 30 minutes (ASME Section 5, Article 11).

Figure 5 of Appendix B was generated to display a hit driven channel verse's time graph at the 100% load-hold. This graph indicates that sensors 2, 9, 10 and 13 were higher in activity than the remaining sensors. From this, Figure 1 through 4 were generated which show the hits, counts, energy and amplitude verse's time for the 4 sensors combined. The AE data rate initially follows the anticipated exponential decay with time. For a vessel to be considered structurally stable, the AE rate should

completely decay. Figure 1 of Appendix B also shows burst AE activity occurring about every 2 hours. This type of activity typically represents instantaneous releases of AE energy associated with fiber breakage and delamination propagation.

Figures 5 through 21 of Appendix B represent the hits, counts, energy and amplitude verse's time for each of the 4 sensors separately. The x-axis of the hit graphs for channels 2 and 13 (figure 6 and 18) display a continuous low level AE activity rate. While the hit graphs for channels 9 and 10 (figure 10 and 14) lack the continuous low level activity. Burst activity denominate these graphs. From these figures it can be seen that the area adjacent to sensors 2 and 13 are responsible for the continuing emission while sensor 9 and 10 are responsible for the burst type emission. It should be noted that the computer was allowed to vary the y-axis scales for maximum resolution. Consider the scaling factor when comparing like graphs from different sensors.

Referring back to Figure 1 of Appendix B (hits verse's time) it can be seen that there is a definite increase in AE activity towards the end of the figure. Upon referring back to the start of test and interpolating, it is found that the point of increase in the background rate corresponds to approximately the time of sunrise. From this it can be referred that the heat from the sun introduced a second form of stress on the vessel. This thermal gradient serves to increase the continuing AE activity and reinforcing the notion that the AE being recorded is stress related.

Second Load-Hold of Limestone Slurry at 100%:

Following the activity above, it was determined that the LS vessel should be left at the 100% stress level in order to further evaluate the continuing AE. The continued tests of the LS were scheduled around the test of the JBR. There was about a 10 hour delay between the end of the first LS test and the start of the second. Only the 4 most active sensors (2, 9, 10 & 13) were refitted on the LS. To assist in isolating the location of the AE sources, 2 additional sensors were mounted on the LS. These sensors were labeled channels 21 and 22 and positioned above sensors 9 and 10 (see Figure 1a Appendix A). On the basis of this sensor pattern, the sources of acoustic emission could be located using the stress wave time of arrival. Graphs generated for this procedure can be found in Appendix C.

Figure 1 of Appendix C shows the hits verses channel for the region around the four original sensors. Referring to Figure 2 of Appendix C, it can be seen that the emissions do not completely die out with time. Although the data rates are fairly low, these hits are still greater that the analysis threshold of 47dB.

To investigate the magnitude of these hits, Figures 3, 4 & 5 were created to look at the amplitude, counts and energy distribution during this period. From these figures we can see that there are definite periods of burst type AE activity on top of the continuing emission. Of concern are hits in the 70dB amplitude range.

Figures 6 through 21 show the hit, counts, energy, and amplitude distribution for channels 2, 9, 10 and 13. These individual channel figures provided additional detail for

both periods continuing activity and burst type emission.

Final Load-Hold of Limestone Slurry at 100%:

Based on the information gained in the second load-hold, it was decided to leave the vessel at the 100% level and continue to acquire data. The main effort at this point in the schedule was to concentrate on the JBR. It was not until 14 hours later that the monitoring of the LS tank resumed. Starting Friday evening, both the JBR and the LS tanks were monitored simultaneously. The SPARTAN-AT software allows for simultaneous independent data acquisition. Both vessels were monitored for more than 15 hours. Due to rain on Saturday morning, some of the data had to be post filtered from the data set. Even with the removal of this data, the file provided more than 12 hours of data for analysis.

Figure 1 through 16 of Appendix D show the hits, counts, energy and amplitudes for each of the four channels. Once again the level of AE activity has not completely stopped. Since monitoring began at about 9:00 PM, potential AE generated by a solar thermal gradient is not considered a factor.

Figures 5 through 9 display the hits, counts, energy and amplitude plots for channel 54 (sensor location 9 on the LS vessel). At approximately 12 hours into the test, a large "spike" is observed. This spike is of extremely long duration and relatively low amplitude. Due to the magnitude of these emissions it is obvious that the vessel is still actively readjusting to the stress level.

Varying trends are observed in to the amplitude and duration plots of the remaining three channels (53, 59 and 60). Based on the variations in amplitude and duration, the origins of this AE activity differ greatly. The point of this acquisition period was to determine whether the AE would eventually decay below the test threshold. After this greatly extended hold at the 100% stress level, the low level continuous and high level burst emission continued.

Overall Behavior and Evaluation of the Limestone Slurry Tank at 100%:

To give a clear representation of the data taken from the LS tank over the entire 60 hour period. all of the data files have been combined to form one continuous file. The appropriate time offsets have been included between files so that the time axis on these plots is representative of the actual AE occurrences.

From this file, Figures 1 through 4 of Appendix E were generated. These figures show the hits, counts, energy and amplitude verse's time for the entire 100% load-hold period. The figures indicate that the acoustic emission activity decayed during the initial portion of the load-hold, but at no point died out completely. Due to the high amplitude and long duration, the burst type emission experienced throughout the load-hold was particularly troubling.

The high amplitude and long duration hits are typical signatures of two different failure mechanisms. Both of these occurrences can be considered detrimental to the integrity of the vessel and/or the internal structures. These emissions continued up to and through the final load-hold period. After 60 hours at the 100% load-hold level, the vessel was still reacting adversely to the applied load.

A further point of interest is the increased emission during periods of daylight. These emissions are indications of the increased thermal stress on the tank and its special ultraviolet protective coating. The additional stress applied by the thermal effects are another indication of the vessel's inability to support the a load under routine operating conditions.

On the basis of the results from the initial test, an extended hold period at the 100% stress level was needed. This extended hold was incorporated to further evaluate the response of the vessel. Results of the initial test can be found in PAC Project 5-343 final report dated July 7, 1991.

5. Conclusions

Jet Bubble Reactor:

During the testing of the JBR, the two 100% load-hold AE data files were used to interpret results. Each file contained over 11 hours of data. On the basis of the emissions recorded during the load-hold periods, it was evident that the JBR continued to emit AE up to, and including the last portion of, the final load-hold. Since a standardized threshold level was used for evaluation, and since the JBR was not subject to any appreciable external stresses other than the hydrostatic stress, it can be concluded that the vessel was continuing to emit due to increasing degradation. The inability of the vessel to completely stabilize indicates that it was dynamically and adversely readjusting to the stress level. A post test visual analysis of the inside of the JBR supported this contention. Of interest to the AE analysis were the various positions where the internal structure of the JBR was attached to the vessel wall. In several areas it was noted that internal delaminations had occurred at these connection points. It is felt that the continuing AE is directly related to this phenomenon. This conclusion is further supported by the low to mid amplitude, long duration hits that are characteristics of delaminations in FRP vessels.

Limestone Slurry Tank:

Testing of the LS tank offered a unique opportunity to evaluate the vessel at the 100% stress level over a period of greater than 60 hours. During this time, a large amount of data was taken to chart the response of the vessel to this constant stress level. As was the case with the JBR. the LS did not become acoustically stable with time. This was confirmed through burst type and low level continuing emissions. An indication of this problem is provided by channel 54 (sensor #9 on the vessel). Extremely long duration and relatively low amplitude signals were received throughout the test. This occurrence was experienced almost 50 hours into the 100% load-hold. Once again, the conclusions indicate that both the low level continuing emission and the burst type emission are indicative of a vessel that is actively seeking a state of equilibrium. It is anticipated that this vessel would continue to emit until the entire structure was stress relieved. Once again. upon visual inspection, the internal attachments (baffle plates) showed discolorations at the wall interface, indicative of delaminations. The delaminations found in the LS tank were more pronounced than the indications found in the JBR. A detailed sketch of these areas are included in the report as Figure 3 of Appendix A.

A general summarization of the tests performed on the on-site fabricated FRP vessels follows. The general conclusions are:

1. Acoustic emission is a viable method to use for the detection, location and classification of acoustic emission sources.

2. Acoustic emission is effective in distinguishing delaminations and

background noise.

3. A baseline of acoustic emission data from both vessels has been attained for future AE tests.

4. Acoustic emission results show internal structure (baffle plates etc.), mounted to the vessel wall, may cause significant breakdown of the bonding material at the wall/internal structure interface upon loading.

5. After extended hold periods at the 100% level, both vessels continued to emit acoustic signals.

6. The photoelastic plates are not a significant source of acoustic emission as was first thought in the initial test and report.

7. It appears that the ambient temperature change during a typical day can influence the AE results.

6. Recommendations

Load-hold periods on both vessels exceeded accepted industry standards by many hours. At no time was there a 30 minute period that either vessel could be considered acoustically silent. However, the extended hold periods should continue until more is learned about this type of construction. In addition, water was used as the primary stressing medium. During operation, the vessels will contain a mixture of water and limestone. This difference is specific gravity will add additional stress to the vessels. It is recommended that both vessels be monitored very closely for any visual signs of degradation. In addition, it is strongly recommended that a 6 month, but no more than 1 year, AE test interval be established. The test would concentrate on those areas identified in this report as being acoustically active.

7. References

ASME Section 5, Article 11 - **Acoustics Emission Examination of Fiber Reinforced Plastic Vessels.**

ASTM E-610 - **Standard Definition of Terms Relating to Acoustic Emission.**

ASTM E-650 - **Standard Guide for Mounting Piezoelectric Acoustic Emission.**

ASTM E-976 - **Standardized Guide for Determining the Reproducibility of Acoustic Emission Response.**

ASNT SNT TC-1A - **A Standardized Guide for NDT Personnel Qualification and Certification.**

Gilbert, B.E., **Acoustic Emission Testing of On-Site Fabricated FRP Vessels**, Final Report, P.O. S-91-001809, Southern Company Services, Birmingham, AL, July 1991.

APPENDIX A

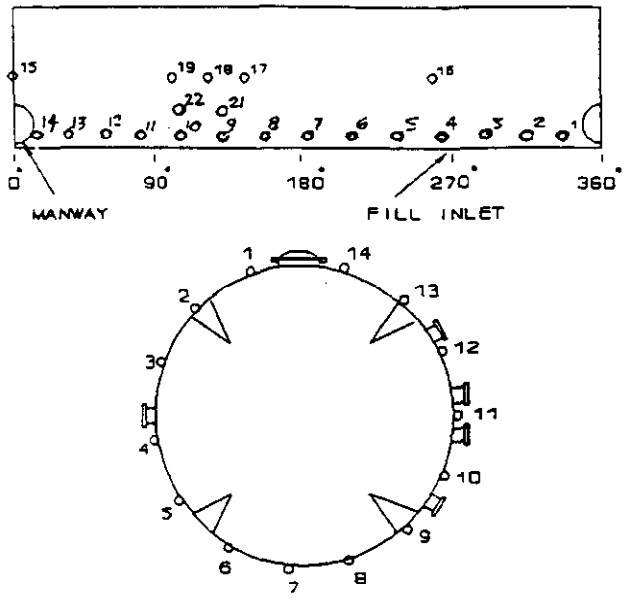

Figure 1a. Sensor arrangement for Limestone Slurry Tank (LS)

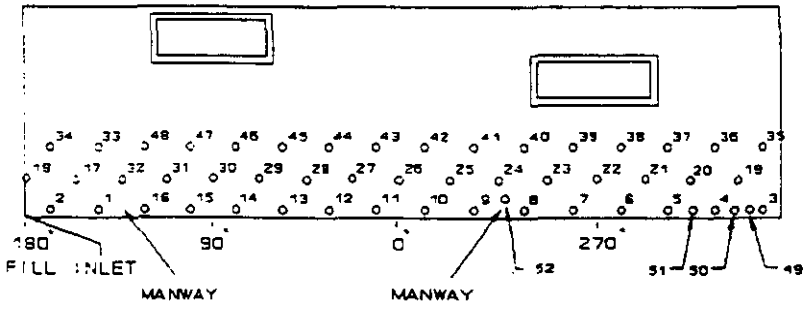

Figure 1b. Sensor arrangement for Jet Bubble Reactor (JBR)

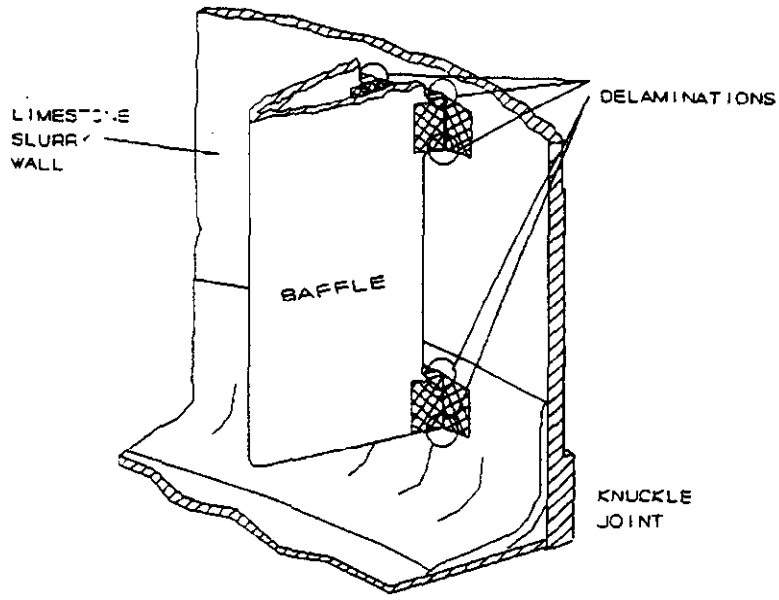

Figure 2. Detail drawing of visual delamination sites

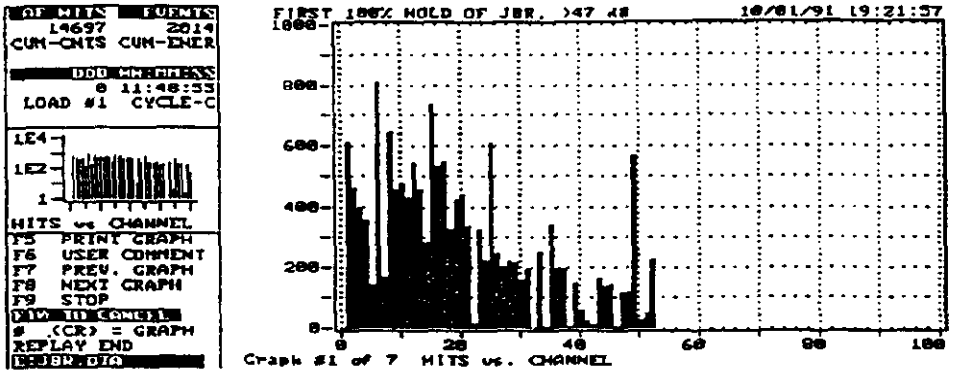

Figure 3. Hits vs Channel for first 100% hold of JBR

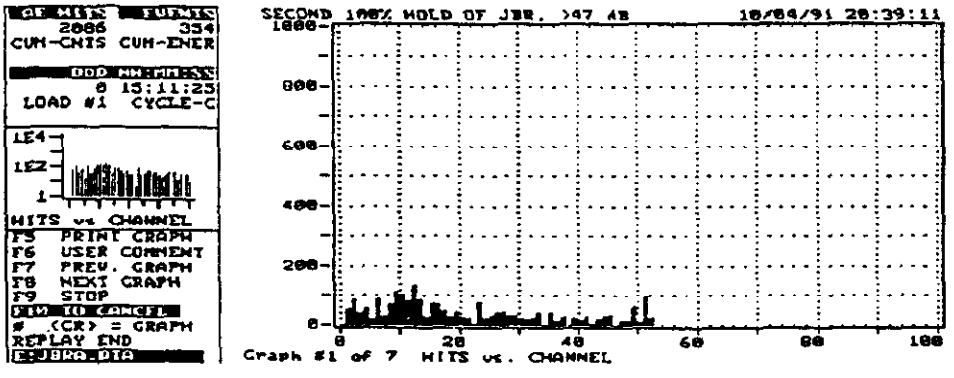

Figure 4. Hits vs Channel for second 100% hold of JBR

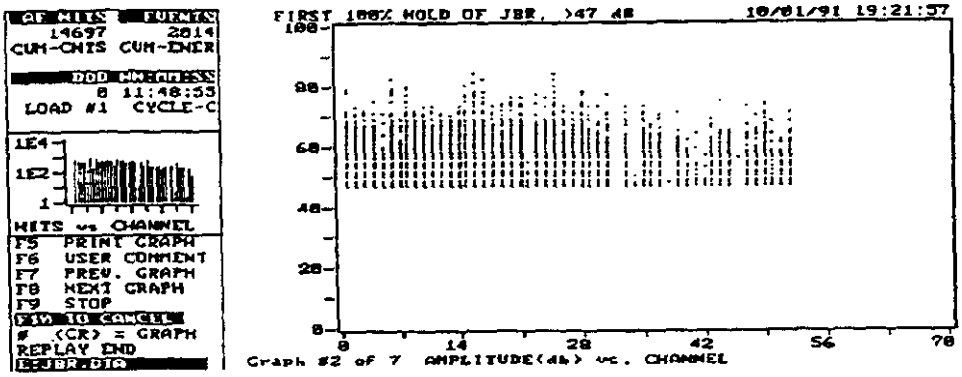

Figure 5. Amplitude vs Channel for first 100% hold of JBR

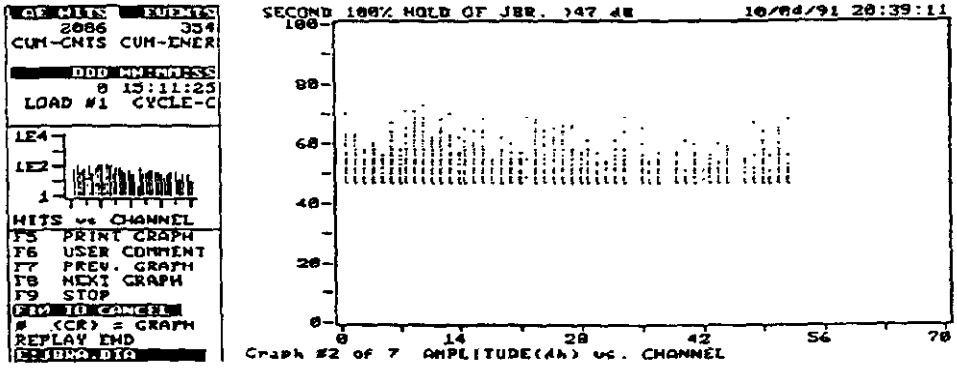

Figure 6. Amplitude vs Channel for second 100% hold of JBR

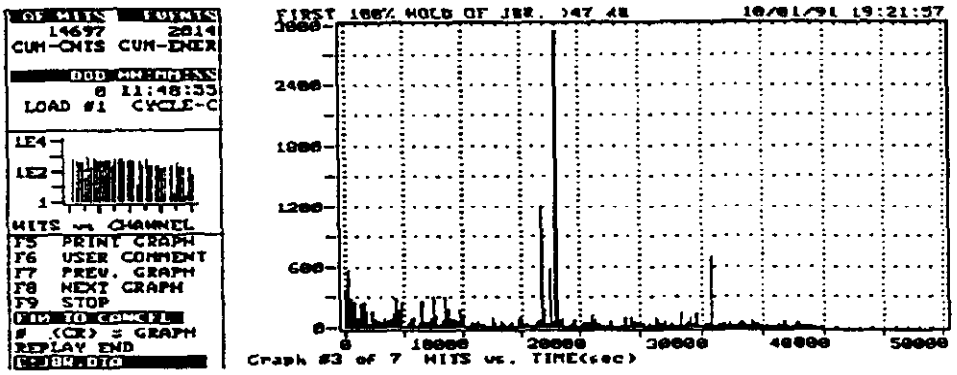

Figure 7. Hits vs Time for first 100% hold of JBR

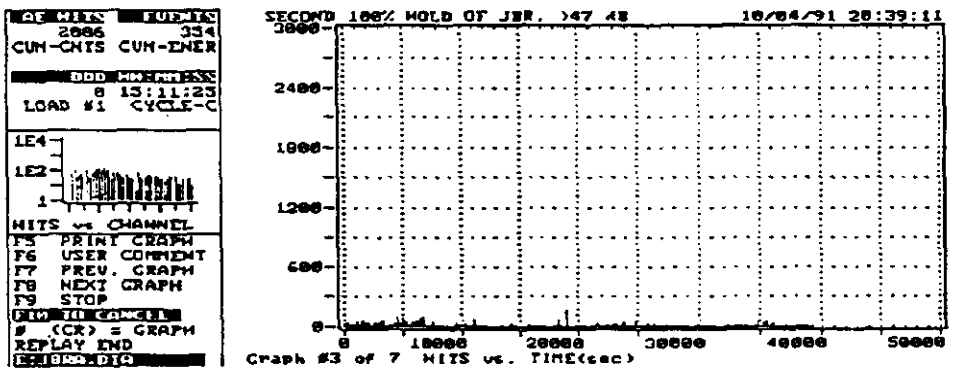

Figure 8. Hits vs Time for second 100% hold of JBR

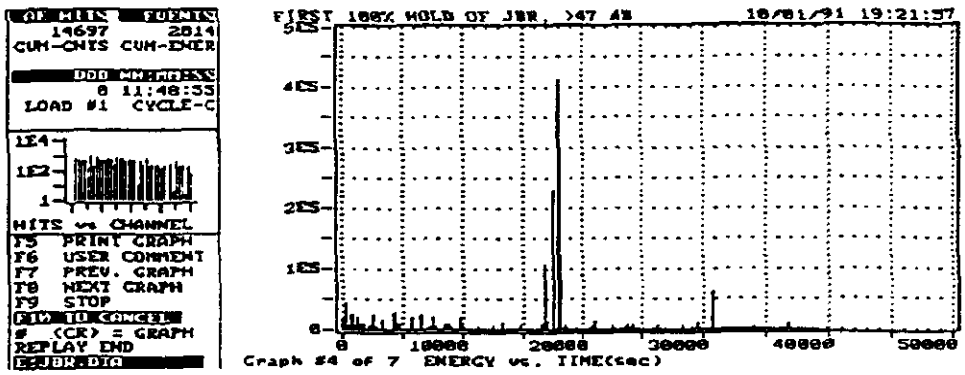

Figure 9. Energy vs Time for first 100% hold of JBR

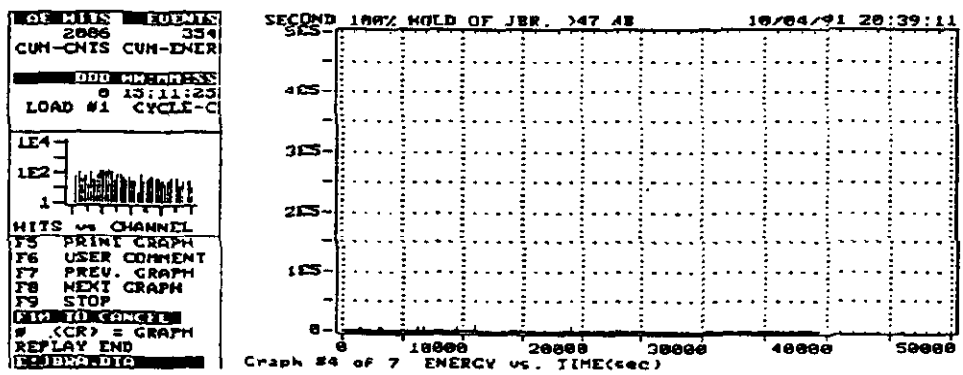

Figure 10. Energy vs Time for first 100% hold of JBR

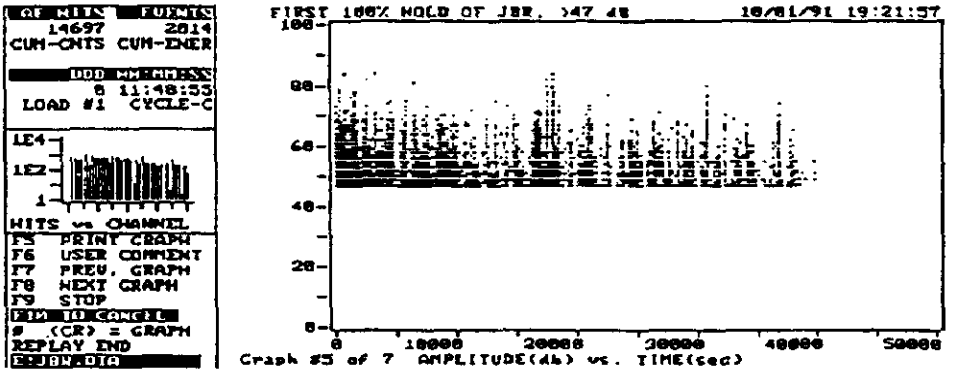

Figure 11. Amplitude vs Time for first 100% hold of JBR

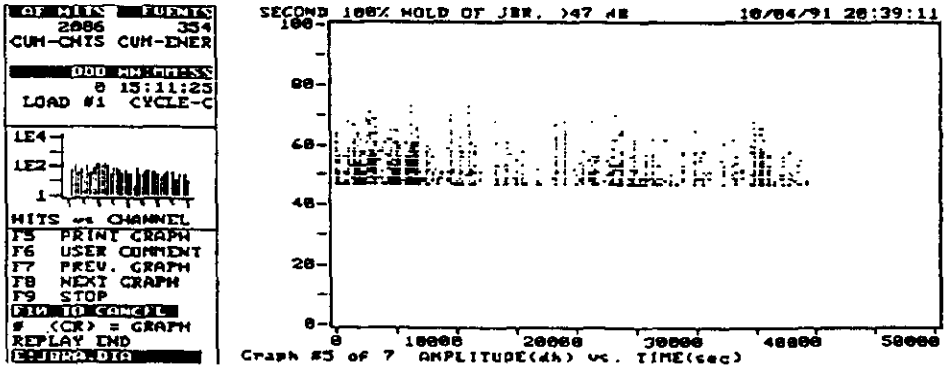

Figure 12. Amplitude vs Time for second 100% hold of JBR

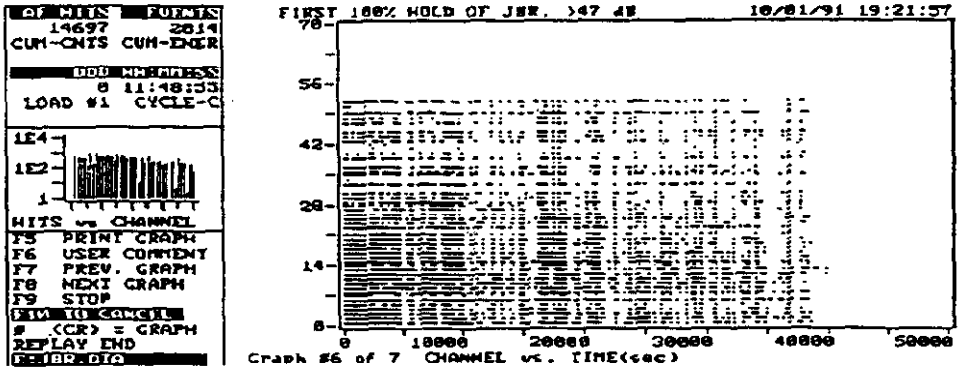

Figure 13. Channel vs Time for first 100% hold of JBR

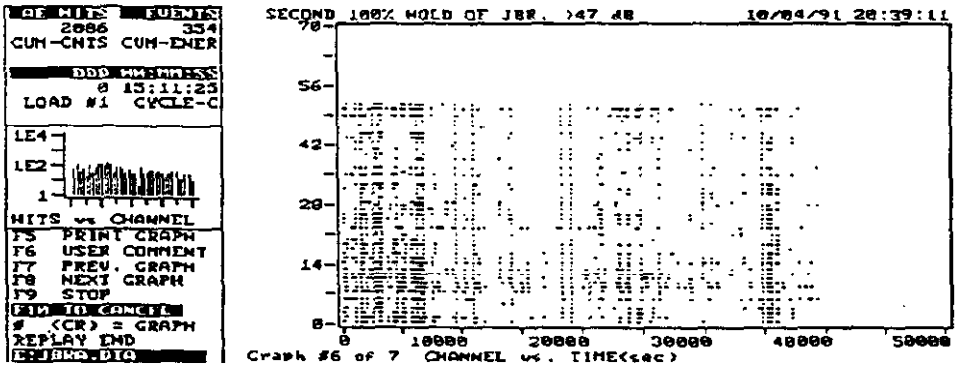

Figure 14. Channel vs Time for second 100% hold of JBR

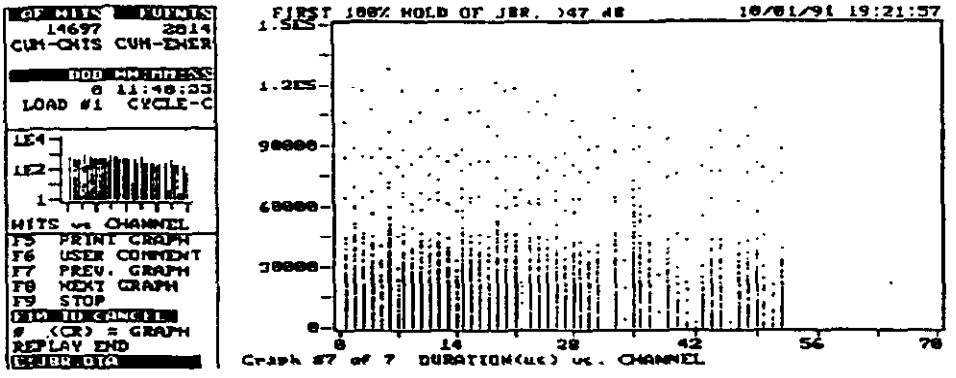

Figure 15. Duration vs Channel for first 100% hold of JBR

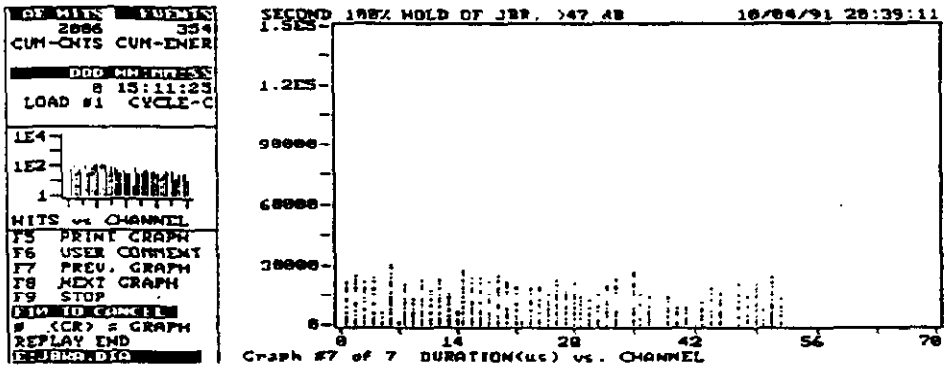

Figure 16. Duration vs Channel for second 100% hold of JBR

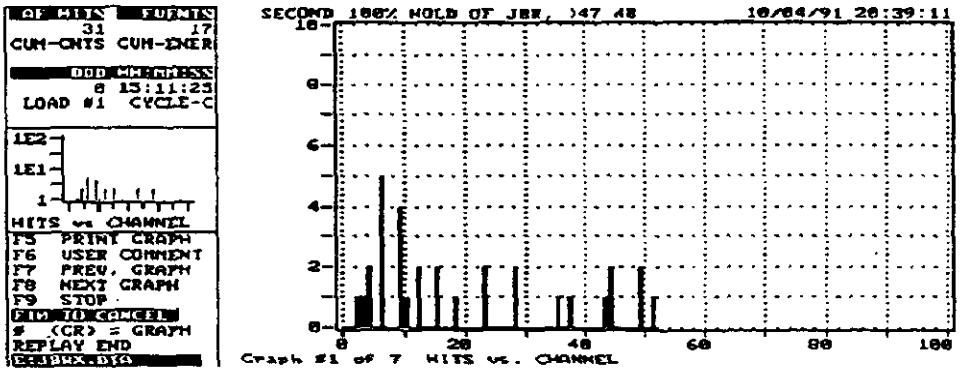

Figure 17. Hits vs Channel for final hour of JBR

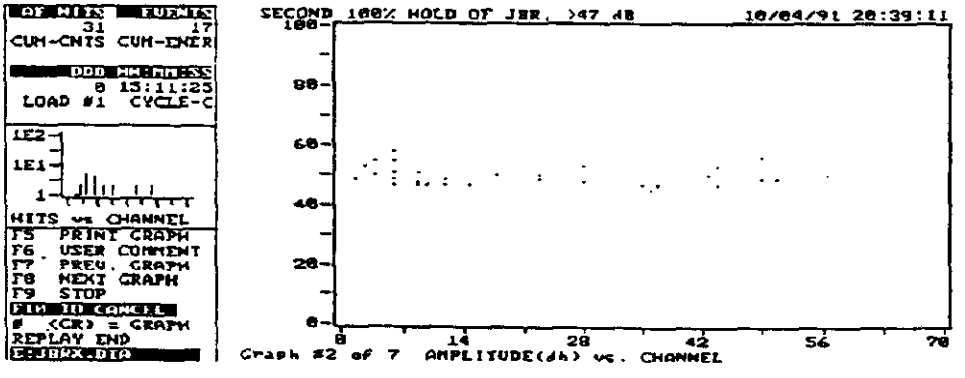

Figure 18. Amplitude vs Channel for final hour of JBR

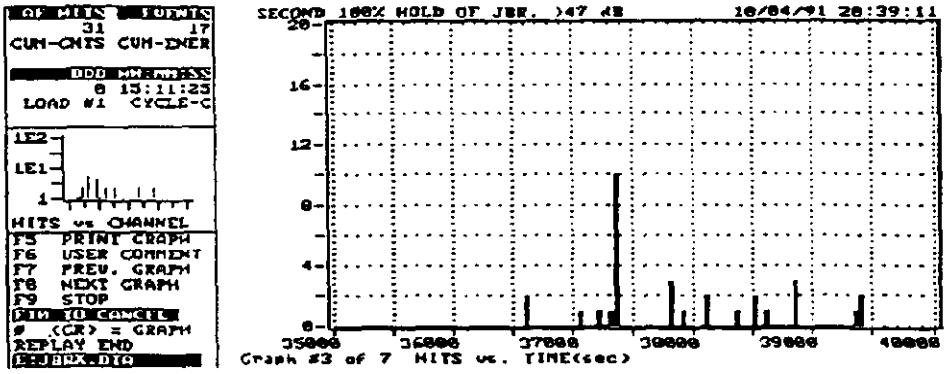

Figure 19. Hits vs Time for final hour of JBR

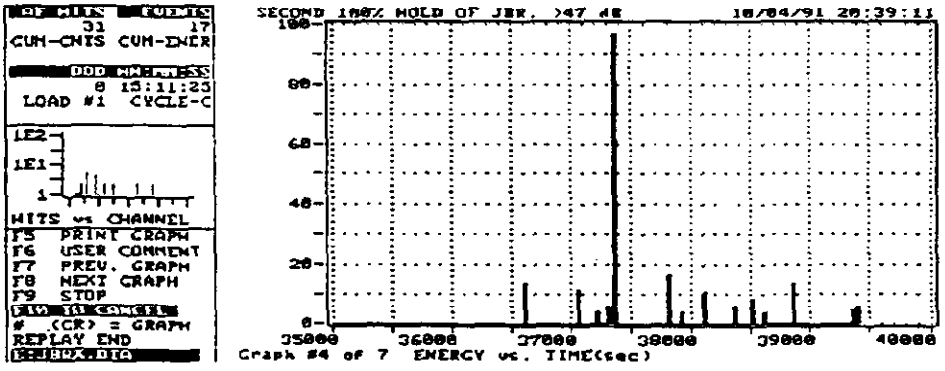

Figure 20. Energy vs Time for final hour of JBR

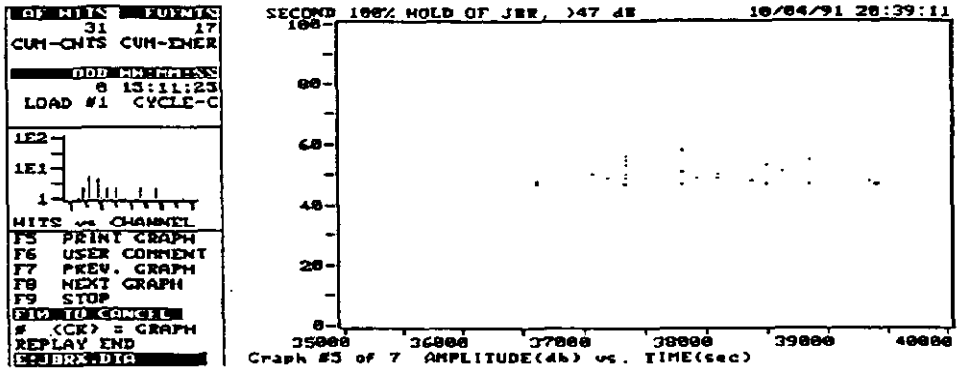

Figure 21. Amplitude vs Time for final hour of JBR

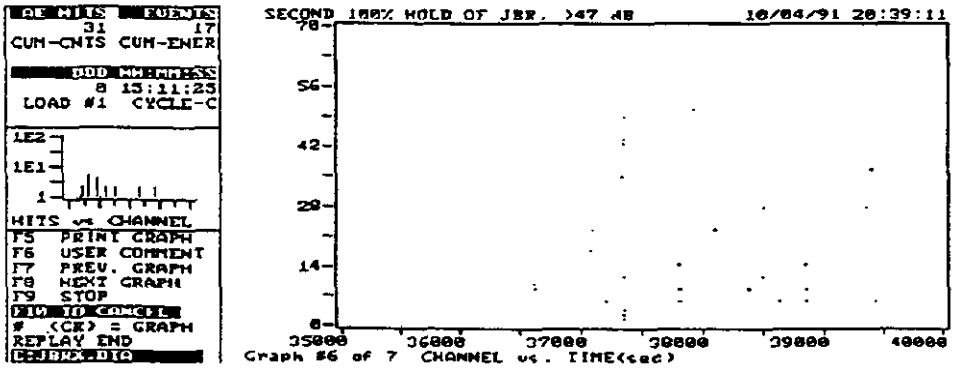

Figure 22. Channel vs Time for final hour of JBR

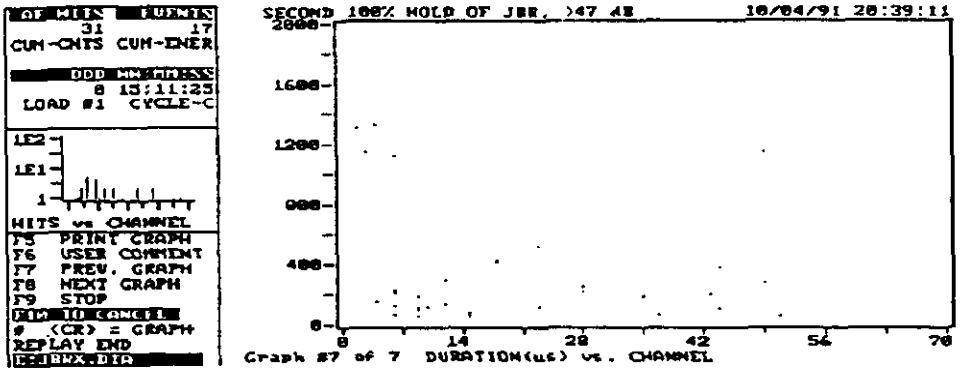

Figure 23. Duration vs Channel for final hour of JBR

APPENDIX B

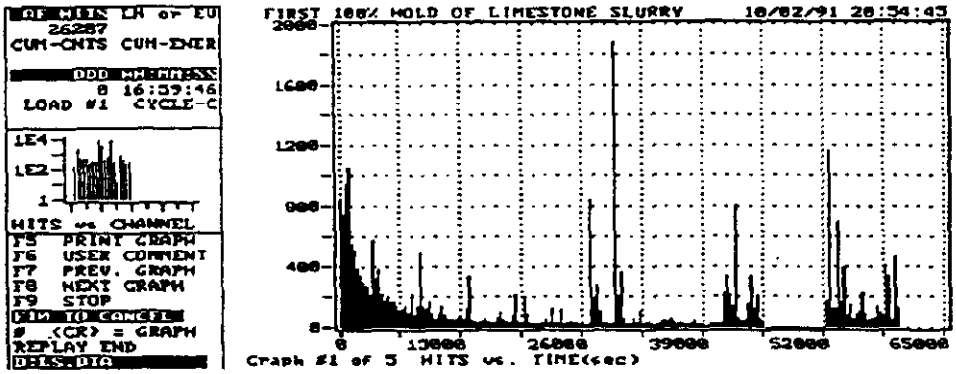

Figure 1. Hits vs Time for first 100% hold of LS

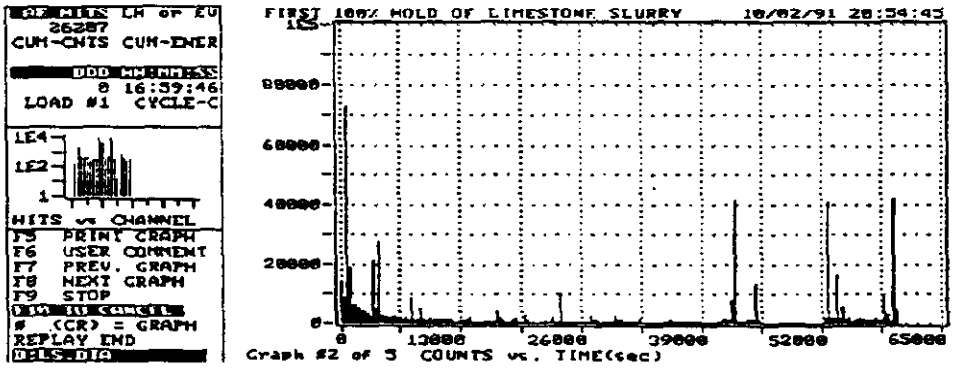

Figure 2. Counts vs Time for first 100% hold of LS

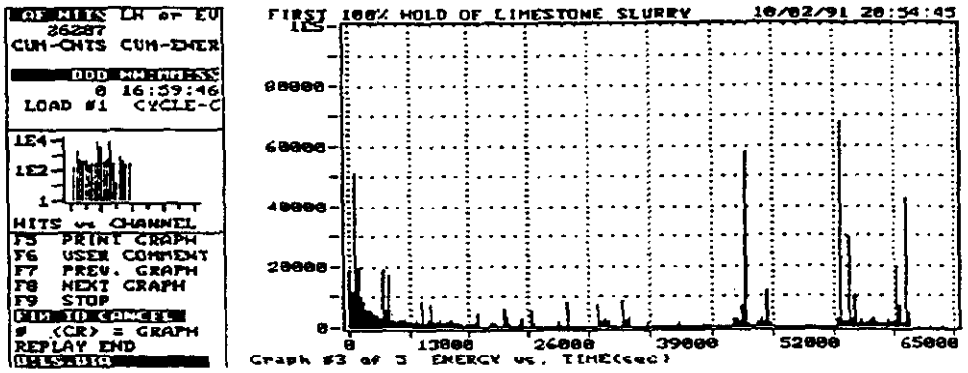

Figure 3. Energy vs Time for first 100% hold of LS

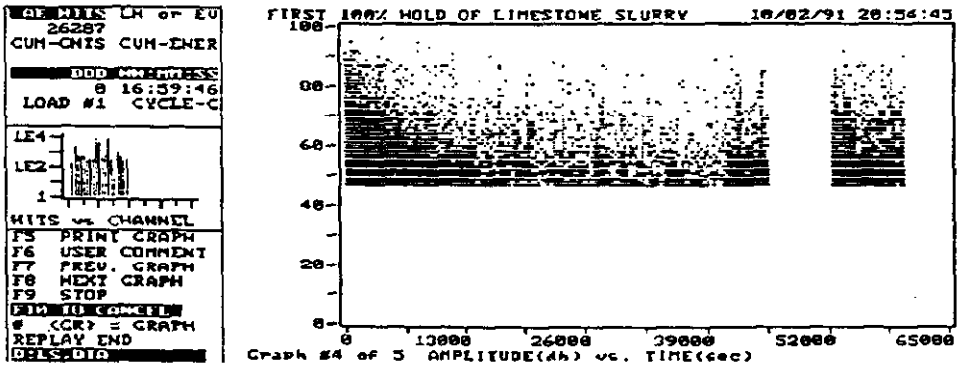

Figure 4. Amplitude vs Time for first 100% hold of LS

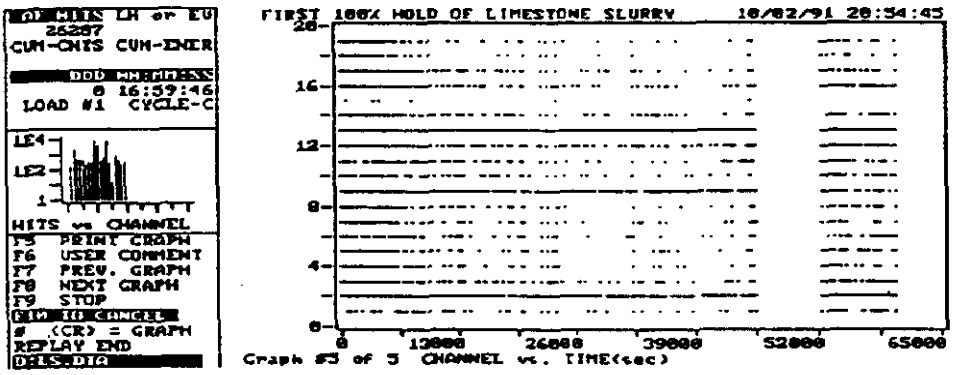

Figure 5. Channel vs Time for first 100% hold of LS

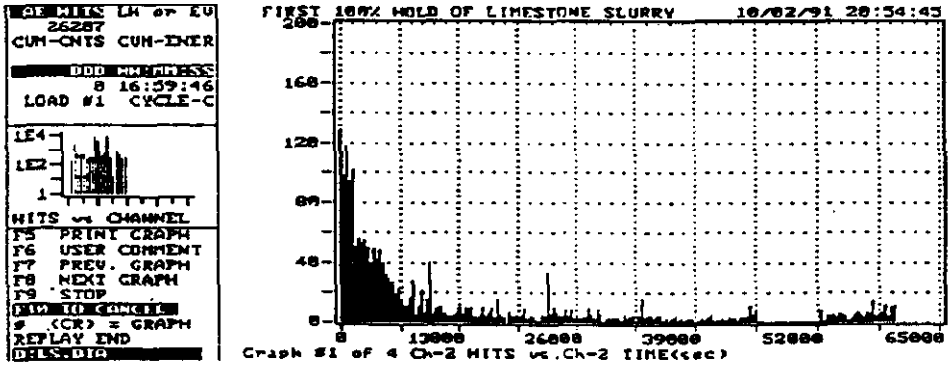

Figure 6. Channel 2 Hits vs Time for first 100% hold of LS

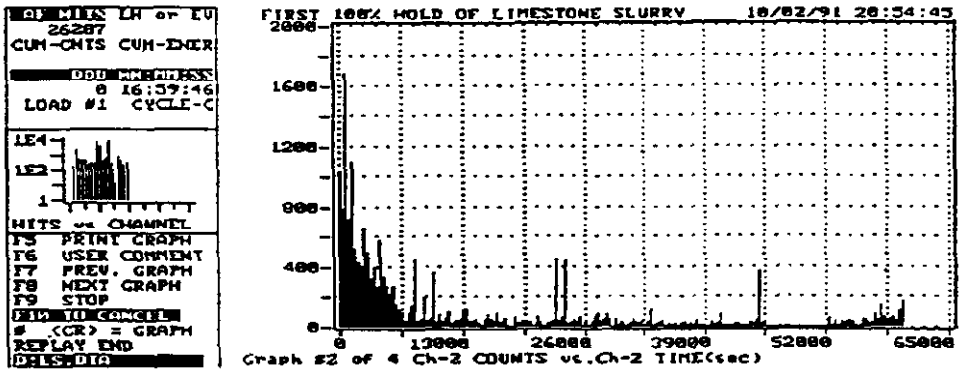

Figure 7. Channel 2 Counts vs Time for first 100% hold of LS

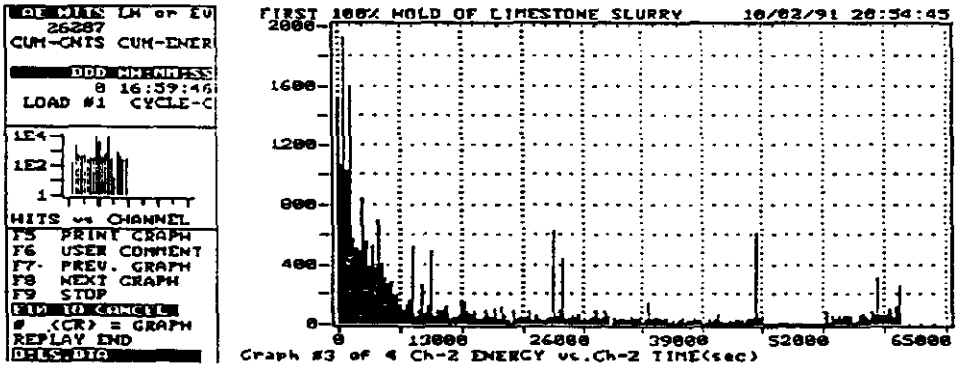

Figure 8. Channel 2 Energy vs Time for first 100% hold of LS

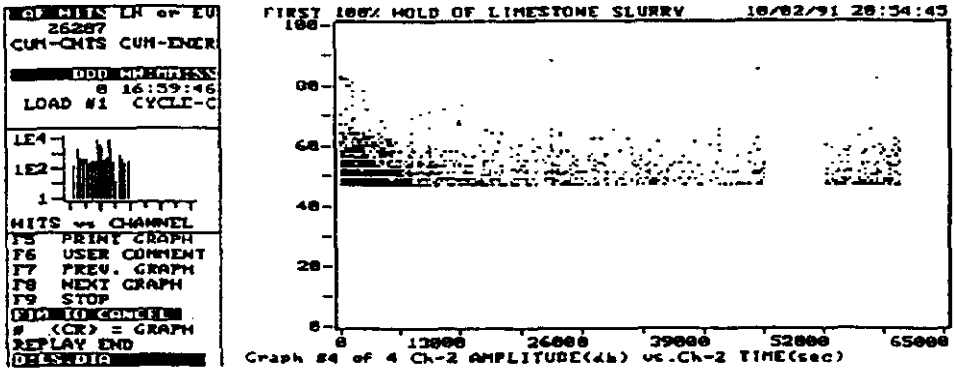

Figure 9. Channel 2 Amplitude vs Time for first 100% hold of LS

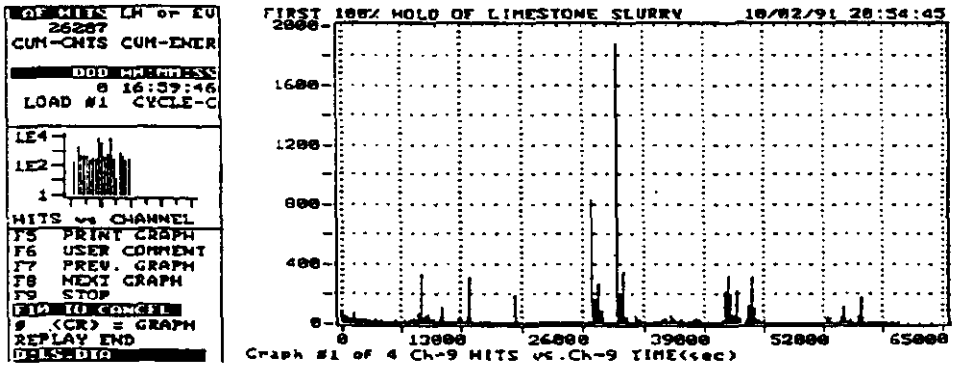

Figure 10. Channel 9 Hits vs Time for first 100% hold of LS

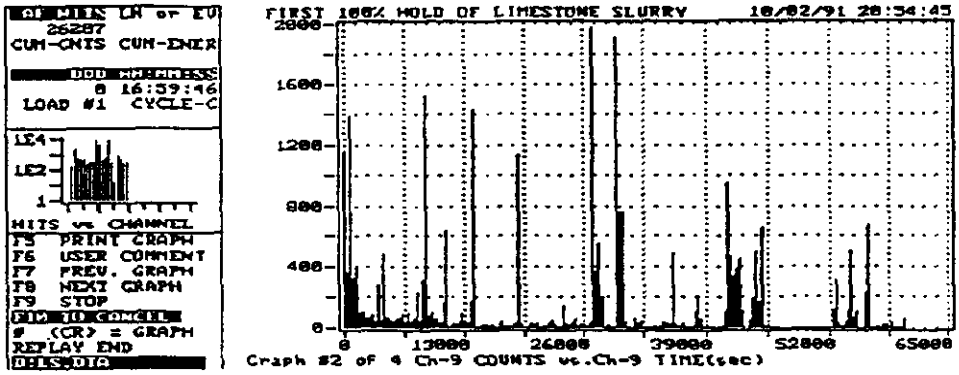

Figure 11. Channel 9 Counts vs Time for first 100% hold of LS

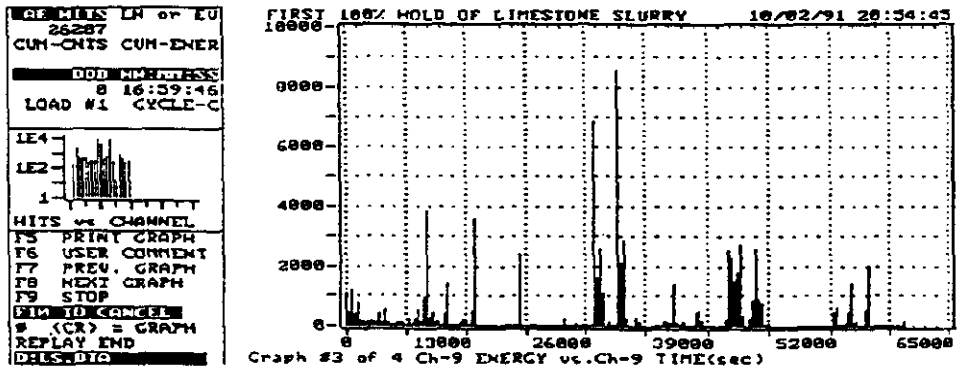

Figure 12. Channel 9 Energy vs Time for first 100% hold of LS

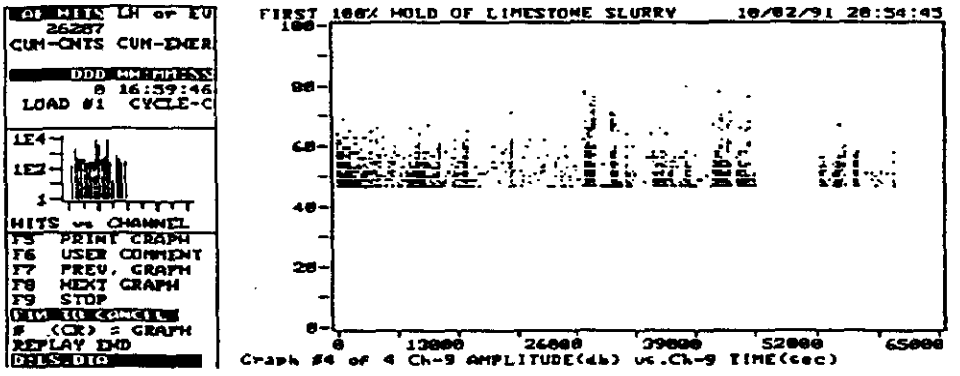

Figure 13. Channel 9 Amplitude vs Time for first 100% hold of LS

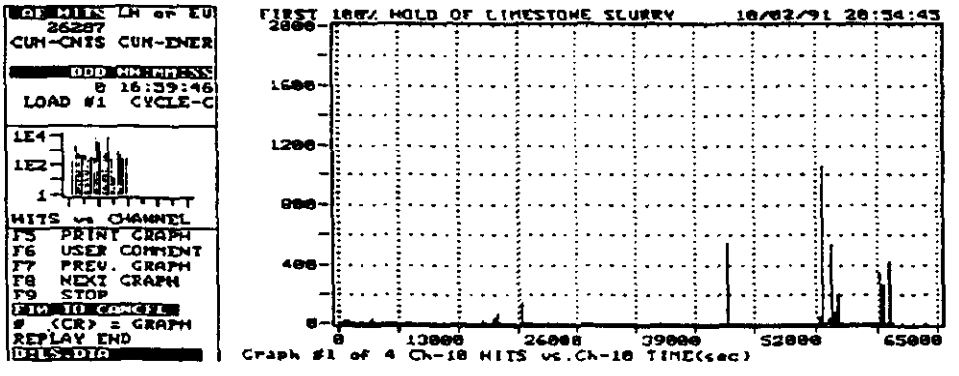

Figure 14. Channel 10 Hits vs Time for first 100% hold of LS

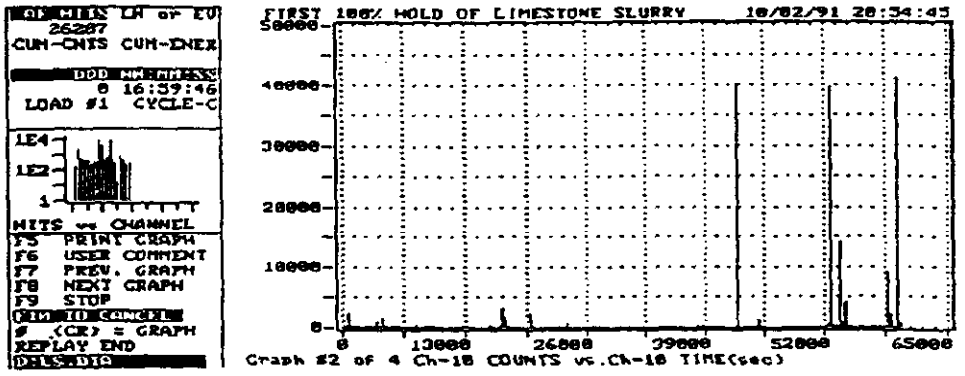

Figure 15. Channel 10 Counts vs Time for first 100% hold of LS

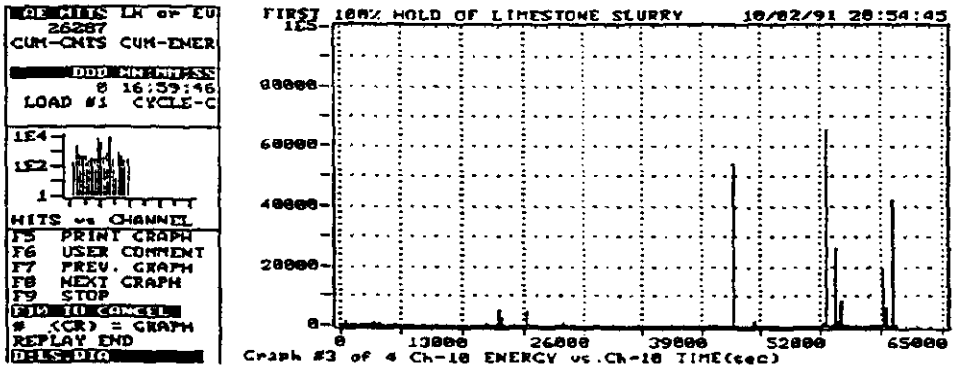

Figure 16. Channel 10 Energy vs Time for first 100% hold of LS

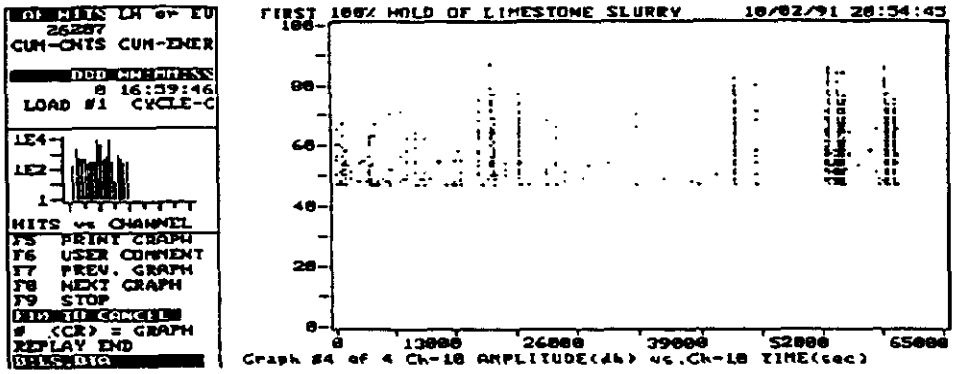

Figure 17. Channel 10 Amplitude vs Time for first 100% hold of LS

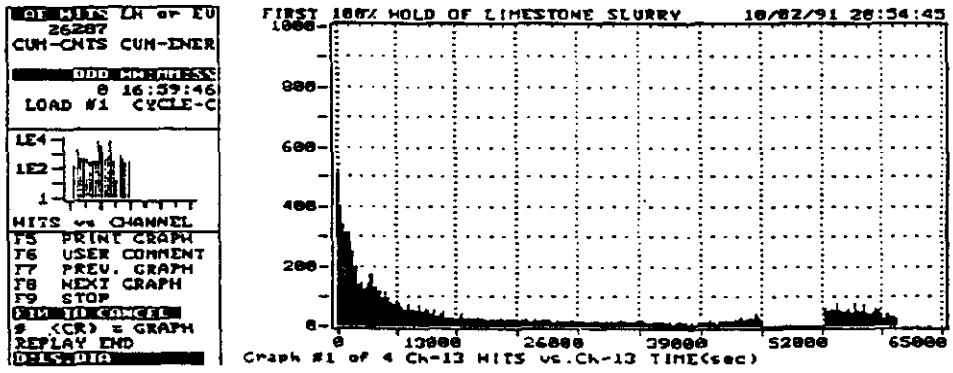

Figure 18. Channel 13 Hits vs Time for first 100% hold of LS

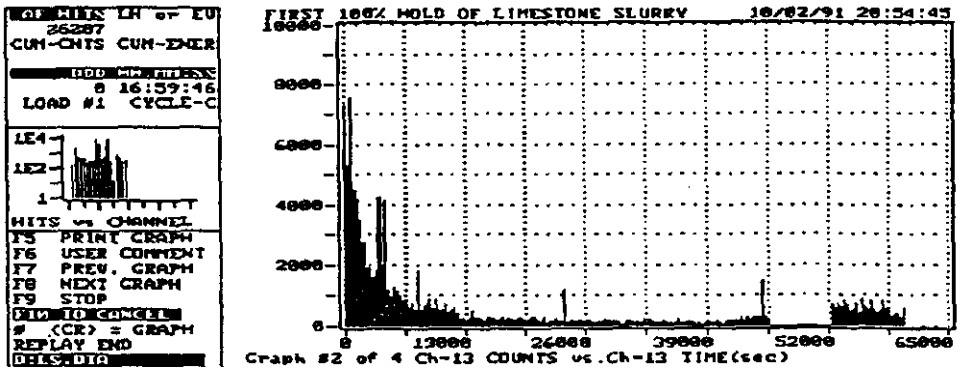

Figure 19. Channel 13 Counts vs Time for first 100% hold of LS

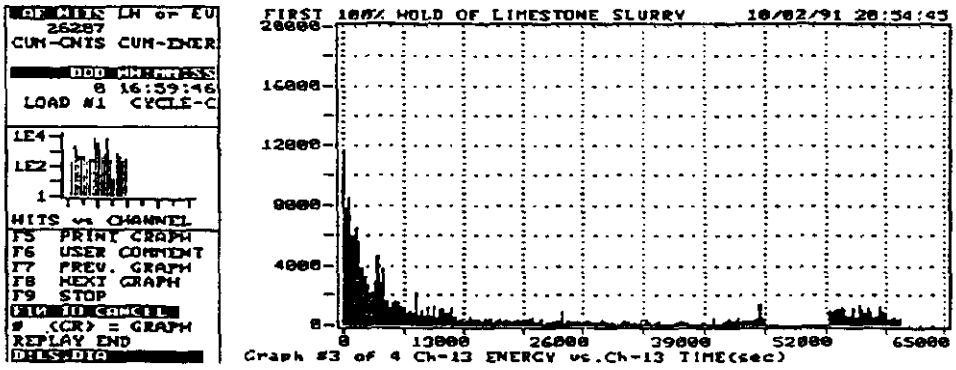

Figure 20. Channel 13 Energy vs Time for first 100% hold of LS

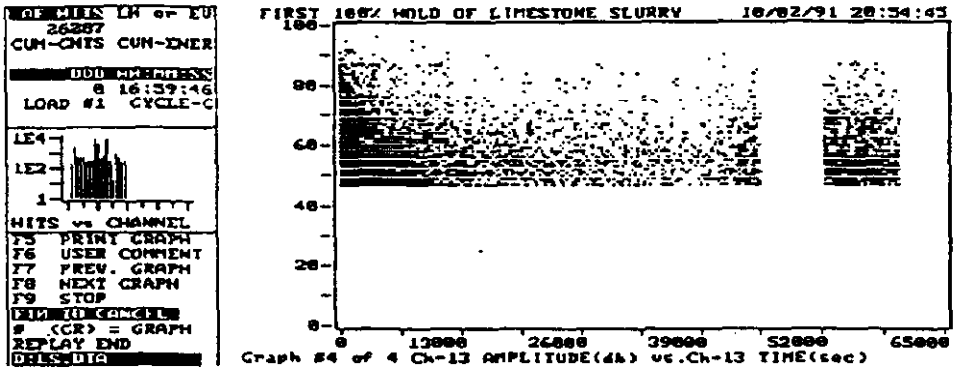

Figure 21. Channel 13 Amplitude vs Time for first 100% hold of LS

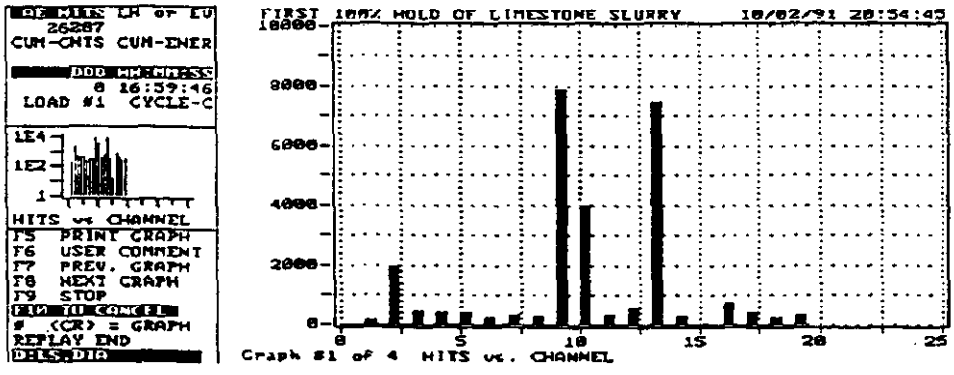

Figure 22. Hits vs Channel for first 100% hold of LS

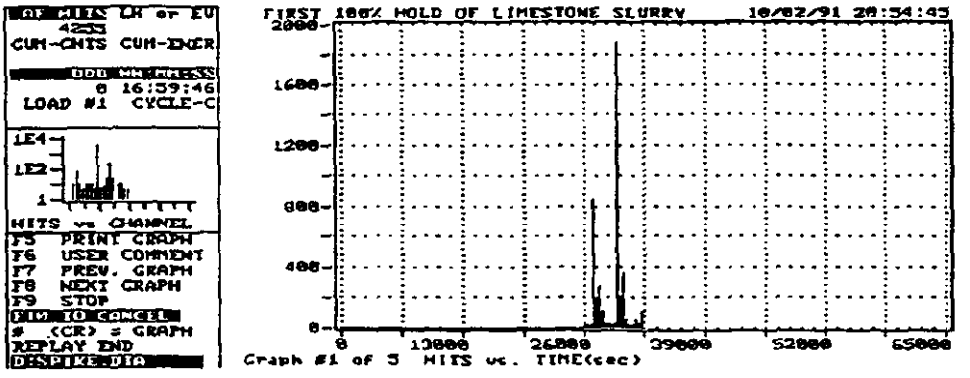

Figure 23. Hits vs Time from 26000-32500 sec, 1st 100% hold of LS

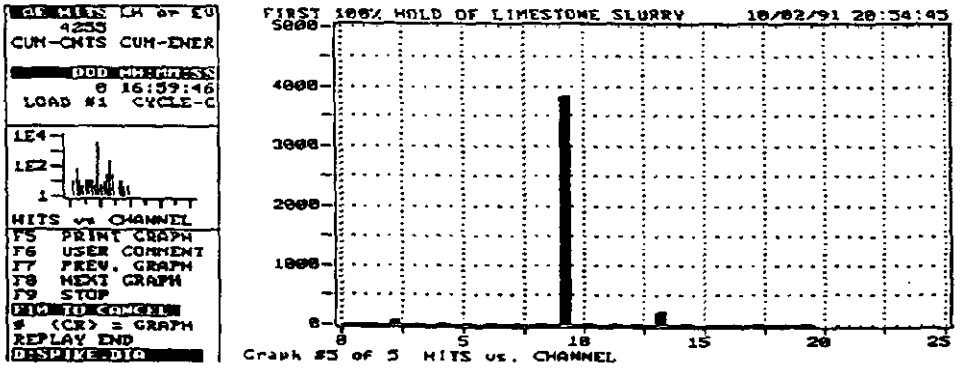

Figure 24. Hits vs Channel of 26000-32500 sec, 1st 100% hold of LS

APPENDIX C

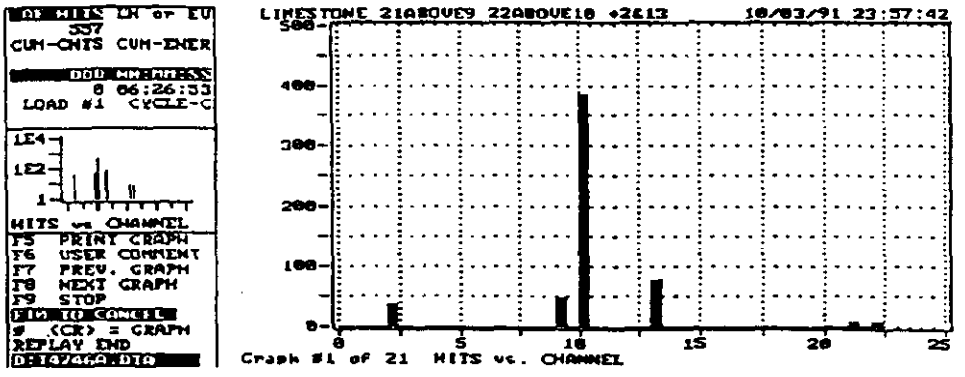

Figure 1. Hits vs Channel for second 100% hold of LS

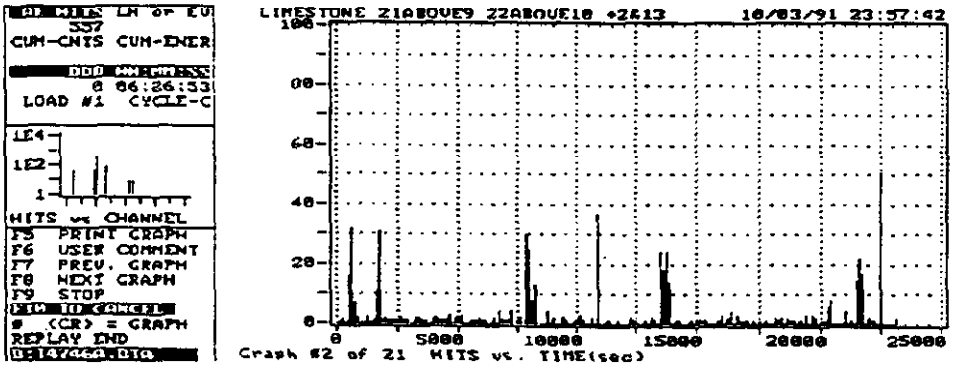

Figure 2. Hits vs Time for second 100% hold of LS

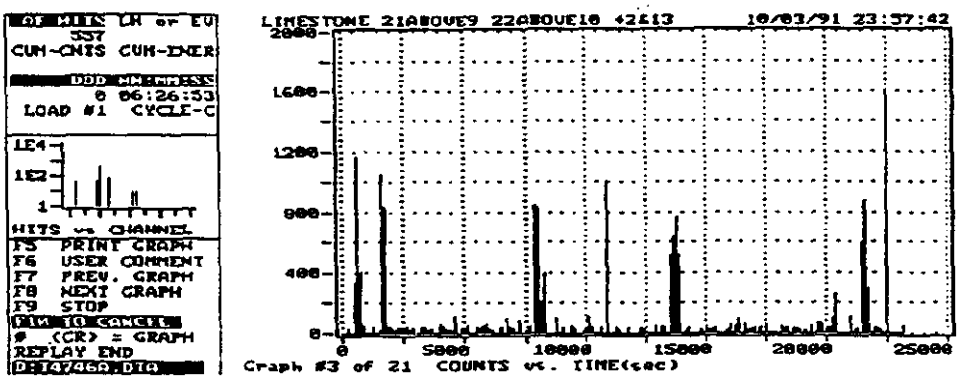

Figure 3. Counts vs Time for second 100% hold of LS

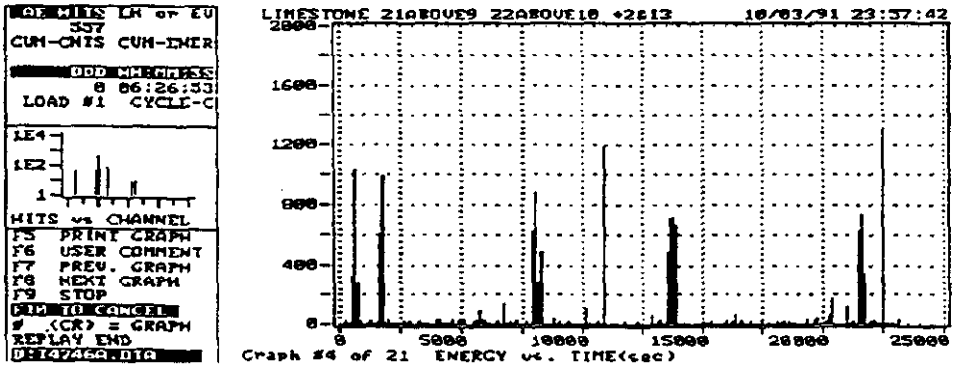

Figure 4. Energy vs Time for second 100% hold of LS

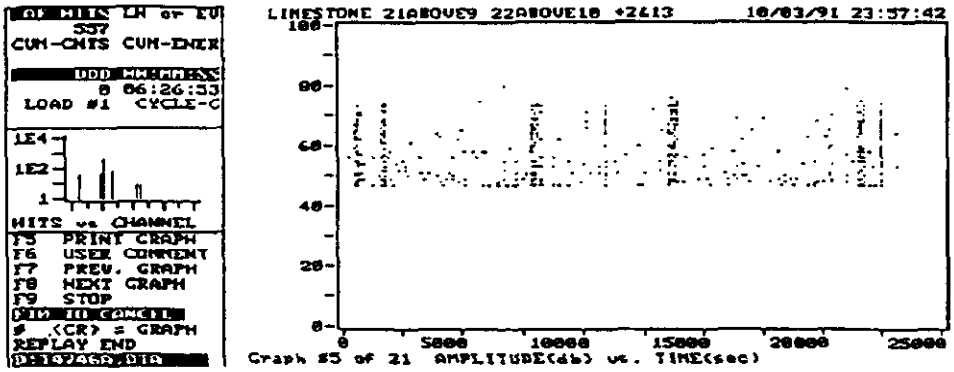

Figure 5. Amplitude vs Time for second 100% hold of LS

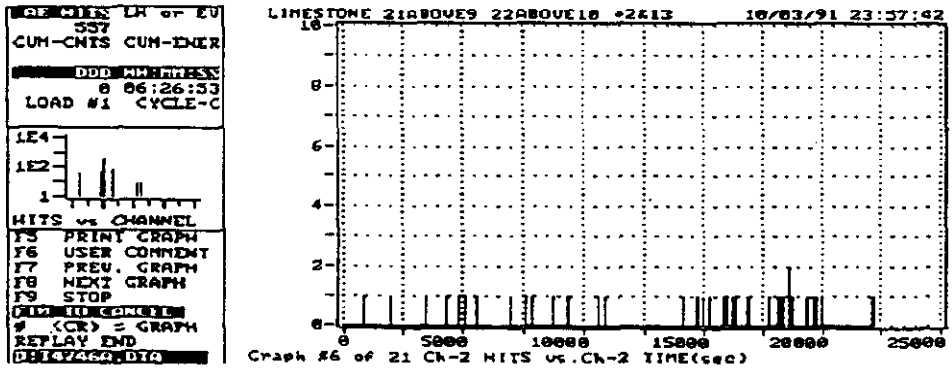

Figure 6. Channel 2 Hits vs Time for second 100% hold of LS

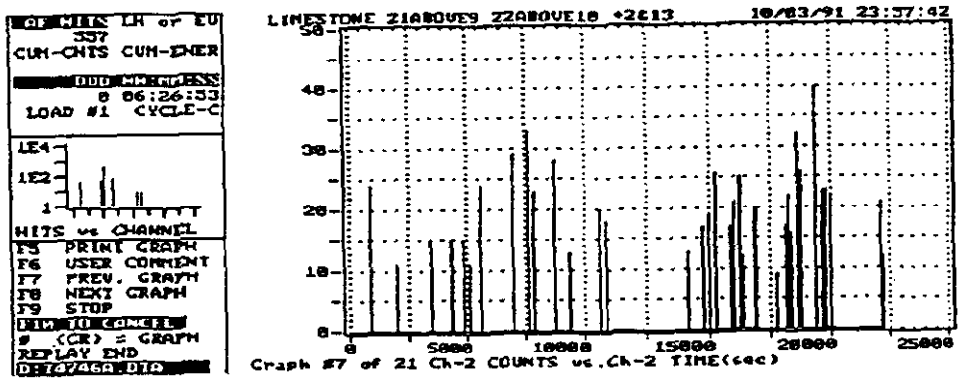

Figure 7. Channel 2 Counts vs Time for second 100% hold of LS

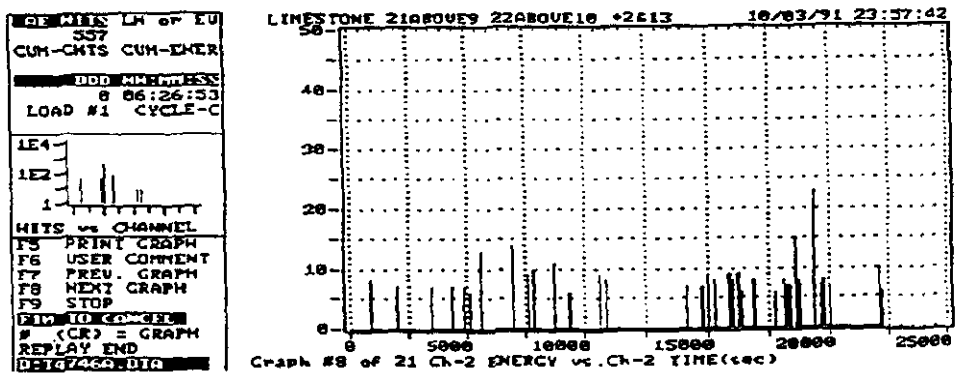

Figure 8. Channel 2 Energy vs Time for second 100% hold of LS

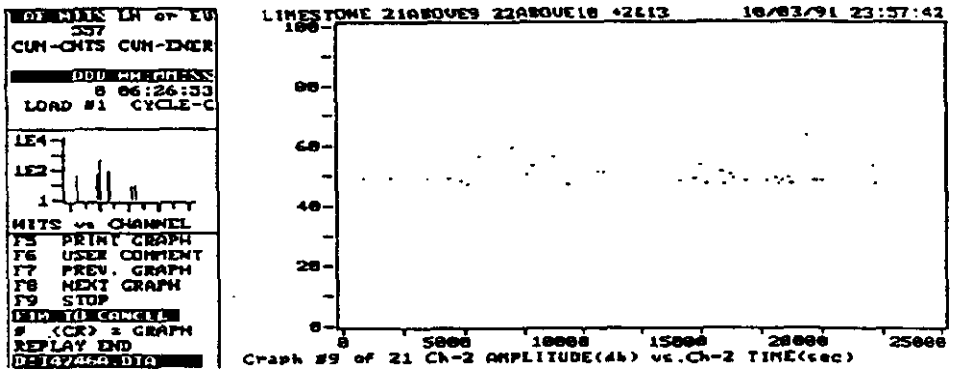

Figure 9. Channel 2 Amplitude vs Time for second 100% hold of LS

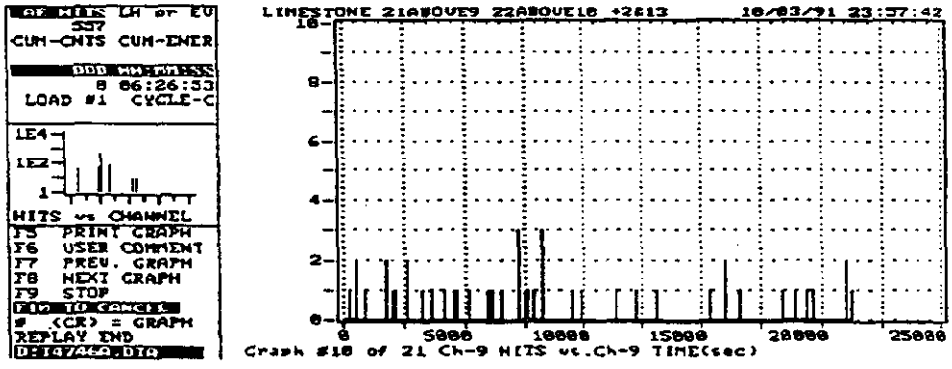

Figure 10. Channel 9 Hits vs Time for second 100% hold of LS

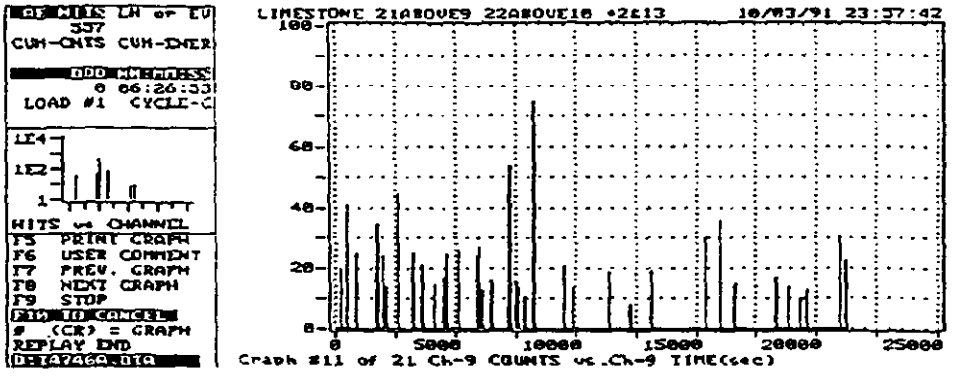

Figure 11. Channel 9 Counts vs Time for second 100% hold of LS

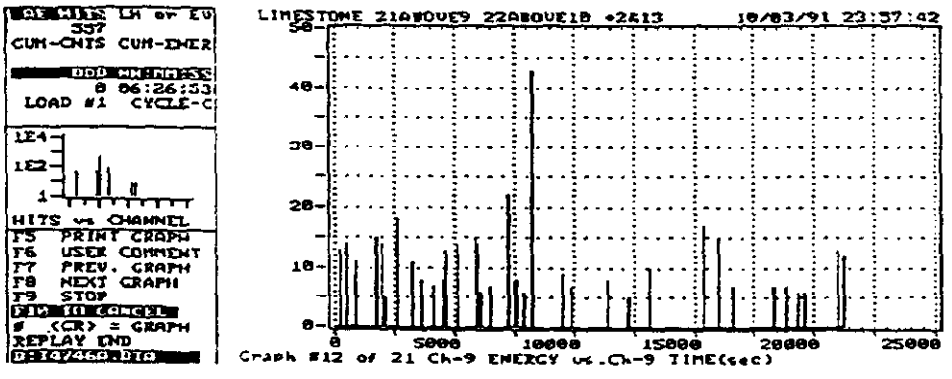

Figure 12. Channel 9 Energy vs Time for second 100% hold of LS

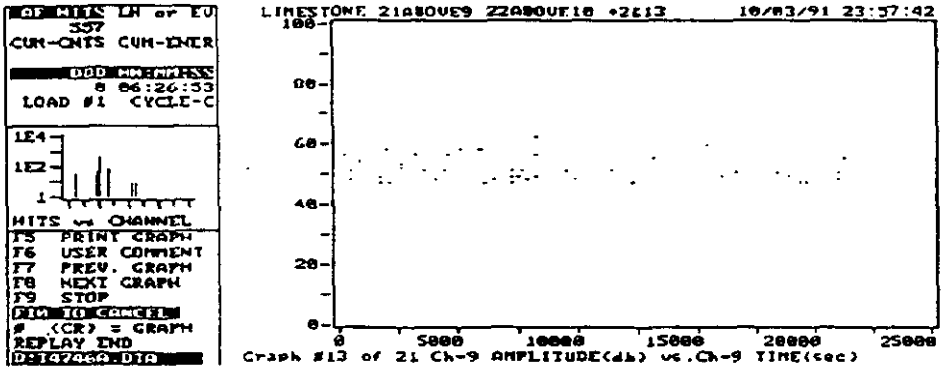

Figure 13. Channel 9 Amplitude vs Time for second 100% hold of LS

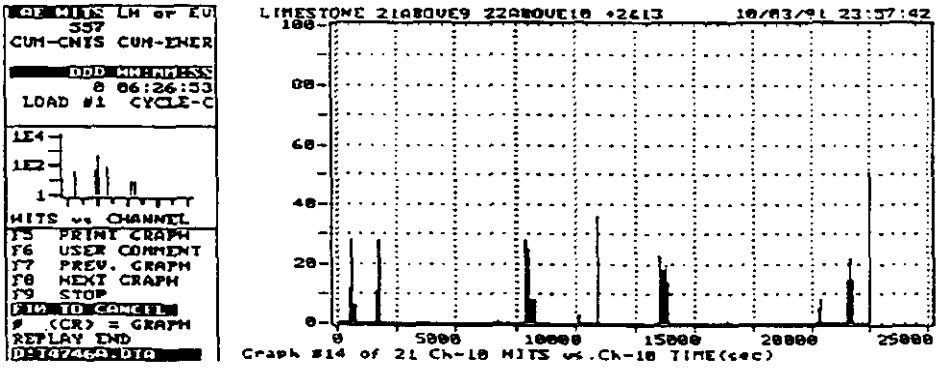

Figure 14. Channel 10 Hits vs Time for second 100% hold of LS

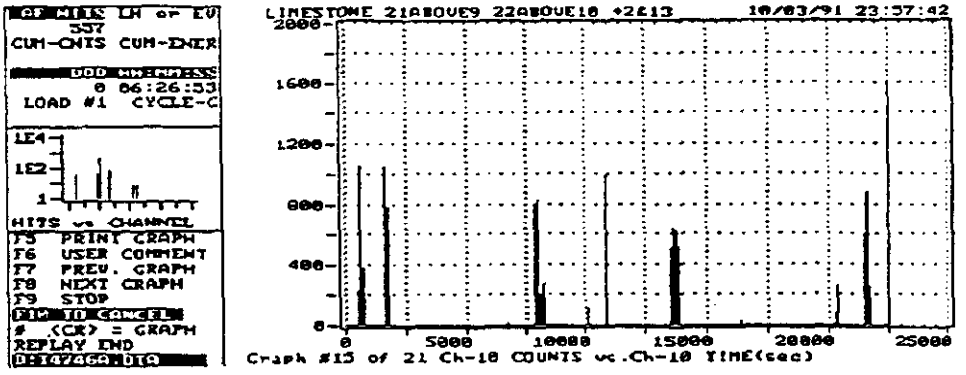

Figure 15. Channel 10 Counts vs Time for second 100% hold of LS

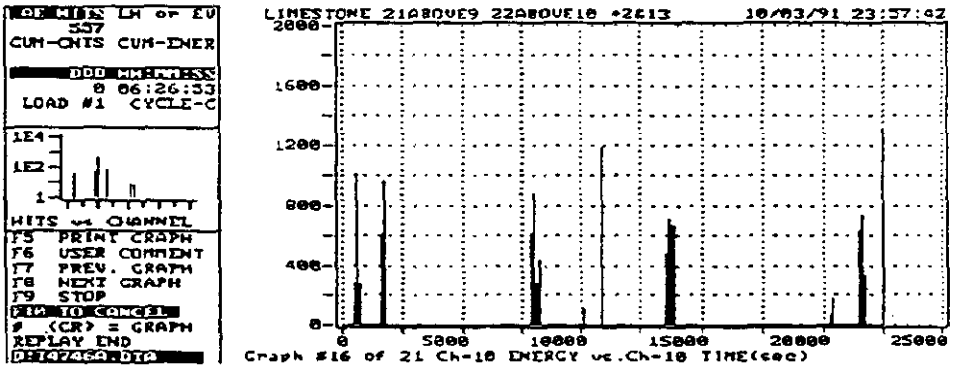

Figure 16. Channel 10 Energy vs Time for second 100% hold of LS

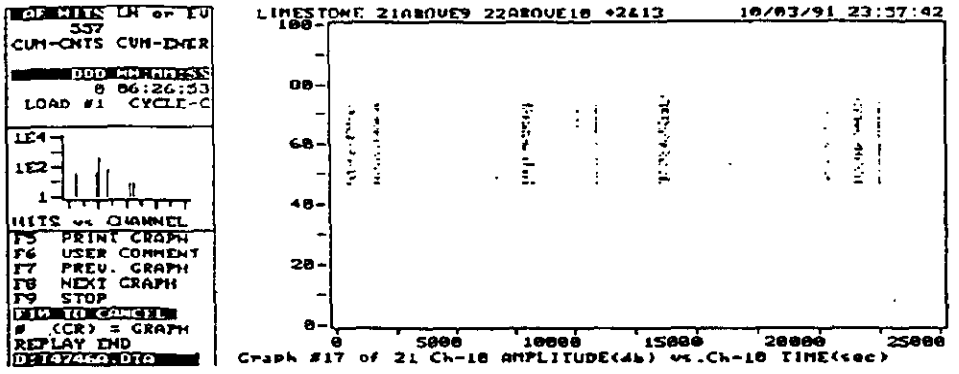

Figure 17. Channel 10 Amplitude vs Time for second 100% hold of LS

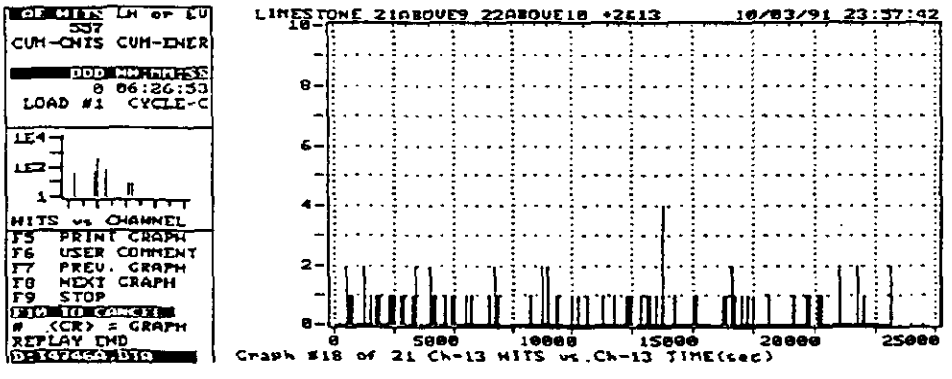

Figure 18. Channel 13 Hits vs Time for second 100% hold of LS

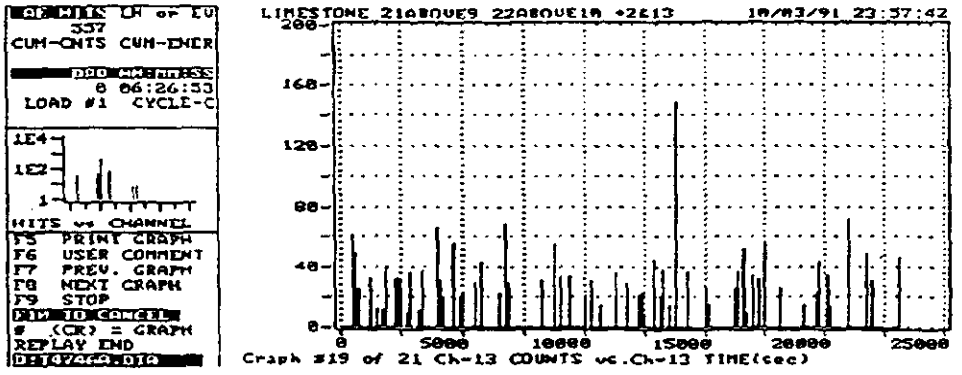

Figure 19. Channel 13 Counts vs Time for second 100% hold of LS

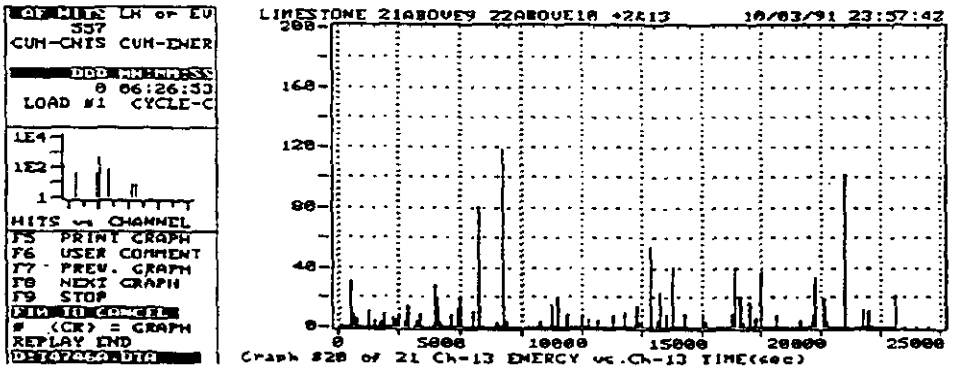

Figure 20. Channel 13 Energy vs Time for second 100% hold of LS

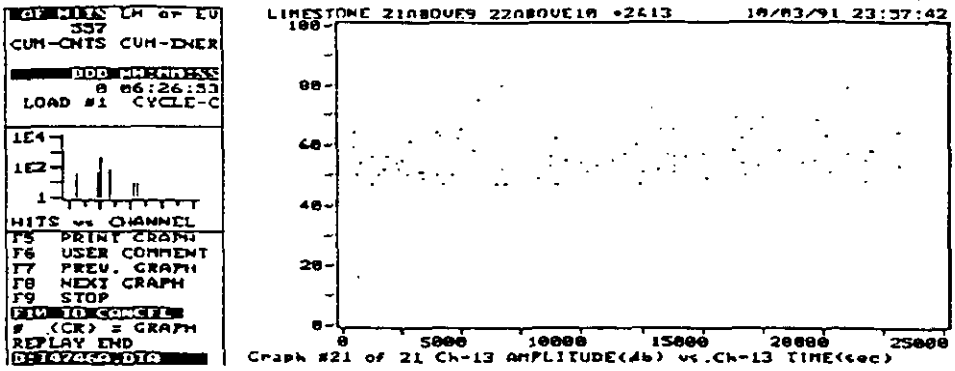

Figure 21. Channel 13 Amplitude vs Time for second 100% hold of LS

APPENDIX D

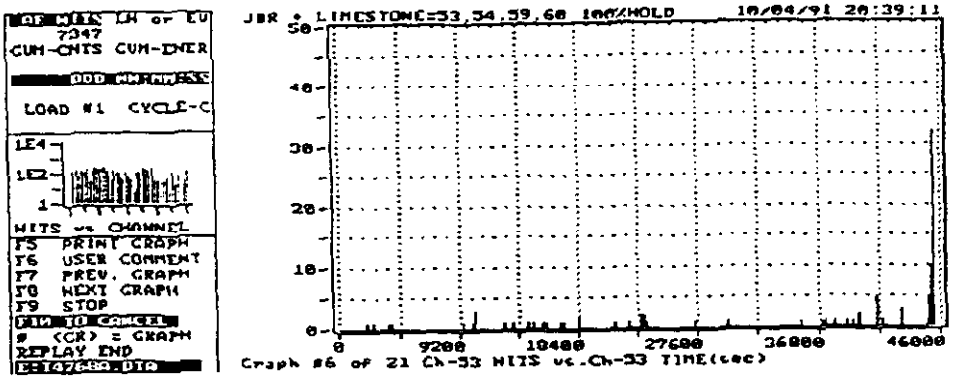

Figure 1. Channel 53 Hits vs Time for third 100% hold of LS

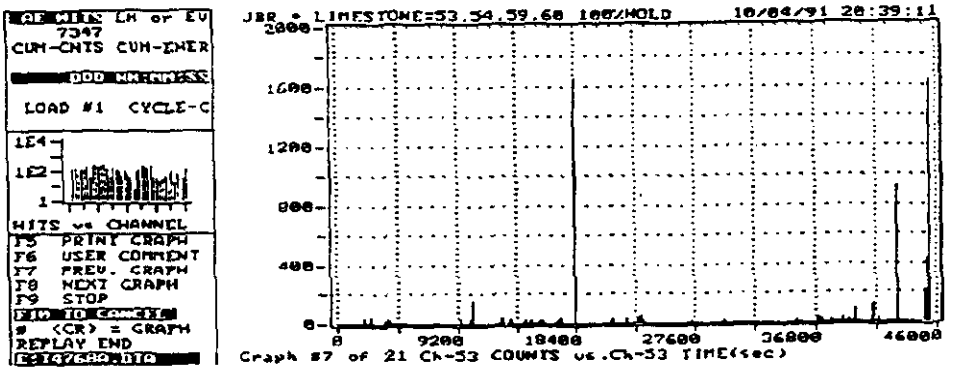

Figure 2. Channel 53 Counts vs Time for third 100% hold of LS

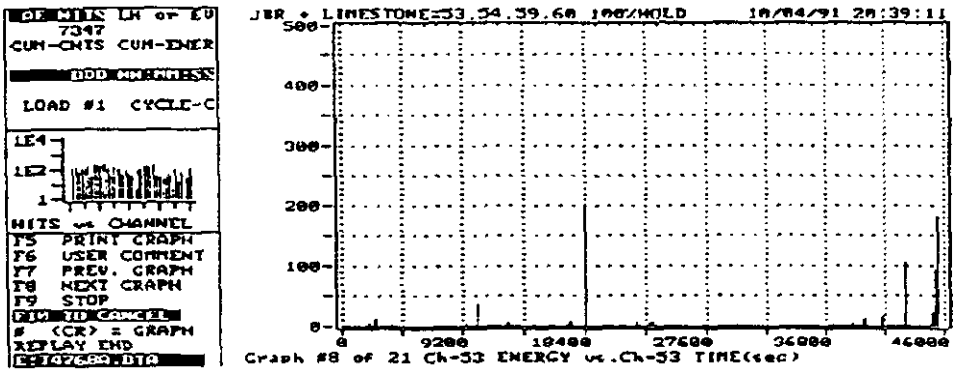

Figure 3. Channel 53 Energy vs Time for third 100% hold of LS

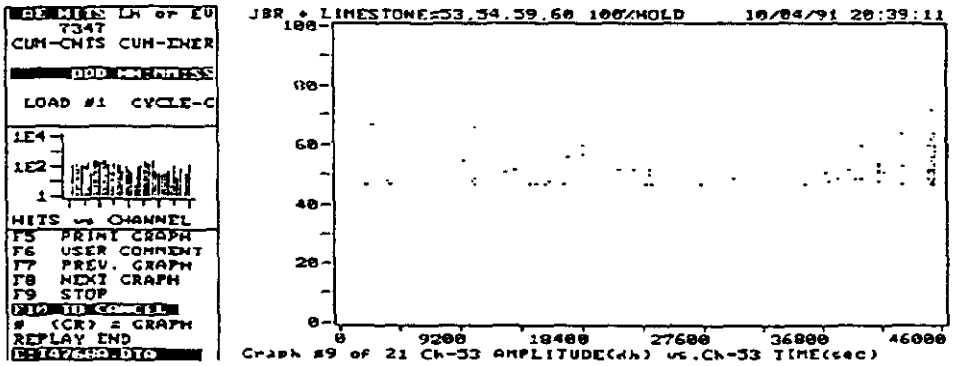

Figure 4. Channel 53 Amplitude vs Time for third 100% hold of LS

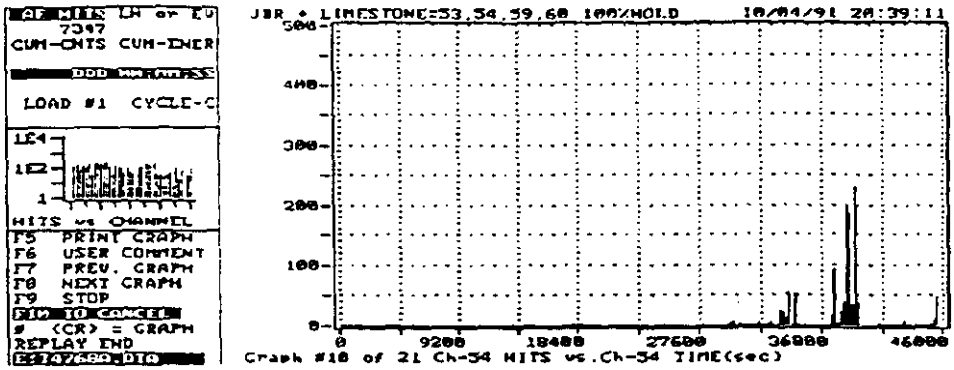

Figure 5. Channel 54 Hits vs Time for third 100% hold of LS

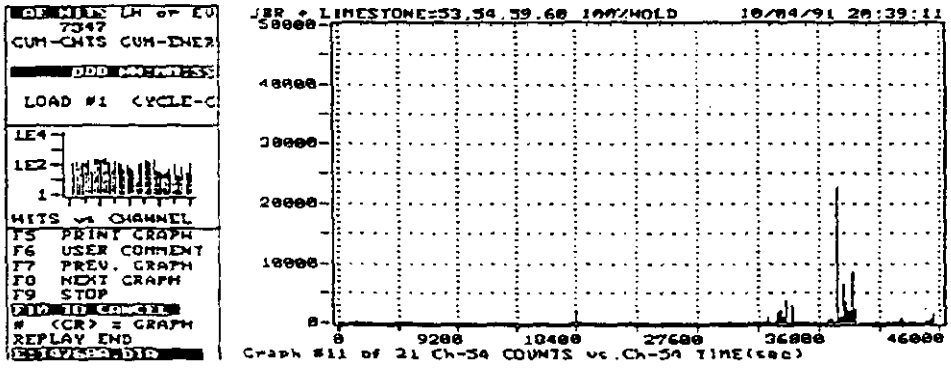

Figure 6. Channel 54 Counts vs Time for third 100% hold of LS

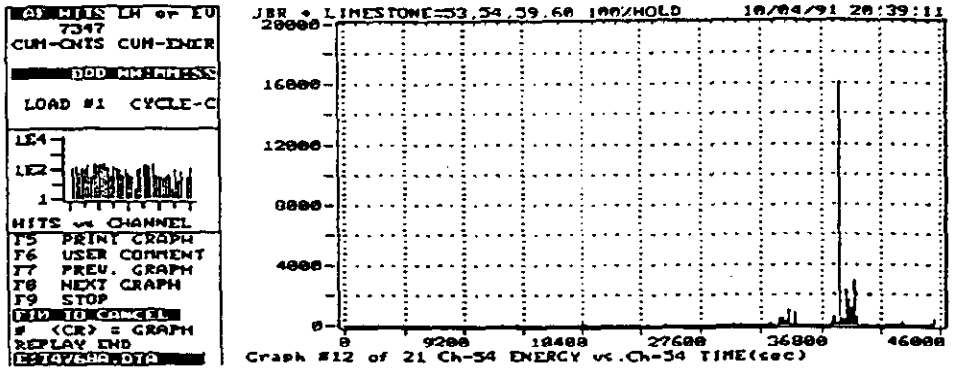

Figure 7. Channel 54 Energy vs Time for third 100% hold of LS

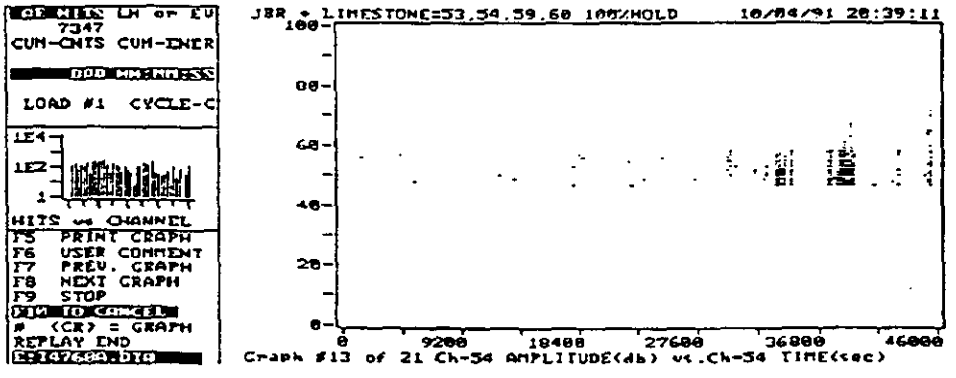

Figure 8. Channel 54 Amplitude vs Time for third 100% hold of LS

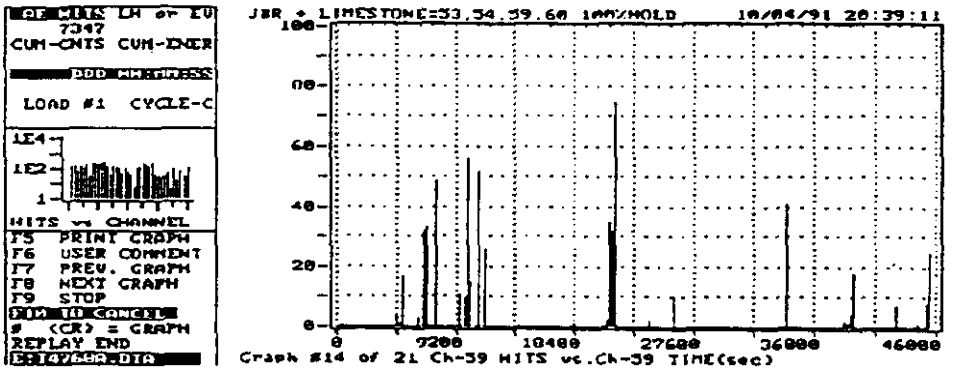

Figure 9. Channel 59 Hits vs Time for third 100% hold of LS

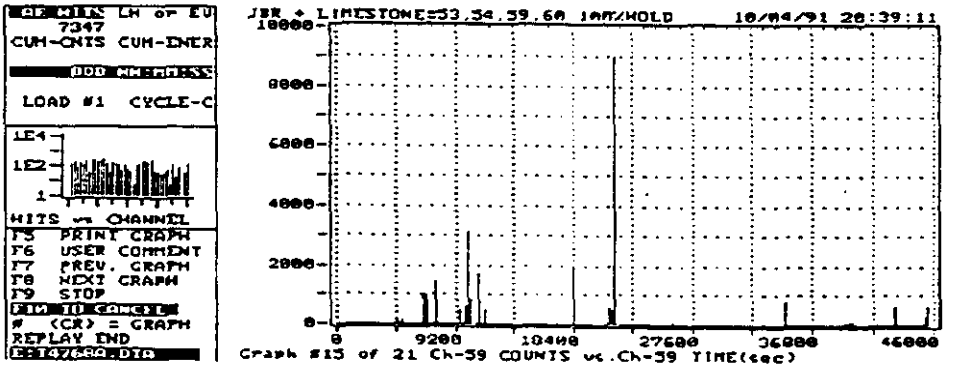

Figure 10. Channel 59 Counts vs Time for third 100% hold of LS

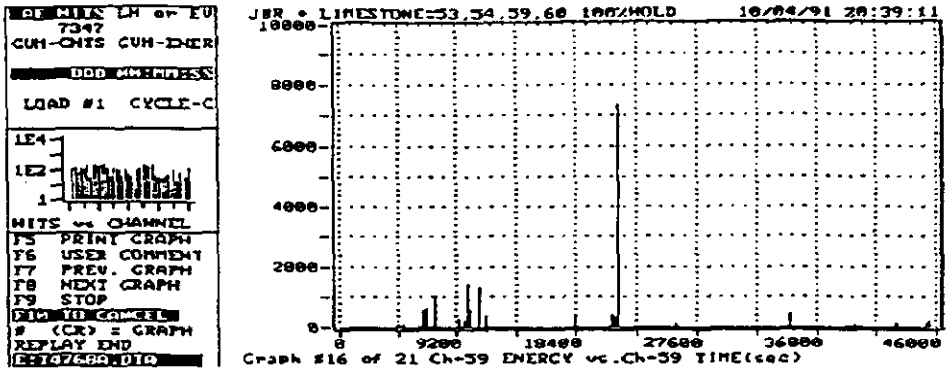

Figure 11. Channel 59 Energy vs Time for third 100% hold of LS

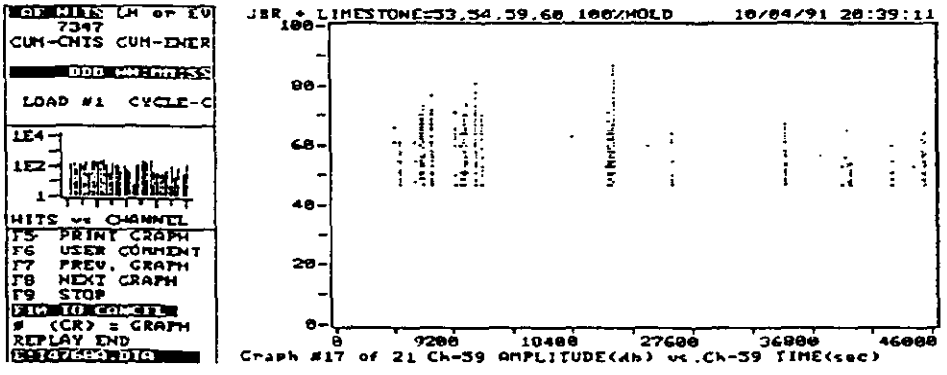

Figure 12. Channel 59 Amplitude vs Time for third 100% hold of LS

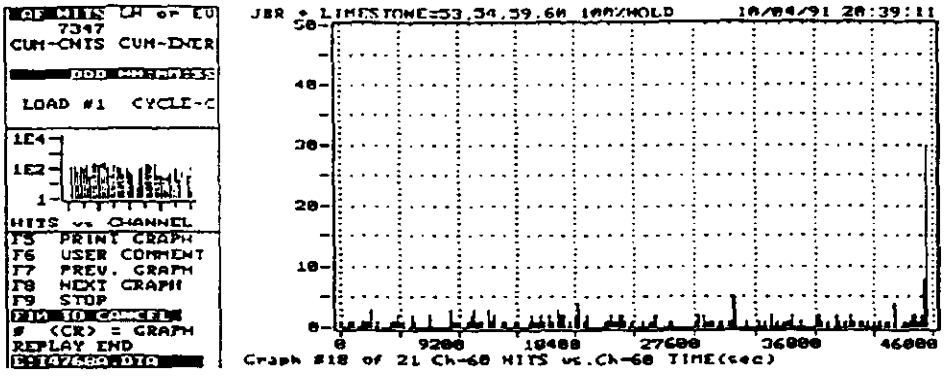

Figure 13. Channel 60 Hits vs Time for third 100% hold of LS

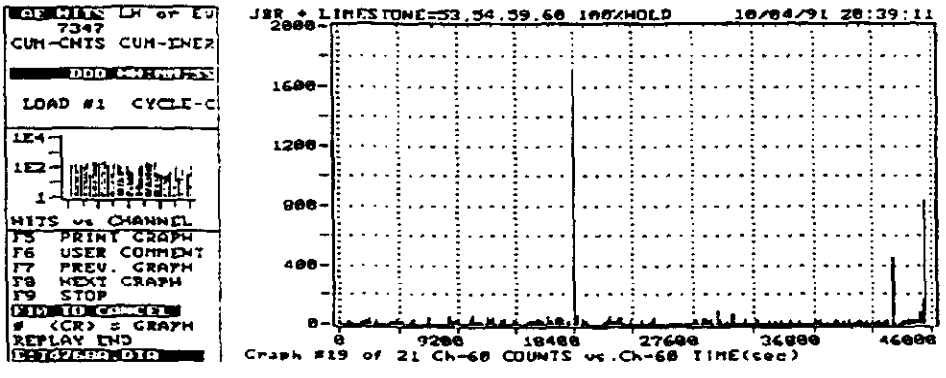

Figure 14. Channel 60 Counts vs Time for third 100% hold of LS

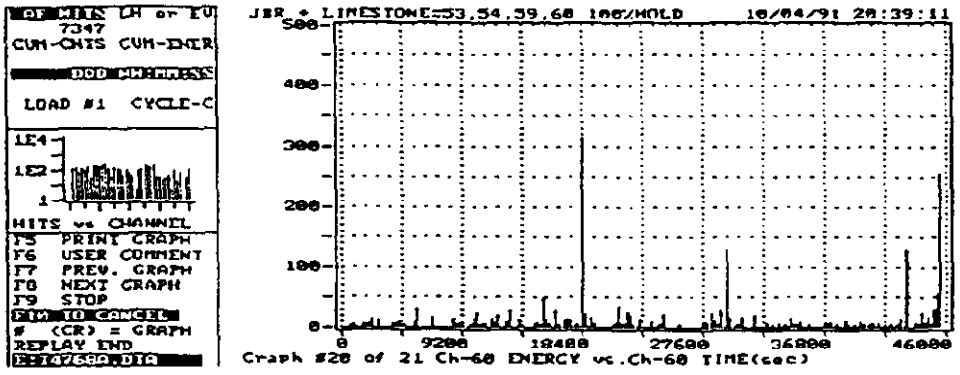

Figure 15. Channel 60 Energy vs Time for third 100% hold of LS

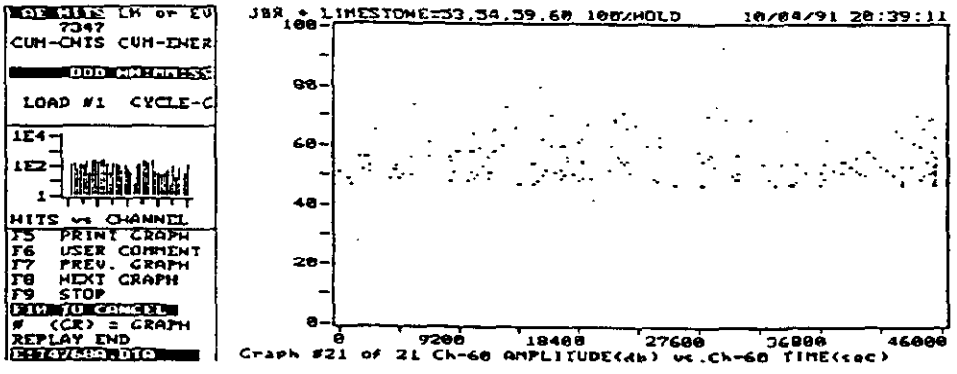

Figure 16. Channel 60 Ampltude vs Time for third 100% hold of LS

APPENDIX E

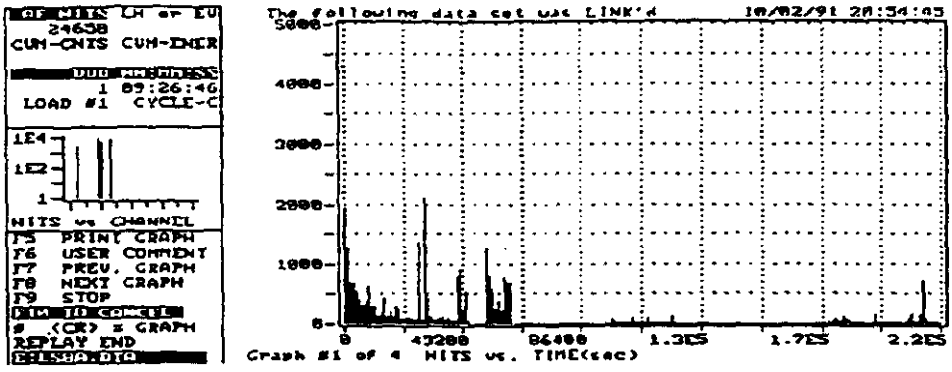

Figure 1. Hits vs Time for entire 100% hold of LS

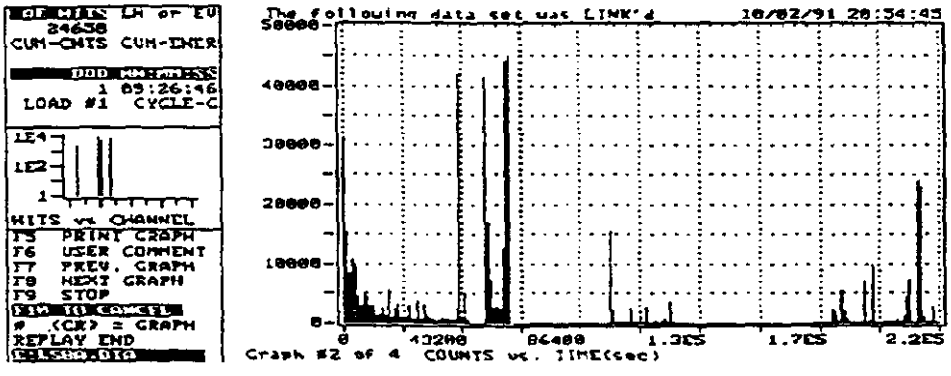

Figure 2. Counts vs Time for entire 100% hold of LS

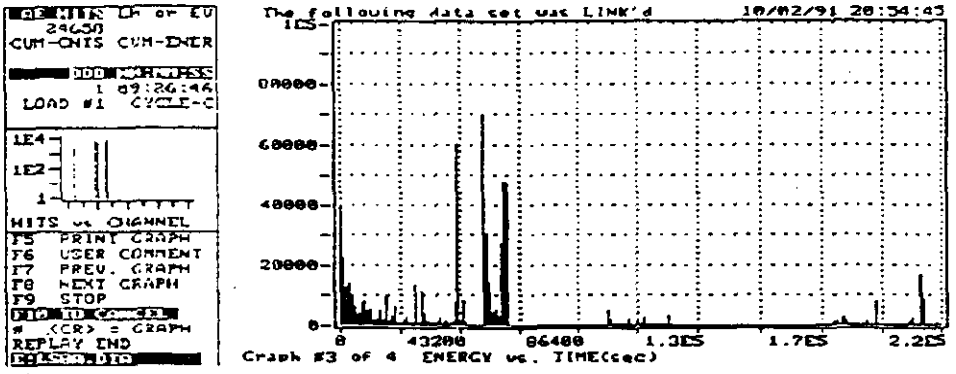

Figure 3. Energy vs Time for entire 100% hold of LS

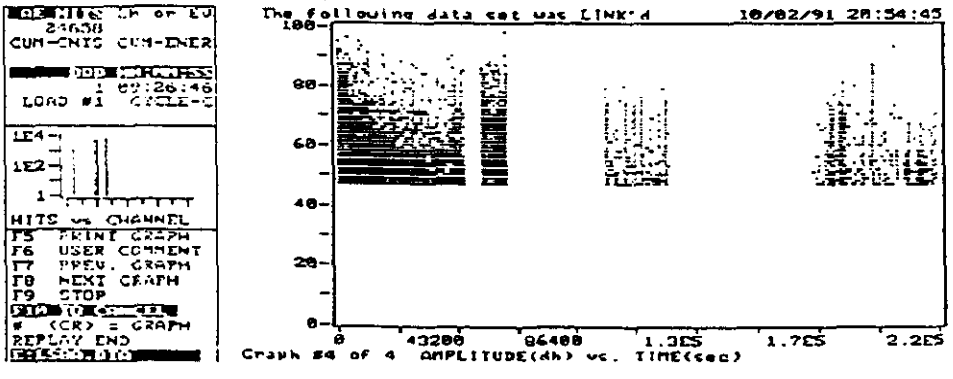

Figure 4. Amplitude vs Time for entire 100% hold of LS

PHYSICAL ACOUSTICS CORPORATION

NDT Instruments, Systems and Services

Acoustic Emission Instruments and Systems
Ultrasonic Imaging Workstations
Eddy Current Digital Instruments
Resistivity Material Testing Equipment
AE/NDT R&D Services, Consultancy and Applications

Spectral Analysis Workstations

Predictive Maintenance Systems
Vibration Measurement Equipment
Acoustic Analysis Instruments
Structural Evaluation Systems
Servo Control System Evaluation
Electronic Circuit Analysis Tools

Active Filters and Front End Processors

Butterworth, Bessel and Elliptic Programmable Filters
0-80dB Gain Front End Signal Conditioning Processors
Transient Recorders

CORPORATE HEADQUARTERS

P O Box 3135, Princeton, NJ 08543-3135 • (609) 844-0800 • Telex 67-17731 • FAX (609) 895-9726

SUBSIDIARIES

DUNEGAN CORP. • 23706B Birtcher Dr • El Toro, CA 92630
(714) 380-0107 • FAX (714) 380-0120

EUROPHYSICAL ACOUSTICS S.A. • 74, rue des Grands Champs • 75020
Paris, France • 33-14-356-2210 • FAX 33-1-43-56-6565

NIPPON PHYSICAL ACOUSTICS CORP. • 6F, Okamoto L.K. Bldg. 2-17-10
Higashi • Shibuya-Ku, Tokyo 150, Japan •
81-3-3498-3570 • FAX 81-3-3498-8450

PHYSICAL ACOUSTICS LTD. • Norman Way, Over,
CB4 5QE England • 44-954-31612 • FAX 44-95

PIEZO KINETICS, INC • P.O. Box 756 • Bellefonte,
(814) 355-1593 • FAX (814) 355-4342

ROCKLAND SCIENTIFIC CORP. • P.O. Box 3135 •
08543-3135 • (609) 844-0800 • FAX (609) 895-

PAC/ROCKLAND SCIENTIFIC GMBH • Ostring 32, 6451 Mainhausen 1,
Germany • 49-6182-32-72 • FAX 49-6182-32-71

Acoustic Emission Testing of On-site Fabricated FRP Vessels

Final Report
Project 5-343
July 7, 1991

Prepared for:

Mr. Kamyer Vakhsoorzadeh
Southern Company Services
P.O. Box 2625
Birmingham, AL 35202

Prepared by:

Bruce Gilbert
Physical Acoustics Corporation
15 Princess Road
Lawrenceville, NJ 08648

INTRODUCTION

Southern Company has recently embarked on the construction of large fiber reinforced plastic (FRP) structures and pressure vessels at Plant Yates (Georgia Power Company). These FRP components are used as the primary parts of the CT-121 flue gas desulfurization (FGD) process. FRP was primarily selected because it provided an economic advantages over other more conventional choices of materials. To verify the integrity of the FRP construction, QC/QA testing was sought. According to the previous experience of FRP equipment users, Acoustic Emission (AE) monitoring of FRP vessels provides the most promising diagnostic tool for FRP vessels. Accordingly, Physical Acoustics Corporation (PAC) was contacted to perform the required testing and verify the integrity of the FRP vessel and its construction. To reach this goal, a hydro-test was scheduled during the pre-operation phase of the Flue gas desulfurization (FGD) process. The primary goal of the hydro-tests were:

a) Detect, locate, and classify emission sources;
b) Evaluate the effectiveness of AE, if active sources are detected, for distinguishing emissions due to fiber cracking, fiber debonding/pull-out, resin cracking, delamination, secondary bond failures, background noise from loose parts, rubbing, etc.

TESTING

The vessel in question was constructed on-site by Ershigs using FRP materials to a size approximately 28'dia x 27'high. The vessel was tested under atmospheric pressure using water at ambient conditions. Prior to filling the vessel a 30 minute background noise check was performed. Loading of the vessel was accomplished with a standardized load-hold schedule. Hold periods were performed at approximately 50%, 75% & 100% fill levels for greater than 5 minutes to insure the integrity of the vessel.

The AE equipment was supplied by PAC and consisted of a 36 channel SPARTAN AT mated to an IBM compatible 386 host computer. The AE system was certified to be in calibration at the factory just prior to shipment to the job site. Sensors used for this test were PAC R15I's which were also calibrated just prior to shipment. Software used was SA-LOC version 3.03 dated 1/24/91. A sketch of the vessel and the approximate sensor location is included in figure 1. Operators from PAC were Dave Kessler (AE level III), Bruce Gilbert (AE level II) and Terry Tamutus.

The testing of the vessel was performed from 4/13 - 4/16/91. Setup was accomplished on 4/13 while actual data acquisition was accomplished on 4/15 and 4/16. Prior to actual loading with atmospheric water a 30 minute background noise check was performed. During this time no appreciable data was recorded and no sources of extraneous data were identified. Following this, loading was initiated at a somewhat controlled pace through a fire hose mated to the bottom of the vessel. After the initial portion of the loading it was verified the turbulence ~~were~~ was not a factor during this testing. Loading up to and including the 50% hold period showed no signs of significant AE, nor were there any burst type emissions which required further consideration.

Loading through 75% showed a similar response. Following this it was decided to load to 87% however for various reasons this loading step was overlooked. Once the water level reached 100% a data file was initiated. This file was intended to run for the entirety of the hold at 100% however there was extraneous noise from various construction and plant personnel to contend with. Within 30 minutes the disruptions to the vessel were concluded and another data file was initiated. This file ran for the next 14 hours until the test was concluded

DATA ANALYSIS AT 100% LOAD

The evaluation of this vessel was based on its' ability to acoustically stabilize over time, thus indicating a reliable vessel. By insuring this simple point it was possible to competently survey the vessel. The ability of the vessel to acoustically stabilize is contrasted to an exponential increase in AE activity during high load - hold periods which indicate a defective vessel and potential failure.

To determine the integrity of the vessel a graphical display of the data was employed. This included 14 graphs which represent the data in either hit based or event based plots. The plots based on hits show any data which crossed the threshold. The event based plots are developed by linking the AE sensors according to their location on the vessel. Using event based plotting it is possible to determine which sensor was closest to the source of the emission. In this manner only the first hit sensor's (the one closest to the source of the AE) data is plotted.

To understand the analysis of the data, each of the 14 graphs will be described. Graph #1 represents the energy of the first hit sensor (event graph) as a function of time. This graph is useful for determining the integrity of the vessel based on its ability to remain acoustically quiet and therefore sustain the load applied. An increase of energy released with time would indicate a defective vessel. Graph #2 is similar to #1 except that it shows the energy for all AE channels (hits) as opposed to graph #1 which is only for the first hit sensor (event). This graph is also useful, in the same manner, for evaluating the integrity of the vessel. Graph #3 shows the amplitude of the first hit sensor as a function of time. This plot shows the peak size of the first hit and helps to determine the severity of the AE activity. Graph #4 is very similar to #3 except that it is for all AE activity (hits) and not just the first hit. Graph #5 shows the number of first hit (event based) counts as a function of channel. This plot is useful for determining which channels are most active and also which are closest to the source of the AE). Graph #6 shows the counts as a function of channel for all hits. It is useful for determining the AE activity at a given sensor. Graph #7 shows the number of events as a function of channel. This graph is used to determine the number of times that a given channel was acoustically nearest the source of the AE. This is a very important graph for the vessel evaluation. Graph #8 shows the number of hits for a given channel and shows which channels were the most acoustically active during a test. Graph #9 shows the event based counts as a function of time. It is useful for determining in time when the activity occurred and its relative magnitude. This plot is also useful for determining the integrity of the vessel. Graph #10 is the cumulative hit based counts as a function of time. It is useful for determining the rate of count release within the vessel and helps to determine whether the vessel will ultimately be able to sustain the loads applied to the vessel over time. Graph #11 shows the events as a function of time. It tells when in time the activity occurred. It is different from #1 or #9 in that this graph does not relate to the magnitude or strength of the signal, but only to the number of occurrences of activity. Graph #13 represents the first hit channels as a function of time. It shows which channels were responsible for the AE activity and when they occurred in time. Graph #14 shows the channel activity as a function of time. It shows which channels were active during which periods of a test.

Since the AE data was recorded in two data files which covered the first 30 minutes and then an additional 14 hours, the graphical analysis was performed on two data files. The first analysis will focus on the initial 30 minutes.

1st 30 minutes at 100%

Two groups of data are included with this section of the report. The first represents the data which was filtered at the 47dB level and is included in Appendix A; the second remains at the threshold level used during the test, which was 40dB and is included as Appendix B. Both groups reveal the same trends, however the absolute numbers for each section differ. The graphs indicate that AE activity was prevalent during the entire 30 minute hold period at 100%. Further there were two periods of time where large bursts of AE were realized. This information is revealed in graphs number 1,2,9,11&12 of appendix A or B. From graphs #13&14 it is difficult to tell which channel is the source of the activity. From graphs #3&4 we can tell that the burst type activity was realized at levels up to approximately 80dB. Using graphs #6&8 it is apparent that sensors number 4 and 23 are the most active. However from graphs #5&7 (which show the first hit channels only) we can see that sensors number 4,9&11 are closest to the source of the emission.

next 14.5 hours at 100%

Following the first 30 minute period, AE data was acquired for an additional 14.5 hours. The data was taken unattended and overnight with a threshold of 40dB. Included with the section of the report are three different groupings of the data using the previously discussed 14 graphs. What differs between the three groups is the minimum threshold for analysis. The first group, included as Appendix C, has the acquisition threshold of 40dB and represents the entirety of the data taken. The second group uses a threshold of 47dB and is seen in Appendix D, while the third group contains only data with a minimum threshold of 60dB and which occurred during a period of burst activity. The last file is included as Appendix E and was used primarily to investigate the source of the data in more detail.

The data analysis for the 14.5 hours is identical to that taken during the initial 30 minute hold period at 100%. In support of this conclusion refer to graphs #5&7 of appendix C or D in which sensors 4 and 9 are again in the region of most of the AE activity. Reviewing the remainder of the graphs it is apparent that a number of regions of burst type activity exist. It is this burst type activity that was of concern during the long term hold at 100% and was the main topic of evaluation for this data file. Since the magnitude of this data is unclear, due to the scattering of amplitudes found in graphs #13&14, it was decided to filter the data at an amplitude level of 60dB. From the majority of the graphs developed as a function of time at the 60dB filtering level, it was revealed that there are 5 sections of data in which burst type activity of substantial amplitude and energy were realized. To simplify the analysis of there 5 sections, the data was further filtered such that the remaining data contained information only greater than 60dB and only during the time of the bursts. From this data file a number of plots were generated for evaluation and included in appendix E. The hand writing on graph #2 of appendix E indicates the time and energy at which these bursts occurred. Graph #7 reveals that sensors 4 and 9 were

responsible for the majority of this data. Comparing graphs #3&4 which in this case show the amplitude distribution as a function of time for events(#3) and hits(#4), it is revealed that the highest amplitude for a given burst is not necessarily the first hit. This information, along with a desire to further investigate the origin of this activity lead to the next group of printouts. This information is the numerical data found in the data file that was used to generate the previous plots. Looking at the times that these burst occurred and referring to the numerical data printouts it can be verified that the labeled sensors on graph #2 were first hit. As eluded to earlier, there are always a number of smaller, precursors to the high energy & count, long duration activity. This explains why the first hit on the graphs was not necessarily the highest amplitude. The overall conclusion to the analysis was again that sensors 4 and 9 were responsible for the noteworthy AE activity.

DISCUSSION

The response of the vessel to the 100% load level was characterized with random AE throughout the hold, as well as periods of burst type activity. The arbitrary, low level activity was not of immediate concern due to its randomness. Of concern however were those periods of burst type AE activity during the overnight hold period. As was conveyed from the results, sensors #4,9&11 were the most active, and responsible for the majority of the AE. With this in mind the vessel schematic released to PAC was reviewed in conjunction with the sensor placement. Although this layout was not identical to the vessel which was tested, it had enough detail to reveal that at least some of sensors #4,9&11 were mounted in the region of vessel fittings. Further, it was found that each of the active sensors were mounted at locations where photoelastic plates were. (Recall that the photoelastic plates were being used as part of testing which was being done independent of the AE work). Suspicion was raised at this point to the following facts:

1.) there were exactly three photoelastic plates mounted on the vessel and each happened to be in the region of the sensors with the highest activity level,

2.) there was relatively no sensor pattern associated with the random continuing activity,

3.) there existed a limited amount of burst type activity generated during the 14 hour hold period which directly related to only those three sensors.

From these facts, it was inferred that the AE generated during this burst mode was probably from the photoelastic equipment. However, there were a number of points to contest the plates as being the source:

1.) the greater than 85dB amplitudes,

2.) durations up to 50 milliseconds combining with secondary hits to form AE activity clusters which ran for seconds at a time, all from a single source,

3.) the fact that almost 90% of the sensors were hit by these single sources.

These fact tend to support that a phenomenon other than the adhesive which bonds the photoelastic plates to the vessel could be the source.

CONCLUSIONS

1.) Sensors #4,9&11 were identified as being the source of relatively high levels of AE activity. As such the immediate area surrounding these sensors, according to figure 1, should be further investigated using an alternative inspection method.

2.) The coincidence between the three most active sensors being in the region of the three photoelastic plates makes it highly likely that at least some, if not all, of the AE was generated from the photoelastic plates.

3.) The high levels of AE activity generated during the periods of burst type activity make it possible that a source other than that identified in point 2, could be the source of the AE. Mainly, a phenomenon associated with the degradation of the vessel.

4.) The random level of AE associated with this vessel at the 100% hold period did not completely decay as anticipated. Although the level of this activity was relatively low, there still remained an ample amount of AE such that standardized inspection criteria could not be applied to this vessel.

5.) The burst type AE that was realized during the hold period overnight would not have been obtained if standard inspection periods had been followed.

RECOMMENDATIONS

1.) During future efforts in which AE is employed, the photoelastic plate effects must be addressed. Potential avenues include performing the photoelastic effort at an alternate time or insuring that no AE is generated from the plate attachments.

2.) As identified above the personnel employed to fill the tank, check for leakage, observe the test, perform the photoelastic measurements, etc. were a source of potential AE. It was not until the overnight hold period that the data was considered to be free of human intervention. In future testing, the area immediately surrounding the vessel must be secured so that human intervention is avoided.

3.) To gain further information about the vessel, the Kaiser effect and the Felicity Ratio, a second loading should be employed. This loading could be applied approximately 12 hours after the 100% level was removed. By decreasing the water level to 50% during for 12 hours and then reloading to 100%, much information could be gained for charting the integrity of the vessel over time.

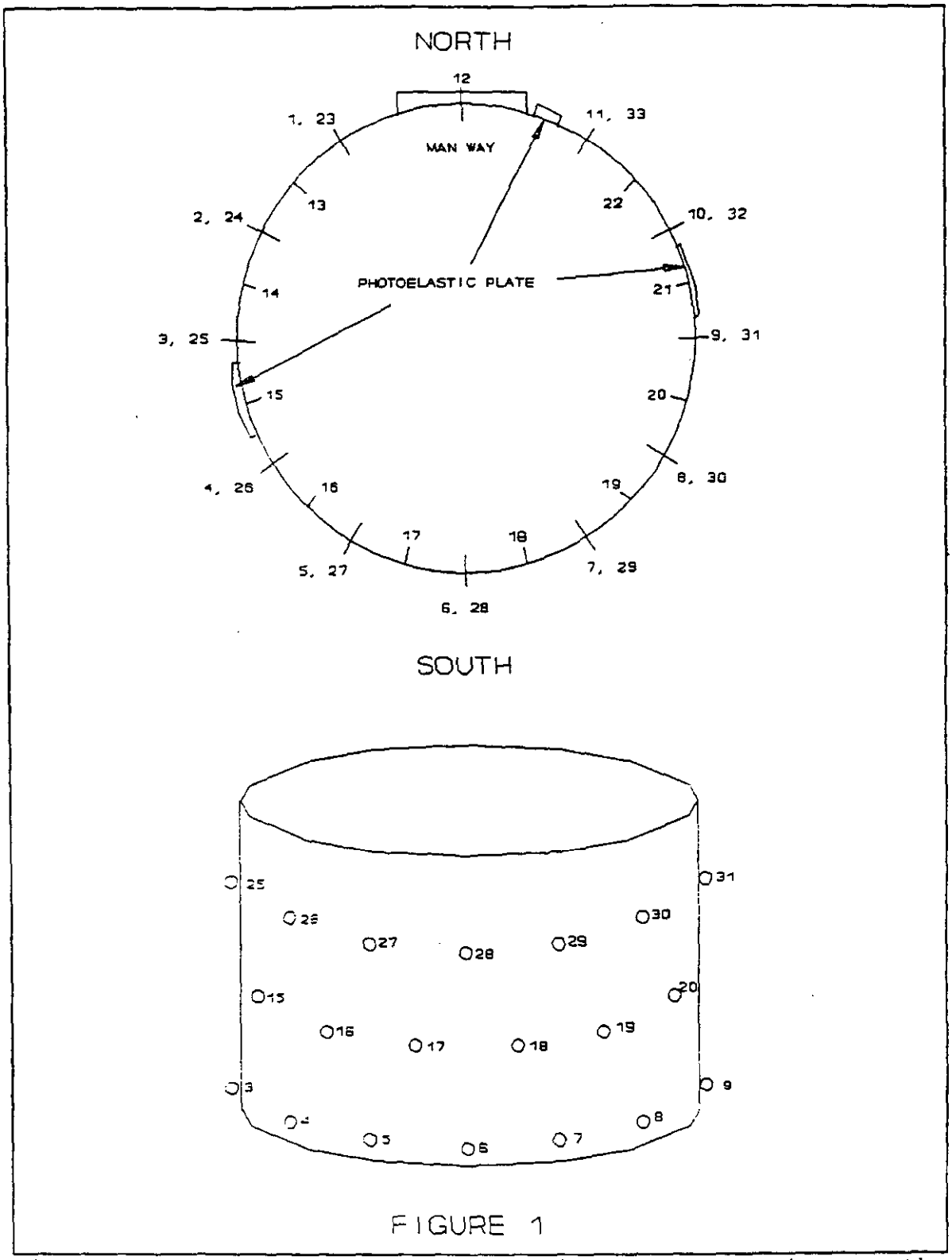

Figure 1: AE Sensor and photoelastic plate location on the vessel.

APPENDIX A

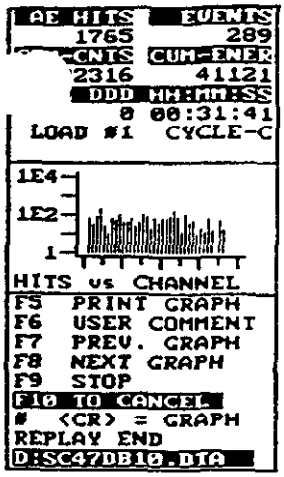
AE HITS EVENTS
1765 289
CNTS CUM-ENER
2316 41121
DDD HH:MM:SS
0 00:31:41
LOAD #1 CYCLE-C
1E4
1E2
1
HITS vs CHANNEL
F5 PRINT GRAPH
F6 USER COMMENT
F7 PREV. GRAPH
F8 NEXT GRAPH
F9 STOP
F10 TO CANCEL
<CR> = GRAPH
REPLAY END
D:SC47DB10.DTA

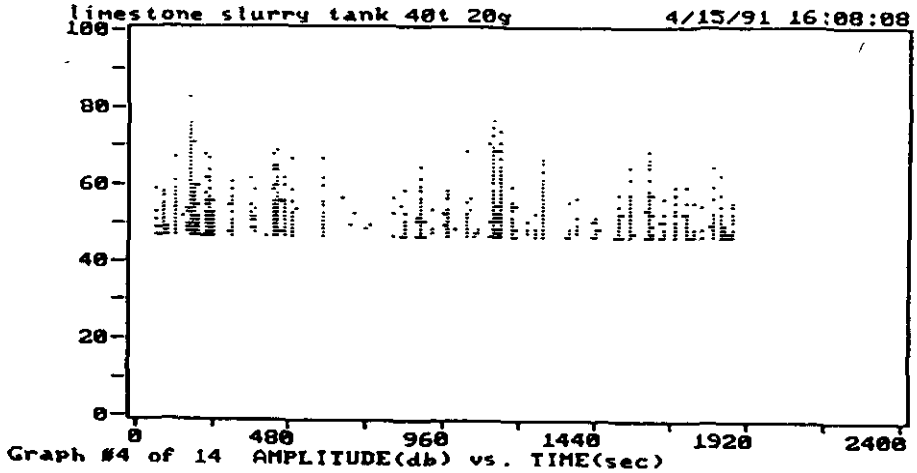
limestone slurry tank 40t 20g
4/15/91 16:08:08
100
80
60
40
20
0
0
480
960
1440
1920
2400
Graph #4 of 14 AMPLITUDE(db) vs. TIME(sec)

AE HITS	EVENTS
1765	289
-CNTS	CUM-ENER
32316	41121
DDD	HH:MM:SS
0	00:31:41

LOAD #1 CYCLE-C

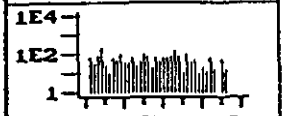

HITS vs CHANNEL

F5 PRINT GRAPH
F6 USER COMMENT
F7 PREV. GRAPH
F8 NEXT GRAPH
F9 STOP
F10 TO CANCEL
<CR> = GRAPH
REPLAY END
D:\SC47\DB10.DTA

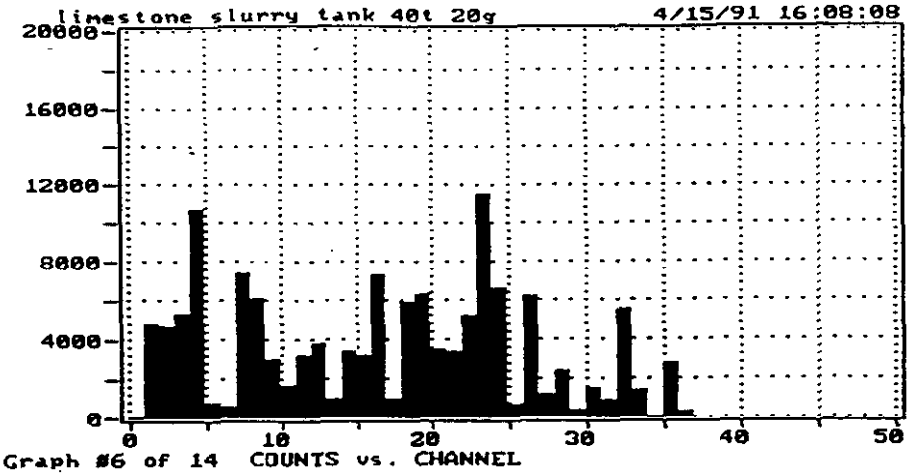

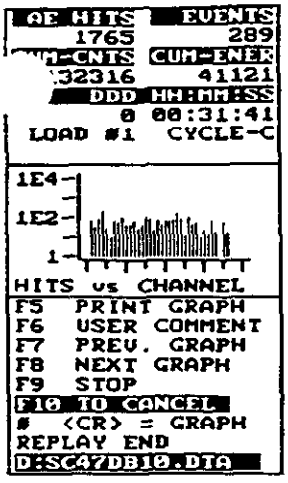
HITS
EVENTS
1765
289
CUM-ENER
32316
41121
DDD HH:MM:SS
0 00:31:41
LOAD #1 CYCLE-C
1E4
1E2
1
HITS vs CHANNEL
F5 PRINT GRAPH
F6 USER COMMENT
F7 PREV. GRAPH
F8 NEXT GRAPH
F9 STOP
F10 TO CANCEL
<CR> = GRAPH
REPLAY END
D:\SC47DB10.DTA

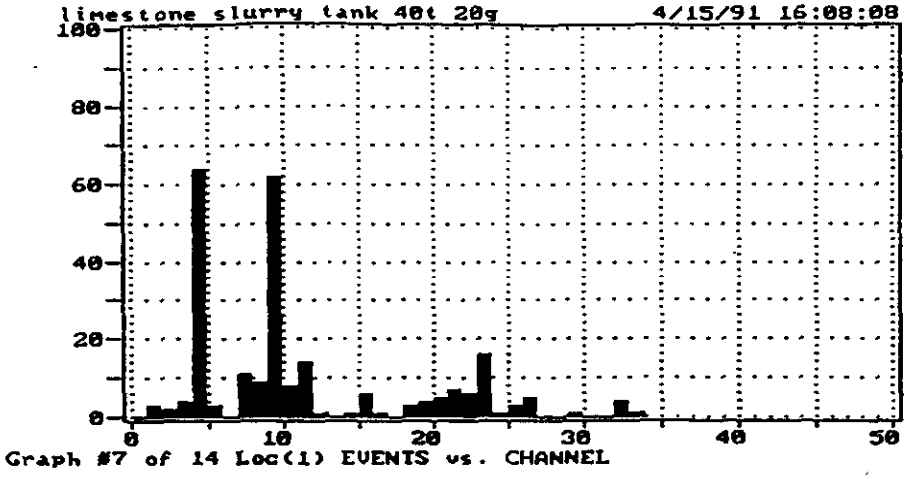
limestone slurry tank 40t 20g
4/15/91 16:08:08
100
80
60
40
20
0
0
10
20
30
40
50
Graph #7 of 14 Loc(1) EVENTS vs. CHANNEL

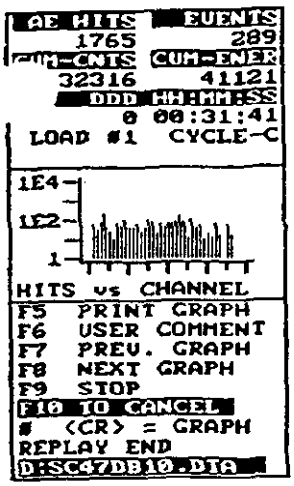
AE HITS
1765
EVENTS
289
M-CNTS
32316
CUM-ENER
41121
DDD HH:MM:SS
0 00:31:41
LOAD #1 CYCLE-C
1E4
1E2
1
HITS vs CHANNEL
F5 PRINT GRAPH
F6 USER COMMENT
F7 PREV. GRAPH
F8 NEXT GRAPH
F9 STOP
F10 TO CANCEL
<CR> = GRAPH
REPLAY END
D:SC47DB10.DTA

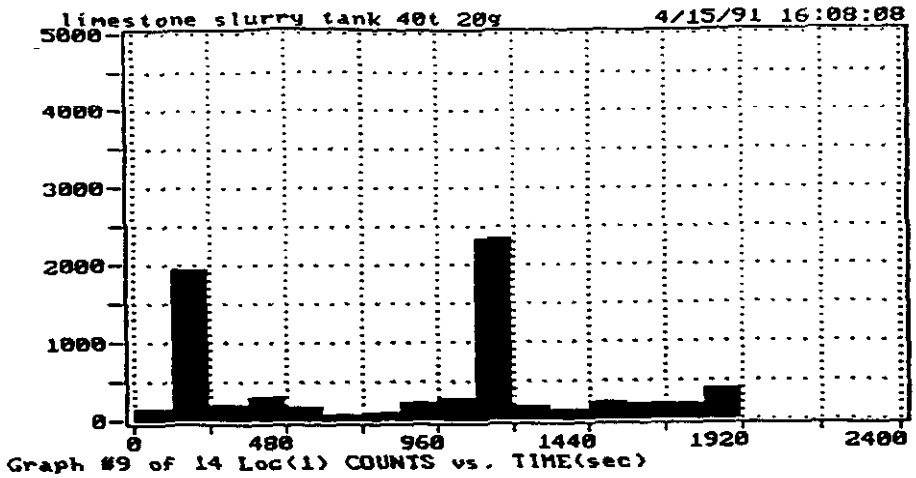
limestone slurry tank 40t 20g
4/15/91 16:08:08
5000
4000
3000
2000
1000
0
0
480
960
1440
1920
2400
Graph #9 of 14 Loc(1) COUNTS vs. TIME(sec)

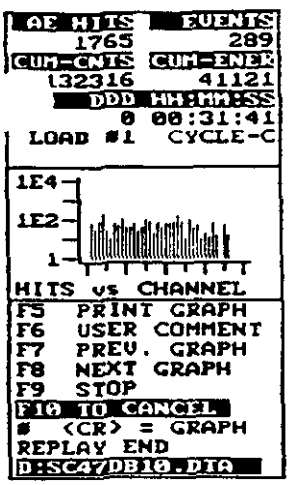
AE HITS
1765
EVENTS
289
CUM-CNTS
132316
CUM-ENER
41121
DDD HH:MM:SS
0 00:31:41
LOAD #1 CYCLE-C
1E4
1E2
1
HITS vs CHANNEL
F5 PRINT GRAPH
F6 USER COMMENT
F7 PREV. GRAPH
F8 NEXT GRAPH
F9 STOP
F10 TO CANCEL
<CR> = GRAPH
REPLAY END
D:SC47DB10.DTA

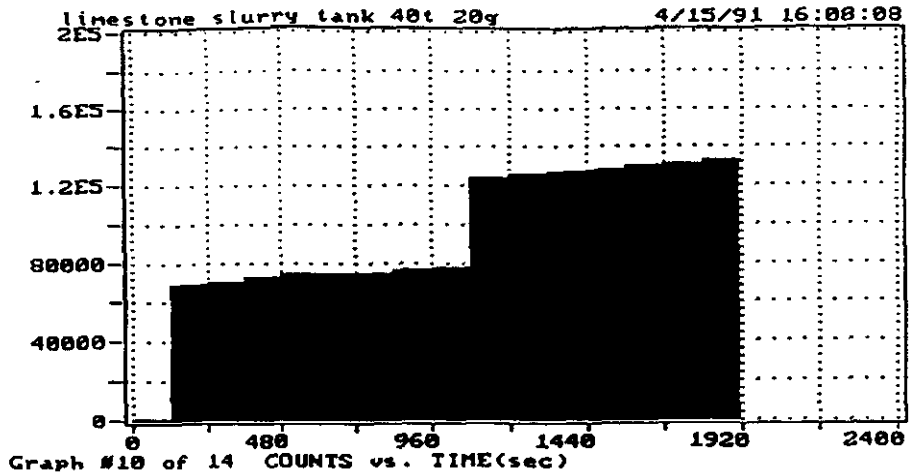
limestone slurry tank 40t 20g
4/15/91 16:08:08
2E5
1.6E5
1.2E5
80000
40000
0
0
480
960
1440
1920
2400
Graph #10 of 14 COUNTS vs. TIME(sec)

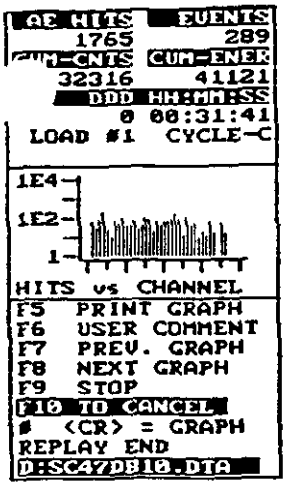

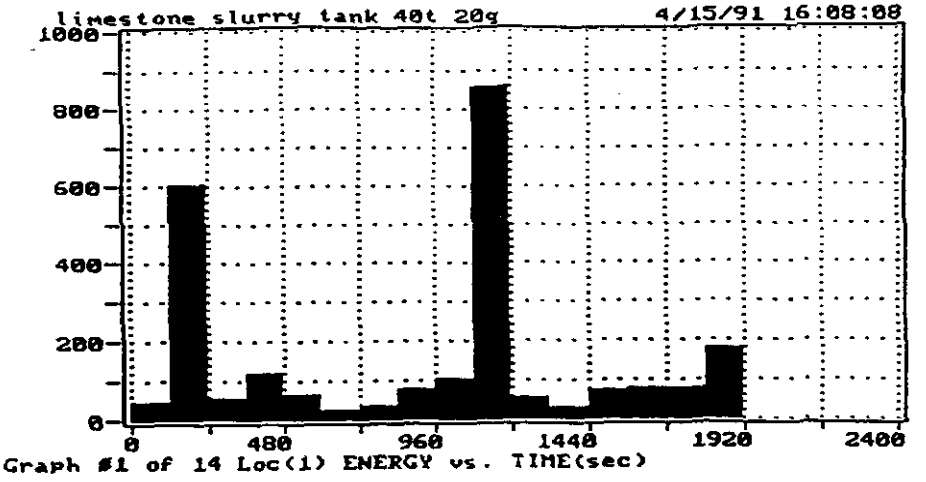

1ST 30-MIN LOAD AT 100%

47dB TRANSIENTS

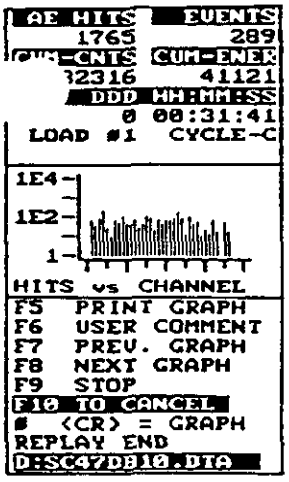
AE HITS
1765
EVENTS
289
CUM-CNTS
32316
CUM-ENER
41121
DDD HH:MM:SS
0 00:31:41
LOAD #1 CYCLE-C
1E4
1E2
1
HITS vs CHANNEL
F5 PRINT GRAPH
F6 USER COMMENT
F7 PREV. GRAPH
F8 NEXT GRAPH
F9 STOP
F10 TO CANCEL
<CR> = GRAPH
REPLAY END
D:SC47DB10.DTA

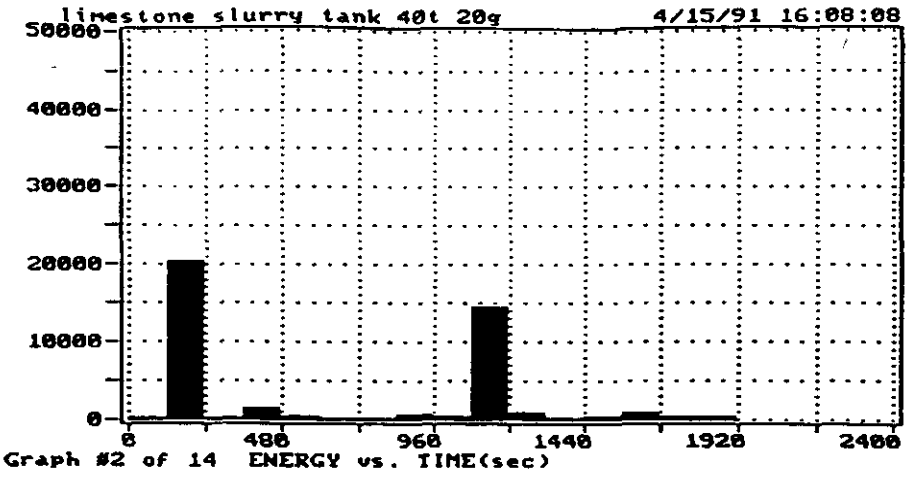
limestone slurry tank 40t 20g
4/15/91 16:08:08
50000
40000
30000
20000
10000
0
0
480
960
1440
1920
2400
Graph #2 of 14 ENERGY vs. TIME(sec)

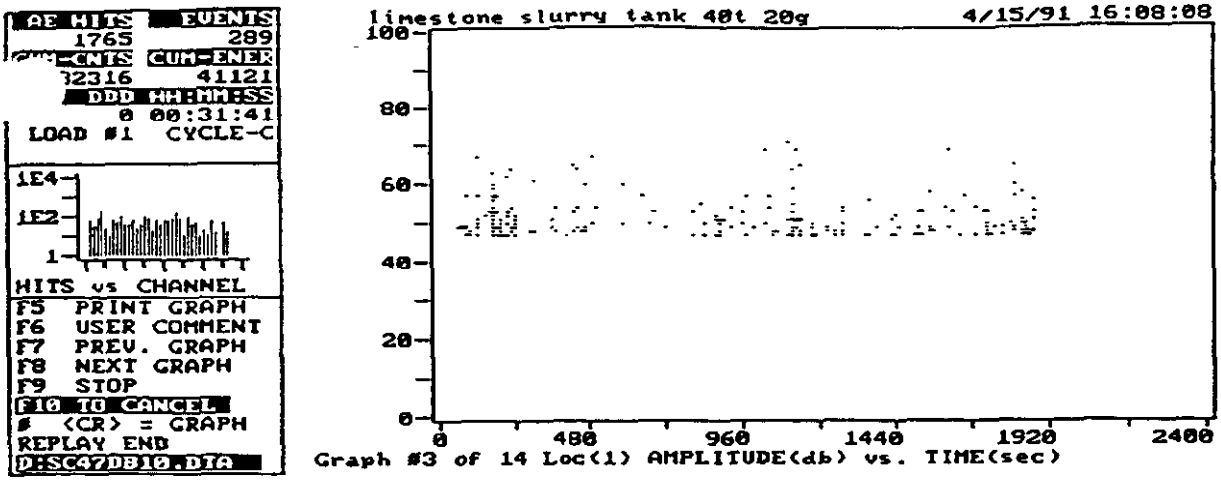
AE HITS
1765
EVENTS
289
CNTS
32316
CUM-ENER
41121
DDD HH:MM:SS
0 00:31:41
LOAD #1 CYCLE-C
1E4
1E2
1
HITS vs CHANNEL
F5 PRINT GRAPH
F6 USER COMMENT
F7 PREV. GRAPH
F8 NEXT GRAPH
F9 STOP
F10 TO CANCEL
<CR> = GRAPH
REPLAY END
D:\SC47DB10.DTA
limestone slurry tank 40t 20g
4/15/91 16:08:08
100
80
60
40
20
0
0
480
960
1440
1920
2400
Graph #3 of 14 Loc(1) AMPLITUDE(db) vs. TIME(sec)

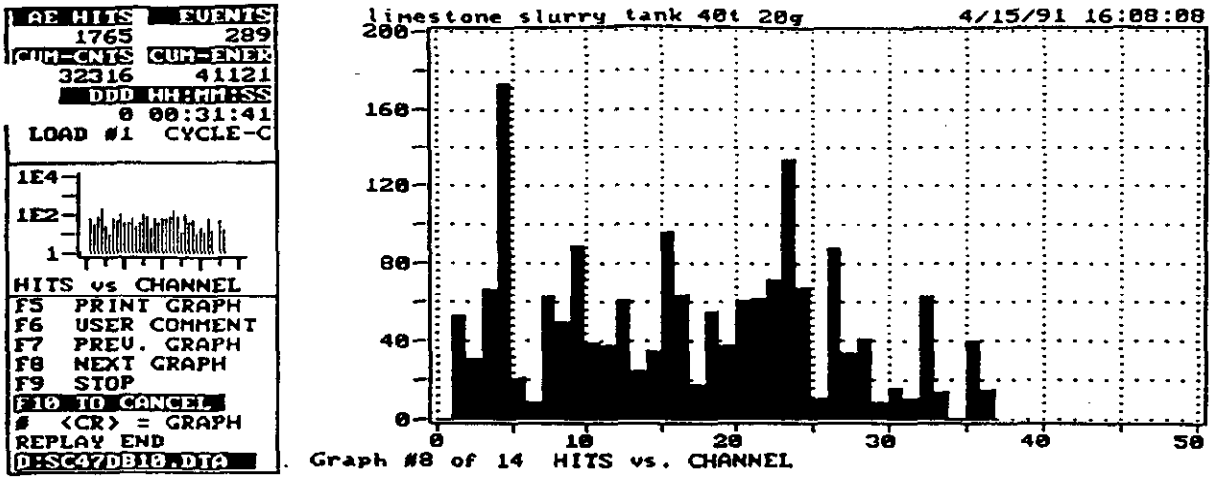
AE HITS
1765
EVENTS
289
CUM-CNTS
32316
CUM-ENER
41121
DDD HH:MM:SS
0 00:31:41
LOAD #1 CYCLE-C
1E4
1E2
1
HITS vs CHANNEL
F5 PRINT GRAPH
F6 USER COMMENT
F7 PREV. GRAPH
F8 NEXT GRAPH
F9 STOP
F10 TO CANCEL
<CR> = GRAPH
REPLAY END
D:SC47DB10.DTA
limestone slurry tank 40t 20g
4/15/91 16:08:08
200
160
120
80
40
0
0
10
20
30
40
50
Graph #8 of 14 HITS vs. CHANNEL

AE HITS	EVENTS
1765	289
CUM-CNTS	CUM-ENER
32316	41121
DDD HH:MM:SS	
0	00:31:41

LOAD #1 CYCLE-C

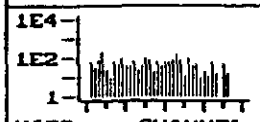

HITS vs CHANNEL

F5 PRINT GRAPH
F6 USER COMMENT
F7 PREV. GRAPH
F8 NEXT GRAPH
F9 STOP
F10 TO CANCEL
<CR> = GRAPH
REPLAY END
D:\SC47DB10.DTA

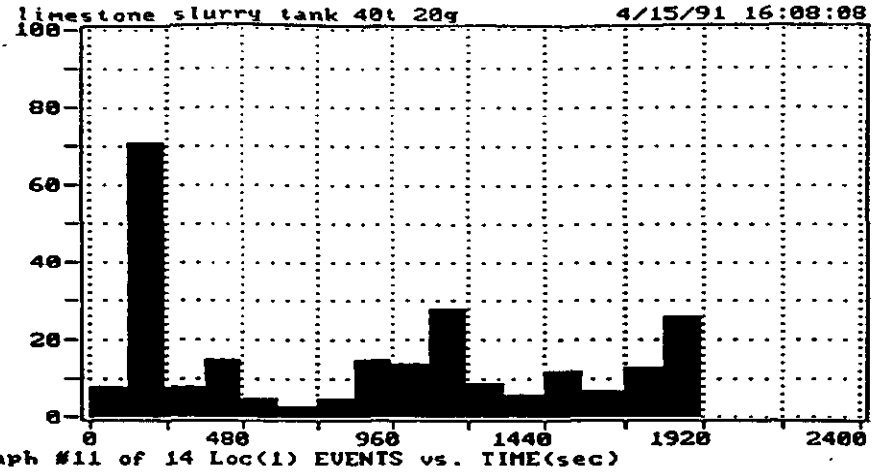

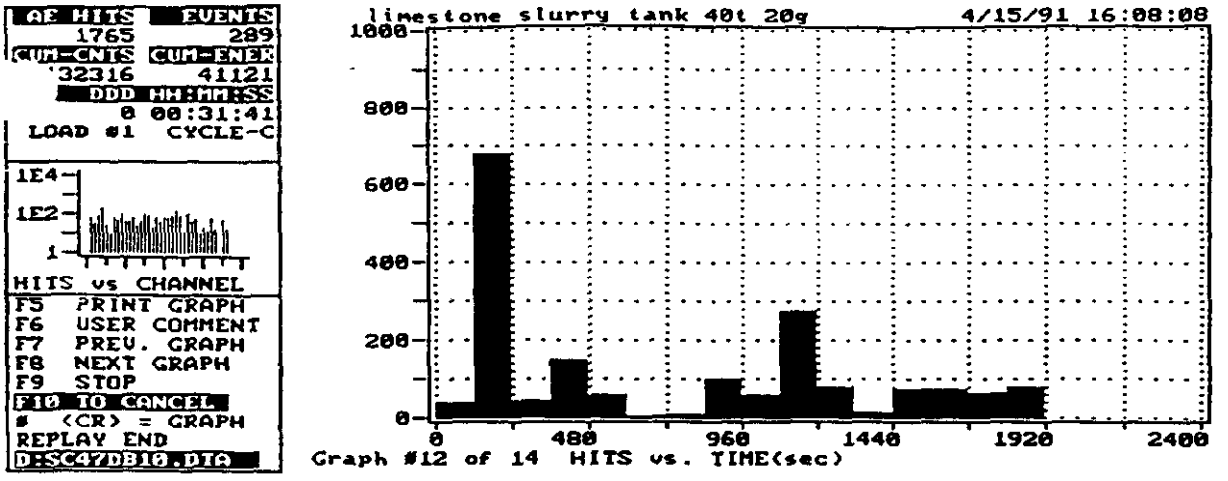
AE HITS
EVENTS
1765
289
CUM-CNTS
CUM-ENER
32316
41121
DDD HH:MM:SS
0 00:31:41
LOAD #1 CYCLE-C
1E4
1E2
1
HITS vs CHANNEL
F5 PRINT GRAPH
F6 USER COMMENT
F7 PREV. GRAPH
F8 NEXT GRAPH
F9 STOP
F10 TO CANCEL
<CR> = GRAPH
REPLAY END
D:\SC47DB10.DTA
limestone slurry tank 40t 20g
4/15/91 16:08:08
1000
800
600
400
200
0
0
480
960
1440
1920
2400
Graph #12 of 14 HITS vs. TIME(sec)

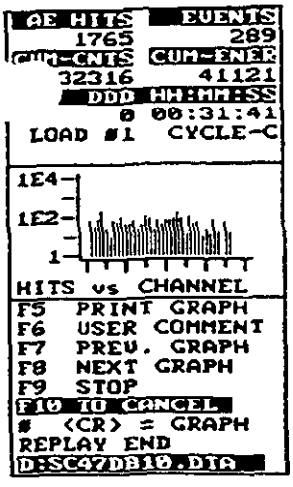
HIT HITS
1765
EVENTS
289
CUM-CNTS
32316
CUM-ENER
41121
DDD HH:MM:SS
0 00:31:41
LOAD #1 CYCLE-C
1E4
1E2
1
HITS vs CHANNEL
F5 PRINT GRAPH
F6 USER COMMENT
F7 PREV. GRAPH
F8 NEXT GRAPH
F9 STOP
F10 TO CANCEL
<CR> = GRAPH
REPLAY END
D:SC47DB10.DTA

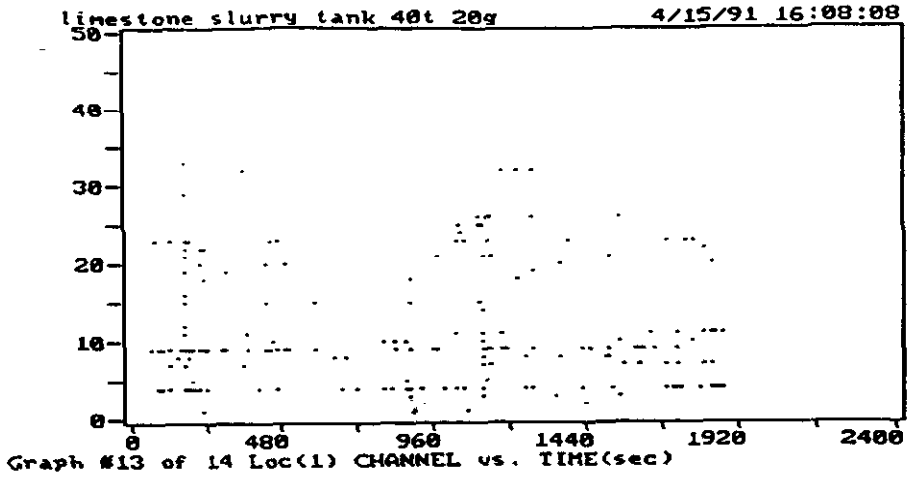
limestone slurry tank 40t 20g
4/15/91 16:08:08
50
40
30
20
10
0
0
480
960
1440
1920
2400
Graph #13 of 14 Loc(1) CHANNEL vs. TIME(sec)

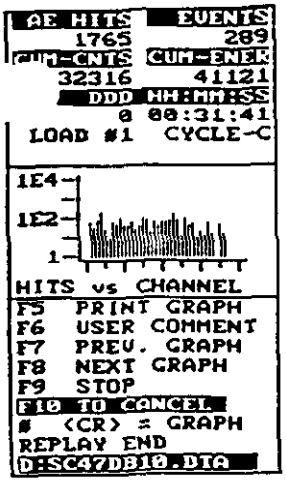
AE HITS
EVENTS
1765
289
CUM-CNTS
CUM-ENER
32316
41121
DDD HH:MM:SS
0 00:31:41
LOAD #1 CYCLE-C
1E4
1E2
1
HITS vs CHANNEL
F5 PRINT GRAPH
F6 USER COMMENT
F7 PREV. GRAPH
F8 NEXT GRAPH
F9 STOP
F10 TO CANCEL
<CR> = GRAPH
REPLAY END
D:SC47DB10.DTA

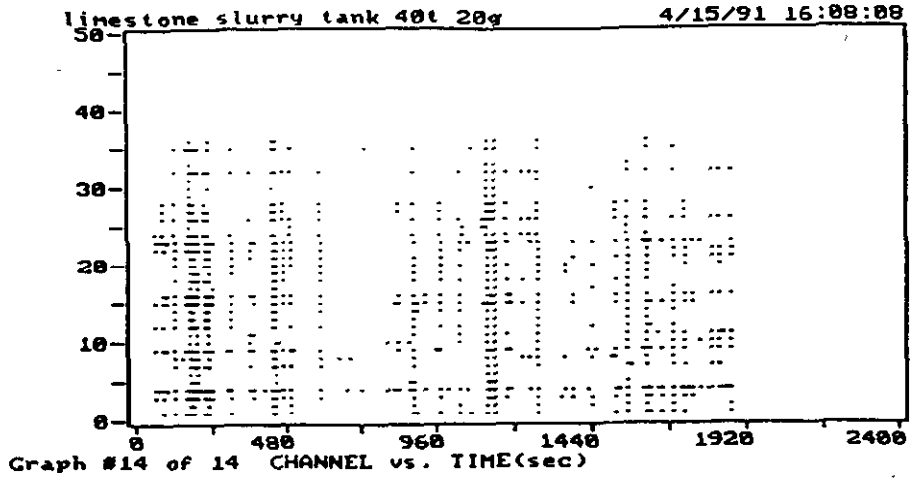
limestone slurry tank 40t 20g
4/15/91 16:08:08
50
40
30
20
10
0
0
480
960
1440
1920
2400
Graph #14 of 14 CHANNEL vs. TIME(sec)

APPENDIX B

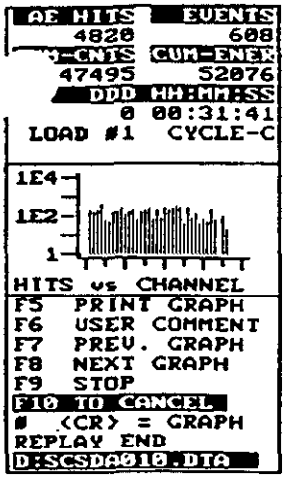

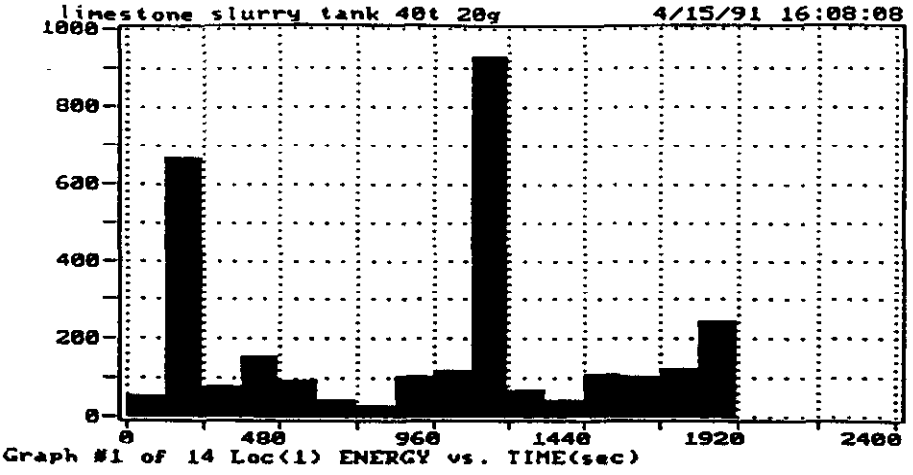

1ST, 30 MIN. HOLD AT 200%

40dB THRESHOLD

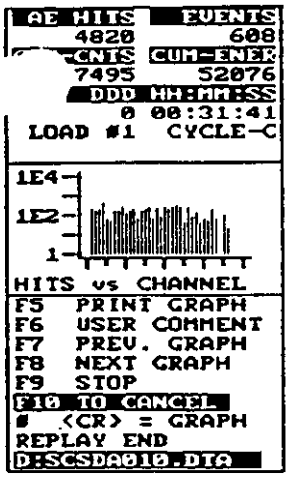
AE HITS
4820
EVENTS
608
CNTS
7495
CUM-ENER
52076
DDD HH:MM:SS
0 00:31:41
LOAD #1 CYCLE-C
1E4
1E2
1
HITS vs CHANNEL
F5 PRINT GRAPH
F6 USER COMMENT
F7 PREV. GRAPH
F8 NEXT GRAPH
F9 STOP
F10 TO CANCEL
<CR> = GRAPH
REPLAY END
D:SCSDA010.DTA

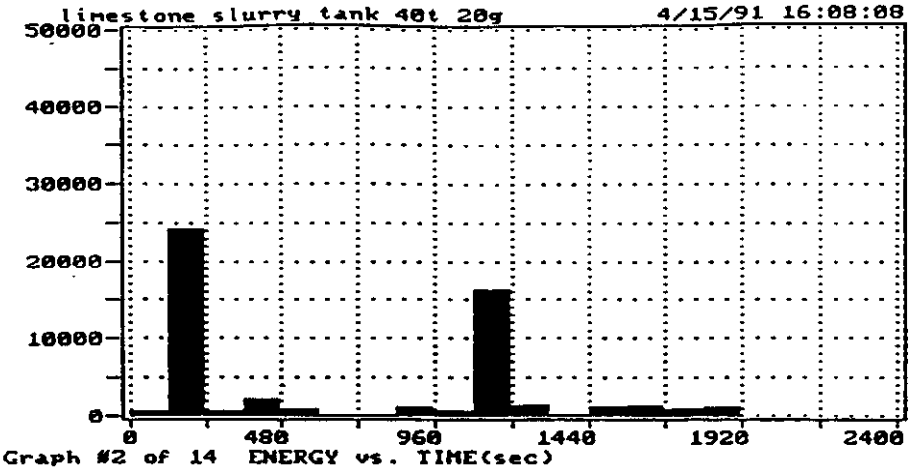
limestone slurry tank 40t 20g
4/15/91 16:08:08
50000
40000
30000
20000
10000
0
0
480
960
1440
1920
2400
Graph #2 of 14 ENERGY vs. TIME(sec)

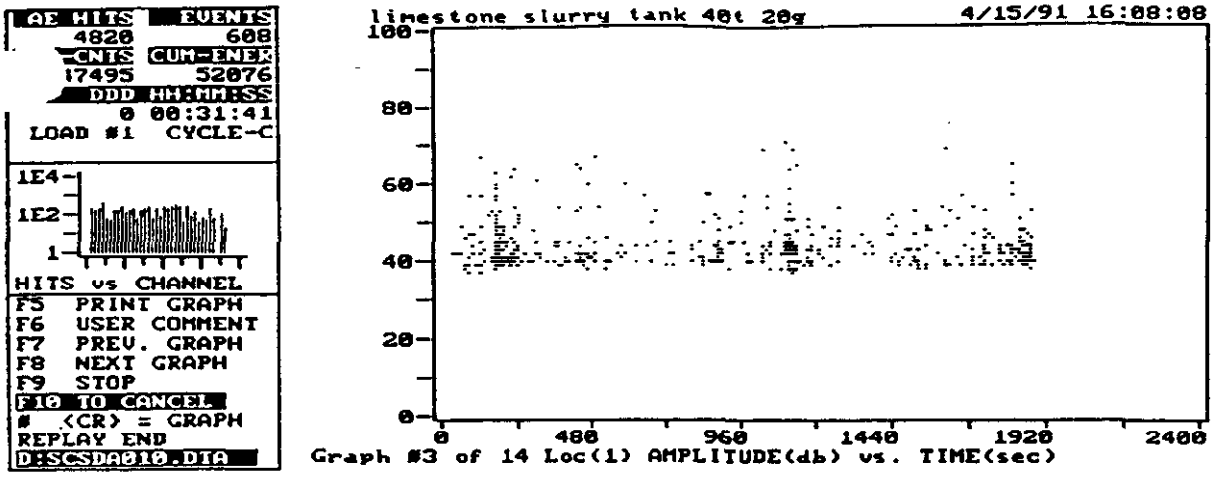
AE HITS
4820
EVENTS
608
CNTS
17495
CUM-ENER
52076
DDD HH:MM:SS
0 00:31:41
LOAD #1 CYCLE-C
1E4
1E2
1
HITS vs CHANNEL
F5 PRINT GRAPH
F6 USER COMMENT
F7 PREV. GRAPH
F8 NEXT GRAPH
F9 STOP
F10 TO CANCEL
<CR> = GRAPH
REPLAY END
D:\SCSDA010.DTA
limestone slurry tank 40t 20g
4/15/91 16:08:08
100
80
60
40
20
0
0
480
960
1440
1920
2400
Graph #3 of 14 Loc(1) AMPLITUDE(db) vs. TIME(sec)

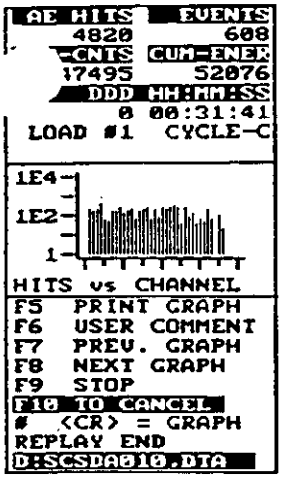
AE HITS
4820
EVENTS
608
-CNTS
17495
CUM-ENER
52076
DDD HH:MM:SS
0 00:31:41
LOAD #1 CYCLE-C
1E4
1E2
1
HITS vs CHANNEL
F5 PRINT GRAPH
F6 USER COMMENT
F7 PREV. GRAPH
F8 NEXT GRAPH
F9 STOP
F10 TO CANCEL
<CR> = GRAPH
REPLAY END
D:\SCSDA010.DTA

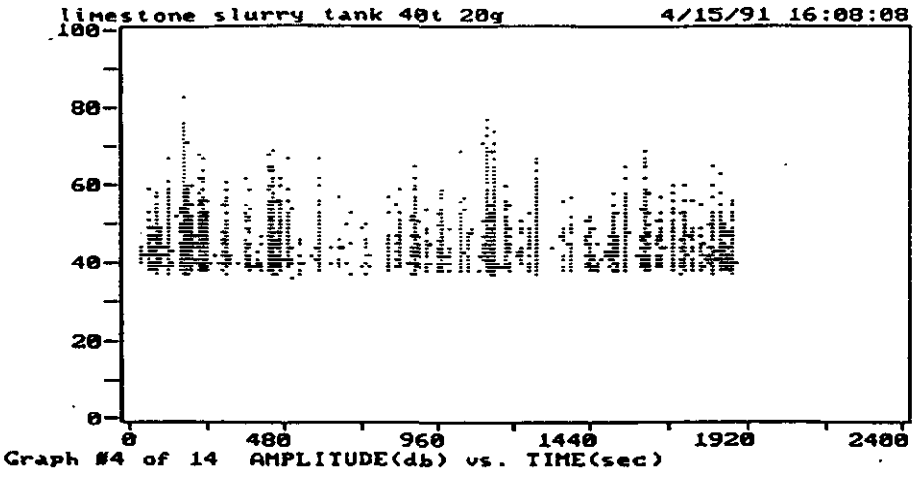
limestone slurry tank 40t 20g
4/15/91 16:08:08
100
80
60
40
20
0
0
480
960
1440
1920
2400
Graph #4 of 14 AMPLITUDE(db) vs. TIME(sec)

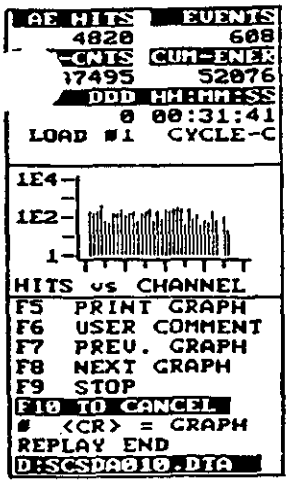
AE HITS
EVENTS
4820
608
CNTS
CUM-ENER
17495
52076
DDD HH:MM:SS
0 00:31:41
LOAD #1 CYCLE-C
1E4
1E2
1
HITS vs CHANNEL
F5 PRINT GRAPH
F6 USER COMMENT
F7 PREV. GRAPH
F8 NEXT GRAPH
F9 STOP
F10 TO CANCEL
<CR> = GRAPH
REPLAY END
D:SCSDA010.DTA

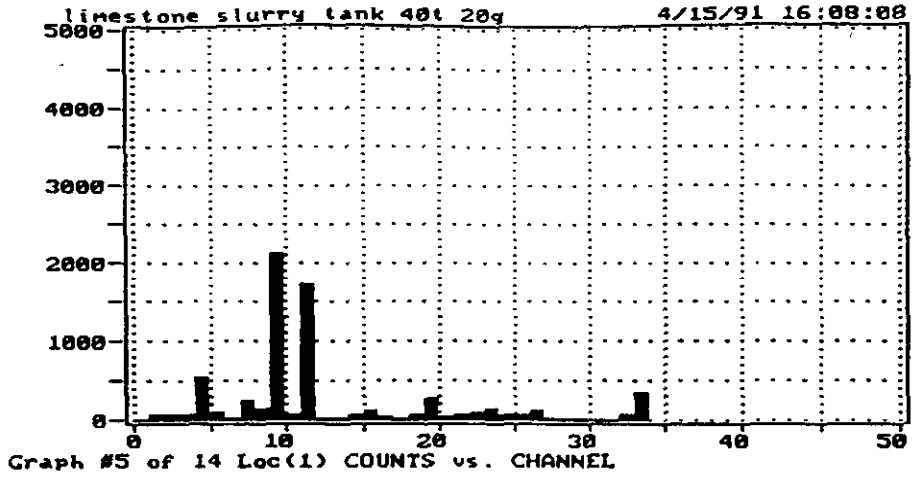
limestone slurry tank 40t 20g
4/15/91 16:08:08
5000
4000
3000
2000
1000
0
0
10
20
30
40
50
Graph #5 of 14 Loc(1) COUNTS vs. CHANNEL

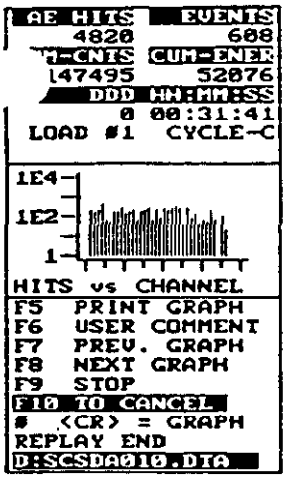
AE HITS EVENTS
4820 608
A-CNTS CUM-ENER
147495 52076
DDD HH:MM:SS
0 00:31:41
LOAD #1 CYCLE-C
1E4
1E2
1
HITS vs CHANNEL
F5 PRINT GRAPH
F6 USER COMMENT
F7 PREV. GRAPH
F8 NEXT GRAPH
F9 STOP
F10 TO CANCEL
<CR> = GRAPH
REPLAY END
D:SCSDA010.DTA

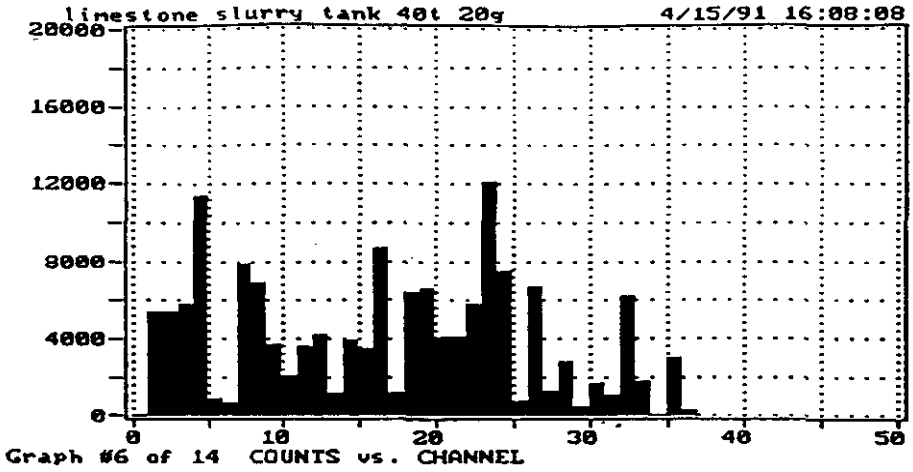
limestone slurry tank 40t 20g
4/15/91 16:08:08
20000
16000
12000
8000
4000
0
0
10
20
30
40
50
Graph #6 of 14 COUNTS vs. CHANNEL

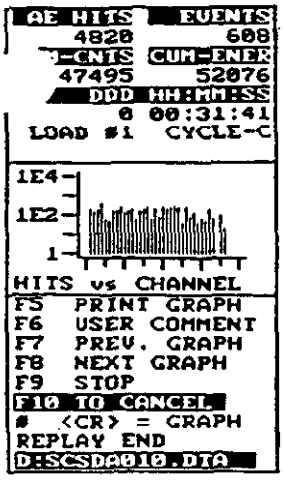
AE HITS EVENTS
4820 608
-CNTS CUM-ENER
47495 52076
DDD HH:MM:SS
0 00:31:41
LOAD #1 CYCLE-C
1E4
1E2
1
HITS vs CHANNEL
F5 PRINT GRAPH
F6 USER COMMENT
F7 PREV. GRAPH
F8 NEXT GRAPH
F9 STOP
F10 TO CANCEL
<CR> = GRAPH
REPLAY END
D:\SCSDA010.DTA

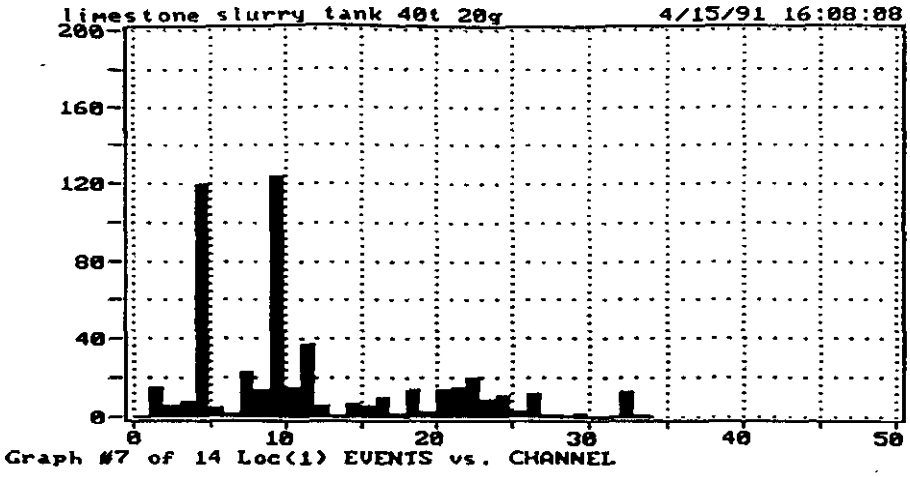
limestone slurry tank 40t 20g
4/15/91 16:08:08
200
160
120
80
40
0
0
10
20
30
40
50
Graph #7 of 14 Loc(1) EVENTS vs. CHANNEL

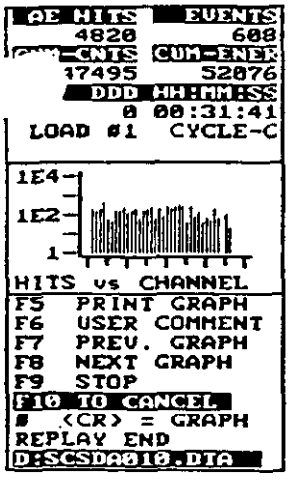
AE HITS
4820
EVENTS
608
CUM-CNTS
17495
CUM-ENER
52076
DDD HH:MM:SS
0 00:31:41
LOAD #1 CYCLE-C
1E4
1E2
1
HITS vs CHANNEL
F5 PRINT GRAPH
F6 USER COMMENT
F7 PREV. GRAPH
F8 NEXT GRAPH
F9 STOP
F10 TO CANCEL
<CR> = GRAPH
REPLAY END
D:\SCSDA010.DTA

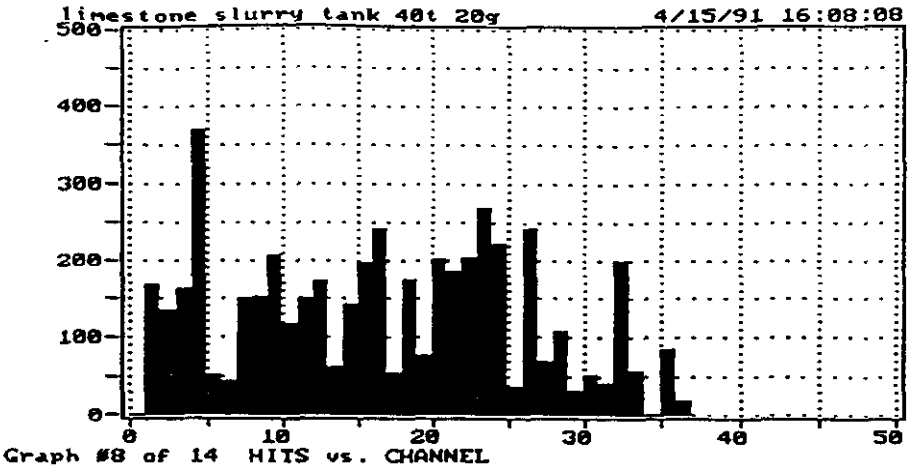
limestone slurry tank 40t 20g
4/15/91 16:08:08
500
400
300
200
100
0
0
10
20
30
40
50
Graph #8 of 14 HITS vs. CHANNEL

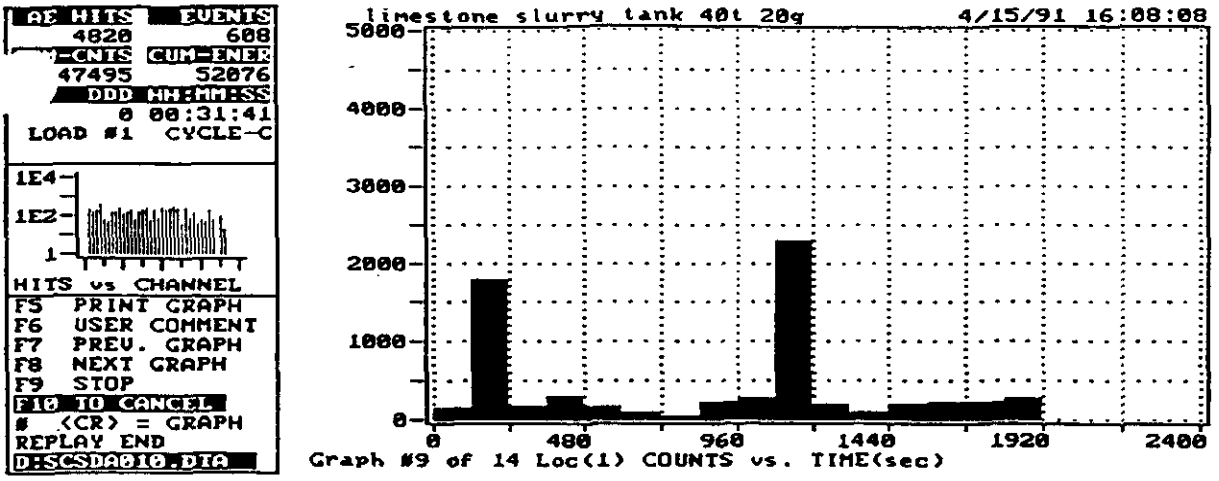
AE HITS
4820
EVENTS
608
CUM-CNTS
47495
CUM-ENER
52076
DDD HH:MM:SS
0 00:31:41
LOAD #1 CYCLE-C
1E4
1E2
1
HITS vs CHANNEL
F5 PRINT GRAPH
F6 USER COMMENT
F7 PREV. GRAPH
F8 NEXT GRAPH
F9 STOP
F10 TO CANCEL
<CR> = GRAPH
REPLAY END
D:\SCSDA010.DIG
limestone slurry tank 40t 20g
4/15/91 16:08:08
5000
4000
3000
2000
1000
0
0
480
960
1440
1920
2400
Graph #9 of 14 Loc(1) COUNTS vs. TIME(sec)

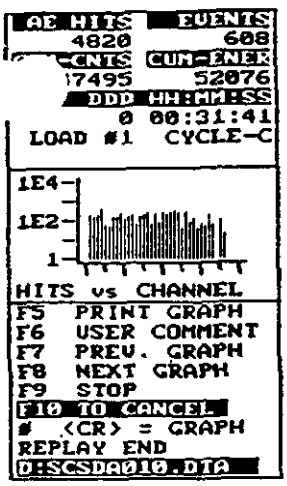
AE HITS
EVENTS
4820
608
CNTS
CUM-ENER
17495
52076
DDD HH:MM:SS
0 00:31:41
LOAD #1 CYCLE-C
1E4
1E2
1
HITS vs CHANNEL
F5 PRINT GRAPH
F6 USER COMMENT
F7 PREV. GRAPH
F8 NEXT GRAPH
F9 STOP
F10 TO CANCEL
<CR> = GRAPH
REPLAY END
D:\SCSDA010.DTA

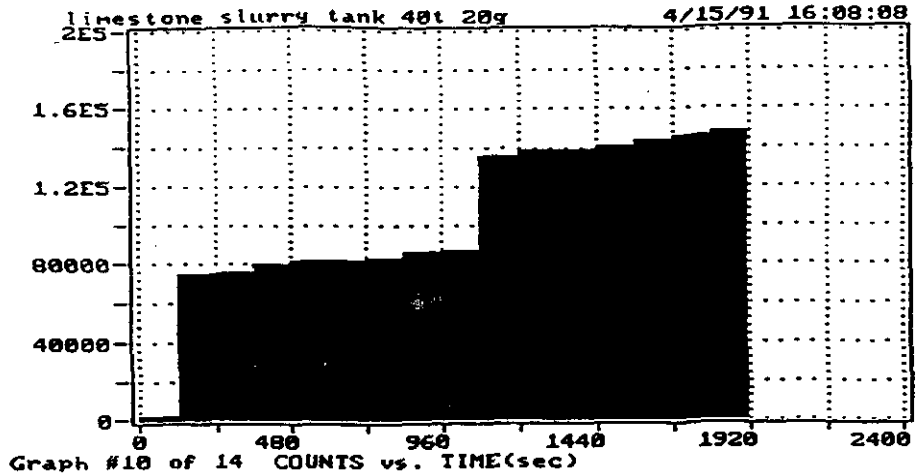
limestone slurry tank 40t 20g
4/15/91 16:08:08
2E5
1.6E5
1.2E5
80000
40000
0
0
480
960
1440
1920
2400
Graph #10 of 14 COUNTS vs. TIME(sec)

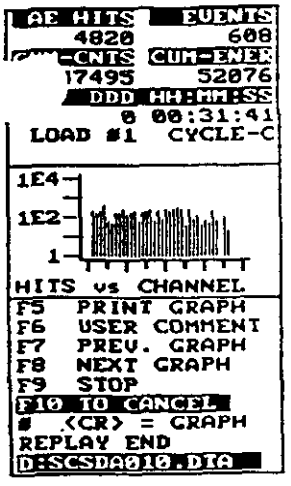
AE HITS
4820
EVENTS
608
CNTS
17495
CUM-ENER
52076
DDD HH:MM:SS
0 00:31:41
LOAD #1 CYCLE-C
1E4
1E2
1
HITS vs CHANNEL
F5 PRINT GRAPH
F6 USER COMMENT
F7 PREV. GRAPH
F8 NEXT GRAPH
F9 STOP
F10 TO CANCEL
<CR> = GRAPH
REPLAY END
D:\SCSDA010.DTA

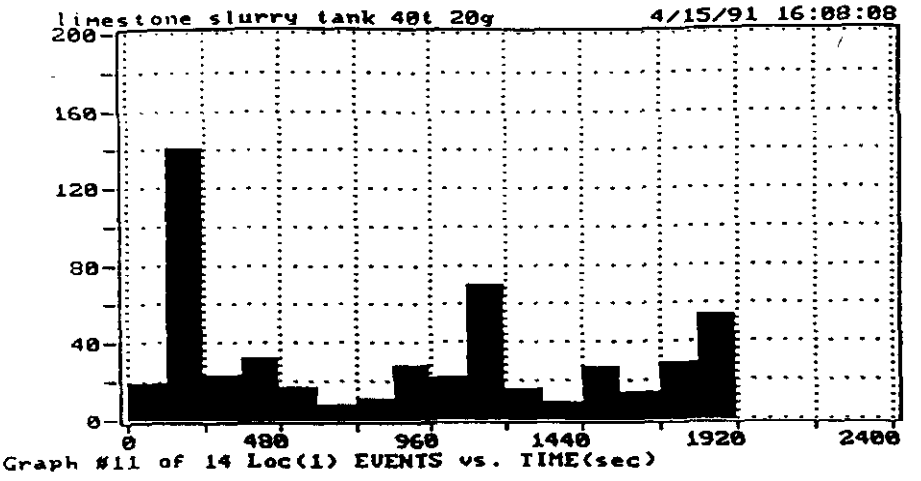
limestone slurry tank 40t 20g
4/15/91 16:08:08
200
160
120
80
40
0
0
480
960
1440
1920
2400
Graph #11 of 14 Loc(1) EVENTS vs. TIME(sec)

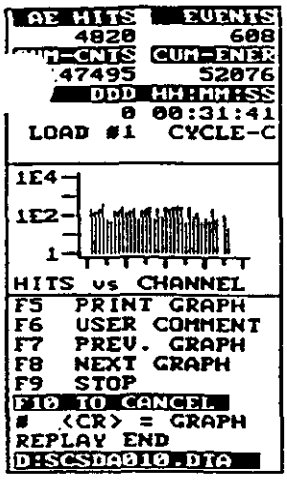
AE HITS
EVENTS
4820
608
M-CNTS
CUM-ENER
47495
52076
DDD HH:MM:SS
0 00:31:41
LOAD #1 CYCLE-C
1E4
1E2
1
HITS vs CHANNEL
F5 PRINT GRAPH
F6 USER COMMENT
F7 PREV. GRAPH
F8 NEXT GRAPH
F9 STOP
F10 TO CANCEL
<CR> = GRAPH
REPLAY END
D:\SCSDA010.DTA

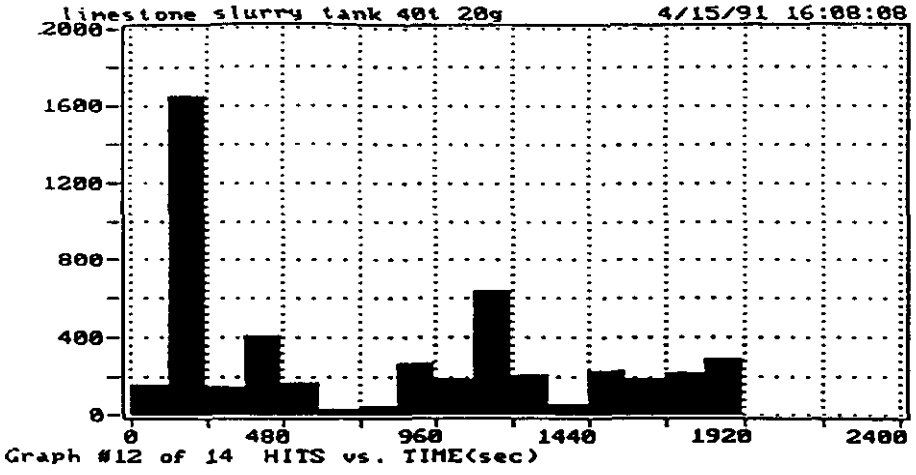
limestone slurry tank 40t 20g
4/15/91 16:08:08
2000
1600
1200
800
400
0
0
480
960
1440
1920
2400
Graph #12 of 14 HITS vs. TIME(sec)

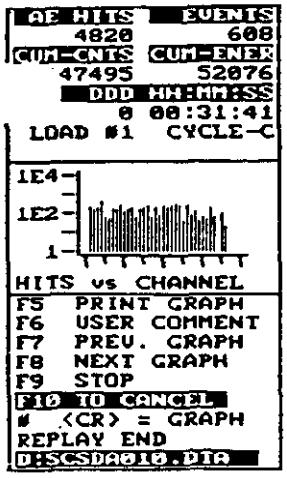
AE HITS
4820
EVENTS
608
CUM-CNTS
47495
CUM-ENER
52076
DDD HH:MM:SS
0 00:31:41
LOAD #1 CYCLE-C
1E4
1E2
1
HITS vs CHANNEL
F5 PRINT GRAPH
F6 USER COMMENT
F7 PREV. GRAPH
F8 NEXT GRAPH
F9 STOP
F10 TO CANCEL
<CR> = GRAPH
REPLAY END
D:\SCSDA010.DTA

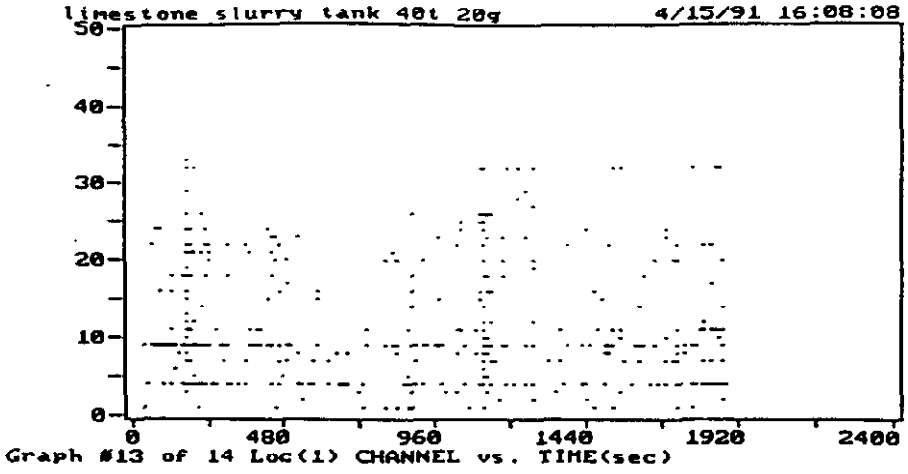
limestone slurry tank 40t 20g
4/15/91 16:08:08
50
40
30
20
10
0
0
480
960
1440
1920
2400
Graph #13 of 14 Loc(1) CHANNEL vs. TIME(sec)

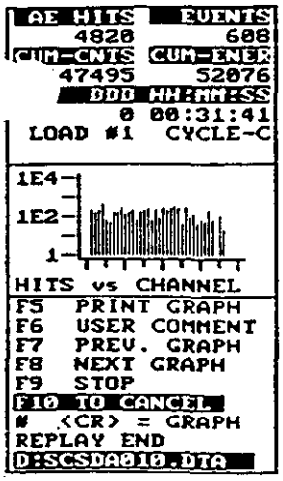
AE HITS
EVENTS
4820
608
CUM-CNTS
CUM-ENER
47495
52076
DDD HH:MM:SS
0 00:31:41
LOAD #1 CYCLE-C
1E4
1E2
1
HITS vs CHANNEL
F5 PRINT GRAPH
F6 USER COMMENT
F7 PREV. GRAPH
F8 NEXT GRAPH
F9 STOP
F10 TO CANCEL
<CR> = GRAPH
REPLAY END
D:SCSDA016.DTA

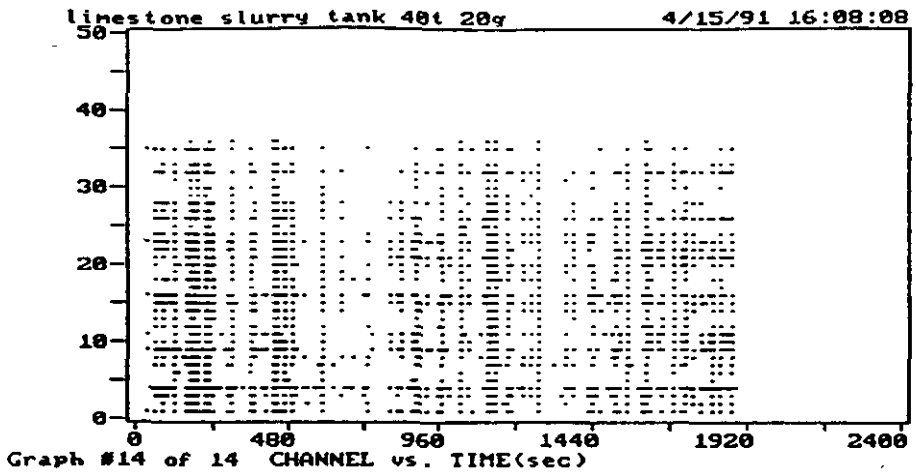
limestone slurry tank 40t 20g
4/15/91 16:08:08
50
40
30
20
10
0
0
480
960
1440
1920
2400
Graph #14 of 14 CHANNEL vs. TIME(sec)

APPENDIX C

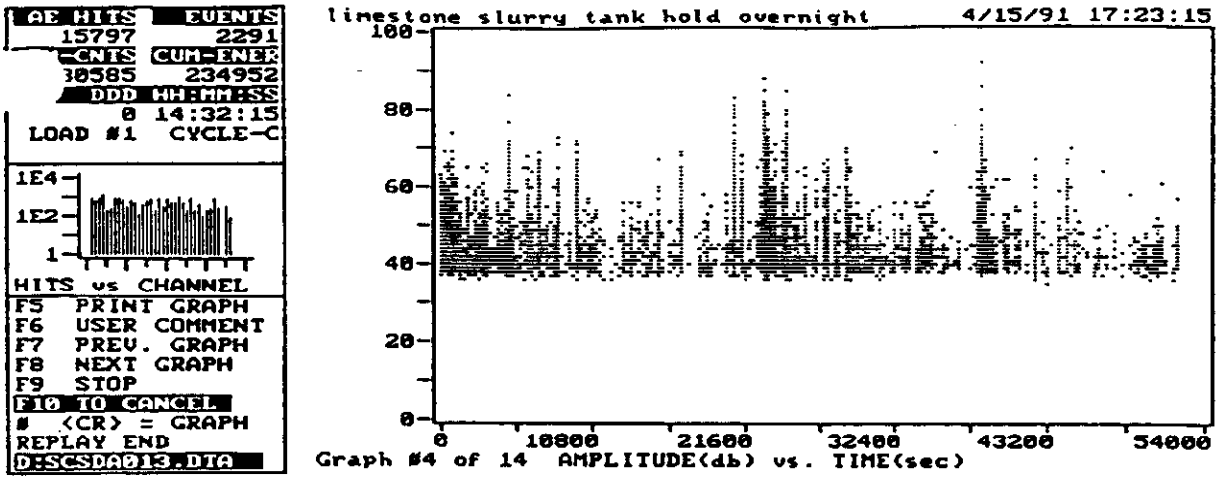
AE HITS
15797
EVENTS
2291
CNTS
30585
CUM-ENER
234952
DDD HH:MM:SS
0 14:32:15
LOAD #1 CYCLE-C
1E4
1E2
1
HITS vs CHANNEL
F5 PRINT GRAPH
F6 USER COMMENT
F7 PREV. GRAPH
F8 NEXT GRAPH
F9 STOP
F10 TO CANCEL
<CR> = GRAPH
REPLAY END
D:\SCSDAQ13.DTA
limestone slurry tank hold overnight
4/15/91 17:23:15
100
80
60
40
20
0
0
10800
21600
32400
43200
54000
Graph #4 of 14 AMPLITUDE(db) vs. TIME(sec)

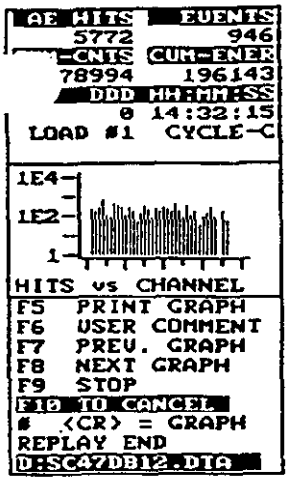
AE HITS EVENTS
5772 946
-CNTS CUM-ENER
78994 196143
DDD HH:MM:SS
0 14:32:15
LOAD #1 CYCLE-C
1E4
1E2
1
HITS vs CHANNEL
F5 PRINT GRAPH
F6 USER COMMENT
F7 PREV. GRAPH
F8 NEXT GRAPH
F9 STOP
F10 TO CANCEL
<CR> = GRAPH
REPLAY END
D:SCA7DB12.DTA

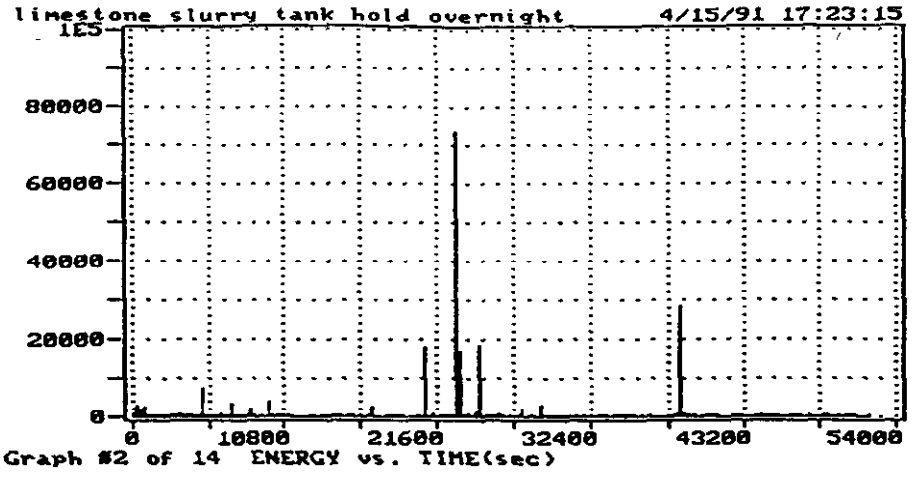
limestone slurry tank hold overnight 4/15/91 17:23:15
1E5
80000
60000
40000
20000
0
0
10800
21600
32400
43200
54000
Graph #2 of 14 ENERGY vs. TIME(sec)

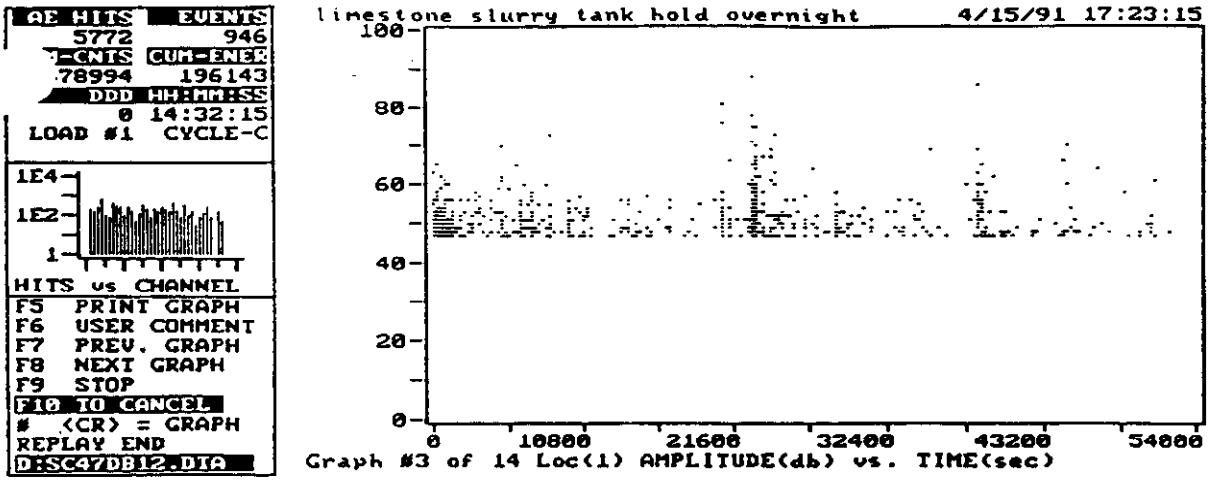
AE HITS
EVENTS
5772
946
-CNTS
CUM-ENER
78994
196143
DDD HH:MM:SS
0 14:32:15
LOAD #1 CYCLE-C
1E4
1E2
1
HITS vs CHANNEL
F5 PRINT GRAPH
F6 USER COMMENT
F7 PREV. GRAPH
F8 NEXT GRAPH
F9 STOP
F10 TO CANCEL
<CR> = GRAPH
REPLAY END
D:SC47DB12.DTA
limestone slurry tank hold overnight
4/15/91 17:23:15
100
80
60
40
20
0
0
10800
21600
32400
43200
54000
Graph #3 of 14 Loc(1) AMPLITUDE(db) vs. TIME(sec)

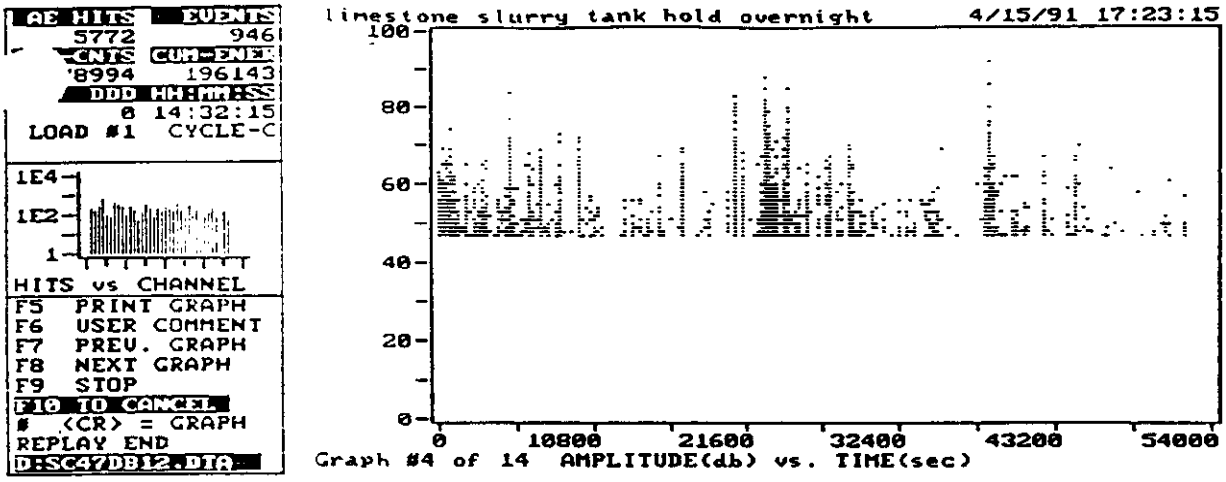
AE HITS
5772
EVENTS
946
CNTS
8994
CUM-ENER
196143
DOD HH:MM:SS
0 14:32:15
LOAD #1 CYCLE-C
1E4
1E2
1
HITS vs CHANNEL
F5 PRINT GRAPH
F6 USER COMMENT
F7 PREV. GRAPH
F8 NEXT GRAPH
F9 STOP
F10 TO CANCEL
<CR> = GRAPH
REPLAY END
D:\SC47DB12.DTA
limestone slurry tank hold overnight
4/15/91 17:23:15
100
80
60
40
20
0
0
10800
21600
32400
43200
54000
Graph #4 of 14 AMPLITUDE(db) vs. TIME(sec)

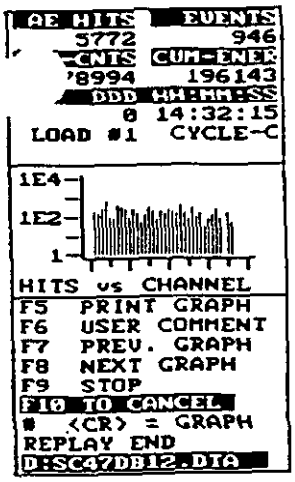
HI HITS
5772
CNTS
8994
DDD HH:MM:SS
0 14:32:15
LOAD #1 CYCLE-C
1E4
1E2
1
HITS vs CHANNEL
F5 PRINT GRAPH
F6 USER COMMENT
F7 PREV. GRAPH
F8 NEXT GRAPH
F9 STOP
F10 TO CANCEL
<CR> = GRAPH
REPLAY END
D:SC07DB12.DTA

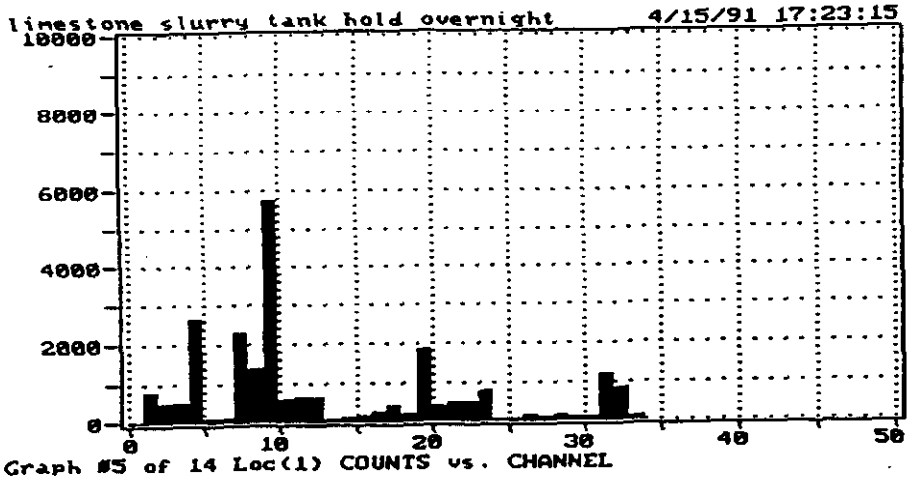
limestone slurry tank hold overnight
4/15/91 17:23:15
10000
8000
6000
4000
2000
0
0
10
20
30
40
50
Graph #5 of 14 Loc(1) COUNTS vs. CHANNEL

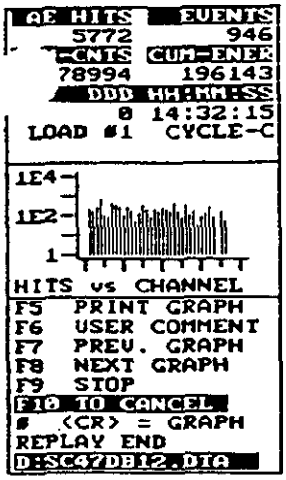
AE HITS EVENTS
5772 946
CNTS CUM-ENER
78994 196143
DDD HH:MM:SS
0 14:32:15
LOAD #1 CYCLE-C
1E4
1E2
1
HITS vs CHANNEL
F5 PRINT GRAPH
F6 USER COMMENT
F7 PREV. GRAPH
F8 NEXT GRAPH
F9 STOP
F10 TO CANCEL
<CR> = GRAPH
REPLAY END
D:SC47DB12.DTA

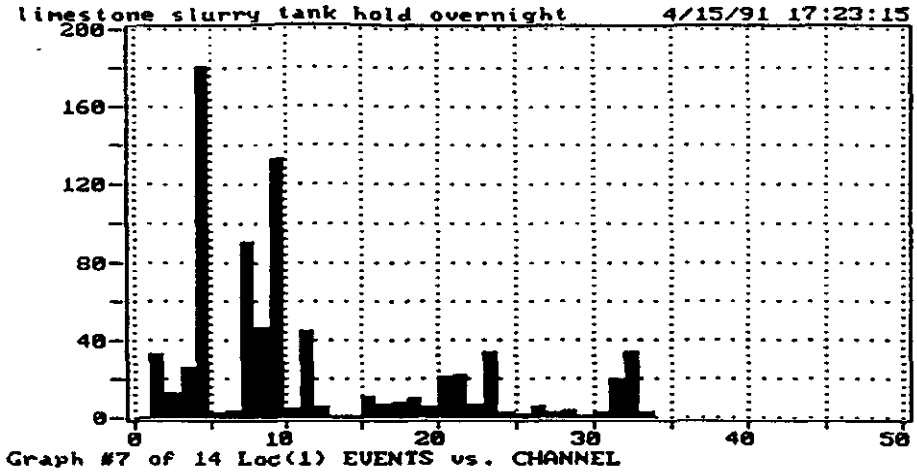
limestone slurry tank hold overnight
4/15/91 17:23:15
200
160
120
80
40
0
0
10
20
30
40
50
Graph #7 of 14 Loc(1) EVENTS vs. CHANNEL

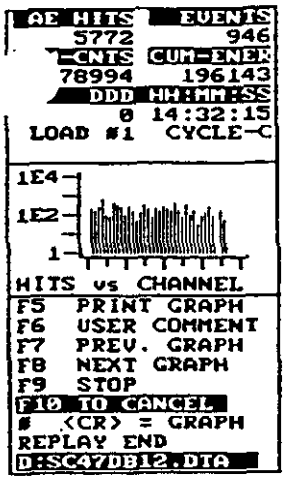
AE HITS
5772
EVENTS
946
CNTS
78994
CUM-ENER
196143
DDD HH:MM:SS
0 14:32:15
LOAD #1 CYCLE-C
1E4
1E2
1
HITS vs CHANNEL
F5 PRINT GRAPH
F6 USER COMMENT
F7 PREV. GRAPH
F8 NEXT GRAPH
F9 STOP
F10 TO CANCEL
<CR> = GRAPH
REPLAY END
D:SC47DB12.DTA

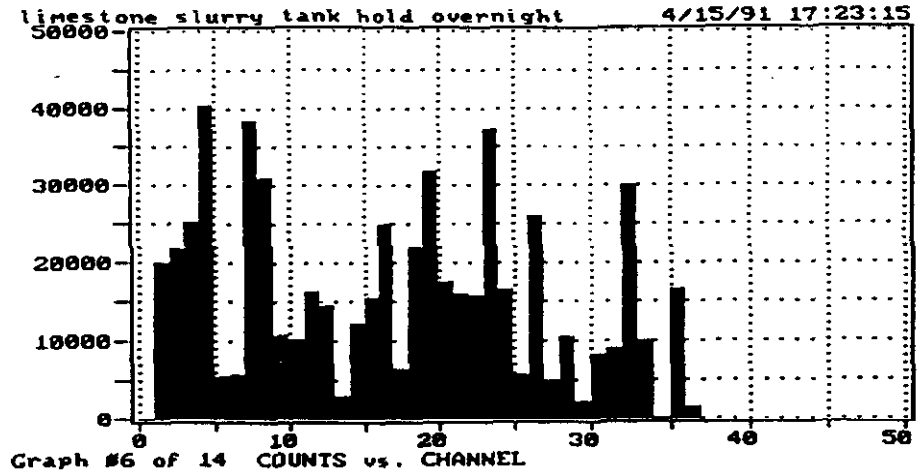
limestone slurry tank hold overnight
4/15/91 17:23:15
50000
40000
30000
20000
10000
0
0
10
20
30
40
50
Graph #6 of 14 COUNTS vs. CHANNEL

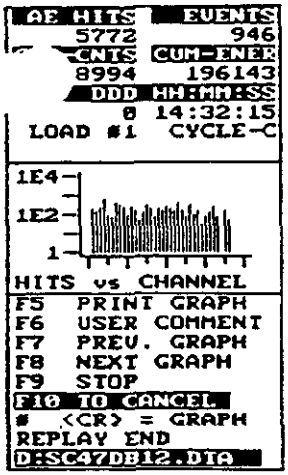
AE HITS
EVENTS
5772
946
CNTS
CUM-ENER
8994
196143
DDD HH:MM:SS
0 14:32:15
LOAD #1 CYCLE-C
1E4
1E2
1
HITS vs CHANNEL
F5 PRINT GRAPH
F6 USER COMMENT
F7 PREV. GRAPH
F8 NEXT GRAPH
F9 STOP
F10 TO CANCEL
<CR> = GRAPH
REPLAY END
D:SC47DB12.DTA

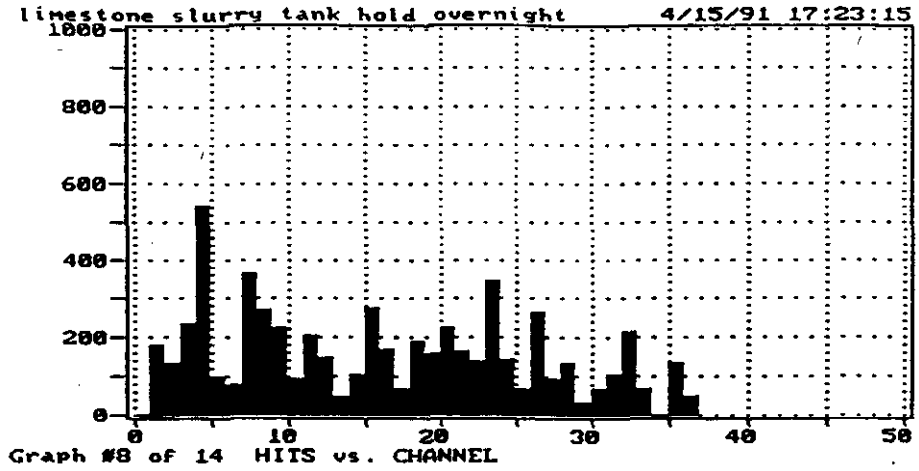
limestone slurry tank hold overnight
4/15/91 17:23:15
1000
800
600
400
200
0
0
10
20
30
40
50
Graph #8 of 14 HITS vs. CHANNEL

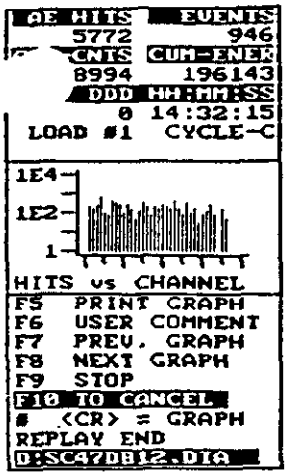

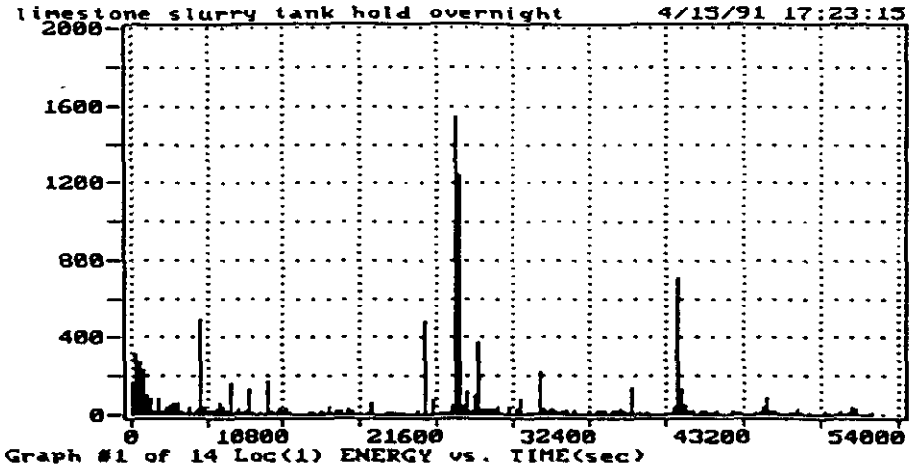

NEXT, 14 HOUR HOLD AT 200 %

47 dB THRESHOLD

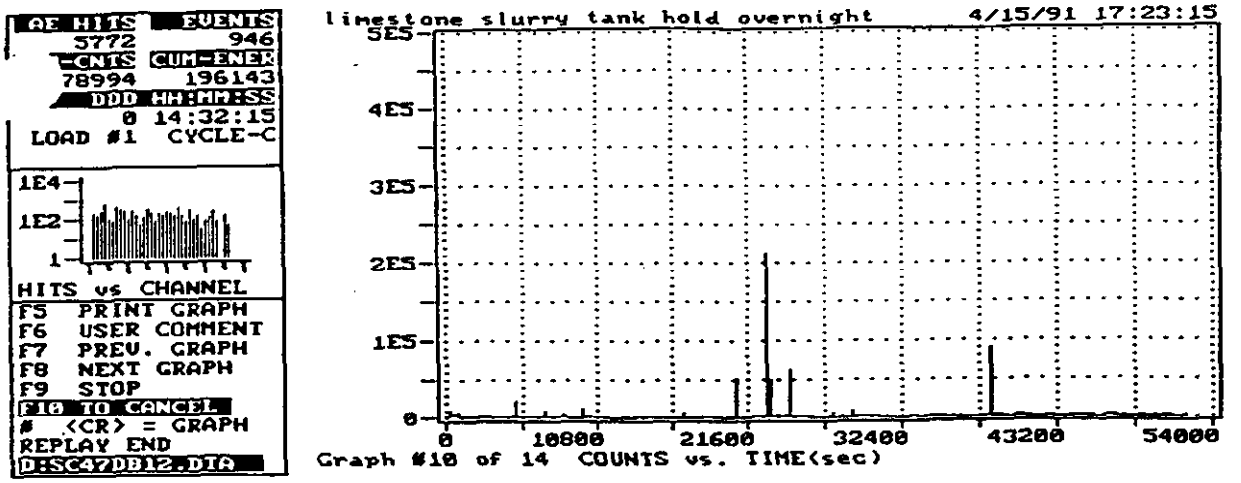
AE HITS
5772
EVENTS
946
CNTS
78994
CUM-ENER
196143
DDD HH:MM:SS
0 14:32:15
LOAD #1 CYCLE-C
1E4
1E2
1
HITS vs CHANNEL
F5 PRINT GRAPH
F6 USER COMMENT
F7 PREV. GRAPH
F8 NEXT GRAPH
F9 STOP
F10 TO CANCEL
<CR> = GRAPH
REPLAY END
D:\SC47\DB12.DTA
limestone slurry tank hold overnight
4/15/91 17:23:15
5E5
4E5
3E5
2E5
1E5
0
0
10800
21600
32400
43200
54000
Graph #10 of 14 COUNTS vs. TIME(sec)

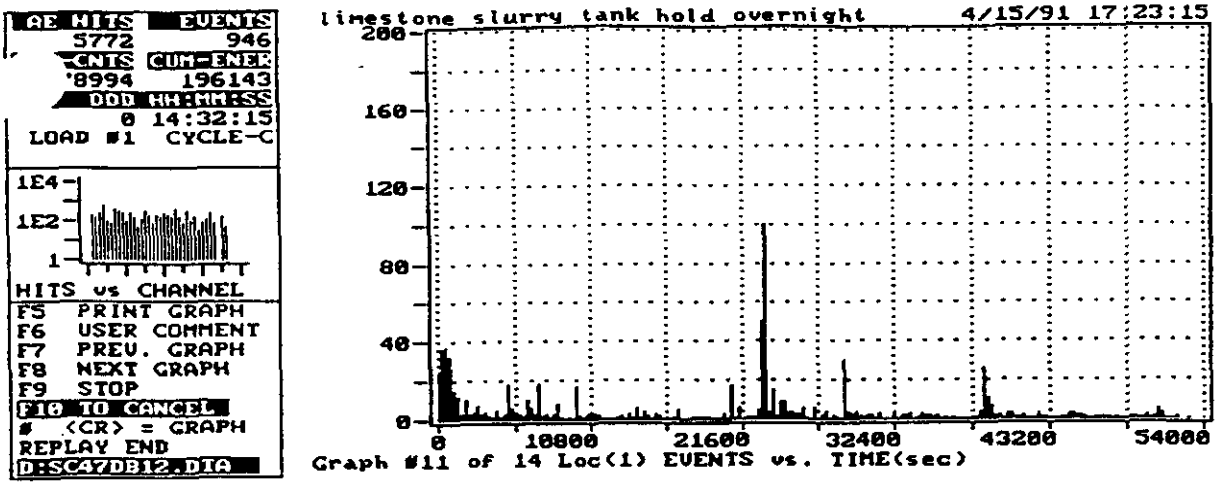
AE HITS
EVENTS
5772
946
CNTS
CUM-ENER
8994
196143
DOD HH:MM:SS
0 14:32:15
LOAD #1 CYCLE-C
1E4
1E2
1
HITS vs CHANNEL
F5 PRINT GRAPH
F6 USER COMMENT
F7 PREV. GRAPH
F8 NEXT GRAPH
F9 STOP
F10 TO CANCEL
<CR> = GRAPH
REPLAY END
D:SC47DB12.DTA
limestone slurry tank hold overnight
4/15/91 17:23:15
200
160
120
80
40
0
0
10800
21600
32400
43200
54000
Graph #11 of 14 Loc(1) EVENTS vs. TIME(sec)

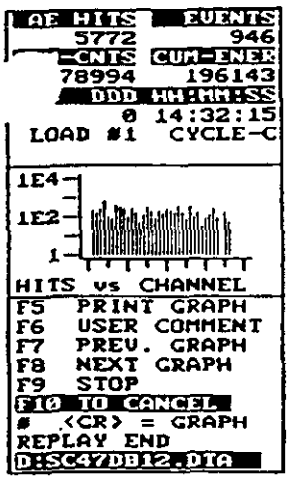
AE HITS
5772
EVENTS
946
CNTS
78994
CUM-ENER
196143
DDD HH:MM:SS
0 14:32:15
LOAD #1 CYCLE-C
1E4
1E2
1
HITS vs CHANNEL
F5 PRINT GRAPH
F6 USER COMMENT
F7 PREV. GRAPH
F8 NEXT GRAPH
F9 STOP
F10 TO CANCEL
<CR> = GRAPH
REPLAY END
D:SC47DB12.DTA

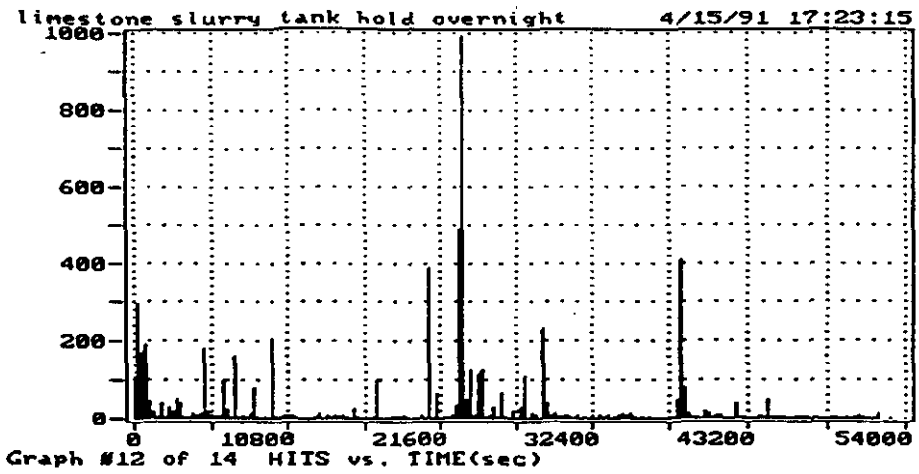
limestone slurry tank hold overnight
4/15/91 17:23:15
1000
800
600
400
200
0
0
10800
21600
32400
43200
54000
Graph #12 of 14 HITS vs. TIME(sec)

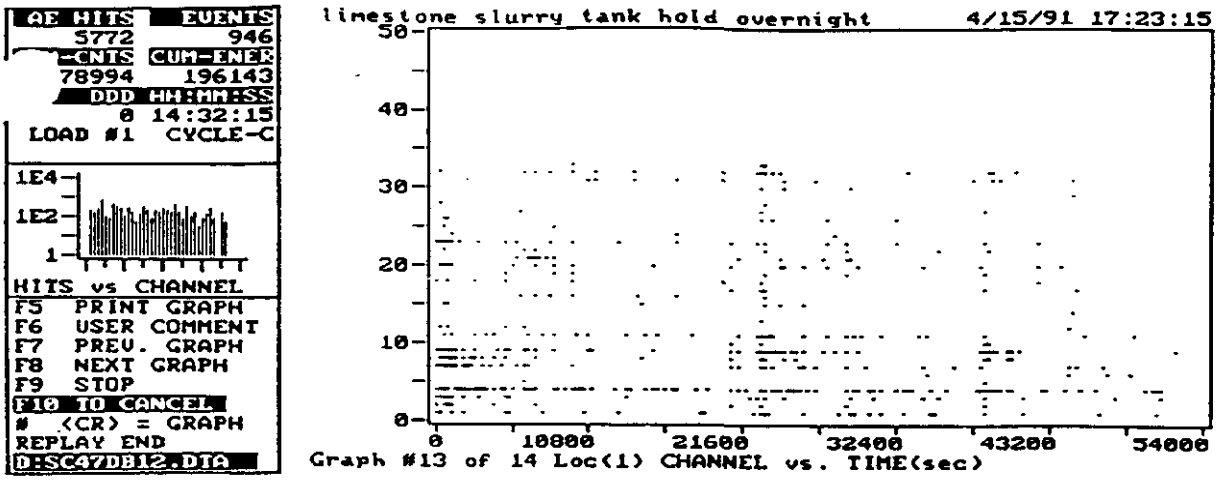
AE HITS
5772
EVENTS
946
-CNTS
78994
CUM-ENER
196143
DDD HH:MM:SS
0 14:32:15
LOAD #1 CYCLE-C
1E4
1E2
1
HITS vs CHANNEL
F5 PRINT GRAPH
F6 USER COMMENT
F7 PREV. GRAPH
F8 NEXT GRAPH
F9 STOP
F10 TO CANCEL
<CR> = GRAPH
REPLAY END
D:\SC47DB12.DTA
limestone slurry tank hold overnight
4/15/91 17:23:15
50
40
30
20
10
0
0
10800
21600
32400
43200
54000
Graph #13 of 14 Loc(1) CHANNEL vs. TIME(sec)

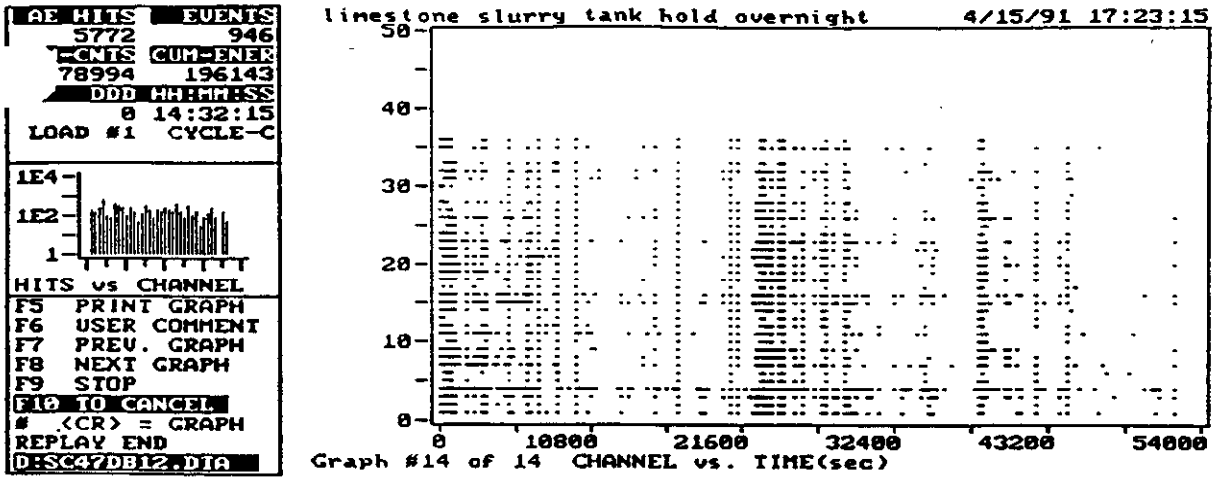
AE HITS
5772
EVENTS
946
CNTS
78994
CUM-ENER
196143
DDD HH:MM:SS
0 14:32:15
LOAD #1 CYCLE-C
1E4
1E2
1
HITS vs CHANNEL
F5 PRINT GRAPH
F6 USER COMMENT
F7 PREV. GRAPH
F8 NEXT GRAPH
F9 STOP
F10 TO CANCEL
<CR> = GRAPH
REPLAY END
DBSC47DB12.DTA
limestone slurry tank hold overnight
4/15/91 17:23:15
50
40
30
20
10
0
0
10800
21600
32400
43200
54000
Graph #14 of 14 CHANNEL vs. TIME(sec)

APPENDIX D

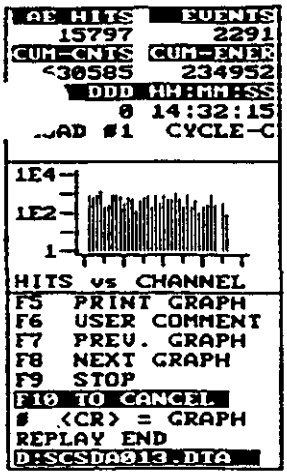

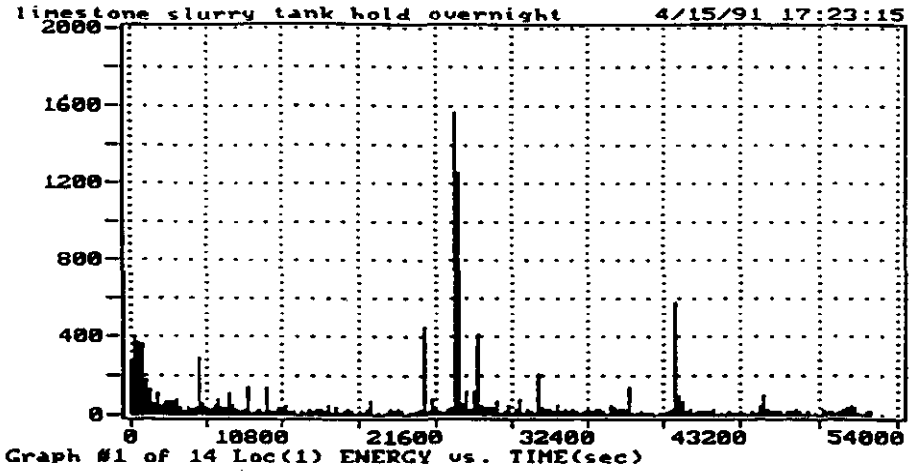

NEXT, 14 HOURS HOLD AT 100%

40dB THRESHOLD

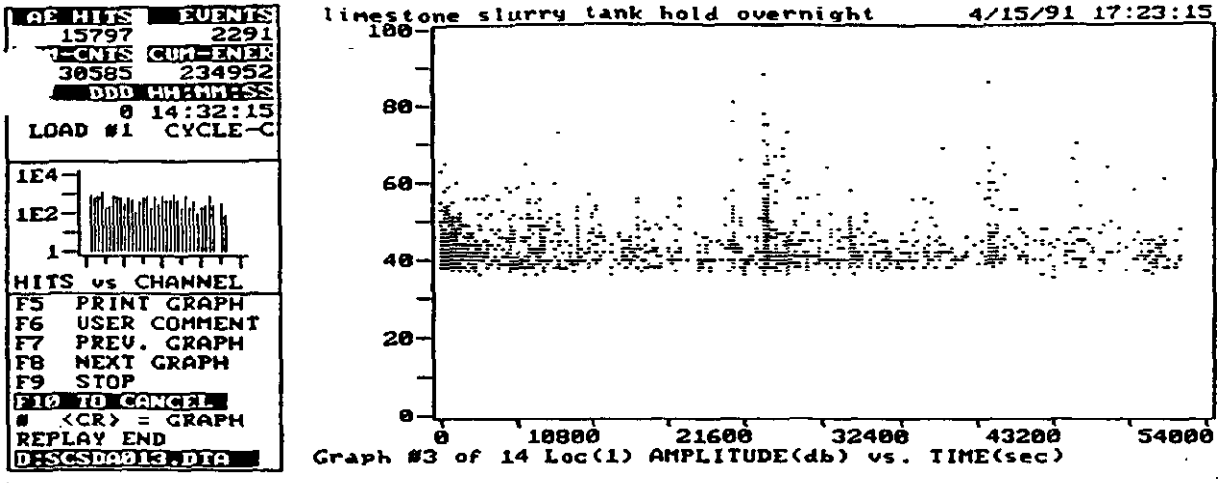
AE HITS
EVENTS
15797
2291
T-CNTS
CUM-ENER
30585
234952
DDD HH:MM:SS
0 14:32:15
LOAD #1 CYCLE-C
1E4
1E2
1
HITS vs CHANNEL
F5 PRINT GRAPH
F6 USER COMMENT
F7 PREV. GRAPH
F8 NEXT GRAPH
F9 STOP
F10 TO CANCEL
<CR> = GRAPH
REPLAY END
D:\SCSDA013.DTA
limestone slurry tank hold overnight
4/15/91 17:23:15
100
80
60
40
20
0
0
10800
21600
32400
43200
54000
Graph #3 of 14 Loc(1) AMPLITUDE(db) vs. TIME(sec)

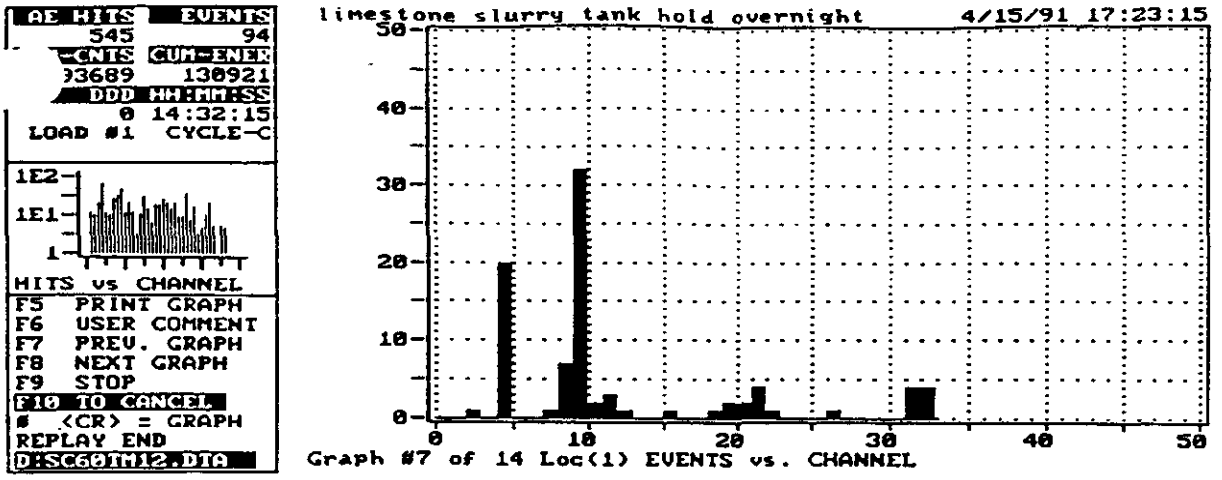
AE HITS EVENTS
545 94
CNTS CUM-ENER
93689 130921
DDD HH:MM:SS
0 14:32:15
LOAD #1 CYCLE-C
1E2
1E1
1
HITS vs CHANNEL
F5 PRINT GRAPH
F6 USER COMMENT
F7 PREV. GRAPH
F8 NEXT GRAPH
F9 STOP
F10 TO CANCEL
<CR> = GRAPH
REPLAY END
D:\SC60TM12.DTA
limestone slurry tank hold overnight
4/15/91 17:23:15
50
40
30
20
10
0
0
10
20
30
40
50
Graph #7 of 14 Loc(1) EVENTS vs. CHANNEL

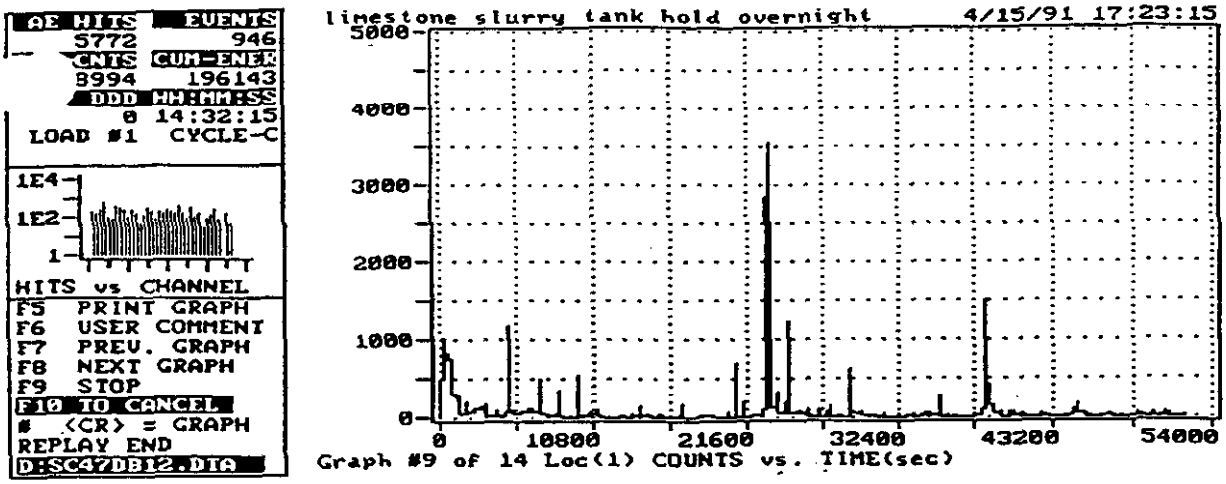
AE HITS
5772
EVENTS
946
CNTS
8994
CUM-ENER
196143
DDD HH:MM:SS
0 14:32:15
LOAD #1 CYCLE-C
1E4
1E2
1
HITS vs CHANNEL
F5 PRINT GRAPH
F6 USER COMMENT
F7 PREV. GRAPH
F8 NEXT GRAPH
F9 STOP
F10 TO CANCEL
<CR> = GRAPH
REPLAY END
D:\SC427DB12.DIG
limestone slurry tank hold overnight
4/15/91 17:23:15
5000
4000
3000
2000
1000
0
0
10800
21600
32400
43200
54000
Graph #9 of 14 Loc(1) COUNTS vs. TIME(sec)

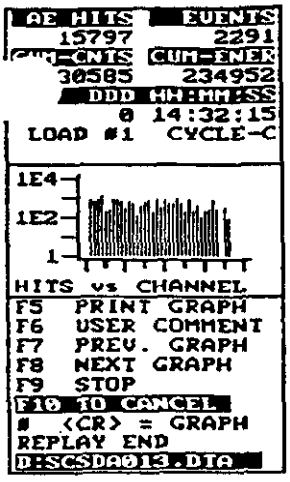
AE HITS
15797
EVENTS
2291
CUM-CNTS
30585
CUM-ENER
234952
DDD HH:MM:SS
0 14:32:15
LOAD #1 CYCLE-C
1E4
1E2
1
HITS vs CHANNEL
F5 PRINT GRAPH
F6 USER COMMENT
F7 PREV. GRAPH
F8 NEXT GRAPH
F9 STOP
F10 TO CANCEL
<CR> = GRAPH
REPLAY END
D:\SCSDA013.DTA

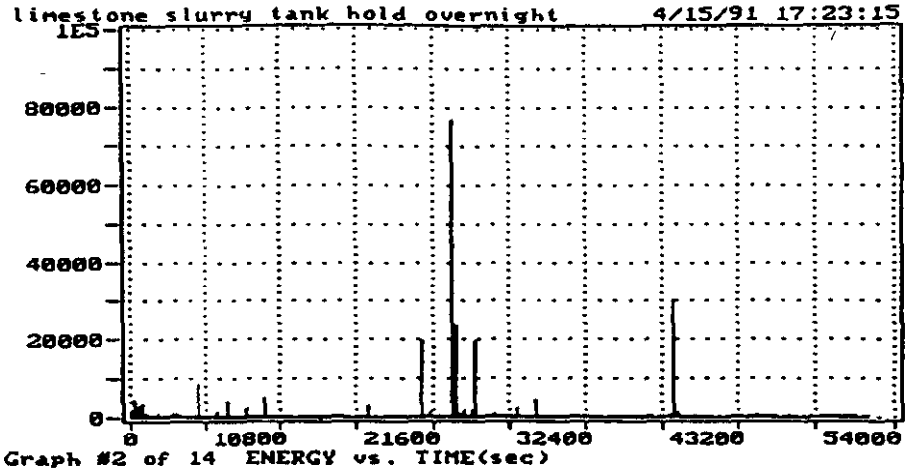
limestone slurry tank hold overnight
4/15/91 17:23:15
1E5
80000
60000
40000
20000
0
0
10800
21600
32400
43200
54000
Graph #2 of 14 ENERGY vs. TIME(sec)

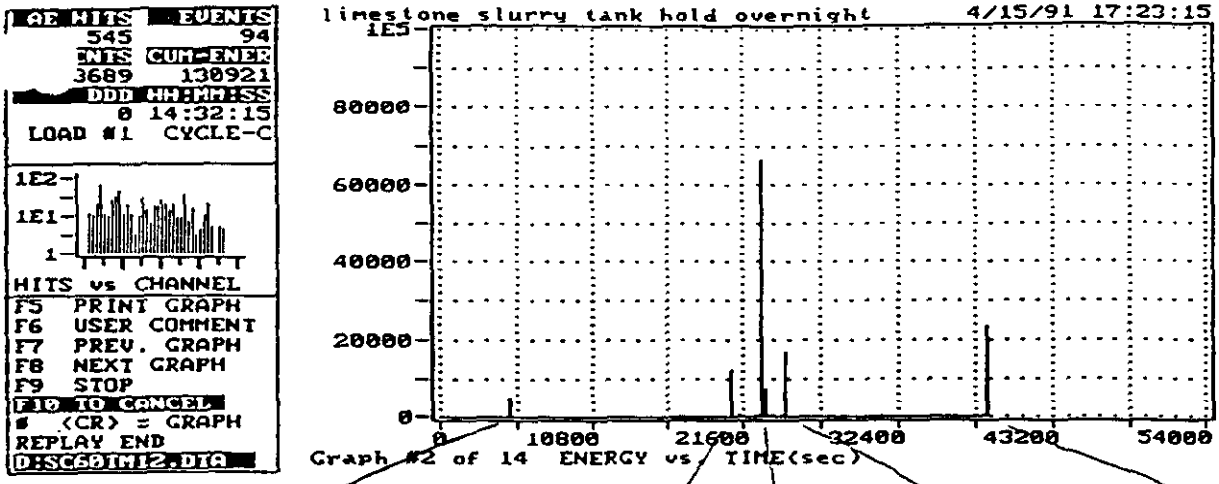

1 22.00 E4

INITIATED AT #9 & 4, MAYBE 23

5 47 58.78

#9, 4 & OTHERS

6.26.21 91

#9, MAYBE 11

6:53 16.04

#9 & 4

10:46 42.17

#9, THEN #4

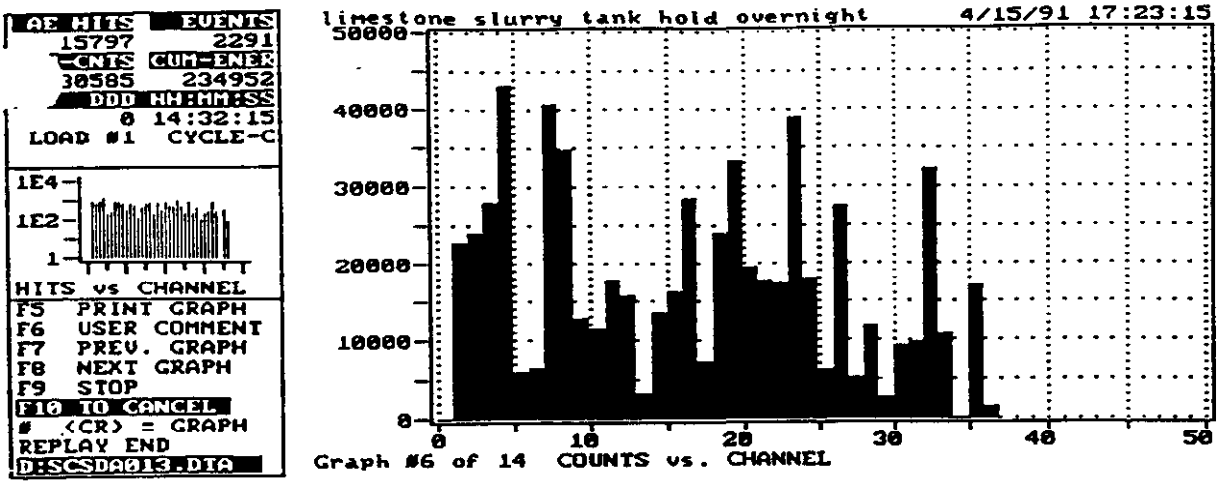
AE HITS EVENTS
15797 2291
CNTS CUM-ENER
30585 234952
DDD HH:MM:SS
0 14:32:15
LOAD #1 CYCLE-C
1E4
1E2
1
HITS vs CHANNEL
F5 PRINT GRAPH
F6 USER COMMENT
F7 PREV. GRAPH
F8 NEXT GRAPH
F9 STOP
F10 TO CANCEL
<CR> = GRAPH
REPLAY END
DHSCSDA013.DIA
limestone slurry tank hold overnight
4/15/91 17:23:15
50000
40000
30000
20000
10000
0
0
10
20
30
40
50
Graph #6 of 14 COUNTS vs. CHANNEL

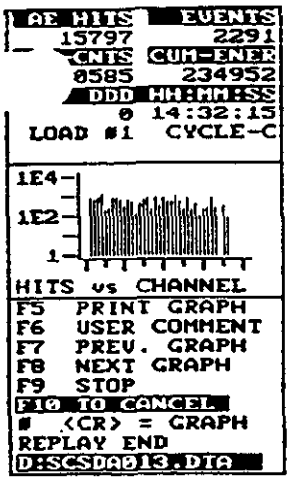
AE HITS
EVENTS
15797
2291
CNTS
CUM-ENER
0585
234952
DDD HH:MM:SS
0 14:32:15
LOAD #1 CYCLE-C
1E4
1E2
1
HITS vs CHANNEL
F5 PRINT GRAPH
F6 USER COMMENT
F7 PREV. GRAPH
F8 NEXT GRAPH
F9 STOP
F10 TO CANCEL
<CR> = GRAPH
REPLAY END
D:SCSDA013.DTA

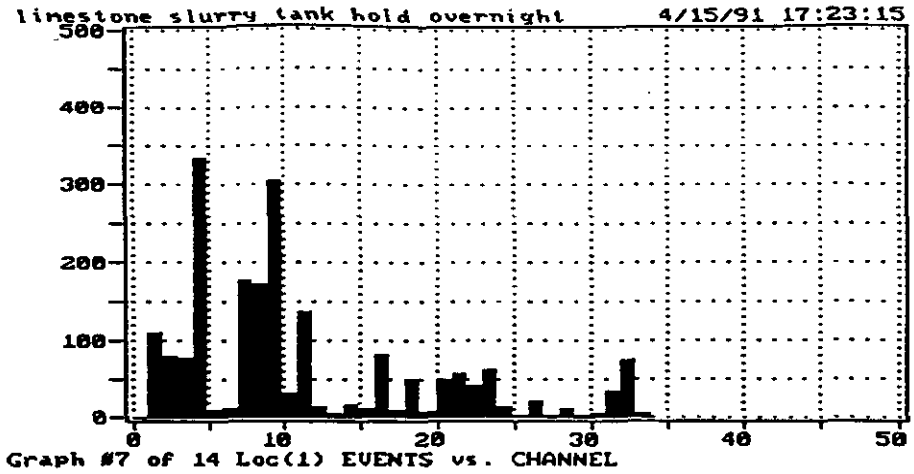
limestone slurry tank hold overnight
4/15/91 17:23:15
500
400
300
200
100
0
0
10
20
30
40
50
Graph #7 of 14 Loc(1) EVENTS vs. CHANNEL

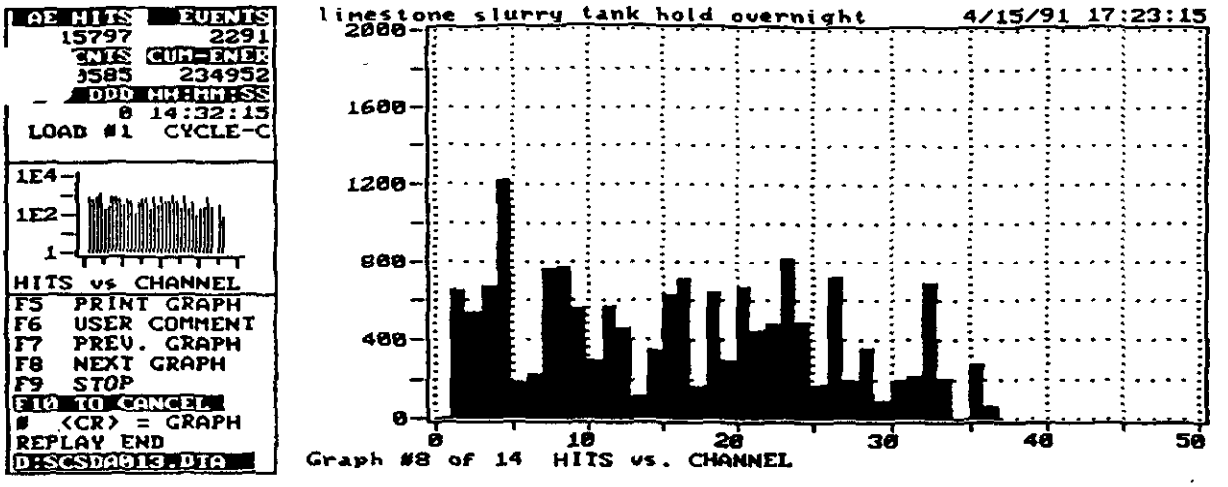
OF HITS
EVENTS
15797
2291
CNTS
CUM-ENER
3585
234952
DDD HH:MM:SS
0 14:32:15
LOAD #1 CYCLE-C
1E4
1E2
1
HITS vs CHANNEL
F5 PRINT GRAPH
F6 USER COMMENT
F7 PREV. GRAPH
F8 NEXT GRAPH
F9 STOP
F10 TO CANCEL
<CR> = GRAPH
REPLAY END
D:\SCSDA013.DTA
limestone slurry tank hold overnight
4/15/91 17:23:15
2000
1600
1200
800
400
0
0
10
20
30
40
50
Graph #8 of 14 HITS vs. CHANNEL

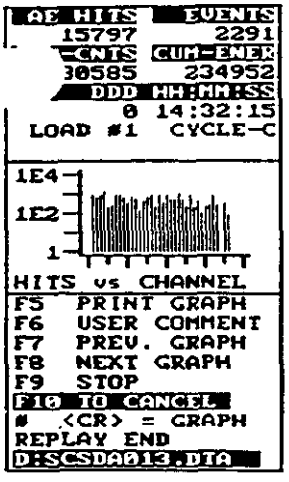
AE HITS
15797
COUNTS
2291
CNTS
30585
CUM-ENER
234952
DDD HH:MM:SS
0 14:32:15
LOAD #1 CYCLE-C
1E4
1E2
1
HITS vs CHANNEL
F5 PRINT GRAPH
F6 USER COMMENT
F7 PREV. GRAPH
F8 NEXT GRAPH
F9 STOP
F10 TO CANCEL
<CR> = GRAPH
REPLAY END
D:\CSDA013.DTA

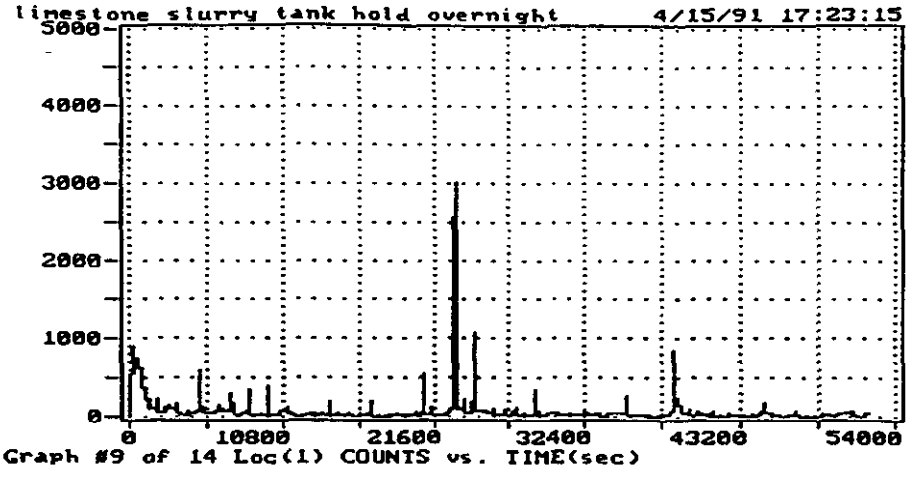
limestone slurry tank hold overnight
4/15/91 17:23:15
5000
4000
3000
2000
1000
0
0
10800
21600
32400
43200
54000
Graph #9 of 14 Loc(1) COUNTS vs. TIME(sec)

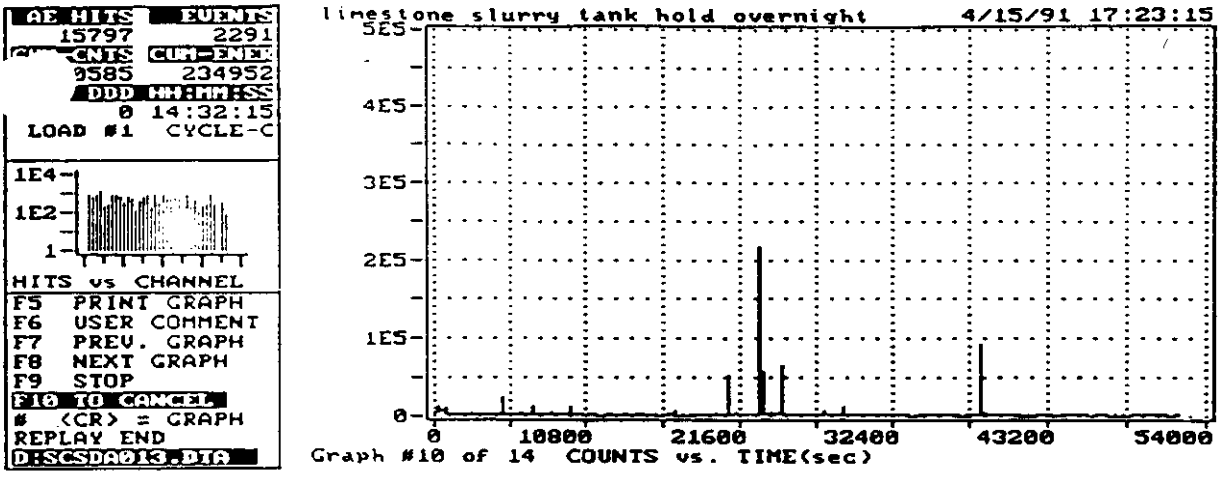
AE HITS
EVENTS
15797
2291
CNTS
CUM-ENER
9585
234952
DDD HH:MM:SS
0 14:32:15
LOAD #1 CYCLE-C
1E4
1E2
1
HITS vs CHANNEL
F5 PRINT GRAPH
F6 USER COMMENT
F7 PREV. GRAPH
F8 NEXT GRAPH
F9 STOP
F10 TO CANCEL
<CR> = GRAPH
REPLAY END
DB:CSDA013.DTA
limestone slurry tank hold overnight
4/15/91 17:23:15
5E5
4E5
3E5
2E5
1E5
0
0
10800
21600
32400
43200
54000
Graph #10 of 14 COUNTS vs. TIME(sec)

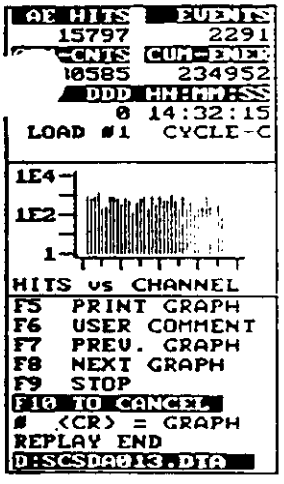
AE HITS EVENTS
15797 2291
CNTS CUM-ENE
10585 234952
DDD HH:MM:SS
0 14:32:15
LOAD #1 CYCLE-C
1E4
1E2
1
HITS vs CHANNEL
F5 PRINT GRAPH
F6 USER COMMENT
F7 PREV. GRAPH
F8 NEXT GRAPH
F9 STOP
F10 TO CANCEL
<CR> = GRAPH
REPLAY END
DASCSDA013.DTA

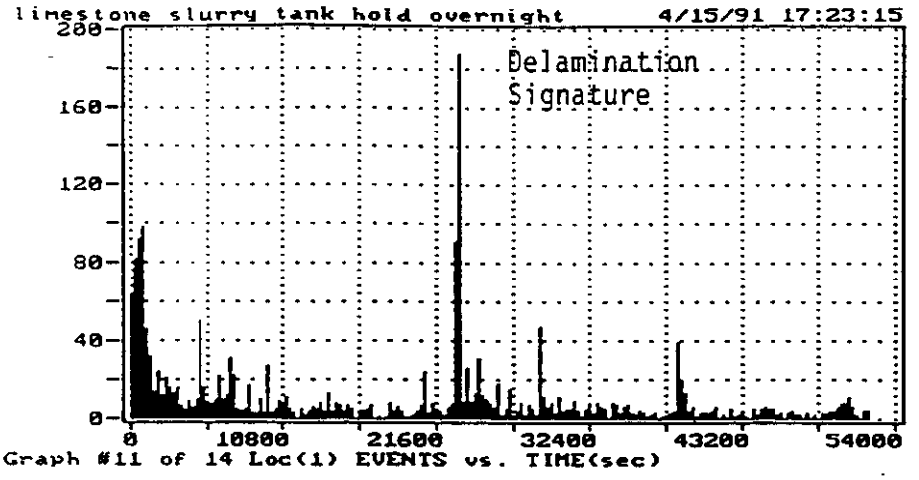
limestone slurry tank hold overnight 4/15/91 17:23:15
Delamination
Signature
200
160
120
80
40
0
0
10800
21600
32400
43200
54000
Graph #11 of 14 Loc(1) EVENTS vs. TIME(sec)

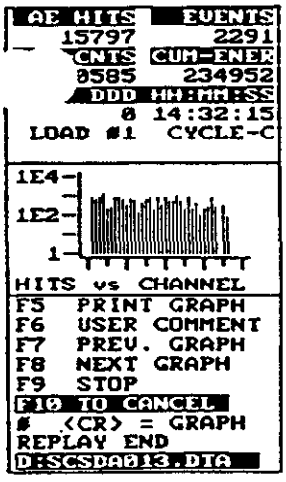
AE HITS
EVENTS
15797
2291
CNTS
CUM-ENER
0585
234952
DDD HH:MM:SS
0 14:32:15
LOAD #1 CYCLE-C
1E4
1E2
1
HITS vs CHANNEL
F5 PRINT GRAPH
F6 USER COMMENT
F7 PREV. GRAPH
F8 NEXT GRAPH
F9 STOP
F10 TO CANCEL
<CR> = GRAPH
REPLAY END
D:SCSDA013.DTA

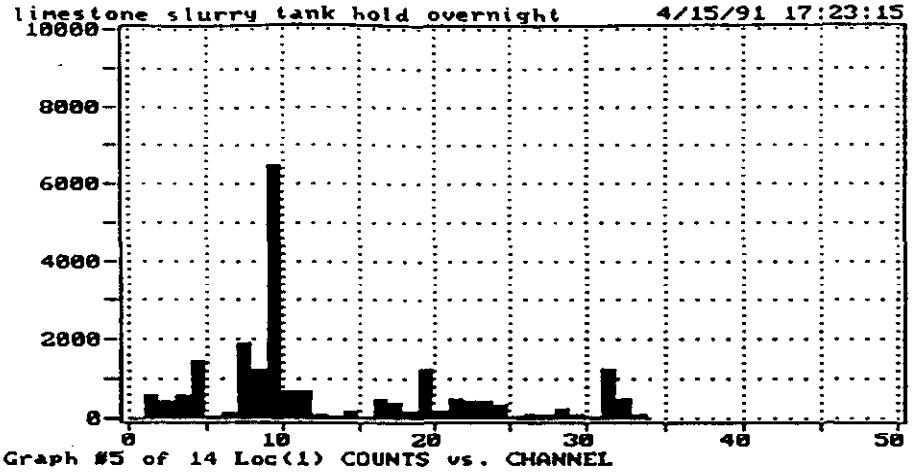
limestone slurry tank hold overnight
4/15/91 17:23:15
10000
8000
6000
4000
2000
0
0
10
20
30
40
50
Graph #5 of 14 Loc(1) COUNTS vs. CHANNEL

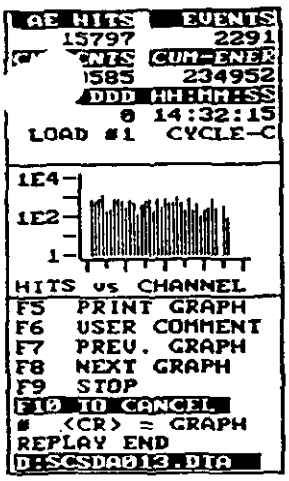
AE HITS
EVENTS
15797
2291
CUM-ENER
1585
234952
DDD HH:MM:SS
0 14:32:15
LOAD #1 CYCLE-C
1E4
1E2
1
HITS vs CHANNEL
F5 PRINT GRAPH
F6 USER COMMENT
F7 PREV. GRAPH
F8 NEXT GRAPH
F9 STOP
F10 TO CANCEL
<CR> = GRAPH
REPLAY END
D:\CSDA013.DTA

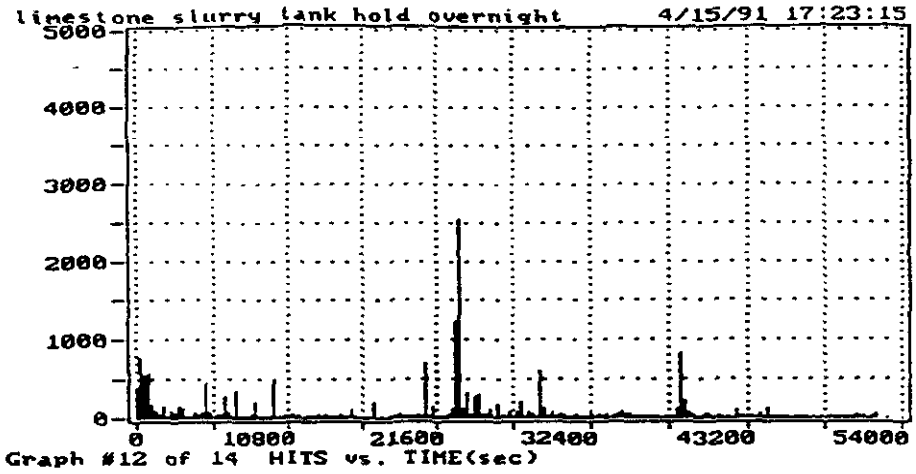
limestone slurry tank hold overnight
4/15/91 17:23:15
5000
4000
3000
2000
1000
0
0
10800
21600
32400
43200
54000
Graph #12 of 14 HITS vs. TIME(sec)

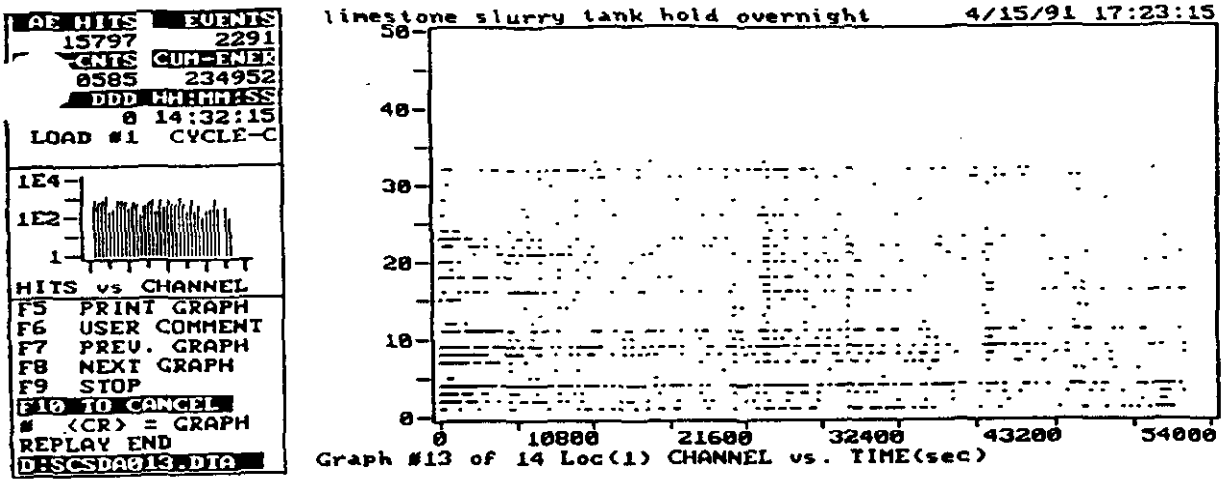
AE HITS
EVENTS
15797
2291
CNTS
CUM-ENER
0585
234952
DDD HH:MM:SS
0 14:32:15
LOAD #1 CYCLE-C
1E4
1E2
1
HITS vs CHANNEL
F5 PRINT GRAPH
F6 USER COMMENT
F7 PREV. GRAPH
F8 NEXT GRAPH
F9 STOP
F10 TO CANCEL
<CR> = GRAPH
REPLAY END
D:\SCSDA013.DTA
limestone slurry tank hold overnight
4/15/91 17:23:15
50
40
30
20
10
0
0
10800
21600
32400
43200
54000
Graph #13 of 14 Loc(1) CHANNEL vs. TIME(sec)

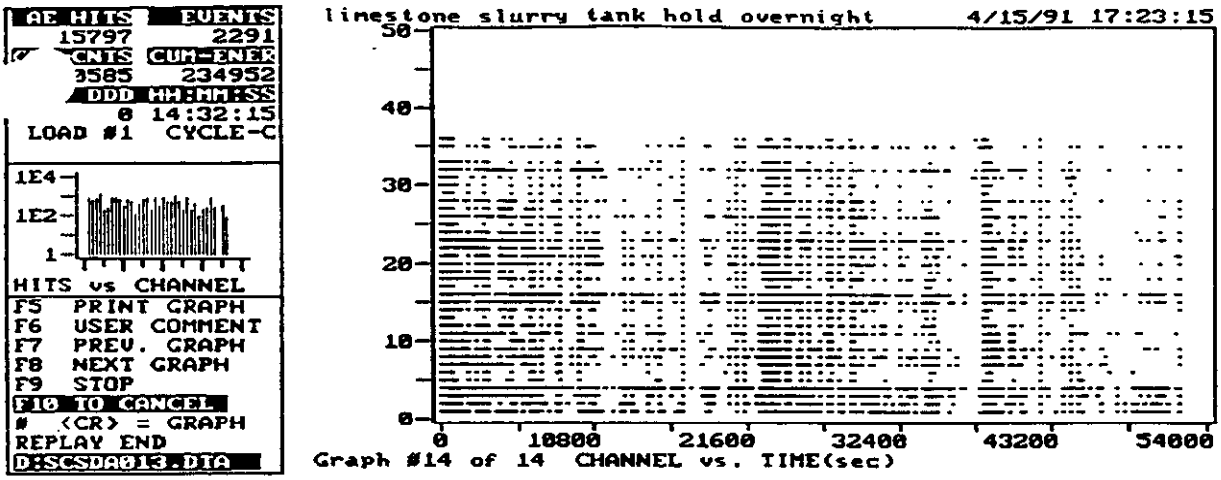
AE HITS
EVENTS
15797
2291
CNTS
CUM-ENER
3585
234952
DDD HH:MM:SS
0 14:32:15
LOAD #1 CYCLE-C
1E4
1E2
1
HITS vs CHANNEL
F5 PRINT GRAPH
F6 USER COMMENT
F7 PREV. GRAPH
F8 NEXT GRAPH
F9 STOP
F10 TO CANCEL
<CR> = GRAPH
REPLAY END
D:\SCSDA013.DTA
limestone slurry tank hold overnight
4/15/91 17:23:15
50
40
30
20
10
0
0
10800
21600
32400
43200
54000
Graph #14 of 14 CHANNEL vs. TIME(sec)

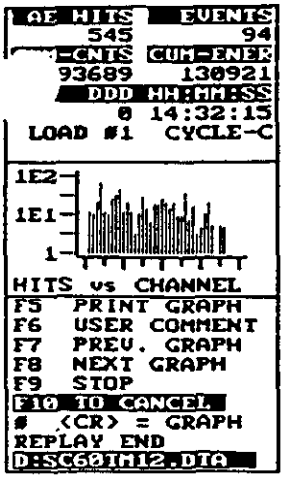
AE HITS EVENTS
545 94
-CNTS CUM-ENER
93689 130921
DDD HH:MM:SS
0 14:32:15
LOAD #1 CYCLE-C
1E2
1E1
1
HITS vs CHANNEL
F5 PRINT GRAPH
F6 USER COMMENT
F7 PREV. GRAPH
F8 NEXT GRAPH
F9 STOP
F10 TO CANCEL
<CR> = GRAPH
REPLAY END
D:SC60TH12.DTA

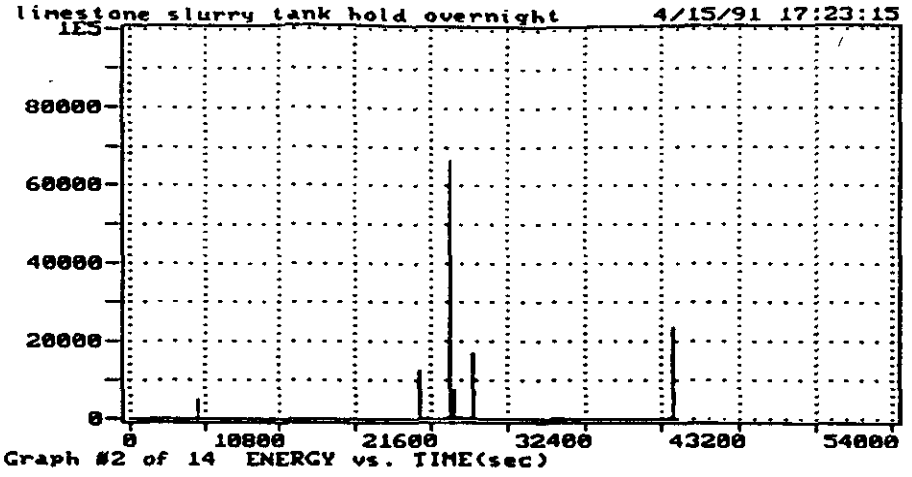
limestone slurry tank hold overnight
4/15/91 17:23:15
1E5
80000
60000
40000
20000
0
0
10800
21600
32400
43200
54000
Graph #2 of 14 ENERGY vs. TIME(sec)

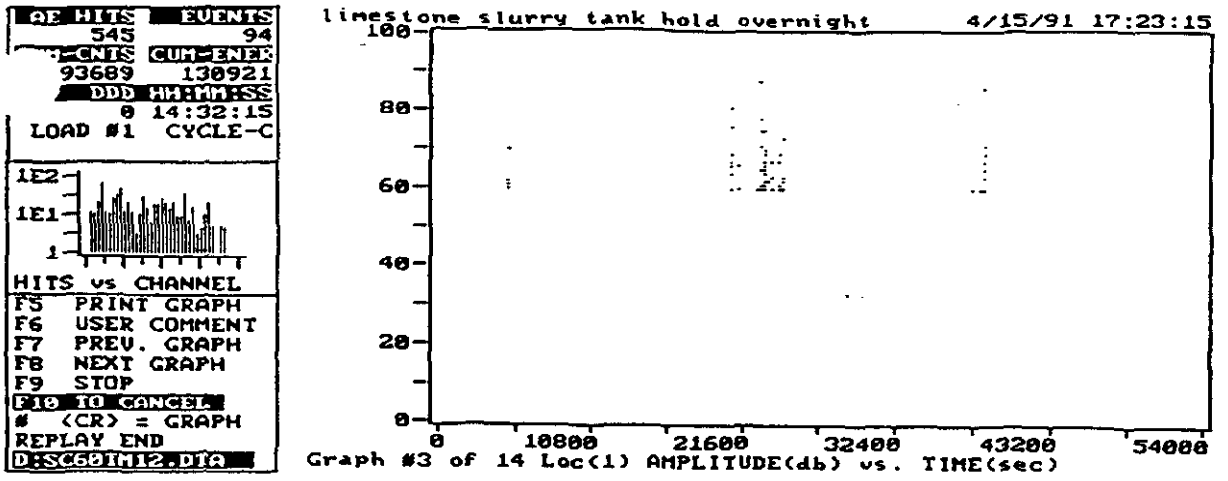
AE HITS EVENTS
545 94
CNTS CUM-ENER
93689 130921
DDD HH:MM:SS
0 14:32:15
LOAD #1 CYCLE-C
1E2
1E1
1
HITS vs CHANNEL
F5 PRINT GRAPH
F6 USER COMMENT
F7 PREV. GRAPH
F8 NEXT GRAPH
F9 STOP
F10 TO CANCEL
<CR> = GRAPH
REPLAY END
D:SC50IM12.DIG
limestone slurry tank hold overnight 4/15/91 17:23:15
100
80
60
40
20
0
0
10800
21600
32400
43200
54000
Graph #3 of 14 Loc(1) AMPLITUDE(db) vs. TIME(sec)

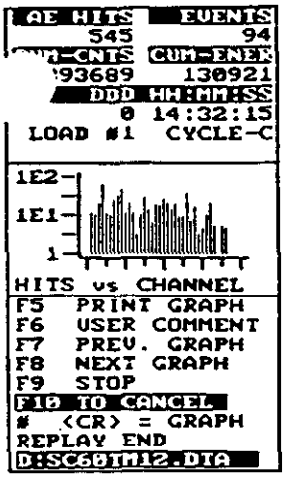
AE HITS EVENTS
545 94
-CNTS CUM-ENER
93689 130921
DDD HH:MM:SS
0 14:32:15
LOAD #1 CYCLE-C
1E2
1E1
1
HITS vs CHANNEL
F5 PRINT GRAPH
F6 USER COMMENT
F7 PREV. GRAPH
F8 NEXT GRAPH
F9 STOP
F10 TO CANCEL
<CR> = GRAPH
REPLAY END
D:SC60TM12.DIA

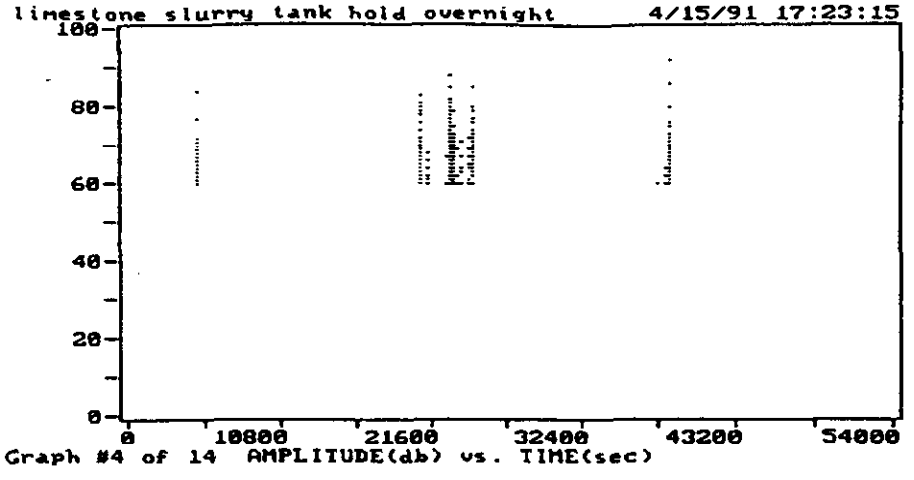
limestone slurry tank hold overnight 4/15/91 17:23:15
100
80
60
40
20
0
0
10800
21600
32400
43200
54000
Graph #4 of 14 AMPLITUDE(db) vs. TIME(sec)

APPENDIX E

FILE NAME	FILE SIZE	FILE DATE & TIME
D:SC60TM12.DTA	14703	4/20/91 19:20:02

TEST LABEL	TEST BEGIN DATE
limestone slurry tank hold overnight	Mon Apr 15 17:23:15 1991

ACTIVE CHANNELS

1	2	3	4	5	6	7	8	9	10	11	12	13	14	15	16	17	18	19	20
21	22	23	24	25	26	27	28	29	30	31	32	33	34	35	36				

ACTIVE AE DATA SET PARAMETERS
ID DDD HH:MM:SS.mmmuuun CH RISE COUN ENER DURATION AMP PCNTS

ACTIVE TIME DRIVEN DATA SET PARAMETERS
ID DDD HH:MM:SS.mmmuuun

AE Data Display is ON TIME Data Display is ON

	DDD	HH:MM:SS.mmmuuun	CH	RISE	COUN	ENER	DURATION	AMP	PCNTS
	Ø	ØØ:ØØ:ØØ.ØØØØØØØ			Test running				
1	Ø	Ø1:22:ØØ.7758145	4	28	27	13	568	6Ø	4
1	Ø	Ø1:22:ØØ.8138635	4	41	56	22	721	62	6
1	Ø	Ø1:22:ØØ.8399545	9	83	98	68	1Ø73	7Ø	13
1	Ø	Ø1:22:ØØ.8408815	1Ø	129	1Ø5	39	1106	65	17
1	Ø	Ø1:22:ØØ.8412695	21	145	111	34	1845	64	23
1	Ø	Ø1:22:ØØ.8421617	22	126	59	29	563	64	17
1	Ø	Ø1:22:ØØ.8422685	11	373	86	35	798	6Ø	55
1	Ø	Ø1:22:ØØ.8425625	7	141	66	26	679	6Ø	19
1	Ø	Ø1:22:ØØ.8428103	32	1Ø9	86	26	764	63	17
1	Ø	Ø1:22:ØØ.8432773	12	128	83	34	832	64	18
1	Ø	Ø1:22:ØØ.8435155	1	157	196	127	3131	72	23
1	Ø	Ø1:22:ØØ.8435357	35	129	187	83	1Ø72	65	22
1	Ø	Ø1:22:ØØ.8443150	13	525	121	32	1650	6Ø	68
1	Ø	Ø1:22:ØØ.8443873	2	176	184	8Ø	2Ø47	67	27
1	Ø	Ø1:22:ØØ.8444227	4	599	1412	619	3Ø849	84	2Ø
1	Ø	Ø1:22:ØØ.8445510	23	118	1814	462	3Ø549	68	18
1	Ø	Ø1:22:ØØ.8447Ø4Ø	28	129	112	34	854	6Ø	18
1	Ø	Ø1:22:ØØ.8448573	3	123	414	195	4840	77	18
1	Ø	Ø1:22:ØØ.8449525	14	131	177	64	2Ø41	65	18
1	Ø	Ø1:22:ØØ.8449783	16	114	927	269	2Ø8Ø8	69	17
1	Ø	Ø1:22:ØØ.8451750	15	12Ø	211	82	3291	7Ø	19
1	Ø	Ø1:22:ØØ.8452570	24	574	119	44	1322	65	71
1	Ø	Ø1:22:ØØ.8456587	26	528	446	124	7375	62	48
	Ø	Ø1:22:ØØ.8488870	22	2Ø	55Ø	2Ø4	15327	67	3
	Ø	Ø1:22:ØØ.8488925	7	123	1291	32Ø	22141	65	17
1	Ø	Ø1:22:ØØ.8490Ø15	8	8	714	167	9886	68	1
1	Ø	Ø1:22:ØØ.8491935	19	84	67Ø	173	9Ø72	65	13
1	Ø	Ø1:22:ØØ.8498733	32	68	958	276	19177	66	5
1	Ø	Ø1:22:ØØ.8499623	12	342	542	215	19657	61	14
1	Ø	Ø1:22:ØØ.8504625	21	462	167	73	2Ø82	71	42
1	Ø	Ø1:22:ØØ.8506667	2Ø	213	264	13Ø	8942	67	23
1	Ø	Ø1:22:ØØ.8509905	3Ø	132	189	69	4366	62	2Ø
1	Ø	Ø1:22:ØØ.8510140	9	2	38	11	612	6Ø	33
1	Ø	Ø1:22:ØØ.8554337	26	3Ø9	428	125	1Ø336	67	8
1	Ø	Ø1:22:ØØ.8564Ø8Ø	3	1	153	58	4615	63	62
1	Ø	Ø1:22:ØØ.8566717	15	Ø	76	16	854	64	27
1	Ø	Ø1:22:ØØ.8610435	19	41	3Ø8	75	2646	62	6
1	Ø	Ø1:22:ØØ.8610920	21	53	169	42	22Ø4	65	8
1	Ø	Ø1:22:ØØ.8616195	2Ø	757	153	66	5373	62	39
1	Ø	Ø1:22:ØØ.8676703	24	514	156	42	1969	62	35
1	Ø	Ø1:22:ØØ.8677ØØØ	15	446	68	21	2ØØ6	61	25
1	Ø	Ø1:22:ØØ.8678130	26	43Ø	76	31	1973	62	28
1	Ø	Ø1:22:ØØ.8737555	21	159	61	18	4Ø9	6Ø	25
1	Ø	Ø5:47:58.7787525	9	164	64	97	1437	76	14
1	Ø	Ø5:47:58.7804797	8	48	85	48	1862	69	8
1	Ø	Ø5:47:58.7813457	19	5Ø	249	99	17Ø7	67	8
1	Ø	Ø5:47:58.7819Ø53	7	74	95	41	1152	64	1Ø
1	Ø	Ø5:47:58.7827670	18	68	66	35	725	67	13
	Ø	Ø5:47:58.7829883	2Ø	84	44	2Ø	832	6Ø	9
	Ø	Ø5:47:58.7831660	6	89	44	21	491	62	12
	Ø	Ø5:47:58.7839120	23	36	62	25	892	64	5
1	Ø	Ø5:47:58.7839405	28	22	63	27	812	67	4
1	Ø	Ø5:47:58.7840580	5	93	55	23	1138	63	13
1	Ø	Ø5:47:58.7843293	4	257	8Ø5	4Ø6	19791	8Ø	36
1	Ø	Ø5:47:58.7844365	16	97	2Ø5	73	2173	66	15
1	Ø	Ø5:47:58.7844535	3	136	143	87	4258	67	21

	DDD	HH:MM:SS.mmmuuun	CH	RISE	COUN	ENER	DURATION	AMP	PCNTS
1	Ø	Ø6:28:46.9556500	18	29	45	19	470	62	5
1	Ø	Ø6:28:46.9573355	4	72	114	83	3203	73	12
1	Ø	Ø6:28:46.9607160	26	417	47	24	2924	60	7
1	Ø	Ø6:28:46.9631443	9	97	76	34	1076	65	12
1	Ø	Ø6:28:46.9666483	7	226	137	35	1589	60	28
1	Ø	Ø6:28:46.9677103	18	22	66	19	754	60	3
1	Ø	Ø6:28:46.9686830	4	842	122	94	4121	71	62
1	Ø	Ø6:28:46.9690875	26	117	77	26	1373	60	16
1	Ø	Ø6:28:47.5869797	9	118	163	117	3284	75	16
1	Ø	Ø6:28:47.5886213	8	10	269	89	4887	65	1
1	Ø	Ø6:28:47.5894853	19	607	359	101	3280	63	22
1	Ø	Ø6:28:47.5897327	20	39	92	47	3574	60	5
1	Ø	Ø6:28:47.5900393	7	93	12	6	126	71	11
1	Ø	Ø6:28:47.5909067	18	13	105	55	2733	65	2
1	Ø	Ø6:28:47.5912947	6	127	73	28	1840	60	14
1	Ø	Ø6:28:47.5920720	23	37	6	2	62	64	5
1	Ø	Ø6:28:47.5920800	28	20	6	5	70	68	3
1	Ø	Ø6:28:47.5921977	5	70	11	2	96	67	7
1	Ø	Ø6:28:47.5925827	16	54	285	88	3669	66	8
1	Ø	Ø6:28:47.5925985	3	121	1020	312	21187	67	12
1	Ø	Ø6:28:47.5925990	4	64	1865	712	36935	79	9
1	Ø	Ø6:28:47.5926105	14	11	5	5	95	60	2
1	Ø	Ø6:28:47.5928180	15	13	441	153	20186	70	2
1	Ø	Ø6:28:47.5928243	24	5	3	3	53	63	1
	Ø	Ø6:28:47.5928707	27	31	8	Ø	48	65	5
	Ø	Ø6:28:47.5931885	26	14	14	6	136	71	2
1	Ø	Ø6:28:47.5933015	2	184	1037	315	23837	63	23
1	Ø	Ø6:28:47.5941857	23	1	1680	404	32730	65	6
1	Ø	Ø6:28:47.5955777	26	1	1022	289	27020	62	10
1	Ø	Ø6:28:47.5974225	9	149	135	45	2545	62	21
1	Ø	Ø6:28:47.5975147	8	41	1113	269	19235	64	6
1	Ø	Ø6:28:47.5976550	1	52	715	284	22290	68	6
1	Ø	Ø6:28:47.5981535	22	32	324	111	8693	62	5
1	Ø	Ø6:28:47.5984070	32	220	1448	377	27001	67	21
1	Ø	Ø6:28:47.5984290	7	855	1469	372	27239	65	61
1	Ø	Ø6:28:47.5984585	20	38	412	159	13488	62	5
1	Ø	Ø6:28:47.5984880	21	92	361	81	11178	62	14
1	Ø	Ø6:28:47.5986500	11	545	325	117	6979	64	31
1	Ø	Ø6:28:47.6106280	11	343	114	64	3851	64	36
1	Ø	Ø6:28:47.6147193	10	46	83	38	1592	63	6
1	Ø	Ø6:28:47.6514063	4	50	52	27	1176	64	4
1	Ø	Ø6:28:47.7418093	9	101	51	26	427	64	15
1	Ø	Ø6:28:47.7468913	28	33	51	19	529	64	6
1	Ø	Ø6:28:47.7474135	4	98	86	55	2033	69	15
1	Ø	Ø6:28:47.7476260	15	45	46	8	454	60	6
1	Ø	Ø6:28:47.7479970	26	42	36	13	411	60	5
1	Ø	Ø6:28:48.2287160	4	97	41	17	290	62	14
1	Ø	Ø6:28:48.2525540	9	107	48	24	450	65	13
1	Ø	Ø6:28:48.2541990	8	20	35	16	461	63	3
	Ø	Ø6:28:48.2556197	7	72	51	20	640	60	10
	Ø	Ø6:28:48.2581710	4	135	88	77	3089	71	20
1	Ø	Ø6:28:48.2583815	15	17	45	9	398	62	3
1	Ø	Ø6:28:48.2587543	26	20	25	14	516	64	3
1	Ø	Ø6:28:49.0085175	4	70	35	19	365	62	11
1	Ø	Ø6:28:50.3725610	8	34	38	17	937	61	5
1	Ø	Ø6:28:50.3765375	4	33	93	46	2301	66	5
1	Ø	Ø6:28:51.9955423	8	154	44	16	748	67	25

	DDD	HH:MM:SS.mmmuuun	CH	RISE	COUN	ENER	DURATION	AMP	PCNTS
1	Ø	Ø6:28:57.6384173	4	6Ø	6Ø	47	395	69	9
1	Ø	Ø6:29:19.2868415	4	53	29	13	217	6Ø	8
1	Ø	Ø6:29:23.1889790	4	119	39	16	275	6Ø	18
1	Ø	Ø6:29:57.2186925	9	129	58	24	451	65	21
1	Ø	Ø6:29:57.2243033	4	34	48	26	669	64	5
1	Ø	Ø6:29:57.2245075	15	88	26	7	366	6Ø	13
1	Ø	Ø6:31:1Ø.1325177	8	2Ø	46	13	416	6Ø	4
1	Ø	Ø6:31:1Ø.1364983	4	9Ø	48	26	412	65	14
1	Ø	Ø6:33:15.6412915	9	116	64	24	536	62	16
1	Ø	Ø6:33:15.6469233	4	12Ø	74	57	1965	69	19
1	Ø	Ø6:33:15.6471310	15	14	33	6	379	6Ø	2
1	Ø	Ø6:36:3Ø.3117493	4	66	28	18	197	63	1Ø
1	Ø	Ø6:37:27.219Ø545	4	66	3Ø	24	222	67	1Ø
1	Ø	Ø6:37:3Ø.Ø297483	9	89	45	21	384	67	14
1	Ø	Ø6:37:3Ø.Ø353625	4	76	55	53	1928	71	12
1	Ø	Ø6:37:3Ø.Ø355665	15	21	29	7	327	64	3
1	Ø	Ø6:37:3Ø.Ø359373	26	23	19	9	151	6Ø	3
1	Ø	Ø6:39:Ø3.4444310	4	61	34	15	255	6Ø	9
1	Ø	Ø6:47:2Ø.4260727	4	39	25	14	163	61	7
1	Ø	Ø6:47:2Ø.4873Ø43	4	33Ø	46	31	656	69	13
1	Ø	Ø6:47:2Ø.4880103	3	17	16	1Ø	115	6Ø	3
1	Ø	Ø6:48:Ø2.6689613	9	82	54	34	365	67	13
1	Ø	Ø6:48:Ø2.67Ø4Ø2Ø	2Ø	33	2Ø	11	185	61	5
1	Ø	Ø6:48:Ø2.6725195	1	4Ø	3Ø	17	723	6Ø	6
	Ø	Ø6:48:Ø2.6738380	3	28	75	33	1949	64	4
-	Ø	Ø6:48:Ø2.6738690	4	43	121	72	3Ø61	72	6
1	Ø	Ø6:48:Ø2.6739433	16	35	123	35	2471	65	5
1	Ø	Ø6:48:Ø2.6741470	15	24	32	8	9Ø9	65	4
1	Ø	Ø6:48:Ø2.6797695	21	41	4Ø	9	911	6Ø	7
1	Ø	Ø6:53:11.3419700	4	1Ø	25	15	174	62	2
1	Ø	Ø6:53:16.Ø428725	9	119	154	89	28Ø7	73	18
1	Ø	Ø6:53:16.Ø441330	8	46	352	83	4963	6Ø	7
1	Ø	Ø6:53:16.Ø442Ø30	21	131	19Ø	95	1921	7Ø	21
1	Ø	Ø6:53:16.Ø442830	2Ø	124	97	77	852	74	19
1	Ø	Ø6:53:16.Ø45Ø363	22	167	83	68	2312	7Ø	19
1	Ø	Ø6:53:16.Ø45Ø8Ø7	19	2Ø9	715	371	4960	71	31
1	Ø	Ø6:53:16.Ø451925	11	57	152	61	25Ø2	65	8
1	Ø	Ø6:53:16.Ø453923	7	197	3744	1ØØ6	5Ø555	71	29
1	Ø	Ø6:53:16.Ø457347	32	92	132	61	1824	68	13
1	Ø	Ø6:53:16.Ø46149Ø	12	432	95	6Ø	956	67	54
1	Ø	Ø6:53:16.Ø463195	18	184	1Ø9	61	1Ø99	67	27
1	Ø	Ø6:53:16.Ø464155	1	1Ø4	2419	736	37661	79	15
1	Ø	Ø6:53:16.Ø464445	35	92	1889	712	28120	71	17
1	Ø	Ø6:53:16.Ø465Ø47	33	143	71	26	55Ø	63	22
1	Ø	Ø6:53:16.Ø465983	6	147	115	39	941	62	21
1	Ø	Ø6:53:16.Ø471447	2Ø	2	33	17	514	63	33
1	Ø	Ø6:53:16.Ø471860	13	124	164	62	2195	67	19
1	Ø	Ø6:53:16.Ø472Ø63	36	64	92	56	1706	65	19
1	Ø	Ø6:53:16.Ø472603	2	125	2556	668	32250	71	19
	Ø	Ø6:53:16.Ø474333	23	143	4123	1176	53189	76	22
	Ø	Ø6:53:16.Ø474397	5	95	179	5Ø	2786	62	15
1	Ø	Ø6:53:16.Ø475450	28	149	926	314	2Ø219	72	23
1	Ø	Ø6:53:16.Ø477Ø4Ø	3	141	2400	7ØØ	32187	8Ø	21
1	Ø	Ø6:53:16.Ø477350	4	132	3348	1Ø99	44557	85	16
1	Ø	Ø6:53:16.Ø477970	14	139	1474	469	3Ø095	72	15
1	Ø	Ø6:53:16.Ø478127	16	89	2481	616	33499	73	14
1	Ø	Ø6:53:16.Ø48Ø125	15	110	1484	459	3Ø419	77	12

	JDD	HH:MM:SS.mmmuuun	CH	RISE	COUN	ENER	DURATION	AMP	PCNTS
1	Ø	Ø6:53:16.Ø484767	26	642	2874	796	41283	73	78
1	Ø	Ø6:53:16.Ø491175	12	2	1875	551	34884	66	1
1	Ø	Ø6:53:16.Ø495685	32	2	3261	87Ø	47352	68	32
1	Ø	Ø6:53:16.Ø496190	22	1Ø4	1647	441	29741	65	9
1	Ø	Ø6:53:16.Ø496795	2Ø	479	1788	6Ø4	34357	73	26
1	Ø	Ø6:53:16.Ø5ØØ997	11	926	1455	437	29219	63	57
1	Ø	Ø6:53:16.Ø512260	8	657	2439	597	33Ø76	7Ø	11
1	Ø	Ø6:53:16.Ø514100	17	1	237	64	5377	62	1
1	Ø	Ø6:53:16.Ø52Ø513	19	53	2451	555	28254	68	8
1	Ø	Ø6:53:16.Ø522690	5	1	2	5	547	6Ø	2
1	Ø	Ø6:53:16.Ø524223	18	2	2445	628	37410	69	57
1	Ø	Ø6:53:16.Ø53Ø710	31	26	587	126	8301	63	4
1	Ø	Ø6:53:16.Ø53Ø727	21	1	1164	286	19955	7Ø	22
1	Ø	Ø6:53:16.Ø533913	3Ø	532	818	287	19780	65	11
1	Ø	Ø6:53:16.Ø534440	29	139	111	35	4413	6Ø	9
1	Ø	Ø6:53:16.Ø535627	9	123	57	32	1370	65	19
1	Ø	Ø6:53:16.Ø572Ø33	25	26	168	66	5594	62	1
1	Ø	Ø6:53:16.Ø5E5687	17	354	192	52	6438	62	22
1	Ø	Ø6:53:16.Ø601853	1Ø	137	166	84	2968	69	21
1	Ø	Ø6:53:16.Ø633927	31	15	186	46	3694	6Ø	2
1	Ø	Ø6:53:16.Ø6E6683	1Ø	15	51Ø	165	1Ø235	64	2
1	Ø	Ø6:53:16.Ø758860	21	878	14Ø	45	6280	62	19
1	Ø	1Ø:32:52.1175647	31	12	29	7	2Ø2	6Ø	2
1	Ø	1Ø:4Ø:33.1103027	2Ø	45	32	12	214	6Ø	7
	Ø	1Ø:4Ø:33.1110535	22	34	35	14	247	6Ø	5
	Ø	1Ø:4Ø:33.1134337	23	4Ø	4Ø	11	6Ø2	6Ø	6
1	Ø	1Ø:4Ø:33.1135353	28	44	47	15	6Ø3	6Ø	7
1	Ø	1Ø:4Ø:33.1137517	4	51	68	35	2Ø4Ø	64	8
1	Ø	1Ø:4Ø:33.1138307	16	23	58	25	2213	62	4
1	Ø	1Ø:45:31.3214535	9	9Ø	217	259	3250	86	16
1	Ø	1Ø:45:31.3273635	2Ø	46	199	92	3907	67	7
1	Ø	1Ø:45:31.3273857	8	48	4Ø8	144	5244	72	9
1	Ø	1Ø:45:31.3283660	19	151	622	372	5Ø67	75	23
1	Ø	1Ø:45:31.3Ø44273	11	176	1Ø4	5Ø	2273	64	26
1	Ø	1Ø:45:31.3Ø45163	7	112	342	119	3813	67	19
1	Ø	1Ø:45:31.3Ø45375	32	94	94	39	2373	62	12
1	Ø	1Ø:45:31.3ØE3297	12	78	73	39	1767	63	11
1	Ø	1Ø:45:31.3ØE3843	18	55	3ØØ4	8Ø5	44934	7Ø	8
1	Ø	1Ø:45:31.3Ø54593	33	39	7Ø	21	653	62	5
1	Ø	1Ø:45:31.3Ø57260	1	135	2958	865	43593	66	19
1	Ø	1Ø:45:31.3Ø57457	35	218	2172	784	34Ø38	64	4Ø
1	Ø	1Ø:45:31.3Ø57735	6	126	95	42	823	66	19
1	Ø	1Ø:45:31.3Ø64877	17	81	129	39	1139	63	11
1	Ø	1Ø:45:31.3Ø6E37Ø	23	112	4476	12Ø8	5Ø211	71	15
1	Ø	1Ø:45:31.3Ø6E547	28	63	138	78	1146	72	11
1	Ø	1Ø:45:31.3Ø6e695	2	86	33Ø7	857	42803	68	12
1	Ø	1Ø:45:31.3Ø6e717	5	6Ø	15Ø	98	2Ø84	73	9
1	Ø	1Ø:45:31.3171545	16	81	2728	779	47Ø23	76	13
1	Ø	1Ø:45:31.3171723	4	99	4Ø93	1486	48388	92	7
	Ø	1Ø:45:31.3171723	3	176	2876	8Ø4	41287	69	26
	Ø	1Ø:45:31.3273837	14	78	166Ø	496	32130	68	11
1	Ø	1Ø:45:31.3272435	15	33	1532	529	32550	8Ø	6
1	Ø	1Ø:45:31.3272570	24	91	2157	581	37796	69	13
1	Ø	1Ø:45:31.3273516	27	59	134	53	1648	69	8
1	Ø	1Ø:45:31.3Ø7e477	25	96	3ØØ	143	6429	71	14
1	Ø	1Ø:45:31.3Ø7e613	26	32	3Ø19	922	43Ø11	8Ø	5
1	Ø	1Ø:45:31.3Ø87595	33	32	1253	378	27358	62	2

	ODD	HH:MM:SS.mmmuuun	CH	RISE	COUN	ENER	DURATION	AMP	PCNTS
1	Ø	1Ø:45:31.3092185	11	77	2Ø51	7Ø1	35348	75	7
1	Ø	1Ø:45:31.3094Ø97	12	653	1942	549	34899	64	6
1	Ø	1Ø:45:31.3099850	28	89	24Ø	95	6239	65	15
1	Ø	1Ø:45:31.3103420	7	5Ø7	3984	1Ø38	39572	73	17
1	Ø	1Ø:45:31.3106140	8	84	3131	795	39ØØ8	7Ø	9
1	Ø	1Ø:45:31.3110553	2Ø	95	1990	565	31957	71	14
1	Ø	1Ø:45:31.3113843	19	92	2568	6Ø8	22267	69	11
1	Ø	1Ø:45:31.3114513	36	229	41	26	617	6Ø	22
1	Ø	1Ø:45:31.3115810	21	1Ø3	1479	374	3Ø733	71	1
1	Ø	1Ø:45:31.3116117	22	32	1Ø9Ø	551	31465	71	4
1	Ø	1Ø:45:31.3116385	31	33	641	163	8490	67	6
1	Ø	1Ø:45:31.3122973	9	2	1Ø6	91	2109	75	2
1	Ø	1Ø:45:31.3126443	3Ø	555	929	314	18337	67	27
1	Ø	1Ø:45:31.3133387	5	1	232	89	6687	69	38
1	Ø	1Ø:45:31.3156123	6	378	267	139	1Ø883	65	6
1	Ø	1Ø:45:31.3160870	25	45	23Ø	92	8374	64	5
1	Ø	1Ø:45:31.3171297	17	345	36Ø	1ØØ	1Ø331	63	9
1	Ø	1Ø:45:31.3185427	27	384	148	44	1996	63	49
1	Ø	1Ø:45:31.3231333	31	1	337	1Ø5	7973	67	1
1	Ø	1Ø:45:31.3242347	9	28Ø	81	47	3129	66	2Ø
1	Ø	1Ø:45:31.3279800	1Ø	5	646	267	9853	75	1
1	Ø	1Ø:45:31.3288950	6	13	119	61	4654	6Ø	2
1	Ø	1Ø:45:31.3418553	15	1	188	44	6382	6Ø	61
1	Ø	1Ø:45:31.3516845	8	4	8Ø	33	2199	61	2
	Ø	1Ø:45:31.4932310	9	63	62	2Ø	437	63	11
	Ø	1Ø:45:31.4988305	16	69	85	28	1375	61	11
1	Ø	1Ø:45:31.4988587	4	4Ø	67	51	1987	7Ø	7
1	Ø	1Ø:45:31.4990675	15	32	36	8	37Ø	63	5
1	Ø	1Ø:45:31.4994365	26	29	26	9	168	6Ø	4
1	Ø	1Ø:46:42.1695357	9	118	1Ø6	76	1616	69	2Ø
1	Ø	1Ø:46:42.1711695	8	42	168	6Ø	2338	7Ø	7
1	Ø	1Ø:46:42.172Ø387	19	1Ø3	141	43	1338	6Ø	16
1	Ø	1Ø:46:42.1725917	7	1Ø7	1Ø6	38	1422	62	17
1	Ø	1Ø:46:42.1734635	18	34Ø	78	32	741	65	45
1	Ø	1Ø:46:42.1746330	28	52	111	41	9Ø5	67	9
1	Ø	1Ø:46:42.1746340	23	457	79	27	1618	63	48
1	Ø	1Ø:46:42.1747477	5	86	54	31	1186	69	13
1	Ø	1Ø:46:42.1751345	16	24	191	77	2387	67	4
1	Ø	1Ø:46:42.1751530	3	138	297	14Ø	8952	68	2Ø
1	Ø	1Ø:46:42.1751560	4	91	329	332	8734	86	6
1	Ø	1Ø:46:42.1751667	14	62	63	31	1121	61	1Ø
1	Ø	1Ø:46:42.1753763	15	25	117	6Ø	2643	71	4
1	Ø	1Ø:46:42.1757470	26	16	25Ø	93	5751	66	2
1	Ø	1Ø:46:42.1782627	23	1	319	86	58Ø1	64	32
1	Ø	1Ø:46:42.1783997	2	817	161	56	3703	61	29
1	Ø	1Ø:46:42.1793355	7	6	393	119	7420	64	1
1	Ø	1Ø:46:42.1795015	11	2	184	1Ø4	7589	67	3
1	Ø	1Ø:46:42.1795823	8	23	3	4	22	67	3
1	Ø	1Ø:46:42.1797620	1	224	132	5Ø	2287	63	22
1	Ø	1Ø:46:42.1799697	32	21	5ØØ	16Ø	8195	67	3
	Ø	1Ø:46:42.1803677	22	513	12Ø	55	1803	66	34
1	Ø	1Ø:46:42.1809423	21	134	1Ø2	34	1390	64	21
1	Ø	1Ø:46:42.1809575	2Ø	129	8Ø	44	1899	65	16
1	Ø	1Ø:46:42.1809640	9	43	49	22	332	67	7
1	Ø	1Ø:46:42.1816605	8	1	319	91	8Ø57	61	21
1	Ø	1Ø:46:42.1841333	26	61	3Ø8	11Ø	11149	66	4
1	Ø	1Ø:46:42.1859Ø23	4	2	348	13Ø	7726	65	7

	DD	HH:MM:SS.mmmuuun	CH	RISE	COUN	ENER	DURATION	AMP	PCNTS
1	Ø	1Ø:46:42.1867280	15	212	83	24	898	61	29
1	Ø	1Ø:46:42.1893675	1	1	65	41	3Ø99	6Ø	7
1	Ø	1Ø:46:42.1919147	8	583	176	76	5869	65	21
1	Ø	1Ø:46:42.1920877	11	232	7Ø	35	1269	66	31
1	Ø	1Ø:46:42.1924640	32	226	31Ø	92	6870	63	29
1	Ø	1Ø:46:42.1966467	4	1	216	93	6489	67	1
1	Ø	1Ø:46:42.1970753	1Ø	275	59	54	1386	69	18
1	Ø	1Ø:46:42.1971665	7	6Ø4	252	88	8547	65	36
1	Ø	1Ø:46:42.1973755	26	1Ø96	88	32	2593	6Ø	36
1	Ø	1Ø:46:42.1978635	3	413	78	3Ø	1Ø6	62	33
1	Ø	1Ø:46:42.2Ø91873	7	245	54	19	494	6Ø	2Ø
1	Ø	1Ø:47:14.68Ø9730	9	73	47	19	381	6Ø	1Ø
1	Ø	1Ø:47:14.68Ø9730	9	73	47	19	381	6Ø	1Ø
1	Ø	1Ø:47:14.6825917	8	2Ø	37	14	344	62	4
1	Ø	1Ø:47:14.6865715	4	56	56	23	433	63	1Ø
	Ø	14:32:15.8199695			Test Paused				
ID	DDD	HH:MM:SS.mmmuuun							
3	Ø	14:32:15.82Ø35ØØ							
	Ø	14:32:52.78Ø481Ø			Test Stop				

"Strain Monitoring Final Report"

Consulting and Testing Services

PLANT YATES

DEPARTMENT OF ENERGY

DEMONSTRATION PROJECT CT-121

STRAIN MONITORING FINAL REPORT

PREPARED BY

CONSULTING AND TESTING SERVICES

AND

RESEARCH AND ENVIRONMENTAL AFFAIRS

JULY 1995

PREPARED BY:	Tom Lantrip	DATE:	7/95
REVIEWED BY:	Phillip Garrett	DATE:	7/95
APPROVED BY:	David McKinney	DATE:	7/95

Executive Summary

The implementation of tighter environmental controls on sulfur dioxide (SO_2) gases has required many utilities to retrofit existing fossil fuel generating plants with scrubbers capable of reducing the stack emissions.

Georgia Power's Plant Yates Unit 1 was selected as a joint project with the DOE to construct a full-scale demonstration project utilizing the Chiyoda reduction process to remove the SO_2 gases. The Chiyoda process involves the "wet scrubbing" of the waste gas, and to facilitate this process, the primary vessels are required to be corrosive resistant. Therefore, the primary process vessels, the Jet-Bubbling Reactor Vessel (JBR) and the Limestone Slurry Tank were both constructed of a filament-wound fiber reinforced plastic (FRP) composite material which is basically inert to the corrosive environment of the Chiyoda chemical process.

As part of the demonstration of this technology, the structural integrity of the FRP vessels was requested to determine the suitability of the material for the designated design duty. Strain testing was adopted as one of the methods to quantify the behavior of the primary vessels for the loadings to be applied during the operating life of the vessels.

This testing proved to be beneficial in calibrating the design practice and quality assurance of the field constructed vessel and structures. Various hydrostatic tests were conducted both prior to and at the completion of the demonstration period, to qualify the integrity of the vessel structure initially, and after the required operating demonstration period.

Results of the testing include the comparison of the design hydrostatic stresses to the experimentally determined stresses, a means of quantification of the safety factors used in design, and discussions on the behavior of the FRP material . These discussions provided insight on life cycle creep which may occur in FRP vessels.

The results and research which occurred in reduction of the data and review of material performance, also demonstrated the importance of unique information applicable for each FRP material. Industry experience has suggested that engineering data and properties of FRP constructed material require a much more comprehensive requirement on the part of the owner to specify carefully many aspects of the design process, quality assurance requirements, and construction requirements. In addition, performance testing of the completed structure is very important to comprehensively test the total system.

The strain testing was successful is providing comprehensive data during the hydro tests and providing insight into the time and duty affects on the FRP vessels. This experimental test data correlated very well with theoretical stresses utilizing the design material properties.

The strain testing provided a full scale verification of the structural integrity of the vessel. In addition, the strain testing provides a tool for the trending of the performance of the structural composite material.

The test data from the hydrostatic tests on the Plant Yates Jet-Bubbling Reactor and Limestone Slurry Tank compared well with the predicted stress levels and material properties provided in the manufacturers design calculations. In addition, the test data provided some valuable insight into the long term behavior of the material properties. This strain testing provides a rational means to evaluate the life cycle behavior of a FRP vessel both at initial loading and a trending tool over time.

Background

In 1991, the Yates/Doe Scrubber Demonstration project was selected as a candidate for quality assurance of the structural integrity of the Fiber-Reinforced Plastic (FRP) vessels at Georgia Powers Plant Yates. Based on the corrosive environment of the chemicals and slurry utilized in the Chiyoda Scrubber process, Fiber-Reinforced Plastic (FRP) was selected as the primary construction material based on its resilience and durability to the "scrubbing" process. Quality assurance of the primary process vessels was deemed to be an important aspect of the evaluation process and strain monitoring was suggested as a logical means to accomplish this activity.

Structural integrity testing included strain gage monitoring, photoelastic monitoring, and acoustic emission testing during hydrostatic loadings in October 1991. This testing provided a mechanism of simulating some of the operating loadings due to be encountered during full-scale operation, expected in mid-1992.

The size and volume of the Chiyoda process in this application at Plant Yates required the primary vessel constructor and designer, Ershigs, Inc. to design and construct one of the largest FRP vessels using a filament winding construction technique. The Jet-Bubbling Reactor (JBR), the primary process vessel, was fabricated as a "wound" cylindrical vessel at the plant site. This process involved winding fiberglass filaments and "mating" on a cylindrical mandrel while turning at a slow speed. The filaments were applied circumferentially in a helical pattern as the mandrel was turning, and thus produced a smooth cylindrical vessel.

Quality assurance requirements, specified in the original contracts for the fiber-reinforced plastic FRP structures, mandated that strain monitoring and testing would be included over the time span of the construction, implementation and operational cycle of the Chiyoda process.

Project Photographs

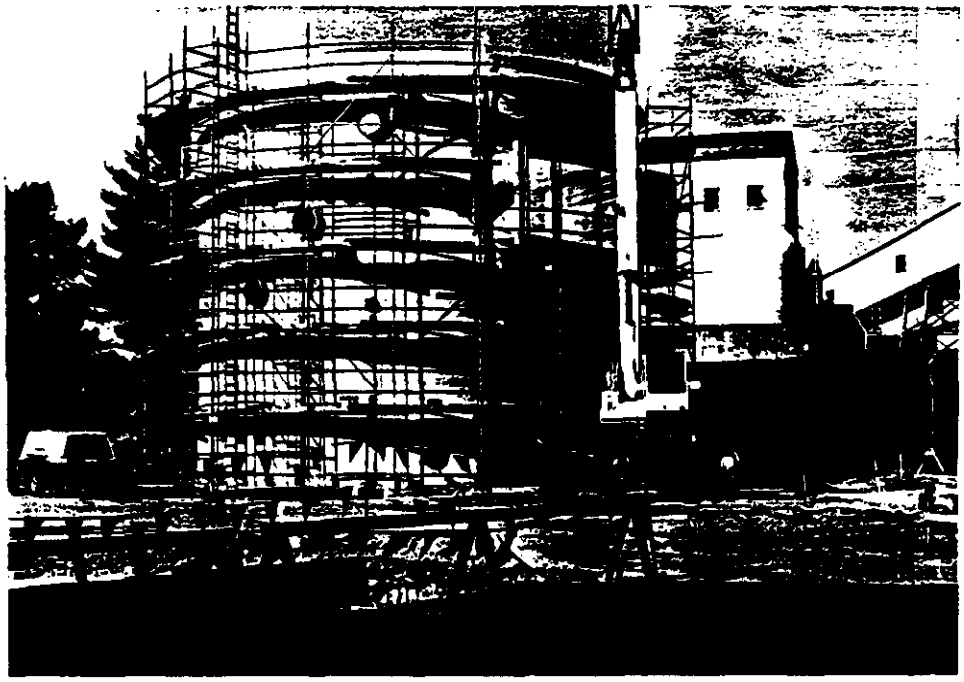

Photo 1 : Construction Photograph of Jet-Bubbling Reactor

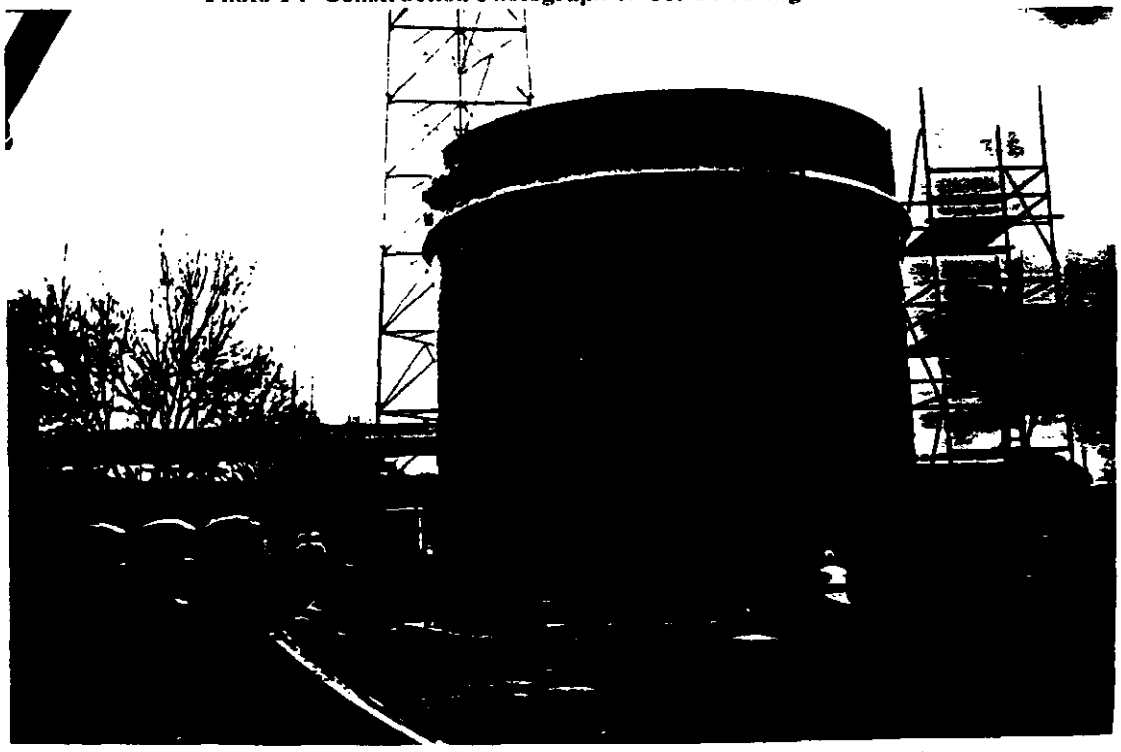

Photo 2 : Photograph of Limestone Slurry Vessel prior to Piping

Photo 3 : Representative Photograph of Strain Gage Installation

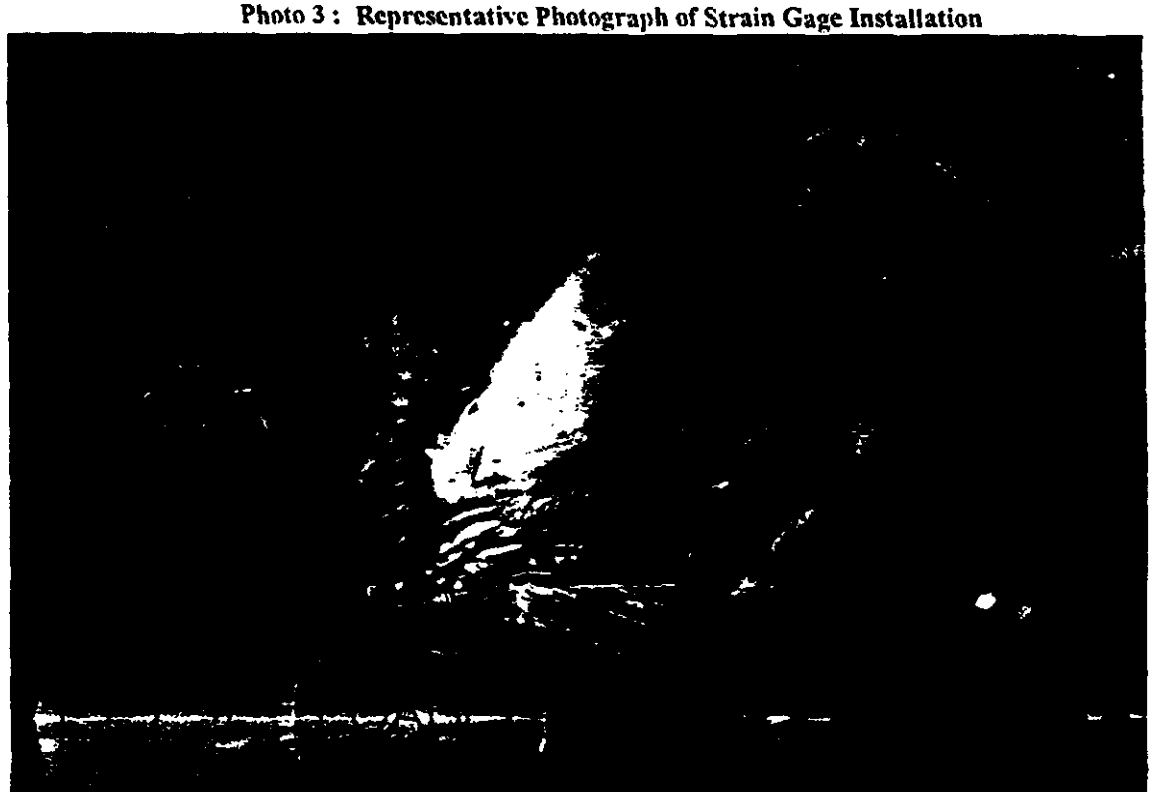

Photo 4 : Representative Photograph of Photoelastic Laminant

Purpose

TEST OBJECTIVES

The primary objectives in the strain monitoring of the FRP structures was to address the following aspects of the design, construction, and operation of the fiber-reinforced vessels:

- Determine flaws, if any, in the construction of the FRP vessels
- Measure strains induced by hydrostatic loading of the JBR and Limestone Slurry Tank using the photolaminant plates and strain gages, and to compare these values to design calculations prepared by the vessel constructor, Ershigs, Inc.
- Identify areas of structural concern within the FRP vessels, which can be associated with any design or construction anomolie.

HYDRO TESTING

To provide for structural acceptance, a hydrostatic test was determined to produce a realistic operational loading for the Jet-Bubbling Reactor and Limestone Slurry Tank. This technique provided several advantages including the structural integrity leak-tight testing as well as providing a mechanism to simulate operational strain levels in a manner similar to that of the fully-loaded vessel.

Both the JBR and the Limestone Slurry vessel were hydrotested to a safe level as documented in the original design calculations. The hydrotest procedure was established by Research and Environmental Affairs. The hydrotesting occurred the week of September 30, 1991, with the first JBR hydro occurring on October 1, 1991 and the second test .

The purpose of the hydrotest was again two fold:

- To evaluate the structural integrity through leak detection.
- to collect strain data and acoustic emission data of the vessels under design loadings.

Instrumentation

Strain Gages

Conventional strain-gaging was selected as one of the suitable techniques for strain monitoring of the process vessels during acceptance hydrodynamic testing and also for long-term trending of strain. The appropriate strain gages were selected for the FRP materials, accounting for the environmental effects of humidity, temperature and corrosion as well.

Figure 1

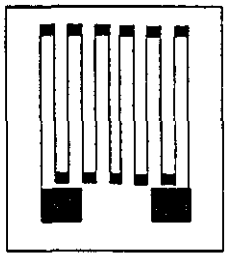

Schematic of Strain Gage

Photo Laminants

Photoelasticity, an optical method of quickly evaluating strain conditions was also selected as an additional technique for quantification of the strain state of the FRP structures. Photoelastic laminants generally provide a more continuous representation of the strain contour, which provides for examination of discontinuities, or imperfections, which may not normally be evident through the use of strain gages alone. Photoelasticity provides an optical strain contour through which strains can be visually identified, particularly at the points of maximum strain.

Strain Gage Testing

Strain gages, of the "bonded resistance " type were selected for the FRP material, expected strain rates, and life-cycle duty of the strain gage testing. The gages selected consisted of both uniaxial and strain rosettes. The unixial gages provide only a strain component in the single direction of placement. The strain rosette provides a three direction planar grid with uniaxial gages in the 45, 90, and 135 degree directions. The actual gages used were 120 ohm resistance gages produced by Micro Measurements, Inc. and of a type to thermally grow with the structure. This type of strain gage, self-temperature-compensating (STC) provides for a more stable signal and eliminates signal noise.

The strain condition measured for the hydro testing of the JBR and limestone slurry vessel, included only static strain measurements. The primary instrumentation for the collection and interpretation of the strain field data was composed of a single channel wide-range strain- indicator, and a 10 channel switch and balance unit. Both of these components were manufactured by Micro Measurements, Inc. of Raleigh, NC.

Gage selection and protective coatings were also based on the environmental effects of temperature, humidity, and corrosion resistance. Both rosettes and single gages were applied on the JBR and Limestone Slurry Tank. The strain rosette provides the full strain condition measurement at the point of attachment to the vessel. Figure 6 provides a close-up view of a strain gage rosette grid pattern and the associated relationship of the measured strain with that of the classic Mohr's Circle of Stress.

The gages selected for this project were purchased with lead wires preattached to the gage solder dots, to minimize the amount of heat typically present during the soldering of the lead wires to strain gage. A photograph of a typical strain gage installation is provided in Photo 3. The in-situ surface of the fiber-reinforced vessels was cleaned, sanded and desensitized to allow for proper adhesion of the strain gage. Surface prepartion is a vital step to insure the success of the strain gage testing.

Coatings/Wiring

Another important aspect of the gage installation included the coating of the gages after all soldering and wiring was complete. This coating is important to insure that the gages stay intact during the project life. The harsh environment of the Chiyoda scrubbber process is an unknown and many precautions were taken to insure long-term service of the strain gages and instrumentation. The strain gage wiring was terminated at a plastic junction box away from the gage site to allow for a terminal point to connect the junction wiring.

A trailer, during the hydrostatic testing, was temporary used at the plant site for sheltering of the strain gage equipment. This allowed the test materials, including the strain gage equipment, to be protected and environmentally controlled to preserve the testing control conditions of the strain gage hardware. All strain gage measurements were monitored and collected from this location adjacent to the FRP vessels.

Photolaminant Testing

Photoelasticity was used in harmony with the strain gage testing. The photolaminant plates were applied to the external surfaces of the JBR and Limestone Slurry Tank at locations deemed appropriate for quantification of strain state and contour. Figures 2 and 3 and Figures 4 and 5 provide the locations of the photolaminants on the Limestone Slurry and JBR vessels respectively.

The photolaminant plates during prepartion, were required to be contoured to conform to the uneven surface of the fiber-reinforced vessels. The photolaminants are composed of an epoxy-resin mixture which is mixed at the photolaminant test site and applied as a pliable sheet to the test surface. After 24 hours, the sheet becomes rigid and can be adhered to the vessel surface with a special reflective adhesive. This adhesive bonds the photolaminant to the vessel surface as well as provides a reflective background underneath the transparent photolaminant plate.

The photolaminant plates are viewed through a reflection polariscope, which is used to observe and measure the surface strains on the photoelastically coated part. The surface strains cause the photoelastic coating to deform. The strains in the photoclastic coating produce proportional optical effects which appear as isochromatic fringes when viewed with a reflection polariscope.

The reflection polariscope provides a quantitative method of determining the directions of the principal strains and ultimately stresses at all points on the photoclastic coating. The magnitude and sign of the difference between the principal maximum and minimum strain at any selected point on the coated surface is possible using this photoelastic method.

Test Setup

TEST CONSIDERATIONS

The FRP structures at Plant Yates are massive, complex structures, each with its own unique design and operational characteristics. The selection process of strain monitoring required several considerations, based on construction schedules, weather, review of design documents and limitations of test materials and resources.

To aid in the determination of the location of the strain gages and photoelastic plates, the original design calculations, including design details and finite-element models were reviewed. These tools helped to focus in on those areas of the process vessels that would produce the highest strain patterns as well as the most predictable. The selection was also based on those areas that would be the most important with respect to long-term durability of the finished vessel. The partial goal was to measure the strain on the vessel and structures in-situ, under hydrostatic and operational loading, and to correlate with design information, the actual strains and corresponding stresses in the loaded structures.

This information directly can provide insight into any degradation or change in the structures over time that may have occurred or is likely to occur. This determination provides an important aspect of the completed project, knowing with reasonable assurance the actual strain and stress loadings at selected locations within the structure.

Test Scope and Instrumentation

After initial review of the drawings and calculations provided by Ershigs Inc., it was decided that the structures to be included in the strain monitoring and testing would be the limestone slurry vessel and the jet-bubbling reactor. Based on the various construction schedules for each structure determinations were made on the the best period of testing and instrumentation.

Figure 2

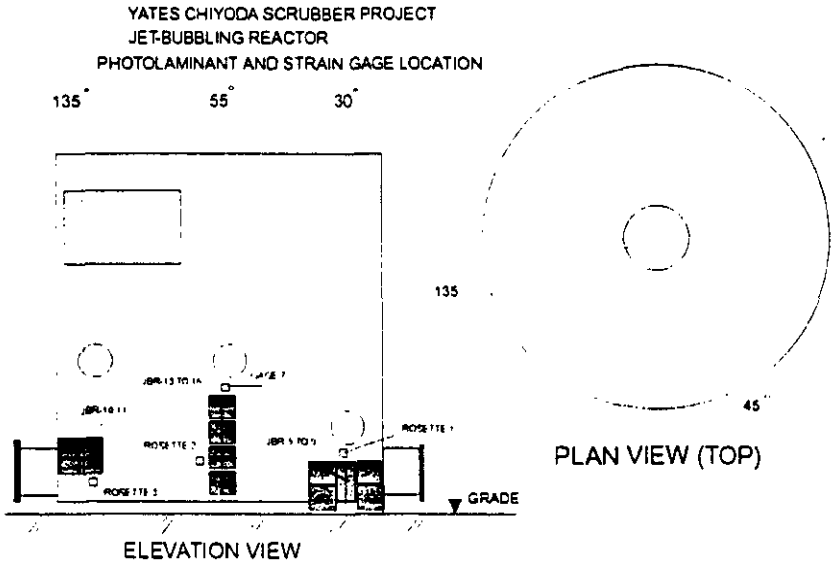

Figure 3

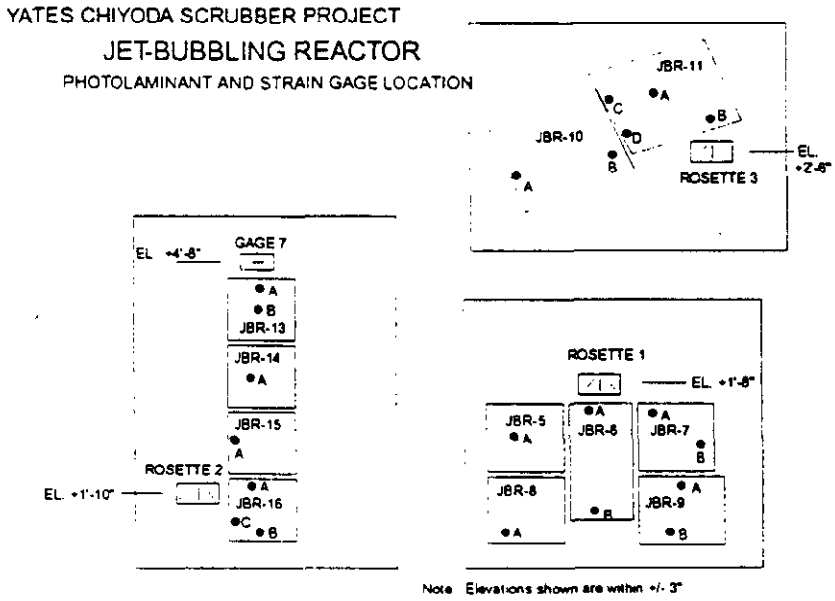

Figure 4

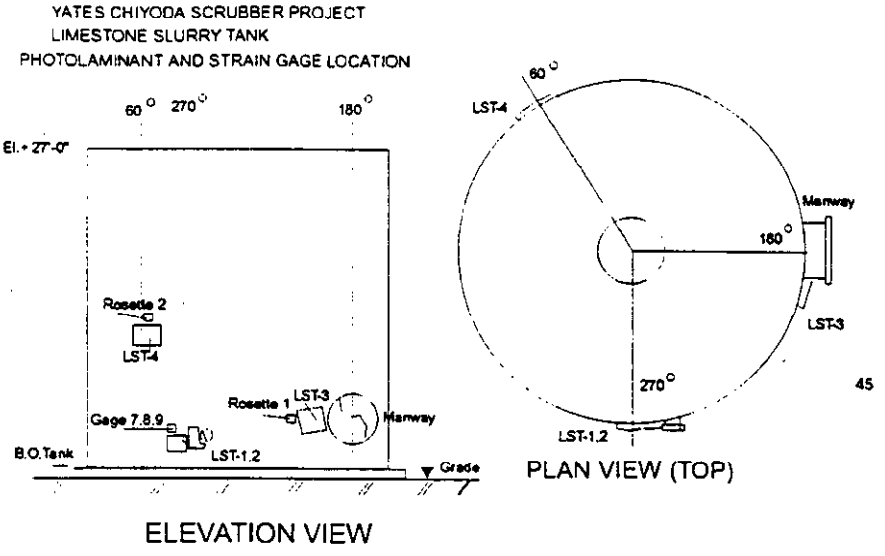

Manway

Figure 5

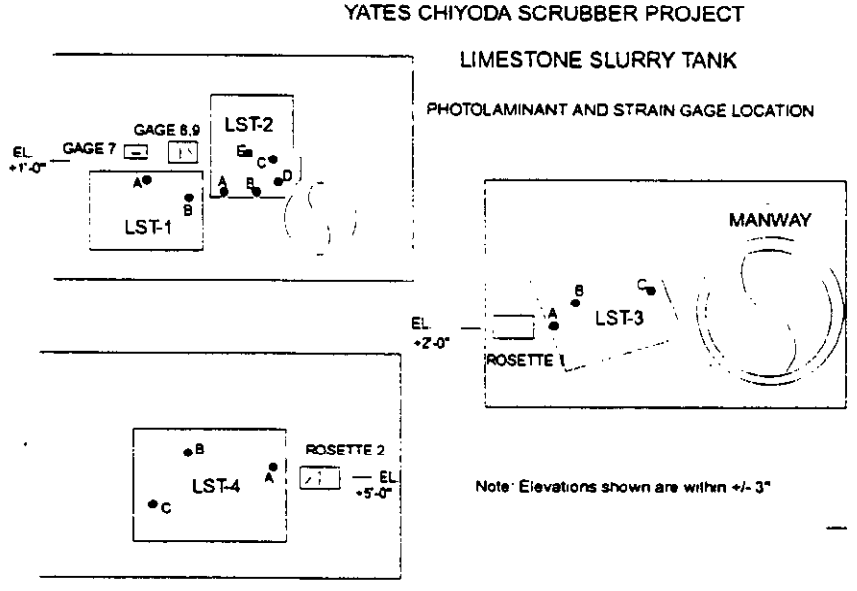

Description of Structures

Limestone Slurry Tank

The limestone slurry vessel is a secondary stucture which produces the limestone slurry liquid necessary in the "scrubbing" process. The limestone slurry tank was instrumented with both photolaminants and strain-gages as shown in Figures 4 and 5.

Jet-Bubbling Reactor (JBR)

The jet-bubbling reactor JBR as it is commonly known, required the largest portion of planning and study with respect to the strain-gage monitoring and photolaminant testing. The JBR is more than a fiber-reinforced pressure vessel which contains the process chemicals.

The JBR is indeed a complex reactor, made-up of a cylindrical tank, with numereous piping penetrations and a complex internal structure, providing support for associated process piping and equipment. The JBR includes a interstitial section, composed of small sparger tubes which transport and mix hot flue gases and process chemicals. Also, a large mixing vane is located symmetrically in the center of the JBR vessel, which promotes the mixing process.

The JBR was instrumented with both photolaminants and strain-gages, at locations on the external surface of the vessel. Figures 2 and 3 provide some details and locations associated with the strain monitoring.

Test Configurations

Water Levels

Several water levels were used throughout the sequence of the testing that occurred between 1991 and 1994. The water levels for the limestone slurry tank ranged from 24 ft. in 1991 to 24.5 ft. in 1994. The JBR levels ranged from 14 ft. in 1991 to 16.6 ft. in 1994.

Rate of Loading

The rate of water loading was generally dependent on the flow rates of the pumping equipment during the hydro testing. In general, the loading rate for the limestone and JBR was around 8 to 12 hours for the full respective heights of the two vessels.

Hold Periods

Generally, the vessels were filled and left overnight to hold. The strain measurements were collected during the filling process and held overnight. The strain measurements were taken just at a filled condition and after a hold period, prior to unloading.

Hydro Dates

The limestone slurry tank and JBR were first hydrostatically testing in September and October of 1991. The latest hydro tests were performed in November of 1994. The vessels have been in operation between these dates, with full operating conditions, containing slurries denser than water.

Strain Gage Results

The results of the strain gaging are provided in several spreadsheets, tables, and figures. The strain gage measurements are presented in several formats, including the raw strain measurements, the resulting principal strains and corresponding angles of principal strain and the corresponding hoop and longitudinal stresses at discrete measurement locations.

Strain Gage Sign Convention

Figure 6

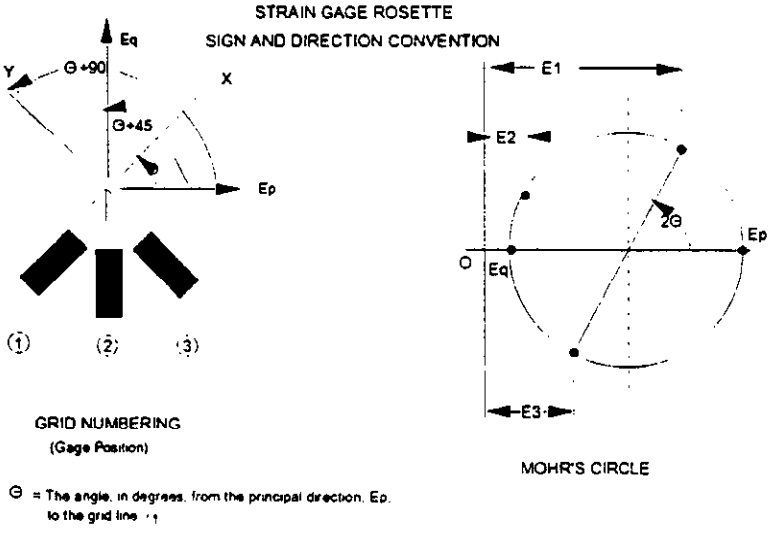

(+) angle indicates a counterclockwise direction on the grid numbering figure.

(-) angle indicates a clockwise direction on the grid numbering figure.

Principal Strains

The principal strains are obtained from the free-field strain measurements. The three element rosette provides the raw data to describe the principal strain magnitude and principal axis.

The principal strains were calculated using the following formulaes.

$$\varepsilon_{p,q} = \frac{\varepsilon_1 + \varepsilon_3}{2} \pm \frac{1}{\sqrt{2}} \sqrt{(\varepsilon_1 - \varepsilon_2)^2 + (\varepsilon_2 - \varepsilon_3)^2}$$

and

$$\phi_{p,q} = \frac{1}{2} \tan^{-1} \left(\frac{(\varepsilon_2 - \varepsilon_3) - (\varepsilon_1 - \varepsilon_2)}{\varepsilon_1 - \varepsilon_3} \right)$$

$\phi_{p,q}$ represents the reference angle from the strain gage grid line (gage 1) to one of the principal strain axis. The reference to this angle is arbitrarily determined from this equation, and depending on the magnitude of the component strains, the location of the maximum principal strain can be determined.

The principal strains values are listed in Tables 1 and 2. The sign convention for the listed principal strains are oriented according to Figure 6 and 7. Note that the angle computed in Tables 1 and 2 is the negative value of $\phi_{p,q}$ as derived above. The location of the major principal strain axis is oriented from the reference grid by this angle. A positive angle represents a counterclockwise movement from the reference grid and a negative angle represents a clockwise movement. This is represented in Figure 7.

Body Stresses

Figure 7

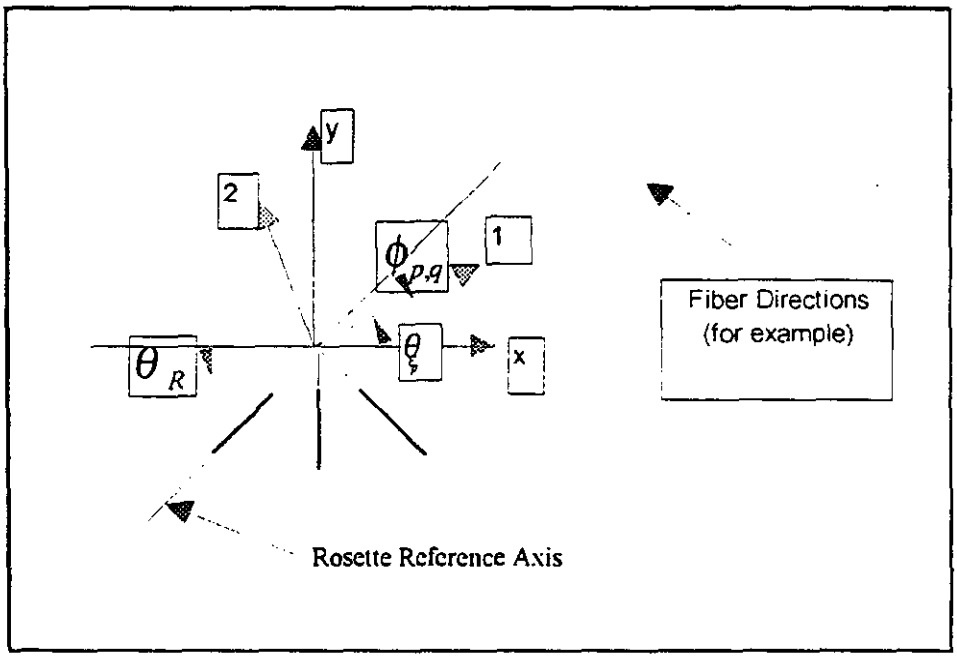

Equations for Body Stress Calculation

$$\varepsilon_x = m^2\varepsilon_p + n^2\varepsilon_q + mn\gamma_{pq}$$

and

$$\varepsilon_y = n^2\varepsilon_p + m^2\varepsilon_q - mn\gamma_{pq}$$

where

$$\gamma_{12} = -2mn\varepsilon_p + 2mn\varepsilon_q + \left(m^2 - n^2\right)\gamma_{pq}$$

where $m = \cos\theta_{\varepsilon_p}$; $n = \sin\theta_{\varepsilon_p}$

and

$$\sigma_x = \frac{E_x\varepsilon_x}{\left(1 - \upsilon_{xy}\upsilon_{yx}\right)} + \frac{\upsilon_{yx}E_x\varepsilon_y}{\left(1 - \upsilon_{xy}\upsilon_{yx}\right)}$$

and

$$\sigma_y = \frac{\upsilon_{xy}E_y\varepsilon_x}{\left(1 - \upsilon_{xy}\upsilon_{yx}\right)} + \frac{E_y\varepsilon_y}{\left(1 - \upsilon_{xy}\upsilon_{yx}\right)}$$

and

$$\tau_{xy} = G_{xy}\gamma_{xy}$$

x direction represents the material axis and y represents the orthogonal material axis for an orthotropic composite material. Directions 1 and 2 are the principal strain axes, determined from the strain test data.

Test Results

General

Test data was collected throughout the various hydro tests and is provided in Tables 1 thru 6 and Figures 9 thru 38. This data has been summarized in various ways, but in general the following procedure is provided for analysis of the data.

Figure 8

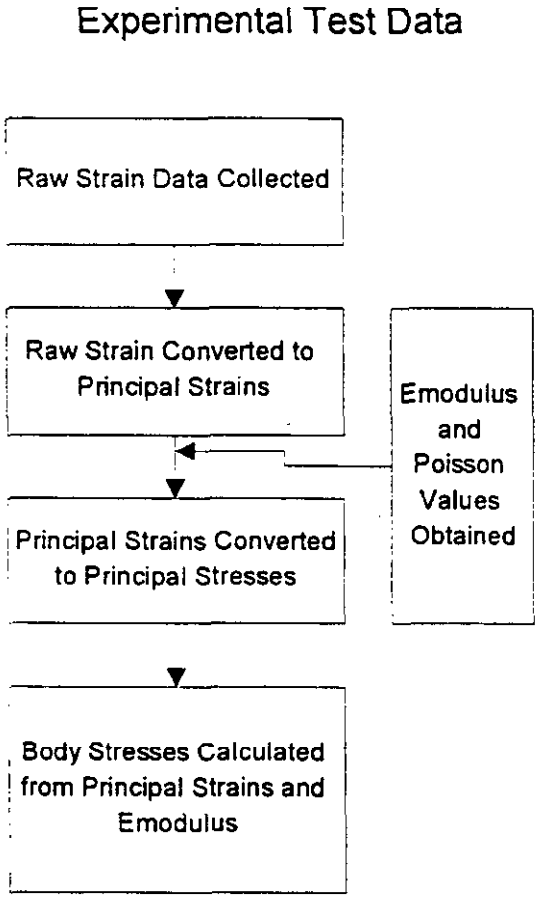

Also, the raw test data is provided in Appendix I.

Listing of Principal Strains for Jet-Bubbling Reactor

Table 1

JBR Hydro 1

		PRINCIPAL STRAINS									
		ROSETTE 1			ROSETTE 2			GAGE 7	ROSETTE 3		
		1	2	3	4	5	6	7	8	9	10
0.0	0.0	0.0	0.0	NA	0.0	0.0	NA	0.0	0.0	0.0	NA
45.0	3.8	261.6	58.4	-50.1	210.6	38.4	-48.5	-60.0	120.1	102.9	-50.0
90.0	7.5	349.2	138.8	-61.1	259.0	70.0	-44.5	80.0	225.2	158.8	55.6
95.0	7.9	421.6	173.4	-57.5	245.4	119.6	-41.6	101.0	239.3	160.7	52.4
95.0	7.9	409.9	135.1	-62.2	249.3	91.7	-36.7	91.0	182.2	103.8	35.3
95.0	7.9	387.2	156.8	-60.4	234.9	107.1	-36.3	77.0	176.4	120.6	26.9
95.0	7.9	421.1	180.9	-60.0	248.9	137.1	-32.9	111.0	150.0	86.0	19.3
135.0	11.3	566.5	285.5	-59.5	267.9	214.1	-22.5	207.0	287.4	176.6	36.6
135.0	11.3	593.1	314.9	-57.5	281.6	237.4	-14.2	234.0	326.0	224.0	45.0
168.0	14.0	702.2	400.6	-56.6	328.4	278.6	15.1	316.0	419.8	290.2	49.4
168.0	14.0	787.0	435.0	-53.1	376.7	305.3	39.3	393.0	524.4	354.6	47.9

JBR Hydro 2

		PRINCIPAL STRAINS									
		ROSETTE 1			ROSETTE 2			GAGE 7	ROSETTE 3		
		1	2	3	4	5	6	7	8	9	10
0.0	0.0	NA	NA	NA	NA	NA	NA	NA	NA	NA	NA
48.0	4.0	271.2	54.8	-49.3	166.1	-10.1	-43.7	-24.0	85.4	69.6	-80.8
84.0	7.0	295.6	68.4	-57.5	135.3	-30.3	-38.2	-30.0	87.4	44.6	39.6
84.0	7.0	191.4	-32.4	-65.9	114.2	-70.2	-37.5	-79.0	32.7	-18.7	6.7
90.0	7.5	317.6	74.4	-60.6	146.0	22.0	-34.6	14.0	66.0	27.0	-45.7
125.0	10.4	391.5	134.5	-59.7	151.0	57.0	-31.7	62.0	154.0	81.0	27.0
158.0	13.2	553.3	350.7	-56.3	335.9	272.1	-24.4	280.0	347.5	165.5	32.5
168.0	14.0	707.1	394.9	-57.7	342.6	296.4	-10.8	301.0	378.7	225.3	39.0
168.0	14.0	734.9	400.1	-55.1	339.5	301.5	6.8	321.0	425.9	311.1	52.3
168.0	14.0	786.8	423.2	-55.8	327.2	299.8	27.9	332.0	507.0	320.0	44.5

JBR Hydro 3

		PRINCIPAL STRAINS									
		ROSETTE 1			ROSETTE 2			GAGE 7	ROSETTE 3		
		1	2	3	4	5	6	7	8	9	10
0.0	0.0	0.0	0.0		0.0	0.0		0.0	0.0	0.0	
77.0	6.4	214.6	68.4	-62.8	92.2	8.8	-67.5	81.0	124.1	-27.1	-8.3
95.0	7.9	260.3	105.7	-65.1	140.3	39.7	-40.5	140.0	97.4	-160.4	64.0
110.8	9.2	297.0	123.0	-66.8	178.3	63.7	-48.4	178.0	129.2	-77.2	64.2
119.8	10.0	323.6	135.4	-66.2	222.2	109.8	-47.6	222.0	192.5	-23.5	62.0
153.5	12.8	420.0	182.0	-72.3	308.0	151.0	-45.2	308.0	317.1	-51.1	69.0
154.6	12.9	424.2	182.8	-71.5	308.1	142.9	-43.4	308.0	310.4	-40.4	68.2
179.4	14.9	494.7	227.3	-70.5	364.4	164.6	-42.5	384.0	392.4	-62.4	73.3
201.9	16.8	569.2	262.8	-71.1	444.0	180.0	-44.6	444.0	452.6	-57.6	71.6
201.9	16.8	567.7	270.3	-72.6	456.6	179.4	-42.3	456.0	468.6	-63.6	71.9
196.3	16.4	560.8	296.2	-68.1	423.8	166.2	-52.0	420.0	475.2	-10.2	74.2
196.3	16.4	476.4	239.6	-82.2	380.3	151.7	-47.1	380.0	419.3	-49.3	75.0
182.8	15.2	472.2	214.8	-75.5	360.2	142.8	-46.7	360.0	345.6	-45.6	73.8
155.8	13.0	399.7	184.3	-74.3	272.3	122.7	-52.2	270.0	285.3	-46.3	75.4
142.3	11.9	368.6	166.4	-73.4	245.8	113.2	-49.6	245.0	244.3	-46.3	72.8
90.5	7.5	256.3	93.7	-65.6	160.3	75.7	-36	125.0	75.4	-27.4	48.4

Plots of Raw Strain Data vs. Water Height

Figure 9 : Final Hydro Test

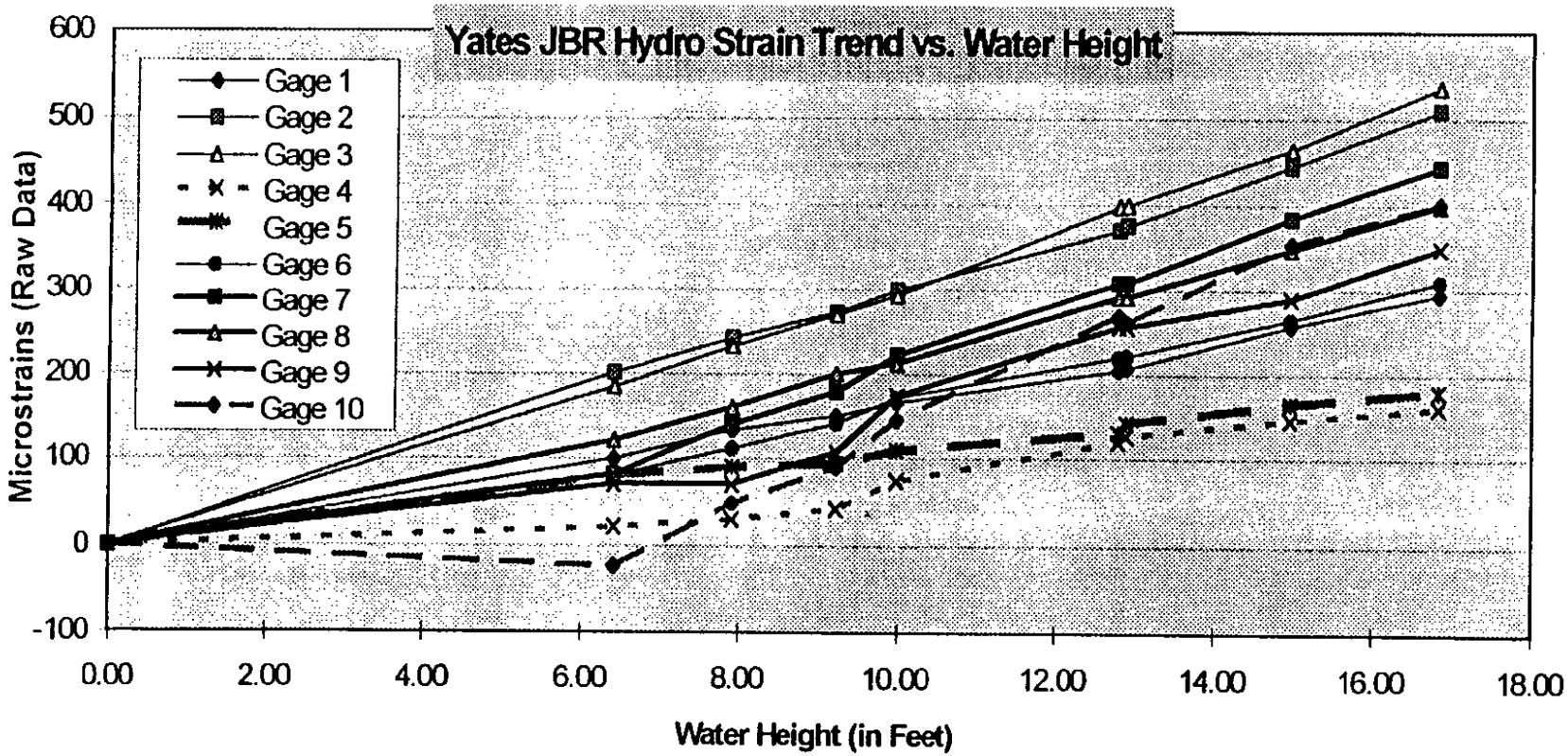

Figure 10 : Final Hydro Test

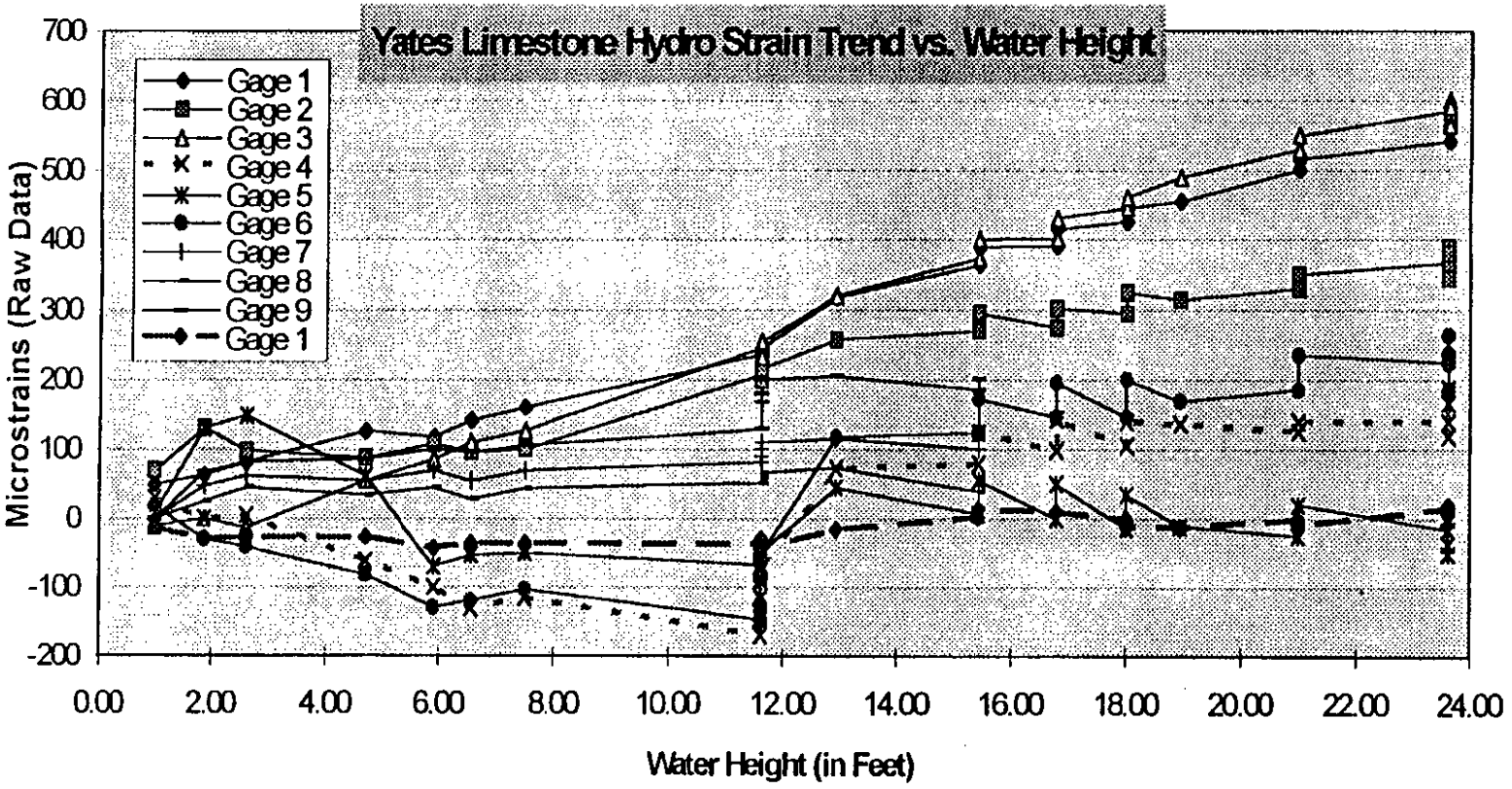

Plots of Principal Strains vs. Water Height (JBR)

Figure 11: Major Principal Strain

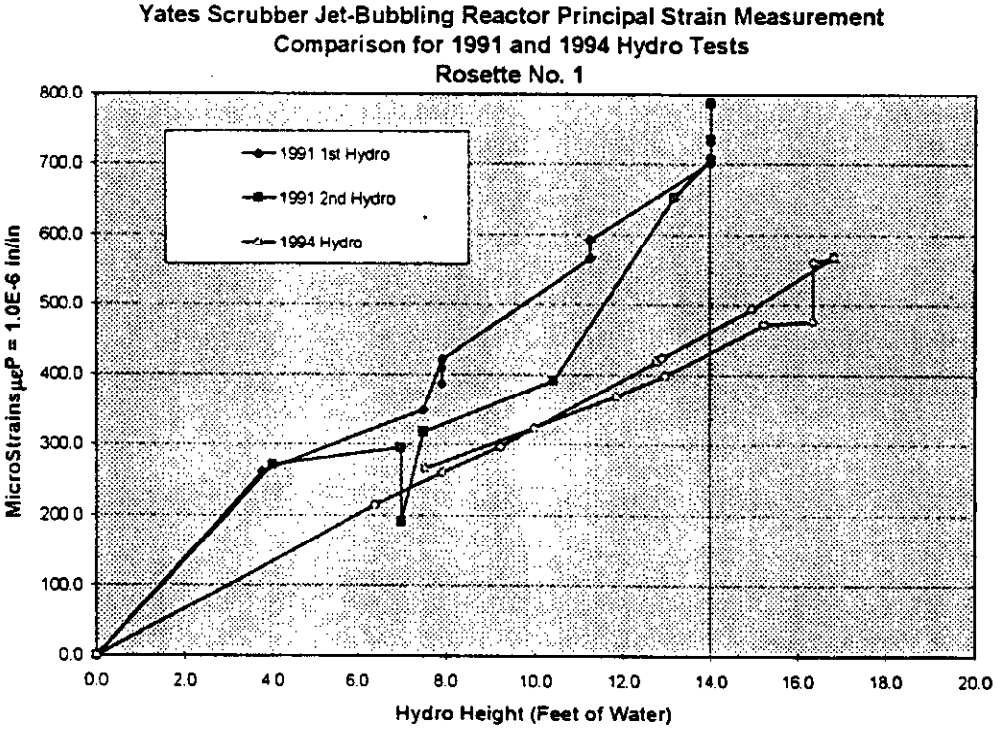

Figure 12 : Minor Principal Strain

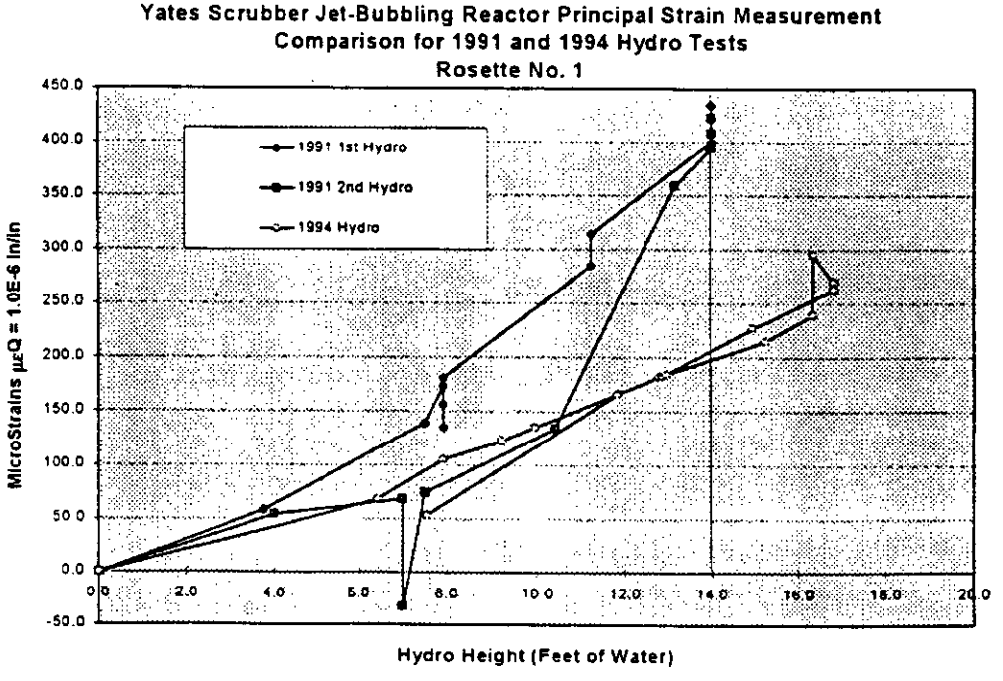

Figure 13 : Major Principal Strain

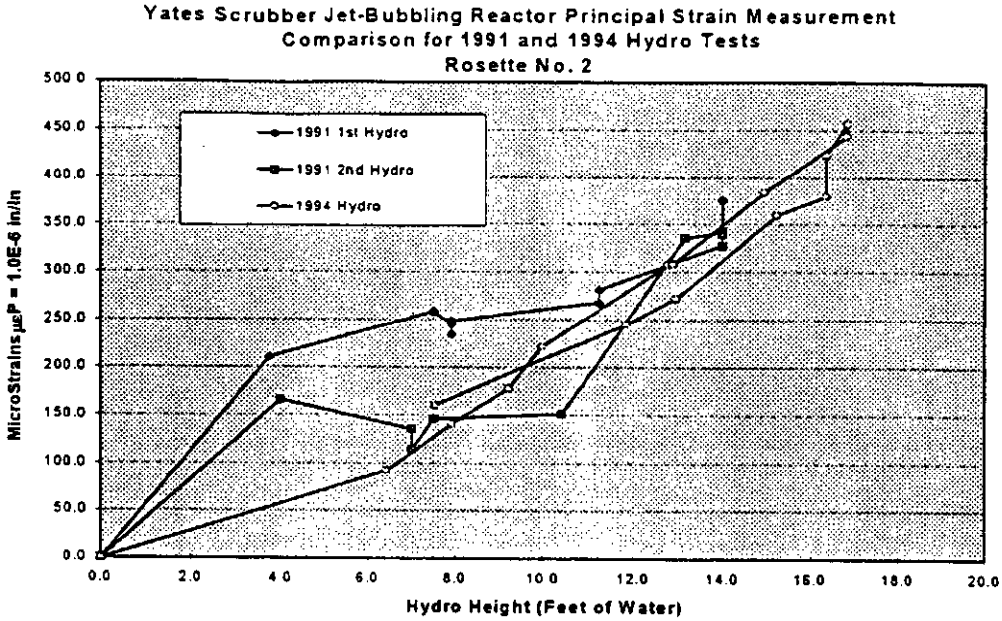

Figure 14 : Minor Principal Strain

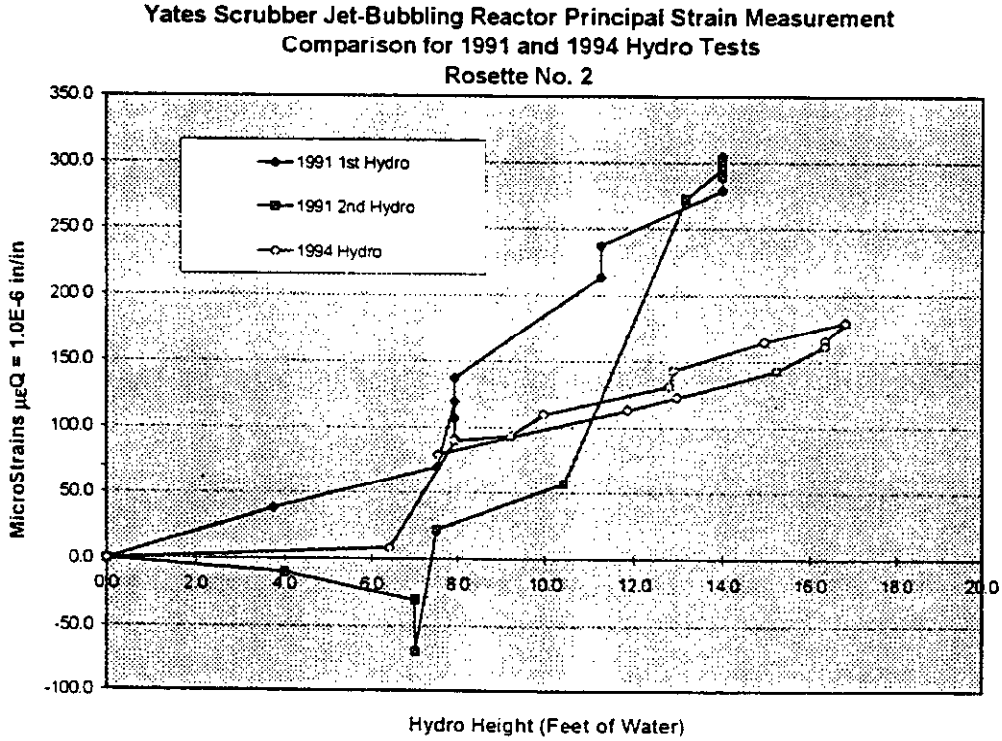

Figure 15 : Major Principal Strain

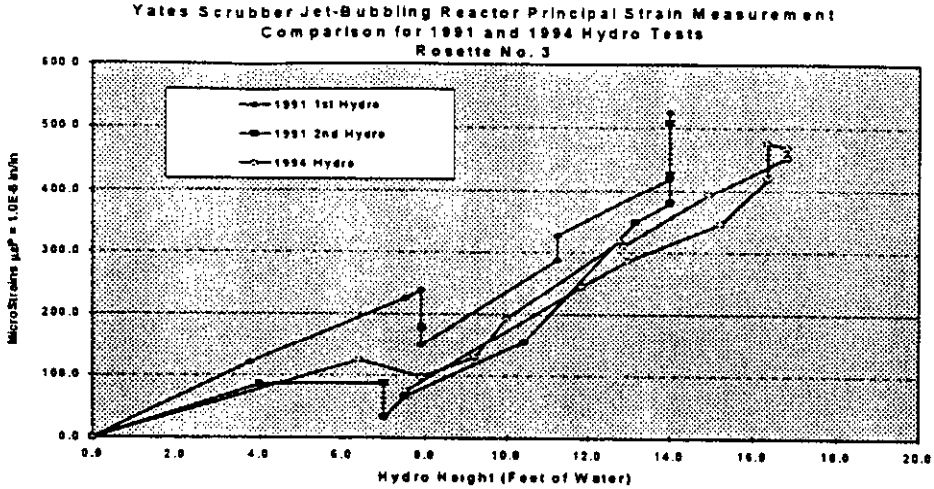

Figure 16 : Minor Principal Strain

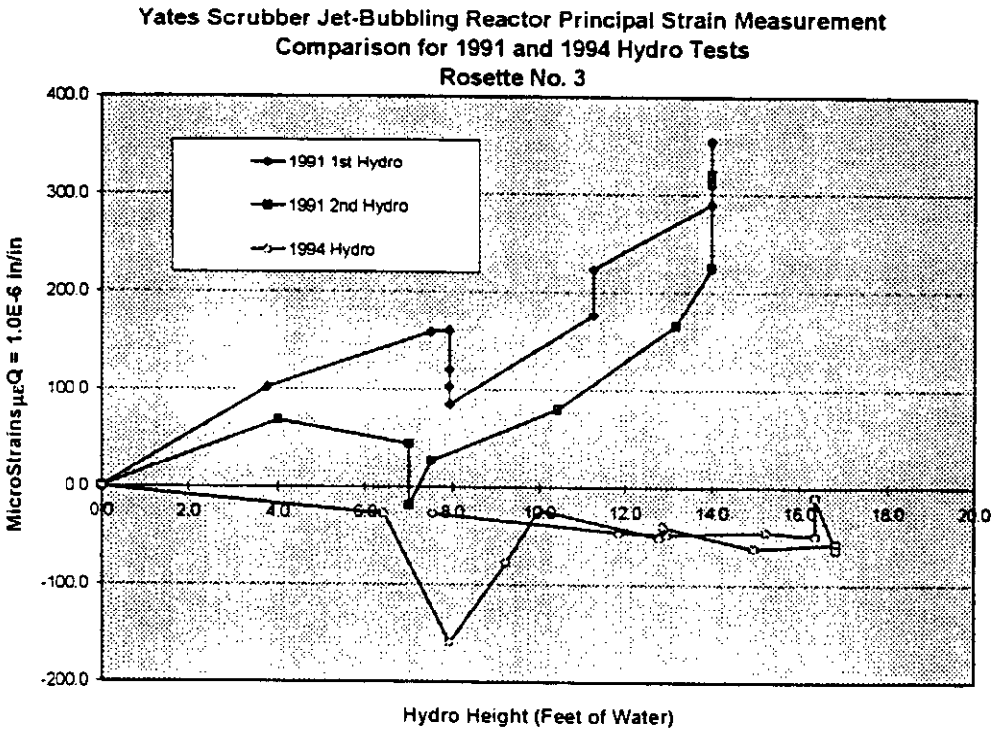

Figure 17

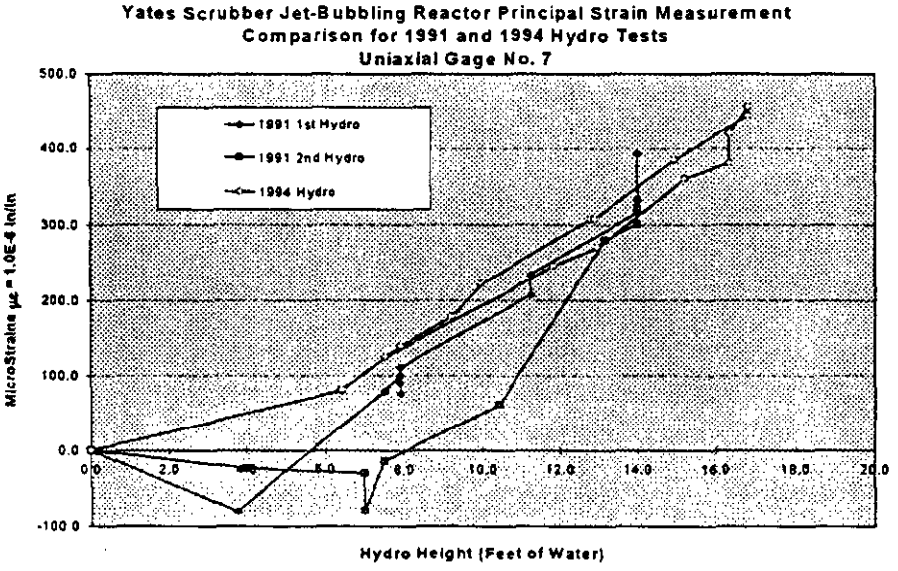
Yates Scrubber Jet-Bubbling Reactor Principal Strain Measurement
Comparison for 1991 and 1994 Hydro Tests
Uniaxial Gage No. 7
1991 1st Hydro
1991 2nd Hydro
1994 Hydro
MicroStrains με = 1.0E-6 in/in
500.0
400.0
300.0
200.0
100.0
0.0
-100.0
0.0
2.0
4.0
6.0
8.0
10.0
12.0
14.0
16.0
18.0
20.0
Hydro Height (Feet of Water)

Listing of Principal Strains for Limestone Slurry Vessel

Table 2 : 2nd and Final Hydro

LIMESTONE Hydro 2

		PRINCIPAL STRAINS								
		ROSETTE 1			ROSETTE 2			GAGE		
WATER HEIGHT (INCHES)	WATER HEIGHT (FEET)	1 με P	2 με Q	3 Θ	4 με P	5 με Q	6 Θ	7 με	8 με	9 με
0	0.0	NA	NA	NA	NA	NA	NA	-9	-8	-9
36	3.0	2.2	-38.2	-4.3	-5.9	-31.1	-48.4	9	-148	-88
60	5.0	72.3	-22.3	42.0	-25.6	-44.4	74.0	91	-126	-29
108	9.0	258.1	39.9	43.9	149.0	-210.0	44.4	215	-100	68
150	12.5	405.1	95.9	46.0	259.0	-215.0	44.5	323	-44	150
205	17.1	625.0	176.0	46.2	353.1	-253.1	44.2	452	-14	236
225	18.8	640.0	167.0	45.1	407.2	-307.2	44.0	480	0	263
290	24.2	832.0	250.0	45.1	526.1	-313.1	44.6	610	36	343
290	24.2	761.0	224.0	45.3	402.4	-356.4	43.7	512	-42	225
290	24.2	748.1	206.9	45.6	344.2	-357.2	44.0	547	-64	223
290	24.2	784.1	199.9	44.2	78.9	-375.9	47.6	565	-35	261

LIMESTONE Hydro 3

		PRINCIPAL STRAINS									
		ROSETTE 1			ROSETTE 2			GAGE 7	ROSETTE 3		
WATER HEIGHT (INCHES)	WATER HEIGHT (FEET)	1 με P	2 με Q	3 Θ	4 με P	5 με Q	6 Θ	7 με	8 με P	9 με Q	10 Θ
12.00	1.00	13.00	13.00	NA	0.00	0.00	0.00	0.00	0.00	0.00	0.00
22.50	1.88	88.00	-7.00	-44.70	73.54	-94.54	-41.75	88.00	44.60	-29.60	26.33
31.50	2.63	61.12	19.88	-19.55	89.92	-120.42	-40.28	149.00	3.06	-13.06	3.56
56.25	4.69	150.69	13.31	42.60	3.69	140.19	-42.91	321.50	117.86	-67.86	-32.75
70.88	5.91	170.30	76.70	54.02	-17.46	-115.54	30.03	373.00	161.40	-91.40	-29.79
78.75	6.56	223.38	58.62	50.25	-95.44	-129.56	-67.50	421.00	187.32	-112.32	-33.30
90.00	7.50	252.97	64.03	49.11	-85.73	109.27	93.87	456.00	206.59	-109.59	-31.76
139.50	11.63	351.08	165.92	56.27	-112.70	-180.30	-59.61	723.00	325.30	-170.30	-33.04
139.50	11.63	338.57	171.43	55.52	-95.86	-144.14	66.61	773.00	328.86	-183.86	-33.94
139.50	11.63	331.34	151.66	54.92	-88.64	-137.36	58.61	808.00	336.11	-181.11	-34.52
139.50	11.63	368.78	181.22	55.96	-7.46	-92.46	54.04	823.00	365.82	-198.82	-33.15
155.25	12.94	430.42	198.08	52.93	201.46	-28.46	52.05	15.00	18.52	-5.52	-22.50
185.06	15.42	500.16	192.84	51.68	234.40	-83.40	49.98	44.00	64.10	-26.10	-43.09
185.06	15.42	512.42	206.58	51.90	264.91	-46.91	50.55	47.00	67.01	-9.01	-44.25
201.38	16.78	540.84	195.16	51.01	271.30	-97.30	49.53	44.00	74.00	-27.00	-45.28
201.38	16.78	568.27	216.73	51.33	315.84	-47.84	50.07	39.00	89.21	-31.21	-42.62
216.00	18.00	610.26	220.74	51.00	403.62	-100.62	49.62	55.00	95.38	-54.38	-42.13
216.00	18.00	627.01	262.99	51.03	358.18	-41.18	50.12	82.00	121.17	-64.17	-36.37
227.25	18.94	678.47	251.53	51.50	367.07	-85.07	47.79	94.00	145.48	-80.48	-36.91
252.00	21.00	737.25	256.75	50.40	378.60	-111.60	49.18	91.00	170.53	-105.53	-40.73
252.00	21.00	758.89	283.11	50.82	407.05	-63.05	51.52	109.00	191.24	-118.24	-39.13
283.50	23.63	780.32	276.68	50.90	407.31	-120.31	50.19	95.00	185.45	-106.45	-42.74
283.50	23.63	794.76	296.24	50.61	511.97	-141.97	48.87	97.00	187.54	-100.54	-42.51
283.50	23.63	805.02	261.98	48.51	487.79	-116.79	49.14	93.00	177.10	-124.10	-43.95
283.50	23.63	786.26	283.74	50.30	425.25	-108.25	49.48	98.00	181.02	-110.02	-44.51

Plots of Principal Strains vs. Water Height (Limestone Slurry Vessel)

Figure 18 : Major Principal Strain

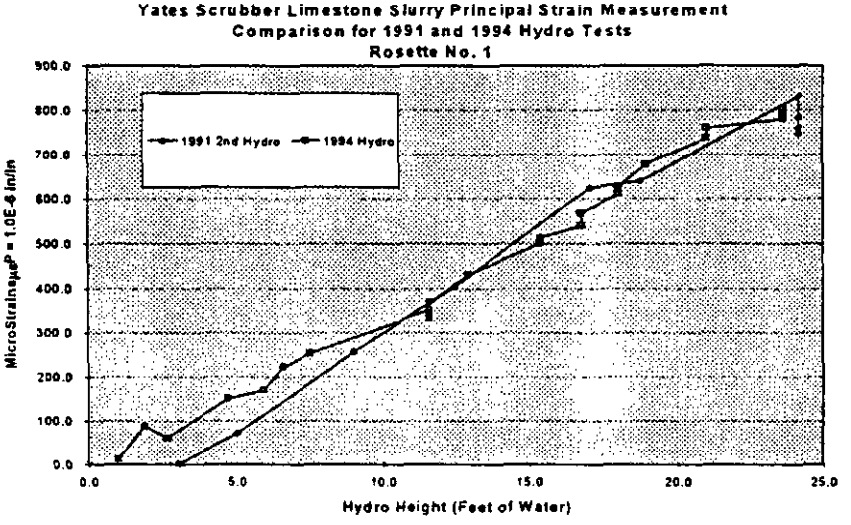

Figure 19 : Minor Principal Strain

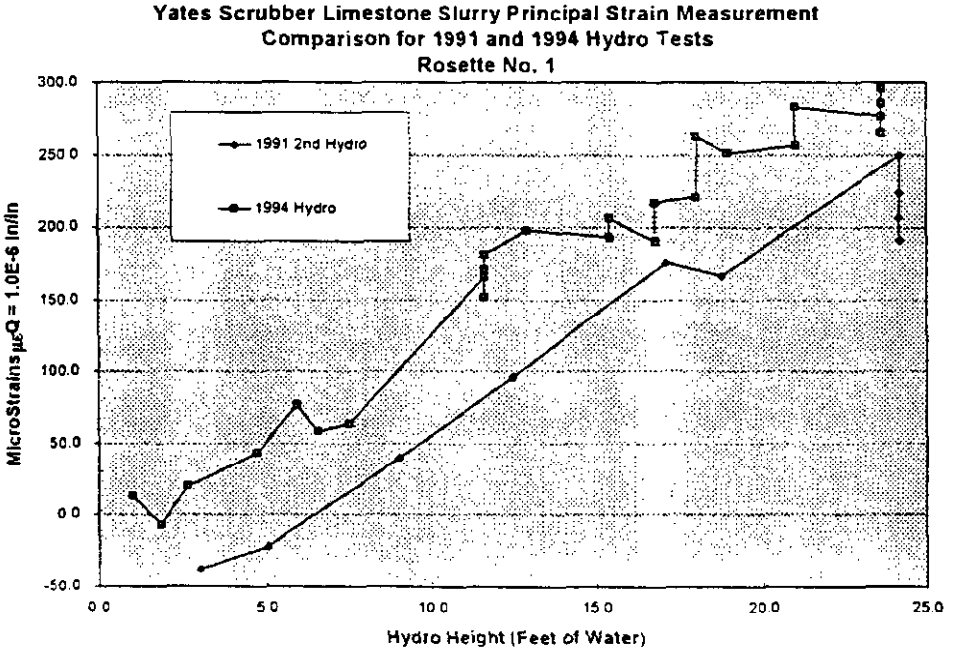

Figure 20 : Major Principal Strain

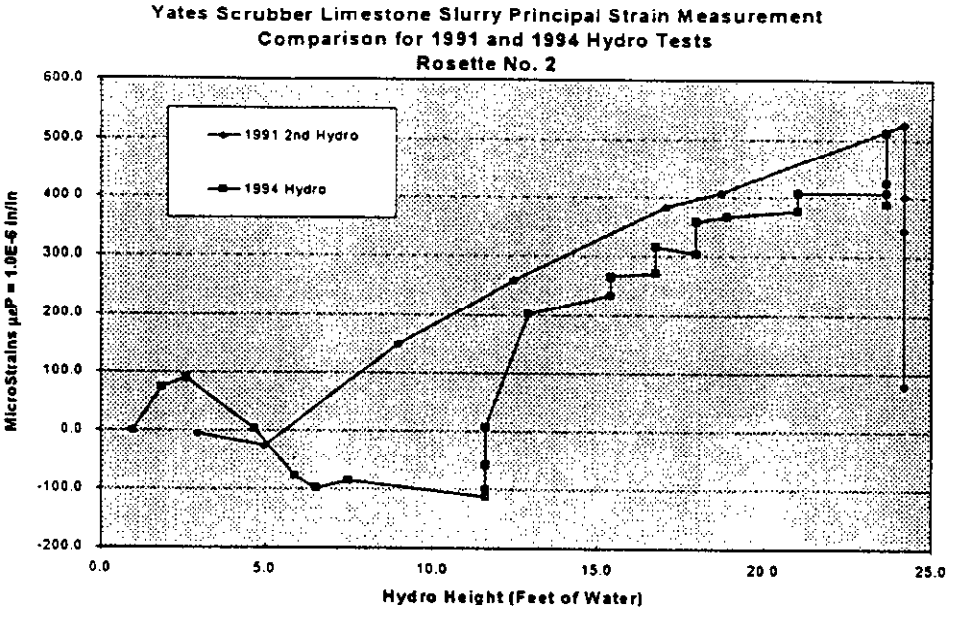

Figure 21 : Minor Principal Strain

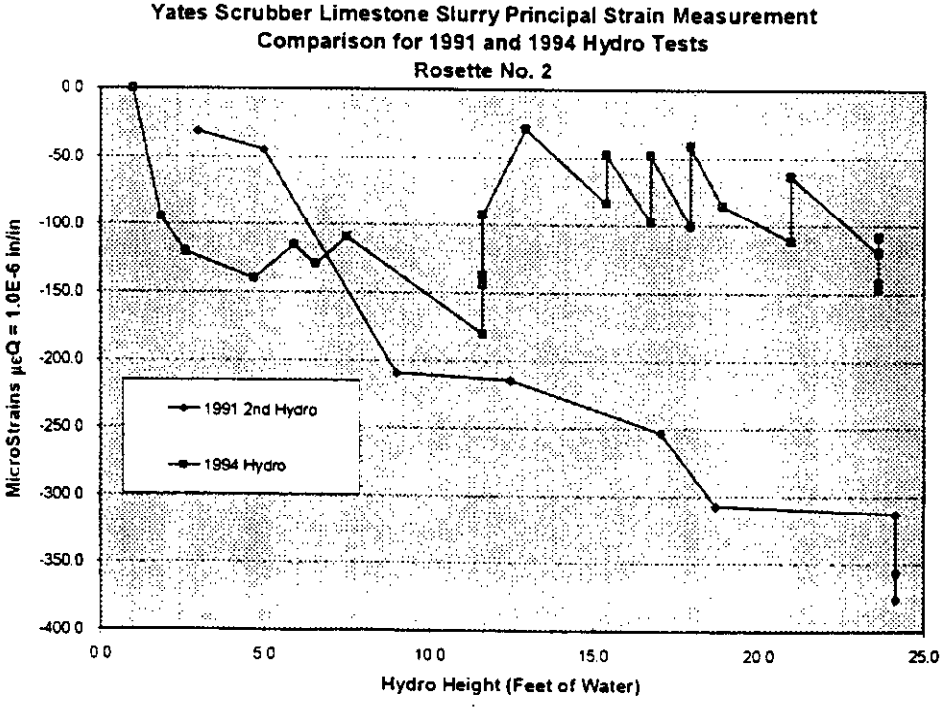

Figure 22 : Major Principal Strain

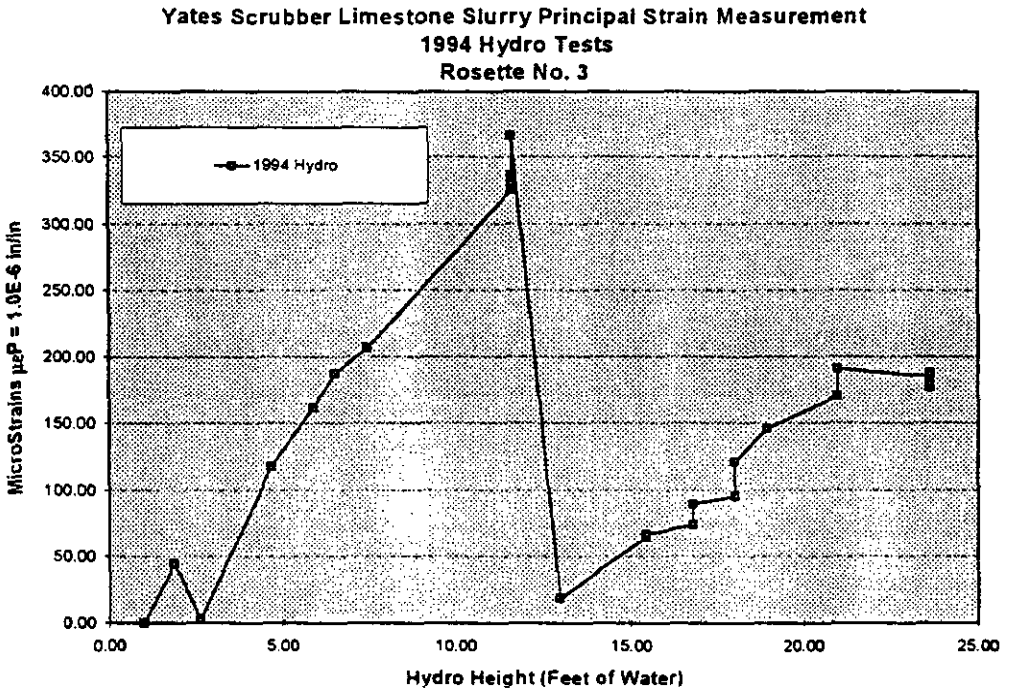

Figure 23 : Minor Principal Strain

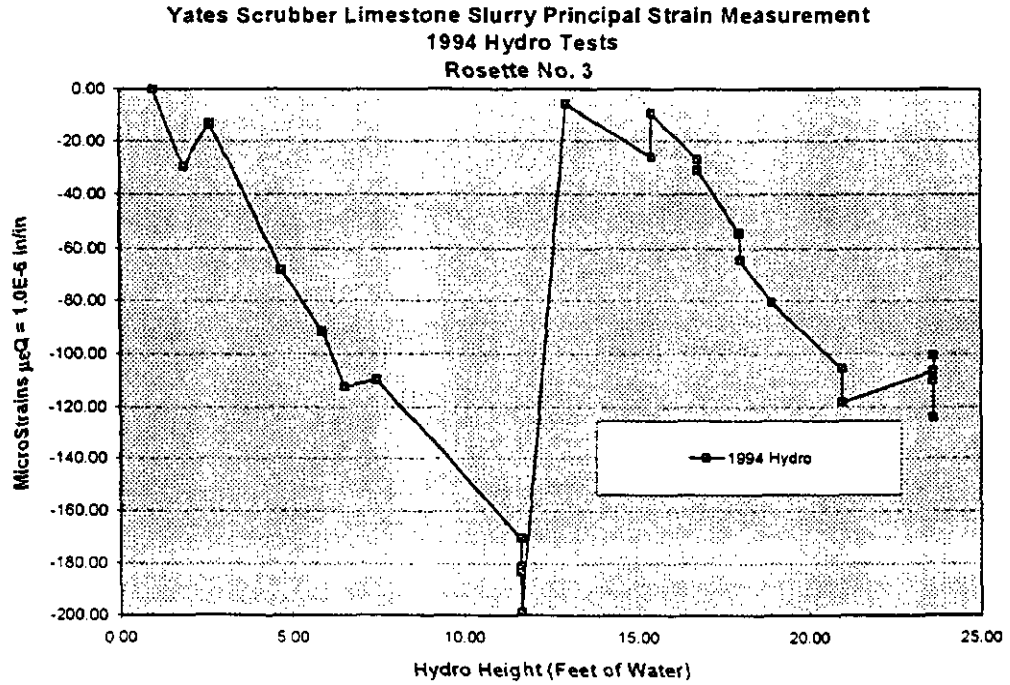

Calculated Actual Body Stresses vs. Water Height

The calculated body stresses oriented with the hoop (circumferential) perpendicular to the gravity axis can be calculated using the methodology provided in Figure 7. This methodology basically transforms the principal strains oriented along the principal axis into the body stresses that are normally oriented with respect to a geometric material axis. In this case, since the vessel is cylindrical and oriented vertically, the body stresses follow oriented in the hoop and longitudinal direction.

Table 3 : Jet-Bubbling Reactor

JBR Hydro 1																	
			Rosette 1		Body Stresses			Rosette 2			Body Stresses		GAGE 7	Rosette 3			Body Stresses	
Wtr Ht (inch)	Wtr Ht (ft)	με P	με Q	ϕ (degrees)	σx	σy	με P	με Q	ϕ (degrees)	σx	σy	με	με P	με Q	ϕ (degrees)	σx	σy
0 0	0 0	0 0	0.0	NA			0.0	0 0	NA			0.0	0.0	0.0	NA		
45 0	3 8	261 6	58.4	-50.1	791.4	88 6	210 6	38 4	-48.5	638 1	62.6	-80.0	120 1	102 9	-50.0	374 5	112 1
90 0	7 5	349 2	138 8	-61.1	1023 3	187 4	259 0	70 0	-44.5	789 7	98 0	60 0	225 2	158.8	55 6	692.3	179 5
95 0	7 9	421 8	173 4	-57 5	1259 2	225 2	245 4	119 8	-41 6	753 6	143 5	101.0	239 3	160.7	52 4	737 6	182 3
95 0	7 9	409 9	135 1	-62 2	1165 8	197 7	249 3	91 7	-36 7	755 5	120.0	91.0	182 2	103 8	35 3	555.8	122 3
95 0	7 9	387 2	156 8	-60 4	1140 1	209.0	234 9	107 1	-36 3	713 2	132 4	77 0	176 4	120.6	26.9	531 2	140 1
95 0	7 9	421 1	180 9	-60 0	1245 8	235 9	248 9	137 1	-32 9	753 3	164 2	111.0	150 0	66.0	18 3	428 2	109 6
135 0	11 3	566 5	285 5	-59.5	1692 8	353.7	267 9	214 1	-22 5	811 3	241 7	207 0	287.4	176.6	38 6	861 5	204.1
135 0	11 3	593 1	314 9	-57.5	1769 4	381 2	261 6	237 4	-14 2	844 8	268 4	234.0	326 0	224 0	45 0	1010 6	251 7
168 0	14 0	702 2	400 8	-56 6	2131.6	475.0	326.4	278 6	15 1	988 7	313 8	316.0	419 8	290 2	49.4	1299.3	326 4
168 0	14 0	787 0	435 0	-53.1	2406 5	513 5	378 7	305.3	39 3	1171 5	335.3	393.0	524 4	354 6	47.9	1623 8	399 6

JBR Hydro 2																	
		Rosette 1			Body Stresses		Rosette 2			Body Stresses		GAGE 7	Rosette 3			Body Stresses	
Wtr Ht (inch)	Wtr Ht (ft)	με P	με Q	ϕ (degrees)	σx	σy	με P	με Q	ϕ (degrees)	σx	σy	με	με P	με Q	ϕ (degrees)	σx	σy
0 0	0.0	NA	NA	NA			NA	NA	NA			NA	NA	NA	NA		
48 0	4 0	271 2	54 8	-49 3	821 1	86 1	166.1	-10 1	-43.7	499.4	10.9	-24.0	85.4	69 6	-80 8	250.5	80.7
84 0	7 0	295 6	68.4	-57.5	869 2	109 7	135 3	-30 3	-38 2	397.6	-10.1	-30.0	87.4	44.6	39 6	267.9	53 2
84 0	7 0	191 4	-32 4	-65.9	491 1	16 2	114 2	-70 2	-37 5	328.5	-49 7	-79 0	32.7	-18 7	6.7	39.3	2 5
90 0	7 5	317 6	74 4	-60.6	918 0	123 8	148.0	22 0	-34 6	431 4	42.0	-14 0	66.0	27.0	-45.7	202 4	33 6
125 0	10 4	391 5	134.5	-59.7	1149 4	188.7	151 0	57 0	-31 7	447.9	78 5	62 0	154.0	81.0	27.0	454.1	101 2
158 0	13 2	653 3	359 7	-56 3	1981 6	429 4	335 9	272 1	-24.4	1023.5	304.9	280.0	347.5	185.5	32 5	1043 7	206 1
168 0	14 0	707 1	394 9	-57.7	2137 2	472 4	342 8	298 4	-10 8	1027 3	334 2	301.0	378 7	225.3	39 0	1164 8	260.8
168 0	14 0	734 9	409 1	-55.1	2237 8	485.0	339 5	301 5	6 8	1018 9	338 5	321.0	425.9	311.1	52.3	1317.1	347 8
188.0	14 0	786 8	423 2	-55.8	2387 7	507.1	327 2	289 8	27 9	1013.1	316.7	332.0	507.0	320.0	44.5	1568 3	364 7

Last Hydro 1994																	
		Rosette 1			Body Stresses		Rosette 2			Body Stresses			Rosette 3			Body Stresses	
Wtr Ht (inch)	Wtr Ht (ft)	με P	με Q	ϕ (degrees)	σx	σy	με P	με Q	ϕ (degrees)	σx	σy	με	με P	με Q	ϕ (degrees)	σx	σy
0.0	0.0																
77.0	6 4	214 8	68.4	-62.8	616.2	102.2	92.2	8.8	-67.6	243.8	29.7	81.0	124.1	-27.1	-8 3	214.4	34.1
95.0	7.9	260 3	105.7	-65.1	745.0	146.9	140.3	89.7	-40.5	433.3	102.2	140.0	97.4	-160.4	64.0	194.6	-117.1
110.8	9 2	297.0	123.0	-66.6	841.3	172 4	178.3	93.7	-48 4	548.3	110.7	178.0	129.2	-77.2	64.2	315.9	-38.6
119 8	10 0	323 6	135 4	-66 2	921.3	187.9	222 2	109.8	-47 6	683.0	131.2	222.0	192 5	-23.5	62 0	524.1	16.6
153 5	12 8	420 0	182 0	-72.3	1144 3	264.7	308.0	131 0	-45 2	944.9	161.6	308.0	317.1	-51.1	89.0	773 2	40 9
154 6	12 9	424 2	182.8	-71 5	1162 3	264 5	306.1	142 9	-43 4	946.4	173 0	308 0	310.4	-40.4	88.2	773 7	44 7
179 4	14 9	494 7	227.3	-70 5	1376 0	316.4	364 4	164 6	-42.5	1176 3	203.1	364.0	392 4	-62 4	73.3	879 5	73.4
201 9	16 8	569 2	262.8	-71.1	1577 8	368 9	444 0	180 0	-44.6	1381.1	224 6	444.0	452 6	-57.6	71.6	1061 0	85 5
201 9	16 8	567 7	270.3	-72.6	1580 9	377.5	456 8	179 4	-42.3	1397.3	226.1	456.0	466.6	-63.6	71 9	1091.2	86 7
196 3	16 4	560 8	298.2	-66.1	1609 6	382.3	423.6	186.2	-52.0	1287.5	212.2	420.0	475.2	-10 2	74.2	1098 5	143.4
198 3	16 4	476 4	239.6	-82 2	1218 2	355 9	380.3	181 7	-47 1	1165 9	199.8	380.0	419.3	-49.3	75.0	919.1	101.4
182 8	15.2	472 2	214.8	-75 5	1258 9	315 4	380 2	142 8	-46.7	1103.2	179.5	380 0	345.6	-45.6	73 8	774 5	73 8
155 6	13 0	399 7	184 3	-74 3	1078 4	265 7	272 3	122 7	-52 2	829 6	151.3	270 0	285 3	-48.3	75 4	807 7	59 5
142 3	11 9	366 6	166 4	-73 4	1000.1	240 0	245 6	113 2	-49 8	752.8	137 6	245 0	244.3	-48.3	72 8	547 9	38 3
90 5	7.5	266 3	53.7	-65 6	733 6	105 1	160.3	79 7	-3 6	391 1	124.0	125 0	75.4	-27 4	48 4	222 9	-16.3

Table 4 : Limestone Slurry Tank

Limestone Slurry 2nd Hydro 1991					Body Stresses					Body Stresses						
WATER HEIGHT (INCHES)	WATER HEIGHT (Feet)	ROSETTE 1 Ep με	Eq με	φ degree	σx psi	σy psi	PRINCIPAL STRAINS ROSETTE 2 Ep με	Eq με	φ degree	σx psi	σy psi	Gage 7 ε1 με	Gage 8 ε2 με	Gage 9 ε3 με		σx psi	σy psi
0	0.0	NA	NA	NA			NA	NA	NA			-9	-8	-9			
36	3 0	2.2	-38 2	-4 3	-47.81	-21 69	-5 9	-31.1	-48.4	-21.90	-30 03	9	-148	-88			
60	5 0	72 3	-22 3	42 0	214.43	-11 94	-25 6	-44 4	74.0	-95.38	-41 48	91	-126	-29			
108	9 0	258 1	39 9	43 9	782 96	69.49	149 0	-210.0	44.4	423 54	-180 13	215	-100	68			
150	12 5	405 1	95 9	46 0	1233.14	140 46	259 0	-215 0	44 5	754 65	-171 34	323	-44	150			
205	17 1	625 0	176 0	45 2	1906 42	243 08	383 1	-253 1	44.2	1123.93	-192 02	452	-14	238			
225	18 8	640 0	187.0	45 1	1950.55	236.42	407 2	-307.2	44.0	1189.67	-240 09	480	0	263			
290	24 2	832.0	250 0	45.1	2539.76	338 43	526 1	-313.1	44.8	1547.80	-231.14	610	36	343			
290	24.2	761.0	224.0	45 3	2322.45	305.14	402 4	-356 4	43.7	1168.57	-287 01	512	-42	225			
290	24 2	748.1	208 9	45 6	2281.18	287.48	344 2	-357.2	44.0	993.54	-295 08	547	-54	223			
290	24.2	784 1	190 9	44 2	2387 8	276 8	78 9	-375 9	47.6	189.2	-344 6	585	-35	261			
Limestone Slurry Hydro 1994					Body Stresses					Body Stresses						Body Stresses	
HEIGHT (inches)	HEIGHT (feet)	Ep με	Eq με	φ degree	σx psi	σy psi	Ep με	Eq με	φ degree	σx psi	σy psi	0	Ep με	Eq με	φ degree	σx psi	σy psi
		ROSETTE 1					ROSETTE 2					ROSETTE 3					
12 00	1 00	13 00	13 00	0 00	40.8	13.9	0 00	0 00	0.00	0 0	0.0	0 00	0.00	0.00	0.00	0.0	0.0
22 50	1 88	88 00	-7 00	-44 70	264.5	4.2	73 54	-94.54	-41.75	208.8	-79.9	88 00	44.60	-29.60	26.33	108.9	-16.2
31 50	2 63	61.12	19 68	-19 55	164.7	32 8	89 92	-120 42	-40.28	252.3	-101 6	149.00	3 08	-13.06	3.56	-12.8	-6.2
56 25	4 69	150 69	43 31	42.60	459.2	59 8	3.69	-140 19	-42 91	-6.6	-131 9	321.50	117.86	-67.86	-32 75	322.9	-42.8
70 88	5 91	170.30	78 70	54 02	616 3	95.3	-77.46	-115.54	30.03	-255.1	-116 6	373.00	161.40	-91.40	-29.79	425.2	-52.2
78 75	6 56	223 38	58 62	50 25	676 9	84.0	-98 44	-129 56	-67 50	-326.0	-130 6	421.00	187.32	-112.32	-33 30	515.5	-73 0
90 00	7 50	252 97	64 03	49 11	787 9	92 4	-85 73	-109 27	83 87	-290 8	-106 2	455 00	206.59	-109.59	-31.78	561.6	-84 5
139 50	11 63	351 08	165 92	58 27	1058 8	205 7	-112 70	-180 30	-59 61	-374 5	-180 7	723 00	325 30	-170 30	-33 04	898.5	-103.4
139 50	11 63	338 57	171 43	55 52	1028 0	208 2	-98 86	-144 14	88 81	-333 6	-143 3	773 00	328 86	-183 86	-33 94	914 6	-117 6
139 50	11 63	331 34	151 86	54 92	1002 4	188 4	-58 64	-137 36	58.81	-206 3	-133 4	808 00	336.11	-181.11	-34 52	941.9	-115 6
139 50	11 63	368 78	181 22	55 98	1114.8	222 1	7.48	-92 46	54 04	4 0	-84 4	823.00	385.62	-198.62	-33 15	1009.9	-123.3
155 25	12 94	430 42	198 08	52 93	1309 6	243 7	201 46	-28 46	52.05	594.0	0 7	15 00	16.52	-5.52	-22 50	45.0	0.0
185 06	15 42	500 18	192 84	51 68	1520.0	247 1	234 40	-85 40	49 98	669 7	-48 0	44.00	84.10	-26.10	-43.09	189.8	-16.7
185.06	15.42	512 42	206 58	51.90	1557.9	261 8	264 91	-46 91	50.55	784.7	-9 4	47 00	87.01	-9.01	-44.25	200.9	-0.3
201 38	16 78	540 84	190 16	51.01	1643 3	249 3	271.30	-97 30	49.53	799.5	-56.7	44 00	74.00	-27.00	-45.28	219.8	-16.4
201 38	16.78	566 27	216 73	51 33	1728.0	278.1	315 84	-47.84	50 07	938.4	-4 1	59.00	89.21	-31.21	-42.62	264.8	-18.4
216 00	18 00	610 28	220 74	51.00	1855.1	287 0	303.62	-100.62	48.62	898.6	-56.4	55.00	95.38	-54.38	-42.13	279.9	-39.4
216 00	18 00	627 01	262 99	51.03	1911.6	328.6	358 18	-41.18	50.12	1065.9	7.7	82.00	121.17	-84.17	-36.37	345 5	-42.3
227 25	18.94	678 47	251 53	51 50	2061.1	325 5	367 07	-85.07	47.79	1093.4	-34.4	94 00	145.48	-80.48	-36.91	415.9	-54 5
252 00	21.00	737 25	256.75	50 40	2242.6	336 7	376.60	-111.60	49.18	1114.5	-57 1	91.00	170.53	-105.53	-40 73	496 9	-77.5
252 00	21.00	758 89	283.11	50.82	2309.2	364.6	407.05	-83.05	51 52	1202.3	-4.6	109.00	191.24	-118.24	-39 13	552.8	-85.6
283 50	23.63	780.32	276.68	50 90	2371 6	361.7	407 31	-120.31	50.19	1201.1	-80.1	95.00	185.45	-106.45	-42.74	544.9	-77.4
283 50	23 63	794 78	298.24	50.81	2419.4	381.5	511 97	-141.97	48.87	1517.0	-88.8	97.00	187.54	-100.54	-42.51	551.6	-71.5
283.50	23.63	805.02	264.98	48.51	2454.4	350 9	387.79	-146.79	49.14	1143.3	-86.8	93.00	177.10	-124.10	-43.95	516.5	-95.4
283 50	23.63	786.26	285.74	50.30	2393.9	370 1	425.25	-108.25	49.48	1259.7	-47.4	98.00	181.02	-110.02	-44.51	532.3	-81.7

Body Stress Summary Figures

Figure 24

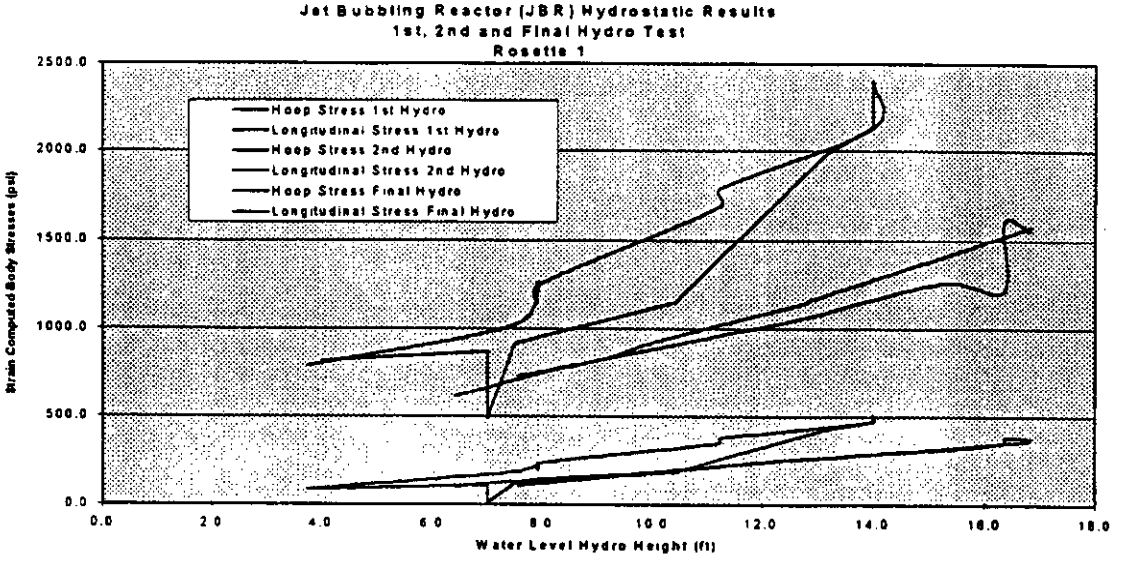

Figure 25

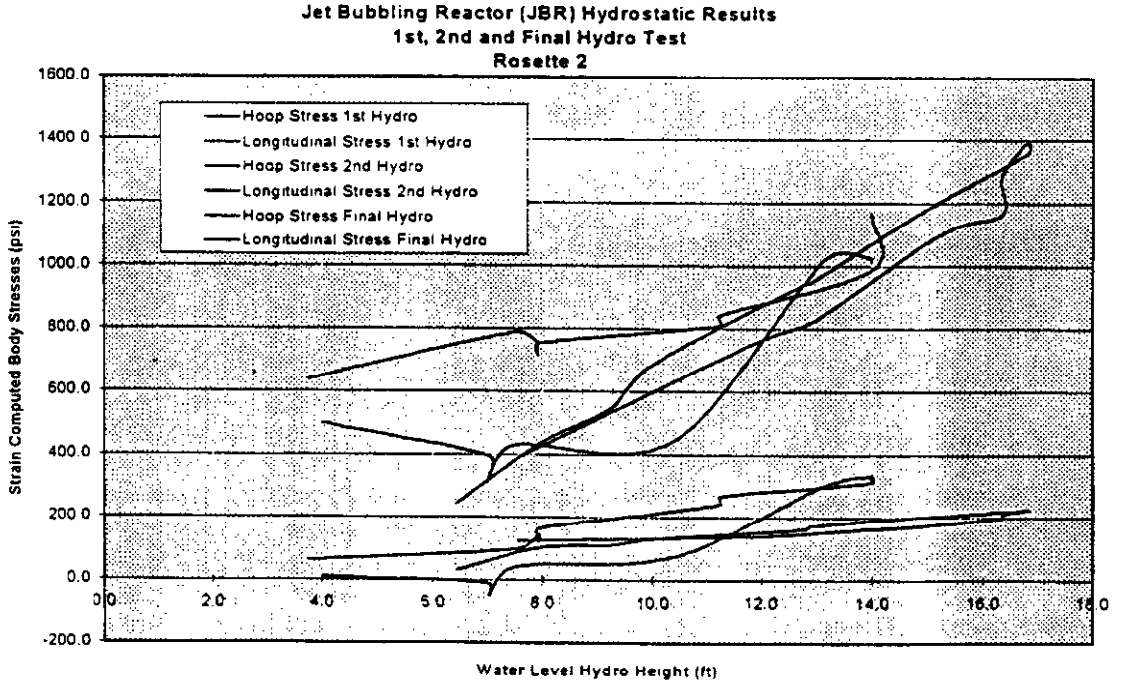

Figure 26

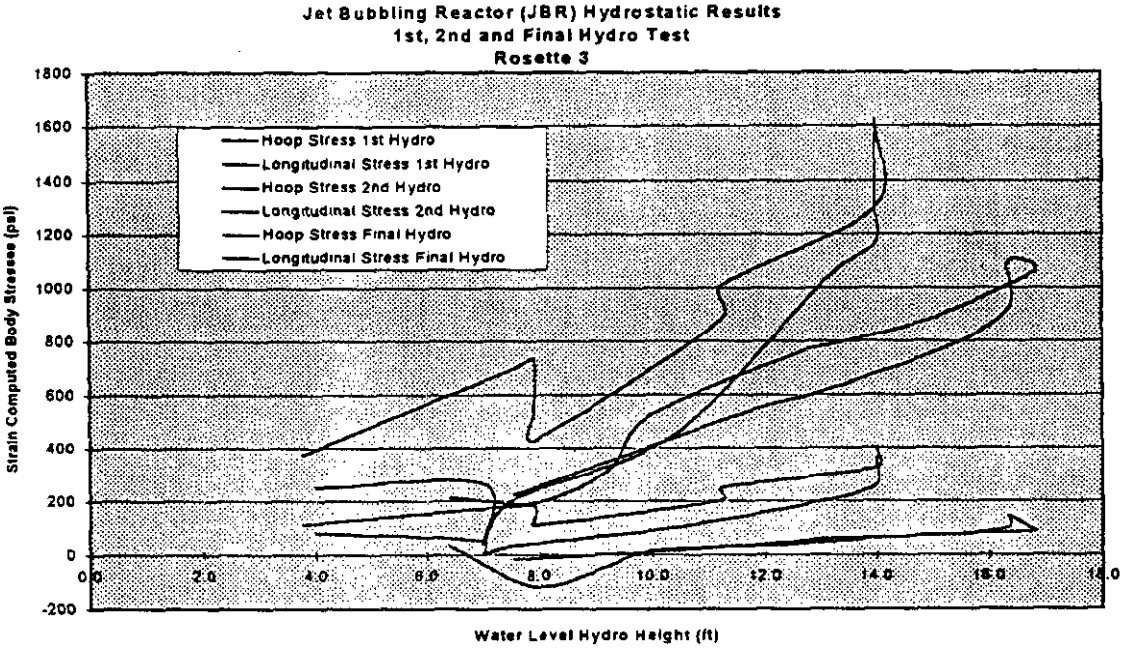

Figure 27

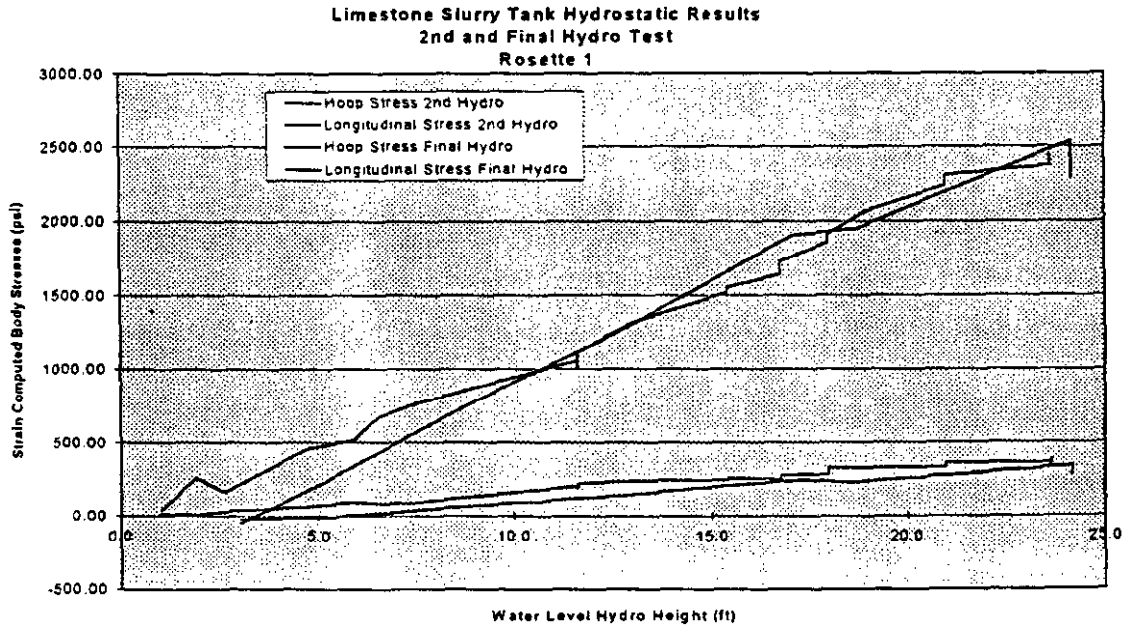

Figure 28

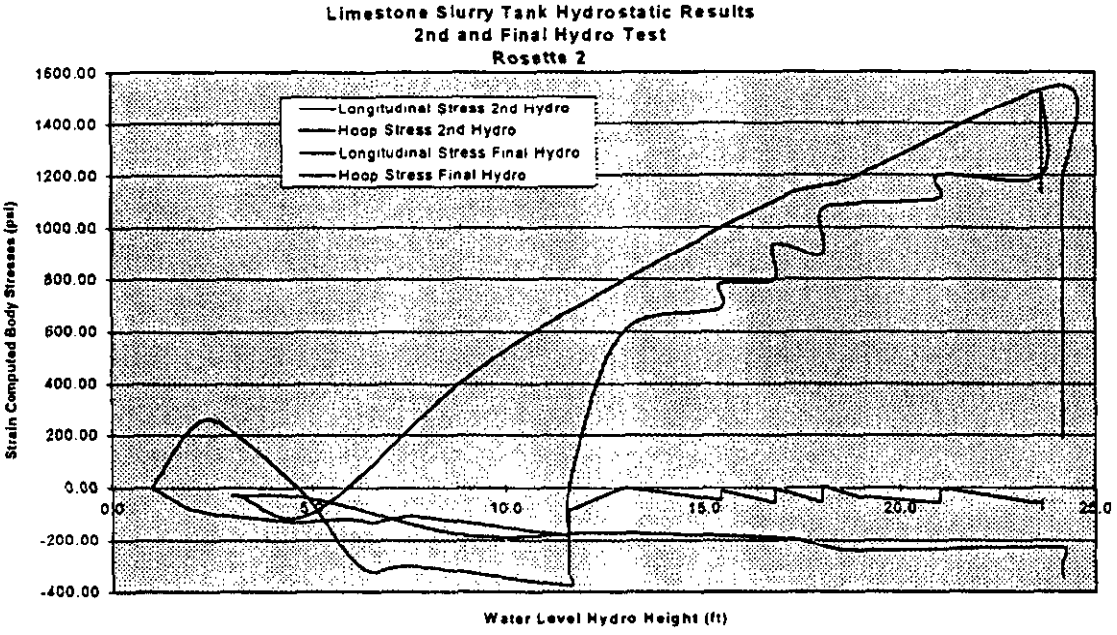

Figure 29

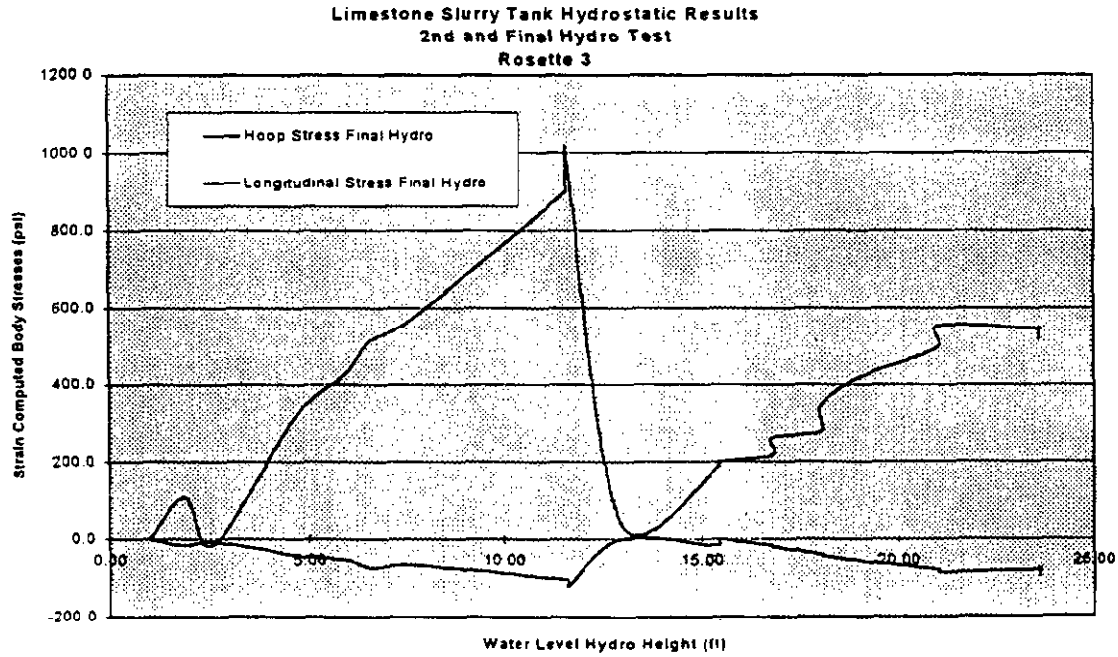

Tested Hoop Stress vs. Theoretical Hoop Stress

Figure 30

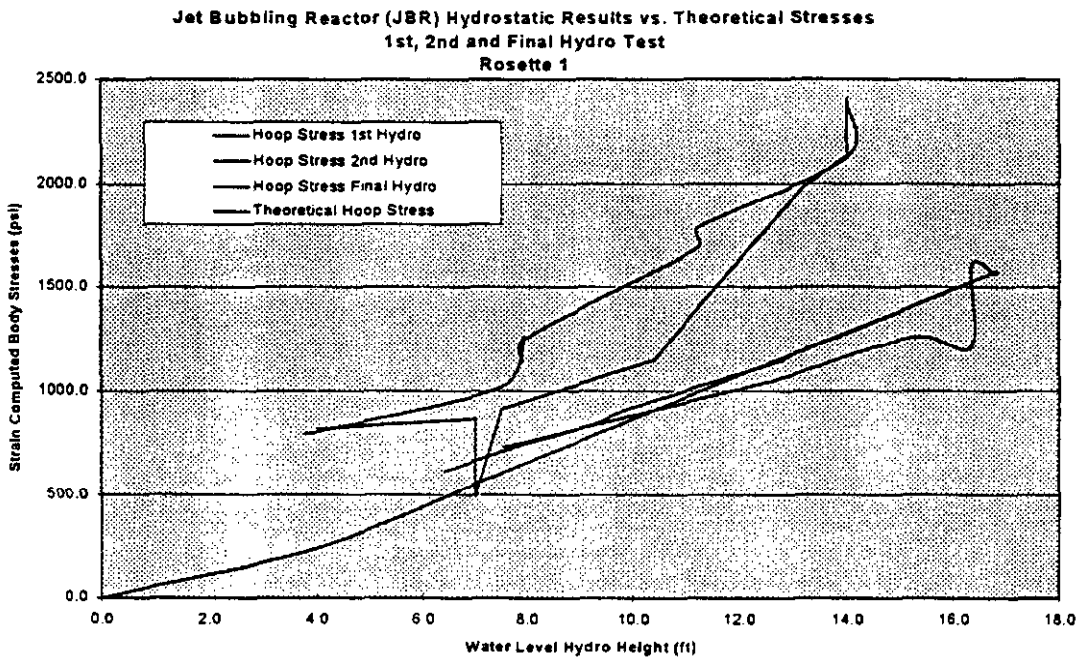

Figure 31

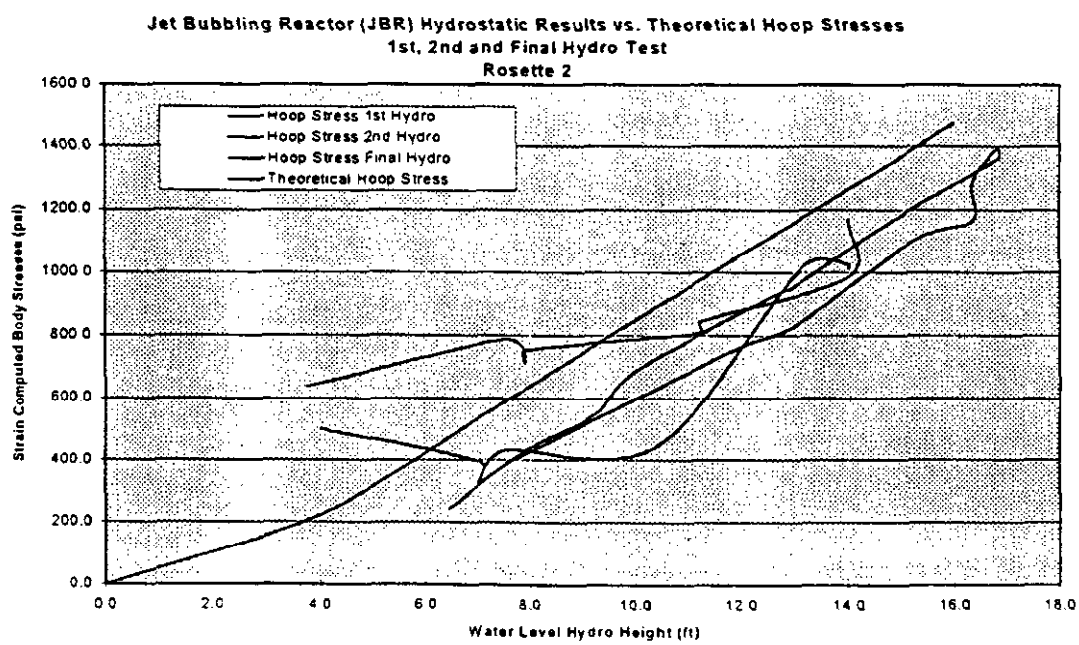

Figure 32

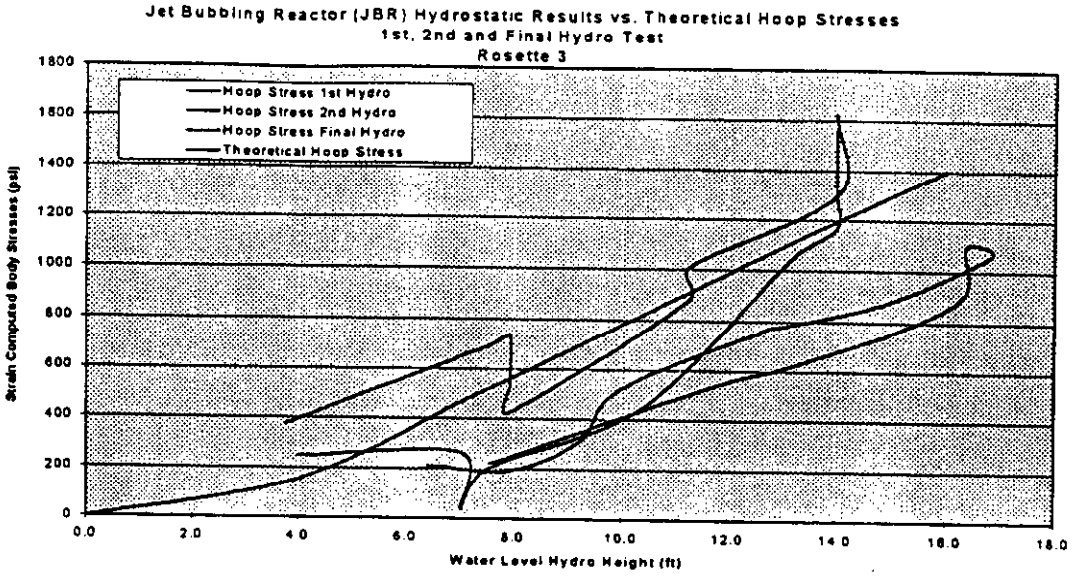

Figure 33

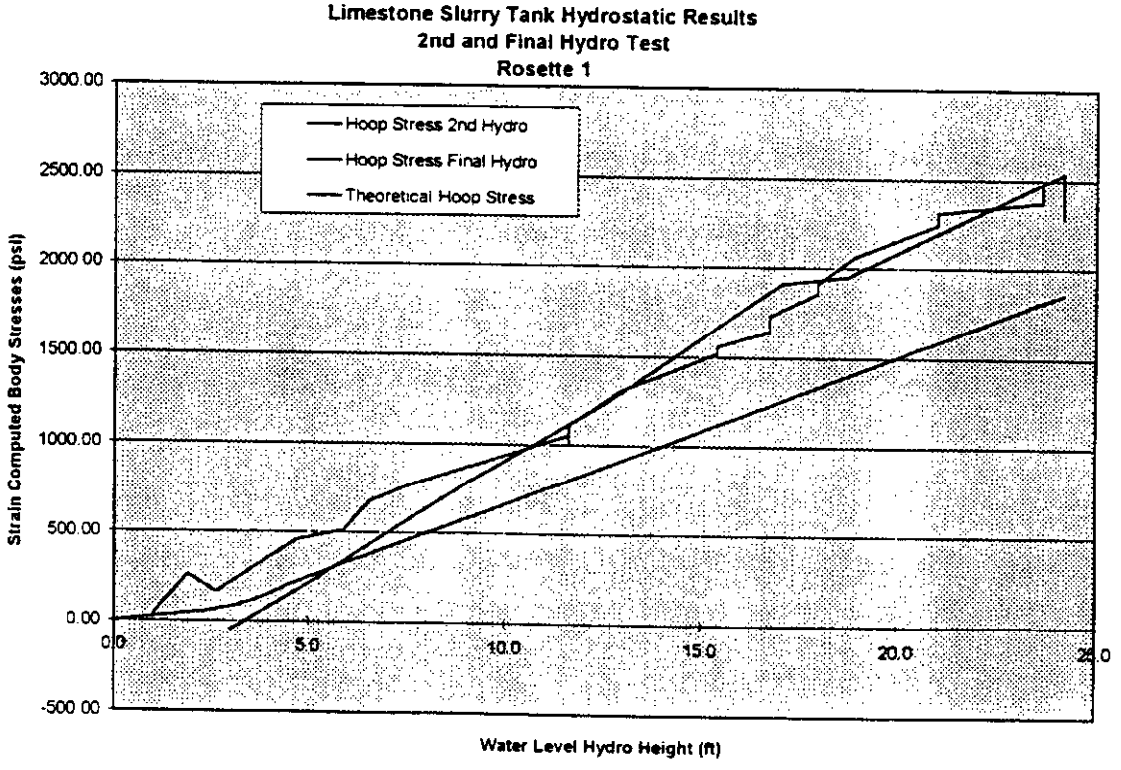

Figure 34

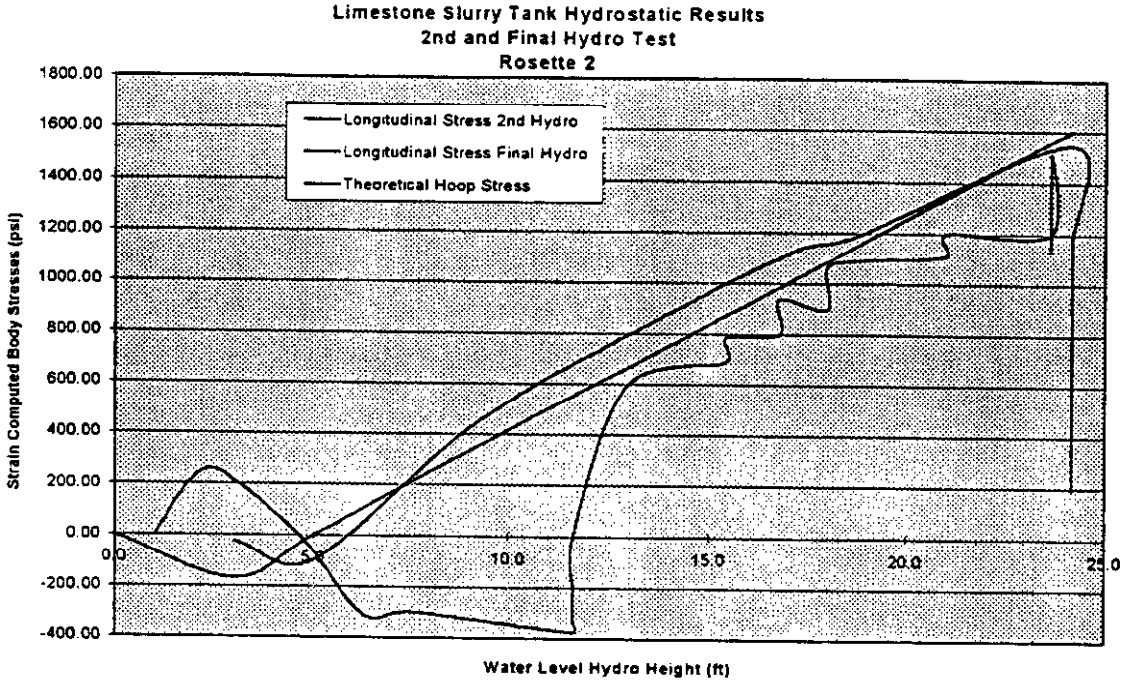

Figure 35

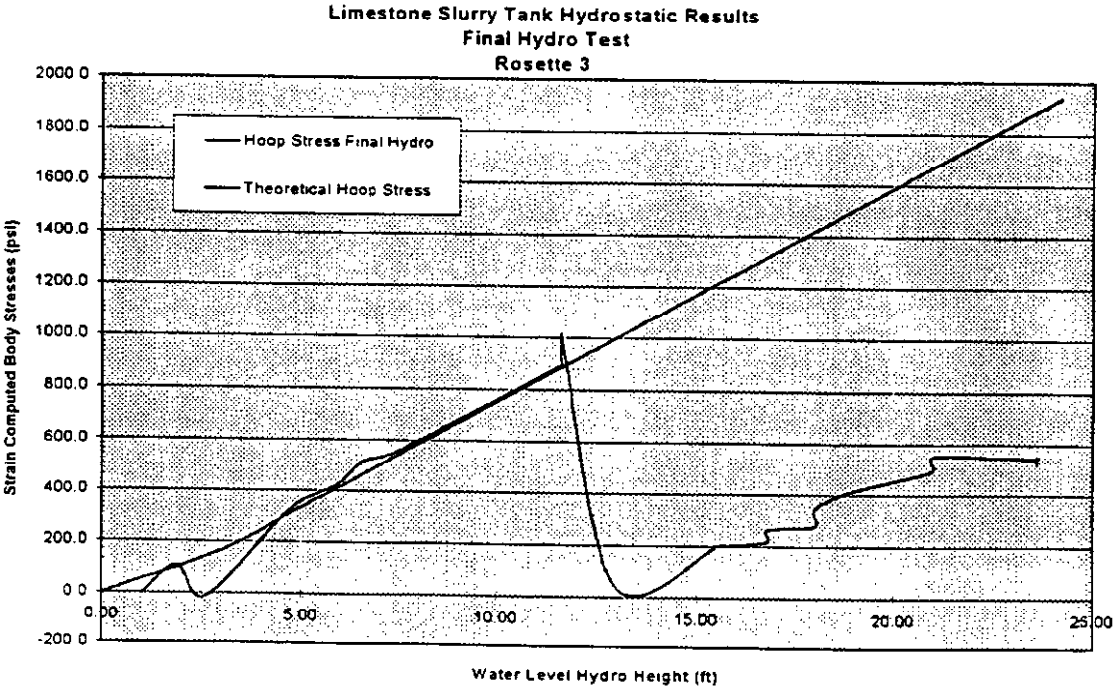

Theoretical Calculated Stresses

$$\sigma = \frac{Pr}{t}$$

For thin-walled vessels, which are qualified with a radius to thickness ratio R/t > 10.0 where ***R*** is the Radius of the vessel and ***t*** is the thickness of the vessel shell, and ***P*** is the pressure inside the vessel.

The actual R/t for the Yates Limestone Slurry and JBR vessels will be minimum for the limestone slurry vessel as R=168 inches and t = 0.87 inches, therefore R/t = 193.

Since the primary vessels are both cylindrical and for simplicity assummed to be of constant vessel thickness, the formula for hydrostatic stress can be re-written as

$$\sigma = \frac{Pr}{t} \quad = \quad \sigma = Px\left[\frac{r}{t}\right] \qquad \text{where } \left[\frac{r}{t}\right]_{JBR} = 332.22$$

$$\text{and } \left[\frac{r}{t}\right]_{Limestone} = 193.1$$

and $P = \gamma x H$ and $\gamma = 62.4$ lb/ft^3

and H = Height of water , in feet (normal)

Therefore, $P = \frac{62.4}{1728} = 0.036$ lb/in^3 x H (inches)

Therefore, $\sigma = 0.036 \times H \times \left[\frac{r}{t}\right]$

$$\sigma = 0.036 \times H \times \left[\frac{r}{t}\right]_{JBR} \qquad \sigma = 0.036 \times H \times \left[\frac{r}{t}\right]_{Limestone}$$

Plot of Hydrostatic Stress vs. Water Height

A generic plot of the hydrostatic stresses vs. water height are provided in the following figure. This plot shows that the hoop stresses are a function of the (R/t) ratio and water height.

Figure 36

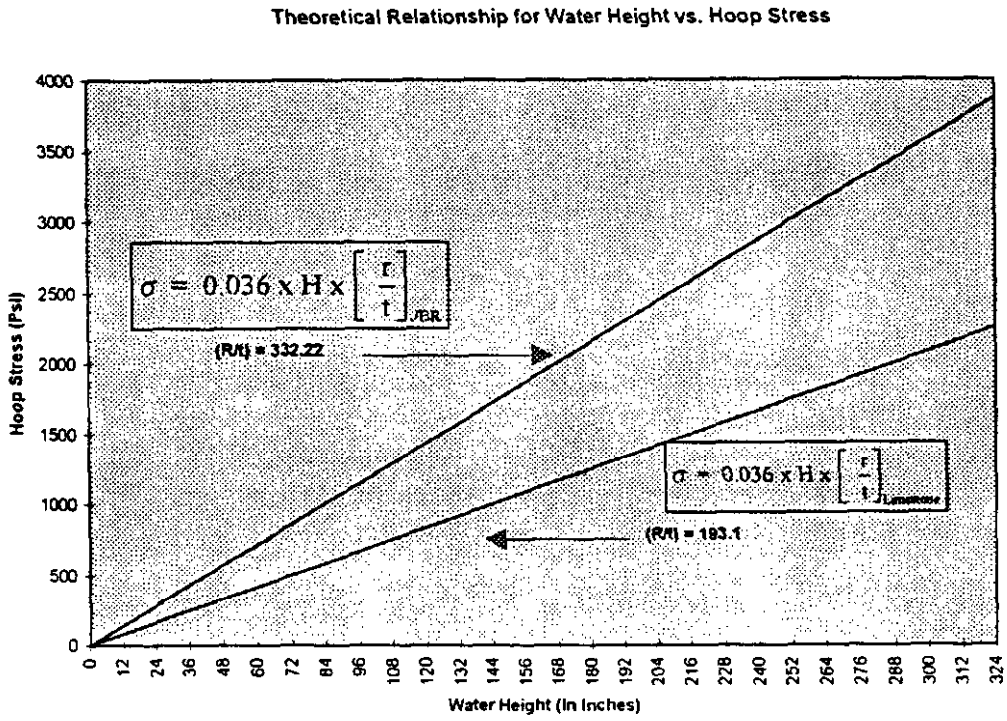

Therefore, the theoretical hoop stress can be calculated or looked up from Figure 36. This relationship is generally found in the experimental test data. Comparison plots between the theoretical stresses and the experimental obtained stresses can be found in Figures 30 to 35.

Comparison of Test Data with Calculated Stresses

Figure 37

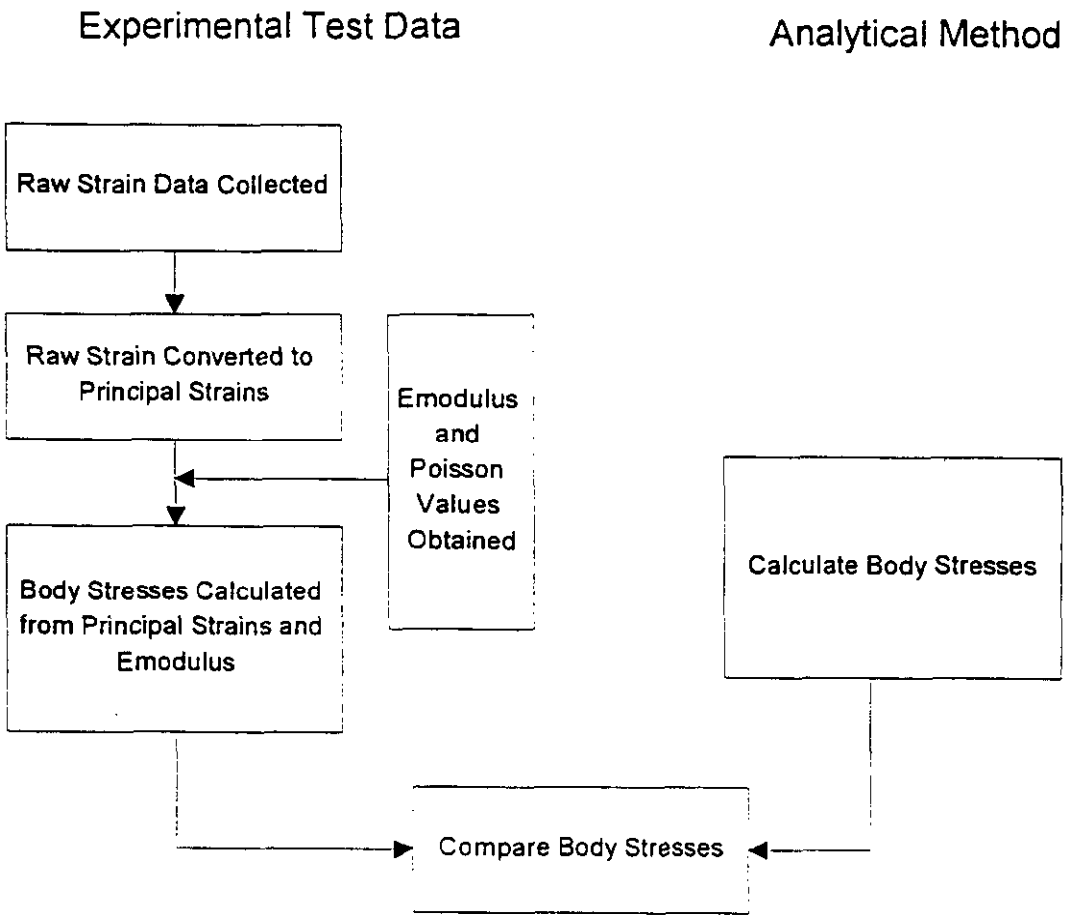

JBR and Limestone Slurry Strain and Stress Results

Strain gage results for the JBR and Limestone Slurry Tank are listed in (Tables 1 and 2) respectively. The results of the strain measurements indicate that the principal strain directions and corresponding body stress directions occur generally in the hoop and vertical directions.

By inspection of the principal strain angle , listed in Table 1and 2, the angle "theta or phi" represents the angle, in degrees, from the reference grid to the principal strain direction. (see Figure 6). These angles "theta" basically align the maximum principal strain (Ep) in the hoop direction, within 8 degrees. Likewise, the minimum principal strain (Eq) is aligned in the vertical direction. The corresponding stresses have been calculated in the pure horizontal (hoop) or pure vertical (longitudinal) directions.

The amplitude of the strain in Tables 1 and 2 show that the predominant strains occur in the hoop direction, but that there are significant strains in the vertical direction. It is our assumption that since the strain gages were applied to the vessel after the majority of the vertical loadings were in-place, dead loads of the vessel, and structure were already present and in general no considerable vertical strains should be seen by the strain gages under hydrostatic loadings.

These plots provide the strain as a function of hydrostatic loading. As seen from this plot, the slope of the line with the relationship of maximum principal strain to water height, is fairly linear.

Photolaminant Results

Table 5

YATES / CHIYODA DOE PROJECT JET-BUBBLING REACTOR
PHOTOLAMINANT TESTING FULL HYDRO LOAD

LAMINANT ID (Note 4)	LOCATION (SUB)	FRINGE LEVEL (FRINGE NO.) (Note 2)	(Ep-Eq) micro strains (Note 3)	THETA (DEGREE) (Note 1)	ROSETTE NO.	STRAIN GAGE RESULTS Ep Strain	Eq Strain	(Ep-Eq) micro strains	Theta (Degree) (Note 5)
JBR-5	A	0.24	336	-15	1				
JBR-6	A	0.26	364	-10		744.60	417.90	326.70	-64.65
	B	0.32	448	-12		742.94	409.06	333.89	-56.19
JBR-7	A	0.2	280	-10					
	B	0.24	336	-10					
		Average	352.8	-11.4			Average	330.29	-55.52
JBR-8	A	0.42	588	90					
JBR-9	A	0.28	392	80					
	B	0.64	896	-90					
						472.10	322.40	149.70	48.66
JBR-10	A	0.2	280	-10	3	437.19	285.48	151.71	45.28
	B	0.1	140	90			Average	150.71	46.97
JBR-11	A	0.68	952	0					
	B	0.42	588	0					
	C	0.14	196	80					
	D	0.1	140	90					
JBR-13	A	0.24	336	-80	2				
	B	0.22	308	-80					
JBR-14	A	0.38	532	10					
JBR-15	A	0.42	588	-5					
JBR-16	A	0.34	476	80		352.53	291.97	60.56	27.22
	B	0.44	616	85		336.46	295.87	40.59	8.00
	C	0.54	756	10					
		Average	457.33	31.67			Average	50.57	17.61

Table 6

YATES / CHIYODA DOE PROJECT LIMESTONE SLURRY VESSEL
PHOTOLAMINANT TESTING FULL HYDRO LOAD

LAMINANT ID (Note 4)	LOCATION (SUB)	FRINGE LEVEL (FRINGE NO.). (Note 2)	(Ep-Eq) micro strains (Note 3)	THETA (DEGREE) (Note 1)	ROSETTE NO.	STRAIN GAGE RESULTS Ep Strain	Eq Strain	(Ep-Eq) micro strains	Theta (Degree) (Note 5)
LST-1	A	0.62	868	5		407.31	-120.31	527.62	50.19
	B	0.76	1064	-25	3	511.97	-141.97	653.95	48.87
						387.79	-146.79	534.57	49.14
LST-2	A	0.4	560	-30		425.25	-108.25	533.50	49.48
	B	1.4	1960	0					
	C	0.96	1344	-28			Average	562.41	49.42
	D	0.8	1120	-25					
	E	1.66	2324	-12					
						832.00	250.00	582.00	45.10
LST-3	A	0.5	700	0	1	761.01	223.99	537.02	45.27
	B	0.32	448	-90		748.06	206.94	541.11	45.58
	C	0.44	616	-58		784.12	190.88	593.24	44.16
						780.32	276.68	503.64	50.90
						794.76	296.24	498.53	50.61
						805.02	264.98	540.06	46.51
						786.26	285.74	500.53	50.30
							Average	537.02	47.56
LST-4	A	0.46	644	0	2	526.05	-313.05	839.10	44.56
	B	0.54	756	0		402.38	-356.38	758.76	43.72
	C	0.64	896	-5		344.22	-357.22	701.45	43.98
						78.93	-375.93	454.86	47.59
						407.31	-120.31	527.62	50.19
						511.97	-141.97	653.95	48.87
						387.79	-146.79	534.57	49.14
						425.25	-108.25	533.50	49.48
							Average	625.48	47.19

Notes

1) The angle theta represents the measured angle of the principal axis with respect to the vertical axis in the clockwise direction (See Figure 29)

2) A single fringe order of 1.0 represents 1400 micro-strains. Example, therefore 0.50 f represents 700 micro-strains, etc.

3) By definition, the photoelastic laminant measurement provides the value of the difference between (Ep-Eq)

4) JBR-"n" or LST-"n" represents the photolaminant identification, example, JBR-5 is the Jet Bubbling Reactor photolaminant no. 5. The location sub "A" provides the identification for a discrete point on the laminant where photoelastic measurements were taken.

5) The Angle Theta for the Strain Gage Orientation is consistent with Figures 6 and 7.

Figure 38

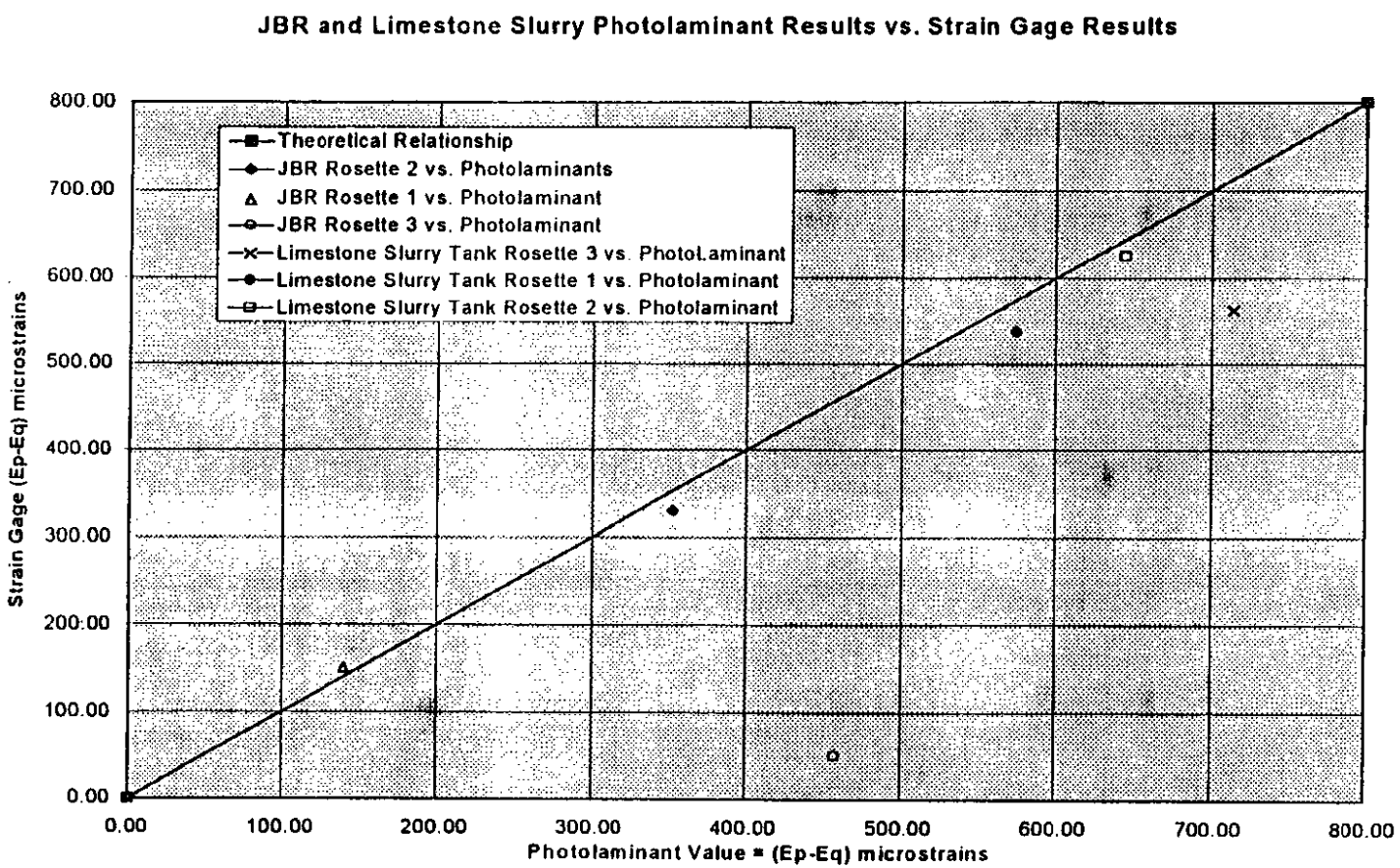
JBR and Limestone Slurry Photolaminant Results vs. Strain Gage Results
Theoretical Relationship
JBR Rosette 2 vs. Photolaminants
JBR Rosette 1 vs. Photolaminant
JBR Rosette 3 vs. Photolaminant
Limestone Slurry Tank Rosette 3 vs. PhotoLaminant
Limestone Slurry Tank Rosette 1 vs. Photolaminant
Limestone Slurry Tank Rosette 2 vs. Photolaminant
Strain Gage (Ep-Eq) microstrains
800.00
700.00
600.00
500.00
400.00
300.00
200.00
100.00
0.00
0.00
100.00
200.00
300.00
400.00
500.00
600.00
700.00
800.00
Photolaminant Value = (Ep-Eq) microstrains

Figure 39

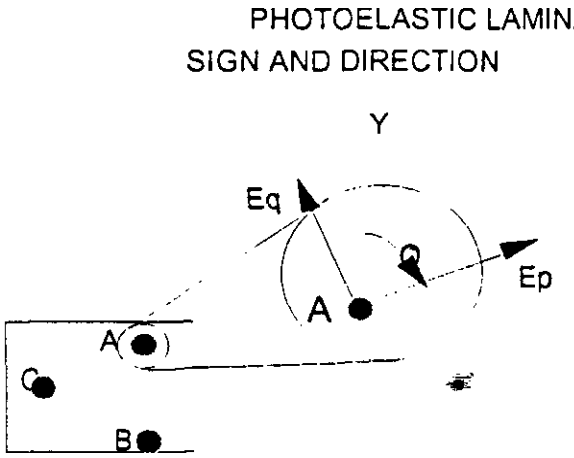

PHOTOLAMINANT GAGE

Photolaminant Comparison Results

Photolaminant amplitudes are provided in Tables 4 and 5 for the initial 1991 hydro tests. A plot of the comparison between the strain gage data (Ep - Eq), major principal - minor principle strain , and the photolaminant (Ep-Eq) is provided in Figure 38. With the exception of one data point, JBR Rosette No. 3, the correlation is very good. Therefore, the photolaminant provides a good method of optically obtaining the strain state and also verification of strain or other NDE data.

Results

Observed Strain Values

Behavior of the strain curve vs. water height

Evaluation of the various strain gage data and corresponding plots provides insight into the behavior of the vessel during the several hydro tests. These plots generally show that the curves are linear in nature, and

comparison of microstrain and/or stress are proportional to the hydro test water height. From presentation of previous theoretical relationships, the linear relationship between stress vs. water height is well accepted for basic tank structures.

Figure 9 and 10 provide the raw strain vs. water height for the last hydrostatic test on the project. These strain trends generally follow a linear trend with water height.

Observations from the strain curve for different hydro tests

JBR Strain Data

Review of Jet-Bubbling Reactor (JBR) trend plots in Figures 11 thru 17 provide the principal strains vs. hydro test heights. These plots provide two hydro tests in 1991 just prior to scrubber operation, and a single hydro test that was performed in late 1994.

Rosette No. 1 is located at 1'-8" above the tank floor which is physically shown in Figures 2 and 3. Figure 11 and 12 indicates a general offset of strain measured in 1994 such that the slope of the curve is more shallow than the 1991 tests. Also, the highest principal strain measured in 1994 was significantly lower than that measured in 1991.

Rosette No. 2 shows a similar trend in the offset of the minor principal strain from Figure 14. Figure 13 however indicates a not so significant difference in the major principal strain between 1991 and 1994 tests.

Rosette No. 3 shows a very similar trend to that of Rosette No.2, where the minor principal strain in Figure 16 from the 1994 curve diverges from the 1991 curve. Another interesting point is that Figure 16 strain actually becomes negative with increased water height. Similar to Rosette No. 2, the major principal strain from Figure 15 traces very well with the 1991 curves.

Also, the uniaxial gage trends in a very linear fashion for the 1994 hydro but seems to lag at lower hydro heights in the 1991 tests, as seen from Figure 17.

Limestone Slurry Vessel Strain Data

Figures 18 thru 23 provide the similar information on the Limestone Slurry Vessel as that contained for the JBR vessel in Figures 11 thru 17. Similarly, these plots provide one hydro test in 1991 and one hydro test in 1994.

Rosette No. 1 in Figures 18 and 19 shows very repeatable results for the major principal strain, and a small shift in the microstrain offset for the minor principal strain. 1994 minor principal strains are actually higher than 1991 strains

Rosette No. 2 indicates very close to the same maximum principal strain from Figure 20 from 1991 and 1994 tests, but a very poor correlation with the minor principal strain from Figure 21.

Rosette No. 3 major and minor principal strains are approximately inversely proportional to each other. The major principal increases with hydro loading, but the minor principal decreases with hydro loading. Additionally, the curve has an interesting step change in principal strain values.

Observations from the Body Stress Curve

Figures 24 thru 29 provide a comparison of the hoop and longitudinal stresses for the different hydro tests.

JBR

Hoop stresses and longitudinal stresses were generally higher during the 1991 test than the 1994 test. Also, the 1994 test hoop and longitudinal stresses were very repeatable.

Limestone Slurry Vessel

Figure 27 shows very similar behavior between 1991 and 1994. Longitudinal stress is higher for 1991 hydro as provided in Figure 28. Figure 29 shows the hoop stresses increasing up to 11 feet and then dropping off to zero and then increasing again.

Comparison of Experimental vs. Theoretical Stress

Computation of Stresses

The calculation of the principal stresses for isotropic materials is a very difficult problem. Generally, composite materials are classified as either anisotropic or orthotropic. For ease of calculations, laminant composites are designed as orthotropic, which requires two sets of Moduli of Elasticity and two sets of poisson ratios. Generally, this will include an Ex and Ey with corresponding poisson ratios vx and vy. These material properties with a full-field strain measurement at a point, allow for the computation of the major body stresses in a laminant. These calculations are expressed in principal by the matrix notation shown below:

Comparison of Body Stresses

Figures 30 and 35 provide a comparison of the hydrostatic results vs. the theoretical stress levels.

JBR

Figure 30 indicates a very good comparison of the 1994 test, but the 1991 test produced stresses approximately 50 to 100 % higher than theory. Figure 31 indicates the actual stress was lower than the theoretical value.

Limestone Slurry Vessel

Figure 33 shows the actual stress slope is steeper than the theoretical slope. Figure 34 indicates good correlation at higher loadings. Figure 35 indicates very similar behavior at lower levels, but has an offset and then a restress behavior. From the restress behavior, it is possible that the strain gage pulled apart from the surface.

Conclusions

Structural Integrity of Scrubber Vessel

Strain Testing

Strain testing provided a good method for comparison of strain and stress levels and verification of engineering properties used in the design calculations.

Hoop stresses determined for the JBR and Limestone Slurry Tank correlated very well with the theoretical hoop stresses with a few exceptions. Rosette 1 on the JBR had a significantly higher stress than the theoretical value. Also, the Limestone Slurry Tank indicated a much steeper slope than the theoretical stress-strain slope at higher levels of water height.

Cyclic Loading on Vessel

Data from the various figures and tables continues to reinforce the fact that the strain does appear to generally trend similarly from hydro to hydro, but there does appear to be some differences in both the principal strain magnitudes and principal strain angles. These cycles of loading and unloading do appear to take some toll on the load response of the vessel.

Another explanation for some of the differences in the 1991 and 1994 loadings may be a consequence of a creep phenomenon, which is quite common in some traditional structures that are significantly stressed.

Evaluation of Material Properties

The general practice of determination of FRP material properties appears to be the computation of the global section material properties using the many layers of the laminant profile. This practice has been observed by several FRP manufacturers, and appears to be the general trend for calculating the elastic modulus and poisson ratios for the composite cross-sections.

FRP as an Engineering Material

Design requirements for FRP structures are not widely controlled as traditional construction materials. Since FRP laminants are constructed as a series of many layers of resins, fiber glass, and coatings, the quality assurance of the raw materials and bonding procedures, and curing have many variables.

The construction of two identically designed vessels, if constructed at different times or by different construction personnel could potentially have a much different quality of workmanship. In summary, quality assurance requirements are much more important for a FRP material than a traditional material construction.

FRP does not have the application experience in massive structures as does steel and concrete structures. Aerospace and automotive industry design personnel have a much extensive experience base in the use of composite plastic materials. Lack of confidence and knowledge in the use of a material is a self-perpetuating problem which prevents a quick acceptance of a new material.

Specifications should be written to include the evaluation of the material, and performance of the constructed component. Specifications for a product to be constructed of FRP requires an extreme effort on the part of the specifying engineer. Not only do the materials have be tightly specified, but also the construction of the component, and the performance requirements for the completed system should also be mandated. This requires a tremendous investment on the part of the owner to enter into a proposal in which the terms of the specification may be very controversal.

Finally, the use of FRP as an engineering material has many aspects that require a more deliberate effort on the part of the owner, the engineer, and the construction party. In certain cases, as is demonstrated by the environment required to construct and operate wet SO_2 scrubbers, only the use of very expensive alternative materials to FRP are acceptable. In these types of applications, the FRP material has tremendous promise.

In the final analysis, the FRP vessel used at Georgia Power Plant Yates for the Chiyoda Wet Scrubber has demonstrated its merit as a viable alternative material for full-scale scrubber vessels.

Additional strain testing and research is ongoing throughout the engineering community, to make FRP structures viable, trustworthy materials, that can be used without hesitation by design engineers.

Normally, the engineer must make many simplifying assumptions about boundary conditions and physical situations that are difficult to quantify with exact numbers. Therefore, the data provided by testing can both lead and support the analytical assumptions used in normal design practice.

Recommendations

Strain testing of a full-scale structure provides actual data on the performance of the installed structure. The testing on fiber-reinforced plastics becomes much more important due to the additional uncertainties and requirements induced by the non-isotropic nature of the composite laminant.

Composite materials provide significant benefits over traditional materials. However, due to the limited experience with composites such as Fiber Reinforced Plastic (FRP), construction with these materials is difficult to specify. As a general rule, however, FRP requires additional surveillance during the design, manufacturing, construction, operation, and maintenance of the subject structure.

For design, it is recommended that the material properties for a proposed laminant be computed by rational engineering methods. Currently, there does not appear to be an engineering standard that has been adopted as a legal basis for an FRP design. Continued monitoring of industry working groups within the area of composites and FRP design are advisable. Also, the use of finite element analysis provides many useful capabilities including good visual methods of quickly determining critical stress locations on or in composite vessels and structures, design optimization of cross sections, and quick loading simulations.

For manufacturing, it is recommended that quality assurance requirements be specified such that controls during the fabrication of the FRP are documented as much as possible, and that the materials and material properties are tested according to at a minimum ASTM D3039-76.

For construction, it is recommended that hand lay up details be documented. This would include such items as environmental conditions, such as weather, resin mix designs, mixing times, and quality assurance testing of field connections , to try and determine the workmanship concerns during the actual construction.

For operations and maintenance, it is recommended that a log of repairs, replacements, painting, cleaning, etc. be kept. Also, the loading history of the vessel would be important for determination of significant cycling of the loading on the structure.

Good non-destructive testing techniques, such as strain monitoring, acoustic emissions testing, modal testing, vibration monitoring provide methods for long term trending of the behavior of the structure.

Additionally, current techniques involving the embedding of continous fiber optic tendons inside composite materials has the potential for providing either a global or local sensor for strain monitoring.

The most successful use of composite materials, such as FRP, will require that several of these recommendaitons be adopted. The costs of materials and labor are such that the efficient use of the composites and/or traditional materials will require more optimum designs be followed in order to reduce costs.

As a trending tool, strain testing provides a way of quantifying the behavior of the vessel over time. As such, a monitoring program of every five years may be advisable. Also, as more and more test data is collected, the trend interval could be expanded or reduced based on the results of the testing.

Appendix I : Raw Data

Raw Strain Data Listing

Hydro 1994

JBR

4.00	0.00	0	0	0	0	0	0	0	0	0	0	0
7.20	6.42	99	201	184	21	80	80	81	121	70	-24	-125
8.00	7.92	133	242	233	30	90	111	140	160	70	48	-133
8.70	9.23	150	273	270	42	94	141	178	200	107	90	-55
9.10	9.98	166	299	293	74	110	171	222	212	174	145	-5
10.60	12.79	204	370	398	120	131	220	308	292	256	270	10
10.65	12.89	207	376	400	127	143	221	308	292	256	262	14
11.75	14.95	257	445	465	146	165	265	384	348	290	355	40
12.75	16.82	295	510	537	161	180	310	444	400	350	402	45
12.75	16.82	297	504	541	165	180	305	456	406	360	417	45
12.50	16.35	333	520	524	125	170	326	420	407	360	439	105
12.50	16.35	244	390	472	138	162	279	380	386	302	388	68
11.9	15.23	231	406	456	110	143	258	360	335	255	315	45
10.7	12.98	200	348	384	84	125	216	270	250	200	264	37
10.1	11.85	183	323	352	85	114	190	245	231	181	219	17
7.8	7.54	90	240	230	25	115	80	125	85	75	30	-27

Limestone Slurry Tank

4	1.00	50	70	-11	29	8	18	6514	3588	3672	-13
5	1.88	63	130	1	0	130	-30	6574	3590	3622	-28
5.4	2.63	81	98	-13	5	148	-41	6637	3565	3640	-26
6.5	4.69	125	87	55	-61	62	-82	6809	3625	3755	-27
7.15	5.91	117	107	85	-100	-70	-130	6845	3645	3774	-42
7.5	6.56	141	95	110	-131	-53	-120	6900	3650	3812	-35
8	7.50	160	100	126	-115	-50	-103	6934	3672	3827	-35
10.2	11.63	237	207	247	-170	-68	-148	7201	3730	3940	-36
10.2	11.63	238	210	237	-145	-90	-125	7250	3720	3945	-37
10.2	11.63	233	199	233	-115	-76	-90	7294	3730	3963	-28
10.2	11.63	247	215	256	-72	-48	-52	7294	3742	3971	-43
10.9	12.94	318	258	320	73	45	118	0	0	0	-15
12.225	15.42	364	270	374	80	7	124	47	25	67	3
12.225	15.42	388	296	400	123	56	172	62	45	82	15
12.95	16.78	390	275	402	98	1	145	55	34	85	11
12.95	16.78	415	302	431	142	51	195	70	45	100	11
13.6	18.00	425	295	445	105	-14	145	55	28	95	0
13.6	18.00	445	325	460	140	35	200	70	44	105	-12
14.1	18.94	455	315	490	136	-11	169	82	52	129	-12
15.2	21.00	501	330	530	125	-25	185	90	52	168	-1
15.2	21.00	515	350	550	140	20	235	101	60	180	-8
16.6	23.63	542	367	584	140	-16	224	110	66	200	15
16.6	23.63	565	389	601	188	-36	265	115	74	205	18
16.6	23.63	560	345	565	119	-51	185	101	40	185	8
16.6	23.63	560	380	591	166	0	238	118	58	201	20
11.3	13.69	346	299	348	85	69	127	35	23	29	90
11.3	13.69	390	308	375	124	73	168	48	31	50	90
	12.00										

Hydro 1 1991

JBR

				JET BUBBLING REACTOR						
				FIRST HYDRO TEST						
				DATE = 10/1/91						
				GAGE FACTOR (TOTAL SYSTEM) = 1.898						
				EXCITATION = 2 VOLTS						
				INDICATOR BALANCE = 90						
				STRAIN GAGE CHANNEL						
GAGE WIRE NO	1	2	3	4	5	6	7	8	9	10
GAGE ANGLE	135	90	45	135	90	45	0	135	90	45
GAGE POSITION	E3	E2	E1	E3	E2	E1	E	E3	E2	E1
WATER	ROSETTE 1			ROSETTE 2			GAGE 7	ROSETTE 3		
HEIGHT	(m e)	(m e)	(m e)	(m e)	(m e)	(m e)	(m e)	(m e)	(m e)	(m e)
(INCHES)	micro e									
0	0	0	0	0	0	0	0	0	0	0
45	178	260	142	135	210	114	-80	113	120	110
90	300	333	188	163	259	166	80	204	161	180
95	350	410	245	175	245	190	101	210	162	190
95	350	386	195	148	246	193	91	130	106	156
95	331	371	213	152	232	190	77	132	126	165
95	361	405	241	170	244	216	111	93	98	143
135	494	549	358	222	260	260	207	216	179	248
135	513	580	395	240	270	279	234	275	224	275
168	611	690	492	282	291	325	316	365	291	345
168	660	780	562	334	306	348	393	448	355	431

Limestone Slurry Tank

		STRAIN GAGE MEASUREMENTS									
NO HYDRO TEST											
(TOTAL SYSTEM) = 1.902											
ATION = 2 VOLTS											
TOR BALANCE = 90											
TIME	CONDITION	RAW DATA				STRAIN CHANNEL					
RAW DATA		1	2	3	4	5	6	7	8	9	10
	DIRECTION DEGREES	45	90	135	45	90	135	0	90	135	compare
		e1	e2	e3	e1	e2	e3	e1	e2	e3	e1
08:15 PM	INITIAL BALANCE	390	410	386	390	410	362	600	438	362	428
	VERNIER SETTING										
08:15 PM	START OF FILLING	-5	-2	-5	-17	-16	-15	-9	-8	-9	-23
08:45 PM	HEIGHT = 36"	2	-15	-38	-20	-6	-17	9	-148	-88	-12
04:07 PM	HEIGHT = 60"	30	-22	30	-43	-40	-25	91	-126	-29	-2
04:55 PM	HEIGHT = 108"	153	40	146	-27	-210	-34	215	-100	68	-6
05:25 PM	HEIGHT = 150"	245	96	256	36	-215	18	323	-44	150	16
07:10 PM	HEIGHT = 208"	309	176	402	74	-253	56	452	-14	236	-12
07:30 PM	HEIGHT = 225"	418	167	434	63	-305	35	480	0	263	-5
09:15 PM	HEIGHT = 250"	540	250	502	113	-313	100	610	36	343	0
11:53 AM	HEIGHT = 297"	490	224	495	80	-356	6	512	-42	225	-2
01:54 PM	HEIGHT = 297"	472	207	483	6	-357	-19	547	-54	223	-8
04:46 PM	HEIGHT = 297"	396	191	479	-109	-375	-128	565	-35	201	-3

2nd Hydro 1991

			JBR HYDRO TEST									
			STRAIN GAGE MEASUREMENTS									
SECOND HYDRO TEST												
DATE = 10/4/91												
GAGE FACTOR (TOTAL SYSTEM) = 1 962												
EXCITATION = 2 VOLTS												
INDICATOR BALANCE = 90												
TIME	CONDITION		RAW DATA			STRAIN CHANNEL						
RAW DATA			1	2	3	4	5	6	7	8	9	10
	DIRECTION(DEGREES)		45	90	135	45	90	135	0	45	90	135
			E3	E2	E1	E3	E2	E1	e	E3	E2	E1
07:00	INITIAL BALANCE		446	592	646	300	606	330	532	148	434	378
	VERNIER SETTING	HEIGHT										
09:09 AM	START OF FILLING	0	20	28	12	12	3	2	6	6	6	6
10:09 AM	HEIGHT = 48"	48	179	270	147	74	166	82	-24	85	80	70
11:09 AM	HEIGHT = 84"	84	230	285	134	33	133	72	-30	62	45	70
01:43 PM	HEIGHT = 84"	84	154	163	5	-2	111	46	-79	-18	1	32
02:43 PM	HEIGHT = 90"	90	259	300	133	62	142	106	-14	47	66	46
03:06 PM	HEIGHT = 125"	125	326	375	200	83	146	125	62	96	88	139
05:17 PM	HEIGHT = 158"	158	563	642	450	283	328	325	280	218	174	295
05:45 PM	HEIGHT = 168"	168	618	692	484	298	328	341	301	286	227	318
07:45 PM	HEIGHT = 168"	168	628	725	516	302	316	339	321	383	313	354
09:41 AM	HEIGHT = 168"	168	672	774	538	298	293	319	332	412	320	415

Appendix II: Photographs

Photo 1 : Typical Test Setup during Strain Gage Testing

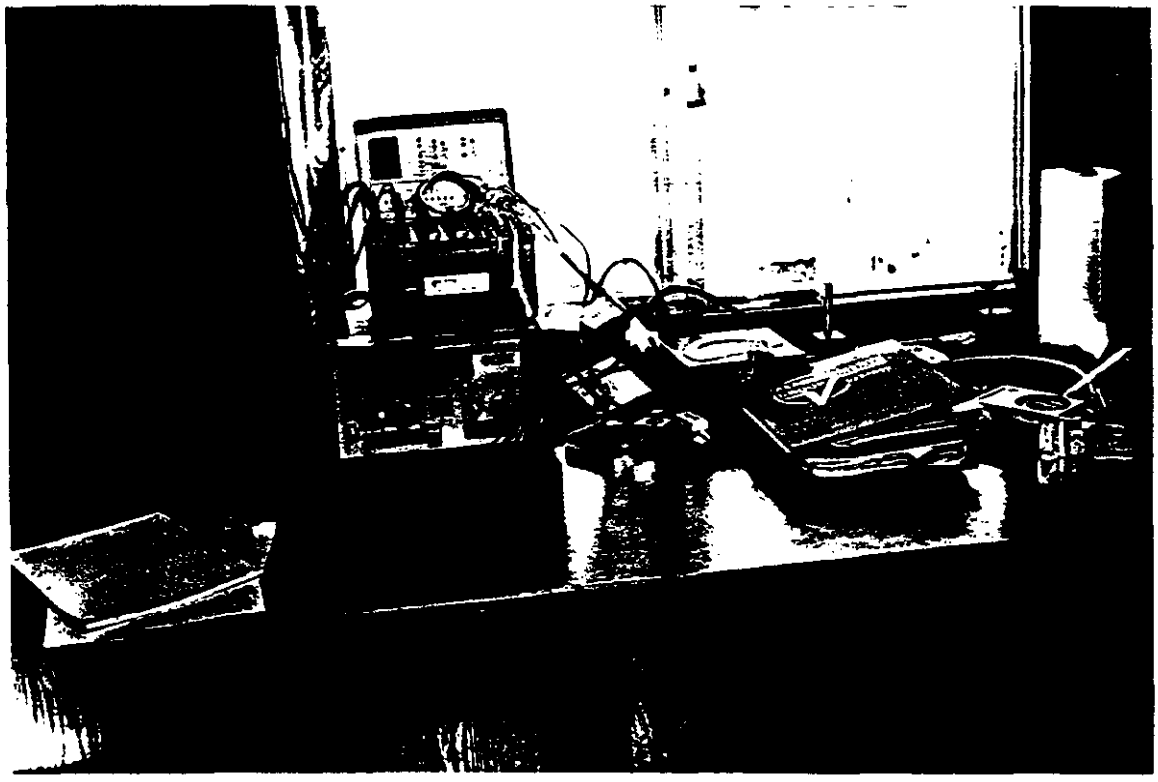

Photo 2 : Construction Photo during JBR fabrication prior to Strain Gage Testing

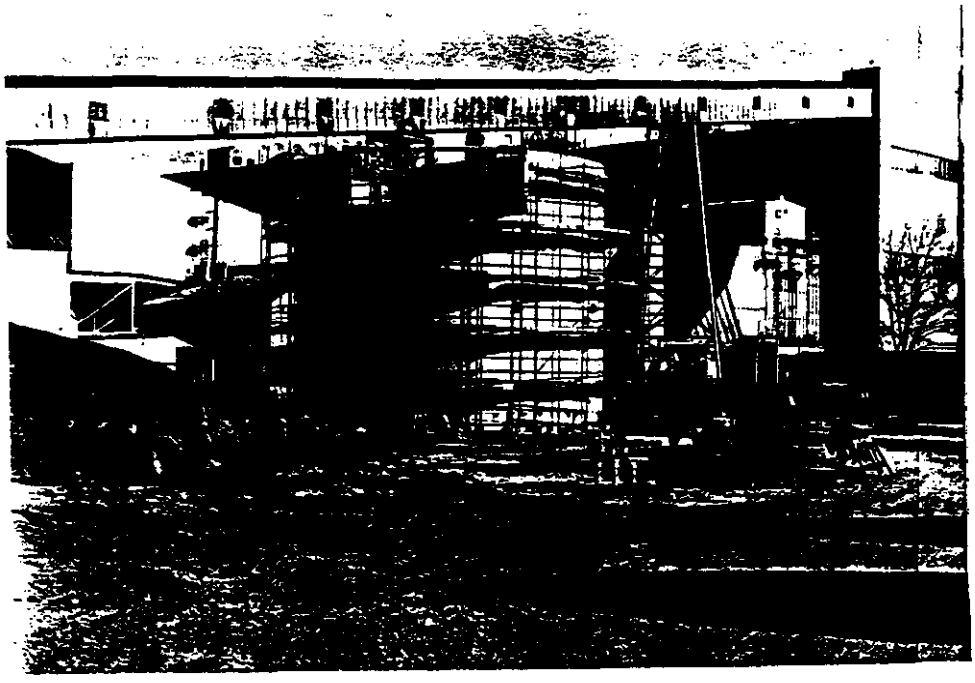

Photo 3: Construction Photograph of JBR with Duct Penetration

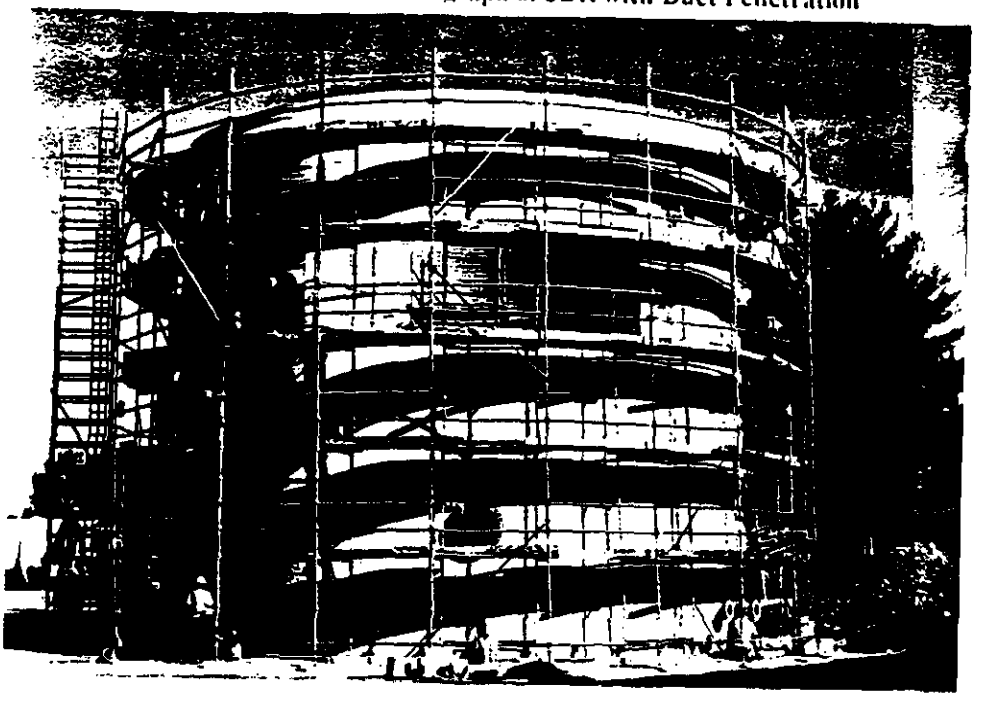

Photo 4 : Construction of JBR Vessel (Inside)

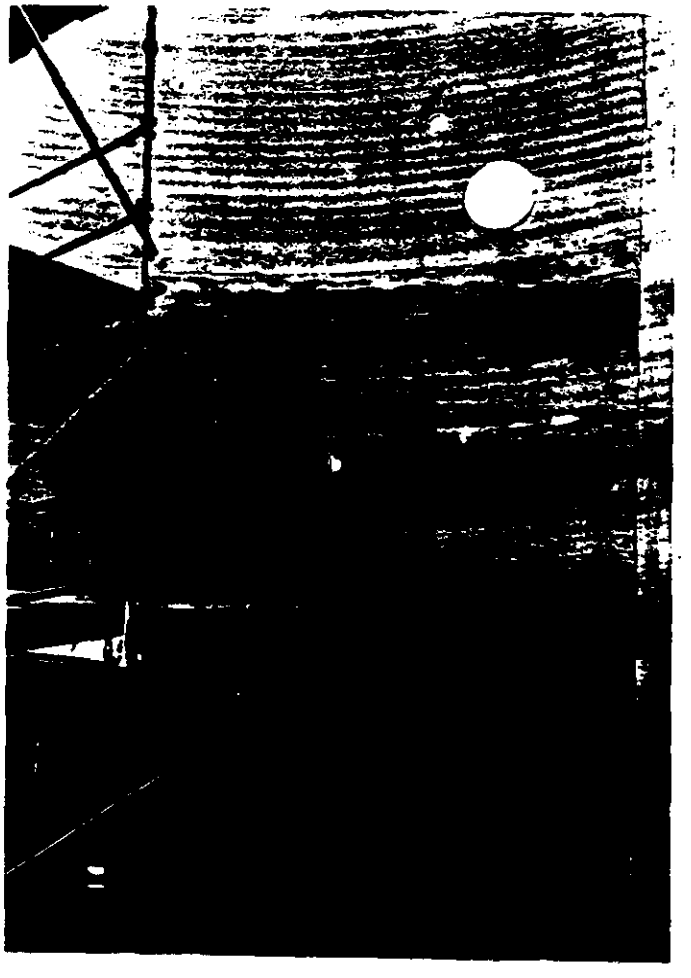

Photo 5 : Photolaminant and Strain Gage Layout Installation on Manway of JBR Vessel

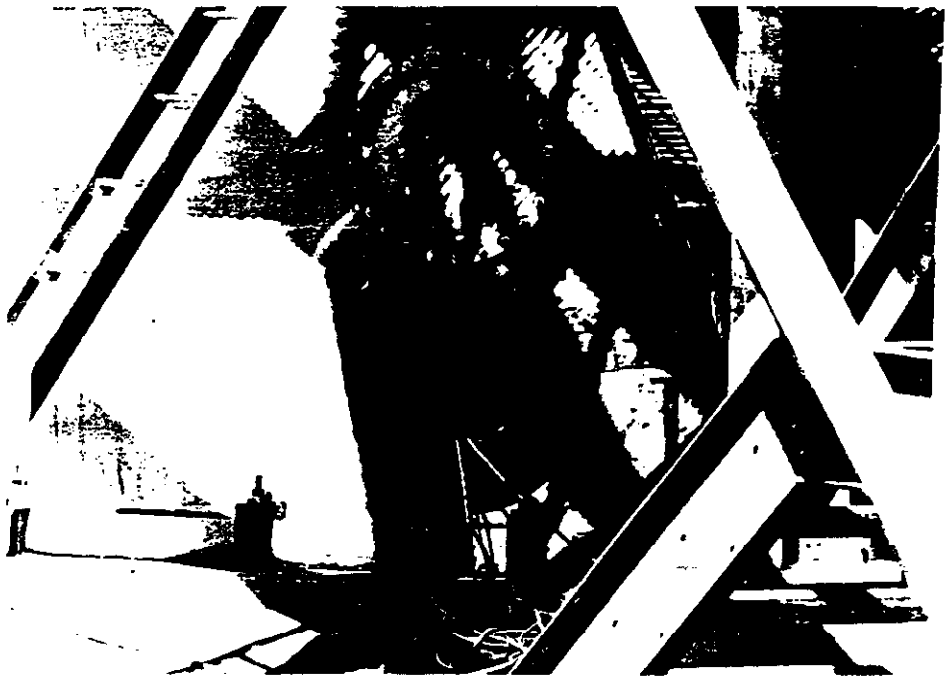

Photo 6: Photolaminant Installation at "Dog Leg" Holdown Anchorage of JBR Vessel

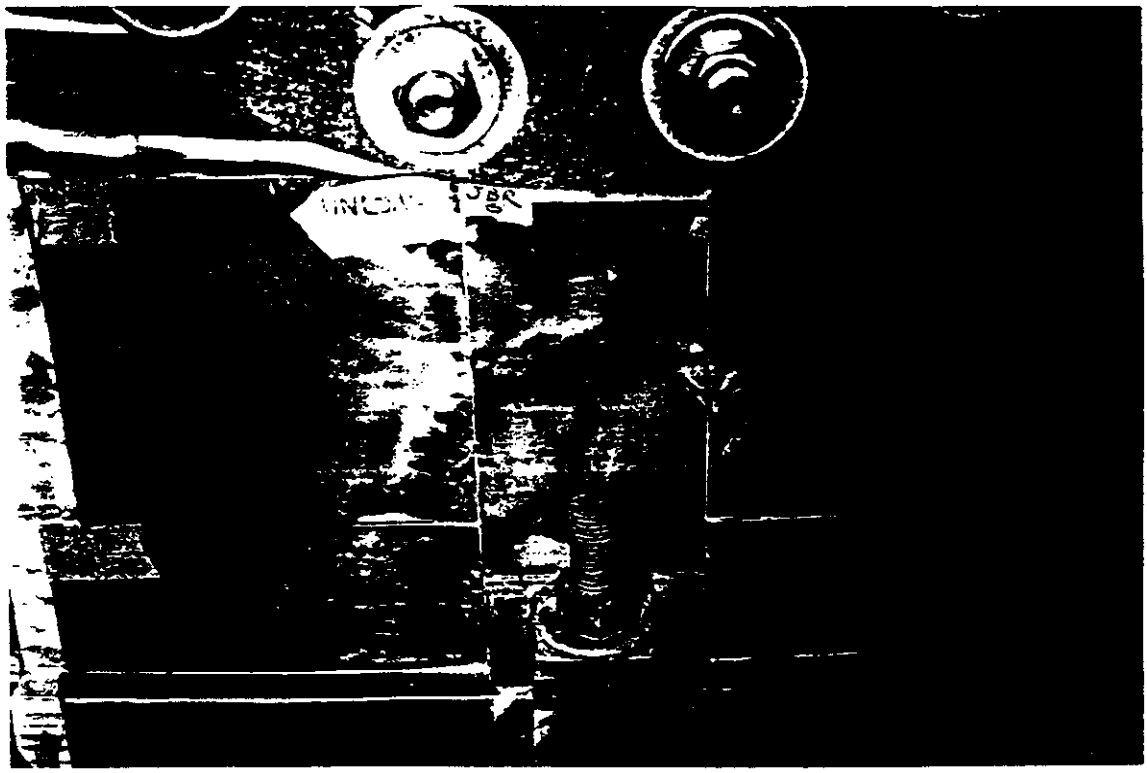

Photo 7 : Photolaminant Layout on Vertical Section of JBR Vessel

Photo 8: Photolaminant Layout on Vertical Section of JBR Vessel

Photo 9 : Construction Photograph of Limestone Slurry Vessel during Photolaminant Construction

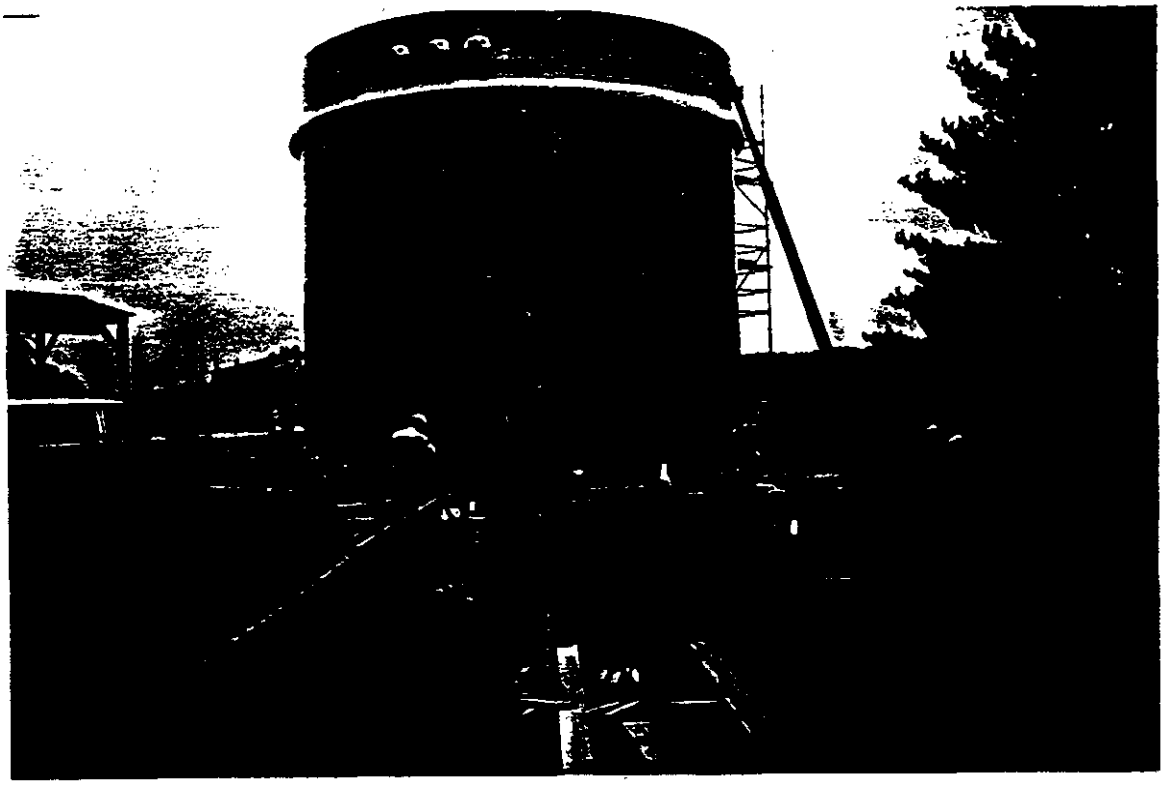

Photo 10 : Photolaminant measurement during Hydrostatic Loading of Limestone Slurry Vessel

"Abrasion and Corrosive Coupons for JBR and Ductwork"

Southern Company Services, Inc.

Southern Company Services Inc
Post Office Box 2625
Birmingham, Alabama 35202
Telephone 205 870-6011

Southern Company Services
the southern electric system

August 22, 1991

To: David Washke, Ershigs
Simon Scott, Ashland Chemical Company

From: Kamyar Vakhshoorzadeh, SCS

Re: Abrasion and Corrosion Coupons for JBR and Ductwork

Gentlemen

Please review the proposed designs for abrasion and corrosion coupons for JBR reaction zone, gas inlet (post-quench), duct area (pre-quench), and exhaust plenum.

1. Corrosion Testing

Corrosion coupons for JBR reaction zone, gas inlet area, and exhaust plenum are shown in Figure 1. The coupon construction schedules are also shown in Figure 1. The test samples are to be flat plates to be installed on pre-fabricated racks using tie-wraps or Fiberbolt. Suggested assembly and rack design for the test coupons are shown in Figures 2, 3, and 4. Figure 3 shows the mounting plate for the all the corrosion coupons to be tailored to the location of testing.

Overall, I expect to install 80 to 100 samples at each location. The current request deals only with samples that are fabricated using Ashland Chemical Hetron Series resins. However, SCS may include, in the corrosion monitoring task, test coupons that are made of pultruded FRP, untested future resins from different manufacturers, and exotic alloys (C276, C22).

I don't have data concerning the overall velocity profile in the vessel. However, based on my discussions with SCS colleagues, I believe that the agitator establishes a downward flow near the center of the vessel and an upward flow near the vessel walls (Figure 4). Because of high slurry viscosity, the boundary layer is expected to be fairly large. This means that the near-wall flow velocities are small in comparison to main agitator velocity. Therefore, the corrosion samples are not expected to experience any abrasion. Please let me know if you have any information that can verify this.

We had not discussed samples in the exhaust plenum or pre-quench areas. However, I am told that the chlorine concentration in JBR is nearly 14000-15000 ppm. The exhaust gas may carry some concentration of chlorine to this chamber. Therefore, the exhaust plenum may also be a good candidate for corrosion testing. Furthermore, for future reference, it is appropriate to include high-temperature FRP coupons for testing in the pre-quench ductwork.

2. Abrasion Testing:

The abrasion samples are designed to provide maximum consistency in terms of impact on flow parameters: velocity profile and boundary layer, velocity gradients and shear rates at the test sample surface, surface temperatures, and chemistry. This condition provides an experimental platform for comparing abrasion resistance of different materials without additional theoretical modeling. The samples are also designed for easy installation and retrieval.

Both the pre-quench and post-quench samples may experience significant abrasion during the proposed high-ash loading period. It is therefore essential that the fasteners be designed to out-perform the abrasion samples.

a) Reaction Zone

The test samples for JBR reaction zone are half cylinders (Figure 5) to be joined together around the structural columns to form a full cylinder (Figure 6). Figure 5 also gives the construction schedule for the abrasion tests coupons in the reaction zone.

The samples are to be constructed of 10 layers of specified construction, each nearly 10 mils thick. The layers will be pigmented to establish a black-white-black-..-black-white color code sequence. The color code will be used for measuring the abrasion depth.

The current drawings are not showing the OD dimension on the support columns. So, please fill in the information lacking and send it back to me for final review.

The designs are believed to have negligible impact on the flow patterns around the supports. The four tabs, laminated on the four corners of each coupon section, will be used to assemble the two cylindrical halves around the existing support columns (Figure 6). Some of the samples will be assembled around the supports closest to the agitator. These samples will be used to gage the effects of different resin fillers. The four smaller supports that are farthest from the agitator tip (Figure 7), will be used to determine the effects of different resins. Standard pultruded 3/8" FRP fasteners will be used to assemble the coupons.

The samples are to be installed right across from the agitator tip. This was reported to be the primary location of abrasion on the structural columns in the Abbott Vessel.

b) Post Quench Zone

The proposed abrasion test samples are shown in Figure 8. These will be installed on the structural columns supporting the cutout section of the vessel (gas inlet area).

The construction of the test coupons is similar to those used in the JBR reaction zone. The samples will be 6" wide. Just as in the JBR samples, the current drawings are missing the OD dimension on these

columns. So, please fill in the information lacking and send it back to me for final review. The samples are to be constructed of 10 layers of specified construction, each nearly 10 mils thick. The layers will be pigmented to establish a black-white-black- .. - black-white color code sequence. The color code will be used for measuring the abrasion depth. The test samples are secured in their place using standard pultruded FRP fasteners (Figure 6).

Five samples of each construction schedule will be randomly distributed on the columns located at the gas inlet area. However, two of the seven supports, which are partially masked by the flow around the duct support columns (Figure 9), will not have any samples attached.

c) Pre-quench Zone

These samples are to be assembled around the support columns located in the steel ductwork preceding the quenching system. The test sample construction will be similar to other abrasion samples. However, these samples will be secured around the support poles by means of stainless steel bands. The ID of the test samples is not currently known and will be provided at a later time. The gas temperature in this area requires will require a choice of high temperature resin. Could you provide me with a list of suggested resin and reiforcment for abrasion and corrosion monitoring.

I request that the corrosion sample mounting racks for the reaction zone, and the inlet and outlet plenums be installed prior to Ershigs departure from the field. The corrosion samples will be installed at a later time, after all the test samples are fabricated and cataloged. The abrasion samples can also be installed at a later time.

I appreciate your time and assistance in reviewing the attached drawings. I'd like to also add that Ms. Donna Hill of SCS R&EA will be assisting me in the Plant Yates corrosion and abrasion monitoring and evaluation tasks. She will be responsible for organizing all the field activities under this subtask. She can be reached at (205) 868-5234. Please feel free to call me if you have any comments or suggestions.

Sincerely

Kamyar Vakhshoorzadeh

Kamyar Vakhshoorzadeh
Senior Research Engineer

CC: (w/att.)

Southern Company Services
D. M. Boylan
D. P. Burford
Donna Hill

Georgia Power Company
R. M. Rhodes

FIGURE 5: IMMERSION SAMPLES

ABRASION SAMPLES FOR JBR REACTION ZONE POSTS

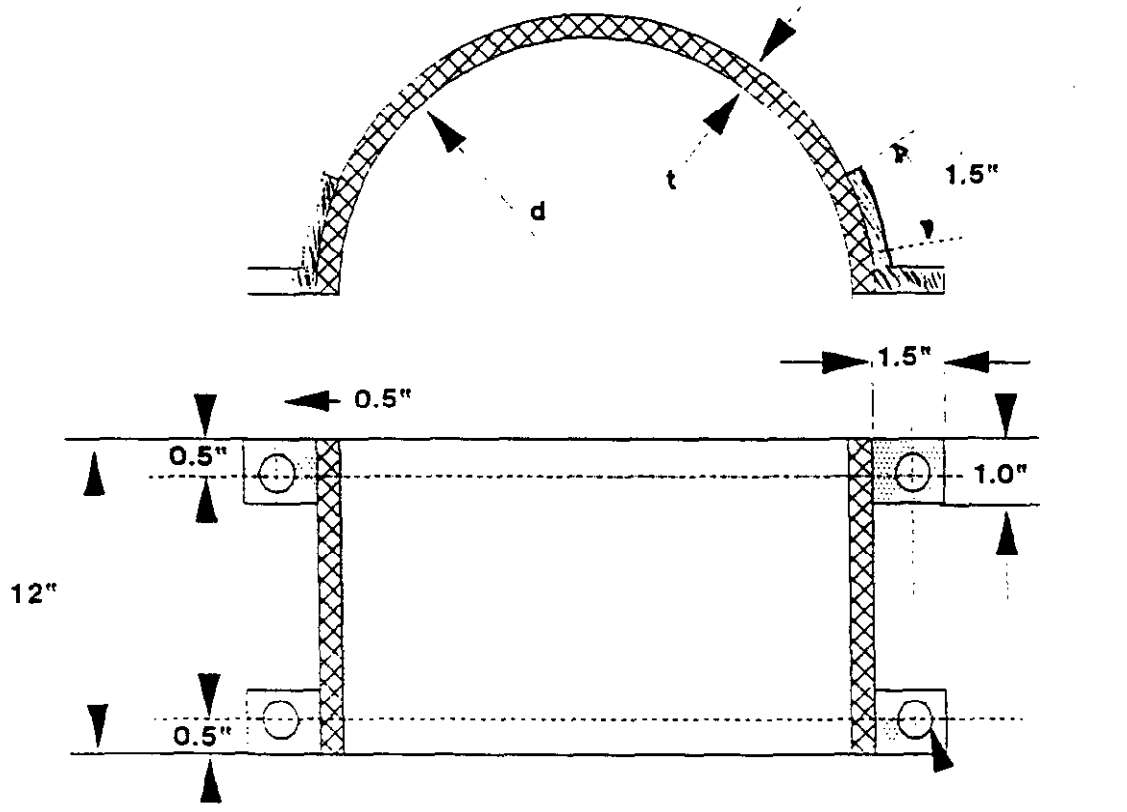

DRILL FOR 3/8"-16 UNC
FIBERBOLT

location	d	t	resin	construction	quantity
near supports			FR992	"C" veil	6
				carbon veil	6
				carbon veil + milled fibers	6
				Ershigs fufu dust	6
far supports			FR992	carbon veil + milled fibers	6
			FR992 +	carbon veil + milled fibers	6
			FR992 An.	carbon veil + milled fibers	6

FIGURE 1: CORROSION SAMPLES FOR JBR REAC. ZONE, INLET AND EXHAUST PLENUMS, AND PRE-QUENCH DUCT AREA.

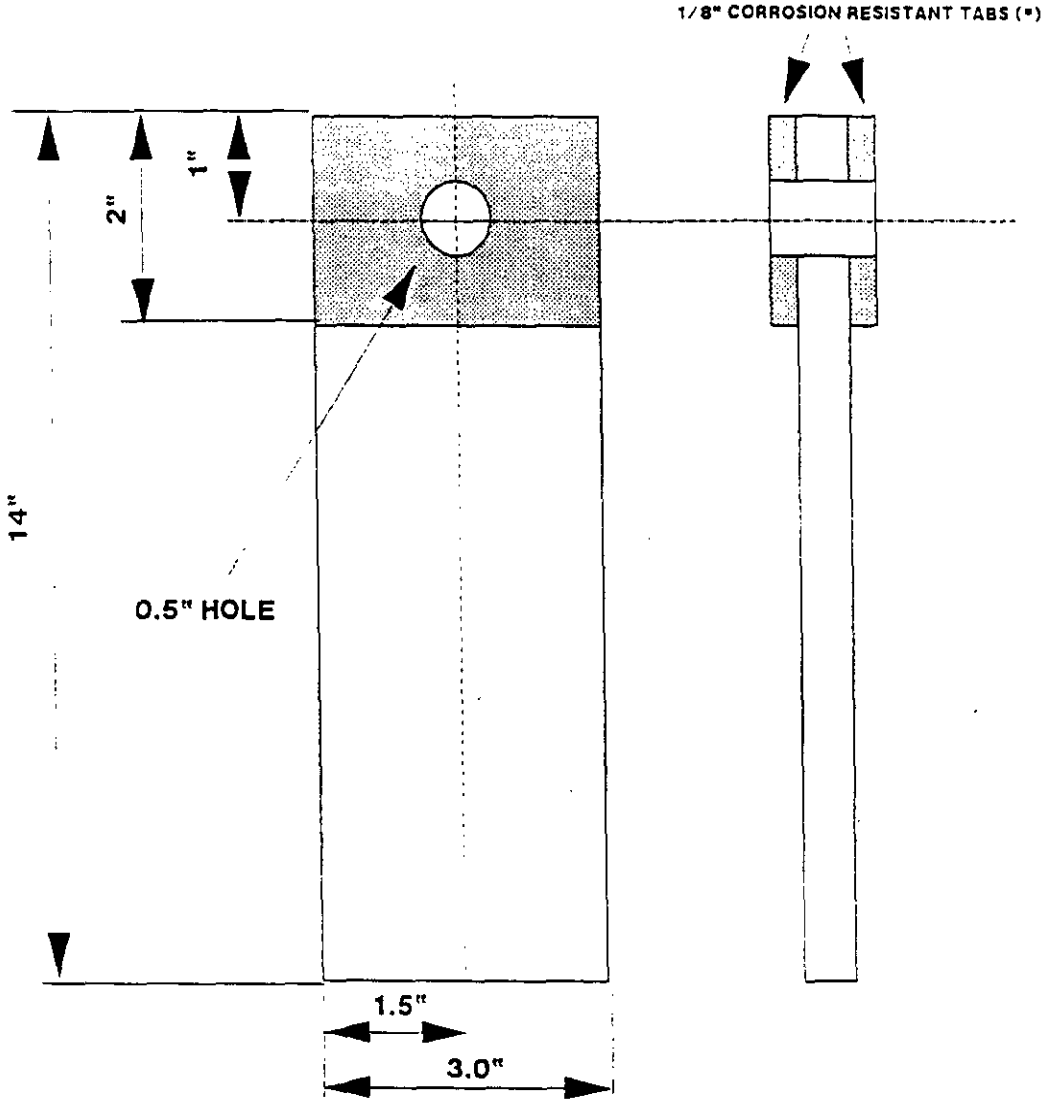

resin	construction	quantity
FR992	VMMV (M=GLASS MAT, V=GLASS VEIL)	24
	CARBON VEIL	24
	CARBON VEIL,MM,CARBON VEIL	24
	CARBON VEIL/MILLED, MM, CARBON VEIL/MILLED	24
FR992 +	VMMV	24
	CARBON VEIL/MILLED, MM, CARBON VEIL/MILLED	24
FR992 AN.	VMMV	24
	CARBON VEIL/MILLED, MM, CARBON VEIL/MILLED	24

* NOTE FOR ERSHIGS: PLEASE ADD ANY OTHER COMBINATIONS THAT MAY BE USED AT WANSLEY, OR ANY COMBINATION THAT YOU CONSIDER APPROPRIATE.

FIGURE 8: POST-QUENCH ABRASION SAMPLES

ABRASION SAMPLES FOR SUPPORT POSTS AT THE JBR INLET

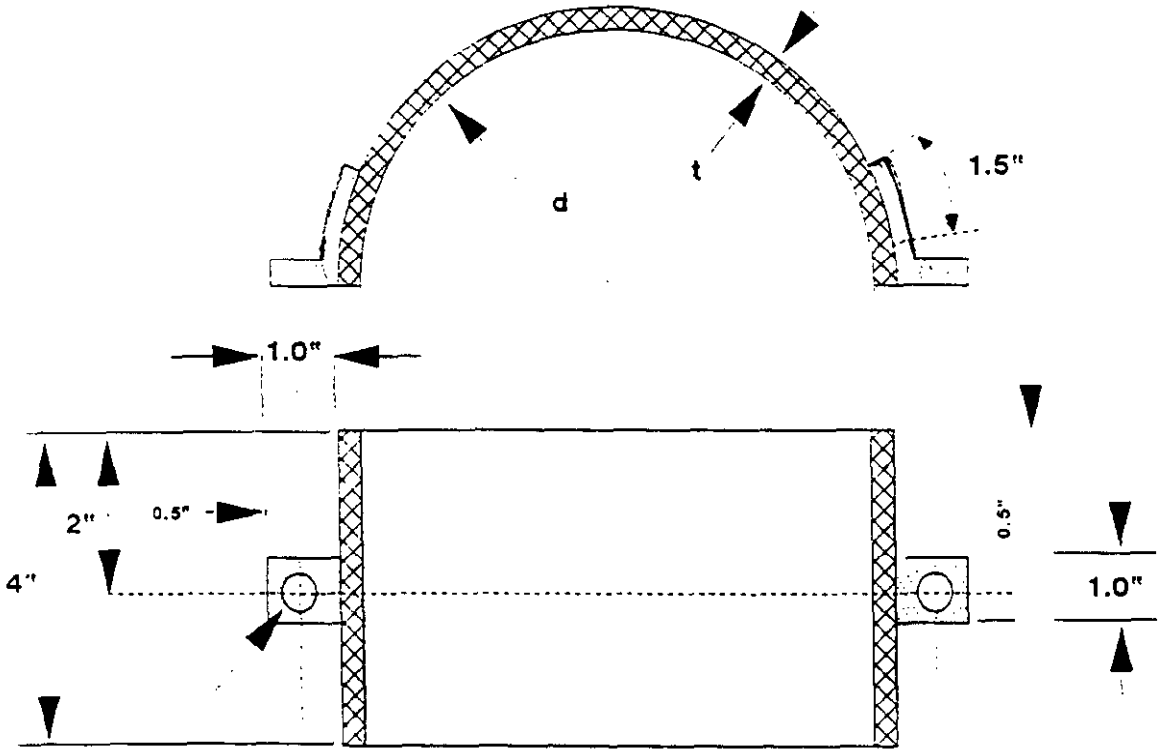

— DRILL FOR 3/8"-16 UNC FIBERBOLT

location	d	t	resin	construction	quantity
SUPPORT POSTS AT THE JBR INLET		*	FR992	"C" veil	6
		*		carbon veil	6
		*		carbon veil + milled fibers	6
		*		Ershigs fufu dust	6
		*	FR992 +	"C" veil	6
		*		carbon veil + milled fibers	6
		*		Ershigs fufu dust	6
		*	FR992 An.	"C" veil	6
		*		carbon veil + milled fibers	6
		*		Ershigs fufu dust	6
		*	197AT-T	"C" veil	6
		*		carbon veil + milled fibers	6
		*		Ershigs fufu dust	6

* 10 layers of veil in this series. layers are to be color coded B/W/B/W/...., (B=Black, W=White) to allow visual checking of abrasion.

FIGURE 3: SPACING OF THE HOLES ON THE SAMPLE MOUNTING BRACKETS

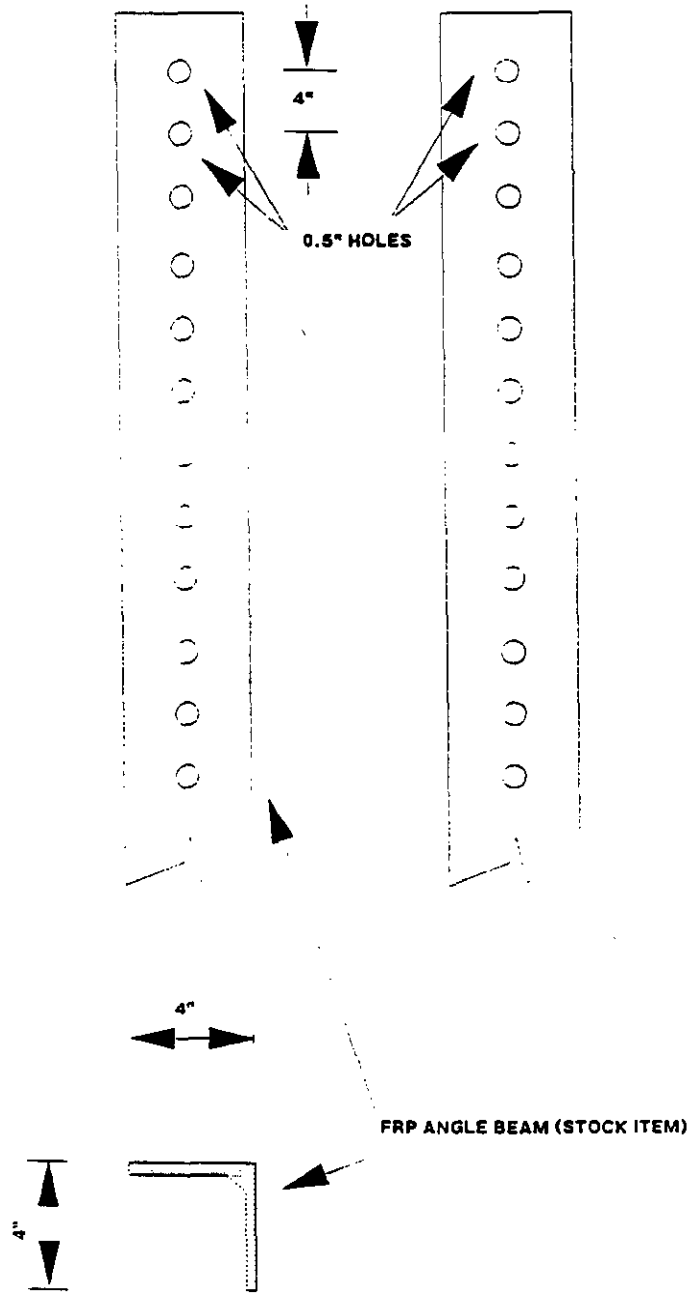

MAT. SPEC.	LOCATION	DESIRED LENGTH	QUANTITY
FRP STD. BRACKET	REACTION ZONE	CUT TO SPACING OF THE PIPING SUPPORTS	4
	INLET PLENUM	10 FT	2
	EXHAUST PLENUM	10 FT	2

FIGURE 2: ASSEMBLY OF CORROSION SAMPLES IN JBR REACTION ZONE

SAMPLES IMMERSED IN CHLORINE-LADEN (14,000 PPM) SLURRY OF GYPSUM AND LIMESTONE.

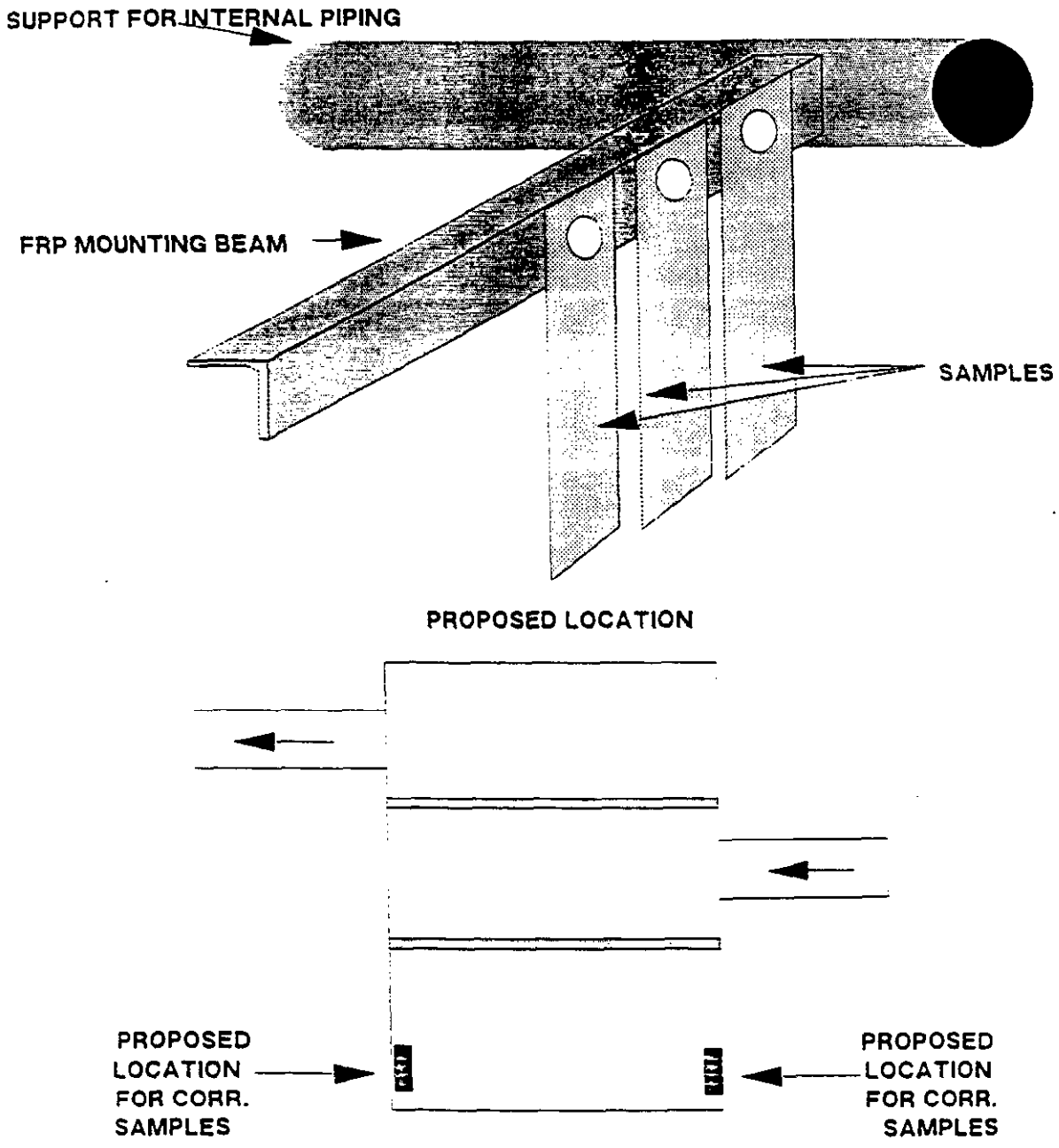

CRITERIA FOR LOCATION:

EASY TO REACH
AWAY FROM MAIN FLOW
SUSPENDED IN LIQUID SLURRY

FIGURE 4a: ASSEMBLY OF SAMPLES IN THE INLET PLENUM

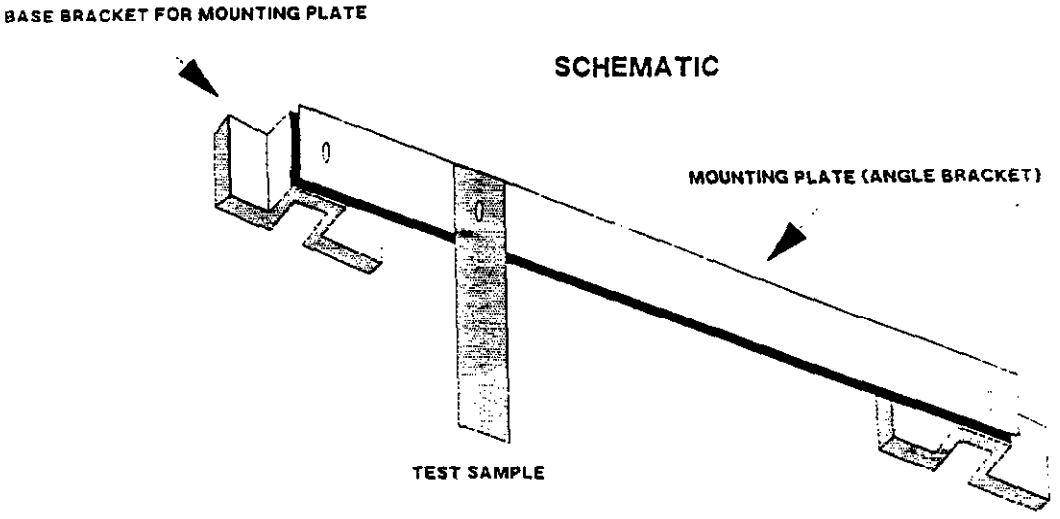

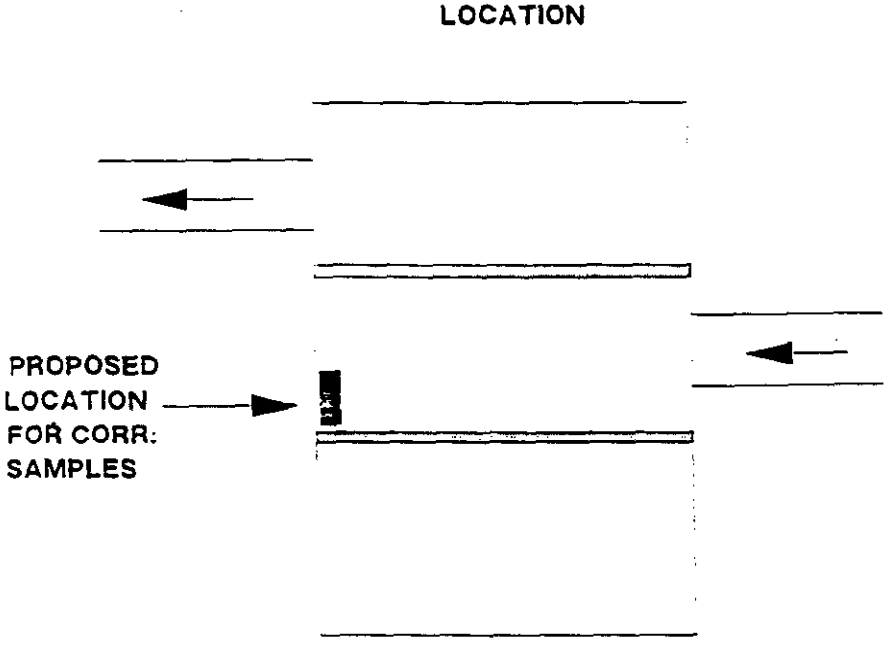

CRITERIA FOR LOCATION:

EASY TO REACH
AWAY FROM MAIN FLOW
ABOVE DECK WASH PIPING

FIGURE 4b: ASSEMBLY OF SAMPLES IN THE EXHAUST PLENUM

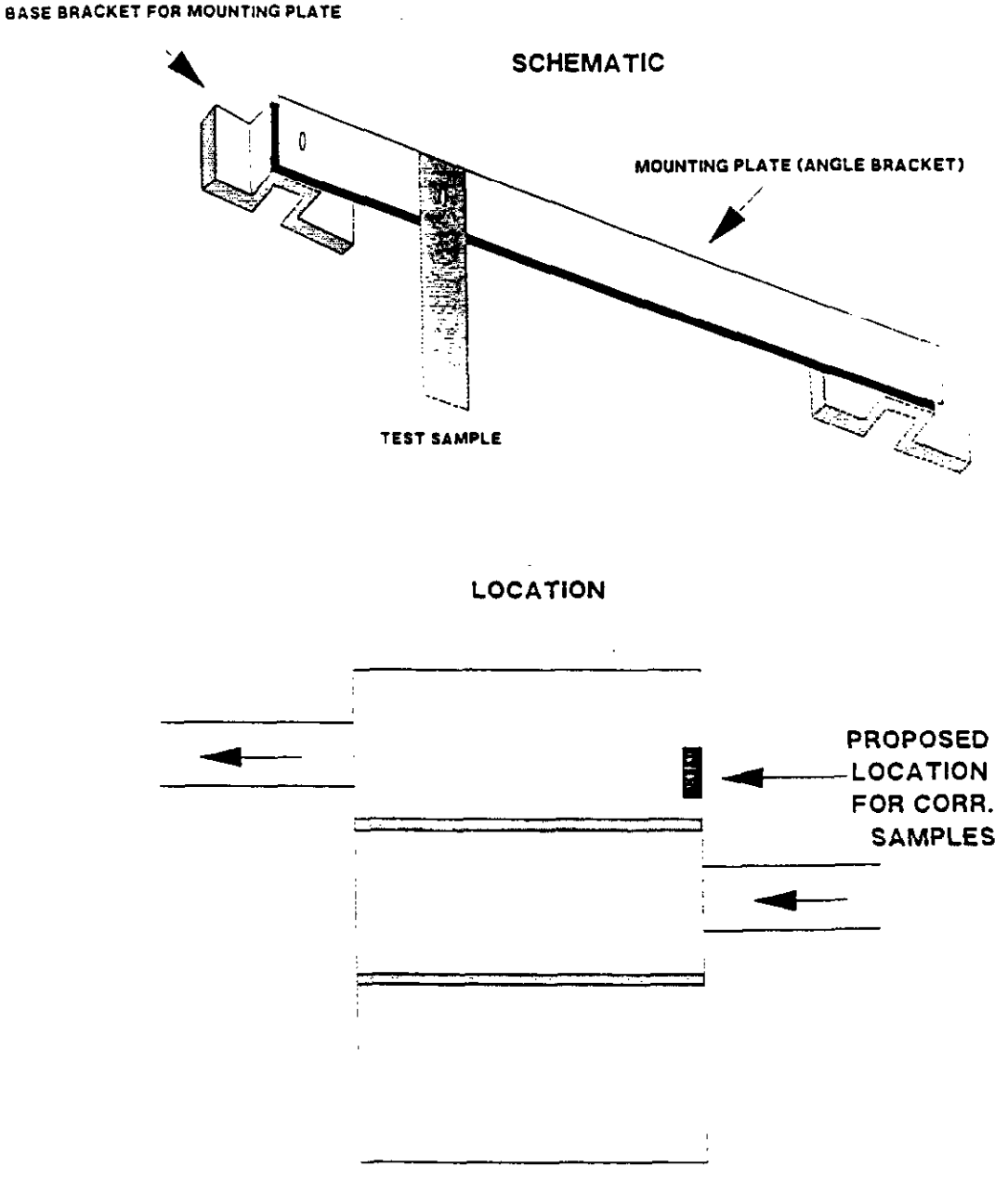

CRITERIA FOR LOCATION:

EASY TO REACH
AWAY FROM MAIN FLOW
ABOVE DECK WASH PIPING

Figure 3: ASSEMBLY OF THE ABRASION SAMPLES IN THE JBR REACTION ZONE

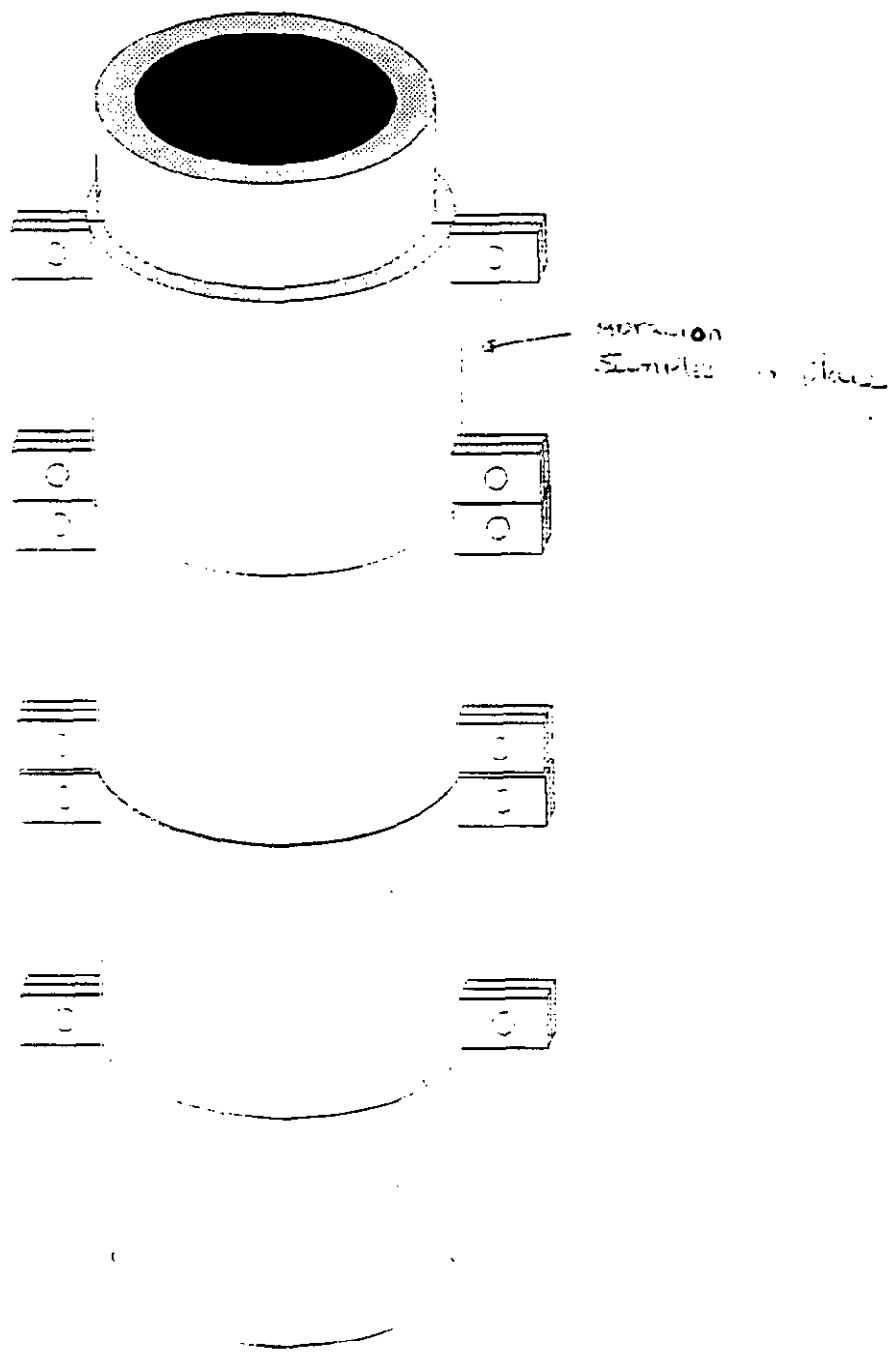

FIGURE 7: VELOCITY PROFILE IF NO SPARGER TUBES WERE PRESENT. VELOCITY NEAR WALL AREA IS PROBABLY VERY SMALL BECAUSE OF VISCOSITY. BOUNDARY LAYER THICKNESS IS ALSO EXPECTED TO BE LARGE. SO VELOCITY GRADIENT IS FLOW SHEAR RATES ARE ALSO SMALL. WITH THE SPARGER TUBES, THE FLOW PATTERN IS NOT KNOWN. THE FLOW IS, HOWEVER, EXPECTED TO BE SMALL NEAR THE VESSEL WALL.

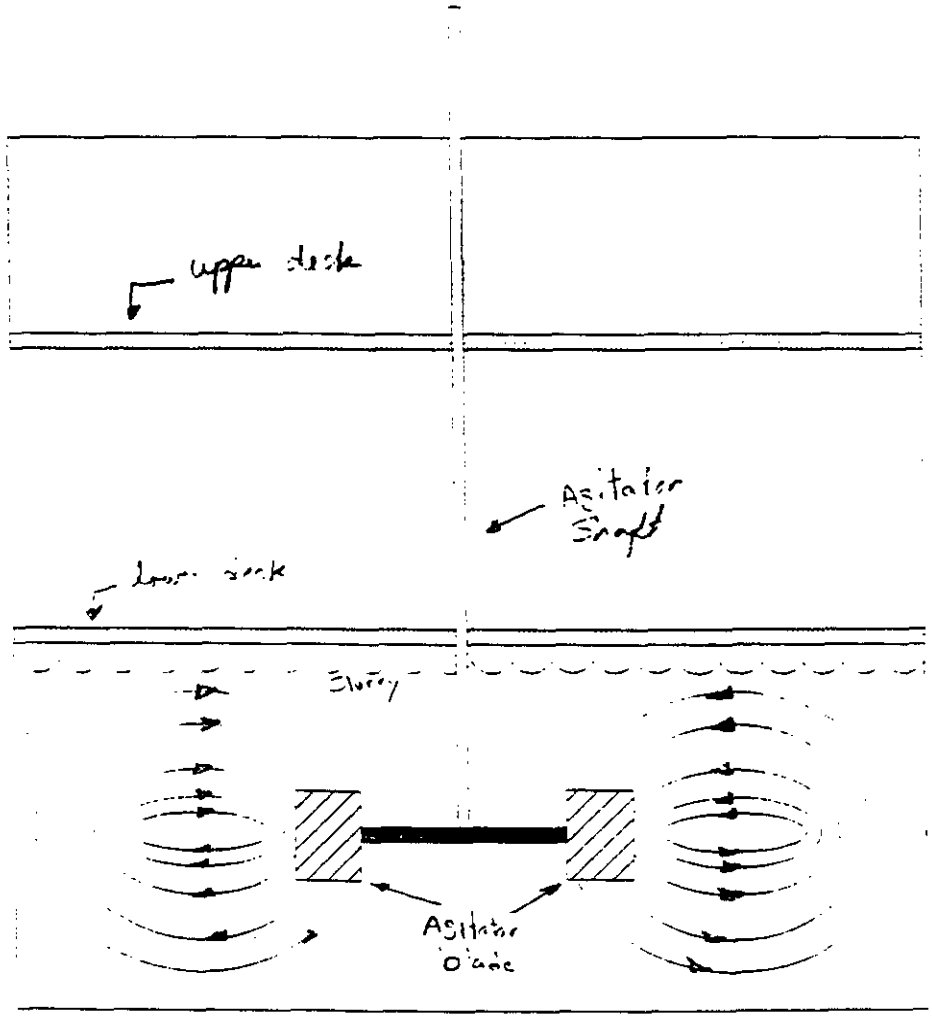

Figure 9:

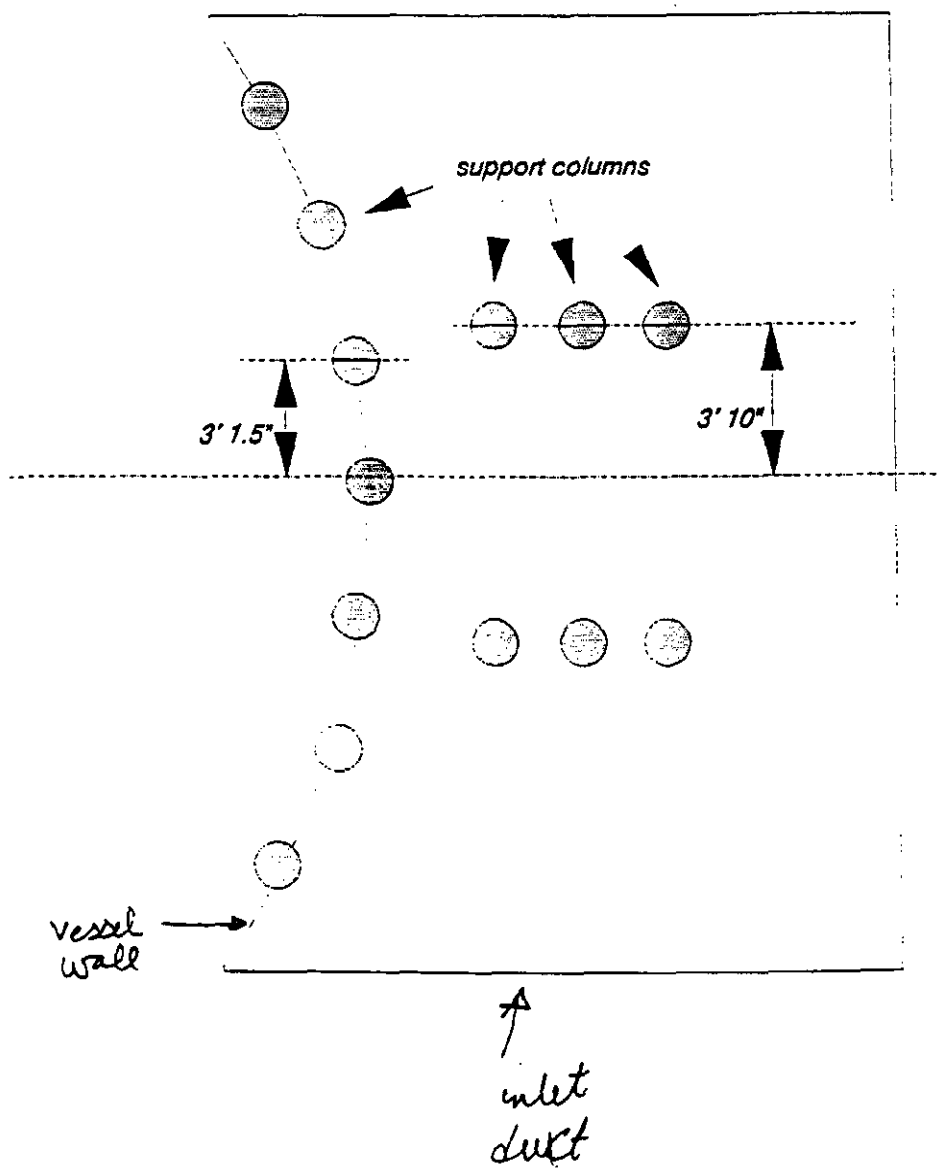

Attachment B

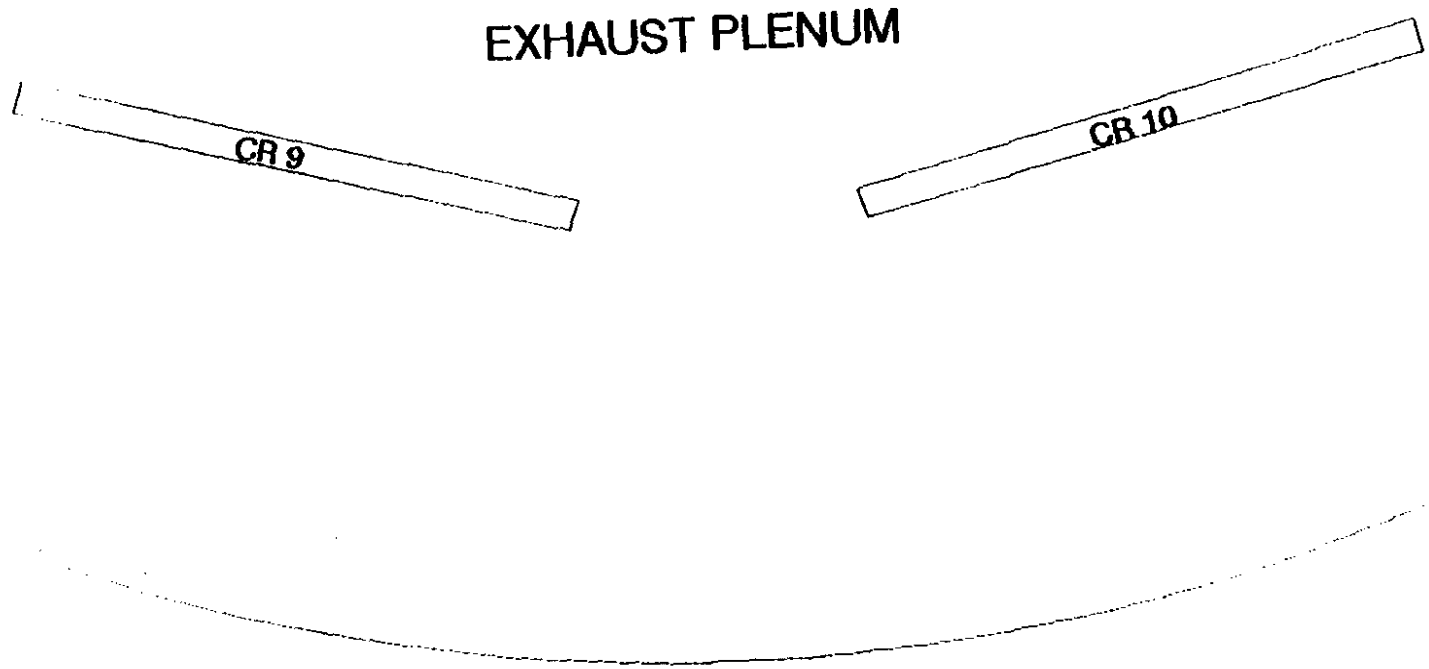

CR 9 (left to right)
163, 164, 165, 166, 167, 168, 169, 170, 171, 172, 173, 174, 175, 176, 177, 178, 179,180, 181, 182, 183, 184, 185, 186

CR 10 (left to right)
187, 188, 189, 190, 191, 192, 193, 194, 195, 196, 197, 198, *205, 206, 207, 208, 209, 210, 211, 213, 213, 214, 215, 216

ACCESS DOOR

NOTCHING CORROSION SAMPLES

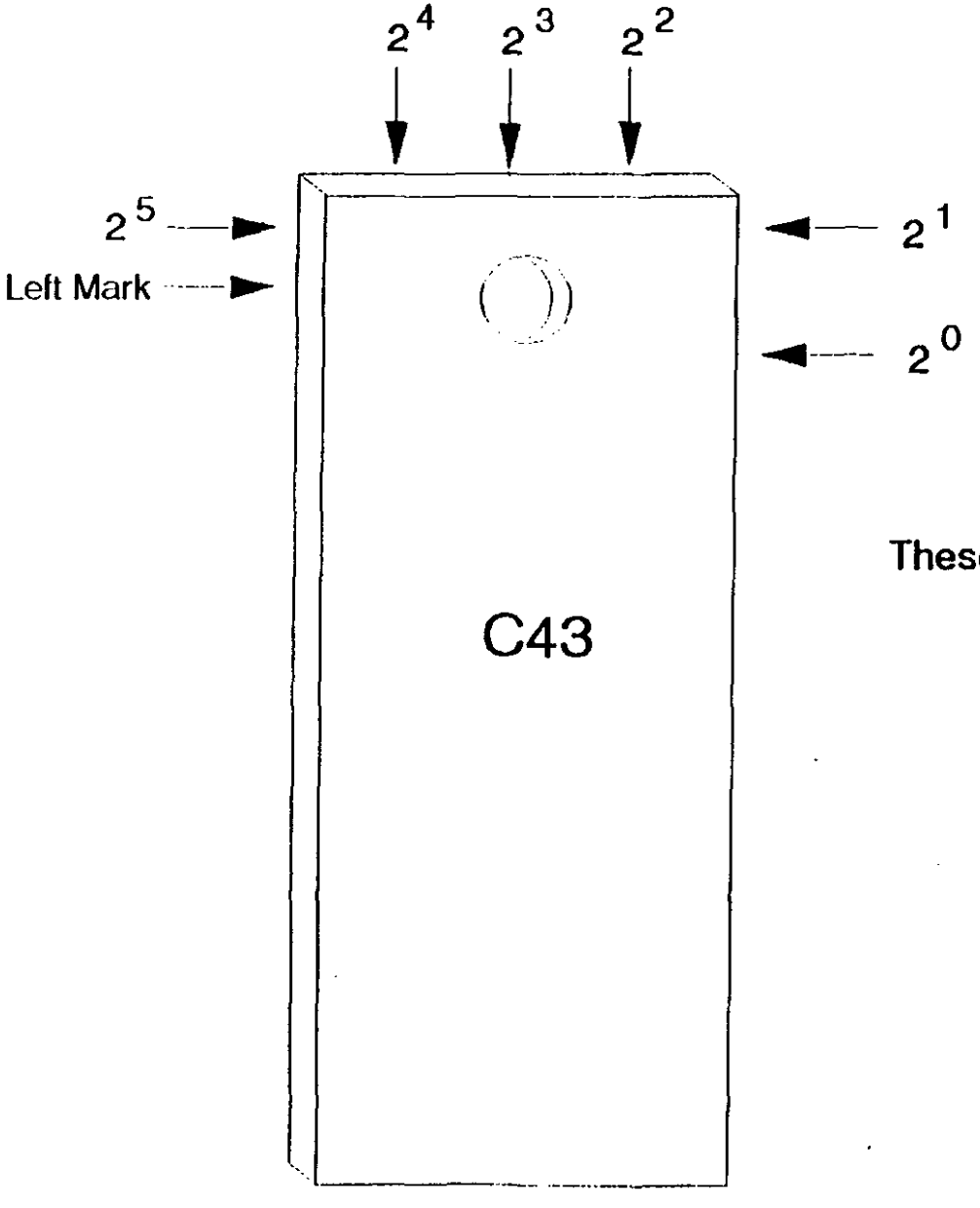

These notches should be read as:
1 + 2 + 8 + 32 = 43

Notch / Cut

FIGURE 1

NOTCHING ABRASION SAMPLES

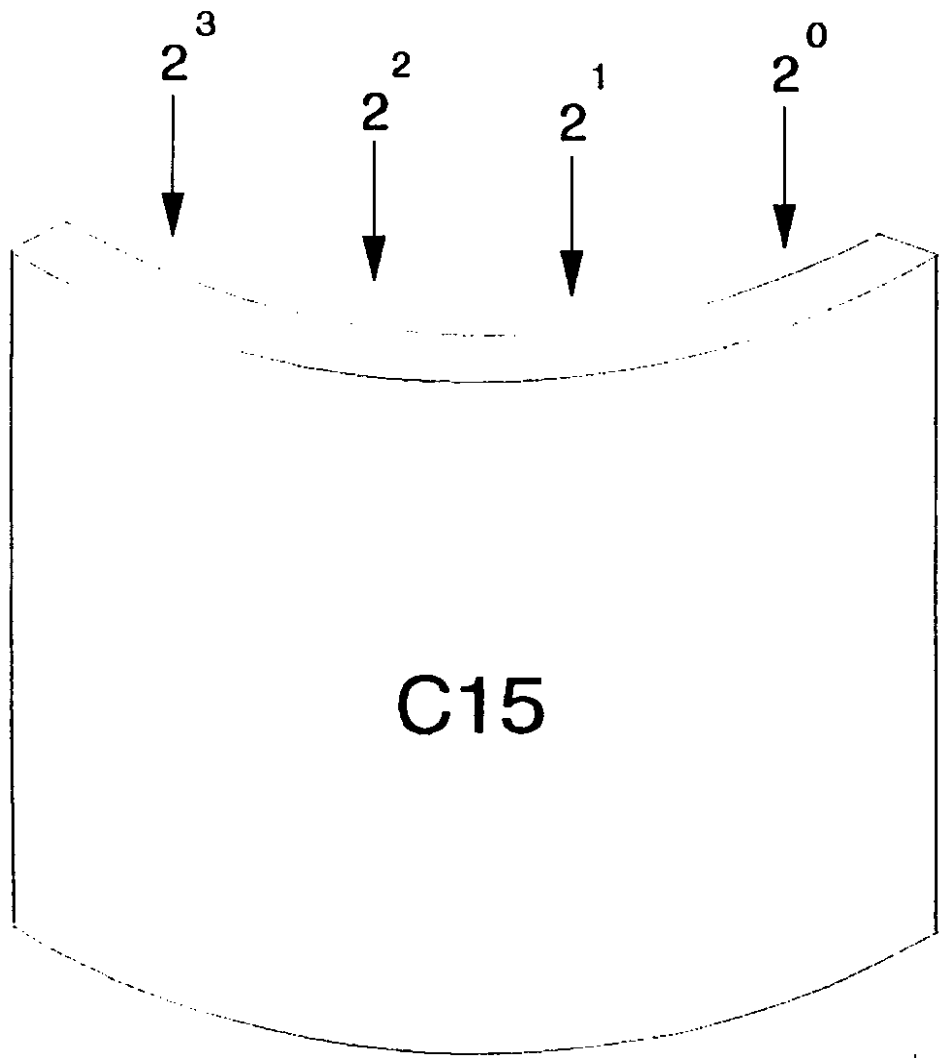

These notches should be read as:

$1 + 2 + 4 + 8 = 15$

Notch / Cut

FIGURE 2

NOTCHING ABRASION SAMPLES

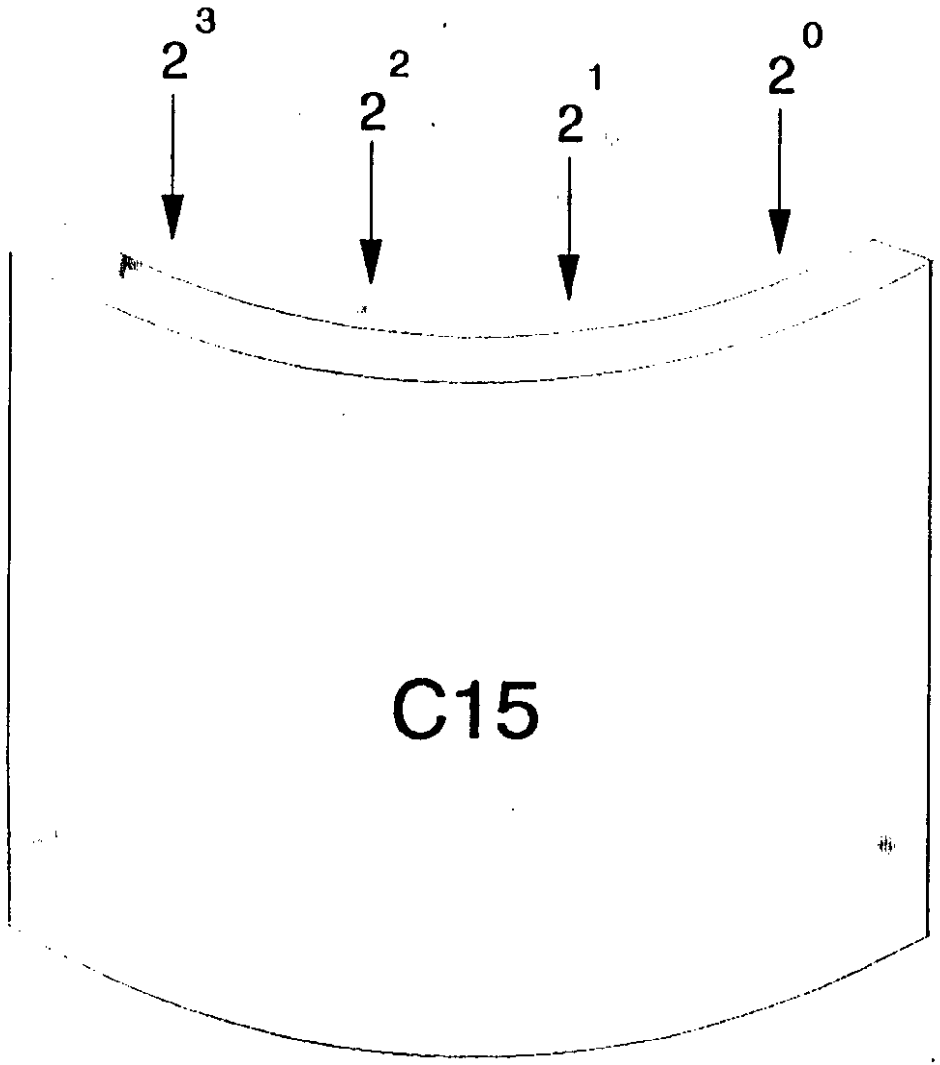

These notches should be read as:

$1 + 2 + 4 + 8 = 15$

Notch / Cut

NOTCHING CORROSION SAMPLES

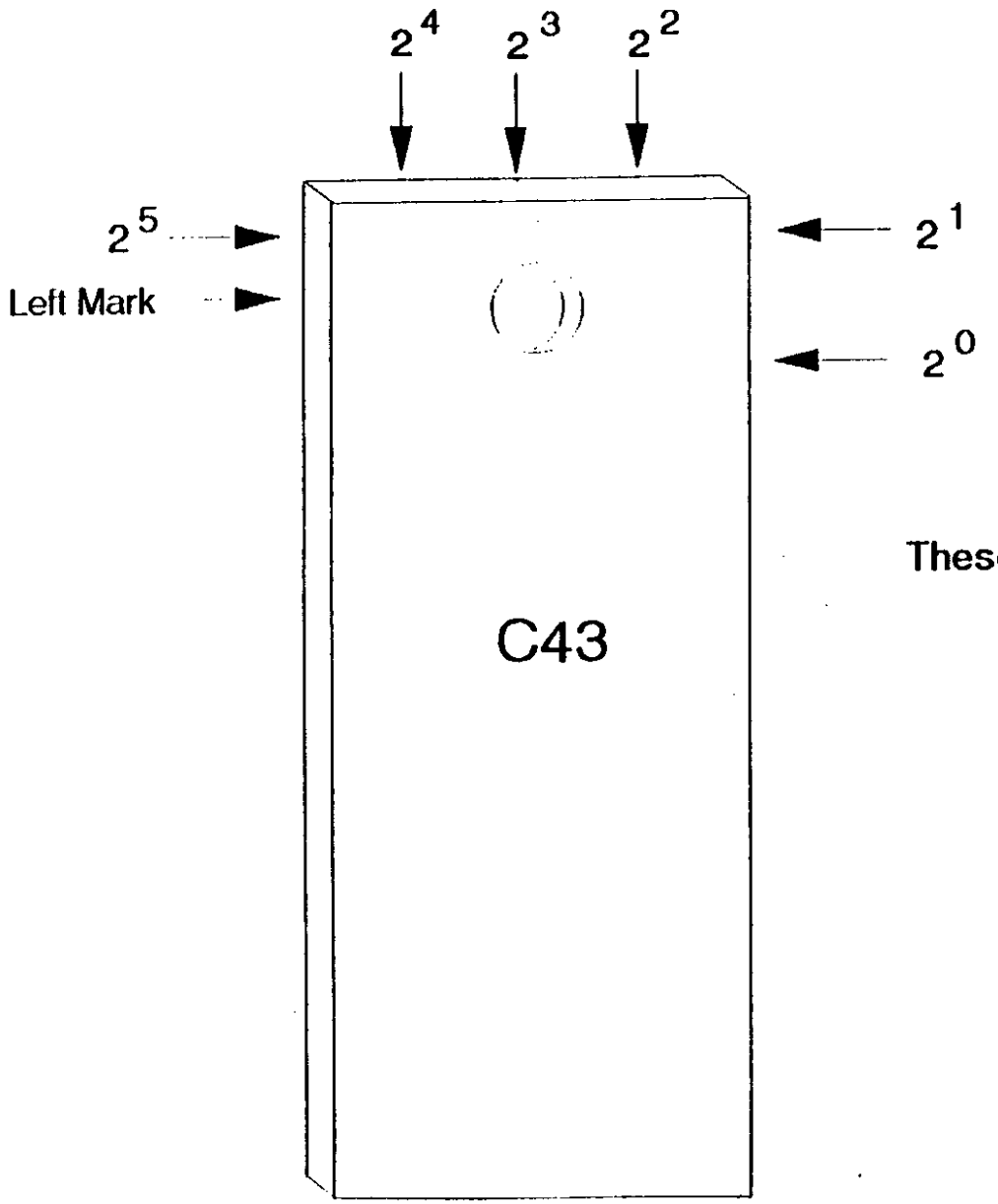

These notches should be read as:
1 + 2 + 8 + 32 = 43

Notch / Cut

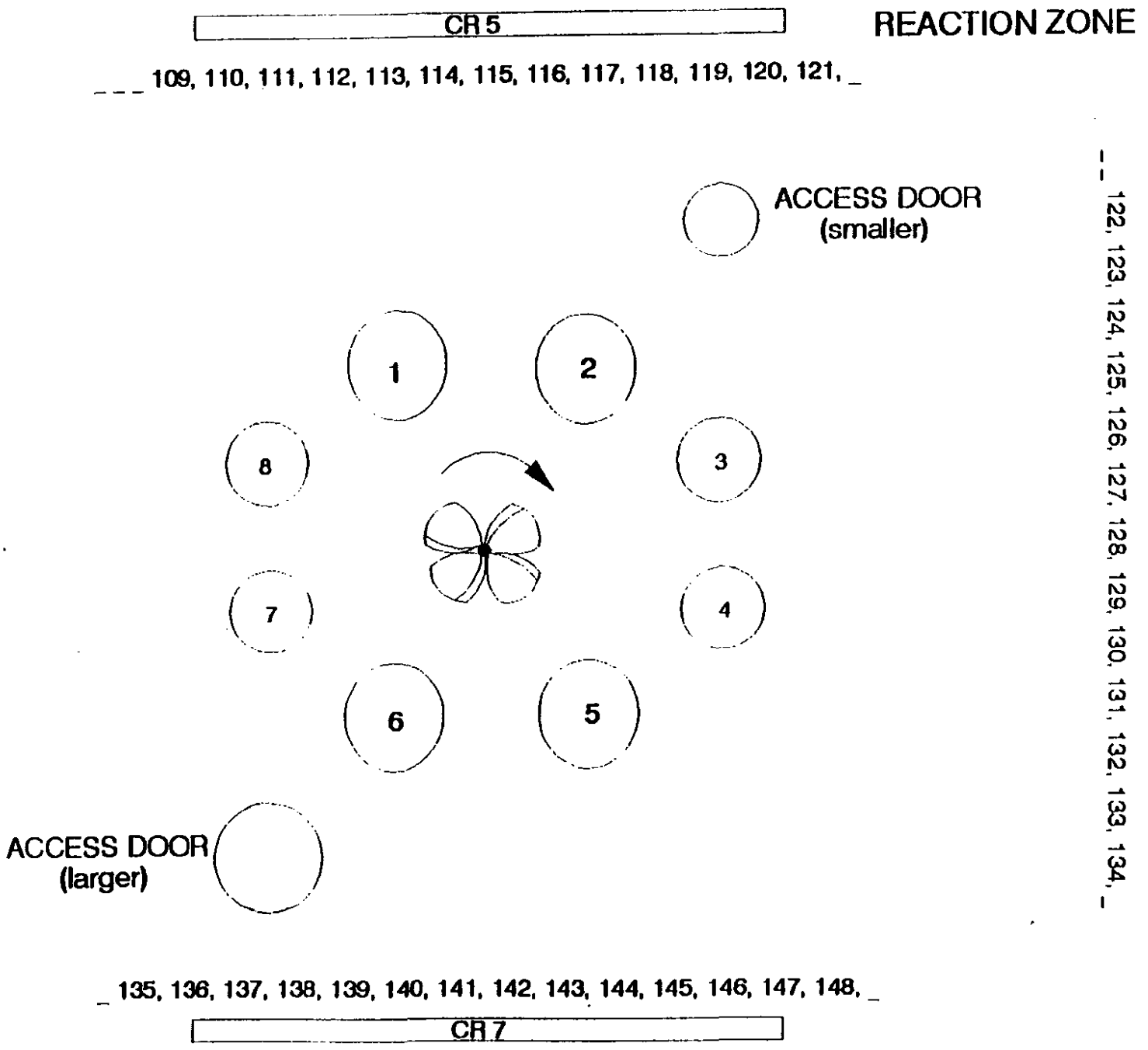
CR 5
REACTION ZONE
109, 110, 111, 112, 113, 114, 115, 116, 117, 118, 119, 120, 121,
122, 123, 124, 125, 126, 127, 128, 129, 130, 131, 132, 133, 134,
CR 6
149, 150, 141, 152, 153, 154, 155, 156, 157, 158, 159, 160, 161, 162
CR 8
ACCESS DOOR
(smaller)
1
2
3
4
5
6
7
8
ACCESS DOOR
(larger)
135, 136, 137, 138, 139, 140, 141, 142, 143, 144, 145, 146, 147, 148,
CR 7

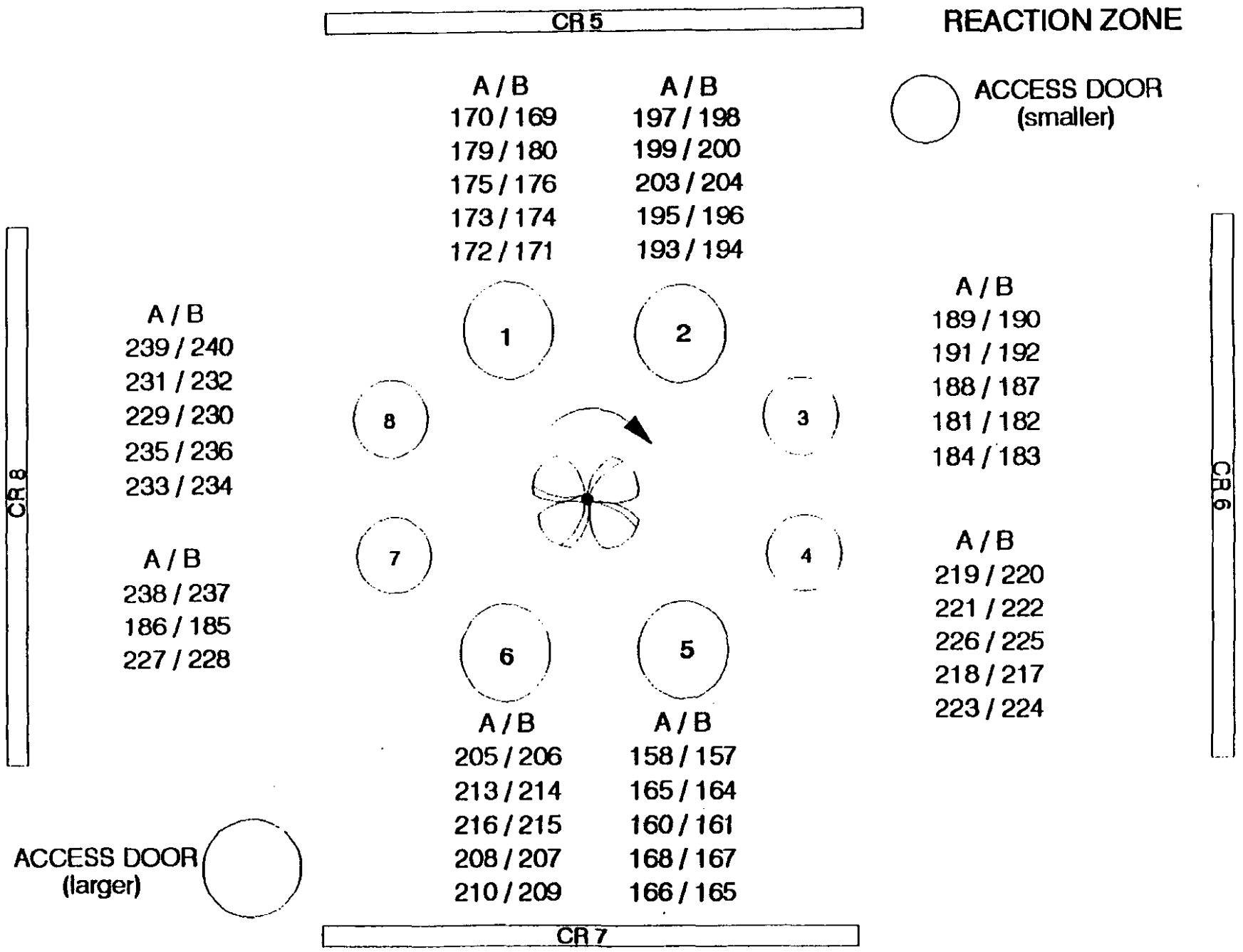
CR 5
REACTION ZONE
ACCESS DOOR
(smaller)
A / B
170 / 169
179 / 180
175 / 176
173 / 174
172 / 171
A / B
197 / 198
199 / 200
203 / 204
195 / 196
193 / 194
CR 8
A / B
239 / 240
231 / 232
229 / 230
235 / 236
233 / 234
A / B
238 / 237
186 / 185
227 / 228
1
2
3
4
5
6
7
8
A / B
189 / 190
191 / 192
188 / 187
181 / 182
184 / 183
A / B
219 / 220
221 / 222
226 / 225
218 / 217
223 / 224
CR 6
ACCESS DOOR
(larger)
A / B
205 / 206
213 / 214
216 / 215
208 / 207
210 / 209
A / B
158 / 157
165 / 164
160 / 161
168 / 167
166 / 165
CR 7

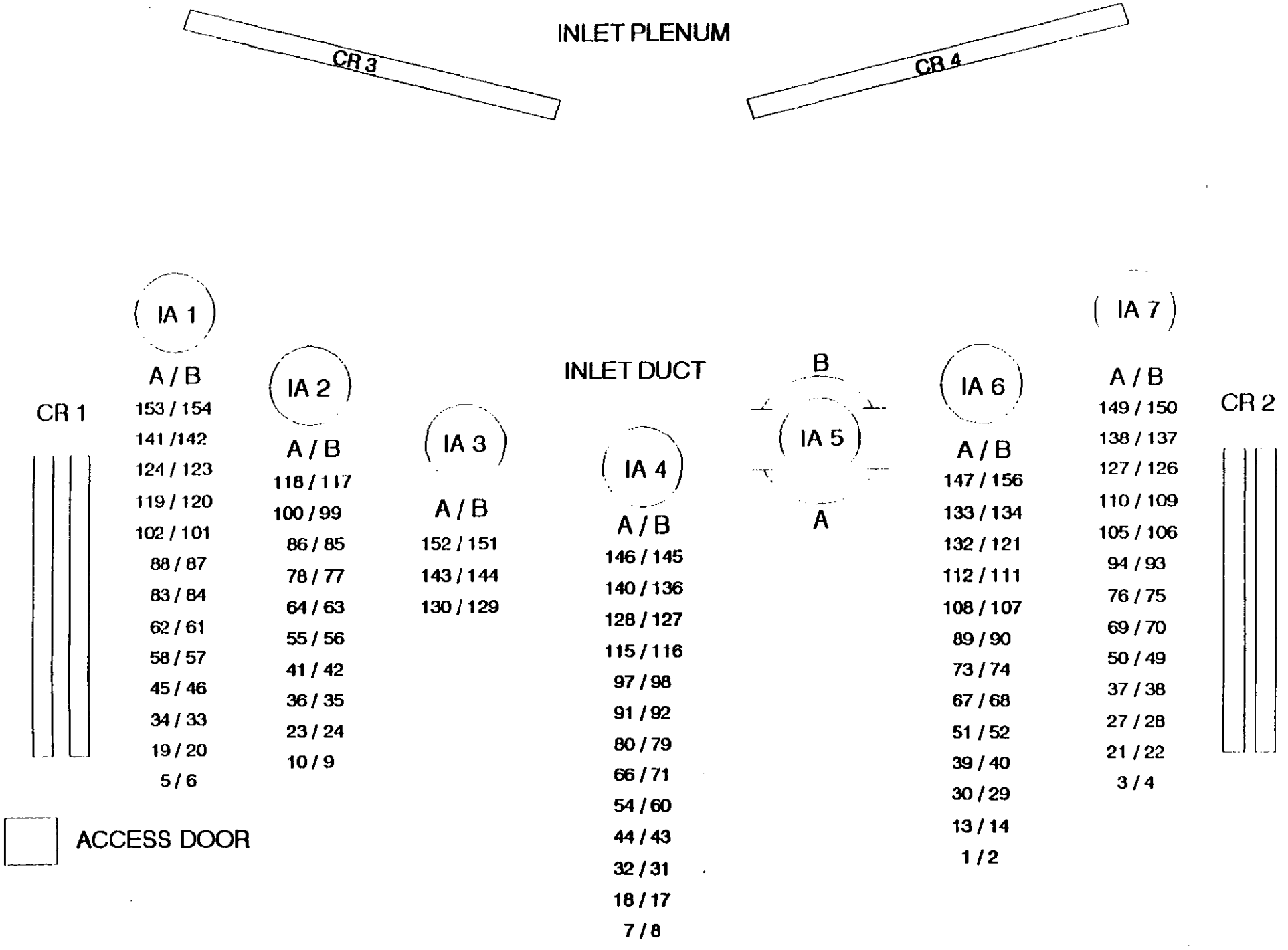
INLET PLENUM
CR 3
CR 4
IA 1
A / B
153 / 154
141 /142
124 / 123
119 / 120
102 / 101
88 / 87
83 / 84
62 / 61
58 / 57
45 / 46
34 / 33
19 / 20
5 / 6
CR 1
IA 2
A / B
118 / 117
100 / 99
86 / 85
78 / 77
64 / 63
55 / 56
41 / 42
36 / 35
23 / 24
10 / 9
IA 3
A / B
152 / 151
143 / 144
130 / 129
INLET DUCT
IA 4
A / B
146 / 145
140 / 136
128 / 127
115 / 116
97 / 98
91 / 92
80 / 79
66 / 71
54 / 60
44 / 43
32 / 31
18 / 17
7 / 8
B
IA 5
A
IA 6
A / B
147 / 156
133 / 134
132 / 121
112 / 111
108 / 107
89 / 90
73 / 74
67 / 68
51 / 52
39 / 40
30 / 29
13 / 14
1 / 2
IA 7
A / B
149 / 150
138 / 137
127 / 126
110 / 109
105 / 106
94 / 93
76 / 75
69 / 70
50 / 49
37 / 38
27 / 28
21 / 22
3 / 4
CR 2
ACCESS DOOR

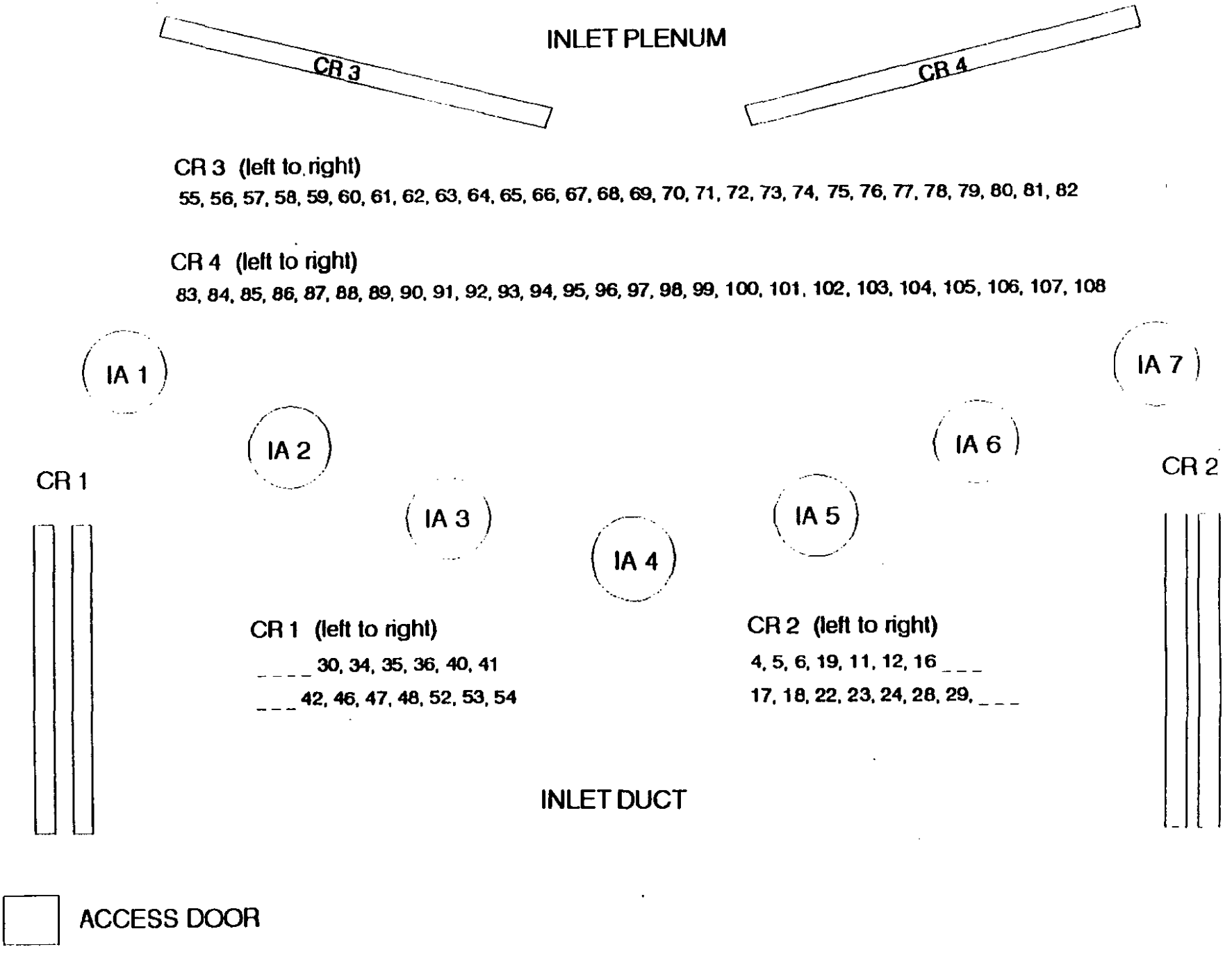
INLET PLENUM
CR 3
CR 4
CR 3 (left to right)
55, 56, 57, 58, 59, 60, 61, 62, 63, 64, 65, 66, 67, 68, 69, 70, 71, 72, 73, 74, 75, 76, 77, 78, 79, 80, 81, 82
CR 4 (left to right)
83, 84, 85, 86, 87, 88, 89, 90, 91, 92, 93, 94, 95, 96, 97, 98, 99, 100, 101, 102, 103, 104, 105, 106, 107, 108
IA 1
IA 2
IA 3
IA 4
IA 5
IA 6
IA 7
CR 1
CR 2
CR 1 (left to right)
_ _ _ _ 30, 34, 35, 36, 40, 41
_ _ _ 42, 46, 47, 48, 52, 53, 54
CR 2 (left to right)
4, 5, 6, 19, 11, 12, 16 _ _ _
17, 18, 22, 23, 24, 28, 29, _ _ _
INLET DUCT
ACCESS DOOR

Southern Company Services, Inc.
Post Office Box 2625
Birmingham, Alabama 35202
Telephone (205) 870-6011

KV

Southern Company Services

The Southern Electric System

March 31, 1993

Mr. David C. Washke
Contract Administrator
Ershigs, Inc.
742 Marine Drive
Bellingham WA 98225

Dear David:

Per our phone conversation, enclosed are photographs of the FRP abrasion phenomenon observed in the FRP duct inlet to JBR. The photographs show the visual abrasion damage in the duct work. The following summarizes our discussions on this topic as well as other SCS concerns:

1. Duct Wall Abrasion: As shown in the pictures, there is significant visual abrasion in the down-comer trough area (downstream of quenching system) and at the duct wall immediately adjacent to the side-wall spray nozzles. In various areas, the depth of abrasion has exceeded the thickness of the protective coating. This is signified by the disappearance of the green coating. It is suspected that the abrasion is caused by the slurry spray from the adjacent nozzles on the top wall.

   The structural integrity of the damaged areas need to be evaluated to determine the type of maintenance that needs to be performed. The least maintenance required would be to resurface the damaged areas with abrasion-resistant coating. This repair should be performed as soon as the scrubber is shut down for maintenance (within the next two to three weeks).

   As we discussed, one goal of the Yates demonstration project is to monitor and report on the performance and longevity of FRP in FGD scrubber environment. The reported abrasion does have the potential to void all benefits from FRP use, if the problem cannot be fixed. Further, the scrubber is about to start a six months continuous operation without any scheduled outage. SCS is eager and interested to perform this task without significant risk to the scrubber and its material of construction. Therefore, the abrasion-resistant coating should be selected to last for a long time.

   If sufficient data does not exist to support the selection of a reliable coating, SCS recommends a sacrificial abrasion-resistant protective plate to be installed around the nozzle area (preferably

with mechanical fasteners), the trough surface, and the structural support columns. These can be replaced on a per-need basis as they wear out. Pete Honeycutt will later transmit a design idea for these protective plates.

2. Limestone Slurry Piping: The 3" limestone slurry pipe has developed a leak at the elbow area, most likely due to severe abrasion of the inner surface. This elbow needs to be replaced during the upcoming maintenance outage. In parallel, other FRP elbows in the limestone and gypsum slurry lines need to be inspected for abrasion to insure their fitness for service.

3. Abrasion of the JBR Wall: There is a concern that surface abrasion may also be occurring on the JBR wall in the reaction zone (across from the agitator blade). As I recall, there is no abrasion protective overlay in this area. However, the protective coating in the reaction zone is also laced with green color dye. There is a need to inspect this area for abrasion damage. However, it may not be possible to drain the vessel for such test. Do you know of any alternative methods?

4. Retrofit FRP Down-Comer: As discussed, the retrofit to reduce vibration of the FRP down-comer needs to be installed during this outage. SCS and Ershigs have already exchanged design ideas on this subject and are in agreement on the modification. For our records, please provide us with a final detail of the design modifications.

5. General Inspection: Based on the general agreement, Ershigs is to perform routine general inspection of the vessel. In conjunction with this outage, SCS requests that Ershigs perform an inspection of the FRP vessels including measurement of Barcol hardness at various strategic sites (including inlet duct). Also, we do not have any record of hardness readings on the unexposed FRP sections. We would appreciate a copy of these records for our internal files.

6. Material Performance Testing: For your information, the following test activities have been planned for the upcoming outage:

   a. Corrosion Monitoring: SCS plans to remove the first batch of corrosion samples from scrubbers. These are samples of Ashland resins Hetron 992, D-1619, and D-1620. New corrosion samples received from DOW Chemical Company (Derakane 470-36) and MMFG will also be installed.

   b. Abrasion Monitoring: To the extent possible, we will monitor and document the abrasion performance of test coupons installed at the gas inlet to JBR and on the structural columns in the reaction zone.

The collected performance data will be reported to DOE and, as appropriate, the participating resin and FRP vendors. Ershigs participation in these tests is most welcome and encouraged, as long as such does not present additional costs or violate existing agreements.

Should you have any comments or questions, feel free to call me at 205/877-7805.

Sincerely,

Kamyar Vakhshoorzadeh

Kamyar Vakhshoorzadeh
Senior Research Engineer
Research & Environmental Affairs

Attachment

cc(w/o att): Southern Company Services
Kerry Bowers
Dave Burford
Pat Evans
Pete Honeycutt

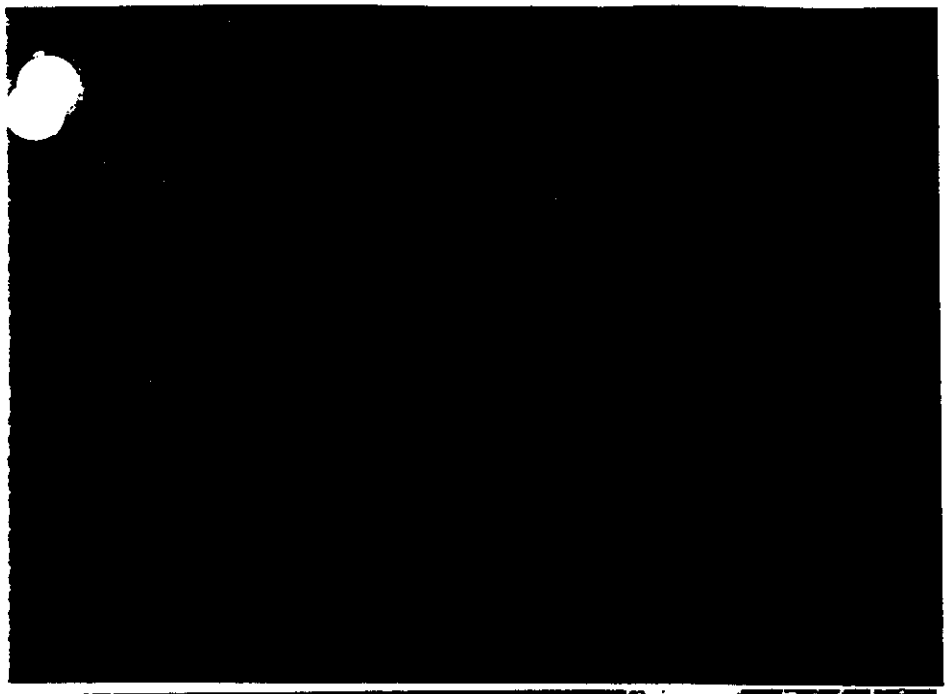

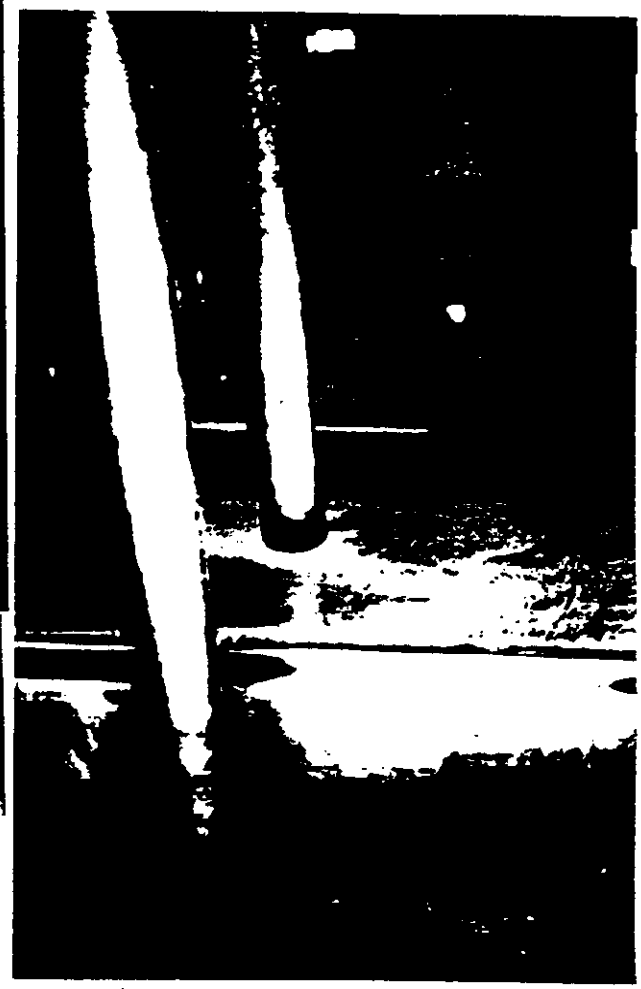

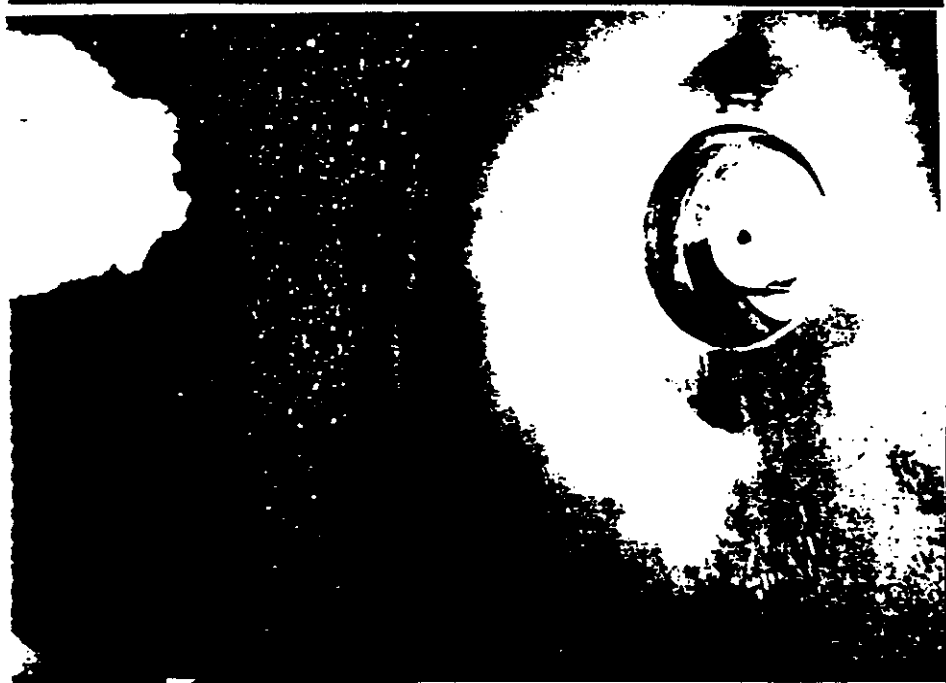

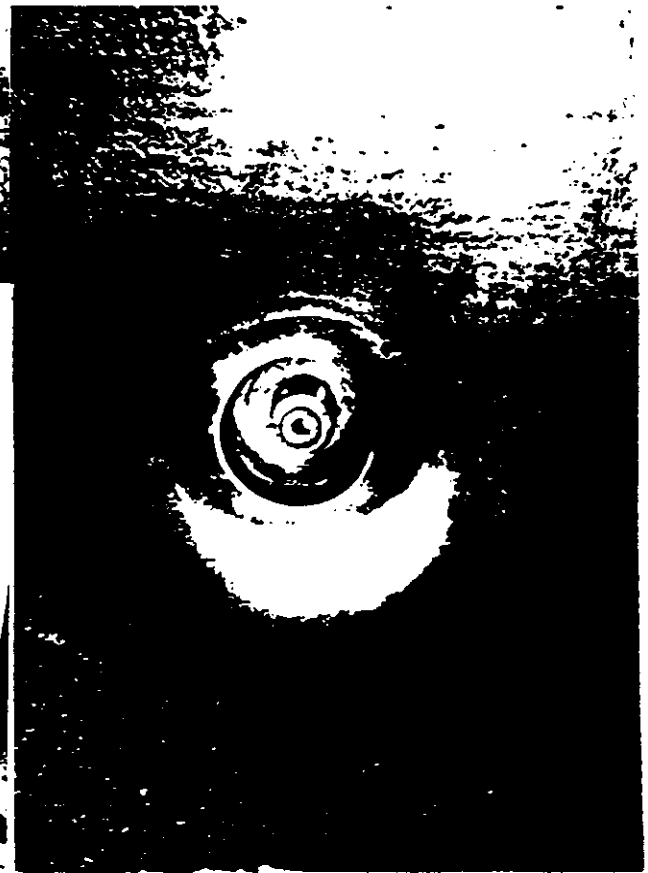

Attachment 1

Table 3

row-wise coupon performance (abrasion depth / average abrasion per row) versus location								
		columns						
rows	material	1	2	3	4	5	6	7
1	M	0.82		1.20	0.71		1.18	1.29
2	L	0.80		1.40	0.91		1.14	1.14
3	K	0.94		1.40	0.94		1.18	0.94
4	J	0.96	0.77		1.15		1.35	0.77
5	I	1.15	0.77		0.96		1.35	0.77
6	H	0.69	0.86		1.20		1.54	0.51
7	G	0.60	1.00		1.20		1.40	0.40
8	F	0.60	1.00		1.20		1.40	0.40
9	E	0.56	1.30		1.48		1.30	0.37
10	D	0.50	1.38		1.38		1.25	0.50
11	C	0.56	1.25		1.53		1.11	0.56
12	B	0.61	1.34		1.34		1.22	0.49
13	A	0.68	1.25		1.25		1.25	0.57
column average		0.73	1.09	1.33	1.17		1.28	0.67

row-wise comparison of abrasion

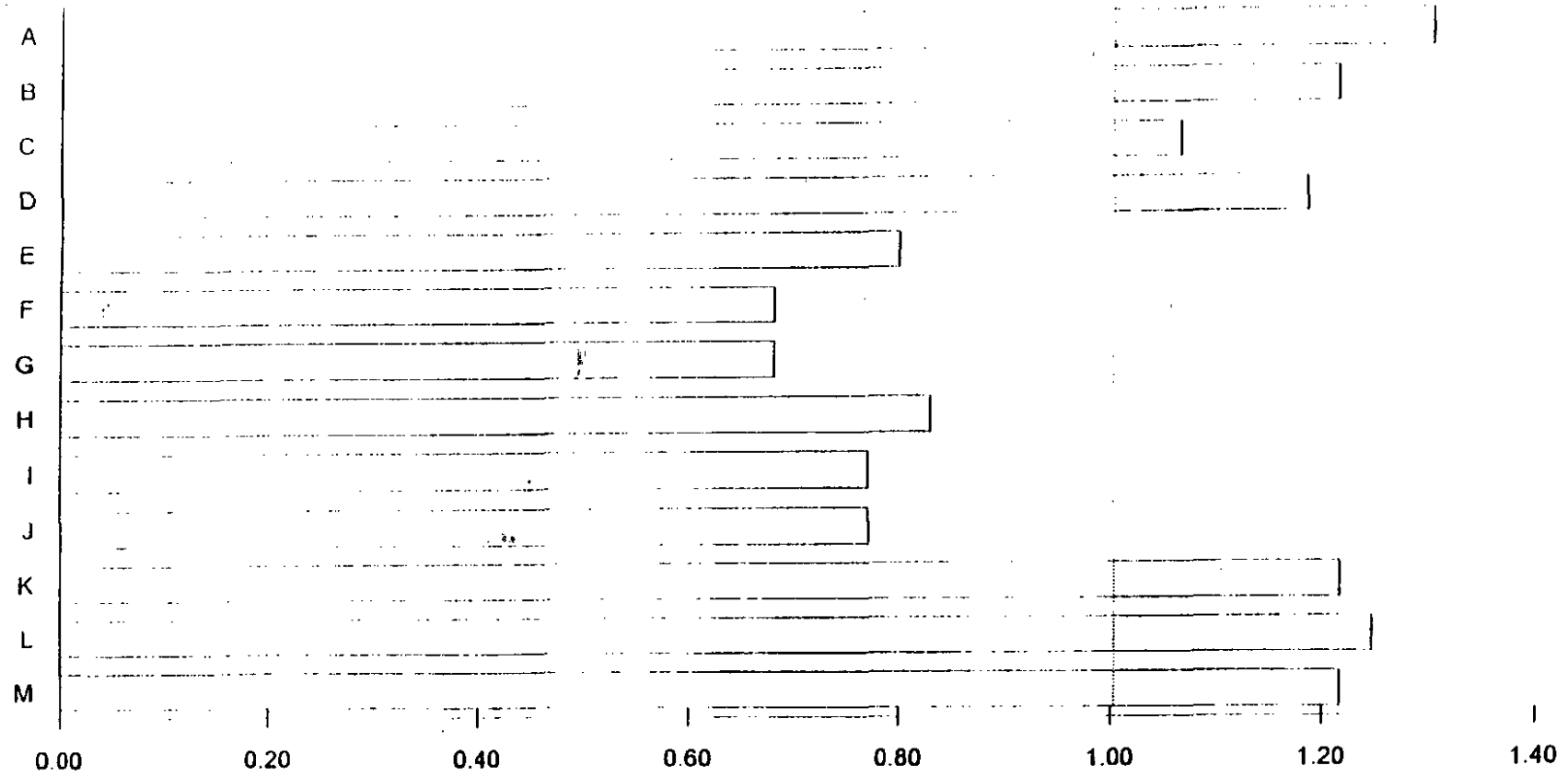

5/12/93

Table4

overall coupon performance (abrasion depth / average abrasion) versus location									
		columns							row
rows	material	1	2	3	4	5	6	7	average
1	M	1.04		1.04	0.89		1.48	1.63	1.22
2	L	1.04		1.04	1.19		1.48	1.48	1.25
3	K	1.19		1.04	1.19		1.48	1.19	1.22
4	J	0.74	0.59		0.89		1.04	0.59	0.77
5	I	0.89	0.59		0.74		1.04	0.59	0.77
6	H	0.59	0.74		1.04		1.34	0.45	0.83
7	G	0.45	0.74		0.89		1.04	0.30	0.68
8	F	0.45	0.74		0.89		1.04	0.30	0.68
9	E	0.45	1.04		1.19		1.04	0.30	0.80
10	D	0.59	1.63		1.63		1.48	0.59	1.19
11	C	0.59	1.34		1.63		1.19	0.59	1.07
12	B	0.74	1.63		1.63		1.48	0.59	1.22
13	A	0.89	1.63		1.63		1.63	0.74	1.31
column average		0.74	1.07	1.04	1.19		1.29	0.72	1.01

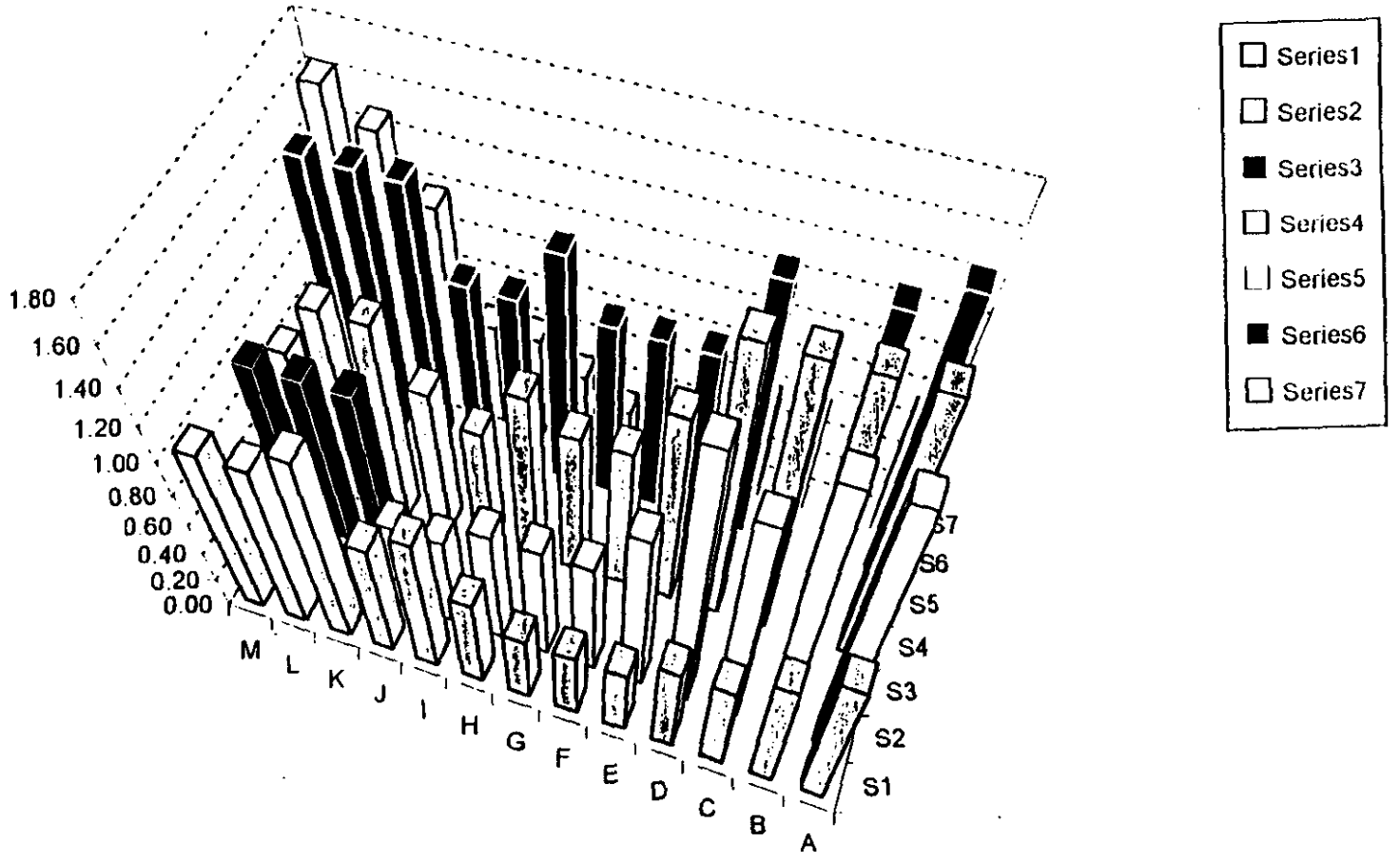
1.80
1.60
1.40
1.20
1.00
0.80
0.60
0.40
0.20
0.00
M
L
K
J
I
H
G
F
E
D
C
B
A
S7
S6
S5
S4
S3
S2
S1
Series1
Series2
Series3
Series4
Series5
Series6
Series7

5/12/93

Attachment 2

DATE: May 11, 1993

RE: **YATES CT121 DEMO FIBERGLASS DESIGN CRITERIA**

FROM: P. M. Honeycutt PMH

TO: K. Vakhshoorzadeh

Per David Waschke's request dated April 27, 1993, please find below our responses:

1. What has been the operating temperature of:
   A. The inlet flue gases prior to the spray chamber? **250 - 280°F**
   B. The flue gas after the spray chamber? **130-135°F**
   C. The flue gas exiting the JBR? **130-135°F**

2. What is the slurry flow rate through the spray chamber nozzles?
   There are a total of 56 nozzles rated at 80 GPM each. The actual flow rate to each nozzle has not been analyzed.

3. What is the operating pressure of the slurry nozzles?
   The nozzles operate at 30 PSI.

4. What is the velocity of the flue gas?
   The spray chamber velocity is 45 feet/sec.

5. Have you analyzed the actual air flows?
   Yes, at the inlet and outlet.

6. How do the spray patterns of the limestone slurry affect the gas flow?
   This is unknown.

PMH/esw51193

xc: D. Burford

Attachment 3

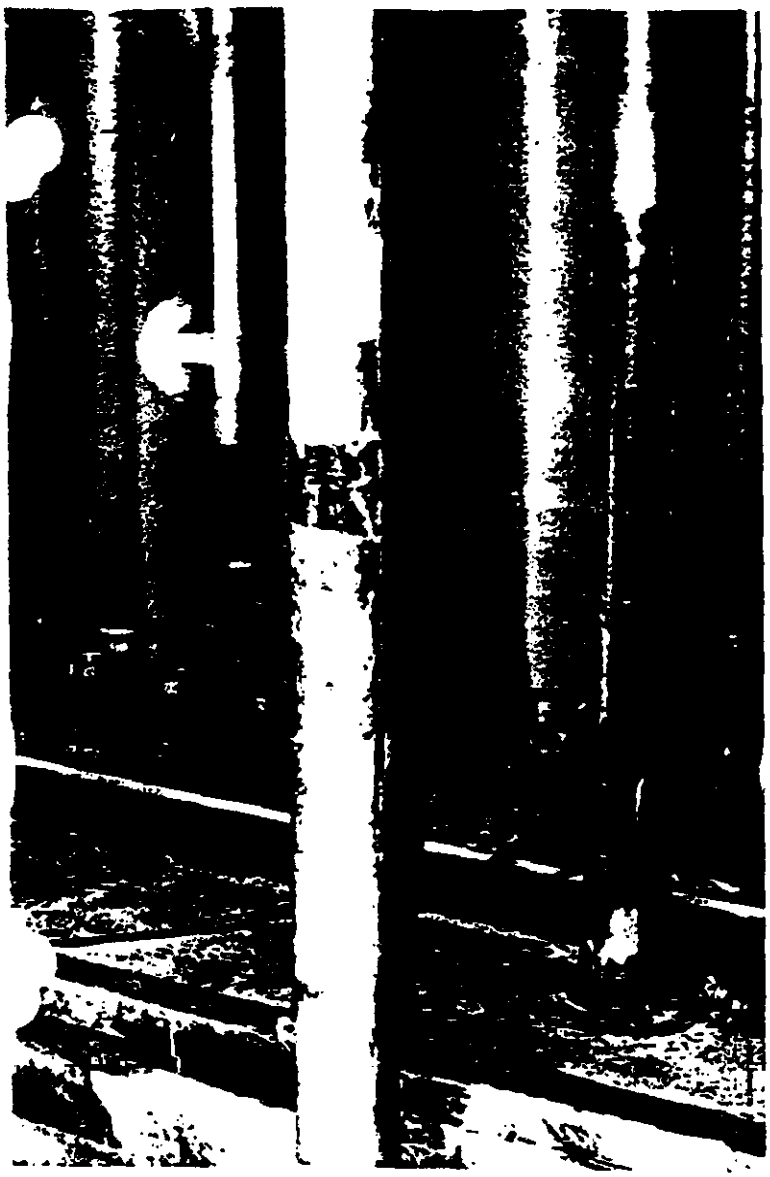

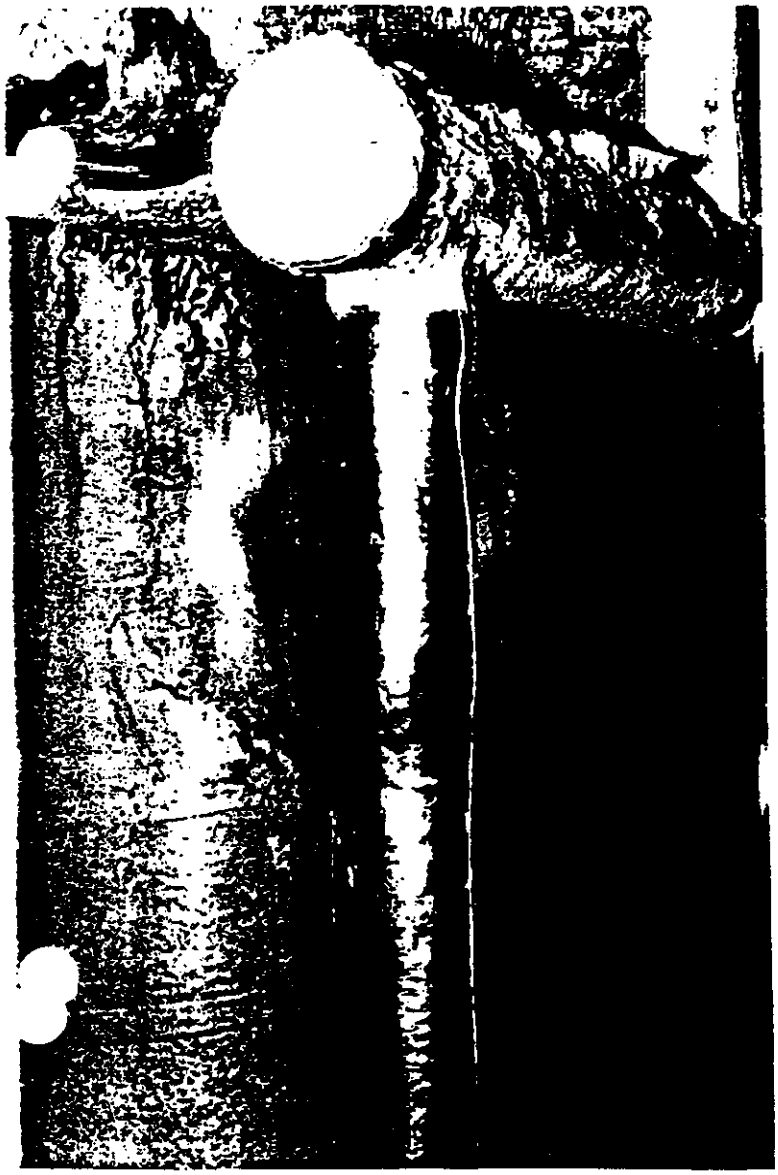

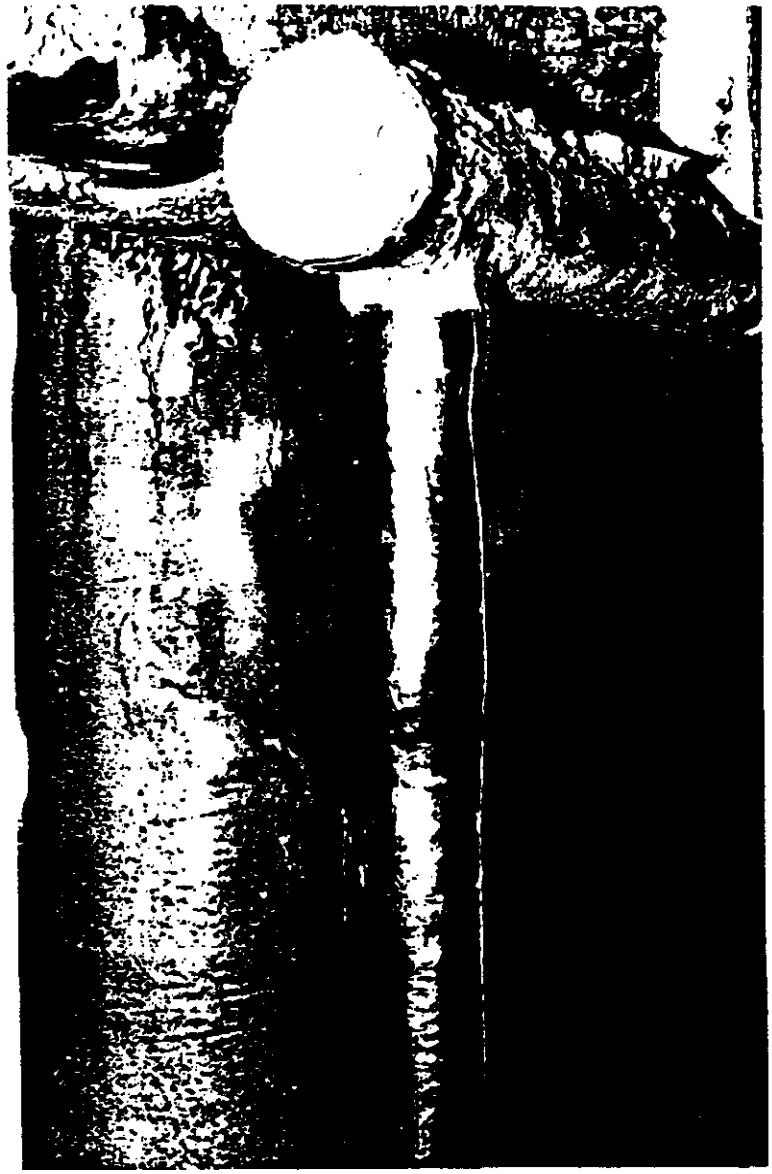

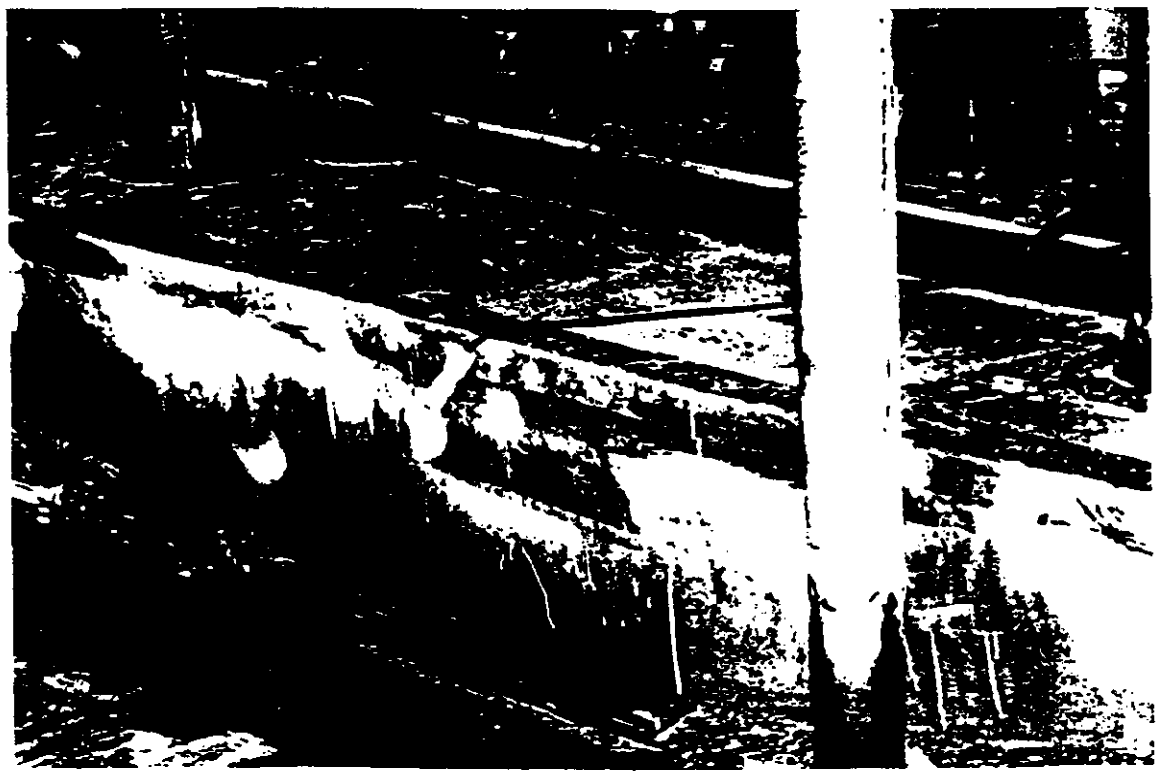

Exhaust plenum

matrix	sample #	days	weight (g)	Weight Change
1619-C	c170	0	135.92	
		790	141.9	5.98
	c173	0	138.8	
		790	141.2	2.4
	c174	0	128.69	
		790	132.5	3.81
1620-C	c188	0	133.48	
		790	139.4	5.92
	c191	0	160.21	
		790	166.3	6.09
	c192	0	151.91	
		790	158.1	6.19
620MC-C	c194	0	136.26	
		790	138.5	2.24
	c197	0	139.95	
		790	146.2	6.25
	c198	0	144.68	
		790	151	6.32
1620-CV	c206	0	102.02	
		790	108.7	6.68
	c207	0	128.33	
		790	137.2	8.87
	c210	0	137	
		790	144.2	7.2
1619-CV	c214	0	122.7	
		790	143.5	20.8
	c215	0	130.05	
		790	137.1	7.05
	c216	0	122.86	
		790	129.6	6.74
992-CV	c176	0	135.04	
		790	140.8	5.76
	c180	0	123.99	
		790	129.7	5.71
992-C	c183	0	123.2	
		526	132.2	9
	c185	0	126	
		790	131.8	5.8
	c186	0	118.7	
		790	135.8	17.1
Derakane 470-36	c229	0	107.34	
		580	107.4	0.06
	c230	0	145.27	
		580	145.5	0.23

Exhaust Plenum: The weight of all samples increased.

Inlet Duct

matrix	sample #	days	weight (g)	Weight change
1619MC-CV	c3	0	127.47	
		790	119.4	-8.07
	c6	0	134.51	
		790	103	-31.51
1619-C	c9	0	136	
		790	127.8	-8.2
	c12	0	129.58	
		790	128.2	-1.38
1620-C	c27	0	156.77	
		790	116.9	-39.87
992-C	c21	0	125.41	
		790	110.8	-14.61
	c24	0	135.53	
		790	122.3	-13.23
992-CV	c15	0	133.49	
		790	142	8.51
	c18	0	134.48	
		790	140.7	6.22
Derakane 470-36	c217	0	127.17	
		790	99.5	-27.67
	c218	0	127.18	
		790	86.2	-40.98

Inlet Plenum

matrix	sample#	days	weight (g)	Weight change
1619MC-CV	c58	0	117.93	
		790	129.7	11.77
1619-CV	c106	0	130.9	
		790	135.2	4.3
	c107	0	128.88	
		790	133.4	4.52
	c108	0	126.26	
		790	132	5.74
1620-C	c82	0	155.16	
		790	164.2	9.04
	c83	0	161.92	
		790	171.2	9.28
	c84	0	157	
		790	163.5	6.5
1620MC-CV	c87	0	160.38	
		790	166.6	6.22
	c88	0	129.24	
		790	135.2	5.96
	c89	0	119.13	
		790	125.3	6.17
992MC-CV	c93	0	122.05	
		790	128.3	6.25
	c94	0	124.03	
		790	131.3	7.27
	c95	0	124.64	
		790	132	7.36
	c96	0	137.37	
		790	144.6	7.23
992-CV	c70	0	136.88	
		790	142.9	6.02
Drakane 470-36	c224	0	126.58	
		580	126.8	0.22
	c225	0	141.82	
		580	142.3	0.48

Inlet Duct: The weight of all samples decreases except that of the 992-CV Matrix.

Inlet Plenum: The weight of all samples increases.

INLET DUCT

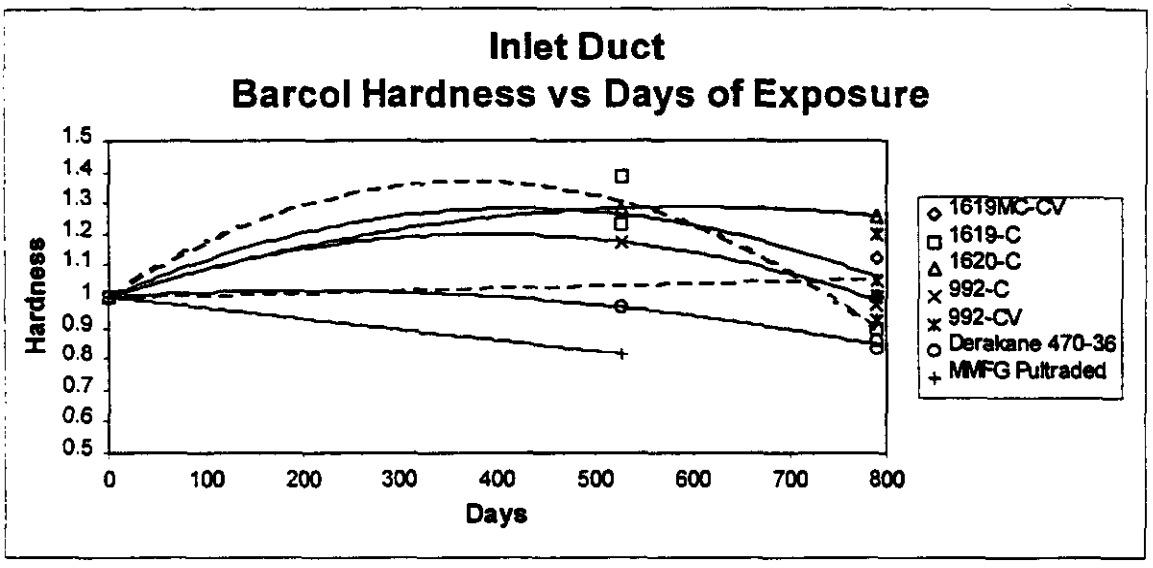
Inlet Duct
Barcol Hardness vs Days of Exposure
Hardness
1.5
1.4
1.3
1.2
1.1
1
0.9
0.8
0.7
0.6
0.5
0
100
200
300
400
500
600
700
800
Days
1619MC-CV
1619-C
1620-C
992-C
992-CV
Derakane 470-36
MMFG Pultraded

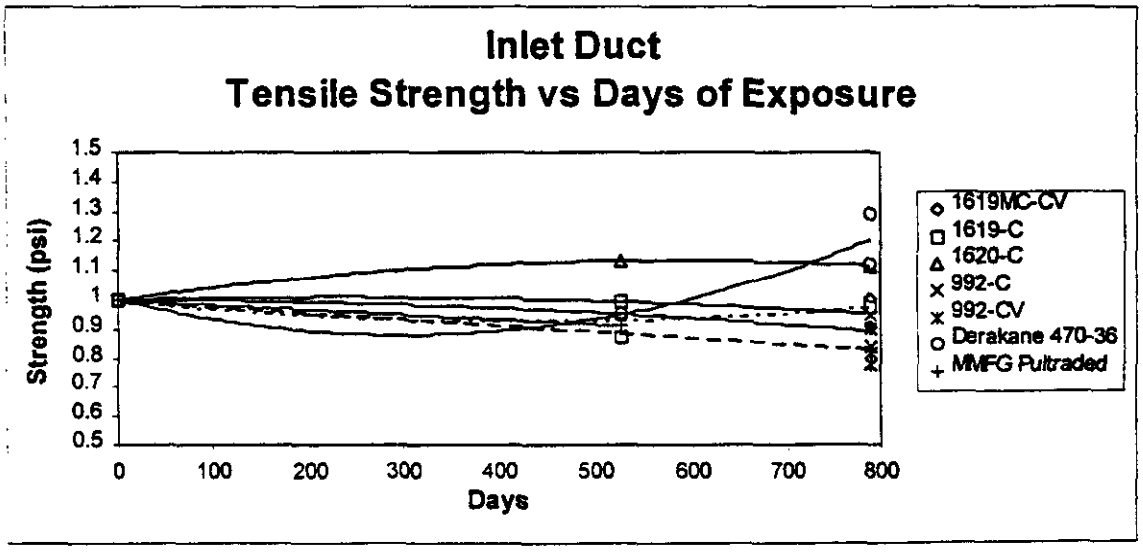
Inlet Duct
Tensile Strength vs Days of Exposure
Strength (psi)
1.5
1.4
1.3
1.2
1.1
1
0.9
0.8
0.7
0.6
0.5
0
100
200
300
400
500
600
700
800
Days
1619MC-CV
1619-C
1620-C
992-C
992-CV
Derakane 470-36
MMFG Pultraded

INLET DUCT

1619-C Matrix

Hardness increases by 38% over first 375 days then decreases.
Final hardness is less than the initial hardness.
Tensile strength decreases by 7% over the 450 days and then increases.
Final; strength less than the initial strength.

1619MC-CV Matrix

Hardness increases by 28% over first 400 days then decreases.
Final hardness is greater than initial hardness.
Tensile strength increases by 2% over first 250 days then decreases.
Final strength less then the initial strength.

1620-C Matrix

Hardness increases by 29% over first 600 days then decreases.
Final hardness is greater than the initial hardness.
Tensile strength increases by 13% over first 550 days then decreases.
Final strength greater than initial strength.

992-CV Matrix

Hardness increases at a rate of .9%/day.
Tensile strength decreases at a rate of 2%/day.

992-C Matrix

Hardness increases by 20% over the first 375 days and then decreases.
Final hardness is less than the initial hardness.
Tensile strength decreases at a rate of 1.4%/day.

Derakane 470-36 Matrix

Hardness increases by 2% over the first 225 days and then decreases.
Final hardness is less than the initial hardness.
Tensile strength decreases by 12% over the first 300 days and then increases.
Final strength is greater than the initial.

MMFG Pultraded Matrix

Hardness decreases at a rate of 3.7%/day.
Tensile strength decreases at a rate of 1.7%/day.

INLET PLENUM

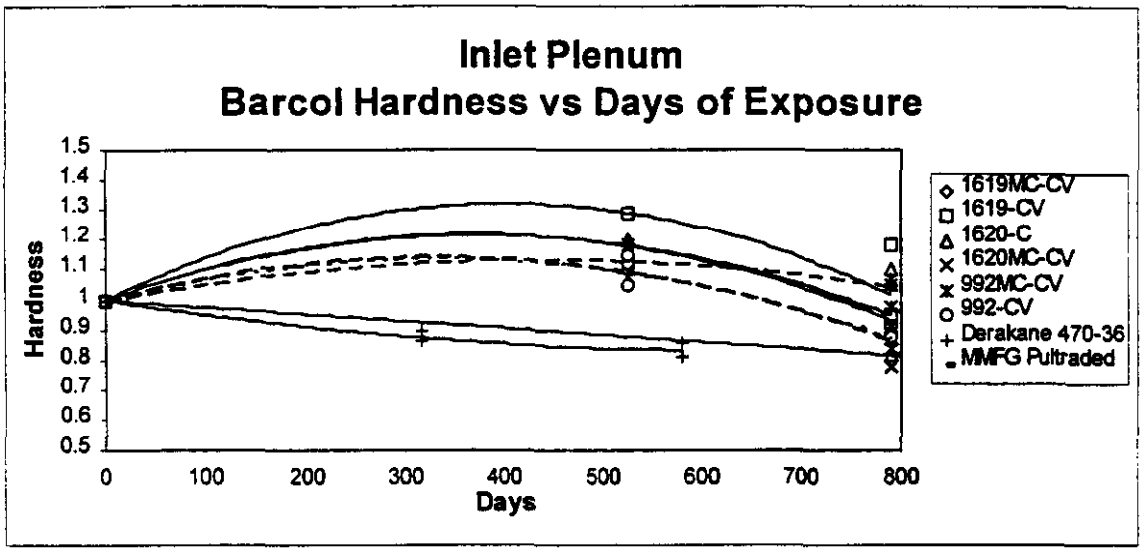

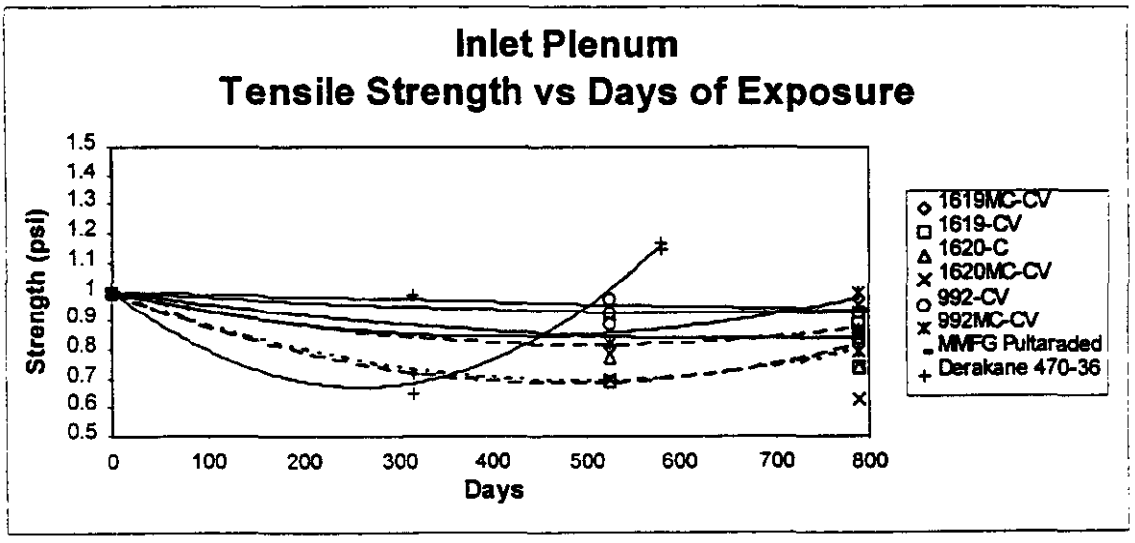

INLET PLENUM

1619MC-C Matrix

Hardness increases by 14% over first 450 days then decreases.
Final hardness is greater than the initial hardness.
Tensile strength decreases by 15% over the first 450 days and then increases.
Final strength is less than the initial strength.

1619-CV Matrix

Hardness increases by 32% over first 425 days then decreases.
Final hardness is greater than initial hardness.
Tensile strength decrease by 31% over first 450 days then increases.
Final strength less then the initial strength.

1620-C Matrix

Hardness increases by 22% over first 375 days then decreases.
Final hardness is less than the initial hardness.
Tensile strength decreases by 16% over first 650 days then increases.
Final strength less than initial strength.

1620MC-CV Matrix

Hardness increases by 15% over first 325 days then decreases.
Final hardness is less than the initial hardness.
Tensile strength decreases by 30% over the first 500 days and then increases.
Final strength is less than the initial strength.

992-CV Matrix

Hardness increases by 14% over first 325 days then decreases.
Final hardness is less than the initial hardness.
Tensile strength decreases by 8% over first 700 days and then increases.
Final strength is less than the initial strength.

992MC-CV Matrix

Hardness increases by 22% over first 375 days then decreases.
Final hardness is less than the initial hardness.
Tensile strength decreases by 18% over first 525 days and then increases.
Final strength is less than the initial strength.

Derakane 470-36 Matrix

Hardness decreases at a rate of 2.9%/day.
Tensile strength decreases by 32% over the first 275 days and then increases.
Final strength is greater than the initial strength.

MMFG Pultraded Matrix

Hardness decreases at a rate of 2.4%/day.
Tensile strength increases at a rate of 1%/day.

EXHAUST PLENUM

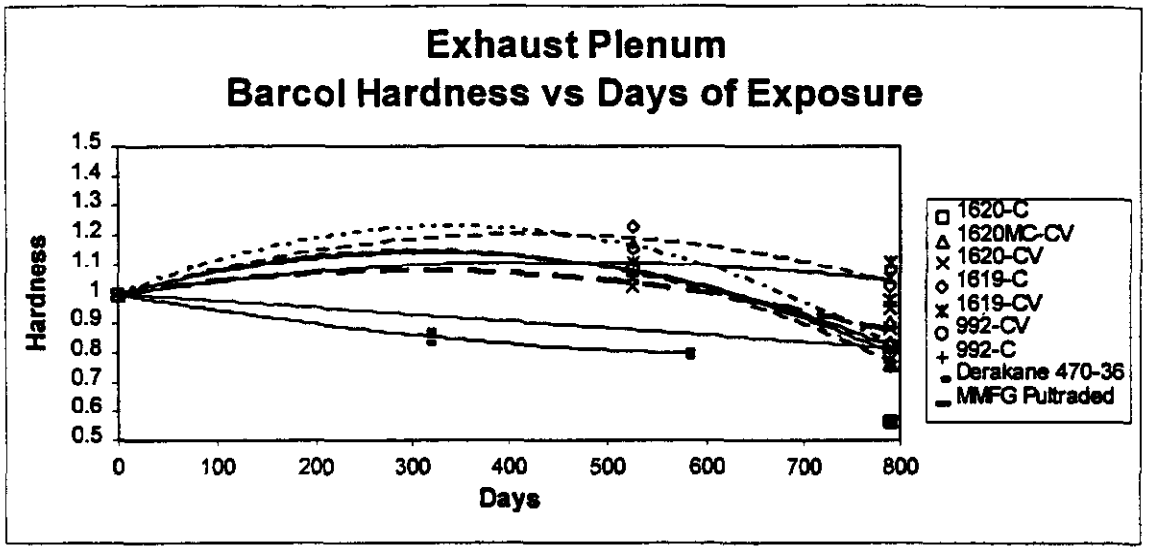

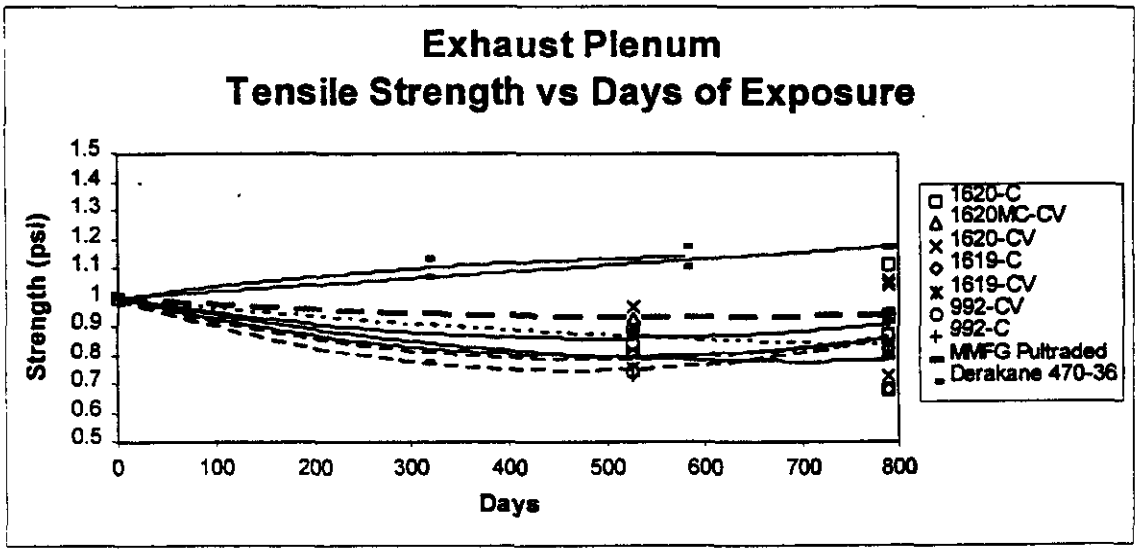

EXHAUST PLENUM

1619-C Matrix

Hardness increases by 21% over first 450 days then decreases.
Final hardness is greater than the initial hardness.
Tensile strength decreases by 22% and then levels off.
If test done over longer period strength may increase again.

1619-CV Matrix

Hardness increases by 11% over first 450 days then decreases.
Final hardness is greater than initial hardness.
Tensile strength decrease by 25% over first 450 days then increases.
Final strength less then the initial strength.

1620-C Matrix

Hardness increases by 14% over first 325 days then decreases.
Final hardness is less than the initial hardness.
Tensile strength decreases by 13% over first 450 days then increases.
Final strength less than initial strength.

1620MC-CV Matrix

Hardness increases by 24% over first 325 days then decreases.
Final hardness is less than the initial hardness.
Tensile strength decreases at a rate of 2%/day.

1620-CV Matrix

Hardness increases by 9% over first 325 days then decreases.
Final hardness is less than the initial hardness.
Tensile strength decreases by 7% over first 525 days and then increases.
Final strength is less than initial.

992-CV Matrix

Hardness increases by 14% over first 325 days then decreases.
Final hardness is less than the initial hardness.
Tensile strength decreases by 21% over first 475 days and then increases.
Final strength is less than the initial strength.

992-C Matrix

Hardness increases by 16 % over first 325 days then decreases.
Final hardness is less than the initial hardness.
Tensile strength decreases by 20% over first 500 days and then increases.
Final strength is less than the initial strength.

Derakane 470-36 Matrix

Hardness decreases at a rate of 3.4%/day.
Tensile strength increases at a rate of 2.5%/day.

MMFG Pultraded Matrix

Hardness decreases at a rate of 2.4%/day.
Tensile strength increases at a rate of 2%/day.

Attachment C

Post-it™ brand fax transmittal memo 7671 | # of pages ▸ 4

To Kamyar	From Pat K. Evans
Co.	Co. SCS
Dept.	Phone # 8-821-6134
Fax # 5367	Fax # 8-821-5103

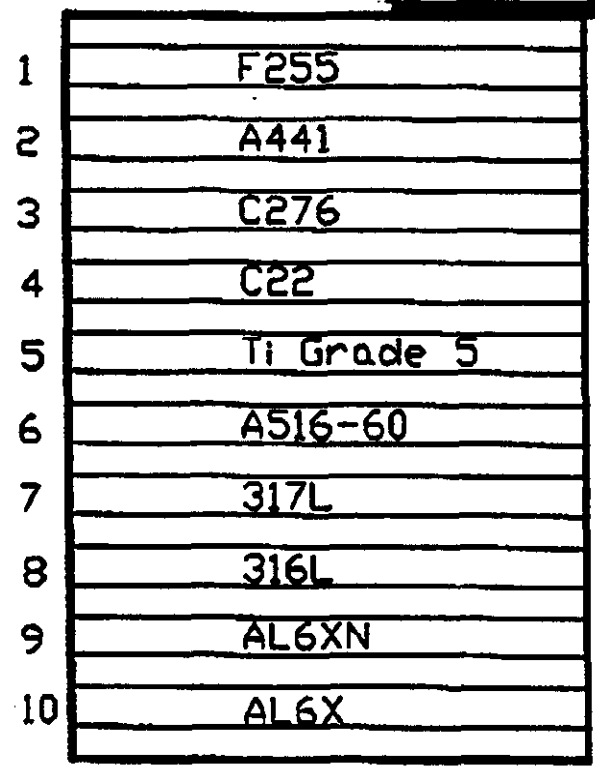

Fully Annealed

Fully Annealed

SAMPLE RACK

All samples are 1/8" except #10 (AL6X)
AL6X is slightly less than 1/8"
Teflon crevice washer between each sample

YATES SCRUBBER

CORROSION SAMPLES
METAL SAMPLES COMPANY

CAD AUTOCAD CDI-Q EVANS92.DWG

ME. L SAMPLES CO.

P.O. BOX 8
RT 1 BOX 152
MUNFORD, AL 36268
(205) 358-4202
FAX (206) 358-4515

MATERIAL TE. REPORT

DATE: 08/26/92

CUSTOMER: SOUTHERN COMPANY SERVICES

CUST. ORDER: VERBAL-P. EVANS

M.S. ORDER: 924007

DEAR CUSTOMER:
WE CERTIFY THAT THIS MATERIAL TEST REPORT IS CORRECT TO THE BEST OF OUR KNOWLEDGE AND THAT THE MATERIAL SUPPLIED MEETS THE REQUIRED SPECIFICATIONS.
THANK YOU.

QUALITY CONTROL DEPARTMENT

CHEMICAL PROPERTIES

ALLOY	HEAT													
255	G646		0.02	25.30	1.90		1.00	3.20	5.10	0.023	0.003	0.50		N-0.19
41	B956		0.19		0.238		1.11			0.016	0.020	0.025		V-0.060
AST.C276	J018		0.003	15.26		5.35	0.48	15.39	BAL	0.007	0.002	0.02		CO-1.35; V-.13; N-3.34
AST.C22	H159		0.003	21.20		4.50	0.25	13.30	BAL	0.006	0.003	0.38		CO-1.96; V-.14; N-3.02
IGR5	F180	6.20	0.02			0.20							BAL	V-3.90; O-0.141; N-0.0
														5; H-<0.005; Y-<0.005
516GR60	F175		0.12			BAL	0.63			0.01	0.026	0.26		
17L	B309		0.017	18.29	0.28	BAL	1.63	3.13	14.0	0.026	0.011	0.59		CO-0.20; N-0.072
16L	H980		0.019	16.30			1.90	2.13	10.18	0.03	0.001	0.50		N-.03
L6XN	J042		0.021	20.52	0.21	BAL	0.34	6.22	23.90	0.026	0.001	0.44		N-.20
L6X	0177	0.006	0.020	20.45	0.19	BAL	1.47	6.30	24.65	0.030	0.002	0.50	0.005	N-0.042; CO-0.19; B-0.(
														008

PHYSICAL PROPERTIES

ALLOY	HEAT									
255	G646	128	95	25 (2")		RC 26	ANNLD	S32550	HAYNES
41	B956	78.6/79.0	57.7/57.9	21.0/25.0				S44100	AMERICAN ALLOY
AST.C276	J018	109	53	60 (2")		RB 90	ANNLD	N10276	CORROSION MATERIALS
AST.C22	H159	115	53	58 (2")		RB 90	ANNLD	N06022	HAYNES INT'L
IGR5	F180	149.2	139.1	14.0				R56400	TICO TITANIUM
516GR60	F175	66.2	49.3	24.0(8.0")				K02100	ARMCO
17L	B309	88.8	45.5	46.0		Rb 78		S31703	EASTERN
16L	H980	85.5	40	57 (2")		RB 78	CR ANN	S31603	REYNOLDS ALUMINUM
L6XN	J042	108	58.5	46		RB 87	ANNLD	N08367	ROLLED ALLOYS
L6X	0177							N08366	ALLEGHENY

Date: 08/26/92 Sheet: 1

Metal Samples Co., Inc.
Phone: (205) 358-4202
Initial Weight Log

Customer : SOUTHERN CO.SERVICE Shop Order : 924007
Purchase Order : VERBAL

Material : 316L

Serial No.	Weight(g)	Len.(in.)	Wid.(in.)	Thick(in.)	Hole(in.)
B0001	16.2474				

Material : 317L

Serial No.	Weight(g)	Len.(in.)	Wid.(in.)	Thick(in.)	Hole(in.)
01	16.2249				

Material : A441

Serial No.	Weight(g)	Len.(in.)	Wid.(in.)	Thick(in.)	Hole(in.)
01	18.0140				

Material : A516-60

Serial No.	Weight(g)	Len.(in.)	Wid.(in.)	Thick(in.)	Hole(in.)
01	17.0638				

Material : AL6X

Serial No.	Weight(g)	Len.(in.)	Wid.(in.)	Thick(in.)	Hole(in.)
01	9.4109				

Material : AL6XN

Serial No.	Weight(g)	Len.(in.)	Wid.(in.)	Thick(in.)	Hole(in.)
01	17.1741				

Material : C22

Serial No.	Weight(g)	Len.(in.)	Wid.(in.)	Thick(in.)	Hole(in.)
01	19.0074				

Material : C276

Serial No.	Weight(g)	Len.(in.)	Wid.(in.)	Thick(in.)	Hole(in.)
A0036	18.8909				

Date: 08/26/92 Sheet: 2

Metal Samples Co., Inc.
Phone: (205) 358-4202
Initial Weight Log

Customer : SOUTHERN CO.SERVICE Shop Order : 924007
Purchase Order : VERBAL

Material : F255

Serial No.	Weight(g)	Len.(in.)	Wid.(in.)	Thick(in.)	Hole(in.)
01	16.4359				

Material : TI-5

Serial No.	Weight(g)	Len.(in.)	Wid.(in.)	Thick(in.)	Hole(in.)
01	10.2437				